



**UNIVERSITY OF
BIRMINGHAM**

**THE STUDY OF PHARMACEUTICAL POWDER MIXING THROUGH IMPROVED FLOW
PROPERTY CHARACTERISATION AND TOMOGRAPHIC IMAGING OF BLEND
CONTENT UNIFORMITY**

by

Brian Armstrong

A thesis submitted to
The University of Birmingham
for the degree of
Engineering Doctorate

Department of Chemical Engineering
School of Engineering
The University of Birmingham
April 2011

UNIVERSITY OF
BIRMINGHAM

University of Birmingham Research Archive

e-theses repository

This unpublished thesis/dissertation is copyright of the author and/or third parties. The intellectual property rights of the author or third parties in respect of this work are as defined by The Copyright Designs and Patents Act 1988 or as modified by any successor legislation.

Any use made of information contained in this thesis/dissertation must be in accordance with that legislation and must be properly acknowledged. Further distribution or reproduction in any format is prohibited without the permission of the copyright holder.

Summary

The regulatory framework in which pharmaceutical companies have to work has changed significantly since the late 1990's. The development and implementation of risk based approaches to processing pharmaceutical powders allows the pharmaceutical manufacturers the freedom to adopt real-time release for their products whilst reducing the regulatory burden for both the statutory bodies and the manufacturers.

This thesis has been a collaboration between Buck Systems and the University of Birmingham School of Chemical Engineering to evaluate and develop methods which would enhance the way in which Buck Systems can, in co-operation with their clients, enhance their understanding of how powder properties affect their products that are used in pharmaceutical manufacturing to better comply with the changes in the regulatory environment.

To this end simple and quick screening methods for characterisation of customers' powders with a view to identifying potential problems prior to blending tests have been developed to replace the current *ad hoc* approach. These include the use of tests that have been relied on historically as well as newer, more universal and robust techniques such as automated shear cells and powder rheometers. Detailed characterisation trials have shown where these techniques can be successfully applied and where their limitations lie. Further work has shown how powder systems can be better evaluated within the existing HAZOP framework. Specific evaluation of the hopper design methodology has resulted in the development of an expert system to enable the rapid sensitivity analysis of design options. In addition the limits of the hopper design method have been explored and some limitations identified where significant overdesign may occur.

The evaluation of content uniformity in a laboratory scale blender using specialist Positron Imaging equipment available at the University of Birmingham has also been undertaken. The unique study of the blender contents using Positron Emission Tomography has provided a range of insights into the way binary and ternary powder systems interdisperse.

Dedicated to

Evaline May Armstrong

**my recently departed mother who always
inspired and supported me**

John Armstrong

**my father who's resilience and
dry wit have kept me grounded**

and to

Sally Ann Brain

for all her support and understanding

Acknowledgements

I would like to thank all those at the University of Birmingham who helped me with this project; Dr Xiangfeng Fan; Dr David Parker; Dr Richard Greenwood; Dr Andy Ingram; Dr Neil Rowson; Dr Charley Wu; Professor Jonathan Seville; and Professor Mike Adams.

I would also like to thank all those at NIRO/GEA Pharma Systems for initiating this project and for their support, both financial and technical. I would especially like thank Trevor Page; Vejay Jeckmohan; Stephen Boswell and Mike Waldron.

The staff at Freeman Technology must also be mentioned for their support, ideas and for access to a powder rheometer to undertake many of the tests reported here. Reg Freeman, Tim Freeman and Carl Duckels deserve special thanks.

Finally I would like to thank the EPSRC for financial support through the excellent Engineering Doctorate programme.

Table of Contents	Page
List of Figures.....	iv
List of Tables	xvi
Chapter 1 – Introduction	1
1.1 The aims and goals of the project.....	2
1.2 Background to solid dose manufacturing in the pharmaceutical industry.....	3
1.3 History of Buck Systems	6
1.4 Key Market Segments.....	8
1.5 Market Structure and Size.....	10
1.6 Manufacturing for pharmaceutical processing.....	17
1.7 Recent FDA initiatives that affect the development of pharmaceutical processing systems	19
1.8 Thesis Outline	25
1.9 References.....	26
Chapter 2 – Powder Characterisation	27
2.1. Introduction	28
2.2. Powder Characterisation Testing	31
2.3. Powder Testing Equipment.....	40
2.3.1. Shear Cell.....	40
2.3.2. Angle of repose	83
2.3.3. Jolting Volumeter.....	92
2.3.4. Flow through an orifice & Flowability Tester Model BEP2 tester	98
2.3.5. Powder rheometry	109
2.4. Comparative evaluation of powder testers	140

2.5.	An evaluation of the comparative effectiveness of universal powder testers	149
2.5.1.	Pharmaceutical grade Zinc Oxide	151
2.5.2.	Pharmaceutical excipients	158
2.5.3.	Pharmaceutical blends	164
2.5.4.	Pharmaceutical Excipient	166
2.5.5.	Summary of comparison testing	169
2.6.	Summary & conclusions	169
2.7.	Instrument Manufacturers	174
2.8.	References	176
Chapter 3 – Powder Mixing		180
3.1.	Introduction	181
3.2.	Mixing in the pharmaceutical industry	182
3.2.1.	Influences on blending	186
3.2.2.	Modes of flow & mechanisms of dispersal in a tumble blender	190
3.2.3.	Stress levels in IBC blenders	195
3.2.4.	The measurement of powder cohesion and its influence on tumble blender performance	199
3.3.	Positron Emission Tomography	205
3.3.1.	Tomographic evaluation of mixing behaviour	211
3.3.2.	Sample preparation	212
3.3.3.	PEPI Studies	214
3.3.4.	PEPT studies	221
3.3.5.	PET Studies – Siemens ECAT Camera	232
3.4.	Summary	264
3.5.	References	266
Chapter 4 – Powder Systems Evaluation		272
4.1.	Introduction	273
4.2.	Powder systems and their analysis	273
4.2.1.	The extension of the HAZOP methodology	279

4.2.2. Additional considerations	285
4.2.3. Summary	287
4.3. Sensitivity analysis of storage system design	288
4.3.1. Review of bin design using standard protocols.....	291
4.3.2. Sensitivity of outlet size to variations in yield loci.....	300
4.3.3. The use of alternate evaluations of the Flow Function on hopper design parameters.	305
4.3.4. Summary	318
4.4. Perceptual mapping	320
4.5. Evaluation of the Decel system	339
4.5.1. Results and observations.....	345
4.5.2. Powder characterisation study	353
4.5.3. Powder system analysis.....	358
4.5.4. Summary and discussion	362
4.6. Conclusions.....	364
4.7. References	365
Chapter 5 – Final conclusions & suggested future work.....	369
5.1. Main conclusions	370
5.2. Suggested Future Work	376

Appendix 1. Background to Shear Cell Testing

Appendix 2. Hopper Design Software Tool

List of Figures	Page
Figure 1.1: Organogram of GEA Niro Pharma Systems.....	7
Figure 1.2: Order value by year for Buck Systems.....	10
Figure 1.3: Split of Buck Systems customer type between ethical.....	12
Figure 1.4: Split of contracts 1997 -1999.....	13
Figure 1.5: Split of contract by region 1997-2000 and 2000-2005.....	14
Figure 1.6: Order Value by Country 1997-2005.....	15
Figure 1.7: Order Value by Customer 1997-2005.....	16
Figure 1.8: A graphical representation of the concepts	24
Figure 2.1: RST-XS and FT4 shear cells.....	42
Figure 2.2: Screenshot of RST-XS performing a shear test. The blue trace shows the progress of the shear stress on the left axis; the red trace shows the height of the lid on the right axis; the green line indicates the end of the test	44
Figure 2.3: Screenshot of FT4 performing a shear test. The top trace shows the evolution of the force, measured by the load cell, during the test; the lower trace indicates the torque measurement during the same time period. Both graphs scroll right to left during the test.....	44
Figure 2.4: Filling of the RST-XS Shear Cell	45
Figure 2.5: Force and torque traces for a shear test on Limestone at 3kPa consolidating stress with the carriage undertaking each shear test at a fixed height once the target consolidating force has been achieved, generated using an FT4 shear cell attachment.....	47
Figure 2.6: Yield loci for shear tests on Limestone at 3kPa consolidating stress with the FT4 carriage undertaking each shear test at a fixed height (blue trace) and with the carriage under normal force control parameters (green trace).	48

Figure 2.7: Comparison of force control techniques for the FT4 shear cell for a highly dilating powder. In the top graph, the Blue trace is simple proportional control where the instrument attempts to maintain a constant force but fails to do so; the red trace shows a modulated back off algorithm where the normal force is maintained at a constant level through the incipient failure (shown in the lower torque graph).....	49
Figure 2.8: Comparison of force control techniques for the FT4 shear cell for a highly dilating powder. Blue trace is simple proportional control; green trace shows a modulated back off algorithm	50
Figure 2.9: Yield locus for Lactose using recommended procedure for RST-XS shear cell at a consolidating load of 2kPa. The software creates a 'bent' locus which significantly increases the derived cohesion and ff_c values for the powder compared to a linear regression fit.....	51
Figure 2.10: Graphical description of the yield locus and the parameters derived from the fitting of Mohr Circles to the σ/τ data set.....	53
Figure 2.11: A yield locus derived from 5 measurement points fitted to linear and polynomial regressions for Limestone CRM116, generated using an FT4 shear cell attachment.	55
Figure 2.12: A yield locus derived from 7 measurement points fitted to linear and polynomial regressions for Limestone CRM116, generated using an FT4 shear cell attachment.	56
Figure 2.13: Flow Functions of exemplar powders using data from tests on the RST-XS at 8kPa consolidating stress	60
Figure 2.14: Comparison of the Flow Function values derived for the exemplar powders using data from tests on the RST-XS at 8kPa consolidating stress and the FT4 at 9kPa consolidating stress	61

Figure 2.15: Yield loci for Celphere 102 generated using the RST-XS shear cell at 2, 4 & 8kPa consolidating loads	63
Figure 2.16: Yield loci for Celphere 102 generated using the RST-XS shear cell	63
Figure 2.17: Yield loci for Celphere 305 generated using the RST-XS shear cell at 2 & 4kPa consolidating loads.....	65
Figure 2.18: Yield loci for Celphere 305 generated using the RST-XS shear cell at 2, 4 & 8kPa consolidating loads	65
Figure 2.19: Flow Function for Celphere 305 generated using the RST-XS shear cell at 2, 4 & 8kPa consolidating loads	66
Figure 2.20: Yield loci for Mannitol generated using the RST-XS shear cell at 2kPa consolidating load	67
Figure 2.21: Yield loci for Starch generated using the RST-XS shear cell at 2kPa consolidating load	67
Figure 2.22: Three repeat shear tests at 9kPa consolidating load for Tablet Blend Placebo generated using an FT4 shear cell attachment.....	70
Figure 2.23: Average of three repeat tests at 9kPa consolidating load for Tablet Blend Placebo generated using an FT4 shear cell attachment.....	71
Figure 2.24: Three repeat tests at 9kPa consolidating load for Tablet Blend Placebo showing Mohr's circles fitted to the linear fit yield loci generated using an FT4 shear cell attachment.	72
Figure 2.25: Average of three repeat tests at 9kPa consolidating load for Tablet Blend Placebo showing Mohr's circles fitted to the linear fit yield loci generated using an FT4 shear cell attachment.....	73
Figure 2.26: Four repeat shear tests at 9kPa consolidating load for Limestone generated using an FT4 shear cell attachment.	76
Figure 2.27: Average of 4 repeat tests at 9kPa consolidating load for Limestone generated using an FT4 shear cell attachment.....	76

Figure 2.28: Screenshot of normal stress and shear stress traces from shear cell tests of Limestone (trace [a]) and micro-crystalline cellulose (Avicel PH200) (trace ([b]) @ 9kPa consolidating stress generated using an FT4 shear cell attachment in which single and multiple pre-shears are required to achieve critical consolidation respectively	79
Figure 2.29: Yield loci of Celphere 305 at a consolidating load of 3kPa showing the effect of single and two pre-shears generated using an FT4 shear cell attachment.....	80
Figure 2.30: Raw data of Celphere 305 at a consolidating load of 3kPa showing the effect of single and two pre-shears, generated using an FT4 shear cell attachment.....	81
Figure 2.31: The definition of (poured) angle of repose.....	83
Figure 2.32: Various determinations of the Angle of Repose; (a) the poured angle of repose; (b) the impacted, wet or cohesive materials where multiple angles of repose [α_1 and α_2 for example] are observed; (c) easily aerated materials; (d) drained; (e) sliding; (f) compacted [σ is an applied consolidating stress]; (g) aerated: (h) rolling; (i) feeder discharge [α_s is the static angle of repose – feeder stationary; α_d is the dynamic angle of repose – feeder operational]	84
Figure 2.33: Geldart AOR tester (left) and Hosokawa Powder Tester – including an AOR test (right).....	85
Figure 2.34: Angles of repose of a range of pharmaceutical excipients	86
Figure 2.35: Angles of repose for the exemplar powders generated using the Geldart Angle of Repose Tester.....	89
Figure 2.36: Single Vessel Jolting Volumeter	93
Figure 2.37: Results from testing exemplar powders using a Jolting Volumeter (n=3 for all tests)	97
Figure 2.38: Glass flow funnel as shown in the British Pharmacopoeia	99
Figure 2.39: Alternative flow funnel and nozzle made from acid resistant stainless steel (V4A, CrNi) as shown in the British Pharmacopoeia.....	99

Figure 2.40: The Flowability Tester Model BEP2 Powder Flowability Tester	100
Figure 2.41: Measured Data from Flowability Tester Model BEP2 (n=3 for all tests)	105
Figure 2.42: Calculated Coefficient of Friction (K) and Drained Angle Repose – Flowability Tester Model BEP2	106
Figure 2.43: The Powder Flow Analyser (left) and the FT4 Powder Rheometer (right).....	109
Figure 2.44: Example of Cohesion Test raw data – the trace follows the blade as it passes down through column of powder (from zero to the 70mm maximum travel point) and is designated by the positive force (compression) and then as it traverses back up through the powder (lifting) to reach its original start point.....	112
Figure 2.45: Example of raw data from a PFSD Test – the trace follows the blade as it passes down through column of powder (from zero to the 70mm maximum travel point) and is designated by the positive force (compression) and then as it traverses back up through the powder (lifting) to reach its original start point. The different traces represent the different speeds of the PFSD test from 10 to 100 mm/s	114
Figure 2.46: PFA compaction coefficient for a range of exemplar powders	116
Figure 2.47: PFA compaction coefficient for three tests of Sodium Benzoate.....	117
Figure 2.48: Shear cell data and flow functions for two Lactose/Avicel 102 systems, one with added magnesium stearate (MgSt).....	119
Figure 2.49: PFSD results for two Lactose/Avicel systems one with added	120
Figure 2.50: Motion and pathway of the FT4 blade during a test	121
Figure 2.51: A dynamic test for 4 of the test powders showing 7 repeat tests at a blade tip speed of 100mm/s to evaluate the powders flow stability, followed by 4 tests at reducing blade tip speed from 100mm/s to 10mm/s	126
Figure 2.52: An aeration test where the flow energy of the sample is evaluated whilst increasing quantities of air are passed through the base of the test vessel....	126

Figure 2.53: The compressibility of samples evaluated by change in volume with respect to an applied normal stress	127
Figure 2.54: The pressure drop across the powder bed with respect to an applied normal stress.....	127
Figure 2.55: Dynamic test data generated by the FT4 Powder Rheometer	131
Figure 2.56: Action of test blade on a cohesive/compressible powder	136
Figure 2.57: Action of test blade on a non-cohesive/non-compressible powder	137
Figure 2.58: Comparison of the Flow Function, BFE and Carr's Compressibility Index for the exemplar powders.....	144
Figure 2.59: Comparison of results from shear cell, powder rheometer and Jolting Volumeter	145
Figure 2.60 Ranking of exemplar powders according to flowability defined by the test method	147
Figure 2.61: Comparison of relative flowability by additive combination of ranking levels for all tests shown in Table 2.19	148
Figure 2.62: A dynamic test for the zinc oxide powders showing 7 repeat tests at a blade tip speed of 100mm/s to evaluate the powders flow stability, followed by 4 tests at reducing blade tip speed from 100mm/s to 10mm/s	153
Figure 2.63: Comparison of the Basic Flowability Energy for the two Zinc Oxide materials at three different feeder speeds.	154
Figure 2.64: Relative Flow Energies of.....	155
Figure 2.65: Yield loci for Zinc Oxide samples generated using the FT4 shear cell at 9kPa consolidating load	156
Figure 2.66: Comparison of the Flow Function for the two Zinc Oxide materials at three different feeder speeds.	156

Figure 2.67: A dynamic test for the Vanillin and Ethyl Vanillin powders showing seven repeat tests at a blade tip speed of 100mm/s to evaluate the powders flow stability, followed by 4 tests at reducing blade tip speed from 100mm/s to 10mm/s.....	159
Figure 2.68: Yield loci for Vanillin and Ethyl Vanillin samples generated using the FT4 shear cell at 9kPa consolidating load.....	160
Figure 2.69: Photographs of the particles of Vanillin (l) and Ethyl Vanillin (r).....	160
Figure 2.70: Selection of CCD images of Vanillin generated by Sympatec Qicpic.....	161
Figure 2.71: Selection of CCD images of Ethyl Vanillin generated by Sympatec Qicpic.....	162
Figure 2.72: Aspect ratio vs particle size for three tests each of Ethyl Vanillin & Vanillin collected by Sympatec Qicpic – note the dramatic split at 300microns between the high aspect ratio Vanillin and the low aspect ratio Ethyl Vanillin.....	162
Figure 2.73: Yield loci for two tablet blends generated using the FT4 shear cell at 9kPa consolidating load	165
Figure 2.74: A dynamic test for two tablet blends showing 7 repeat tests at a blade tip speed of 100mm/s to evaluate the powders flow stability, followed by 4 tests at reducing blade tip speed from 100mm/s to 10mm/s	165
Figure 2.75: A dynamic test for two samples of DCP showing 7 repeat tests at a blade tip speed of 100mm/s to evaluate the powders flow stability, followed by 4 tests at reducing blade tip speed from 100mm/s to 10mm/s	167
Figure 2.76: Yield loci for for two samples of DCP generated using the FT4 shear cell at 9kPa consolidating load	167
Figure 2.77: The compressibility of samples evaluated by change in volume with respect to an applied normal stress for two samples of DCP	168
Figure 3.1: Examples of IBCs	182
Figure 3.2: A tumble blender in operation.....	182

Figure 3.3: Laboratory scale (left) and production scale (right) blenders equipped with NIR sensing head (GEA Pharma Systems 2010a)	184
Figure 3.4: Laboratory Scale Blender in-situ prior to PET experiment	188
Figure 3.5: Isometric drawing of the 10litre mini-IBC	189
Figure 3.6: Modes of flow in a rotating drum with respect to rotational speed – fastest to slowest, R to L – after (Pirard et al. 2009).....	190
Figure 3.7: Example of the balance of the mechanisms occurring within a mixing process after (Miyunami 2006)	194
Figure 3.8: Normal loads generated at the base of a column of powder derived for three common pharmaceutical excipients using Janssen’s equation.....	196
Figure 3.9: The vertical stress in a half filled 1.35mx1.6m cylinder with respect to the depth in the cylinder for lactose, using a wall friction angle of 25° derived from a wall friction test using stainless steel coupon ($R_a = 0.28\mu\text{m}$) from Janssen’s Equation.....	198
Figure 3.10: The GEA Prism™ intensifier bar shown schematically in plan view in an IBC fitted to a post hoist (left) and a photo of the Prism™ in-situ (right)	200
Figure 3.11: Detector block and the ring block of a PET camera	207
Figure 3.12: The data collection process from a PET camera.....	208
Figure 3.13: The ADAC gamma camera	209
Figure 3.14: ECAT scanner in a medical application.....	210
Figure 3.15: Example of PEPI test using MCC in plastic tub showing two orthogonal views of the system – colours at the bottom of the scale show (relatively) lower concentration to those at the top of the scale.	215
Figure 3.16: Experimental set up for PEPI testing.....	217
Figure 3.17: Normalised PEPI image showing side view	219
Figure 3.18: Normalised PEPI image showing top view.....	220
Figure 3.19: Schematic of dispersion calculation method	222

Figure 3.20: Screen shot of dispersion analysis for Sodium Benzoate	224
Figure 3.21: Cumulative dispersion for MCC tracer in Sodium Benzoate	226
Figure 3.22: Cumulative dispersion for MCC tracer in Lactose	227
Figure 3.23: Statistical representation of dispersion in	228
Figure 3.24: Statistical representation of dispersion in	229
Figure 3.25: Cumulative dispersion of a tracer particle in binary systems.....	230
Figure 3.26: Mini-IBC located in its support frame prior to insertion into the measurement cavity inside the camera.....	234
Figure 3.27: Screenshot of ImageJ software	236
Figure 3.28: Re-constructed sinogram of a blending experiment showing the 62 slice images of the powder in the test vessel moderated for the background and vessel transmission scans.....	238
Figure 3.29: An example of the image noise on a medical scan (left) and the resultant processed image (right)	239
Figure 3.30: Views of the blender contents after 5, 20 (top left, top right) 55 & 100 revolutions (bottom left, bottom right)	240
Figure 3.31: Pixel intensity for an unmasked data set, taken after 15 revs, for an experiment where a 2% MCC bolus was mixed in 5litres of Lactose at 15rpm	241
Figure 3.32: Pixel intensity for a masked data set, taken after 15 revs, for an experiment where a 2% MCC bolus was mixed in 5litres of Lactose at 15rpm	241
Figure 3.33: Raw data set exported from ImageJ into a spreadsheet for 2% MCC bolus in 5litresof Lactose at 10rpm.....	242
Figure 3.34: Normalised data set for 2% MCC bolus in 5litres	243
Figure 3.35: All normalised data sets for 2% MCC bolus in 5litres	243
Figure 3.36: Continuity graph for 2% MCC bolus in 5litresof Lactose at 15rpm	245
Figure 3.37: Regression fit to data from blending experiment using ~2% labelled MCC in 5.5litres of Sodium Carbonate Light at 15rpm.....	246

Figure 3.38: Summary graph of all the mixing experiments	251
Figure 3.39: Effect of substrate volume on blending rate at 15rpm	253
Figure 3.40: Effect of IBC rotational speed on blending rate	254
Figure 3.41: Photograph of the Sodium Benzoate powder showing the high concentration of platelets within the sample	255
Figure 3.42: Effect of IBC rotational speed on plate like particles	256
Figure 3.43: Comparison of binary and ternary systems at 15rpm	258
Figure 3.44: Graphical representation of the standard Dynamic test using the FT4 Powder Rheometer comparing three substrates	259
Figure 3.45: The BFE values from the standard Dynamic test using the FT4 Powder Rheometer comparing three substrates	259
Figure 3.46: Graphical representation of the shear test at 3kPa consolidating stress using the FT4 Powder Rheometer comparing three substrates	260
Figure 3.47: the shear stress from the first and last shear points together with the derived functions (FF, C, and UYS) comparing three substrates	260
Figure 3.48: How scale of scrutiny can effect the perception of mixedness	262
Figure 3.49: Effect of scale of scrutiny for 5 litres of Lactose + 120ml of irradiated MCC, blended at 10rpm, after 100revs	263
Figure 4.1: Flowsheet for a coal processing facility	276
Figure 4.2: Normal loads generated at the base of a column of powder based on Janssen's equation for three common pharmaceutical excipients	292
Figure 4.3: Example of linear and polynomial curve fitting to two repeat 7 point yield loci for Limestone	298
Figure 4.4: Three repeat shear tests of Gypsum at 9kPa consolidating load	301
Figure 4.5: Averaged data sets from three yield loci	302
Figure 4.6: Three repeat shear tests of Limestone at 9kPa consolidating load	303
Figure 4.7: Averaged data sets from three yield loci	303

Figure 4.8: Extent of extrapolation required for linear fit Flow Function (derived from yield loci measured at 3, 6, 9 and 15kpa) to achieve intersection with maximum and minimum flow factor limits expressed in Roberts (Roberts 1993).	308
Figure 4.9: Flow Function for Limestone CRM116 derived from yield loci	312
Figure 4.10: Flow Function for FlowLac 100 derived from yield loci.....	313
Figure 4.11: Assumed trajectories of the major principal stress respectively for filling state of stress (a), for initiation of discharge state stress for the mass flow regime(b), the fully developed discharge stress state for the mass flow regime (c) and for discharging state of stress for the core flow regime (d) (where the 'dead zone' is also shown) (Schulze 2007).....	317
Figure 4.12: Perceptual Maps for Automotive Brands and Breakfast Cereals	321
Figure 4.13: Geldart's representation of the relationship between the particle size and density with respect to its likely fluidisation behaviour.....	322
Figure 4.14: Similarities and differences between different methods of powder flow measurement – from Lee et al	324
Figure 4.15: McGee's Spider Diagram showing idealised easy flowing (left hand side) and poor flowing (right hand side) materials	326
Figure 4.16: Examples of McGee's Spider diagram for four sample materials.....	327
Figure 4.17: A spider diagram created in Microsoft Excel for four materials	329
Figure 4.18: Spider diagram representing the powder rheometry data for the exemplar powder set.....	330
Figure 4.19: The representation of the features of a single substrate as a function of 6 characteristics d_1 to d_6	332
Figure 4.20: PolyViz representation of all the powder rheometry and shear cell results for all the exemplar powders.....	334
Figure 4.21: PolyViz representation of all the powder rheometry results for all the exemplar powders.....	336

Figure 4.22: PolyViz representation of all the shear cell results for all the exemplar powders	337
Figure 4.23: GEA Vibroflow™ flow promoter.....	340
Figure 4.24: Discharge Station and Decel Tube with IBC containing the placebo located in position before operation with a load cell frame located under the discharge point to monitor the flow rate of the powder	342
Figure 4.25: Detail of the discharge point of the Decel test rig	343
Figure 4.26: Rathole formed in IBC containing Avicel 102 during Test 1	346
Figure 4.27: Rathole formed in IBC containing Avicel 102 during Test 2	347
Figure 4.28: Schematic of the ‘vacuuming’ of the powder	348
Figure 4.29: Contraction of the layflat due to ‘vacuuming’ in the tube	349
Figure 4.30: Rathole formed in IBC containing Avicel 102 during Test 3	350
Figure 4.31: Rathole formed in IBC containing Avicel 102	353
Figure 4.32: Dynamic testing for Avicel Samples	355
Figure 4.33: Permeability for Avicel Samples	356
Figure 4.34: Normalised Aeration Energy for Avicel Samples.....	356
Figure 4.35: Flow Functions for Avicel Samples.....	357
Figure 4.36: Yield loci for Avicel Samples generated by the RST-XS shear cell @ 4kPa consolidating stress.....	357
Figure 4.37: Flowsheet/P&I schematic for the Decel discharge station.....	359

List of Tables	Page
Table 1.1: Key decision making factors for equipment purchase by company type	11
Table 2.1: Classification of powder flowability after Jenike where σ_1 is the major principal stress; σ_h is the resultant horizontal stress; σ_c is the unconfined yield strength; and FF is the Flow Function defined as σ_1/σ_c	33
Table 2.2: Classification of powder flowability after Carr	34
Table 2.3: Carr's Flowability Index as supplied by Hosokawa Micron Ltd	36
Table 2.4: Carr's Floodability Index as supplied by Hosokawa Micron Ltd.....	37
Table 2.5: List of exemplar powders chosen for characterisation testing and their relevance to this project.....	39
Table 2.6: Comparison between the two shear cells testers used during this project. The cell volumes in brackets show optional configurations for each instrument (which were not used in this study)	43
Table 2.7: Parameters derived from the yield locus	52
Table 2.8: FT4 shear test derived data under 9kPa consolidating load (n=3)	58
Table 2.9: RST-XS shear test derived data under a range of consolidating loads	59
Table 2.10: Variation in derived parameters based on different averaging methodologies for Tablet Blend Placebo	74
Table 2.11: Variation in derived parameters based on different averaging methodologies for Limestone.....	77
Table 2.12: Angle of repose and bulk density data generated from the test samples using the Geldart angle of repose tester (n=3 for all tests).....	90
Table 2.13: Results from testing exemplar powders using a jolting volumeter (n=3 for all tests)	96

Table 2.14: Measured and derived data for the Flowability Tester Model BEP2 (n=3 for all tests)	104
Table 2.15: Descriptions of the standard suite of test routines available for the FT4 Powder Rheometer	124
Table 2.16: Results for dynamic testing of the exemplar powders in aerated and non-aerated states (n=3 for all tests).....	129
Table 2.17: Results for bulk property testing of exemplar powders (n=3 for all tests).....	130
Table 2.18: Interpretation of FT4 Powder Rheometer parameters for dry, unlubricated powders.....	134
Table 2.19: Ranking of exemplar powders according to flowability defined by the test method	141
Table 2.20: Summary of Zinc Oxide materials tested.....	152
Table 3.1: Results of AFM experiment after Lam and Newton (Lam & Newton 1992) for spray dried lactose for the pull off forces required to remove a particle from a steel surface following an initial press-on force	204
Table 3.2: Results of exponential regression fit to PET data sets	247
Table 3.3: Summary of process conditions and results for PET blending experiments.....	250
Table 4.1: Disciplines associated with powder processing.....	274
Table 4.2: Range of Guide Words Used in HAZOP Studies.....	280
Table 4.3: Examples of the Combination of Parameters, Guide Words and perturbations Used in HAZOP Studies.....	281
Table 4.4: Risk Assessment Matrix	284
Table 4.5: Various stages of Hazard and Operability Study	286
Table 4.6: Hopper design parameters generated by Fitzpatrick <i>et al</i> / using a Stainless Steel 304 wall materials (Ra unknown).....	294

Table 4.7: Typical hopper design parameters generated from the FT4 hopper design software tool.....	296
Table 4.8: Sensitivity of derived hopper design parameters to variation in the yield locus for an axi-symmetric conical hopper using a stainless steel wall friction material with a 1.2micron surface roughness.....	304
Table 4.9: Comparison of derived outlet sizes from two Flow Function models.....	315
Table 4.10: Parameters suggested by the tests reported in McGee 2005.	326
Table 4.11: Results from Restricted Powder Testing Methods.....	354

Chapter 1 – Introduction

Abstract

This chapter outlines the nature of the thesis and undertakes a review of the sponsoring company, Buck Systems, with respect to its place in the market, the technical and regulatory drivers that have influenced the choice of project and how the intended outcomes will shape the way the company does business in the future.

1.1 The aims and goals of the project

This Engineering Doctoral project has been a collaboration between Buck Systems and the University of Birmingham School of Chemical Engineering.

Buck Systems, a division of GEA Process Engineering (NPS) Ltd, was founded in 1990 as Gallay Systems Ltd. The Birmingham-based company was initially established to meet the specific needs of the pharmaceutical market, where it still has almost all its sales. It has developed and introduced a range of products and services based around the batch manufacturing focus of the solid dose segment of the industry (tablets, capsules, caplets); blending in intermediate bulk containers (IBC), washing, discharge and dosing, dispensing and post-hoists.

Recent regulatory initiatives combined with ongoing moves to outsource both fabrication and assembly functions by the equipment manufacturing industry have required the company to evaluate and improve the 'value added' to its range of standard products. To this end it has decided to develop its focus on the characterisation of the powdered materials used by the pharmaceutical industry and how that impacts on its main product line – dry powder, batch, tumble blenders.

The specific goals of this thesis were

- Develop simple and quick screening methods for characterisation of customers' powders with a view to identifying potential problems prior to blending tests – this replaces the current *ad hoc* approach and should reduce

the amount of effort that goes into blending trials and would be performed at Buck Systems.

- Detailed characterisation using specialist equipment available at the University of Birmingham and elsewhere to inform of the efficacy and limitations of specific tests and testers.
- Characterisation of powder and systems for customer specific troubleshooting.
- Evaluate the applicability of powder testing to the other Niro group companies which manufacture equipment for other powder processing unit operations.
- Evaluation of blending using specialist equipment available at the University of Birmingham – Positron Imaging of powder blending

In order to put these goals into context, a review was undertaken of the Buck Systems position within the pharmaceutical equipment supply sector and the drivers that shape the specific needs of that sector.

1.2 *Background to solid dose manufacturing in the pharmaceutical industry*

There are several historic drivers relating to manufacturing in the pharmaceutical industry being geared towards batch manufacturing.

- The need to manufacture (relatively) small quantities of product (compared to the general chemical industry).
- The large number of products and formulations within any given company's portfolio

- The cost and time of R&D and Clinical Trials for each product means that the quicker the process plant starts turning out saleable product, the quicker the return on investment and the longer the period of production before the end of the patent period.

Thus simple, batch unit operations – that are often just larger versions of laboratory bench chemical manufacturing – are prevalent.

A more detailed description of this approach can be found in (Bennett & Cole 2005) and (Aulton & *et al* 2002).

An additional driver for this batch manufacturing approach has been the regulatory mantle applied by the various national and supra-national bodies such as the Food & Drug Administration (FDA – US), Medicines and Healthcare Products Regulatory Agency (MHRA – UK), European Directorate of the Quality of Medicines & Healthcare (EDQM – Europe) and Pharmaceutical & Medical Devices Agency (PMDA – Japan). These bodies licence the manufacture of drug substances for sale and for prescription within their own geographic zone of influence. Historically they have, in conjunction with the pharmaceutical companies, relied upon Standard Operating Procedures (SOPs) as a means of Quality Assurance (QA), backed up by strict Quality Control (QC) requirements to achieve the goals of pharmaceutical products that are both safe and efficacious. Invariably this involves a significant amount of paperwork, known as the ‘New Drug Application’ (NDA), to be submitted and approved before a drug can be manufactured for sale. From an engineering

perspective, this can lead to the need to specify the manufacturing process and the SOPs prior to full evaluation of the plant using a production size batch of the active pharmaceutical ingredient (API) due to the lead times for submission and approval of the NDA.

However, such a manufacturing control strategy has a number of drawbacks. Firstly the use of SOP control is based upon the following logic

Constant Feedstocks + Constant Process Conditions → Constant Products

This assumes that any variability in the processing is the major source of variability in the end product and dictates that there is no variation in the process control parameters during manufacture – for example the number of rotations, fill level and rotational speed of a batch tumble blender are all kept constant throughout the manufacturing life of a given product/production line combination. Where this falls down, particularly with respect to particulate materials, is that the feedstocks, whilst usually being chemically consistent, do not necessarily have constant physical properties (such as particle size/size distribution; particle shape/shape distribution; moisture content; particle density; particle porosity etc.) which in turn leads to poor repeatability in any unit operation where the powder is required to flow.

Secondly, it is very unusual to change any SOP unless there is absolutely no other way of solving a problem. This is because of the large amount of paperwork required to re-validate the process. Unlike more conventional chemical processing where the

slight alteration of process conditions is a regular occurrence to maintain product quality, it is very unusual in the pharmaceutical industry's highly regulated environment.

Thirdly, even if a change in SOP did not present the difficulties mentioned above, how would one measure a parameter that could be changed? The number of on-, in- or at-line instruments that can measure powder properties, coupled with the markedly tiny number of mathematical models upon which a control system or even a simple quality specification could be derived, is minimal.

All of these issues cascade down to the equipment manufacturing sector which needs to create components and systems that allow the pharmaceutical companies – the 'end users' – to comply with their regulatory requirements.

Recent initiatives by the FDA are, however, having a significant impact on the way pharmaceuticals are manufactured, and thus on how the equipment suppliers design processing systems to meet these changing requirements. This is discussed later in this chapter.

1.3 *History of Buck Systems*

Gallay was taken over in 1996 by English engineering company GEI and integrated with its other Pharma divisions Collette (granulation) and Courtoy (tablet presses) and, the following year, Buck Valve (high containment valves utilised on the

discharge of Buck Systems IBCs). GEI was, in turn, taken over by GEA, a division of mg technologies ag, in 1999 and associated with GEA's other pharmaceutical operation Aeromatic-Fielder to create an umbrella operating group within GEA - Niro Pharma Systems (Figure 1.1). The synergy between GEA Buck Valve and Gallay Systems resulted in the change of name to Buck Systems in May 2003.

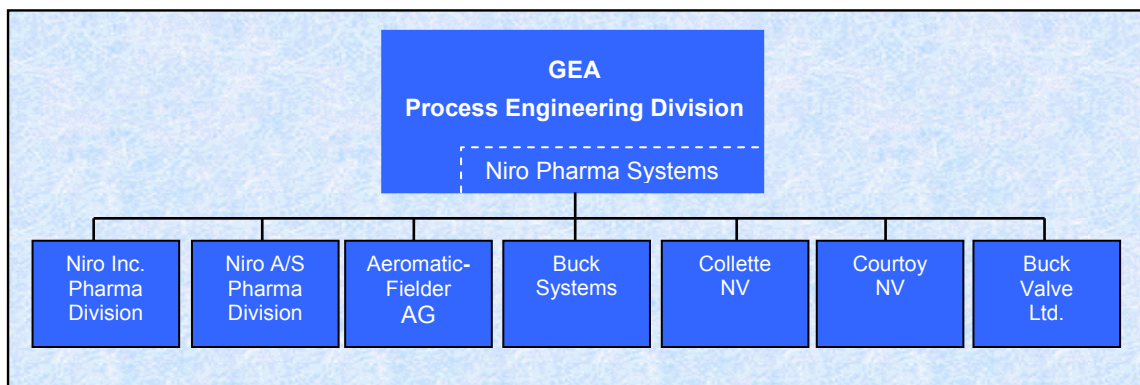


Figure 1.1: Organogram of GEA Niro Pharma Systems¹

The formation of Niro Pharma Systems (NPS) has enabled NPS companies, Niro, Aeromatic Fielder, Collette, Courtoy, and Buck, to provide standardised interfaces providing simple integration between technologies and equipment. This has resulted in the creation of one of the few organisations that can supply most of the unit operations required for the manufacture of pharmaceutical Solid Dosage Forms, and could be considered a 'one-stop-shop' for anyone designing a manufacturing process.

It is also notable that mg technologies ag has divested its chemical manufacturing activities since the start of this project and re-branded itself GEA Group ag (July 2005) to emphasise its focus on process equipment engineering. It is therefore likely

¹ The information presented in Figures 1.1 to 1.7 was kindly supplied by Buck Systems Sales and Marketing Department

that any outcomes from this project would have a range of internal applications within the other process equipment manufacturing divisions of Niro/GEA Group.

1.4 Key Market Segments

The market serviced by Buck Systems and the other Niro companies is segmented into two types of pharmaceutical client, commonly described as 'ethical' and 'generic'. Ethical manufacturers are those pharmaceutical companies that develop their own drugs such as Glaxo Smith Kline, Pfizer, Merck Sharpe and Dohme, Astra Zeneca, Sanofi and many others. These companies are household names and many are regarded as 'blue chip' entities with a significant presence in the various stock market indices (FTSE, Dow, NASDAQ etc) throughout the world. Generic manufacturers are those companies that manufacture pharmaceuticals that do not require development or that are out of patent or other intellectual property rights (IPR). These are less well-known names, but are a significant sector within the market.

Each of these two marketing segments is also sub-divided into two technical sub-segments – primary and secondary manufacture – each with differing emphases on the requirements for process equipment. Primary manufacture is the term used to describe the production of the drug substance (active ingredient), which is usually a small percentage of the overall dose unit such as a tablet or capsule. Secondary manufacture is the stage where the drug material is combined with other substances, known as excipients, to create the finished product. These excipients are

substances that can help the drug material perform its designated task, act as a lubricant for the tableting process, create a pleasing taste or look to the tablet, or are simply there to provide sufficient material to achieve the required size for the application, i.e. a bulking agent.

In broad terms the requirements for the type of materials handling equipment supplied by Buck Systems are; small equipment volume, high containment for primary manufacture; and larger equipment volumes medium/high containment for secondary manufacture. These are generalisations and the installation depends on the potency level of the drug materials being handled.

Additionally the market can also be broken down geographically into the typical world regions Europe, North America, Latin America, Africa, Middle East and Far East. However the geographical nature of the business is tempered by two elements; most of the ethical manufacturers have their headquarters in Western nations and any spending in developing regions will almost certainly be initiated and managed by those head offices; additionally the lure of cheap manufacturing overseas has to be balanced by the need to satisfy the relevant regulatory authority, which in most cases will be the US FDA if the drug is to be sold into the United States. These factors mean that the need to tailor products for regional bias is almost non-existent when selling to ethical manufacturers.

1.5 Market Structure and Size

The size of the global materials handling market in the pharmaceutical sector is estimated to be of the order of \$80-100m (£47-58m) p.a. by Buck Systems, who believed that they had around 15% of the market share in 2000, with a stated goal to achieve 30% by 2010.

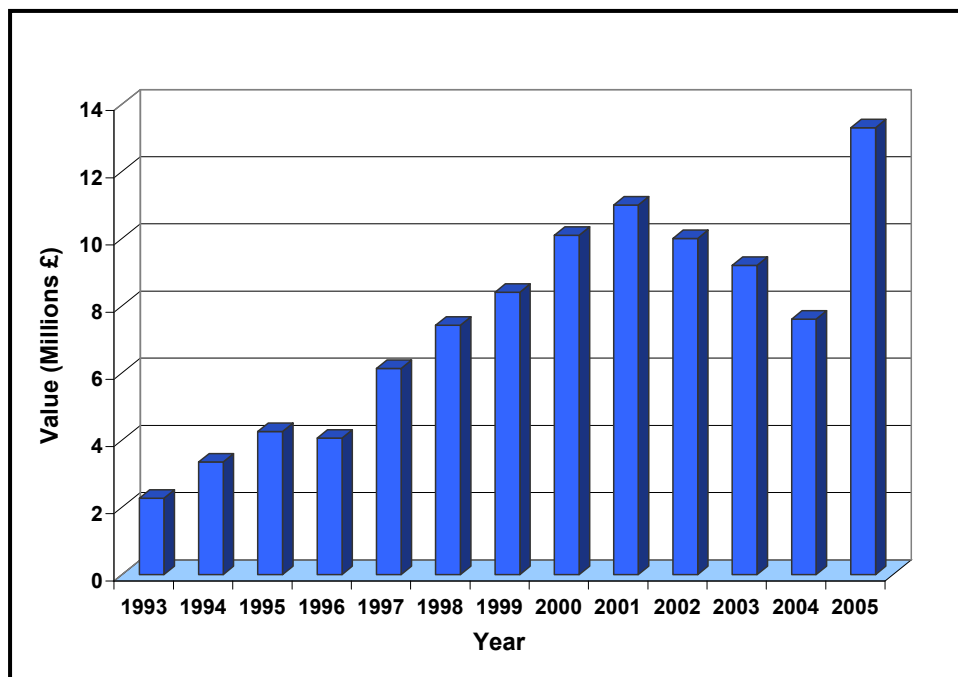


Figure 1.2: Order value by year for Buck Systems

As can be seen from Figure 1.2, sales steadily increased and were on target up to 2001 when a mini-recession hit the whole market. However, as can be seen for the period to mid-2005 (and, although not shown on the graph, continued in 2006) strong orders boosted turnover dramatically and the company is close to achieving its 30% market share target in the near future. The availability of more recent detailed figures is restricted due to their commercial sensitivity.

Each of the market segment's requirements can broadly be defined by examining the needs of each client type – ethical and generic. These requirements tend to dictate both the sales and design approach and are listed in Table 1.1.

Table 1.1: Key decision making factors for equipment purchase by company type

Ethical Companies	Generic Companies
Technology based decisions	Affordable & delivered quickly
Time to market	Quick return on investment
Containment	Ease of use
Potent products	Simplicity
Protection of operators	Lower level of training for operators
GMP / Cross contamination	Easy to maintain
Reliable discharge of product	Flexibility
No operator intervention	Design for worse case
GMP design	Future patent products coming off license
	Reliable discharge of product
	Product yield

The two sets of requirements are not mutually exclusive, both groups would like all of the listed requirements to be met, there is merely a difference in emphasis required.

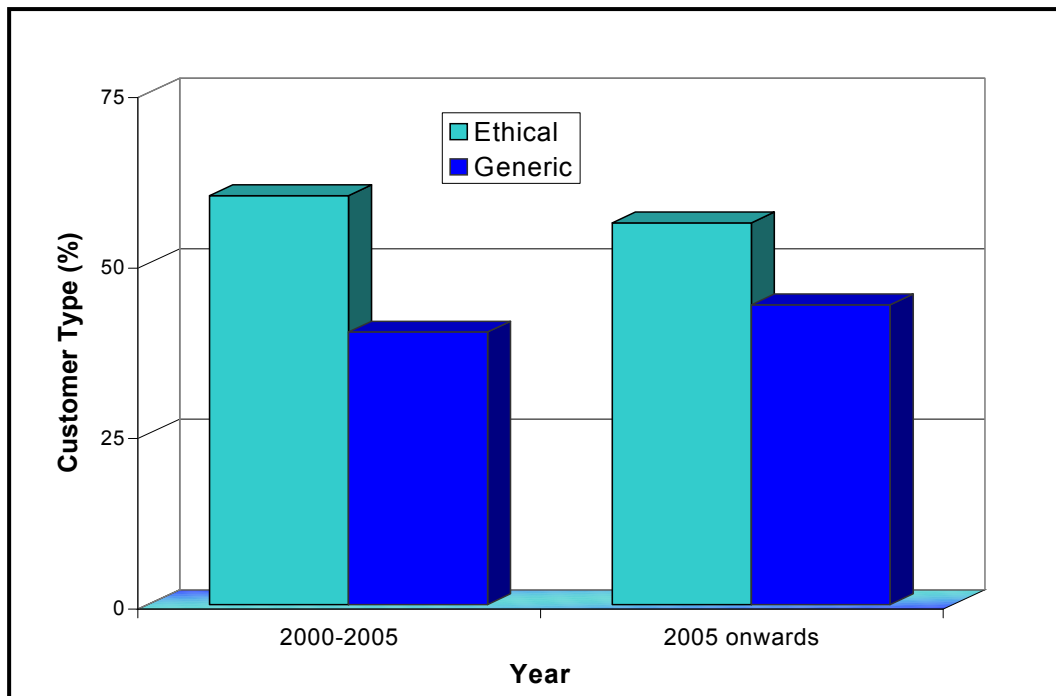


Figure 1.3: Split of Buck Systems customer type between ethical and generic drug manufacturers over the period 2000 to present

Looking at the current and historical splits between the two clients groups, (Figure 1.3), it can be seen that sales into the ethical sector are 20% greater than into the generic sector and this ethical/generic split appears to be broadly constant over the medium term.

Historically the split between primary and secondary, in the early years of Gallay Systems, was biased towards secondary manufacture, but with a significant level of sales into primary manufacturing as shown in Figure 1.4.

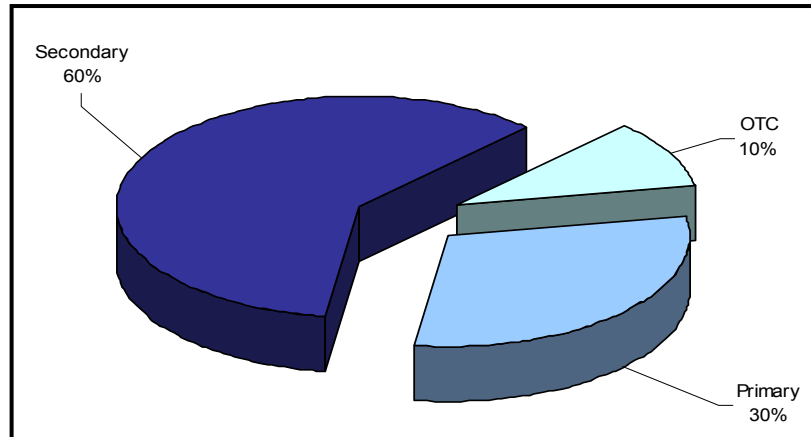


Figure 1.4: Split of contracts 1997 -1999²

Significantly, the creation of the Niro brand has pushed the emphasis towards the secondary sector, as most of the companies within Niro also focus on unit operations related to solid dose preparation and manufacture to such an extent that from 2004 Buck Systems has worked exclusively on contracts for secondary manufacture.

A significant opportunity exists to reassert the Niro/Buck Systems presence in the primary manufacturing sector whilst maintaining the organic growth that has occurred in the secondary sector.

Figure 1.5 shows the regional splits of sales. The region descriptors are slightly different, but the main point to note is the increase in sales to the Far East.

² OTC relates to 'over the counter' medicines, a differentiator that is no longer used. The value can, for the purposes of this review be assumed to be Secondary manufacture

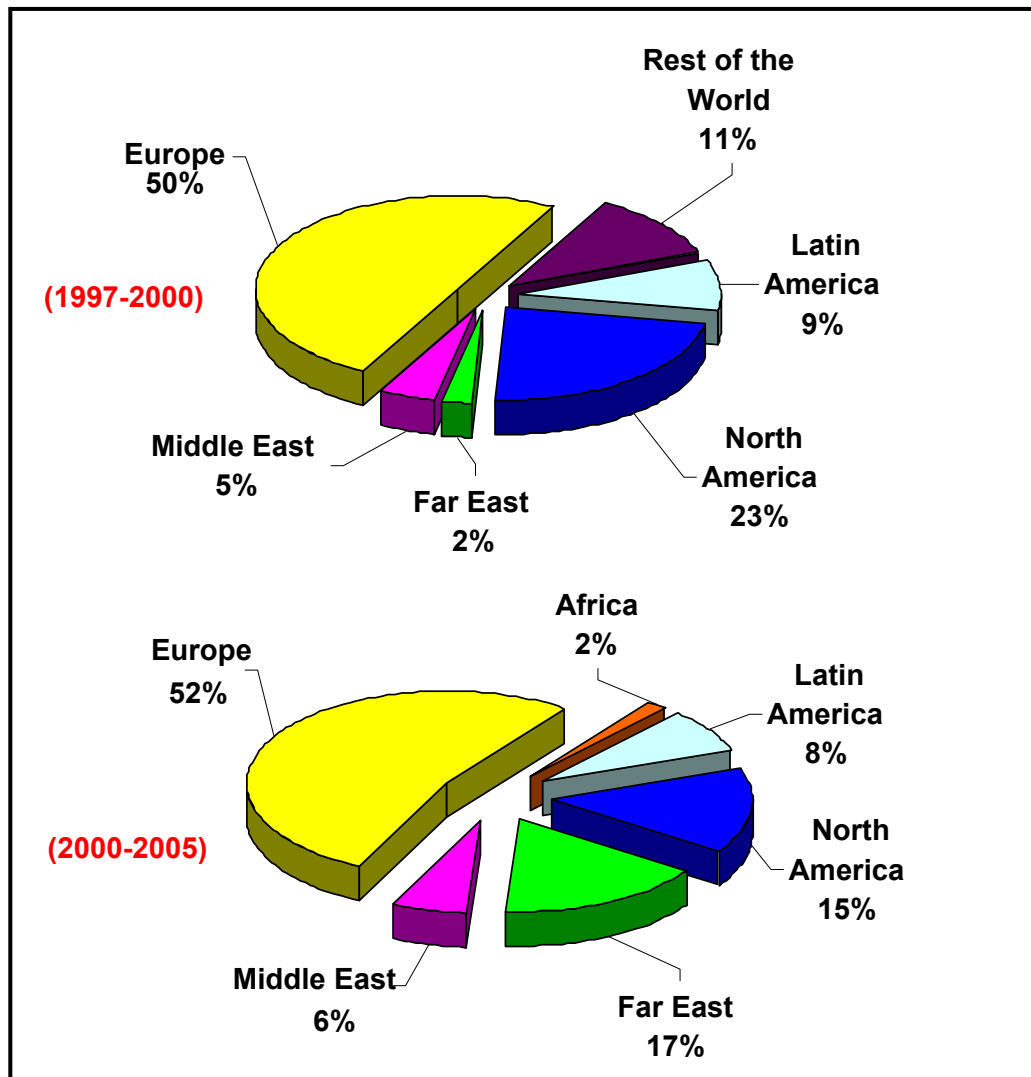


Figure 1.5: Split of contract by region 1997-2000 and 2000-2005

There is also a significant trend in the European marketplace shown in Figure 1.6. The favourable conditions offered by the Irish Government resulted in a massive increase in the number of pharmaceutical companies basing manufacturing operation in the country over the past 10-15 years. These are mostly ethical manufacturers and the growth is, to a limited degree, self-perpetuating. Companies now see the region as a source of high quality operational staff as well as capitalising on the financially advantageous tax environment.

For supplier companies like Buck Systems however, the likelihood of a continuing Irish Pharma boom is unlikely and while business from the region will continue, it is accepted that the growth rates and sales volumes will tail off in the coming years and other geographical markets need to be assessed and targeted.

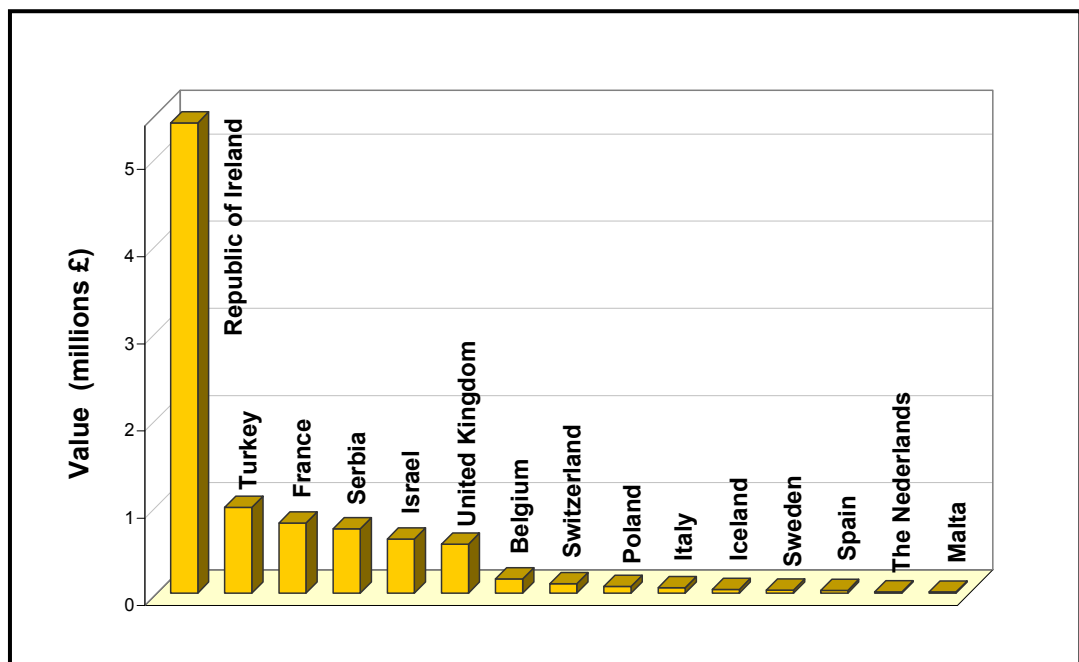


Figure 1.6: Order Value by Country 1997-2005

Figure 1.7 shows the split of business over a four-year period up to 2005 differentiated by client. As can be seen four major projects stand out as being the major sources of revenue from a total of 39 clients. Although this may be perceived as being a hazardous strategy in some industries, the equipment supply business is such that you take work when it comes from whoever provides the contracts.

This appears to be a classic example of the Pareto Principle (i.e. 80% of your sales come from 20% of your clients) (Bookstein 2009; Reed 2001) but the quantity of the data is perhaps on too short a time scale to be definitive. Many of the key blue chip manufacturers barely register on the scale in Figure 1.7, but are still considered to be key clients. What biases this graph is the lead times for large projects and the cyclic

nature of pharmaceutical manufacturing. Often drug companies can have several new drug entities entering the market (c.f. Wyeth in Ireland); sometimes there are several years between approvals (c.f. Pfizer; Glaxo Smith Kline; Astra Zeneca). Thus all the key clients are not necessarily represented in this graph to their overall, long term importance to the company.

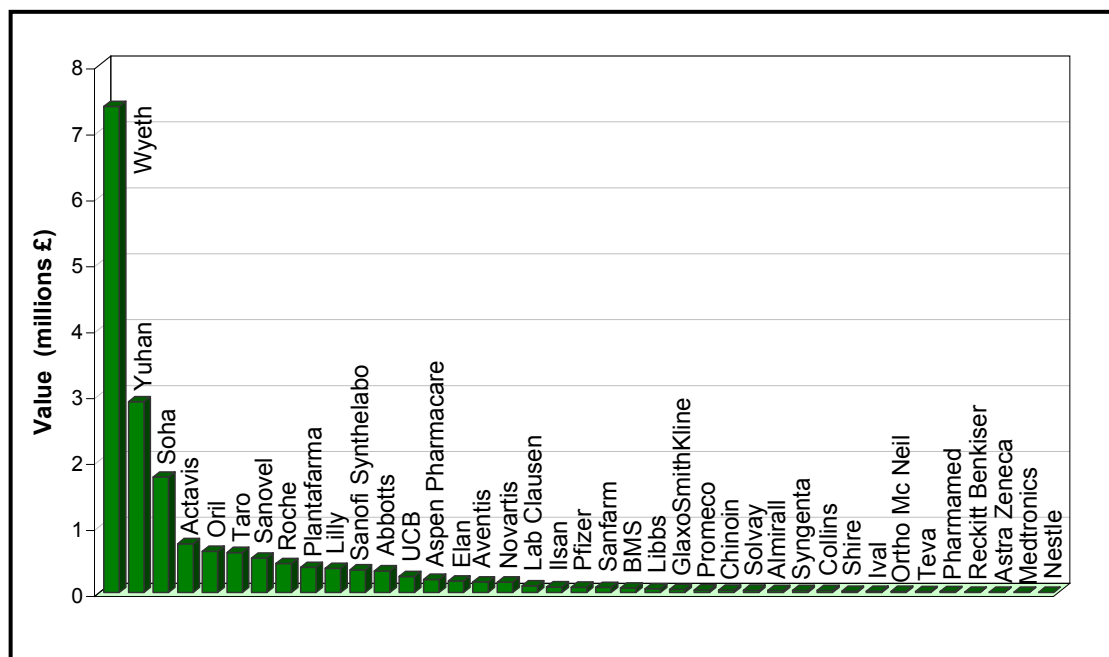


Figure 1.7: Order Value by Customer 1997-2005

Additionally, the way larger contracts are handled within the Niro Group may contribute to the skewed picture above. When a customer comes to Niro for several items as part of a large contract, a main contractor is appointed to co-ordinate all of the work of the individual Niro companies and to provide a single point of contact for the client. Invariably, as Buck Systems products interlink all the other products in the Niro portfolio, a Buck Systems project manager is often appointed and thus all income from the work goes through the Buck Systems accounts.

Thus the importance of understanding the powder characteristics and their relation to a wide range of unit operations and product transfer functions becomes even more pertinent to ensure efficient design and smooth installation.

1.6 *Manufacturing for pharmaceutical processing*

The supply of manufacturing equipment into the pharmaceutical industry is usually by the competitive tender route. It can be categorised into two main types of sale – new manufacturing site and retrofit. The new manufacturing site is self-explanatory; retrofit can either be a new drug manufactured within an existing infrastructure (including buildings, equipment or both) or the transfer of a production line to an alternate facility (typically to a lower cost manufacturing environment when a drug is out of patent).

It is generally believed by those outside the industry that cost is not an issue in specifying equipment for pharmaceutical manufacture. This is not the case. Whilst it is true that pharmaceutical manufacturers do make significant amounts of profit, and they can utilise complex, intricate and costly manufacturing processes to achieve their goals, cost of manufacture is still an issue. Most projects go to competitive tender and most manufacturers of equipment will be required to produce goods that are cost effective. To this end Buck Systems has moved from manufacturing all its goods from scratch to outsourcing several mechanical operations such as machining, IBC construction and most of the fabrication functions, some manufacture is even

undertaken in low cost facilities in the Far East. The company now concentrates on the design, assembly, finishing and testing of the products: the perceived 'value added' areas of the business.

The lifecycle of any given product is not easy to identify. Most systems are semi-bespoke; that is they are assembled from a number of key items that can vary in size from installation to installation and can have differing control systems and ancillaries depending on the operational requirements. It is also not unusual for a client to request additional items that are identical to the ones bought many years ago, despite numerous design improvements to individual components or their materials of construction that are currently available. The restrictions placed on companies from the need to comply with process validation regulations mean that the incorporation of process improvements would entail significant paperwork and testing to re-validate the process. Often this is not cost effective and the client buys non-current versions of equipment. Thus, the concept of product lifecycle is not clear-cut, and it is necessary to keep drawings of all installations well archived to ensure that components can be supplied for plant refurbishment.

There are, however, significant drivers within the pharmaceutical industry that engender product development. These are mostly driven by regulatory authorities such the FDA and MHRA, and recent changes to the way regulation is implemented and how this affects the equipment supply sector is discussed later in this Chapter. Safety concerns are also paramount, especially as the potency of drugs continues to increase, making the elimination of dust release a priority issue. All the products

made by Buck Systems and other Niro companies must also comply with CGMP (current good manufacturing practice) standards making any cross contamination unacceptable, which inevitably means they are manufactured from stainless steel to ensure cleanable surfaces where contact is made with the product.

Thus continual product development is required to ensure client specifications, driven primarily by regulation, are met and where possible exceeded without significant extra cost of manufacture.

1.7 *Recent FDA initiatives that affect the development of pharmaceutical processing systems*

The FDA has the most significant influence on the manufacture of pharmaceutical products of all the regulatory bodies. This is because the US market is the most lucrative in the world, with more products for more ailments than any other country, so the emphasis of many ethical pharmaceutical companies is to develop products that are compatible with US regulatory requirements. Thus manufacturing processes – no matter where they are based – are often subject to (or allow themselves to be subject to) FDA regulatory approval.

The historical regulatory system was based on SOP systems coupled with QC/QA testing to validate batches for sale. Towards the end of the last century, the FDA were coming to the realisation that they were struggling with the amount of regulatory effort required for all the products that were coming to market and that the cost to

maintain the existing regulatory regime would spiral, in-turn increasing the cost of medicines significantly – something that they were keen to minimise. In concert with this realisation by the FDA, the blue chip pharmaceutical manufacturers were also struggling with their product pipeline – the stream of ‘blockbuster’ drugs that had emerged from the R&D laboratories in the 1980’s and 1990’s was slowing down dramatically and ways have to be found to improve revenue and reductions in manufacturing costs would certainly help. Thus pharmaceutical companies were certainly open to any opportunities offered by the regulator that would allow them to cut costs.

However, in order to stimulate a new approach to development and manufacturing, a step change was needed from the FDA, which was often perceived as a roadblock rather than an enabler, to promote innovation and understanding of the processes and (importantly) the risks involved. A similar approach had been achieved in the food industry with the legal adoption of the Hazard and Critical Control Points (HACCP) methodology in the 1990’s (Food & Drug Administration 1995; International Commission on Microbiological Specifications for Foods (ICMSF). 1988; International Organisation for Standardization 2007) and used in the processing and handling of most foodstuffs. This methodology ensures that the producer understands what part of his process is critical to product quality – specifically the safety of the foodstuffs being manufactured. Close scrutiny of the critical manufacturing steps allows the manufacturer to know when his product is in specification and thus safe to send to market without the need to hold the entire batch of product back until QA/QC testing and approval is obtained (as is current practice in pharmaceutical manufacturing).

This method is invaluable when dealing with short shelf life perishable goods and, although most pharmaceuticals have considerably longer 'best before' timescales and full scale QC testing is unlikely to dramatically reduce product saleability, there are clear efficiency, storage and cash flow benefits.

Following extensive collaboration and consultation with the pharmaceutical industry³, the first step was the introduction of an initiative entitled 'Pharmaceutical CGMPs for the 21st Century: A Risk-Based Approach' (Food & Drug Administration 2004b), coupled with an additional Guidance document entitled – 'Guidance for Industry: PAT – A Framework for Innovative Pharmaceutical Manufacturing and Quality Assurance' (Food & Drug Administration 2004a) in 2004. Both documents outlined a way that pharmaceutical companies could reduce the amount of regulatory oversight by using a combination of;

- Process understanding
- PAT tools
- Risk assessment
- Integration of approach from all concerned parties within the company

The end goal of this process was to allow companies to achieve 'real-time release' of products – that is send products to market where the quality was determined by process data **not** subsequent QC checking.

³ A useful timeline is provided by the Watts presentation in 2005 and available from the FDA website (<http://www.fda.gov/downloads/AboutFDA/CentersOffices/CDER/UCM174306.pdf>)

The key part to this was the Process Understanding, but for many systems developed under the existing regulatory framework, this was difficult to achieve as the level of instrumentation fitted to processes was limited to those that provided the set points indicated in the SOP. Other useful process data was simply not collected – the historic emphasis on fixing the process conditions to achieve regulatory approval did not require significant level of process monitoring and control, and therefore costly instrumentation was not added.

Consequently there was anecdotal evidence that a significant level of instrument retrofit to existing process plant and over-specification of instrumentation for new plant to generate sufficient information from which ‘plant understanding’ could be gained (Mathis 2004). Once the initial shock of the quantity and variability of the data that could be collected was over, the use of statistical data analysis methods allowed companies to identify which measurements actually gave them useful data, but also gain significant insight into their operations and how they could be controlled. There are many techniques that can be applied to liquid based systems as on- and in-line sensors to generate such useful data, but when powdered solid systems are considered there are a very limited number of measurement systems that are available. The nature of powdered solids and measurement systems will be discussed and evaluated in Chapter 2.

The experiences acquired during the extended evaluation of ‘Pharmaceutical CGMPs for the 21st Century’ and ‘PAT – A Framework for Innovative Pharmaceutical

Development, Manufacturing and Quality Assurance' (Food & Drug Administration 2004b) review and implementation periods were further supplemented by 'Quality Systems Approach to Pharmaceutical CGMP Regulations' in 2006 (Food & Drug Administration 2009).

Further refinement and expansion of the concepts generated in the FDA work have been assembled in the ICH⁴ (the International Conference on Harmonisation of Technical Requirements) Quality Guidelines – Q8 (2005-2008), Q9 (2005) and Q10 (2007-2008) (INTERNATIONAL CONFERENCE ON HARMONISATION OF TECHNICAL REQUIREMENTS FOR REGISTRATION OF PHARMACEUTICALS FOR HUMAN USE 2005;INTERNATIONAL CONFERENCE ON HARMONISATION OF TECHNICAL REQUIREMENTS FOR REGISTRATION OF PHARMACEUTICALS FOR HUMAN USE 2008;INTERNATIONAL CONFERENCE ON HARMONISATION OF TECHNICAL REQUIREMENTS FOR REGISTRATION OF PHARMACEUTICALS FOR HUMAN USE 2009).

Perhaps the most relevant and useful concept to come out of these guidelines is the concept of 'design space' which is shown schematically in Figure 1.8.

⁴ The ICH is a project that brings together the pharmaceutical regulatory bodies of Japan, the EU and the USA to provide pharmaceutical manufacturers with a single framework within which to develop products, obviating the need for multiple testing and approval for different territories.

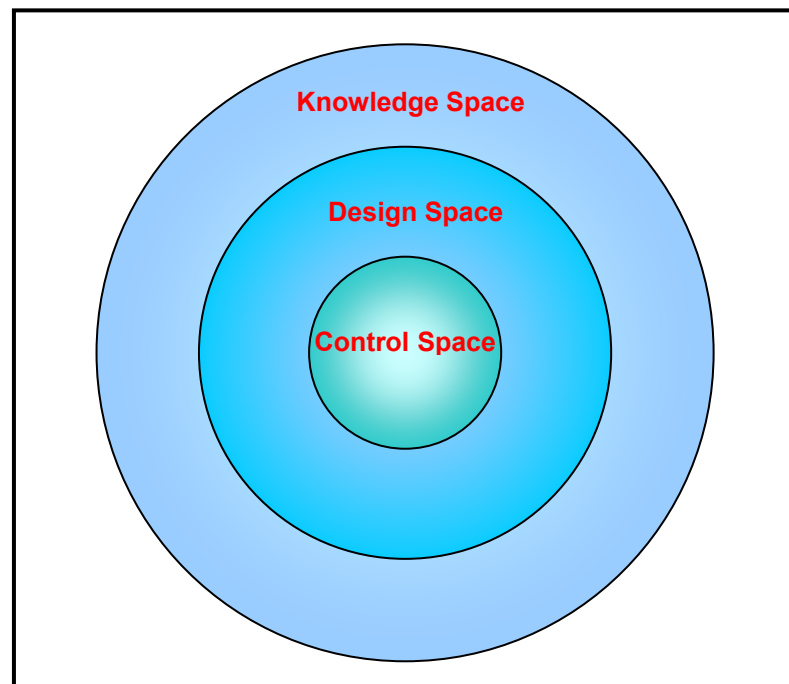


Figure 1.8: A graphical representation of the concepts of knowledge, design and control spaces

The 'knowledge space' contains the entire multi-dimensional understanding of all the properties of the feedstocks, process and product. The design space contains the set of properties that will ensure that the end product meets its safety and efficacy criteria. The control space is the set of parameters that allow the process to operate and be controlled and assure product quality with a margin of safety built in.

The design space is the most important region as it is the one which will be subject to regulatory scrutiny, however, any changes to the system within the design space will be acceptable without the need for regulatory intervention. Thus a manufacturer who has defined the process design space will actually be able to modulate their process to achieve product consistency, minimising waste/re-work and getting the final

product to market without the need to slow every stage down whilst waiting for (necessarily) long QC procedures.

1.8 Thesis Outline

As can be seen the company's history and the regulatory framework in which it has to operate clearly has an impact on the way GEA/Buck Systems approaches the design, development and tendering process for their clients. The ability to develop systems that can assist with the creation of design space through the understanding of the way the process affects the materials will be essential for the long term health of the company.

This project consisted of four parts;

- Establishing a greater understanding of how powders can currently be characterised with an emphasis on the limitations of the types of test and a critical review of specific data analysis and interpretation methods (Chapter 2).
- Providing an improved understanding of powder mixing processes at a greater scale of scrutiny by means of a novel application of Positron Emission Tomography (Chapter 3).
- Developing improved ways of evaluating processes and suggesting ways that powder characteristics can be used to better integrate the company's process equipment into manufacturing schemes (Chapter 4).
- Summarising the project and giving suggestions for further study (Chapter 5).

1.9 References

- Aulton, M. E. & *et al* 2002, *Pharmaceutics, The Science of Dosage Form Design*, 2nd edn, Churchill Livingstone.
- Bennett, B. & Cole, G. 2005, *Pharmaceutical Production An Engineering Guide* Institution of Chemical Engineers.
- Bookstein, A. 2009, "Informetric distributions, part I: Unified overview", *Journal of the American Society for Information Science*, vol. 41, no. 5, pp. 368-375.
- Food & Drug Administration 1995, *21 CFR Parts 123 and 1240. Procedures for the Safe and Sanitary Processing and Importing of Fish and Fishery Products*.
- Food & Drug Administration 2004a, *Guidance for Industry PAT — A Framework for Innovative Pharmaceutical Development, Manufacturing, and Quality Assurance*.
- Food & Drug Administration 2004b, *Pharmaceutical CGMPs for the 21st Century - a Risk Based Approach*.
- Food & Drug Administration 2009, *Guidance for Industry, Quality Systems Approach to Pharmaceutical CGMP Regulations*.
- International Commission on Microbiological Specifications for Foods (ICMSF). 1988, *HACCP in microbiological safety and quality*, Blackwell Scientific Publications, Oxford Mead, UK.
- INTERNATIONAL CONFERENCE ON HARMONISATION OF TECHNICAL REQUIREMENTS FOR REGISTRATION OF PHARMACEUTICALS FOR HUMAN USE 2005, *QUALITY RISK MANAGEMENT, Q9*.
- INTERNATIONAL CONFERENCE ON HARMONISATION OF TECHNICAL REQUIREMENTS FOR REGISTRATION OF PHARMACEUTICALS FOR HUMAN USE 2008, *PHARMACEUTICAL QUALITY SYSTEM, Q10*.
- INTERNATIONAL CONFERENCE ON HARMONISATION OF TECHNICAL REQUIREMENTS FOR REGISTRATION OF PHARMACEUTICALS FOR HUMAN USE 2009, *PHARMACEUTICAL DEVELOPMENT Q8(R1)* .
- International Organisation for Standardization 2007, *ISO 22000:2005. Food safety management systems -- Requirements for any organization in the food chain*.
- Mathis, N. Process Analytical Technology, A First-Birthday Standardization Update. *Pharmaceutical Technology [PROCESS ANALYTICAL TECHNOLOGY]*, 13-1. 2004.
- Reed, W. J. 2001, "The Pareto, Zipf and other power laws", *Economics Letters*, vol. 74, no. 1, pp. 15-19.

Chapter 2 – Powder Characterisation

Abstract

This chapter looks at the type of powder characterisation equipment and methodologies that could be practically employed by Buck Systems and GEA/Niro to evaluate powdered pharmaceutical materials. A critical review of the most appropriate is undertaken and recommendations made for their application.

2.1. Introduction

The pharmaceutical manufacturing sector is unusual in its extensive use of an extremely large variety of powdered materials. This is because these powders are the constituent materials for solid dose forms (tablets, capsules, caplets) which are the preferred method of administering drug entities or API (active pharmaceutical ingredients) where technically possible. This is due to several reasons

- Easier for patients to take a tablet compared to administering an injection.
- Cost per unit dose for many materials
- Shelf life of solids compare to liquids
- Easier to control dose size compared to injections – management of risk

Most other chemical industries handle a few or a few tens of different chemical entities in powdered form, with perhaps the food industry utilising the second highest number of powders.

Solid dose forms are a combination of the API (which is usually a small proportion of the total mass/volume of the dose) and a number of excipients whose variety and proportion are determined by formulators seeking to achieve the optimal delivery of the API to its target within the body. Excipients have a variety of roles where they act as binders, disintegrants, emulsifying agents, diluents, stabilizers, sweeteners, colourings, preservatives, plasticisers, release agents etc. Thus pharmaceutical companies are required to manipulate the constituent powders to produce a solid

dose that, within predetermined limits, contains the required proportion of each component.

Of the 299 chemical entities listed as approved excipients in Rowe (Rowe, Sheskey, & Owen 2005), 199 have a primary form which is granule or powder. Many are also supplied in a variety of grades, for example Lactose, which is one of the more common diluents, has three listings for its chemical forms which are further subdivided into 7 commercial grades of anhydrous Lactose; 8 grades of spray dried Lactose; and 58 grades of the monohydrate form. The listing of commercial grades is not exhaustive and there are many other suppliers of these materials than those listed whose products may subtly differ from those noted in Rowe. In addition, consideration has to be given to the equally, if not greater, number of API ingredients which are also mostly in the form of finely divided solids. This means the number and variety of powdered materials available to the pharmaceutical formulator is very large and the number of possible combinations is vast.

In short, the pharmaceutical industry relies heavily on powders, and hence powder processing, to generate saleable products. Given this reliance, it is perhaps odd to a disinterested observer that their approach to evaluating powder properties, particularly as it relates to flow, is still largely based on a small number of semi-empirical, operator dependent tests – the British Pharmacopeia (British Pharmacopoeia Commission 2005) lists sieve analysis; flow rate through a funnel; and tapped density testing as the ways of testing a powder for flow performance.

However, given the historical regulatory context detailed in Chapter 1, it is also not surprising that the drug companies have not kept up with advances in the evaluation of powder properties. There is no incentive to understand and manage powder properties when, even if the result contradicts the SOP (Standard Operating Procedure), you will not be able to influence the way the powder is processed due to the level of bureaucracy.

Clearly the FDA initiatives mentioned in Chapter 1 are the most significant current industry driver and the ability to generate 'process understanding' is required not only by the pharmaceutical manufacturers but also by their process equipment suppliers. Thus the evaluation of powder characteristics is an important topic.

The characterisation of powders can be undertaken in a variety of ways, however, to be useful to GEA the technique(s) has to be not only cost effective, but be compatible with the type of testing that their clients – pharmaceutical manufacturers – routinely undertake. Ideally, the suggested range of tests should provide a rapid, repeatable, operator independent series of measurements that can be applied to any powdered material. In addition, if the tests can be highly differentiating such that small variance can be accurately quantified, it should be possible to undertake the sensitivity analyses that can be used by process designers to generate 'design space' and ultimately the 'control space'.

2.2. Powder Characterisation Testing

Powders are assemblies of considerable numbers of individual particles and as such can be investigated either as the bulk assembly or as the discrete entities that go to make up the bulk. Many of the physical characteristics of individual particles are difficult to measure as an absolute parameter, for example frictional interactions; Young's modulus; Poisson's ratio; tensile strength etc. Instruments for looking at these properties of discrete particles, such as atomic force microscopy; scanning electron microscopy; x-ray micro tomography; and micro-manipulation are usually found at academic institutions, require very time intensive measurements, carry a high price tag (if you can indeed buy a commercial instrument) and need highly skilled operators to use them. Couple this with the potential variation between individual particles, and collecting sufficient information to provide statistically valid data sets becomes prohibitively expensive. Even if such a data set existed, the means to link the (nano and micro scale) properties across the scale range to normal (macro scale) operational behaviour does not exist.

In the context of the requirements of GEA/Niro, the study of individual particles is less likely to lend itself to the development of relationships with process equipment within a useable time frame, if at all (de Silva 2000; Fitzpatrick, Barringer, & Iqbal 2004) and would require significant capital investment beyond the means of the company for the likely returns that could be made. At the other end of the scale particle size measurement is almost standard in most laboratories in some form – usually through sieve analysis if laser diffraction instrumentation is not available. It's use is often invaluable, but it still cannot, on its own, be used to characterise a powder's flow

behaviour because the size, or size distribution, information does not give full insight into the assembly behaviour – it can only provide a window into the cause of any flow problem, and cannot address the magnitude or the stress level at which such problems may occur.

Thus instrumentation that can evaluate the assembly behaviour of powdered materials is the focus of this study. A list of the instrument suppliers, whose devices are used or mentioned in this thesis, together with their address and website details is given in Section 2.7.

Two observations can be immediately made about the powder flow characterisation instrumentation market

- There are very few laboratory tests or instruments available (compared to, say, the chemical analytics market)
- There are very few process engineering calculations, empirical or otherwise, that make use of a powder characteristic to predict/define performance.

Historically, the development of bulk powder characterisation testing instruments took considerable steps forward in the 1960's with the work of two researchers; A. W. Jenike (Jenike 1964) and R. L. Carr (Carr 1965a;Carr 1965b). Although taking very different approaches to the subject, both created significant testing methodologies that form the basis of most bulk powder characterisation today. Jenike was concerned specifically with the flow of bulk material from storage vessels and used

an adapted civil engineering shear box to characterise the Mohr-Coulomb failure properties of coals and iron ores at the stresses typically found in large storage bins. Carr developed a more experimentally involved, low stress system to characterise powders based on two empirical terms ‘flowability’ and ‘floodability’. These terms allow the user to give a relative ranking to powders and are derived from combinations of a number of individual tests methodologies; bulk density (loose); bulk density (tapped); compressibility (the ratio of packed to loose bulk density); angle of repose; angle of fall; angle of difference (the difference between the angles of repose and fall); angle of spatula; cohesion; and dispersibility.

Tables 2.1 and 2.2 provide a qualitative relationship between parameters derived from the tests specified by each approach to powder characterisation that are frequently quoted in textbooks and academic papers.

Table 2.1: Classification of powder flowability after Jenike where σ_1 is the major principal stress; σ_h is the resultant horizontal stress; σ_c is the unconfined yield strength; and FF is the Flow Function defined as σ_1/σ_c

Type of flow	Flow Function Value	
Easy-flowing	$10 < FF$	
Free-flowing	$4 < FF < 10$	
Cohesive	$2 < FF < 4$	
Very cohesive and non-flowing	$FF < 2$	

A detailed derivation of the Flow Function is presented in Appendix 1.

Ennis *et al* (Ennis *et al.* 2007) detail two measures of flowability that can be derived from shear cell data.

$$\text{Flow Function or } Rel_j = \frac{\sigma_1}{\sigma_c} \quad \text{Equation 2.1}$$

$$Rel_p = \frac{\sigma_1 - \sigma_3}{\sigma_c} \quad \text{Equation 2.2}$$

The *Rel* refers to relative flowability and the subscript to the person who derived the function. The first is the Flow Function as defined by Jenike; the second (where the symbols are the those described in Table 2.1 except σ_3 which is the minor principal stress) is a variant suggested by Peschl and Colijn (Pechl & Colijn 1976). Both ascribe a high value to easy flowing powders and a low value to poor flowing powders. The most commonly used is the Jenike version.

Table 2.2: Classification of powder flowability after Carr

Type of flow	Carr's Compressibility Index, CCI (%)	
Excellent	5-15	<p>How CCI is generated</p>
Good	12-16	
Fair to passable	18-21	
Poor	23-35	
Very poor	33-38	
Extremely poor	>40	

Tables 2.3 and 2.4 show how the parameters derived by Carr can be related to the particular process environments. These are descriptive terms and can only be used to broadly suggest how powders may flow and where specific design measures may be required. Indeed some of the boundaries between one specific measure and another are very small; for example that between 'normal' and 'not good' for the angle of repose is one degree. Such a fine boundary requires that the measurement produces a very repeatable and sharp delineation of the powder behaviour to allow such a boundary to be meaningful, and this will be shown not to be the case later in this Chapter.

Table 2.3: Carr's Flowability Index as supplied by Hosokawa Micron Ltd

Degree of Flowability	Flowability Index	Necessity of Bridge-Breaking Measures	Angle of Repose		Compressibility		Angle of Spatula		Uniformity *		Cohesion **	
			Degree	Index	%	Index	Degree	Index	No.	Index	%	Index
Very Good	90 - 100	Not Required	> 25 26 - 29 30	25 24 22.5	< 5 6 - 9 10	25 23 22.5	< 25 26 - 30 31	25 24 22.5	1 2 - 4 5	25 23 22.5		
Fairly Good	80 - 89	Not Required	31 32 - 34 35	22 21 20	11 12 - 14 15	22 21 20	32 33 - 37 28	22 21 20	6 7 8	22 21 20		
Good	70 - 79	Sometimes vibration is required	36 37 - 39 40	19.5 18 17.5	16 17 - 19 20	19.5 18 17.5	39 40 - 44 45	19.5 18 17.5	9 10 - 11 12	19 18 17.5		
Normal	60 - 69	Bridging will take place at the marginal point	41 42 - 44 45	17 16 15	21 22 - 24 25	17 16 15	46 47 - 59 60	17 16 15	13 14 - 16 17	17 16 15	< 6	15
Not Good	40 - 59	Required	46 47 - 54 55	14.5 12 10	26 27 - 30 31	14.5 12 10	61 62 - 74 75	14.5 12 10	18 19 - 21 22	14.5 12 10	6 - 9 10 - 29 30	14.5 12 10
Bad	20 - 39	Powerful measures should be provided	56 57 - 64 65	9.5 7 5	32 33 - 36 37	9.5 6 5	76 77 - 89 90	9.5 7 5	23 24 - 26 27	9.5 7 5	31 32 - 54 55	9.5 7 5
Very Bad	0 - 9	Special Apparatus and techniques are required	66 67 - 89 90	4.5 2 0	38 39 - 45 > 45	4.5 2 0	91 92 - 99 > 99	4.5 2 0	28 29 - 35 > 35	4.5 2 0	56 57 - 59 > 79	4.5 2 0

Table 2.4: Carr’s Floodability Index as supplied by Hosokawa Micron Ltd

Degree of Floodability	Floodability Index	Measure for Flushing Prevention	Flowability		Angle of Fall		Angle of Difference		Dispersibility	
			Degree	Index	%	Index	Degree	Index	%	Index
Very High	80 - 100	Rotary seal must be used	> 60	25	< 10	25	> 30	25	< 50	25
			59 - 56	24	11 - 19	23	29 - 28	24	49 - 44	24
			55	22.5	20	22.5	27	22.5	43	22.5
			54	22	21	22	26	22	42	22
			53 - 50	21	22 - 24	21	25	21	41 - 36	21
49	20	25	20	24	20	35	20			
Fairly High	60 - 79	Rotary seal is required	48	19.5	26	19.5	23	19.5	34	19.5
			47 - 45	19.5	27 - 29	18	22 - 20	18	33 - 29	18
			44	19.5	30	17.5	19	17.5	28	17.5
			43	19.5	31	17	18	17	27	17
			42 - 40	19.5	32 - 39	16	17 - 16	16	26 - 21	16
39	19.5	40	15	15	15	20	15			
Tends to Flush	40 - 59	Sometimes rotary seal is required	38	14.5	41	14.5	14	14.5	19	14.5
			37 - 34	12	42 - 49	12	12	12	18 - 11	12
			33	10	50	10	10	10	10	10
May Flush	23 - 39	Rotary seal is necessary depending on flow speed and feed conditions	32	9.5	51	9	9.5	9.5	9	9.5
			31 - 29	8	52 - 56	8	8	8	8	8
			28	6.25	57	7	6.25	6.25	7	6.25
Won't Flush	0 - 24	Not Required	27	4	58	6	6	6	6	6
			26 - 23	3	59 - 64	5 - 1	3	3	5 - 1	3
			< 23	0	> 64	0	0	0	0	0

Much debate has taken place over which systems provides the better solution – or even if other approaches, such as the recently developed field of powder rheometry, are more representative. This chapter will evaluate these approaches to powder characterisation and provide a cogent analysis of the benefits and shortcomings of each.

Additionally, what is clear from Tables 2.1 & 2.2 is that there is a distinct attempt to provide a single number approach to the issue of ‘characterising’ powders. Whilst this could be seen as a laudable attempt to keep things simple, it is an unrealistic approach to an exceptionally complex system. This project will also show is that this approach to single parameter quantification of a powders flow characteristics is both naïve and potentially costly in terms of designing process plant which will not achieve its design throughput.

To compare powder characterisation testers, a set of powders were evaluated which relate to the powder mixing study discussed in Chapter 3. However, a significant range of other materials have also been tested which have been of specific interest to GEA/Niro or have particular relevance to one or more of the particular testers. These powders are shown in Table 2.5 together with their size distributions.

Table 2.5: List of exemplar powders chosen for characterisation testing and their relevance to this project

Test Material	Particle size (microns) ¹					Reason for Testing
	d10	d16	d50	d84	d90	
Avicel 102 Sample 1	27.27	37.50	108.94	203.98	229.59	These two samples were provided for testing a GEA IBC discharge station
Avicel 102 Sample 2	27.79	38.09	107.75	201.95	227.97	
MCC	5.83	9.03	35.92	257.51	406.17	Used for mixing experiments
Lactose	11.88	20.99	90.73	198.05	230.90	
Sodium Benzoate	7.00	11.45	124.08	407.95	494.60	
Celphere 102	147.08	150.23	173.03	205.55	228.36	Used in a Departmental tableting experiment (Wu <i>et al.</i> 2007)
Celphere 305	363.31	375.69	421.52	498.27	509.38	
Sodium Bicarbonate	3.34	5.15	23.73	55.18	64.63	Granulation excipients provided by GEA Collette
Fine Salt	13.73	30.94	114.10	198.90	220.91	
Mannitol	1.45	2.06	9.17	40.71	59.56	
Paracetamol Fine	1.13	1.59	6.32	28.01	43.66	Tableting excipients and placebo blends supplied by GEA Courtoy
Paracetamol Extra Fine	1.92	2.89	11.53	10.39	56.53	
Paracetamol blend	10.17	17.24	78.52	315.22	379.72	
Tablet Blend Placebo	31.76	45.4	129.18	231.59	261.71	

¹ Measurements made using a Sympatec Helos laser diffraction particle size analyser and a Rodos dry powder dispersion system.

It was not possible to evaluate all the materials in Table 2.5 using all the powder characterisation methods due to stability issues with some samples over the extended period in which instruments became available, but the majority of materials were tested using all the methodologies. Other samples have been chosen to explore different powder behavioural traits or instrument performance, and these are detailed in the relevant section.

2.3. Powder Testing Equipment

2.3.1. Shear Cell

Shear cell evaluation of powdered materials has been detailed in many standard texts and journal articles (EFCE 1989;Fayed & Otten 1984;Jenike 1964;McGlinchy 2005;Rhodes 1998;Roberts 1993;Schulze 2007) and the concepts behind the methodology, as well as the derivation of the Mohr's circle, are presented in detail in Appendix 1. The use of shear cell testing has been vigorously promoted because of its strong theoretical basis and is to be commended as this advances strong, science based technology into industry. However, there are some details of the measurement and analysis which, when in-depth evaluation is undertaken, have some significant shortcomings that end users should be aware of when testing powders and interpreting the results.

This section will briefly outline shear testing using two different instruments; look at some of the more challenging issues when collecting and interpreting shear data;

and demonstrate some of the strengths and weaknesses of the information derived from shear cell testing of powdered materials.

Shear cell measurements have historically been complex and very time consuming. Personal experience with a Walker annular ring shear cell in the late 1980's showed that it required a day to collect the test measurements and half a day to process the chart recorder output and manipulate the data to produce a yield locus and the associated derived information. The Jenike type shear tester was even more complex requiring the preparation of multiple samples for defining a single yield locus and a manual pre-consolidation of each powder sample. Such testing protocols could easily introduce considerable variability and it was recognised that a skilled and experienced operator was required to achieve usable results.

Although things have improved with the advent of automated and computer controlled shear cells (FT4; Peschl, Shear Scan; Schulze cells; i-shear; and most recently the Brookfield PFT²) there is still reluctance on the part of practitioners and specialists to undertake repeat measurements and to evaluate more than 3 data points per yield locus³. The lack of repeat testing has a clear implication for the understanding of the stability of the test powder and the repeatability of testing method. The use of only three measurements per yield locus also has implications for the applicability of the model from which the derived functions (AIF, UYS, MPS, FF – as defined in Appendix 1) are generated. These issues will be discussed in Section 2.3.1.2.

² The details of the manufacturers are presented in Section 2.7

³ private conversation with Prof D Schulze, University of Braunschweig/Wolfenbuttel, 2007

Two different shear cells have been available during this project. Figure 2.1 shows the Schultz RST-XS shear cell located in the Dept. of Chemical Engineering and the shear cell attachment used in conjunction with the Freeman Technology FT4 Powder Rheometer. It should be noted that another shear cell within the University – the ShearScan – was unavailable throughout this project due to instrument failure and thus such a device cannot be recommended for use by GEA/Niro.

The use of more complex, but arguably more technically robust, biaxial and triaxial shear testers is beyond the scope of this project as there are no commercially available instruments and comparatively little work is available in the literature relating to testing industrially relevant powders at industrially relevant consolidating stresses (Feise 1998; Janssen, Verwijs, & Scarlett 2005; Kamath & Puri 1997; Schwedes 2002; Schwedes & Schulze 1990b).



Figure 2.1: RST-XS and FT4 shear cells

There are several differences between the two instruments which are summarised in Table 2.6.

Table 2.6: Comparison between the two shear cells testers used during this project. The cell volumes in brackets show optional configurations for each instrument (which were not used in this study)

	RST-XS	FT4
Cell volume	30ml ⁴ (9ml)	85ml (10ml, 1ml)
Shear area	2412.75mm ²	1963.5mm ²
Driven section	Shear cell base	Shear head
Consolidation load	'Dead weight'	Motor control
Pre-shear	Single	Can be defined
Order of shear test	Low → High	High → Low
Control method	Custom program on separate dedicated PC located adjacent to instrument	Custom program on PC integrated into instrument
Length of test	700-800 seconds	700-800 seconds
Weighing of sample	Need a separate balance	On board sample weighing
Post processing	Custom program on instrument PC or on remote PC ⁵	Custom program on integrated instrument PC or on remote PC

The figures below show the screen trace of a test in progress for both testers – Figure 2.2, the RST-XS and Figure 2.3 the FT4. Although the two figures are not directly comparable, due to the intrinsic differences in their control program display philosophy, one can see that are one or two significant differences.

⁴ Instrument test volumes highlighted in red indicate that they were used in this project

⁵ The post processing program may be installed on a PC in the user's office rather than the instrument PC located in the laboratory.

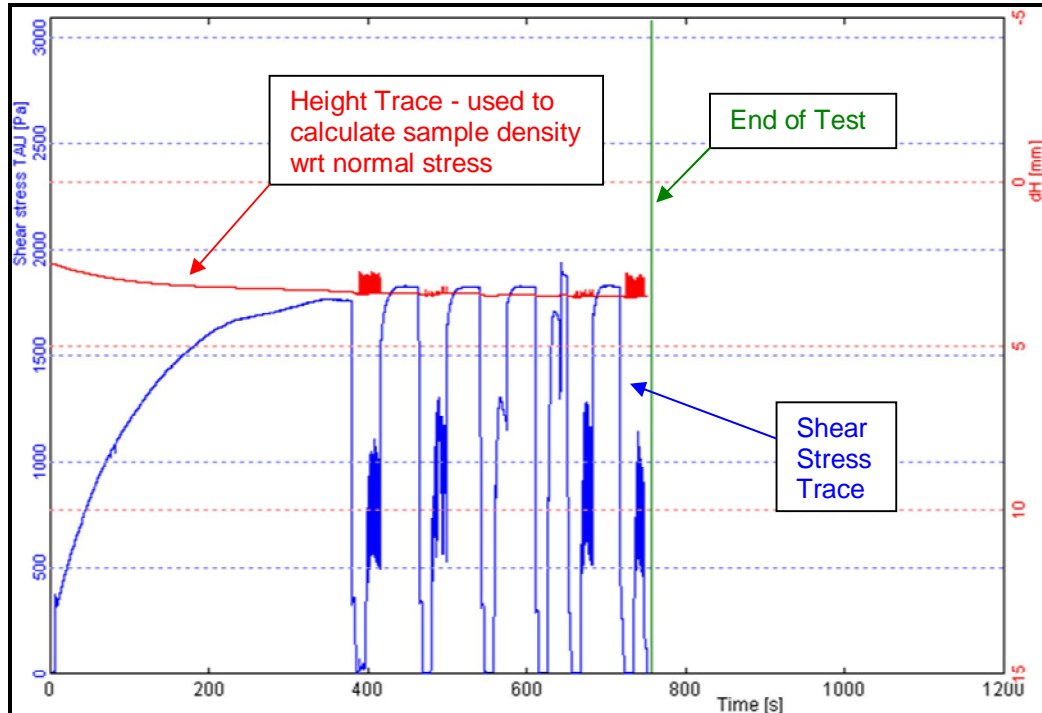


Figure 2.2: Screenshot of RST-XS performing a shear test. The blue trace shows the progress of the shear stress on the left axis; the red trace shows the height of the lid on the right axis; the green line indicates the end of the test

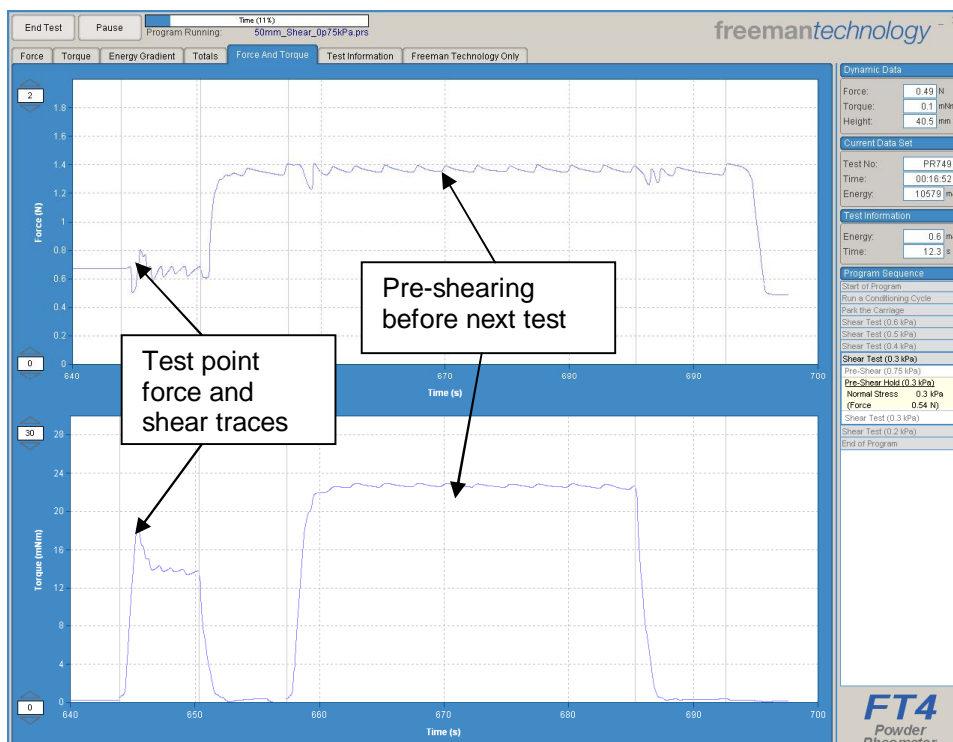


Figure 2.3: Screenshot of FT4 performing a shear test. The top trace shows the evolution of the force, measured by the load cell, during the test; the lower trace indicates the torque measurement during the same time period. Both graphs scroll right to left during the test.

The RST-XS displays shear stress (converted in real time from the torque measurements) and height traces during a test routine. The FT4 displays force and torque traces measured during the test. It also captures the position of the shear head, but does not display this in real time.

Two practical drawbacks with the RST-XS are firstly the sample preparation can be quite messy, as shown in Figure 2.4. The sample cell has to be overfilled and scraped flat. The FT4 accomplishes this with a sample cell splitting mechanism that is described in more detail in Section 2.3.5.2 and results in very little spillage of the material, which is a benefit when testing samples containing API. Secondly, when filled, the RST-XS cell has to be weighed on a separate balance; the FT4 has a built in balance which means the system does not require a separate weighing balance.



Figure 2.4: Filling of the RST-XS Shear Cell
(reproduced from the Schulze web site <http://www.dietmar-schulze.de>)

2.3.1.1. Application and treatment of normal force

One of the more interesting differences between the two testers is the treatment of normal force. The FT4 uses a motorised carriage to apply the normal force to the powder in the cell. The RST-XS uses lever arms to apply a 'dead weight' to the sample. The FT4 records and displays all the force, torque and height profiles during the test at a frequency of 50Hz. The RST-XS records and display only the torque and height profiles and asserts that the normal force remains constant at the set level; the frequency of measurement is unknown. This assumes that the normal force changes very little during the dilation phase of the shearing process. Dilation, as described by Schulze (Schulze 2007), is due to particles having to move over each other because of the stress imposed by the shearing process. To allow this during shearing, particles must move slightly upwards – imagine a trying to roll a single golf ball over the surface of a barrel full of golf balls, the rolling golf ball has to climb up from its location nestling between other golf balls in the lower level and climb to the top of a golf ball before falling down into the next gap. This also has a tendency to create a reaction force which, in conjunction with the normal force that is being applied, results in an increase in the measured force and can be observed clearly if the top cap or lid of a shear cell had been held at a fixed height during shear. Additionally, if the shear head is held at constant height, the torque required to shear the sample also increases as the particles have more difficulty in riding over each other. Figure 2.5 shows the force and torque traces of an FT4 shear held at a fixed height during a shear test of Standard Limestone CRM/BCR116 (Akers 1992). Any dilation of the powder would therefore register as an increase in the force captured by the instrument sensors.

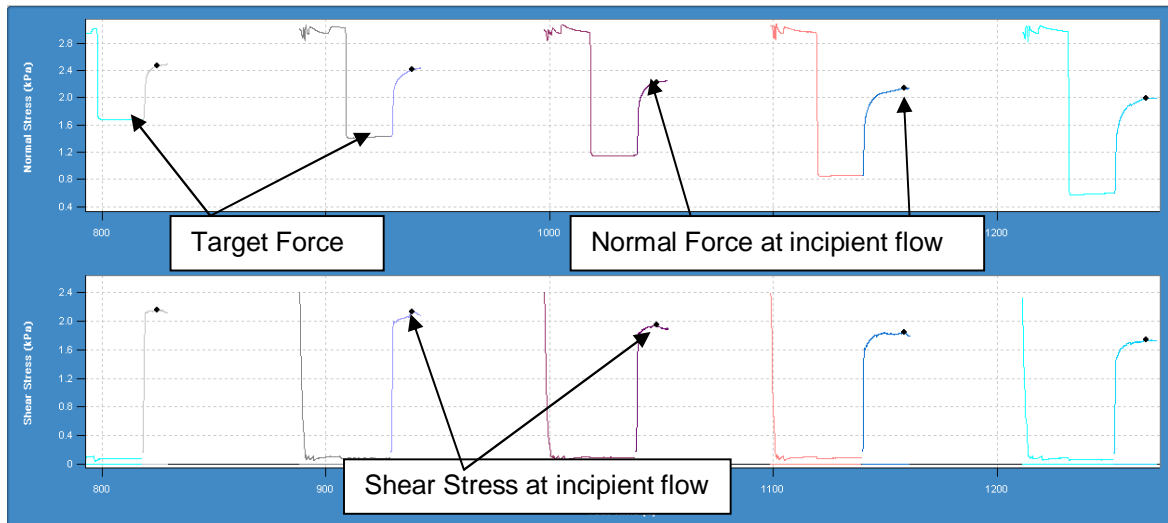


Figure 2.5: Force and torque traces for a shear test on Limestone at 3kPa consolidating stress with the carriage undertaking each shear test at a fixed height once the target consolidating force has been achieved, generated using an FT4 shear cell attachment.

Figure 2.6 shows the resultant yield locus for the test in conjunction with the yield locus for a similar test where the carriage was mobile and utilised the standard force control algorithm.

The application of true 'dead weight' would, of course, have no implication on the treatment of the normal force with respect to powder dilation. However, given the configuration of the RST-XS it can be seen that a 'dead weight' is not directly applied to the powder and force is applied indirectly through the cantilever mechanism, the external components of which are shown in Figure 2.1 (the top of the RST-XS displayed on the left hand side of the diagram). Ideally the force application method should be explicit – which is not the case here – and, if it is not a true dead weight, the force should be monitored and data collected. Assuming that the normal force

remains at a specified set point is, in this instance, simply not good enough as it has implications for the location of the normal stress/shear stress data pairs.

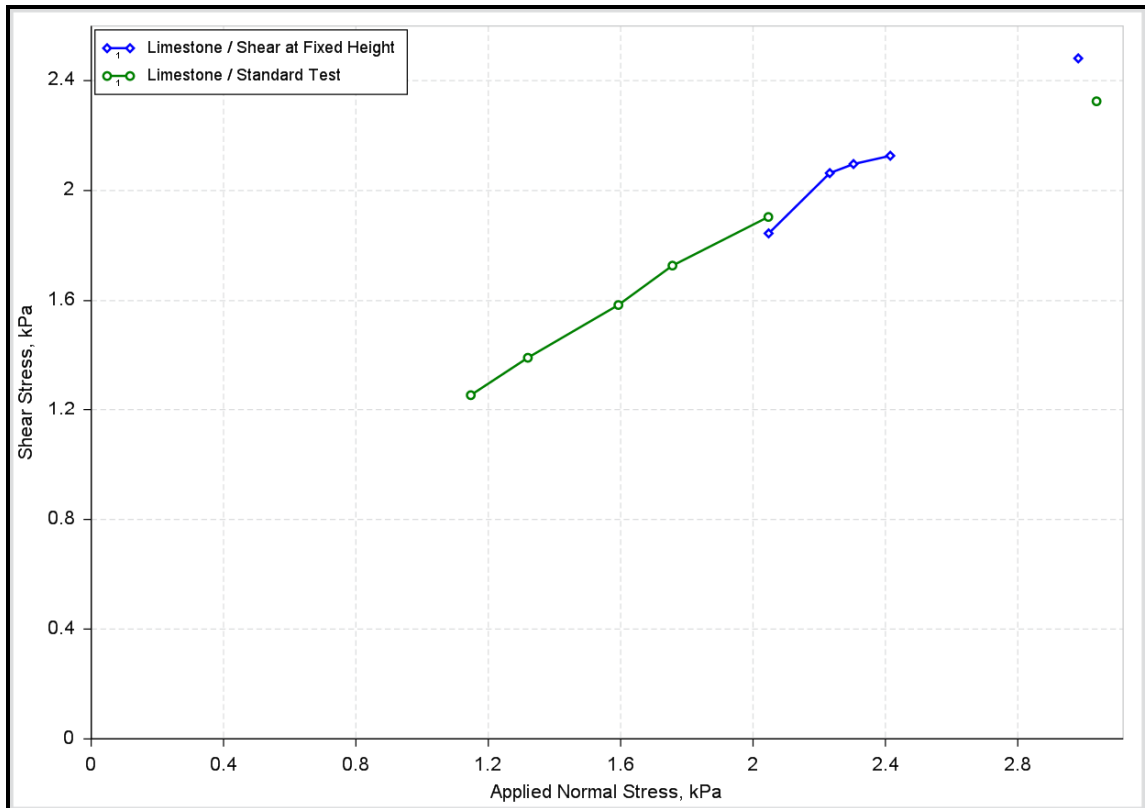


Figure 2.6: Yield loci for shear tests on Limestone at 3kPa consolidating stress with the FT4 carriage undertaking each shear test at a fixed height (blue trace) and with the carriage under normal force control parameters (green trace).

Dilation is a major issue when testing large particles or particles with a high length to diameter (l/d) ratio. In normal operation, the FT4 has to react to this dilation by adjusting the position of the carriage holding the shear head upwards to allow the powder to expand. In Figure 2.7 it can be seen the FT4 attempted to control the over force due to the dilation of the particles using a simple proportional force control algorithm (blue trace) and this trace is compared to a more advanced control method (red trace) where the carriage is controlled using a modulated back off algorithm in order match the rate of dilation of the material.

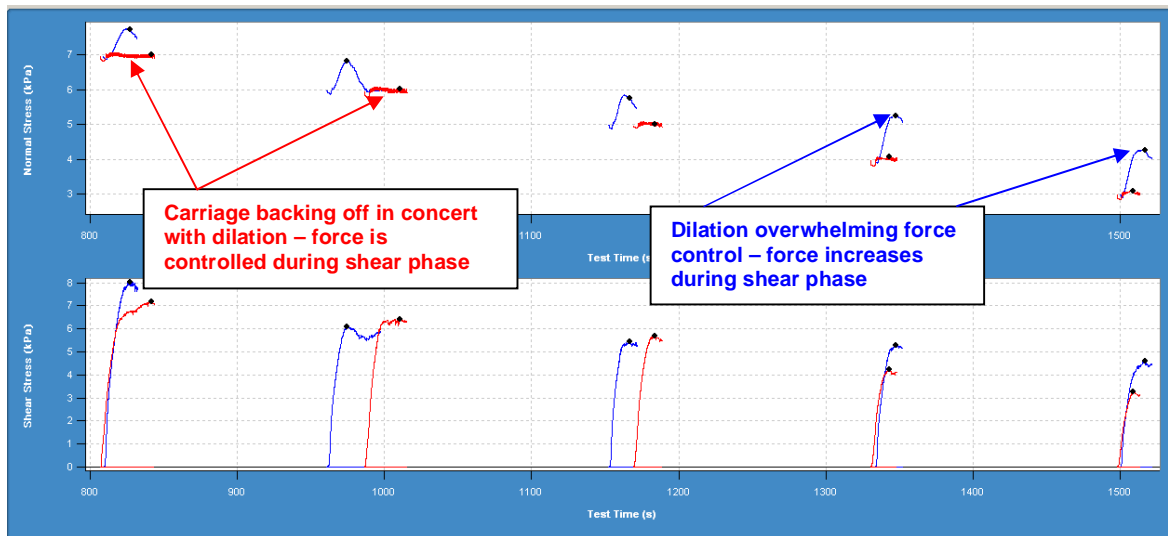


Figure 2.7: Comparison of force control techniques for the FT4 shear cell for a highly dilating powder. In the top graph, the Blue trace is simple proportional control where the instrument attempts to maintain a constant force but fails to do so; the red trace shows a modulated back off algorithm where the normal force is maintained at a constant level through the incipient failure (shown in the lower torque graph).

This clearly shows that dilation is occurring during the shear process and thus can have an effect on the results. Knowledge of the force acting on the powder during the shearing process is useful to understand how the yield point is developed. The FT4 control method has been recently updated to optimise its reaction to the dilating powder and maintain stress on the powder close to the target value set in the test programme. Figure 2.8 shows the yield loci from the same test using the more advanced force control algorithm as well as the original control methodology.

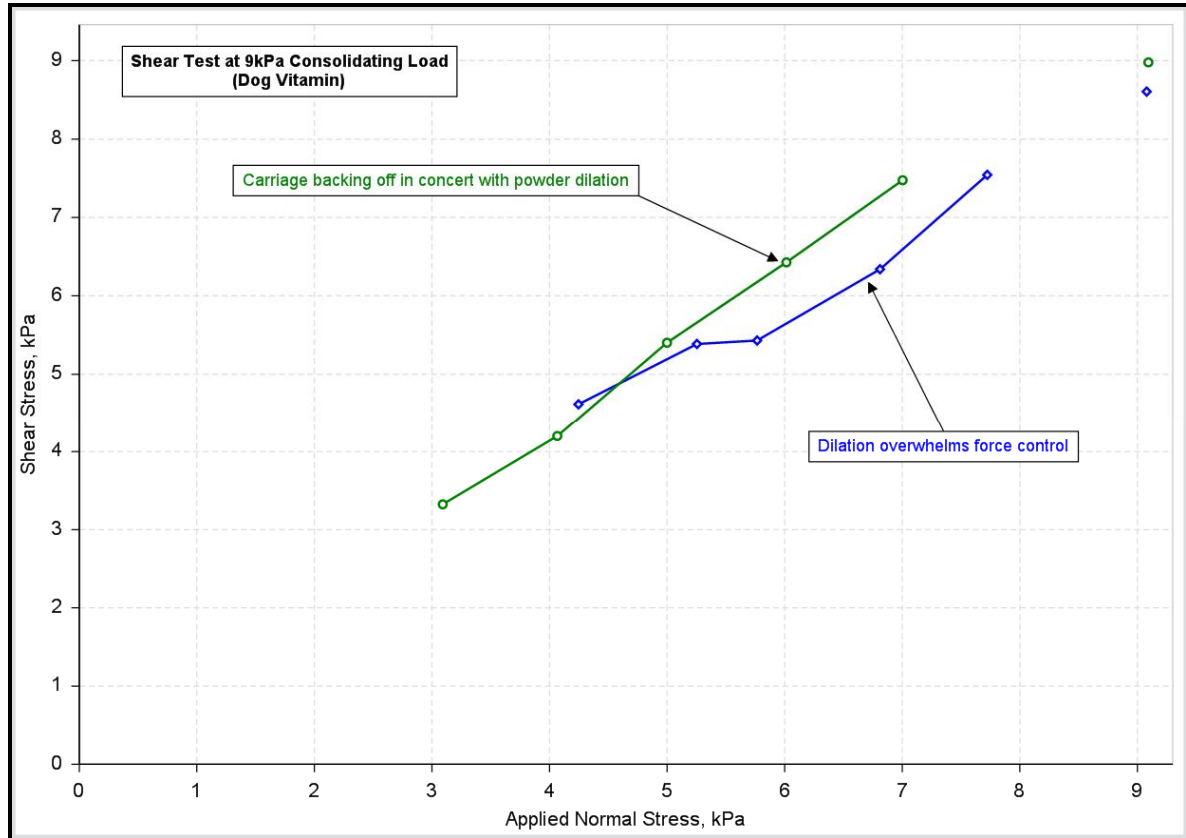


Figure 2.8: Comparison of force control techniques for the FT4 shear cell for a highly dilating powder. Blue trace is simple proportional control; green trace shows a modulated back off algorithm

Additionally, there are some issues when testing with the RST-XS machine at low normal loads, typically below 2kPa, where the tester does not appear to be able to control the force applied to the test cell or that generated by the powder (as shown in Figure 2.9). This may be due to the way that the force is applied to the powder and the ability of the mechanics to respond rapidly enough to the extremely fast dilation that occurs at the point of incipient failure which has been observed in the during testing with the FT4 shear cell. As the RST-XS does not record force, there is no practical way to validate this assumption.

The resultant normal load vs. shear load graph and Mohr's circle construction does not provide the expected straight, or slightly convex curved construction that is observed for higher consolidating loads. The reasons for this system drawing such a 'kinked' yield locus and what it means for the derived data will be discussed in more detail in the next section.

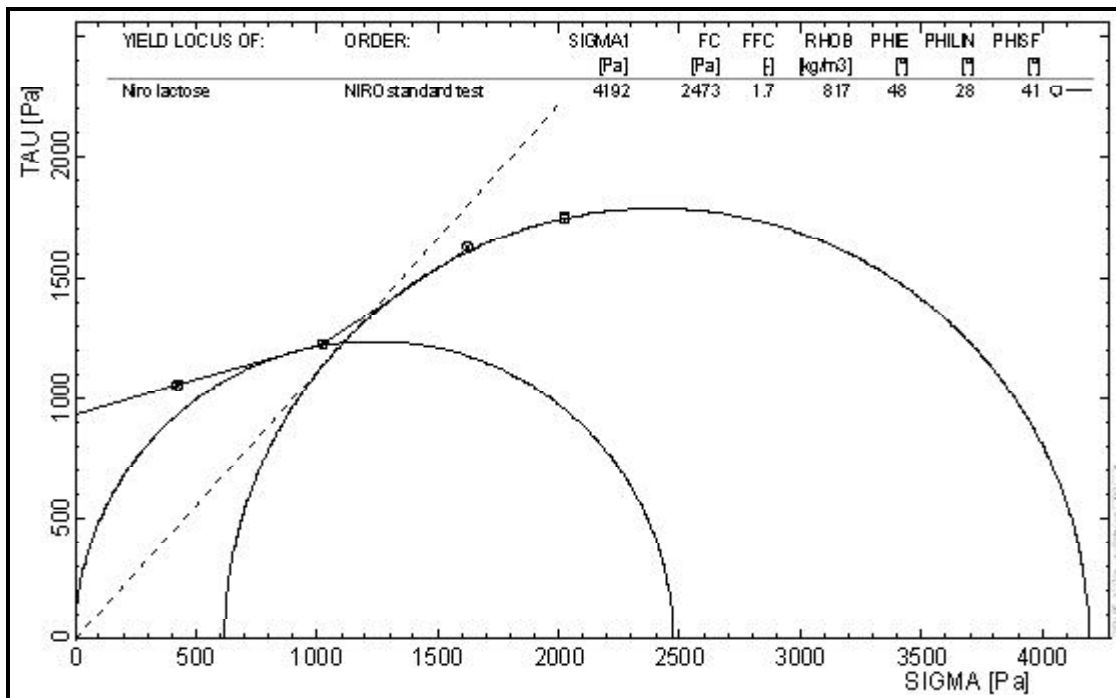


Figure 2.9: Yield locus for Lactose using recommended procedure for RST-XS shear cell at a consolidating load of 2kPa. The software creates a 'bent' locus which significantly increases the derived cohesion and ff_c values for the powder compared to a linear regression fit

Thus the FT4's ability to measure and display the force acting on shear head is an extremely useful tool to enable the understanding of what is going on during a test. It enables the test to be scrutinised to evaluate the validity of each test point and determine if critical consolidation of the sample during testing has been achieved.

The debate over which shear cell provides a ‘true’ shear stress/normal stress relationship will continue in the literature in parallel to the debate regarding the benefits of bi-axial and tri-axial shear testers, over and above the single axis testers described here (Schwedes & Schulze 1990a), and several heated arguments have occurred at conferences and in internet forums (Schulze & Pechl 2009). However, it is not the primary purpose of this project, nor was there sufficient time to investigate this particular issue in detail, other aspects of the treatment and application of shear cell data will now be discussed.

2.3.1.2. Evaluation of shear test data and derived data

Shear cell testing generates a lot of parameters from the mathematical treatment of the normal stress/shear stress data pairs, as described in Appendix 1. These parameters are generated in the post processing data analysis packages associated with both instruments. Table 2.7 lists the parameters together with some typical symbols or abbreviations used and the units where applicable.

Table 2.7: Parameters derived from the yield locus

Parameter	Symbol	Units
Major Principal Stress	σ_1 , MPS	Pa
Unconfined Yield Strength	σ_c , FC, UYS	Pa
Cohesion	C	Pa
Flow Function (σ_1 / σ_c)	ff _c , FF	-
Angle of Internal Friction	δ , AIF	deg
Effective Angle of Internal Friction	δ_e , AIF(E)	deg
Angle of Internal Friction at Steady State Flow	δ_{ss} , AIF(SS)	deg

Figure 2.10 shows how these parameters are derived from a yield locus.

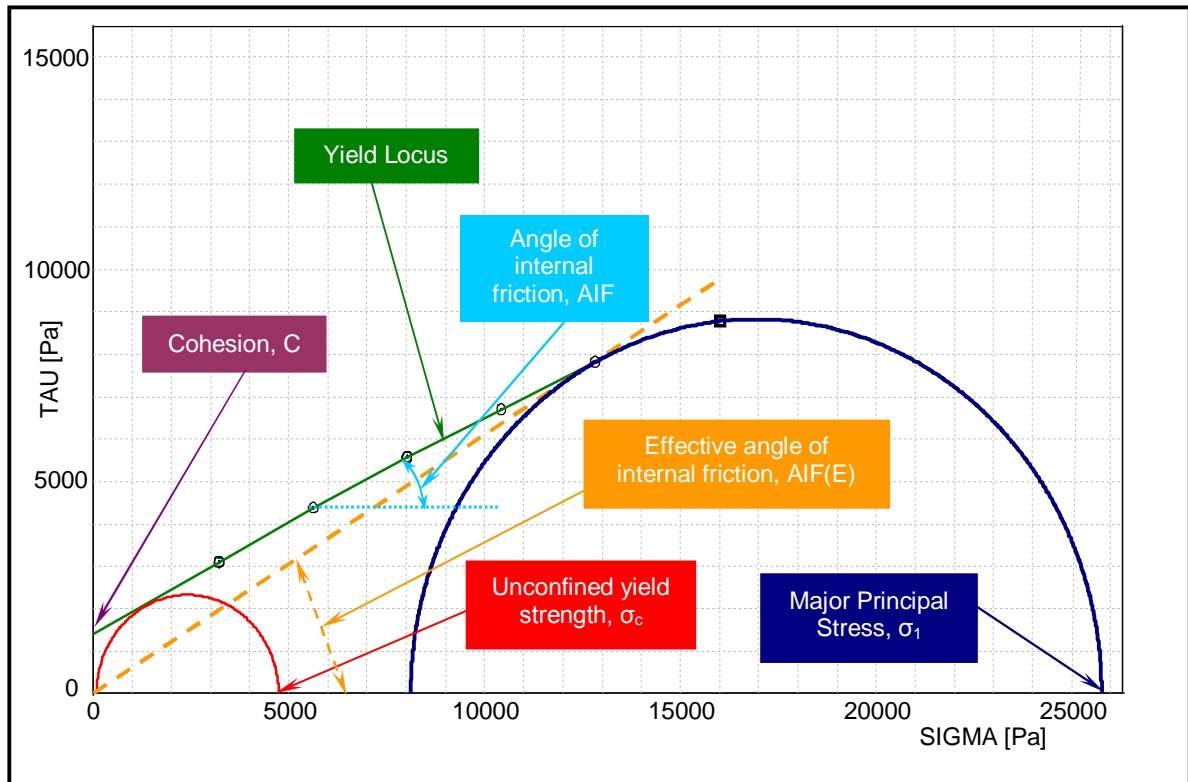


Figure 2.10: Graphical description of the yield locus and the parameters derived from the fitting of Mohr Circles to the σ/τ data set.

Common practice is to provide a linear fit to the data points in order to generate these derived parameters. An alternative is to use the Warren Springs equation (Equation 2.3) which allows the concept of a tensile strength to also be derived (Bundalli 1973; Cheng & Farley 1968; Stainforth, Ashley, & Morley 1971).

$$\left(\frac{\tau}{C}\right)^N = \frac{\sigma + T}{T} \quad \text{Equation 2.3}$$

where τ is the shear stress (kPa)
 σ is the normal stress (kPa)
 C is the cohesion (kPa) – intercept on the Y-Axis
 T is the tensile strength (kPa) – intercept on the X-Axis
 N is the shear index

Schwedes (Schwedes 2003) points out that the authors of the equation also offer a physical explanation for the relationship by considering adhesive and repulsive forces at particle contacts, but despite the equation being well represented in the literature, it was never used for practical applications and the index, N , is no longer used to characterize flowability.

However, a more complex non-linear model should not be dismissed out of hand. The use of only three measurement points to determine a yield locus has been promoted/justified with the view that particles at the shear plane may degrade if subjected to excessive shearing – this may be the case for very friable materials, but in most instances, the periods over which the particles are subjected to stress in the shear plane are relatively short and degradation is rarely an issue and easily spotted if the force/torque trace is carefully analysed. Additionally, the ability to fit non-linear models to data can be difficult, especially if such an analysis has to be completed without the aid of computer based mathematical programs, as was the case during the development of the shear cell methodology, which can now rapidly provide the required regression analysis.

It should also be noted that many materials are likely to generate a linear yield locus, so this approach is, arguably, not unreasonable. This is especially the case for the less cohesive materials.

However, if one considers a test where multiple data points are used to describe a yield locus, the differences between a linear and non-linear curve fit can be seen. In this case Limestone CRM116 has been tested and linear and polynomial regression fits have been used to determine the shape of the locus as shown in Figure 2.11.

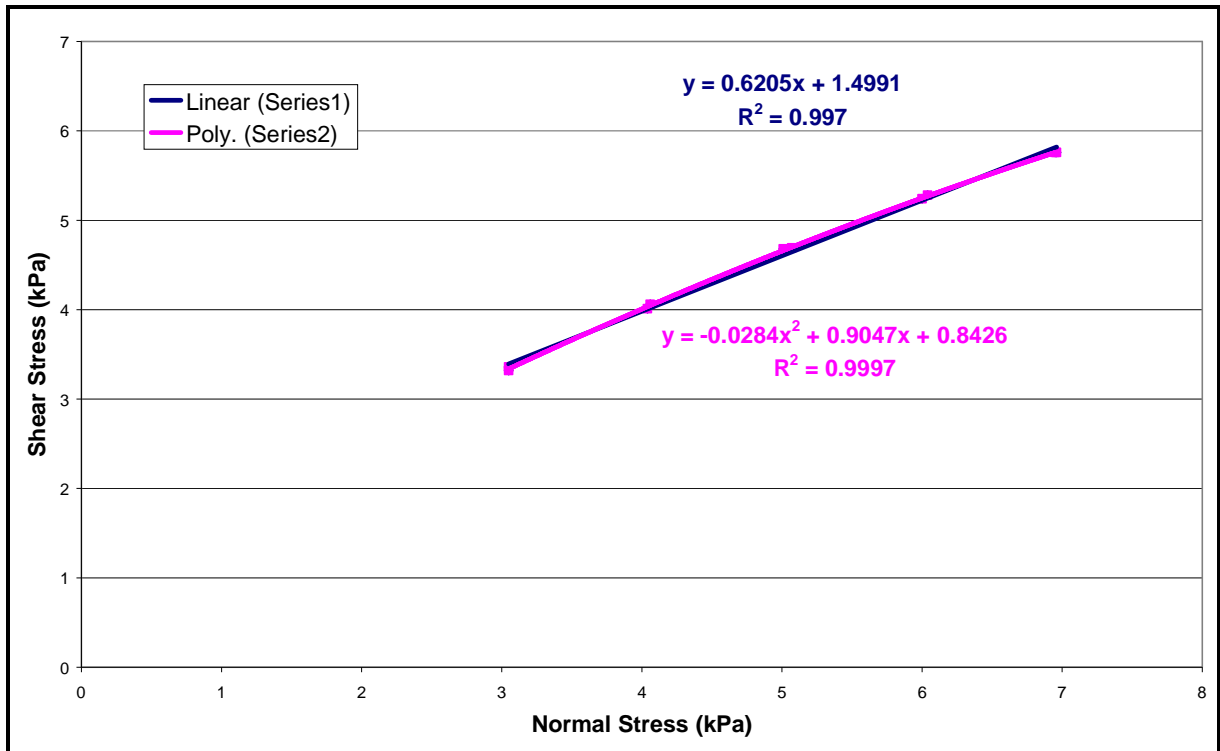


Figure 2.11: A yield locus derived from 5 measurement points fitted to linear and polynomial regressions for Limestone CRM116, generated using an FT4 shear cell attachment.

Comparing the regression analyses presented in Figures 2.11, where only 5 measurements are used to create the loci, what can be immediately seen is that the intercept (Cohesion) value is noticeably different; 0.84kPa for the polynomial fit (which is coupled with a slightly better R^2 value); 1.50kPa for the linear fit. Both models would be described as acceptable given their very high R^2 values, but there is a 78% difference in the derived Cohesion.

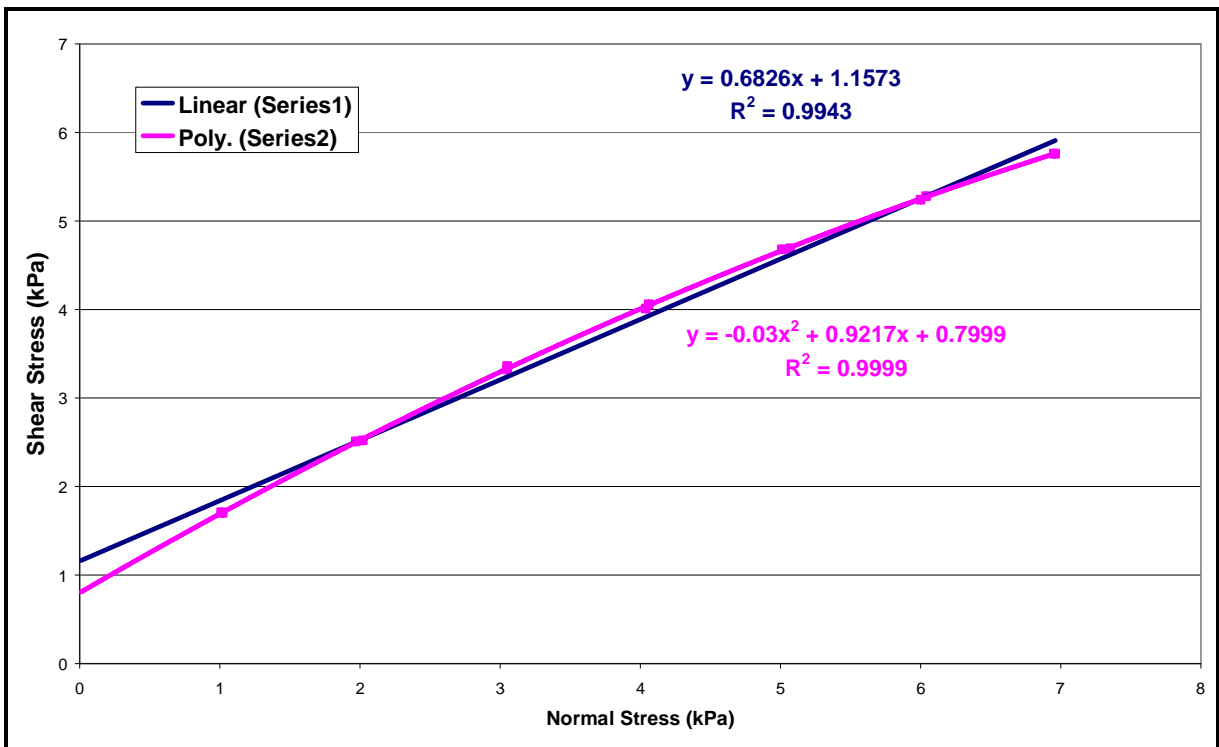


Figure 2.12: A yield locus derived from 7 measurement points fitted to linear and polynomial regressions for Limestone CRM116, generated using an FT4 shear cell attachment.

If one then adds two extra test points at lower normal stresses, (generated during the same test as shown in Figure 2.11, but excluded from that locus creation), as shown in Figure 2.12, then one can see that there is a significant change in the linearly derived cohesion (30% when comparing the cohesion from a 7 point locus to a 5 point locus) compared to the slight change in polynomially derived cohesion (5%). The R^2 value for the linear regression also reduces with additional test points whereas it improves for the polynomial fit. From this analysis it seems that the use of additional (lower stress) test points strongly suggests that a non-linear approach to modelling the yield locus can be appropriate in some cases.

An alternative approach suggested by Berry and Bradley (Berry & Bradley 2005), also suggested by Jenike (Jenike 1964), has shown that, for some powders, a two point yield locus can be used to adequately represent the failure properties of a powder. However, Berry also suggests that this is perhaps more useful in quality control applications where a (very) rapid result is required to qualify acceptance of a batch within a production run. One of Berry's major conclusions is that 'the failure function is strongly dependent on the analysis procedure used', which has also been shown in this study.

Thus it must be concluded that the information derived from the mathematical analysis applied to the yield locus by the instrument suppliers must be interrogated very carefully to ensure that it is interpreted correctly and its limitations understood.

The linear fit is, however, the simplest and is used in most shear cell post processing software, including the two shear cells compared here and will be used in this study for the purposes of comparison.

If one also considers good experimental practice there would be a need to understand the uncertainty associated with the measurements and repeat testing would be the norm. There is an argument put forward that multiple testing takes time (and therefore costs money) but with modern equipment, a shear test takes less than 20 minutes and the cost implications are small. Thus where possible repeat tests have been undertaken and are presented.

Tables 2.8 and 2.9 show the derived data from the testing of the exemplar powders using the FT4 shear cell attachment and the RST-XS shear cell respectively. Figure 2.13 shows the Flow Functions derived from the RST-XS shear cell and Figure 2.14 compares the Flow Functions derived from both shear testers.

Table 2.8: FT4 shear test derived data under 9kPa consolidating load (n=3)⁶

Test Material	σ_1 /MPS (kPa)	σ_c /UYS (kPa)	ff_c	τ_c / C (kPa)	$\phi_{LIN} /$ AIF	$\phi_E /$ AIF (E)	$\phi_{SF} /$ AIF (SS)
Avicel 102 Sample 1	16.0	1.50	10.7	0.38	35.8	38.0	33.9
Avicel 102 Sample 2	16.4	1.64	10.0	0.40	38.3	40.6	35.4
MCC	20.0	6.19	3.23	1.52	37.6	45.5	41.2
Lactose	16.4	3.41	4.81	0.88	35.2	40.5	35.3
Sodium Benzoate	26.7	6.02	4.44	1.37	41	46.3	45.4
Celphere 102	12.4	0.90	13.8	0.29	24.4	26.4	23.2
Celphere 305	12.7	1.25	10.2	0.38	27.8	30.4	25.5
Sodium Bicarbonate	14.9	2.20	6.8	0.59	33.5	37.2	32.2
Fine Salt	11.9	1.19	10.1	0.35	29.6	32.2	23.8
Mannitol	17.2	6.74	2.56	1.71	36.3	46.9	38.7
Paracetamol Fine	17.3	4.59	3.78	1.24	33.3	40.3	36.4
Paracetamol Extra Fine	19.9	5.39	3.69	1.39	35.6	42.6	39.9
Paracetamol blend	18.1	1.72	10.6	0.43	36.9	39.2	36.6
Tablet Blend Placebo	15.5	0.66	23.6	0.18	33.9	34.9	32.2

⁶ For all tests 'n' is the number of repeat measurements carried out to generate the averaged value presented and, where applicable, the variance. In the case of shear data, yield points are averaged and a single yield locus is generated, from which the derived data are determined and presented in the Table – hence no variance is available.

Table 2.9: RST-XS shear test derived data under a range of consolidating loads

Test Material	Cons Stress [Pa]	σ_1 [Pa]	σ_c [Pa]	ff_c	C [Pa]	ρ_B [kg/m ³]	Φ_E [°]	Φ_{LIN} [°]	Φ_{SF} [°]
Avicel 102 Sample 1	8000	10796	1427	7.6	335	409	42	38.9	39.1
	4000	6611	944	7.0	220	404	42.2	38.8	39.5
	2000	4454	696	6.4	162	402	42.8	39.2	40.0
Avicel 102 Sample 2	8000	11453	1563	7.3	363	416	42.8	39.7	40.4
	4000	6766	1001	6.8	231	414	43.8	40.4	40.6
	2000	4582	749	6.1	172	407	43.7	39.9	40.8
MCC	8000	11601	1824	6.4	401	381	44.6	41.0	41.5
	4000	6890	1181	5.8	265	375	44.3	40.4	41.2
	2000	4605	896	5.1	204	368	45.0	40.5	41.5
Lactose	8000	10585	3122	3.4	692	804	46.7	39.4	40.7
	4000	6197	2213	2.8	499	778	47.6	38.4	40.4
	2000	4265	1630	2.6	360	766	49.3	39.5	41.6
Sodium Benzoate	8000	11690	1680	7.0	362	322	45.0	41.7	41.8
	4000	7025	976	7.2	213	320	44.5	41.4	41.6
	2000	4802	750	6.4	159	316	46.4	43.0	42.8
Celphere 102	8000	13910	293	47.5	82	939	32	31.5	30.4
	4000	6871	1291	5.3	471	930	31.8	26.6	30.0
	2000	3562	1276	2.8	441	932	32.4	21.1	30.8
Celphere 305	8000	14075	5	3.1	1	964	34.1	34.1	31.7
	4000	7825	1334	5.9	490	959	33.2	28.6	32.5
	2000	3785	1231	3.1	365	955	34.0	24.2	32.6
Sodium Bicarbonate	8000	10400	2221	4.7	497	888	41.4	36.1	38.2
	4000	6255	1529	4.1	351	858	44.0	37.9	39.3
	2000	4096	1098	3.7	250	828	45.1	38.4	39.3
Fine Salt	8000	9234	130	70.8	34	1314	36.5	36.1	33.7
	4000	5556	173	32.0	45	1321	36.5	35.8	33.7
	2000	3891	83	47.0	20	1317	37.7	37.2	35.0
Mannitol	8000	10505	4062	2.6	900	683	49.3	39.3	41.4
	4000	6488	2913	2.2	622	649	52.3	40.6	42.9
	2000	4176	1970	2.1	435	622	52.1	39.4	42
Paracetamol Fine	8000	11524	4140	2.8	853	487	50.0	41.1	43.5
	4000	6649	3443	1.9	704	462	53.6	39.3	43.8
	2000	4845	2910	1.7	577	458	59.7	43.7	47.1
Paracetamol Extra Fine	8000	13610	6036	2.3	1136	481	51.2	39.5	46.8
	4000	7653	4309	1.8	864	455	56.7	41.4	47.5
	2000	4956	3267	1.5	669	420	61.0	42.2	47.9
Paracetamol Blend	16000	10383	1240	8.4	293	943	41.2	38.4	38.0
	8000	8065	969	8.3	232	927	40.6	37.8	37.3
	4000	6243	889	7.0	212	916	41.8	38.4	38.3
	2000	4383	688	6.4	159	907	42.5	38.8	39.4
Tablet Blend Placebo	16000	10667	531	20.1	125	527	39.8	38.7	37.8
	8000	8773	491	17.9	113	530	40.9	39.7	38.8
	4000	6739	380	17.8	88	523	41.2	40.0	39.3
	2000	4537	270	16.8	62	530	41.9	40.5	39.7

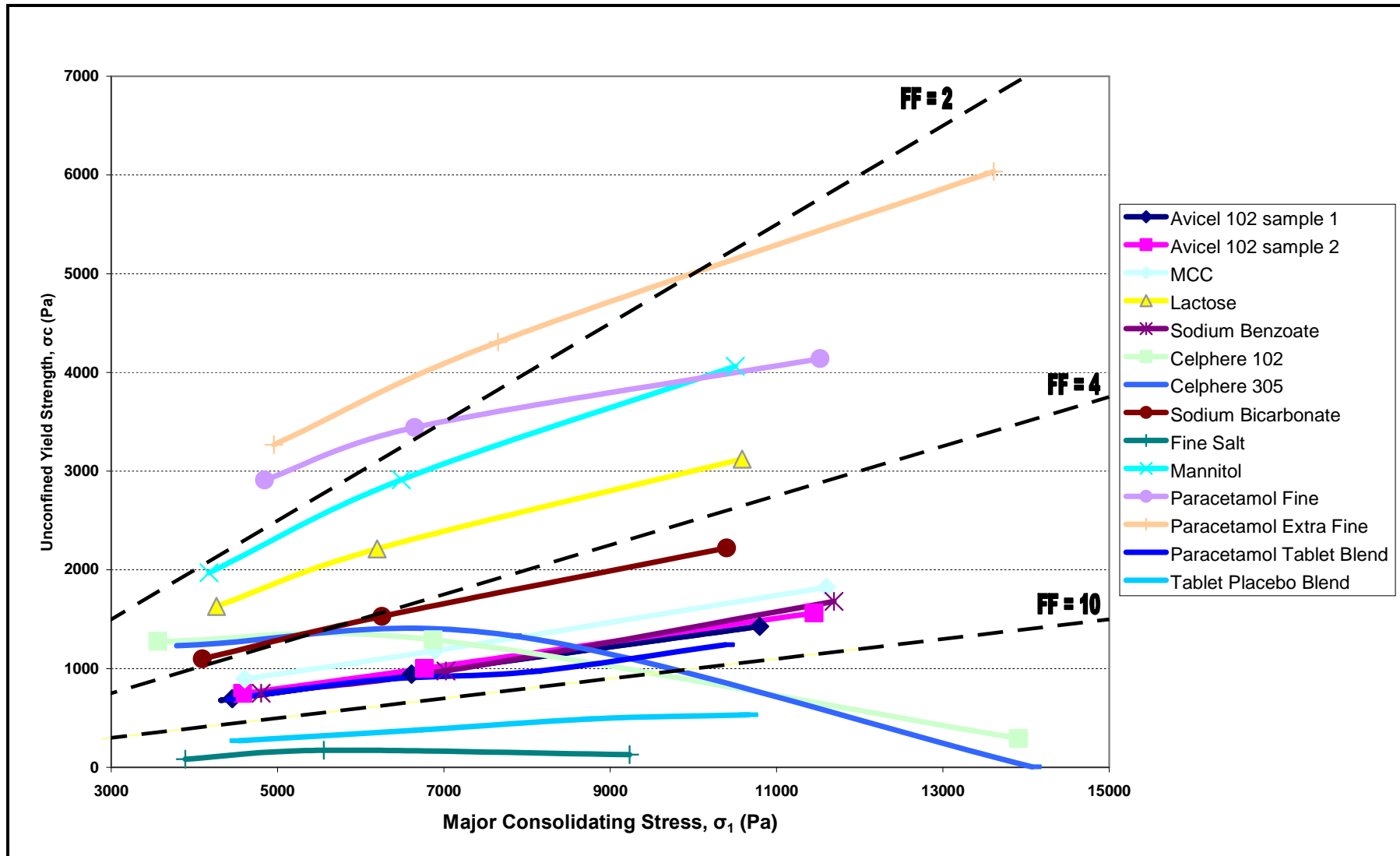


Figure 2.13: Flow Functions of exemplar powders using data from tests on the RST-XS at 8kPa consolidating stress

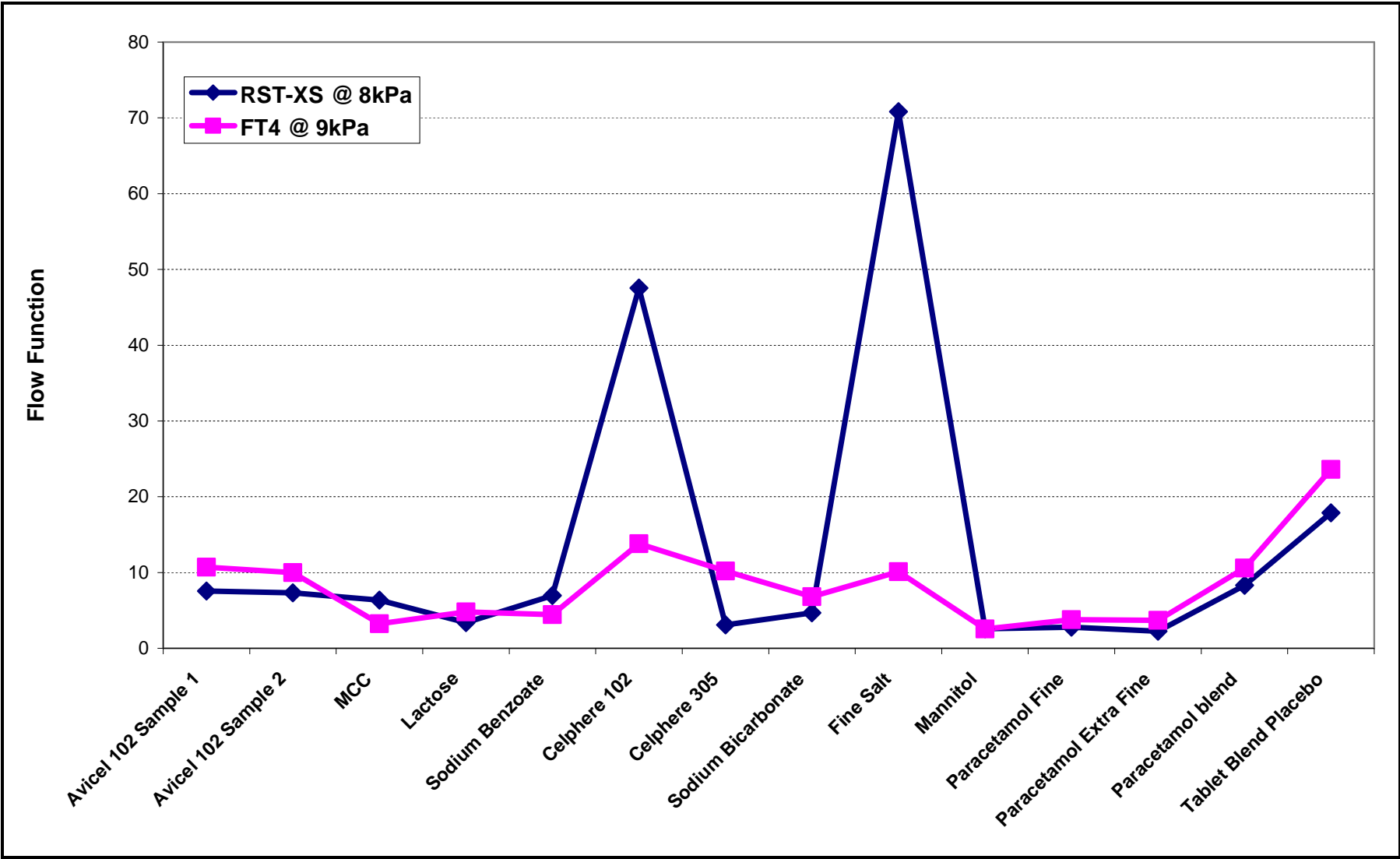


Figure 2.14: Comparison of the Flow Function values derived for the exemplar powders using data from tests on the RST-XS at 8kPa consolidating stress and the FT4 at 9kPa consolidating stress

When the data from the two shear cells are compared, a number of interesting distinctions and similarities can be seen from Table 2.9 and Figure 2.14.

It would be expected that the FT4 Flow Function data be slightly higher than that derived from the RST-XS (due to the slightly higher consolidating stress employed for each set of tests), and this is indeed the case. There two (the MCC and Sodium Benzoate) which could be related to the age of the samples at time of testing (the FT4 data was generated many months after the RST-XS data due to instrument availability). Where there is a significant variation is for the Salt and Celphere 102 tests. This is likely to be due to the RST-XS's ability to handle very free flowing materials.

Considering the Celphere 102 sample specifically; the RST-XS shows very low Flow Function values for both (which is unusual as they are both extremely free flowing) samples – except for the 8kPa test, which is very high. There could be two reasons for this apparent anomaly; firstly, experience with the FT4 shear cell suggests that free flowing materials require multiple pre-shearing to achieve steady state density. Inspecting the resultant yield loci, shown in Figure 2.15, it is clear that there is a dramatic difference between the minor Mohr's circles for the 2 & 4kPa conditions and the 8kPa condition.

Also the derivation of the Mohr's circles for the 2 & 4kPa conditions are not ideal due to the 'kinked' yield loci which are shown in more detail in Figure 2.16.

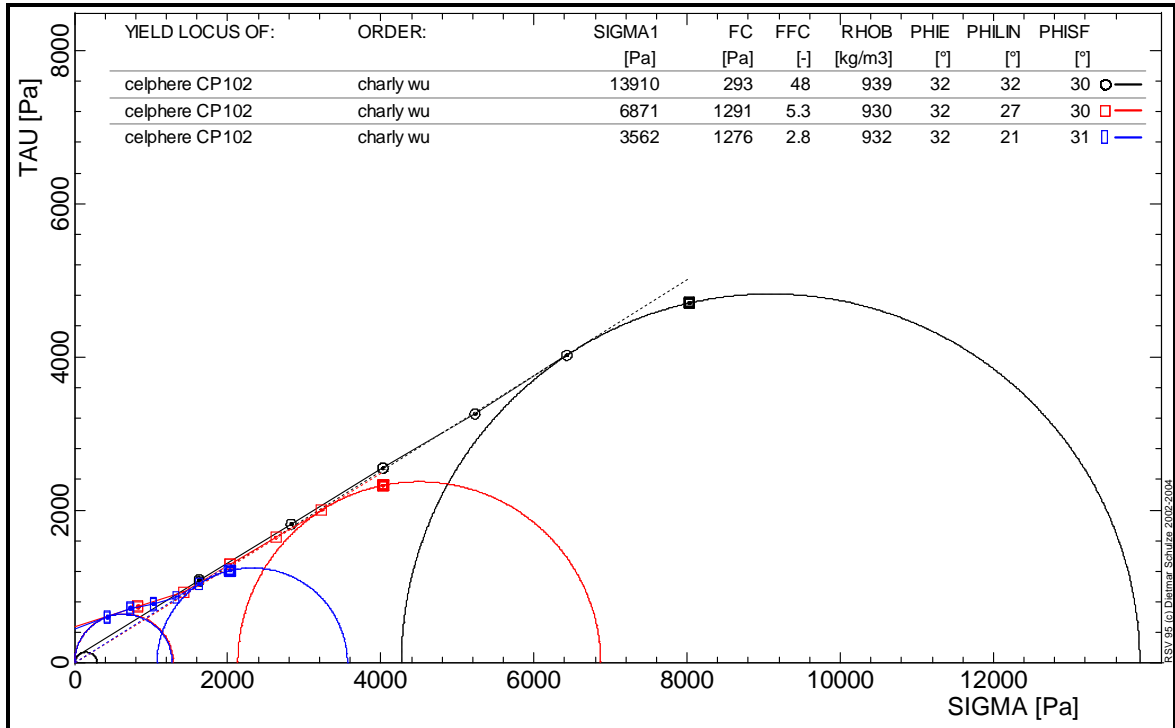


Figure 2.15: Yield loci for Celphere 102 generated using the RST-XS shear cell at 2, 4 & 8kPa consolidating loads

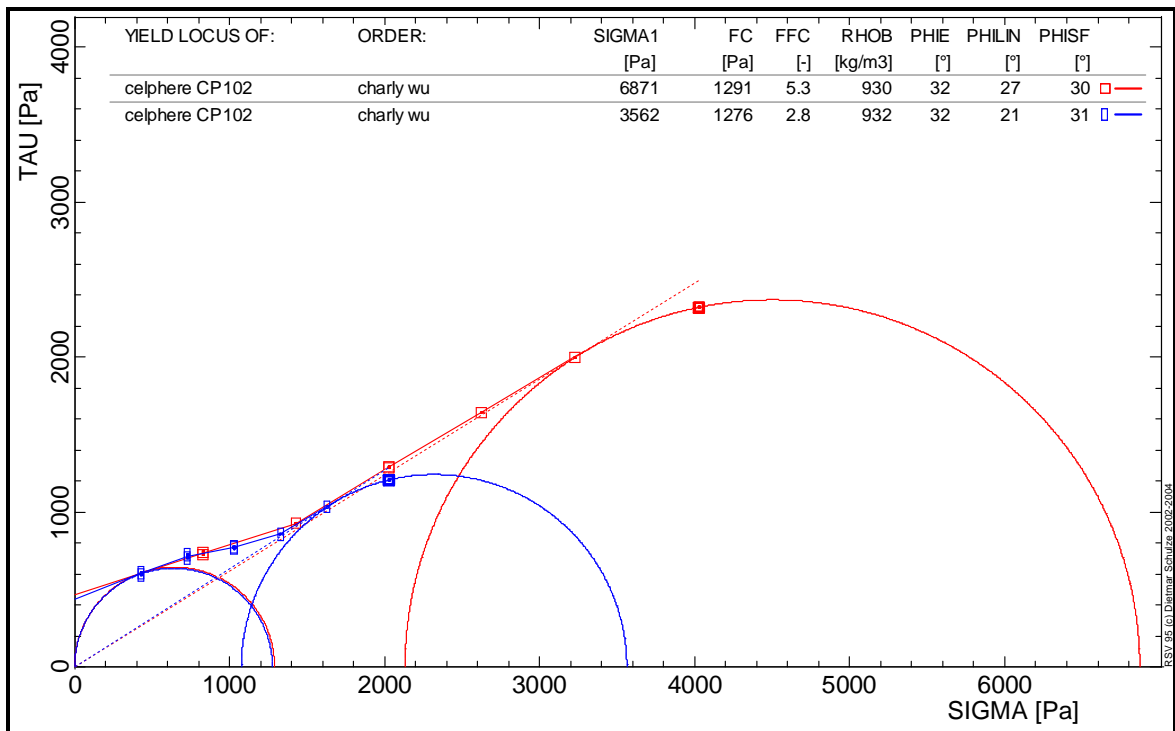


Figure 2.16: Yield loci for Celphere 102 generated using the RST-XS shear cell at 2 & 4kPa consolidating loads

In this case it appears that the analysis program simply joins the data points and fits the Mohr's circles to the resultant trace and extrapolates the trace to the y-axis. Figure 2.9 also shows this treatment of the data points. This is not a usual way of evaluating the data and would generally be described as incorrect. In this case it results in much larger cohesion values and much larger minor Mohr's circles – resulting in very low f_c values indicative of a very cohesive material, which this is clearly not.

The main cause for the kinked yield locus is likely to be dilation during shearing which would result in a commensurate increase in the shear stress and normal stress. This is most likely at lower normal stress tests within the derivation of the locus as shown in Figures 2.9, 2.15-2.18. However, if it is assumed that the target force is the actual force applied at shear, then plotting the measured shear stress at this target normal stress results in a kink such as the one shown in Figures 2.15 and 2.16. If the data points at the lower normal stresses were plotted at the (higher) actual normal stress, they would be shifted to the right on the plot and the resultant locus would be significantly smoother.

This effect can also be seen in the yield loci derived from testing the larger Celphere 305 shown in Figures 2.17 and 2.18 as well as the Flow Function plotted in Figure 2.19.

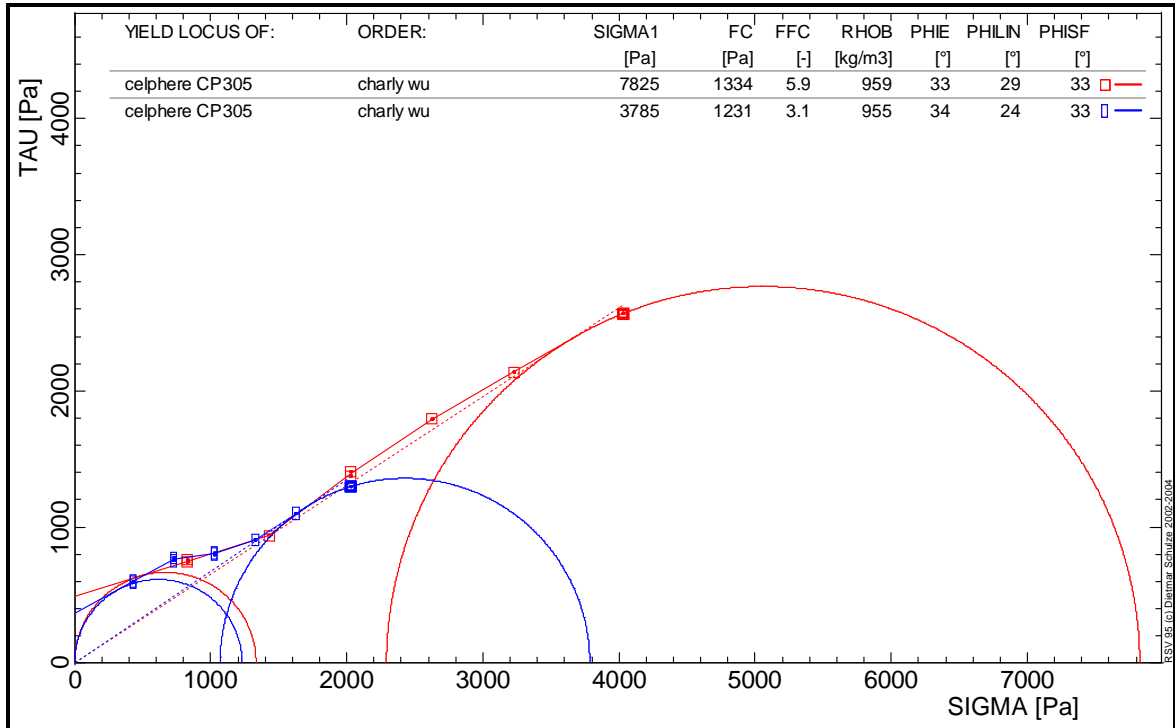


Figure 2.17: Yield loci for Celphere 305 generated using the RST-XS shear cell at 2 & 4kPa consolidating loads

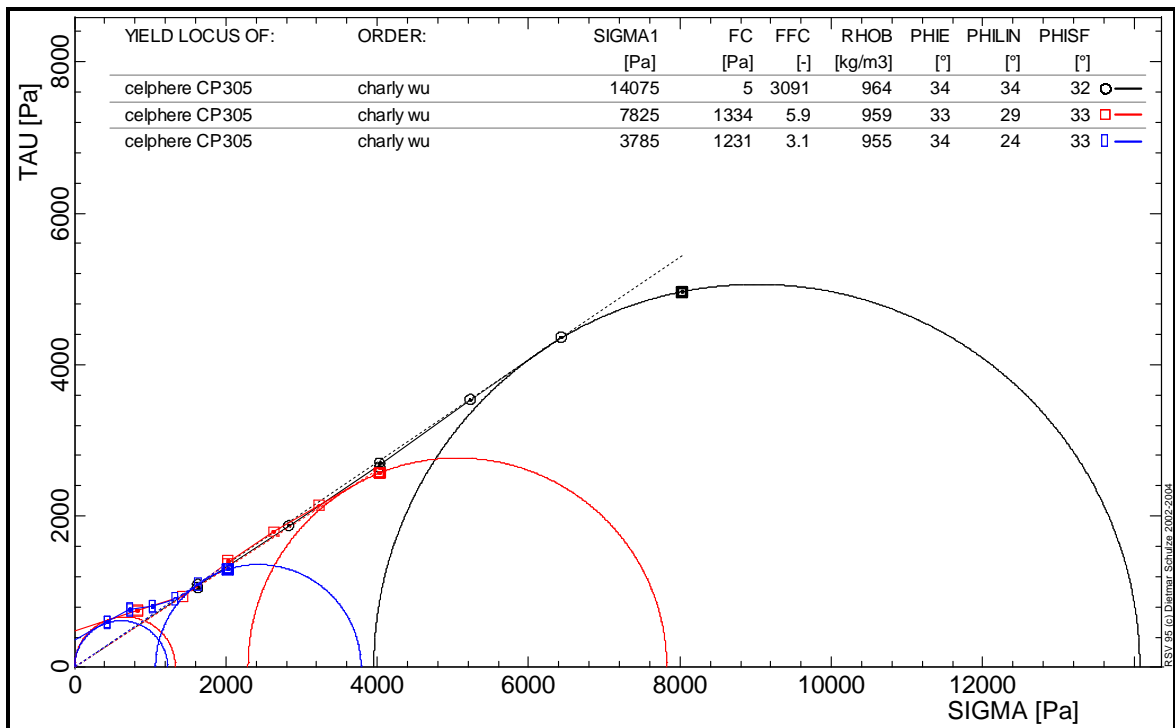


Figure 2.18: Yield loci for Celphere 305 generated using the RST-XS shear cell at 2, 4 & 8kPa consolidating loads

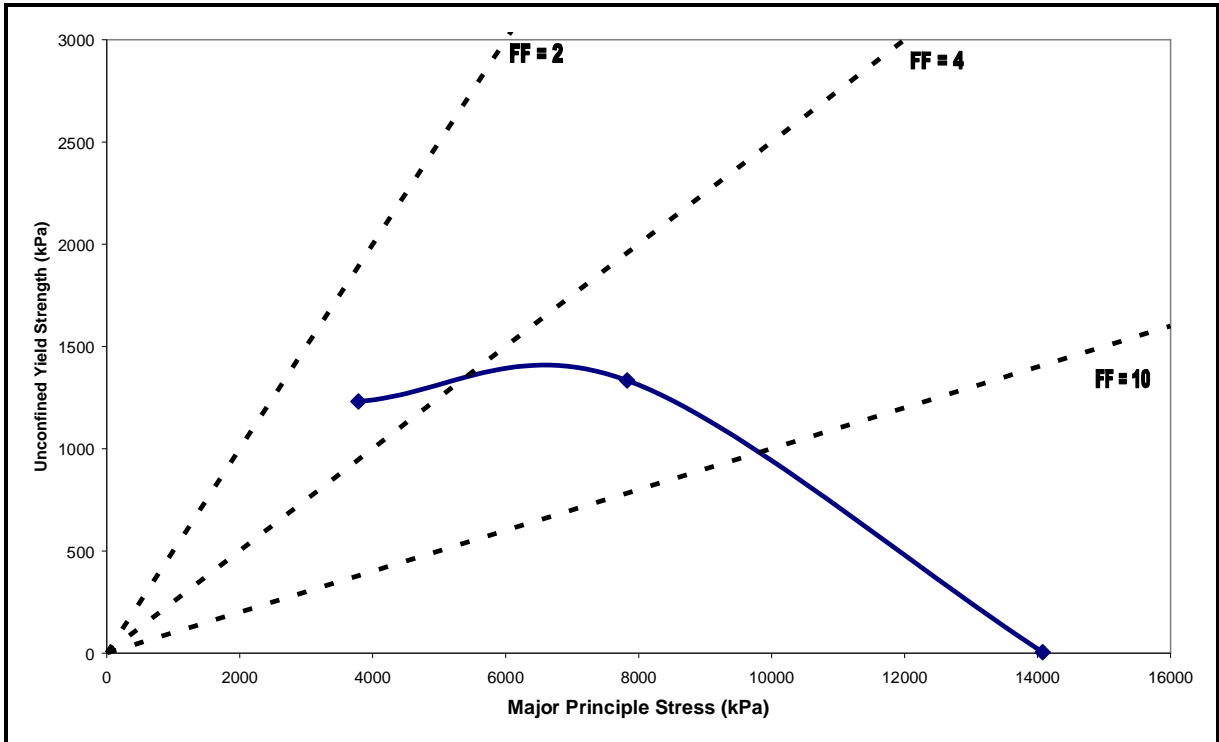


Figure 2.19: Flow Function for Celphere 305 generated using the RST-XS shear cell at 2, 4 & 8kPa consolidating loads

The Flow Function of the Celphere 305, shown in Figure 2.19, goes from 3 (quite cohesive) to 6 (quite free flowing) to 3100 (well beyond the value of 10 designating very free flowing). Clearly there are some issues with the testing as well as with the manipulation of the resultant data.

As can be seen from Figures 2.20 and 2.21 this kinking of the yield locus and the apparent 'connecting the dots' approach to defining the yield locus is not restricted to non-cohesive samples when tested at 2kPa.

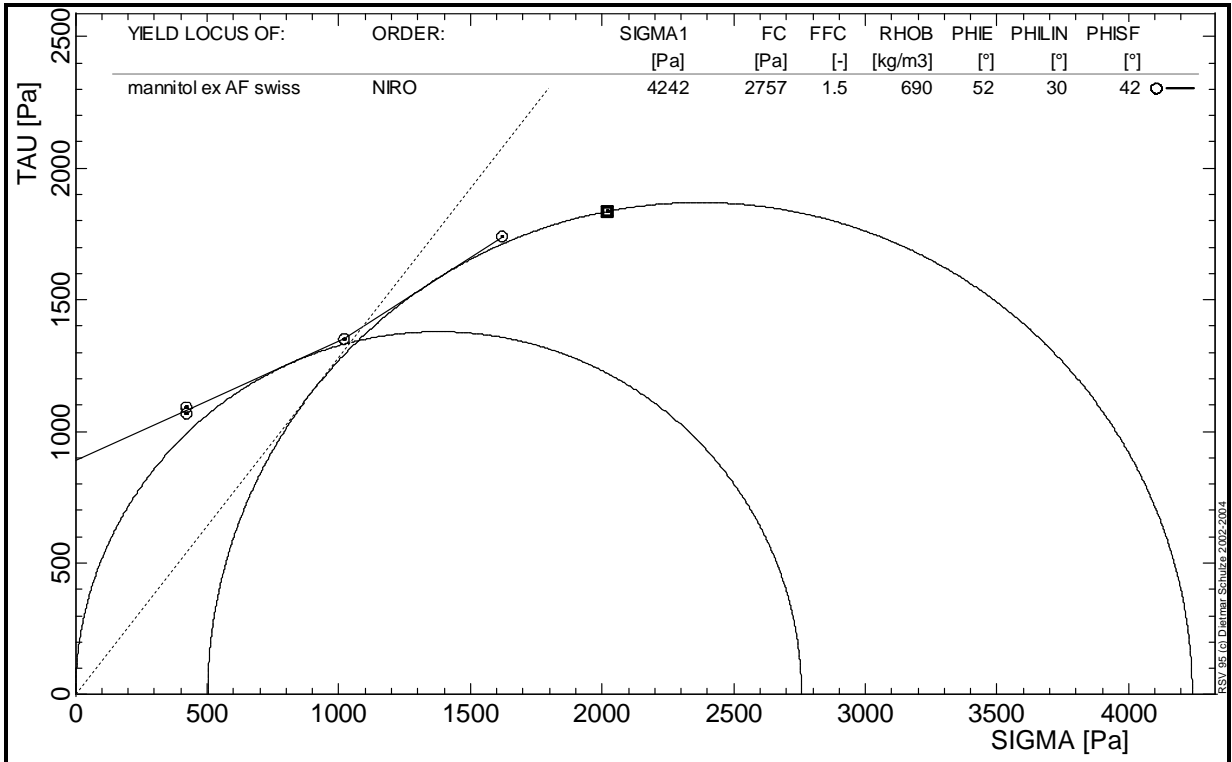


Figure 2.20: Yield loci for Mannitol generated using the RST-XS shear cell at 2kPa consolidating load

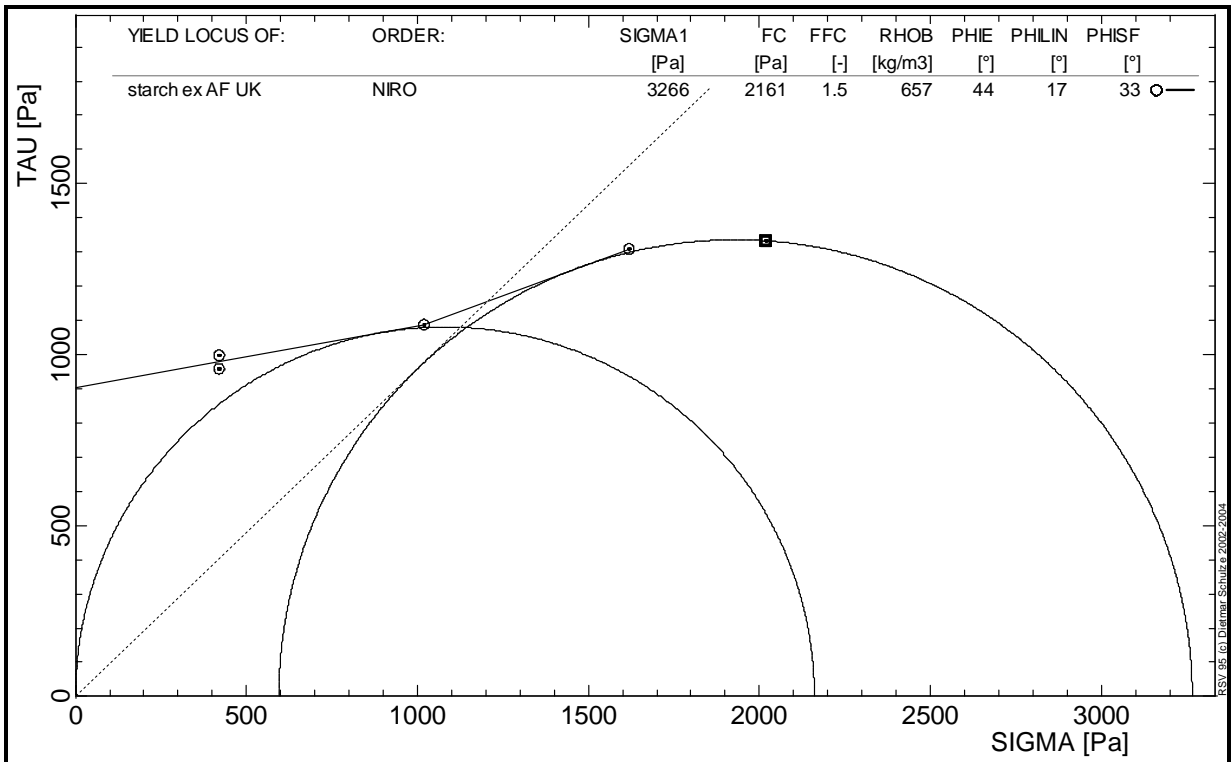


Figure 2.21: Yield loci for Starch generated using the RST-XS shear cell at 2kPa consolidating load

Schulze advocates the use of the linear over the Warren Springs fits to the data in order to describe the yield locus (Schulze 2007;Schweddes & Schulze 1990c), and it is not known why either one of these curve fitting methods is not used within this version of the data analysis program for the RST-XS instrument.

Unfortunately there is no way to inspect the raw data within the RST-XS suite of programs to fully understand what the relationships between force and torque are during the testing. Such an evaluation would be extremely useful as the RST-XS does appear to have issues with tests at lower consolidating stresses for many of the powders tested in this study.

Similar tests using the FT4 shear cell allow much closer inspection of the data and even the opportunity to remove rogue data points – a practice advocated by Jenike (Jenike 1964).

The data for the more cohesive powders – Mannitol, Paracetamol Fine/Extra Fine, Lactose – are broadly in agreement between the two cells (given the slight difference in the consolidation stress). This in itself is an interesting result as it tends to indicate that these two different configurations of shear cell will give similar results with more cohesive powders, helping to confirm that a true state property of the material is being measured.

The differences in test results between the two instruments occur when less compressible (usually freer flowing) powders are evaluated, and the ability of the FT4 to cope with the data derived from testing these materials in a more robust fashion would tend to suggest it could be actively considered by GEA as a suitable the shear tester.

In addition to the instrument variation mentioned above, there are a number of issues with the shear cell technique that should be considered when collecting the data and interpreting the mathematical treatment of the data that are common to all testers.

2.3.1.3. Sensitivity of the derived data to deviations in shear behaviour

It is often the case, especially with the shear testing of freer flowing powders, very slight differences in the yield locus can have a dramatic effect on the derived data. This issue is not usually reported due to the previously discussed historic reluctance to undertake repeat testing. It is, however, germane to the use of shear data when characterising powders that give different process outcomes. Any given powder tester will be used to test all the powders that the particular user has a requirement to process and for the pharmaceutical industry this will include a significant proportion of non-cohesive, freer flowing materials. If the repeatability of the derived shear functions means that multiple data sets for a single powder show significant variability (despite good repeatability in the actual shear test points) then the derived functions cannot be realistically used to characterise such powders and the shear test has a more limited usefulness.

This effect is clearly shown for a non-cohesive sample. Three repeat tests for the Tablet Blend Placebo sample are shown in Figure 2.22.

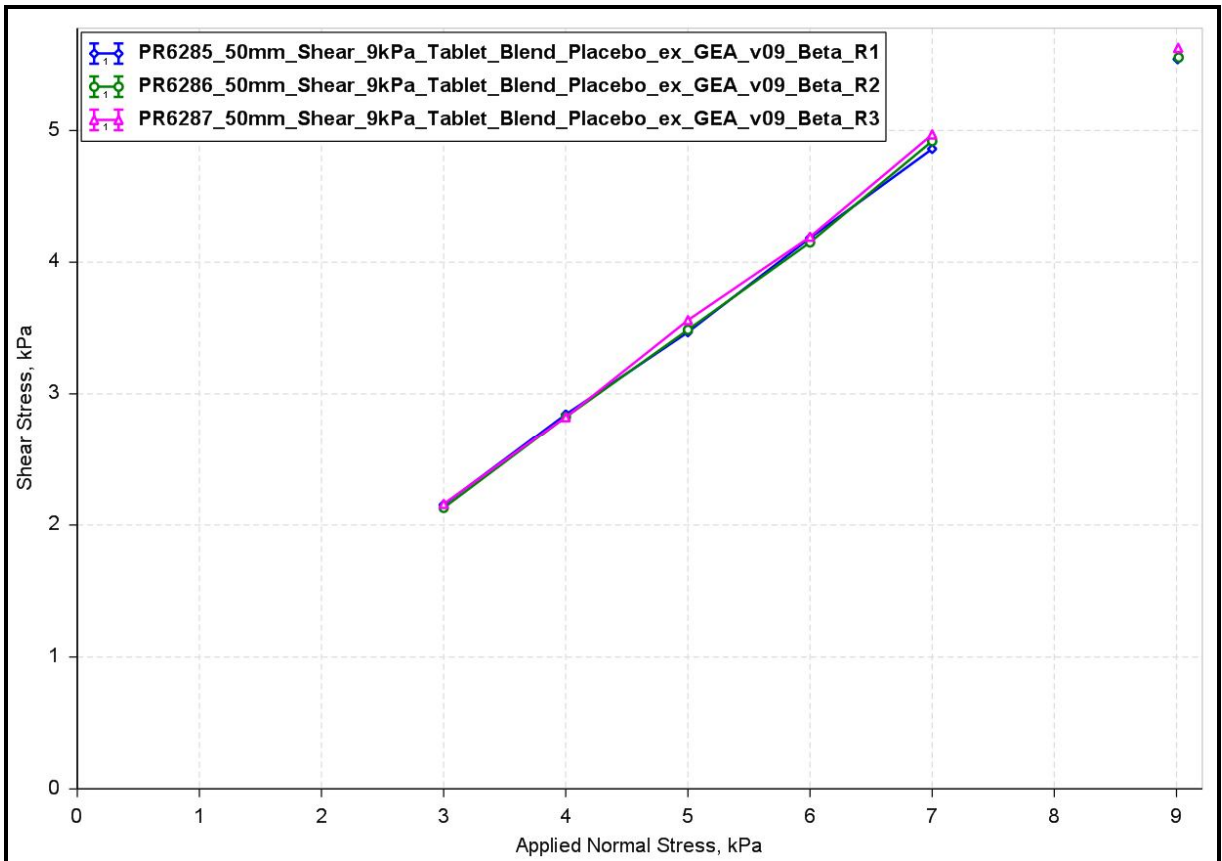


Figure 2.22: Three repeat shear tests at 9kPa consolidating load for Tablet Blend Placebo generated using an FT4 shear cell attachment

The repeatability is excellent and Figure 2.23 shows the three data sets averaged which produces a maximum data point variability of 1.4%.

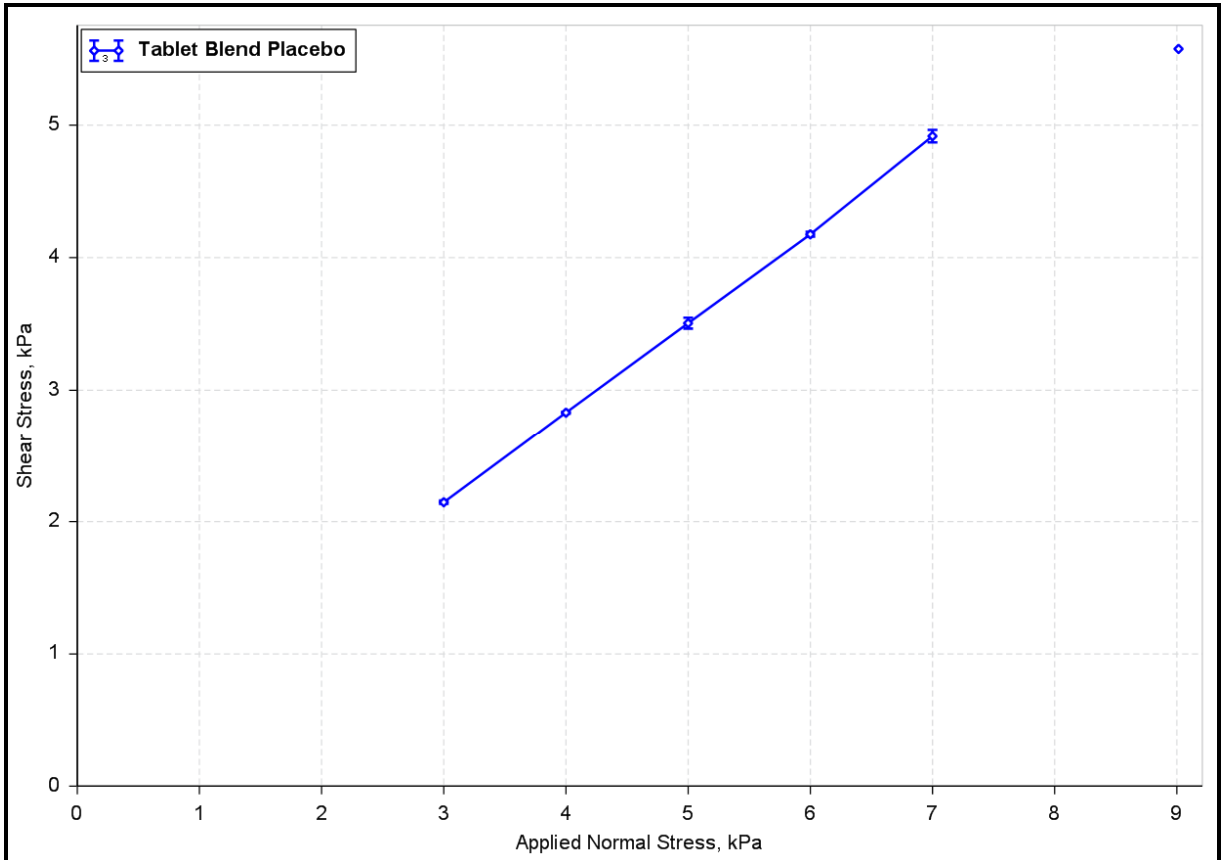


Figure 2.23: Average of three repeat tests at 9kPa consolidating load for Tablet Blend Placebo generated using an FT4 shear cell attachment

When the Mohr's circles are fitted, as shown in Figure 2.24, there is a significant difference between two of the minor Mohr's circles and the third – which is much smaller. This makes the flow function values, indicated in the table within the graph, differ by over 50.

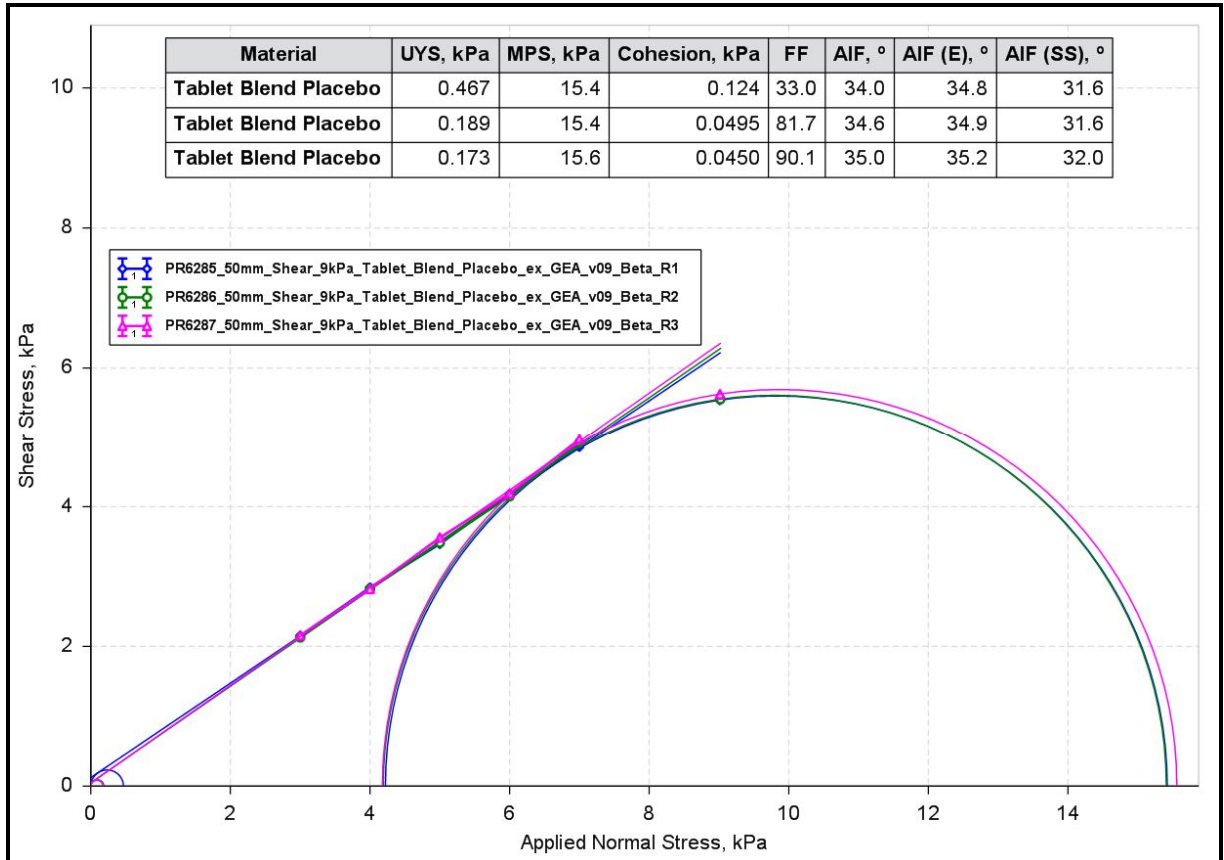


Figure 2.24: Three repeat tests at 9kPa consolidating load for Tablet Blend Placebo showing Mohr's circles fitted to the linear fit yield loci generated using an FT4 shear cell attachment.

In addition, when the three data sets are averaged and the derived parameters calculated from the single yield locus fitted to the averaged data points, shown in Figure 2.25, there is a significant drop in the flow function by around 24 from the largest value from the individual loci.

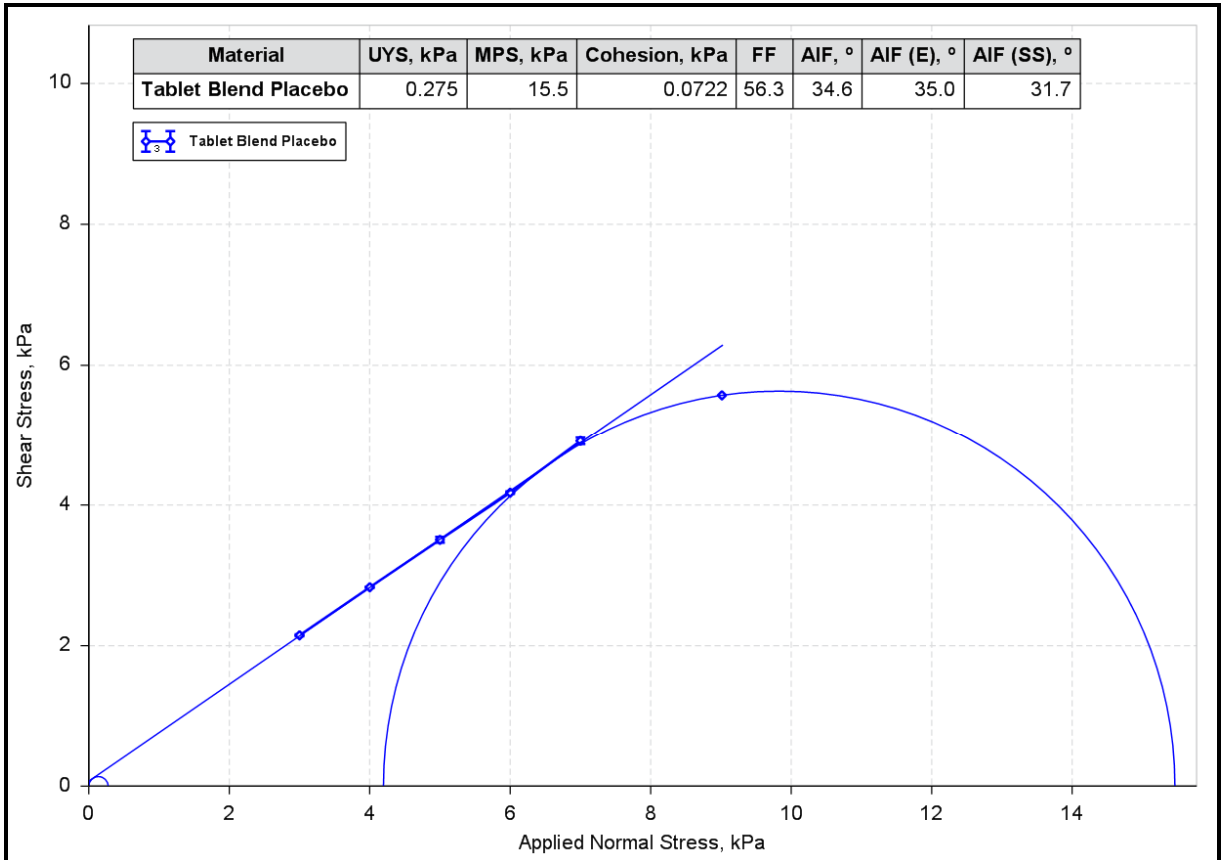


Figure 2.25: Average of three repeat tests at 9kPa consolidating load for Tablet Blend Placebo showing Mohr's circles fitted to the linear fit yield loci generated using an FT4 shear cell attachment.

This poses a number of questions about the way multiple data sets are handled.

The main question is when should any averaging take place? Should a single yield locus be drawn through the data sets? Or should the multiple yield loci be drawn and the derived parameters for each yield locus then averaged? Table 2.10 below shows the variation produced when these options are adopted for the Tablet Blend Placebo example.

Table 2.10: Variation in derived parameters based on different averaging methodologies for Tablet Blend Placebo

Derived parameter	Average from three yield loci	Values from single yield locus derived from averaged data points
UYS	0.28	0.65
MPS	15.5	15.5
C	0.07	0.17
ff_c	68.1	23.6
AIF	34.5	33.9
AIF(E)	35.0	34.9
AIF(SS)	31.7	31.7

The major principal stress for both methods is virtually identical, which in turn means the AIF(E) & AIF(SS) values – which are derived from the MPS – are also very similar. However, it is the values derived from the minor Mohr's circle that show the greatest discontinuity. When the extrapolated (linear) yield locus is close to zero shear stress, any slight variation in plotting the linear regression derived yield locus, due to very minor shifts in the data points, can result in a large variation in the cohesion (C) value and hence the UYS. In the example shown in Figure 2.24 and its embedded table, the difference in the linear extrapolations result in a difference of 0.1kPa in the cohesion value which may not be regarded as large, but represents an almost threefold uplift from the lowest value, which is mirrored in the difference in the UYS values. The resultant ff_c values are consequently equally disparate.

Thus the data handling clearly has a significant influence on the derived results for this type of non-cohesive powder. It could be argued that this is an irrelevance due

to the very low values that are being generated, but that is not the issue if the data is required to compare two very similar materials that process differently. If the 'noise' generated by the variability derived purely from the way the data is processed by 'standard' methods causes significant overlap between the data from the two samples, then shear cells cannot be relied upon to provide any insight into the process problem – they will simply indicate that the two powders are identical and cannot be differentiated.

If this analysis is applied to a more cohesive powder, this effect is virtually eliminated. Four repeat shear tests of Limestone at 9kPa consolidating stress are shown in Figure 2.26 and the averaged data shown in Figure 2.27. Comparing these data to those presented for Tablet Blend Placebo in Figure 2.23, it is noticeable that there is a greater spread of the yield loci for the Limestone. However, the derived parameters do not show the variability for the Limestone that they do for the Tablet Blend Placebo example.

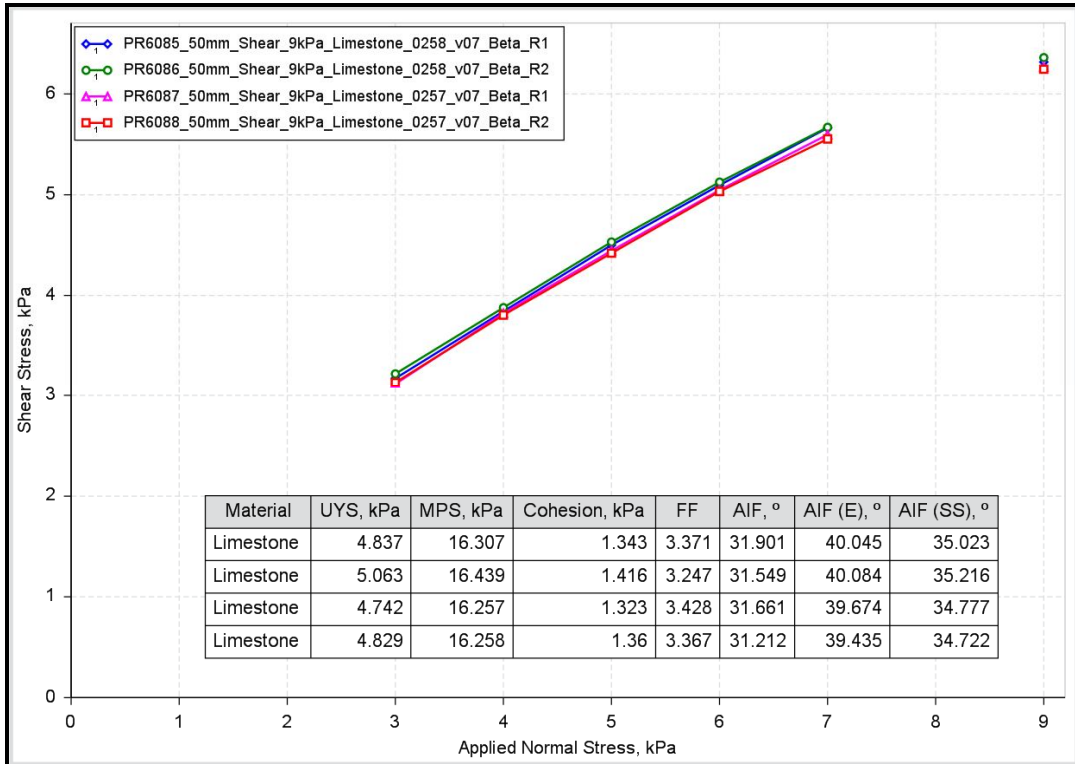


Figure 2.26: Four repeat shear tests at 9kPa consolidating load for Limestone generated using an FT4 shear cell attachment.

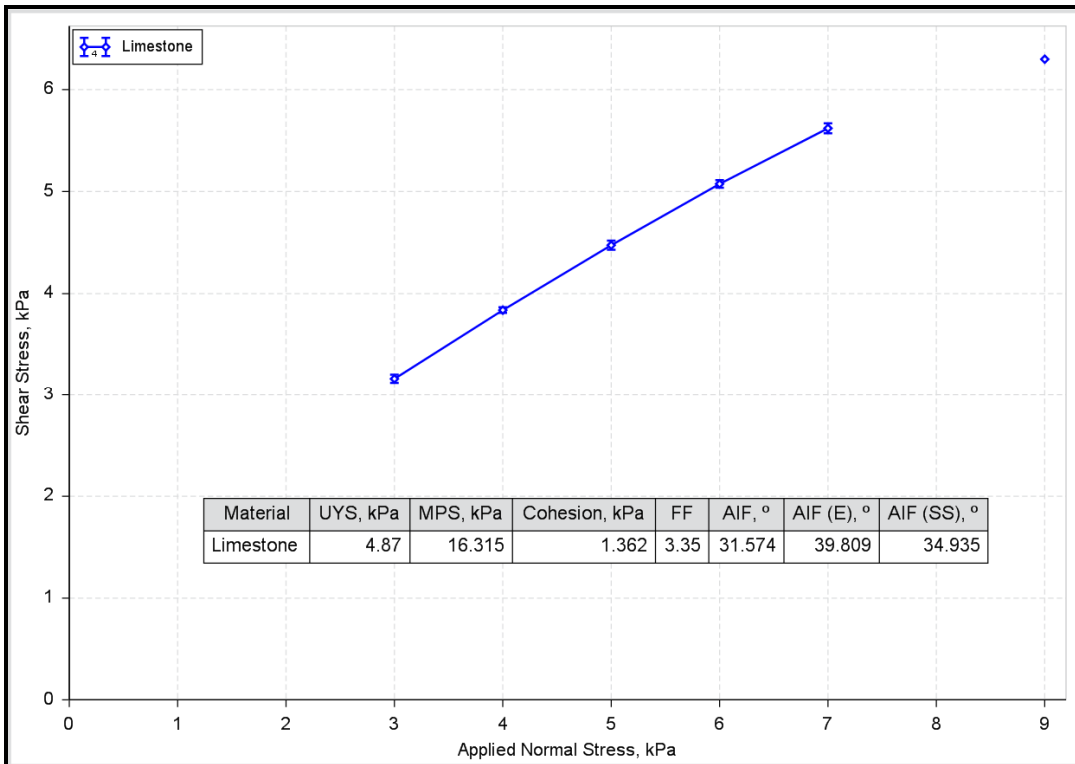


Figure 2.27: Average of 4 repeat tests at 9kPa consolidating load for Limestone generated using an FT4 shear cell attachment

Table 2.11: Variation in derived parameters based on different averaging methodologies for Limestone

Derived parameter	Average from four yield loci	Values from single yield locus derived from averaged data points
UYS	4.87	4.73
MPS	16.32	16.30
C	1.36	1.32
ff_c	3.35	3.45
AIF	31.6	31.9
AIF (E)	39.8	39.8
AIF(SS)	34.9	34.9

There is a 3% variation in the C and ff_c values for these tests which is substantially better than the variation obtained for the evaluation of the Tablet Blend Placebo.

This analysis again shows up some of the practical limitations of shear testing of free flowing materials and attempting to apply theoretical arguments to the data based on a continuum model which should not be applied to such granular materials.

An experienced user may suggest that these differences are trivial – which in term of bin design it could be argued that they are – but in order to actively use a specific test to investigate the influence of powder properties on the performance of the range of process equipment that GEA manufacture, good repeatability in the data and any values derived from it is a necessity. Here the limitations of the shear cell method mean that the variance generated in the derived values (from ostensibly identical

data sets) limits its potential application for a large number of powders used in pharmaceutical manufacture which are freer flowing materials.

2.3.1.4. The effect of multiple pre-shearing on development of critical consolidation

The development of a shear plane within any automated shear tester requires the pre-shearing of the powder to achieve critical consolidation – that state where the shear plane has reached a steady state such that any stresses incurred during the filling process have been normalised and any anisotropy has been minimised (Schulze 2007). What is less often recognised is that for less compressible, less cohesive powders the most practical option is often to undertake multiple pre-shears to achieve critical consolidation. This allows the particles to adjust their relative positions and achieve a critical consolidation level which would not necessarily be the case with a single pre-shear. Figure 2.28 shows the different approaches required for cohesive powders, in this case Limestone, and less compressible powders, in this case a microcrystalline cellulose – Avicel PH200.

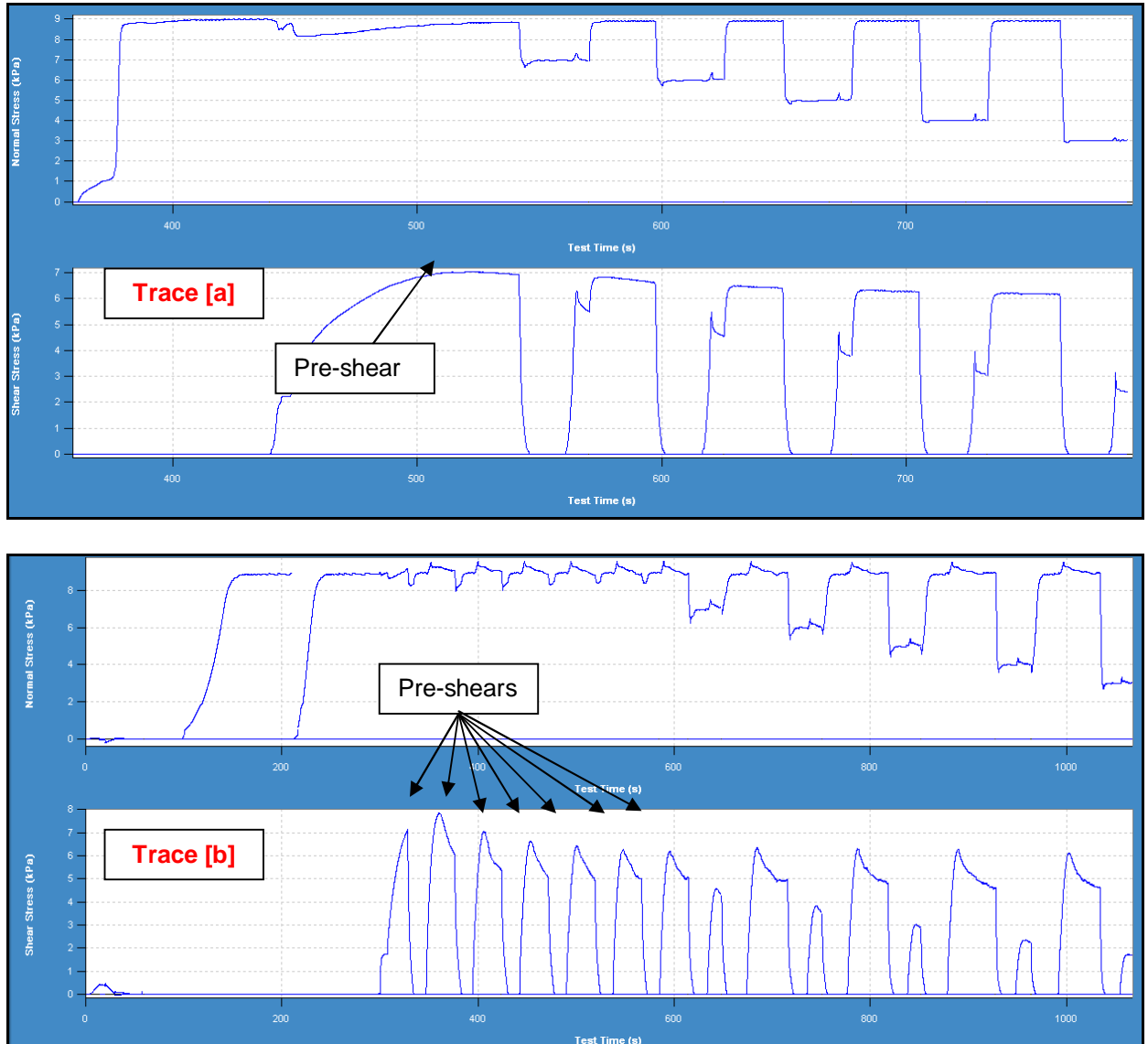


Figure 2.28: Screenshot of normal stress and shear stress traces from shear cell tests of Limestone (trace [a]) and micro-crystalline cellulose (Avicel PH200) (trace [b]) @ 9kPa consolidating stress generated using an FT4 shear cell attachment in which single and multiple pre-shears are required to achieve critical consolidation respectively

The less compressible powder reacts significantly differently to the pre-shearing and only when at least four pre-shears have been completed can a steady state be observed. The subsequent intermediate pre-shears (those undertaken between test points to regain the steady state condition) are at the same level as the last two/three initial pre-shears showing that the powder has indeed reached steady state flow. If

only a single pre-shear had been used, then the subsequent pro-rating (as defined in Appendix 1) would have significantly altered the yield locus calculation.

If we now consider the influence of pre-shearing on the yield locus of Celphere 305, Figures 2.29 and 2.30 show the effect of multiple pre-shearing steps.

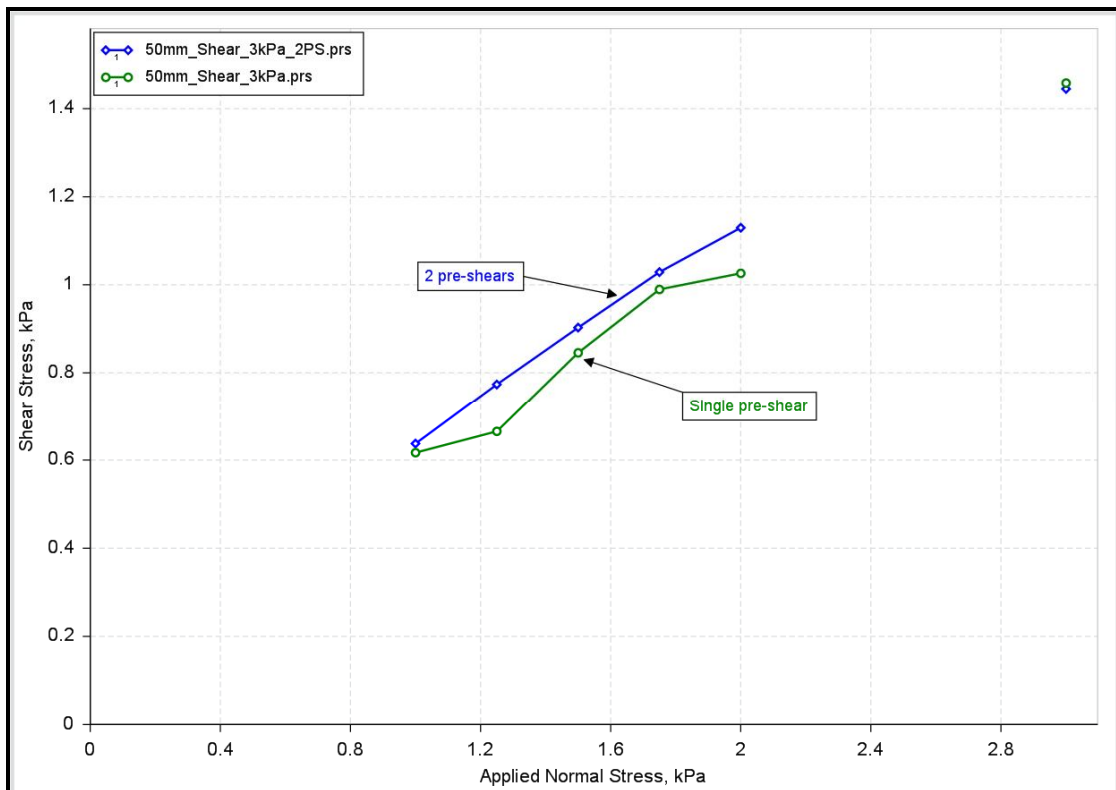


Figure 2.29: Yield loci of Celphere 305 at a consolidating load of 3kPa showing the effect of single and two pre-shears generated using an FT4 shear cell attachment.

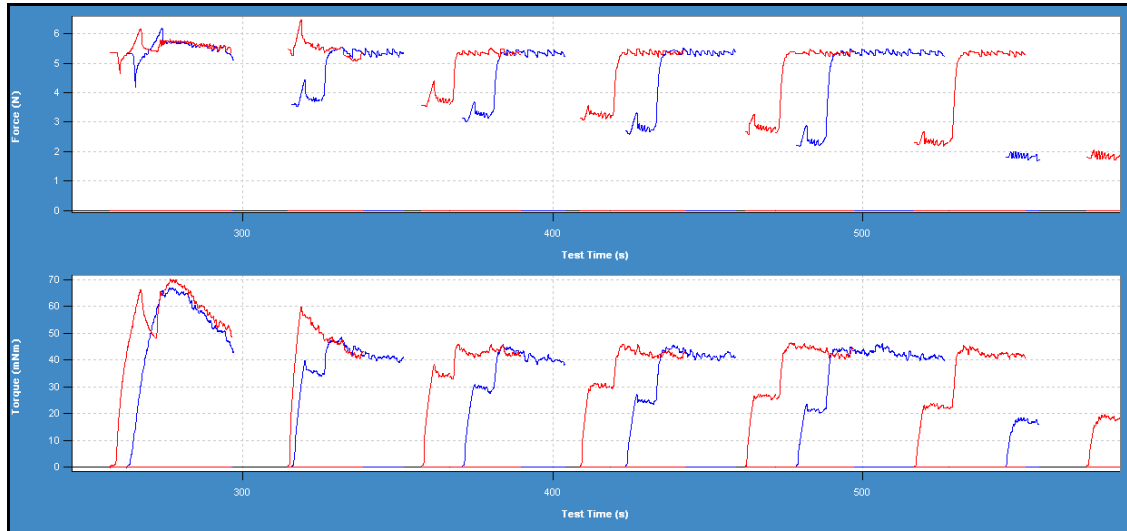


Figure 2.30: Raw data of Celphere 305 at a consolidating load of 3kPa showing the effect of single and two pre-shears, generated using an FT4 shear cell attachment.

As can be seen, the additional pre-shear has the effect of smoothing the yield locus as the material has reached a critical consolidation after two pre-shears, as evidenced by the steady height of the (red) torque trace. The single pre-shear test has a similar low stress kink in the data to that seen when testing this material with the RST-XS and is shown in Figure 2.18.

2.3.1.5. Summary of shear cell evaluation

- Current computer controlled shear cells can generate test data much quicker than was possible 10-15 years ago which provides the user with the ability to generate multiple repeat data sets and a measure of the repeatability of the data and the stability of the sample. It is therefore recommended that shear testing be one of the techniques employed by GEA for powder analysis.

- Pre-shearing protocols can significantly affect the achievement of critical consolidation and the resultant yield locus, especially for non-cohesive powders.
- The testing of freer flowing powders has shown that multiple data sets may generate significant variability in derived data (Flow Function; Cohesion) that are commonly used to characterise materials despite excellent repeatability in the yield loci.
 - There is an argument that the variability in such values is inconsequential as they are (for the Cohesion) close to zero.
 - However if the shear cell is to be used to characterise the process behaviour of all samples likely to be used by GEA (a large proportion of which will be free flowing) then such variability limits the effectiveness of shear testing.
 - This analysis illustrates the limitations of applying the continuum mechanics derived approach to developing a yield locus when testing more non-cohesive, granular materials.
- There are issues with the RST-XS treatment of yield locus at low consolidating/testing stresses with non-cohesive powders which need to be resolved before recommendation of this instrument.
- The results generated from testing the more cohesive of the exemplar powders show good agreement between the two different shear cells, reinforcing the concept that shear cells can provide true state properties of powders (within the limits mentioned above)

2.3.2. Angle of repose

One of the simplest tests that can be undertaken is the measurement of the powders' (poured) angle of repose (AOR).

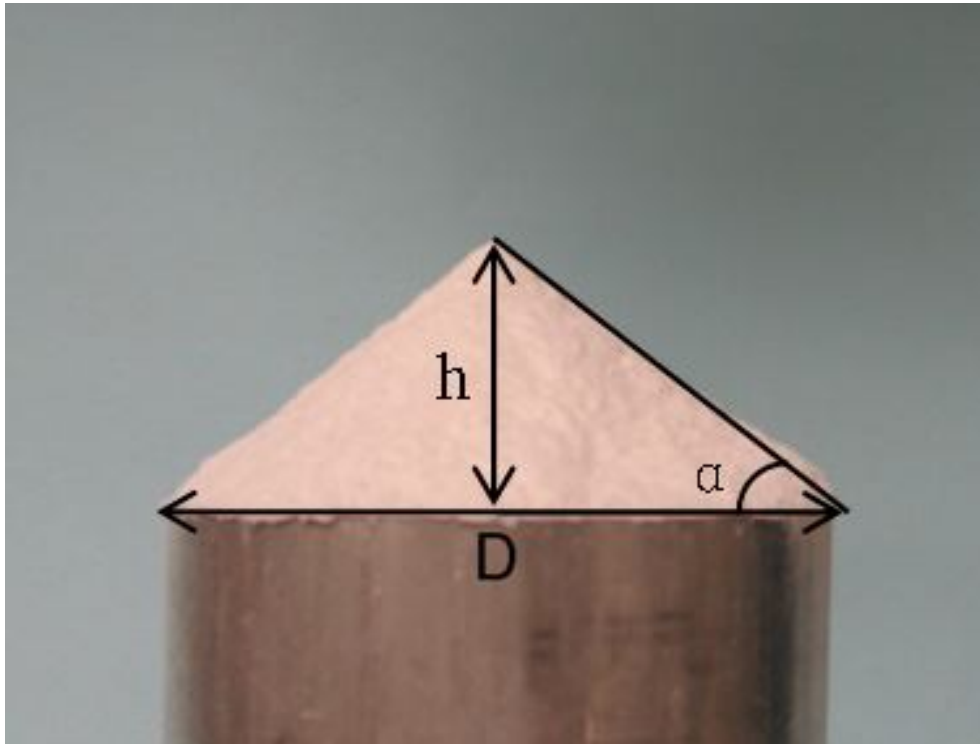


Figure 2.31: The definition of (poured) angle of repose
(photo courtesy of Qi Zhou, Monash University)

As can be seen from Figure 2.31 the angle (α) is simply defined by the height (h) that a powder will reach when poured from a (specified) height onto a surface.

However, there are no current standard methods of determination of the angle of repose. An ASTM Standard has been available, but has been discontinued (ASTM 2005) and AOR is mentioned in USP1174 (United States Pharmacopeia 2007). This is probably due to large variety of angles of repose that can be 'defined', as shown in

Figure 2.32, and the difficulty in generating a standard method suitable for all powders, as will be demonstrated.

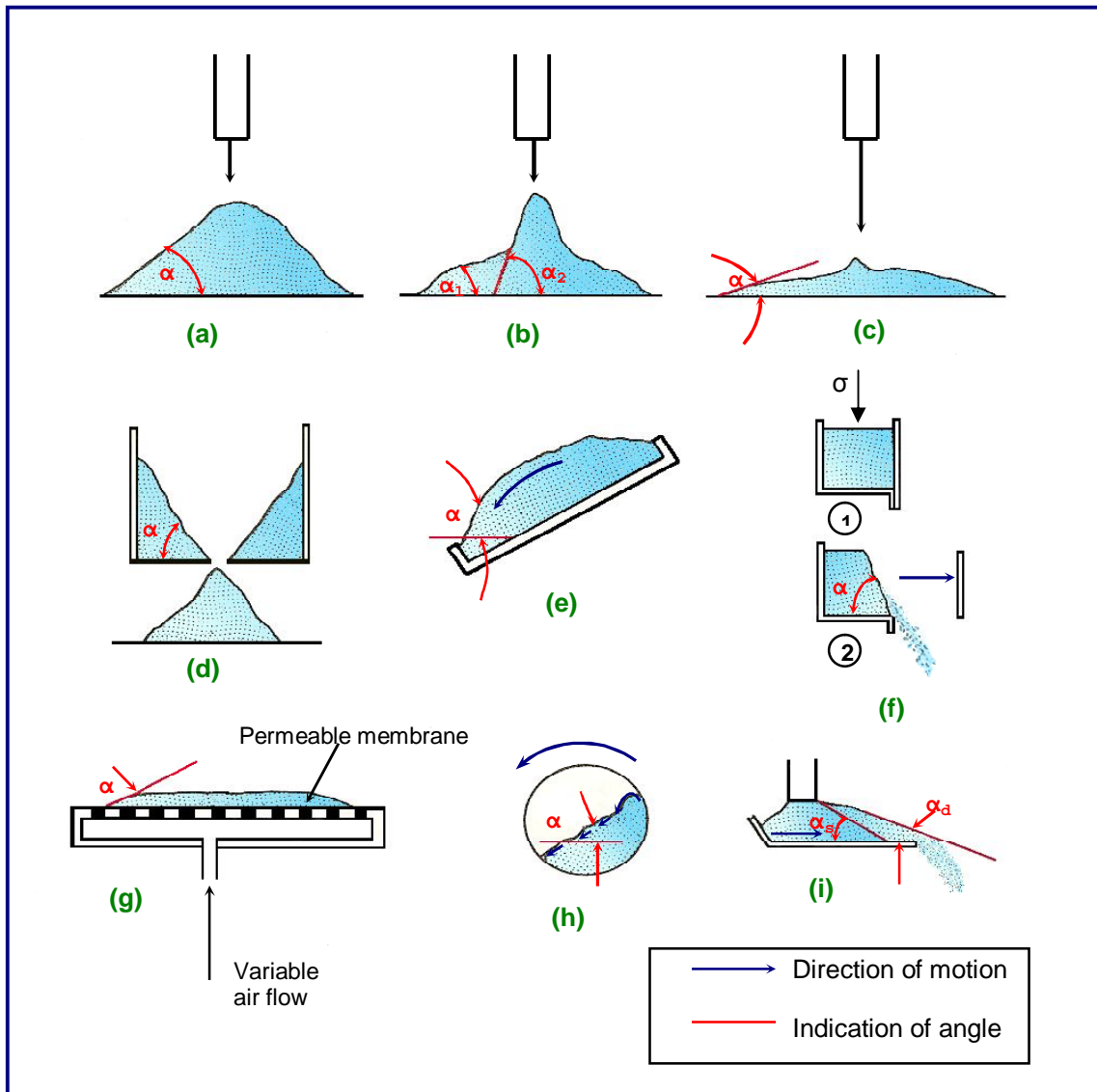


Figure 2.32: Various determinations of the Angle of Repose; (a) the poured angle of repose; (b) the impacted, wet or cohesive materials where multiple angles of repose [α_1 and α_2 for example] are observed; (c) easily aerated materials; (d) drained; (e) sliding; (f) compacted [σ is an applied consolidating stress]; (g) aerated; (h) rolling; (i) feeder discharge [α_s is the static angle of repose – feeder stationary; α_d is the dynamic angle of repose – feeder operational]

Source: Modified from Fayed and Otten (eds).

Several commercial testers are available and employ a poured measure of the AOR such as that employed in the Hosokawa tester (which utilises all of Carr's measurement techniques) and the device developed by Geldart and shown below in Figure 2.33.



Figure 2.33: Geldart AOR tester (left) and Hosokawa Powder Tester – including an AOR test (right).

Many academics still utilise this test for evaluating powder flow and flowability (Geldart *et al.* 2006; Geldart, Abdullah, & Verlinden 2009; Kalson & Resnick 1985; Liu, Specht, & Mellmann 2005; Thalberg, Lindholm, & Axelsson 2004; Zhou *et al.* 2002) and it is still used extensively in industry, primarily due to its simple test methodology and rapidity of the evaluation, coupled with the fact that an angle of repose tester can be constructed very easily.

However, the usefulness of this measurement is limited and this is reflected in Jenike's view of the angle of repose:

"... In fact, it (the angle of repose) is only useful in the determination of the contour of a pile, and its popularity among engineers and investigators is due not to its usefulness but to the ease with which it is measured." (Jenike 1964)

This can be demonstrated by reviewing angles of repose of a range of pharmaceutical excipients as shown in Figure 2.34.

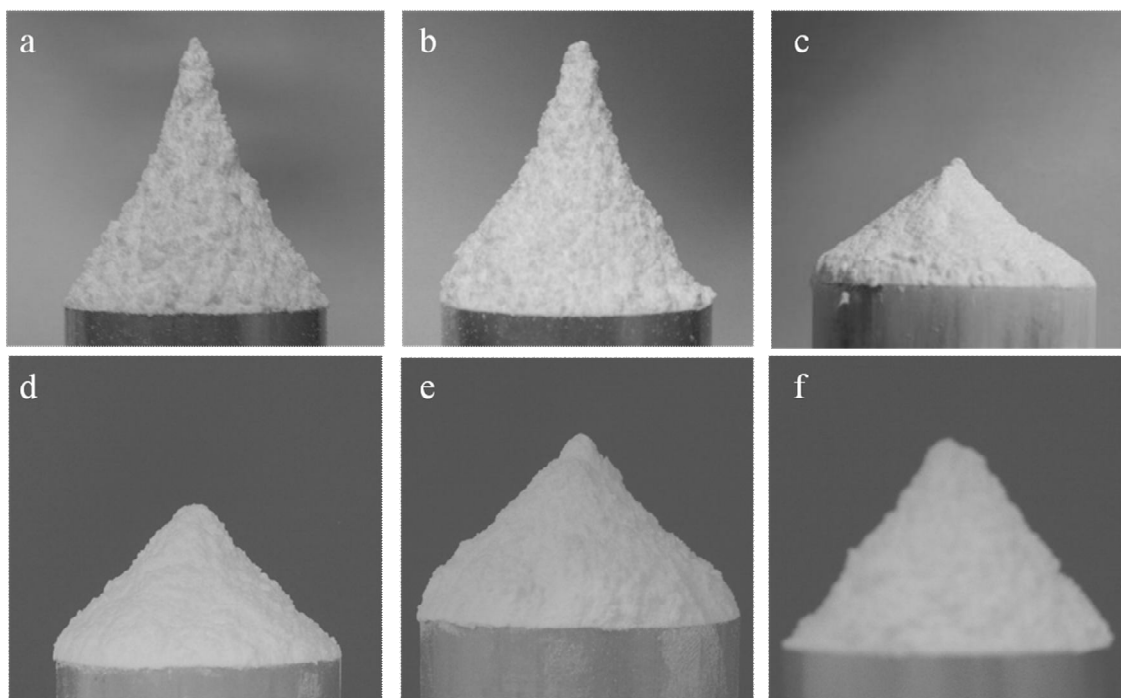


Figure 2.34: Angles of repose of a range of pharmaceutical excipients
(photo courtesy of Qi Zhou, Monash University)

Considering the photographs shown in Figure 2.34, there are several difficulties in precisely quantifying the angle of repose. Powder (a) has a curved face on both the right and left hand sides of the pile; powder (b) is similar but has some steps on the right hand side; powder (c) has very different left and right hand side angles for example. Powders (d) to (f) show additional modes of non-uniform heap formation.

Although a very simple test to perform, there are a number of issues which need to be considered. Firstly the way in which the cone of powder is formed will have an effect on the angle which is produced. To compensate for this a standard method of pouring must be developed – this varies between testers, so the angles generated also vary between testers. Secondly, as can also be seen in Figure 2.34, the actual cone is rarely uniform – several of the powders show multiple angles so specifying which one is the ‘true’ angle of repose is entirely subjective. There may, therefore, be a variation of 5° (or more) within any given pile of sample powder (in the range $20\text{-}55^{\circ}$ in the range of powders tested – i.e. 10-25% of the total). The precision of each test is therefore very low and thus the usefulness as a differentiator is limited. This also makes it difficult to replicate data. The Hosokawa system now employs a camera and image processing to evaluate the AOR, but it still requires an algorithm to decide the actual value – and as this is based on criteria set by the programmer, it is still subjective.

For this evaluation the AOR tester developed by Geldart was chosen (Figure 2.33; left hand side). It consists of two polycarbonate plates bracketed together at 90 degrees onto which powder is poured to form a semi-cone. This design is quite

unusual as most testers are designed to form a full cone. The material of construction is also questionable. If the tester plates were covered with sandpaper (as an extreme example) the generated angles would be significantly larger due to the inability of the sample to move as readily across the horizontal surface.

To initiate a test, the powder is gently poured onto a vibrating chute which channels the powder into the feed cone which is fixed to the top of the vertical polycarbonate sheet. Powder then falls onto a chute (with an adjustable angle) which directs the powder at the vertical polycarbonate sheet and thus it falls centrally onto the horizontal sheet to form the semi-cone. A graticule on both plates allows the size of the base (averaged from up to 10 measurements taken from the perimeter of the semi-cone) and the height of the semi-cone to be evaluated and hence the AOR is derived as indicated in Figure 2.31. The poured bulk density can also be derived from the mass of powder and the volume of the semi-cone. The results for the test powders are shown in Table 2.12 and Figure 2.35.

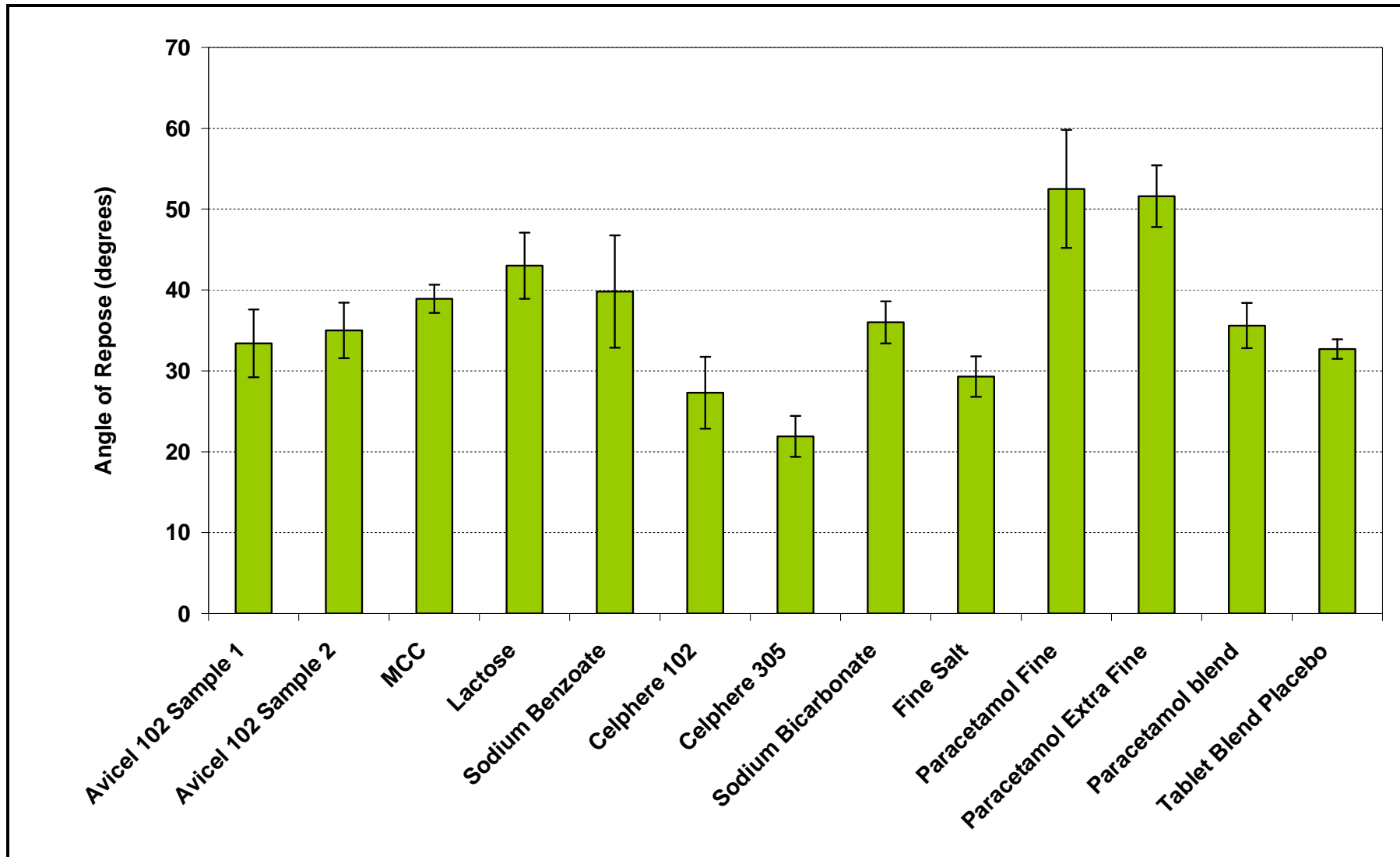


Figure 2.35: Angles of repose for the exemplar powders generated using the Geldart Angle of Repose Tester

Table 2.12: Angle of repose and bulk density data generated from the test samples using the Geldart angle of repose tester (n=3 for all tests)

Test Material	AOR	<i>sd</i>	<i>rsd</i>	Poured bulk density	<i>sd</i>	<i>rsd</i>
Avicel 102 Sample 1	33.4	1.40	4.18	332.8	21.89	6.58
Avicel 102 Sample 2	35.0	1.20	3.44	374.6	21.64	5.78
MCC	38.9	0.68	1.74	314.7	15.73	5.00
Lactose	43.0	1.75	4.08	595.2	42.16	7.08
Sodium Benzoate	39.8	2.76	6.95	282.1	33.01	11.70
Celphere 102	27.3	1.21	4.45	309.2	15.42	4.99
Celphere 305	21.9	0.55	2.53	960.4	22.83	2.38
Sodium Bicarbonate	36.0	0.9	2.6	952.8	30.61	3.21
Fine Salt	29.3	0.7	2.5	1276.8	24.63	1.93
Manitol	Did not flow through feed system under gravity; unable to generate reliable measurement					
Paracetamol Fine	52.5	3.8	7.3	206.0	10.51	5.10
Paracetamol Extra Fine	51.6	2.0	3.8	182.8	16.65	9.11
Paracetamol blend	35.6	1.0	2.8	768.3	38.65	5.03
Tablet Blend Placebo	32.7	0.4	1.2	486.9	14.18	2.91

If one examines the results presented in Table 2.12, there are some interesting outcomes. Firstly a reliable and repeatable measurement could not be generated with the Mannitol sample. This material was too cohesive to flow reliably through the cone and the chute sections of the tester without additional assistance. Thus any data collected for this material was compromised and not presented here.

These results, arguably, show the main limitation of the (poured) angle of repose test – in order to generate an angle of repose, one first needs to have the powder flow through some kind of orifice to eliminate any influence of the operator. This in effect means that the AOR test becomes a test of the feed system and not how the powder actually develops its repose angle – which does seem to defeat the objective.

The calculation of the AOR, based on the averaging of the measurements taken from the spread of powder over the base, effectively creates an ‘envelope’ measurement and does not easily allow the evaluation of the spread angles present in the powder pile. This approach gives a lower angle than the maximum angle (or angles) present within the pile – suggesting a more ‘free flowing’ powder than is actually the case.

There is also a differentiation limit to this type of test. Often many cohesive powders will give virtually identical angles of repose, but when tested using other methods, their properties are dramatically different.

If a powder is too free flowing – such as Celphere 305 – it is often difficult to form a heap of material as the individual particles tend to scatter when they arrive at the base of the tester.

Additionally, the generation of the Angle of Repose requires all the powder to be vibrated down the feed chute and allowed to fall several centimetres onto the measurement area – this can generate dust from the powder which, if the sample contains an API, may constitute a health hazard.

In summary, there are a large number of angles of repose which can be measured; the testers available do not use the same methodology to generate the powder heap even for the same type of AOR; the tests are difficult to perform without operator bias; multiple angles are often present in powder heaps making the measurement imprecise; high cohesion will often render the feed system inoperative; the sensitivity of the measurement to small variations in powder composition is poor, making differentiation difficult.

2.3.3. Jolting Volumeter

The Jolting Volumeter evaluates the variation in powder bulk density in the poured and tapped condition by applying a constant force and displacement to a jolting action on a measuring cylinder containing the powder under test (Figure 2.36).

It is a simple tester and can be described as a universal tester in that it is possible to generate a result from any powder than can be loaded into the test vessel.



Figure 2.36: Single Vessel Jolting Volumeter

There are a large number of reference standards for this particular test which is perhaps indicative of the disparity that can be achieved by varying the amplitude, frequency, number of taps and size of vessel. Like many simple tests there is an emphasis to try to generate a single number characterisation for the material under test – to try to keep it simple!

- ASTM B527: Standard Test Method for Determination of Tap Density of Metallic Powders and Compounds
- ASTM D4164: Standard Test Method for Mechanically Tapped Packing Density of Formed Catalyst and Catalyst Carriers
- ASTM D4781: Test Method for Mechanically Tapped Packing Density of Fine Catalyst Particles and Catalyst Carrier Particles
- ASTM D7481: Standard Test Methods for Determining Loose and Tapped Bulk Densities of Powders using a Graduated Cylinder
- ISO 787-11: General methods of test for pigments and extenders - Part 11: Determination of tamped volume and apparent density after tamping
- ISO 3953:1993 Metallic powders -- Determination of tap density
- ISO 6770: Instant tea - Determination of free-flow and compacted bulk densities
- ISO 8967: Dried milk and dried milk products -- Determination of bulk density
- ISO 8460: Instant coffee - Determination of free-flow and compacted bulk densities
- ISO 10236: Carbonaceous materials for the production of aluminium - Green coke and calcined coke for electrodes - Determination of bulk density (tapped)
- US Pharmacopoeia; USP 616, Bulk Density and Tapped Density
- European Pharmacopoeia; EP 2.9.15

The differences between the methods relate to the number of taps; the amplitude of the tap; the frequency of tapping; and occasionally the size of the measuring vessel. The EP, for example, requires a frequency of 250 ± 15 strokes/minute; amplitude of 3.0 ± 0.2 mm; and requires volume measurements at 10, 500 and 1250 taps. USP has two versions which require 300 strokes/minute with a drop of 14 ± 2 mm (USP I) and 250 ± 15 strokes/minute; amplitude of 3.0 ± 0.3 mm (USP II).

Following the collection of some of the data, it became apparent that further intermediate measurements would be useful as most of the powders tested varied little in volume between 500 and 1250 taps.

Additionally, the filling of the vessel has a significant degree of operator dependant variability. After filling of the cylinder the powder has to be level for an initial volume reading to be taken. Invariably it is not level and the cylinder has to be shaken gently to level the powder or the surface has to be gently swept level using a spatula or similar, which can also compromise the initial volume measurement due to the forced settling. Cohesive materials have a tendency to adhere to the wall of the cylinder during filling, also making it difficult to determine a precise value for the initial volume. This levelling of the powder during the tap testing is much less of an issue than at the start. The precision of the actual volume measurement is also limited to $\pm 2\text{ml}$ due to the graduations on the cylinder itself.

Testing has been completed on a number of powders using non-standard and standard techniques and results are shown in Table 2.13 and Figure 2.37. Carr's Compressibility Index, commonly referred to as Carr's Index, and the Hausner ratio are calculated from the equations below

$$CCI = \frac{\rho_t - \rho_p}{\rho_t} \times 100 \quad \text{Equation 2.4}$$

$$HR = \frac{\rho_t}{\rho_p} \quad \text{Equation 2.5}$$

Where CCI is Carr's Compressibility Index
 HR is Hausner's Ratio
 ρ_t is the tapped density
 ρ_p is the poured density

Table 2.13: Results from testing exemplar powders using a jolting volumeter (n=3 for all tests)

Test Material	Poured density	<i>sd</i>	Density 1000 taps	<i>sd</i>	Density 1250 taps	<i>sd</i>	Carrs Index 1250 taps (* = 1000 taps) (%)	<i>sd</i>	Hausner ratio 1250 taps (* = 1000 taps)	<i>sd</i>
Avicel 102 Sample 1	0.38	0.00			0.46	0.00	18.05	0.62	1.22	0.01
Avicel 102 Sample 2	0.38	0.00			0.46	0.00	17.06	0.05	1.21	0.01
MCC	0.34	0.01			0.46	0.01	25.54	0.91	1.34	0.02
Lactose	0.69	0.01	0.88	0.01			21.31*	0.37	1.27*	0.01
Sodium Benzoate	0.29	0.00	0.37	0.01			20.15*	0.79	1.25*	0.01
Celphere 102	0.86	0.01	0.93	0.00			7.35*	0.50	1.08*	0.01
Celphere 305	0.90	0.01	0.95	0.00			5.27*	1.37	1.06*	0.02
Sodium Bicarbonate	0.76	0.01			1.01	0.02	24.85	1.17	1.33	0.02
Fine Salt	1.23	0.00			1.30	0.00	5.23	0.45	1.06	0.01
Paracetamol Fine	0.36	0.02			0.49	0.01	26.39	2.71	1.36	0.05
Paracetamol Extra Fine	0.34	0.01			0.46	0.01	26.84	1.77	1.37	0.03
Paracetamol blend	0.92	0.07			1.12	0.09	18.23	0.88	1.22	0.01
Tablet Blend Placebo	0.51	0.00			0.59	0.01	13.86	0.89	1.16	0.01

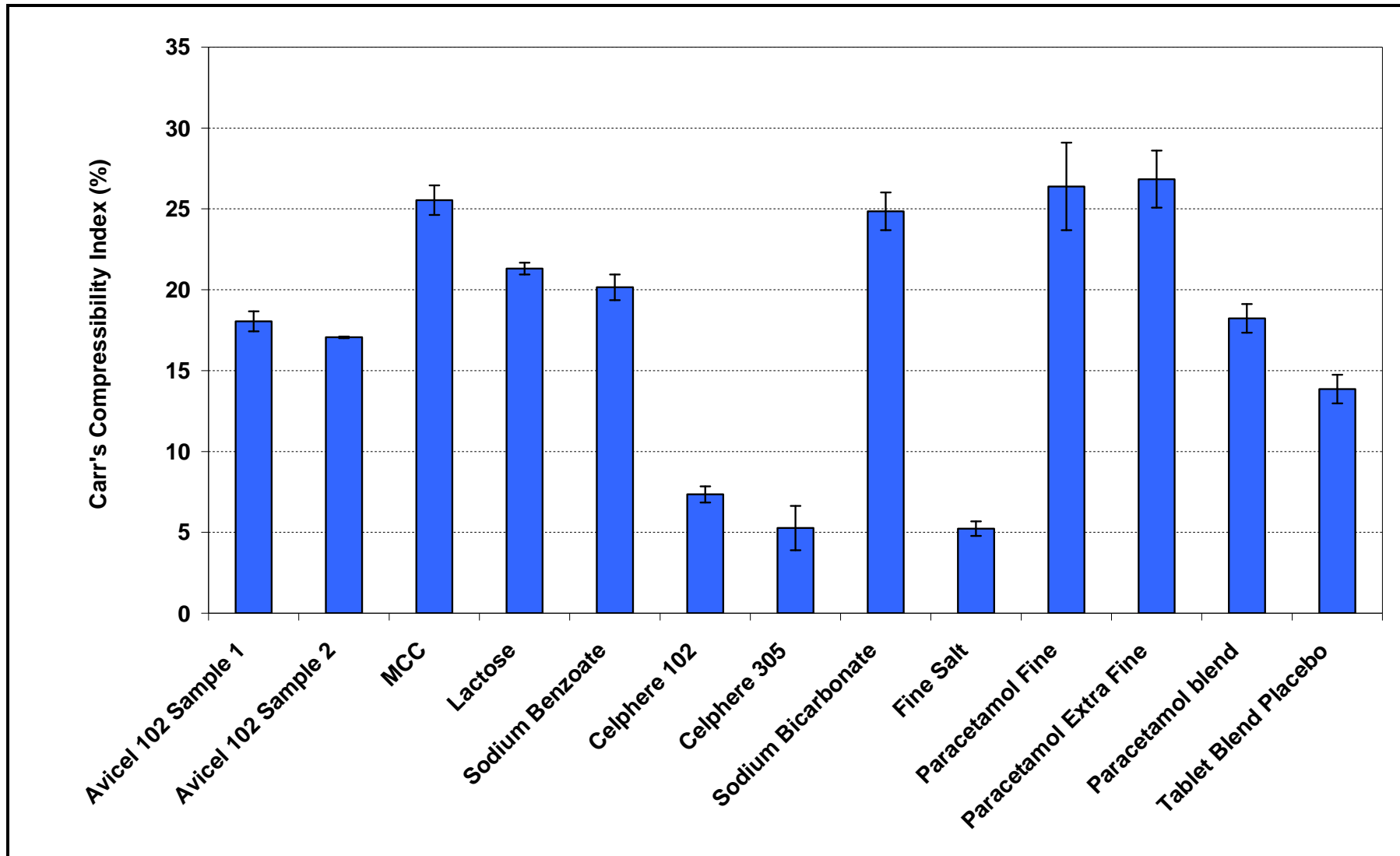


Figure 2.37: Results from testing exemplar powders using a Jolting Volumeter (n=3 for all tests)

The results shown in Table 2.13 & Figure 2.37, and moderated by the flowability descriptors and limits shown in Table 2.2, broadly conform to the expected order of flowability – except for the Sodium Benzoate. This material has a platy shape factor which means that its poured density is lower than expected due to the ordering of the particles within the poured sample which limits the degree of packing. The tapping then allows the particles significant scope to rearrange by expanding the powder bed. The result is a much denser packing structure and hence the Carr Compressibility Index is higher than would be expected for this material.

2.3.4. Flow through an orifice & Flowability Tester Model BEP2 tester

The ability of a powder to flow through an opening, as has been previously detailed in the section on shear cell analysis, requires complex analysis and an instrument that can evaluate the stress states within the powder. However, many simpler testers exist that derive data from actual flow through one or more accurately sized holes.

The British Pharmacopoeia (BP) (British Pharmacopoeia Commission 2005) shows two types of orifice tester. The first – a simple commercial glass funnel shown in Figure 2.38 – is unworkable because most powders will not flow through this item. The outlet is so small that cohesive powders will not flow out of the bottom of the conical section and non-cohesive powders will jam in the long discharge tube. The second device is a more sensible design with three possible outlet sizes and does not have an extended discharge tube is also presented in the BP and is shown in Figure 2.39.

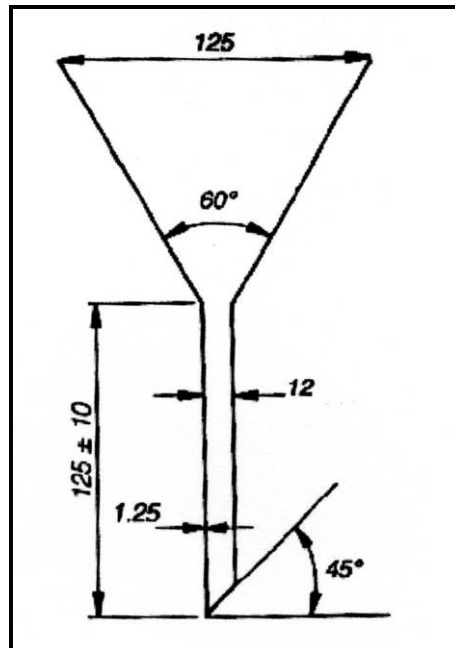


Figure 2.38: Glass flow funnel as shown in the British Pharmacopoeia

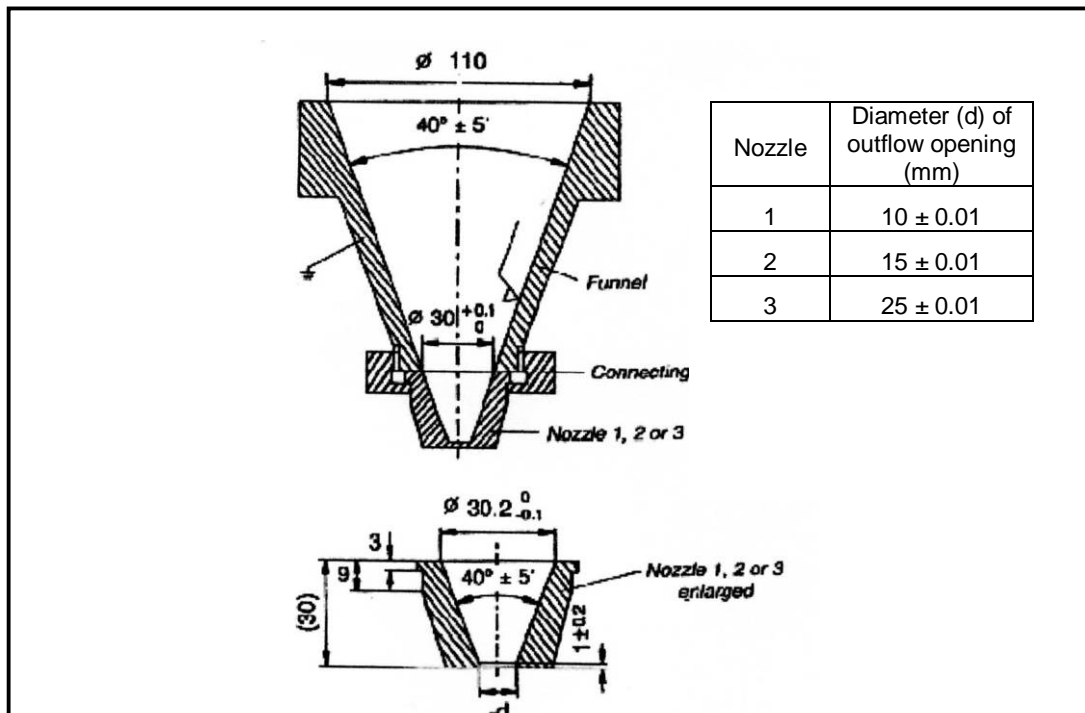


Figure 2.39: Alternative flow funnel and nozzle made from acid resistant stainless steel (V4A, CrNi) as shown in the British Pharmacopoeia

Alternatively there are a number of commercial testers on the market which make use of the ability (or not) of a powder to flow through a specific orifice or range of orifices.

The Flowability Tester Model BEP2 device, Figure 2.40, has been evaluated for this project and consists of a steel cylinder supported on a frame and fitted with a removable base into which a range of discs, with different orifice sizes, can be fitted.



Figure 2.40: The Flowability Tester Model BEP2 Powder Flowability Tester

A valve is located under the cylinder that, when powder has been charged, is opened to allow unrestricted flow through the chosen orifice.

The primary purpose of the test is to find the minimum orifice through which the powder will pass consistently, but the determination of the minimum orifice size is, largely, a trial and error exercise. Some obviously free flowing samples were tested with the smallest orifice first and cohesive samples with the largest. However, powders with intermediate flow properties require multiple tests to accurately determine the correct orifice size. Often the variability of the powder or, more likely, the inconsistent charging of the cylinder by the operator will lead to powder flowing then not flowing through an orifice in consecutive tests. Clearly this occurs close to the flow/no-flow limit of the powder, but this imprecision can lead to significant operator frustration.

An expression is provided by the manufacturer that relates the outlet diameter to a 'coefficient of friction'.

$$\pi r^2 h \rho g \geq 2\pi r h K \quad \text{Equation 2.6}$$

where

- r is the diameter of the outlet
- h is the height of the cylinder of powder
- ρ is the poured bulk density of the powder
- g is the acceleration due to gravity
- K is the coefficient of friction

Clearly this is an oversimplification of the of the flow behaviour as previously described in the section on shear cells, but it is presented here to indicate the limited nature of these types of devices and the way they are represented.

In order to develop the data for this equation, the height of the powder, h , needs to be noted. The operating instructions suggest the cylinder be filled to within 10mm of the top, however no means of measuring such a height is provided and it is left to the end user to provide such a mark.

In addition it has been determined that there are other results that can be obtained from this test. Firstly the flow rate can be measured. Ideally a logged balance under the outlet would provide precise flow rate – especially for very free flowing materials with short discharge times – but the use of a stopwatch sufficed in this instance. This enables further differentiation of powders that flow through the same orifice. Once a flow rate is obtained, comparison with, for example, the Beverloo equation (Rhodes 1998) can be undertaken.

$$W = 0.58\rho_b g^{0.5} (B - kd_p)^{2.5} \quad \text{Equation 2.7}$$

where

- W is the discharge rate (kg/sec)
- ρ_b is the bulk density (kg/m³)
- g is the gravitational constant
- B is the outlet size (m)
- k is an empirical outlet shape constant (typically 1.4) (Mankoc *et al.* 2007)
- d_p is the particle size (m)

The drained angle of repose can also be calculated from knowledge of the weight of powder left in the vessel, the bulk density and the size of the orifice from Equation 2.8.

$$\alpha = \tan^{-1} \left(\frac{16m}{\rho\pi(D^2 - d^2)(D - d)} \right) \quad \text{Equation 2.8}$$

where α is the drained angle of repose (degrees)
 D is the diameter of the cylinder (m)
 ρ is the poured bulk density of the powder (kg/m^3)
 d is the diameter of the orifice (m)
 m is the mass of powder left in the tester (kg)

The results from testing of the range of sample powders are presented in Table 2.14 and Figure 2.41.

Table 2.14: Measured and derived data for the Flowability Tester Model BEP2 (n=3 for all tests)

Test Material	Data				Calculations			
	min orifice (mm)	flow rate (g/s)	<i>sd</i>	<i>rsd</i>	Beverloo predict ⁿ (g/s)	Variation from Beverloo predict ⁿ (%)	K	drained AOR
Avicel 102 Sample 1	30.00	36.59	12.74	34.83	107.28	-68.89	2829.75	85.48
Avicel 102 Sample 2	30.00	37.08	3.83	10.34	106.15	-65.07	2800.35	88.38
MCC*	36.00	37.08	1.64	3.58	168.66	-78.01	3007.62	89.74
Lactose	34.00	28.86	11.17	38.72	258.56	-88.84	5789.35	89.15
Sodium Benzoate	No Flow through largest (36mm) orifice							
Celphere 102	4.00	1.57	0.01	0.80	1.44	8.99	844.76	69.60
Celphere 305	4.00	1.21	0.02	1.74	1.22	-0.93	882.98	68.71
Sodium Bi-carbonate	26.00	157.20	42.80	27.22	149.87	4.89	4841.20	73.01
Fine Salt	4.00	2.31	0.03	1.35	1.84	25.54	1207.36	70.44
Mannitol	No Flow through largest (36mm) orifice							
Paracetamol Fine								
Paracetamol Extra Fine								
Paracetamol blend	34.00	74.97	14.37	19.17	352.40	-79.65	7646.94	89.65
Tablet Blend Placebo	4.00	0.63	0.01	1.61	0.82	-23.94	567.27	78.93

* powder failed to flow for 3 out of 7 tests

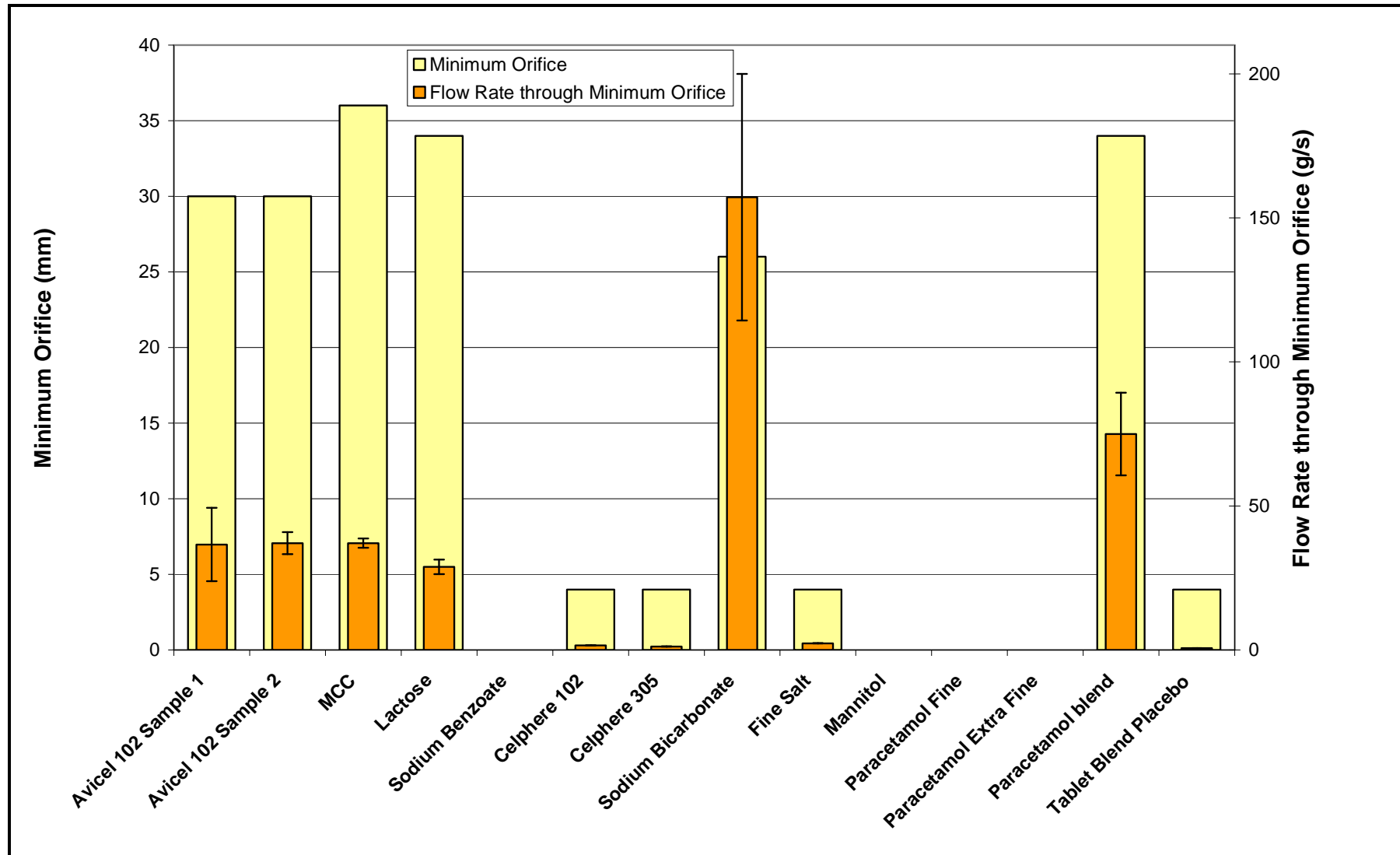


Figure 2.41: Measured Data from Flowability Tester Model BEP2 (n=3 for all tests)

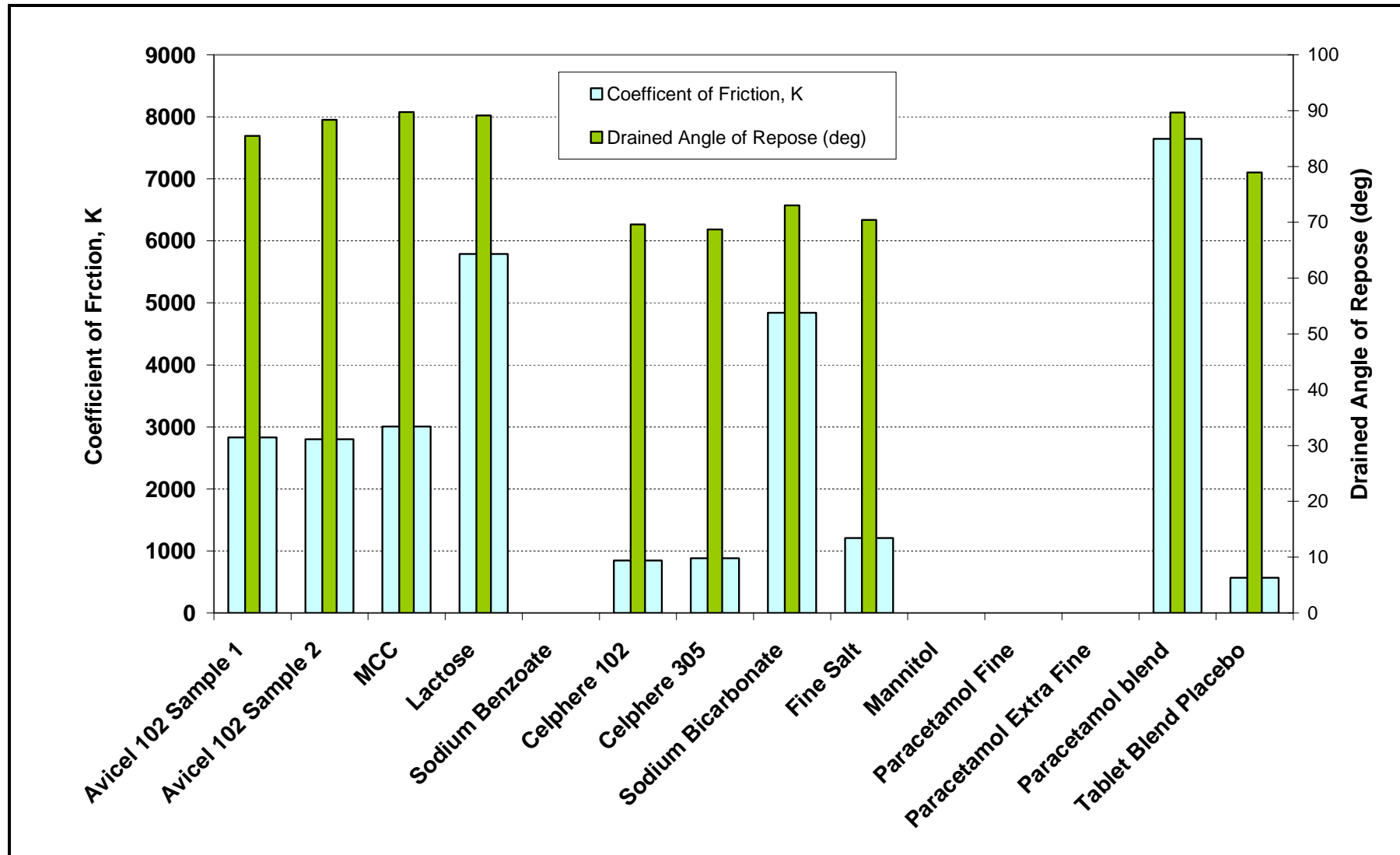


Figure 2:42: Calculated Coefficient of Friction (K) and Drained Angle Repose – Flowability Tester Model BEP2

There are several advantages and disadvantages relating the use of this device and the data collected from it.

Practically there is an issue with dust generation where material, as noted with the AOR tester, is allowed to fall several centimetres which may generate dust and the potential for a health hazard if API materials are present. It is recommended that both of these devices be operated in a fume cupboard or similar environment.

Many cohesive materials will flow through the largest orifice available, but only if the test is done instantaneously – if the powder is left for a short period, even a few tens of seconds, it may not flow through. This was particularly the case for the MCC sample where flow through the 36mm orifice was observed for only 3 of the 7 tests undertaken.

The usefulness of the comparison of flow rate with Beverloo predictions is also moot. The Fine Salt, Sodium Bicarbonate and Celphere samples provide the results which are closest to the predictions. Clearly these back up the assertions that this expression is best used for the most spherical and free flowing materials (Spink & Nedderman 1978).

However, the major problem with this device is that it is a poor differentiator for cohesive powders, four of which generated a null reading when the powders failed to flow through the largest orifice, as shown in Figures 2.41 and 2.42. This does not

allow the user to compare powders if they cannot be tested in this system. The four powders, listed in Table 2.14, which failed are both grades of paracetamol, Mannitol and Sodium Benzoate. The two paracetamol powders and the Mannitol sample can be described as conventionally cohesive, but the Sodium Benzoate would be described by most people as free flowing. In this case it fails this test due to its shape, which can be described as 'platy', and it is clearly forming mechanical bridges over the outlet.

Conversely, free flowing powders will tend to be too free flowing and will pass easily through the minimum orifice available – 4mm. Differentiation in this case has to be based on flow rate through the orifice.

In addition the trial and error nature of finding the minimum orifice size can be time consuming, especially when the flow through a series of similar sized orifices can be influenced by how the powder is loaded into the vessel prior to opening of the outlet.

In summary, this device is a poor differentiator of materials; often requires significant time to generate the correct orifice; needs additional calculation of the throughput to differentiate free flowing powders; but is used within the industry and can be used as a point of reference for clients.

2.3.5. Powder rheometry

Powder rheometry is a relatively new approach to the flow property testing of powders. There are two main suppliers of instruments, Freeman Technology and Stable Micro Systems (SMS), both instruments are shown in Figure 2.43.



Figure 2.43: The Powder Flow Analyser (left) and the FT4 Powder Rheometer (right)

Starting out from the same roots, the two instruments test powder in broadly the same way by passing a propeller shaped blade through the powder under test and measuring the resistance. There is a small difference in the blade design, but the major difference is that the Freeman Technology FT4 tester measures vertical position, blade torque and load on the base of the tester whereas the Stable Micro Systems (SMS) Powder Flow Analyser (PFA) measures only the vertical position and

the load on the base. Additionally the FT4 has a number of optional packages; shear cell; aeration/de-aeration; and wall friction. The PFA itself is an add on unit for the TA.XTPlus Texture Analyser which already has a wide range of food based materials testing options that can also be fitted to the basic instrument.

At this time, there is very little to suggest what these devices are actually measuring in terms of state properties of the powder (compared to the shear cell), which has led to many people dismissing them out of hand. However, they are promoted as being able to provide an insight into powder behaviour that other, better defined devices, fail to characterise. In addition, like the shear cell, both are universal testers in that they will always provide a measurement as long as the powder is compatible with the size of the test vessel – unlike the ‘flow through orifice’ testers, angle of repose testers.

2.3.5.1. SMS PFA

The Department of Chemical Engineering has an existing TA.XTPlus Texture Analyser, and a PFA unit was loaned to the Department for evaluation.

The texture analyser moves its patented helical blade vertically and the rotational motion is provided by a peripheral electronic device via a motor located in the arm of the texture analyser. A powder sample is loaded into a glass powder flow vessel and located on the base of the PFA. The volume of the sample is intended to be 160ml, but the ability to achieve precisely 160ml is, as with the Jolting Volumeter, system is operator dependant. The glass vessel is marked every 20ml giving rise to some

variability in achieving a precise volume especially when the powder is loaded unevenly.

As the blade moves through the powder column during a test, the force (measured by a load cell in the base of the PFA), distance and time data are recorded in Exponent™ software for later analysis. Three types of tests are commonly run on the PFA:

- Cohesion
- Powder Flow Speed Dependency (PFSD)
- Caking

Only the cohesion and PFSD tests have been used because of their simplicity and immediate relevance to the powder mixing part of the project.

One useful feature that is unique to powder rheometers – both the SMS PFA and the Freeman FT4 – is the conditioning cycle. During this process the blade is traversed through the powder in such a way as to gently lift the material and eliminate historical stress features that may have been present during its previous storage period or through the way the powder was introduced into the vessel. This enables a consistent stress state to be achieved prior to running any test routines. In some ways this can be seen as the equivalent to pre-shearing required prior to shear testing and is hugely beneficial in allowing data from different laboratories to be compared as the influence of the operator is all but eliminated, unlike the simple testers (AOR; flow through an orifice; tapped density).

The cohesion test begins with two conditioning cycles to remove any stress history from the powder and to normalise the powder column after filling. The blade then moves down through the powder column using a “cutting” action to minimise compaction. The upward part of the cycle lifts the powder and the force of the powder on the vessel base is recorded.

The PFA measures ‘cohesiveness’ by moving the blade in such a way as to lift the powder. The argument is that a more cohesive powder will cling to itself and to the blade therefore reducing the force exerted on the base of the vessel. A typical trace is shown in Figure 2.44. Here the force seen by the load cell is plotted on the Y-axis against the position of the blade within the vessel.

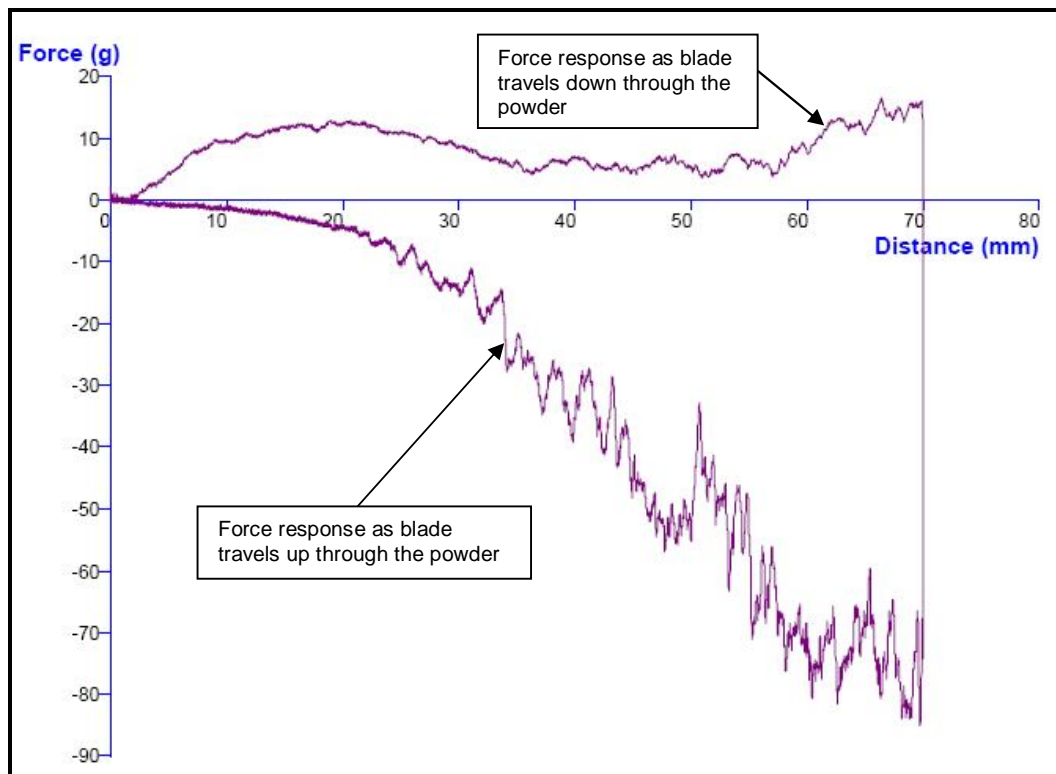


Figure 2.44: Example of Cohesion Test raw data – the trace follows the blade as it passes down through column of powder (from zero to the 70mm maximum travel point) and is designated by the positive force (compression) and then as it traverses back up through the powder (lifting) to reach its original start point

The negative area under the curve is the work required to move the blade through the powder column i.e. to lift the powder and so is related to the weight of the powder sample (and also its density), this is the cohesion coefficient. A cohesion index is calculated by dividing the cohesion coefficient (the upward part of the cycle) by the weight of the sample.

The powder flow speed dependency (PFSD) test begins with two conditioning cycles (as at the start of the cohesion test) followed by 4 sets of 2 cycles at increasing speeds (10, 20, 50 and then the final cycles at 100 mm/sec). The downward parts of the cycles compact the powder and the upward stroke of the cycle uses a lifting action.

Powder flow properties may change with increasing or decreasing blade speeds. For example a powder may become more resistant to flow as it is forced to flow faster or indeed it may become more free flowing as the blade speed increases. The PFA measures this characteristic by assessing the work needed to move the blade through the powder at increasing speeds. An evaluation of the flow stability of the powder is made by comparing the work needed to move the blade through the powder at the start of the test compared to the work required to move the powder at the same speed at the end of the test.

The (positive) area under the compaction curves (a typical PFSD curve is shown in Figure 2.45) is averaged over the two cycles at each speed and gives the compaction coefficient at each of the speeds tested.

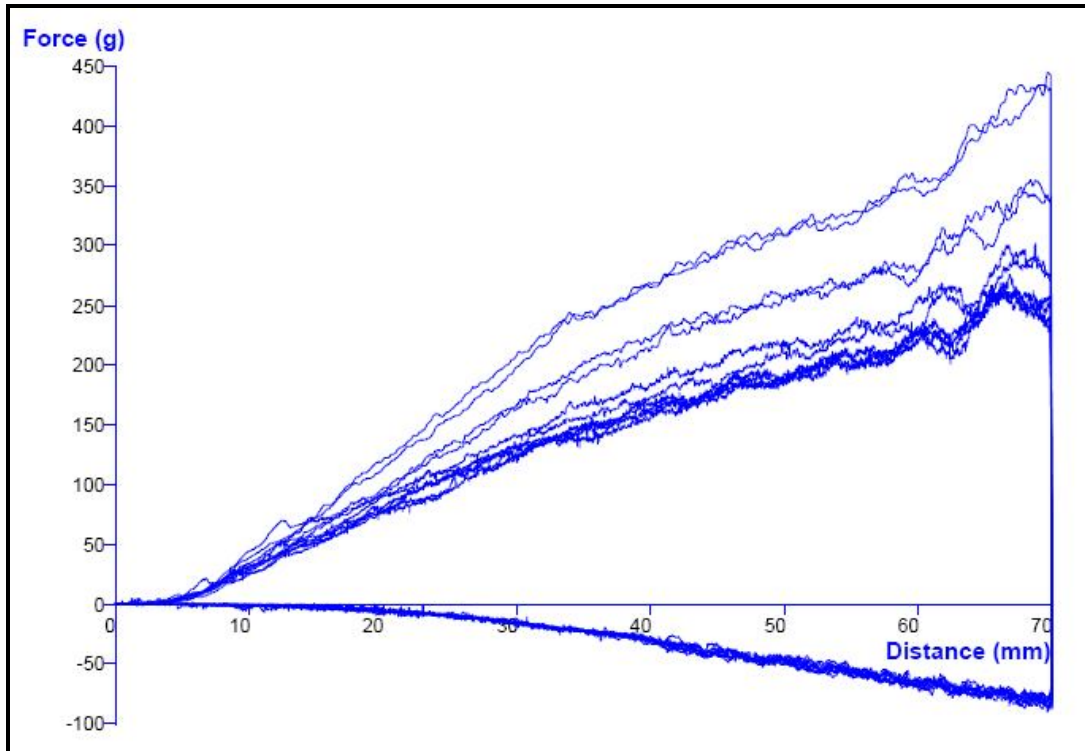


Figure 2.45: Example of raw data from a PFSD Test – the trace follows the blade as it passes down through column of powder (from zero to the 70mm maximum travel point) and is designated by the positive force (compression) and then as it traverses back up through the powder (lifting) to reach its original start point. The different traces represent the different speeds of the PFSD test from 10 to 100 mm/s

The compaction coefficient is the work required to move the blade down through the powder column using a compacting action – a function of the blade direction and the speed of rotation. The area under the upward (negative) section of the first 10mm/sec speed curves are averaged and recorded as a cohesion coefficient. Any increase in cohesiveness or electrostatic forces in the powder would result in a larger negative value and therefore a higher cohesion coefficient. Flow stability is

calculated by dividing the compaction coefficient of the first 10 mm/sec cycles by the compaction coefficient of the last 10 mm/sec cycles.

Data collected from these tests are shown in Figures 2.46 & 2.47.

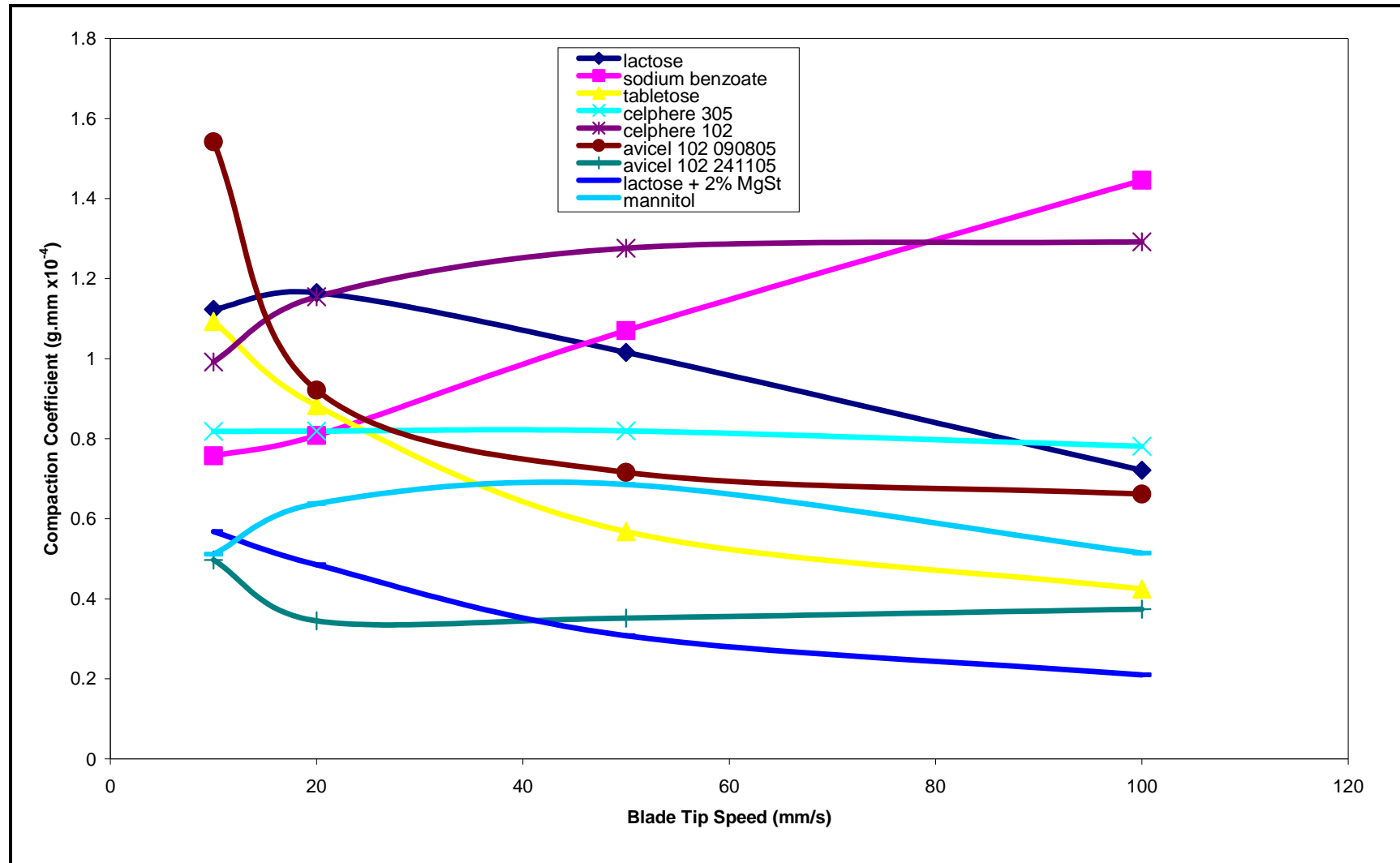


Figure 2.46: PFA compaction coefficient for a range of exemplar powders

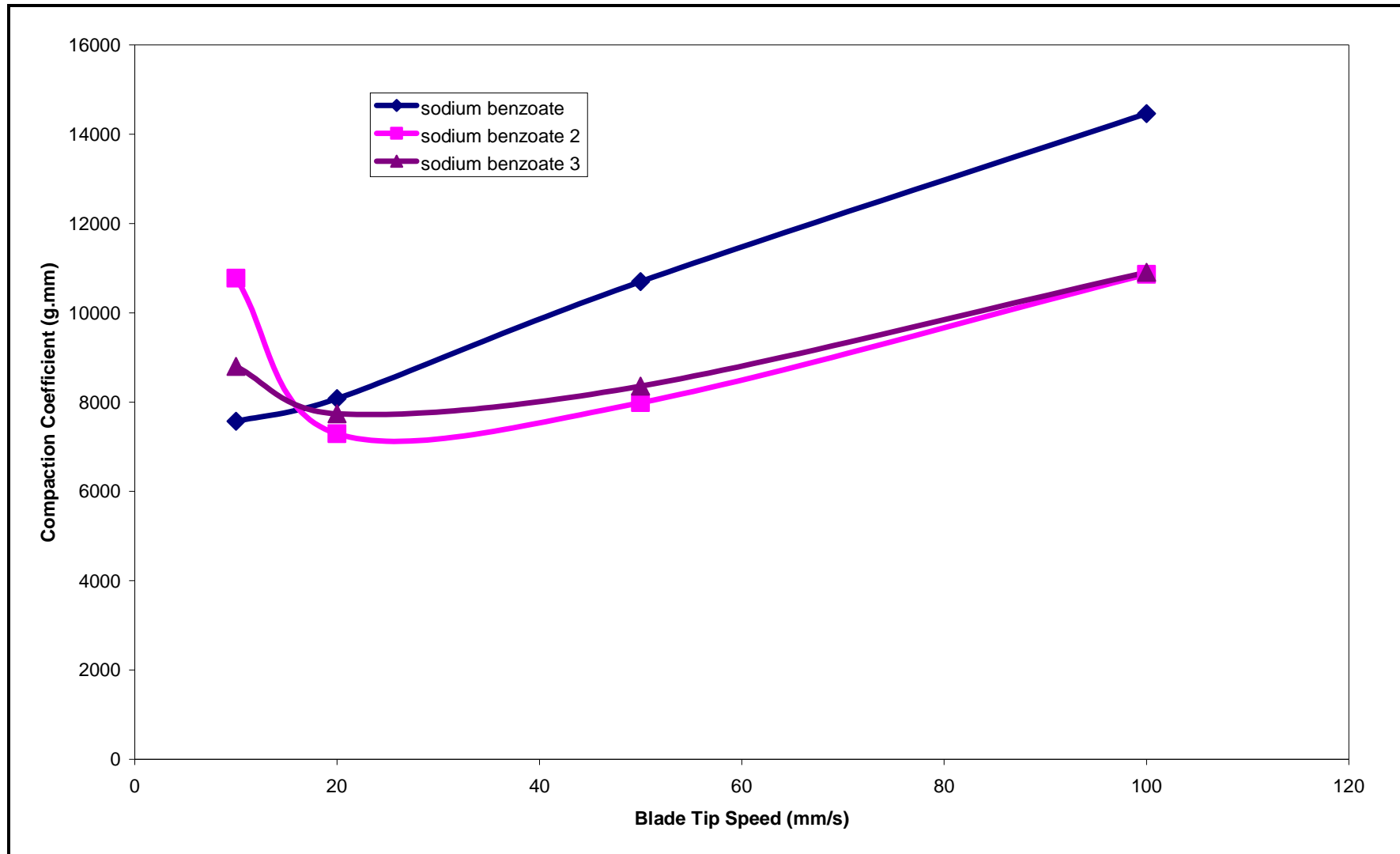


Figure 2.47: PFA compaction coefficient for three tests of Sodium Benzoate

Firstly the behaviour of Sodium Benzoate in this tester is dramatically different to the other powders tested. Figure 2.47 shows three repeats of the PFSD test, showing that passing the blade through the powder at increased speed requires a greater force and therefore more energy. This is at odds with the other powders tested which show the reverse behaviour. Given this result it was postulated that, in a paddle mixer or tumble blender, this material might mix slower at higher rotational speeds. This will be further examined in Chapter 3. However, as can also be seen in Figure 2.47, the repeatability of the test procedure with the PFA is unacceptable. This is most likely due to the difficulty of providing a stable starting condition. The PFT requires a fixed volume of material but provides no means of generating such a volume. This is a feature of the Freeman Technology FT4 powder rheometer that will be discussed later in this Chapter.

Secondly, the tester can, in some instances, differentiate powders that show observable flow differences in real process environments, whereas conventional shear testing cannot. It is well known that the addition of a small quantity of lubricant or flow aid (such as magnesium stearate or fumed silica) can dramatically change the flowability of pharmaceutical formulations (Faqih *et al.* 2007; Liu *et al.* 2008; Velasco *et al.* 1995). Figures 2.48 and 2.49 present two powder systems, based on a formulation containing Lactose and Avicel, with and without low concentrations of magnesium stearate present. When the shear cell testing of the formulations, shown in Figure 2.48, is evaluated the flowability of the powders, as determined by the Flow Function, shows the two samples to be virtually identical. When tested in the PFA there

is considerable variation/differentiation between pure and magnesium stearate doped conditions – correlating with observed process behaviour.

Although this is far from conclusive evidence, it shows the benefits and limitations of having several testing methodologies available and will be explored in more detail in Section 2.5.

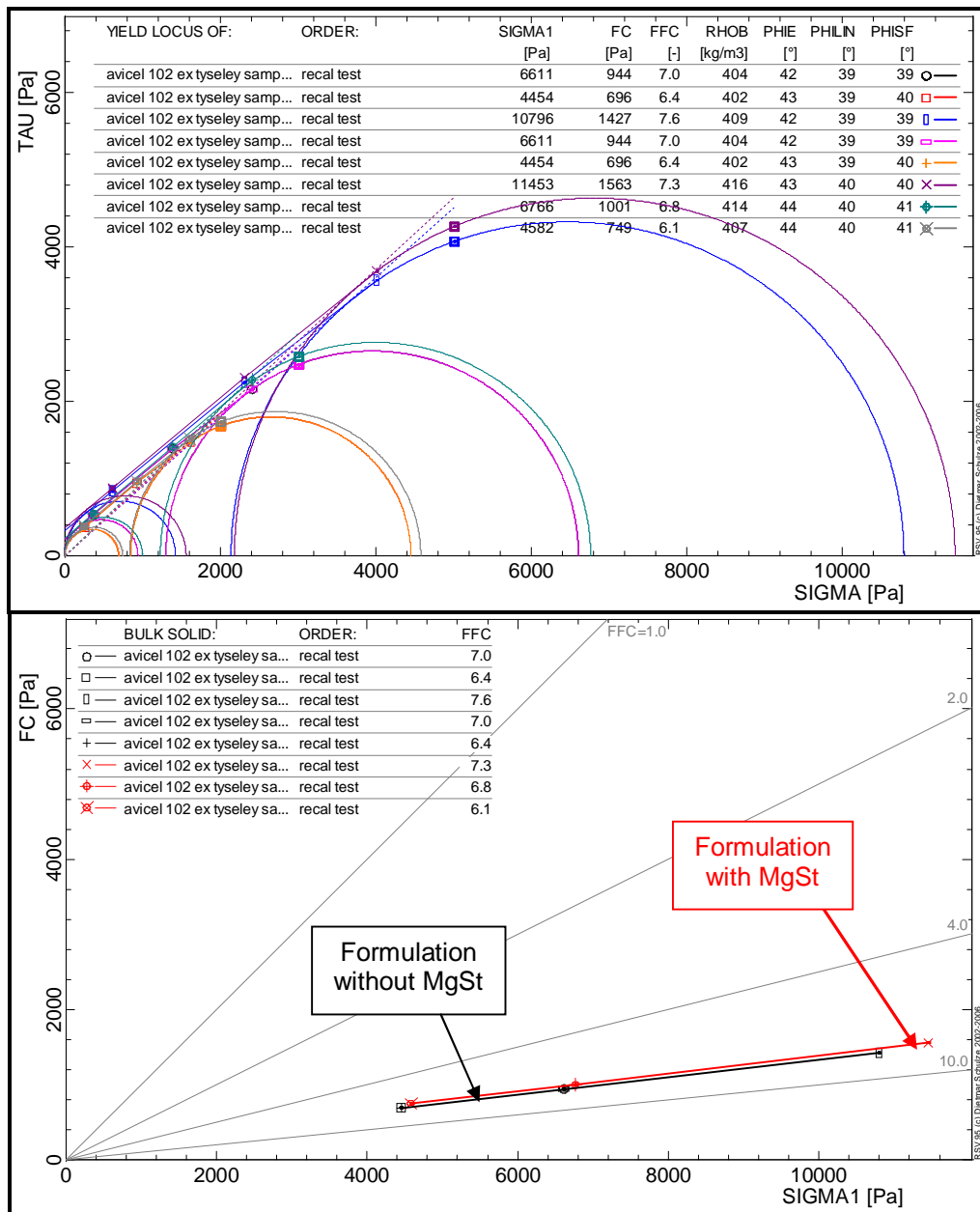


Figure 2.48: Shear cell data and flow functions for two Lactose/Avicel 102 systems, one with added magnesium stearate (MgSt)

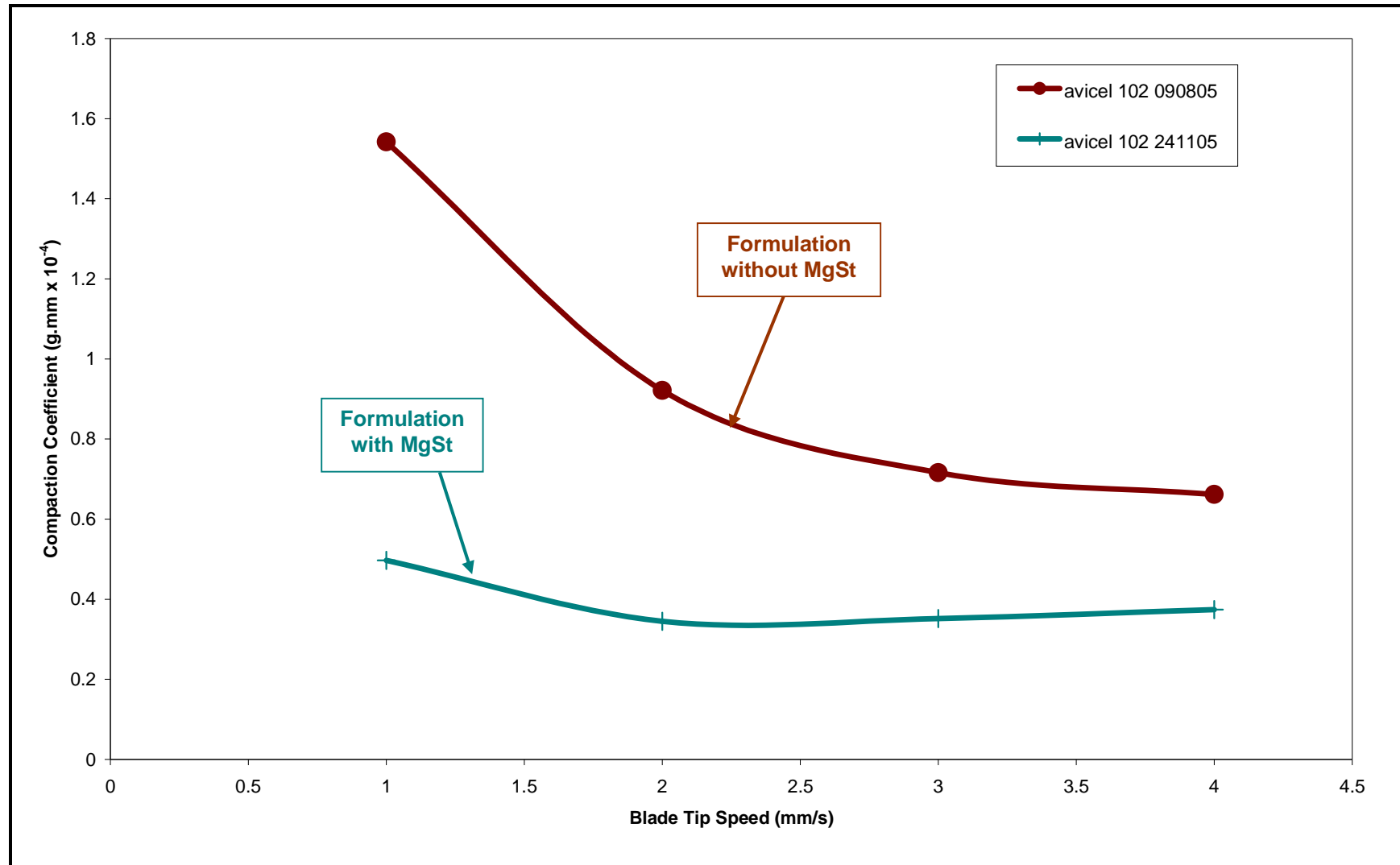


Figure 2.49: PFSD results for two Lactose/Avicel systems one with added magnesium stearate (green trace), one without (brown trace)

2.3.5.2. Freeman Technology Powder Rheometer FT4

The Freeman Technology FT4 is, in many ways, comparable to the Hosokawa powder tester in that it takes a multi-measurement approach to the characterisation of powders. It can evaluate a series of dynamic, bulk and shear properties of a powder for which it has a range of spindle mounted accessories that are easily exchangeable with the standard blade.

The basic blade methodology is similar to the PFA, but there is a slight difference in the actual blade design. The FT4 measures both force and torque during the transit of the blade, whereas the PFA is limited to force measurement only. Figure 2.50 shows the motion of the FT4 blade during a test and the spiral pathway it traverses down the vessel.

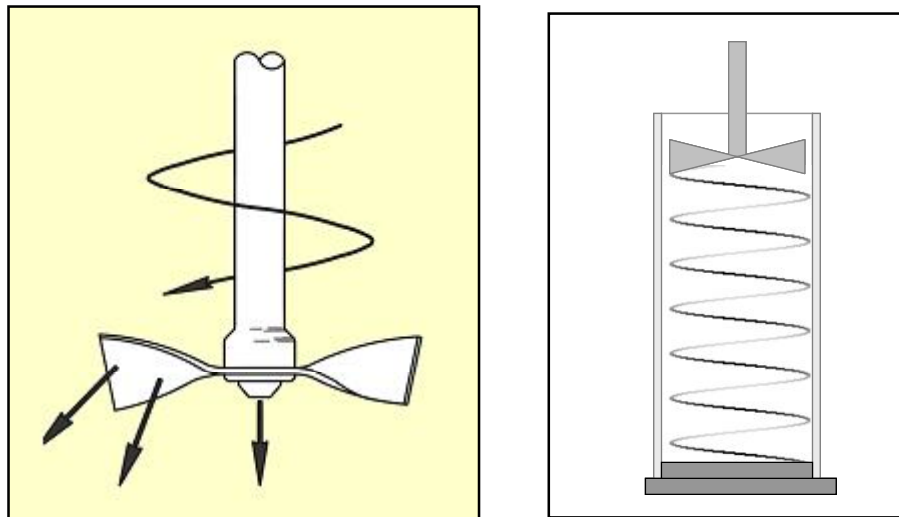


Figure 2.50: Motion and pathway of the FT4 blade during a test

Each test allocates a number of specific attributes to the powder sample based on the analysis of the position, force, torque and air flow measurements taken during

specific test routines, although the entire profile for each test is readily available for examination.

As can be seen from Table 2.15, the number and type of powder characterisation tests that an FT4 can undertake far exceeds that of the SMS PFA. In addition to the dynamic testing with the blade, enhanced by the ability to measure torque and force, additional tests can be undertaken for compressibility, permeability using a vented piston and an aeration unit, and, as has already been discussed, shear testing. Further specialist tests are also available that evaluate segregation, degradation, the effect of vibration, de-aeration, the effect of time consolidation and the effect of direct pressure. These additional tests were not investigated due to time constraints, but the flexibility of the instrument is clear.

A significant feature which is specific to the FT4 is the split vessel assembly, which uses a Delrin plastic fixture to accurately position two glass vessels above each other. The fixture is hinged and allows the top and bottom vessel to separate, enabling the removal of excess powder to a separate beaker, and leaving a very accurately sized volume of powder to be tested. Combine this with the conditioning cycle, described in the previous section, and the repeatability of the testing procedure is almost entirely operator independent and provides an excellent base for enhanced repeatability of testing, especially when compared to the rudimentary procedures provided by other simple testers which were described in earlier sections.

Examples of the graphical output from the FT4, generated in the proprietary post processing software package 'Data Analysis' or DA, are shown in Figures 2.51 to 2.54

Table 2.15: Descriptions of the standard suite of test routines available for the FT4 Powder Rheometer

Sub Group	Test	Parameter	Definition	Units
Dynamic	Stability and Variable Flow rate	Basic flowability Energy (BFE)	The energy needed to displace a conditioned and stabilised powder at a given flow pattern and flow rate – in this investigation at -5° helix and 100 mms^{-1} blade tip speed and a sample volume of 160 ml. BFE = test 7	mJ
		Stability Index (SI)	The factor by which the flow energy requirement changes during repeat testing. SI = test 7/ test 1	-
		Specific Energy (SE)	The energy needed to displace a conditioned powder using a gentle shearing and lifting mode of displacement. This energy is then divided by the split mass	mJ/g
		Flow Rate Index (FRI)	The factor by which the flow energy requirement is changed when the flow rate is reduced by a factor of 10. FRI = test 11 / test 8	-
		Conditioned Bulk Density (CBD)	The bulk density of exactly 160 ml of conditioned powder	g/ml
	Aeration	Aeration Ratio (AR_n)	The factor by which the flowability energy is reduced by aeration at an air velocity of $n \text{ mm/s}$. $AR_n = AE_0 / AE_n$	-
		Aeration Energy (AE_n)	The flowability energy at an air velocity of ' n ' mms^{-1}	mJ
		Normalised Aeration Energy (NAE)	The normalised flowability energy at an air velocity of ' n ' mms^{-1} with respect to the flowability energy at 0 mms^{-1}	-
Aeration Sensitivity (AS)		The maximum rate of reduction of flow energy with increasing velocity.	s/mm	

Table 2.15 contd.

Sub Group	Test	Parameter	Definition	Units
Bulk Properties	Compressibility	Compressibility (CPS _n)	Percentage by which the bulk density has increased with an applied normal stress of 'n' kPa	%
		Bulk Density (BD _n)	The mass per unit volume of the sample at a specified consolidating stress of 'n' kPa	g/ml
	Permeability	Permeability (Perm _n)	The Permeability of a sample as described in Darcy's equation at specified consolidating stress of 'n' kPa	m ²
		Pressure Drop (PD _n)	Pressure drop across the powder bed at a normal stress of 'n' kPa and at an air velocity of 2mm/s (unless stated otherwise)	mbar
Shear	Powder Shear Testing	See Table 2.7		
	Wall Friction Testing	Angle of wall friction (φ)	The angle defined by a series of σ/τ data pairs where $\varphi = \tan^{-1}(\tau/\sigma)$	deg

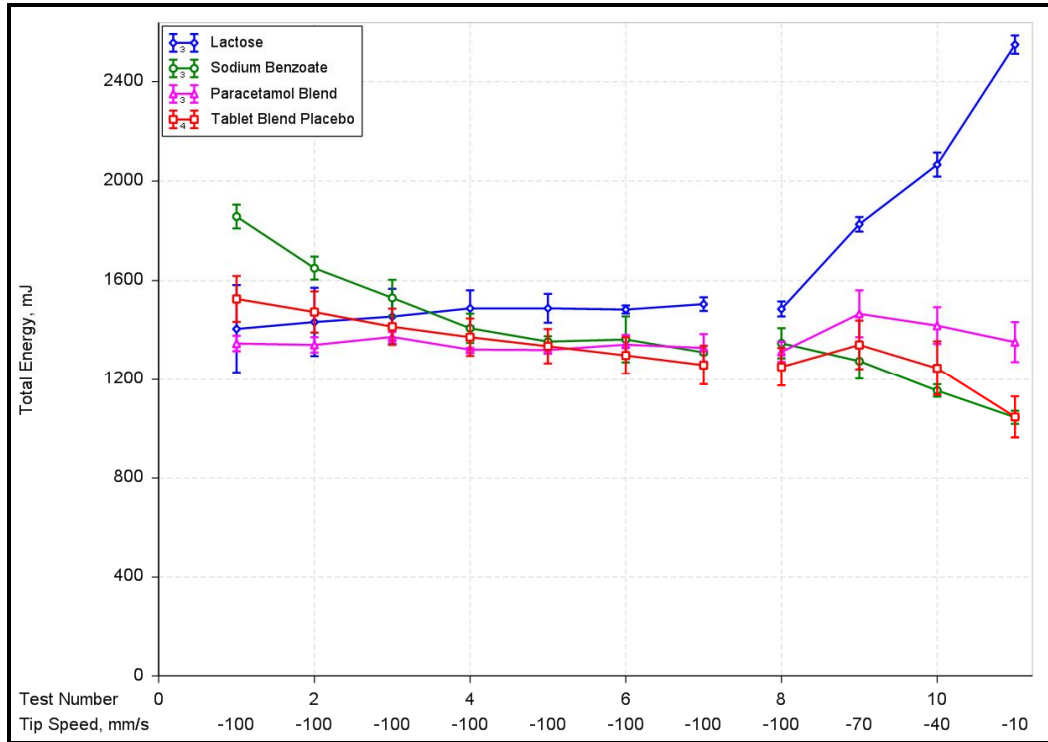


Figure 2.51: A dynamic test for 4 of the test powders showing 7 repeat tests at a blade tip speed of 100mm/s to evaluate the powders flow stability, followed by 4 tests at reducing blade tip speed from 100mm/s to 10mm/s

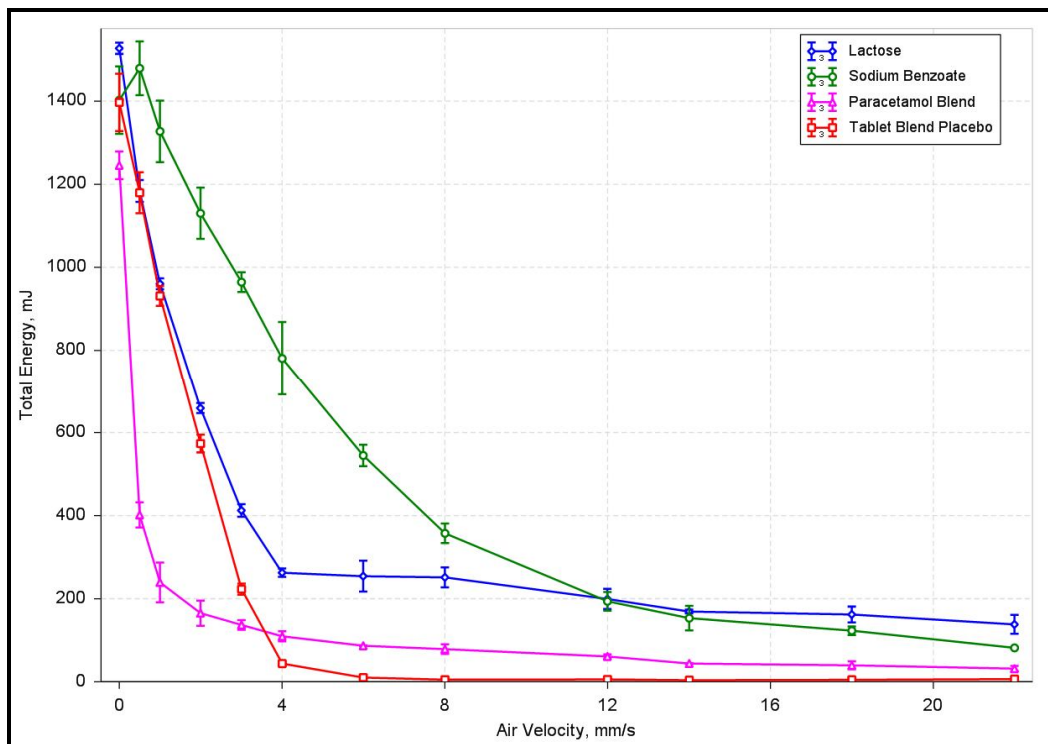


Figure 2.52: An aeration test where the flow energy of the sample is evaluated whilst increasing quantities of air are passed through the base of the test vessel

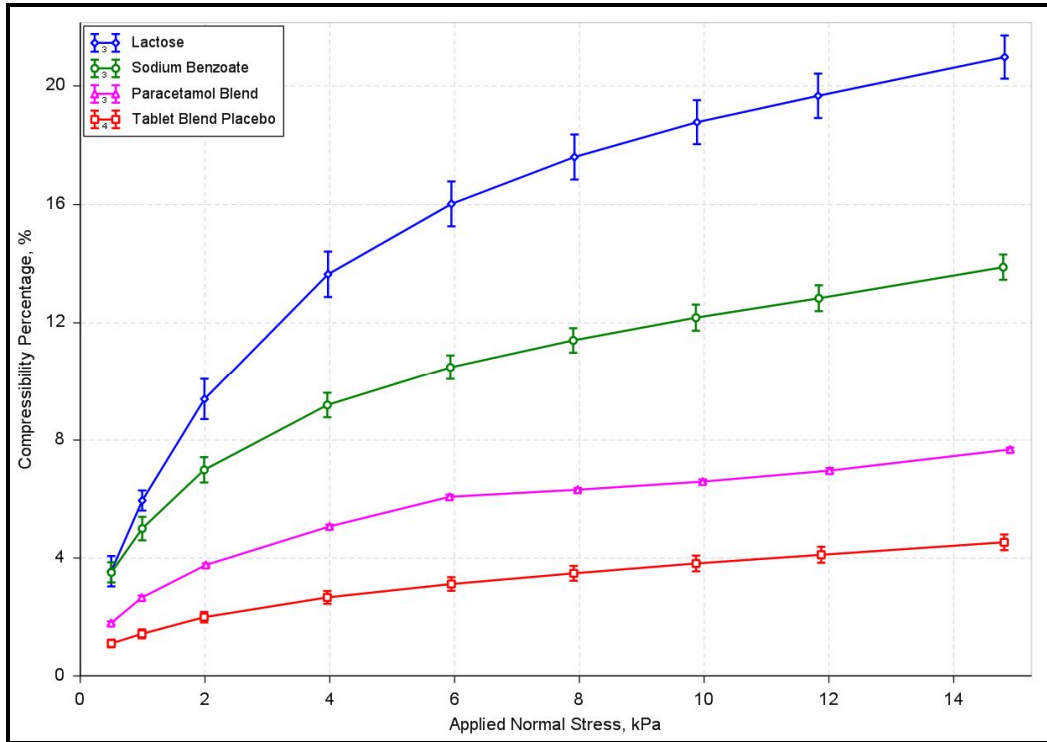


Figure 2.53: The compressibility of samples evaluated by change in volume with respect to an applied normal stress

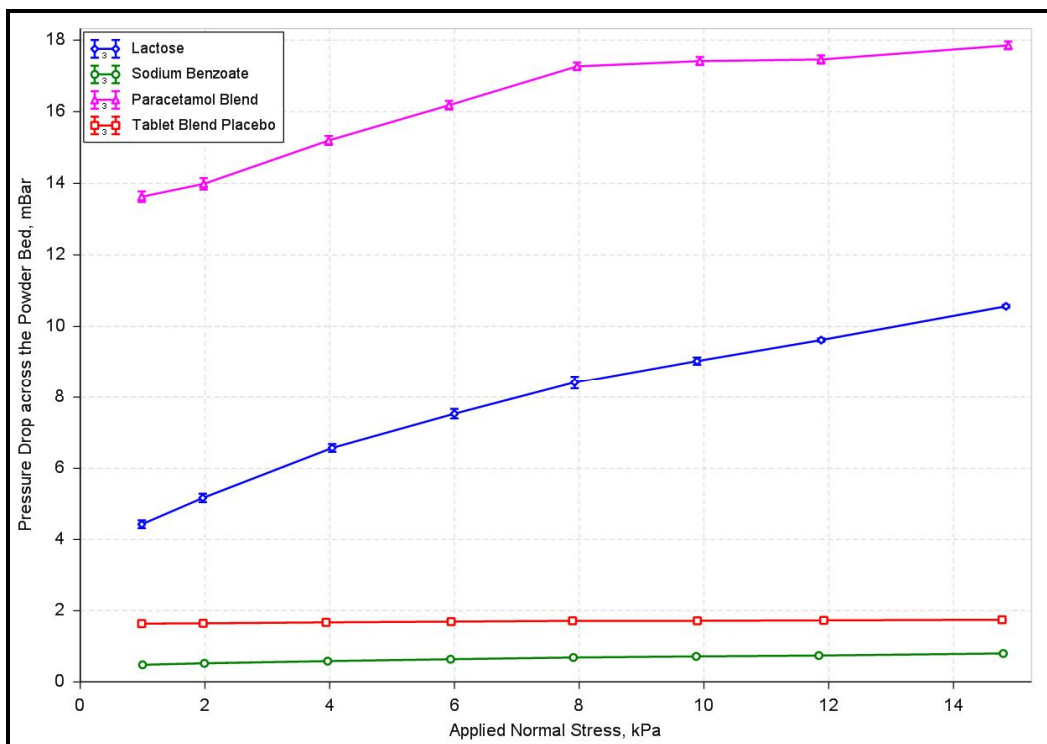


Figure 2.54: The pressure drop across the powder bed with respect to an applied normal stress.

Compared to the SMS PFA, the FT4 is significantly more advanced in its sample preparation and handling procedures, measurement techniques and its interpretation and presentation of data. It also appears to be significantly better at generating repeatable results as can be seen when the data for Sodium Benzoate is compared in Figures 2.47 for the PFA and Figure 2.51 for the FT4.

Further testing was thus carried out on the FT4 only, and data from testing the exemplar powders is shown in Table 2.16 for the dynamic testing results and Table 2.17 for the bulk properties results. Shear data has been previously presented in Table 2.8.

Table 2.16: Results for dynamic testing of the exemplar powders in aerated and non-aerated states (n=3 for all tests)

Test Material	AR ₂₂	<i>sd</i>	AE ₂₂	<i>sd</i>	NAR ₂₂	<i>sd</i>	BFE	<i>sd</i>	SI	<i>sd</i>	FRI	<i>sd</i>	SE	<i>sd</i>	CBD	<i>sd</i>
Avicel 102 Sample 1	426	155	47.6	3.37	0.0026	0.0008	1398	53	1.04	0.0073	1.2	0.0146	7.43	0.224	0.369	0.0014
Avicel 102 Sample 2	216	61.5	40.4	6.1	0.005	0.0013	1265	56.8	0.89	0.0553	1.04	0.125	5.93	0.271	0.372	0.0019
MCC	7.93	1.84	118	28.8	0.132	0.0248	1055	6	1.05	0.0578	2	0.0361	13.4	0.308	0.432	0.0022
Lactose	11.40	1.87	138	22.7	0.09	0.00145	1505	27.8	1.09	0.132	1.72	0.0142	10.3	0.254	0.69	0.0042
Sodium Benzoate	17.10	0.78	81.8	1.44	0.601	0.0153	1311	7.84	0.706	0.022	0.778	0.0447	9.04	0.131	0.292	0.0005
Celphere 102*	50.47	4.7	27.6	1.87	0.0198	0.0013	1606	28.8	1.01	0.0043	0.973	0.0082	3.21	0.0315	0.87	0
Celphere 305*	1.34	0.05	1087	15.1	0.745	0.01	1311	47.6	1.01	0.0032	1.02	0.0201	2.75	0.0754	0.902	0.0005
Sodium Bicarbonate	18.00	5.34	54.3	11	0.0584	0.0026	1195	37.4	1.09	0.0605	1.7	0.0148	8.95	0.244	0.805	0.0041
Fine Salt	21.20	1.04	70	2.99	0.0474	0.0023	1609	51.3	0.923	0.0189	1.06	0.0427	3.75	0.104	1.26	0.0017
Mannitol	5.33	0.292	164	1.72	0.188	0.0102	719	32.2	1.11	0.0372	1.87	0.0111	9.39	0.272	0.484	0.0095
Paracetamol Fine	3.43	0.247	481	4.07	0.293	0.0201	1015	49.5	0.968	0.0402	1.16	0.0443	9.05	0.568	0.369	0.0102
Paracetamol x-Fine	3.06	0.0256	511	13.4	0.327	0.0027	909	37.8	0.892	0.051	1.16	0.0946	9.99	0.205	0.325	0.0062
Paracetamol blend	41	8.15	78.6	11.5	0.0255	0.0058	1329	55.8	0.987	0.0328	1.03	0.0344	5.67	0.17	0.918	0.0037
Tablet Blend Placebo	239	73.3	5.15	1.36	0.0047	0.0017	1223	55.9	0.815	0.0834	0.829	0.0127	4.73	0.0818	0.533	0.0016

Table 2.17: Results for bulk property testing of exemplar powders (n=3 for all tests)

Test Material	CPD ₁₅ (%)	<i>sd</i>	BD ₁₅ (g/cc)	<i>sd</i>	PD ₁₅ (mbar)	<i>sd</i>	Perm ₁₅ (x 10 ⁹ cm ²)	<i>sd</i>
Avicel 102 Sample 1	12.5	0.308	0.415	0.0007	1.05	0.0112	118	0.411
Avicel 102 Sample 2	12.7	0.44	0.420	0.0013	0.95	0.0191	130	2.21
MCC	19.6	0.0908	0.505	0.0022	6.94	0.0506	16.3	0.114
Lactose	21	0.73	0.856	0.003	10.60	0.0391	10.6	0.133
Sodium Benzoate	13.9	0.424	0.344	0.0032	0.80	0.024	149	3.66
Celphere 102	3.11	0.0498	0.883	0.0013	1.21	0.0143	283	3.33
Celphere 305	2.37	0.0722	0.915	0.0011	0.19	0.0073	1802	68.7
Sodium Bicarbonate	15.8	0.574	1.010	0.0062	17.2	0.192	7.03	0.0617
Fine Salt	2.08	0.0925	1.290	0.0035	0.53	0.0175	263	8.67
Mannitol	29	0.687	0.747	0.0002	26.00	0.81	3.73	0.0471
Paracetamol Fine	35.2	0.408	0.551	0.0015	3.83	0.0575	22.7	0.294
Paracetamol Extra-fine	39.6	0.798	0.498	0.0058	4.07	0.0477	20.9	0.563
Paracetamol blend	7.69	0.0644	0.988	0.001	17.90	0.109	7.38	0.0407
Tablet Blend Placebo	4.68	0.0926	0.549	0.0007	1.75	0.0174	77.7	0.758

The data shown in Tables 2.16 and 2.17 and the highlighted data in Figures 2.51 - 2.54 indicate the high degree of repeatability that can be easily achieved by any operator. Figure 2.55 shows the data derived for the dynamic test for all the samples.

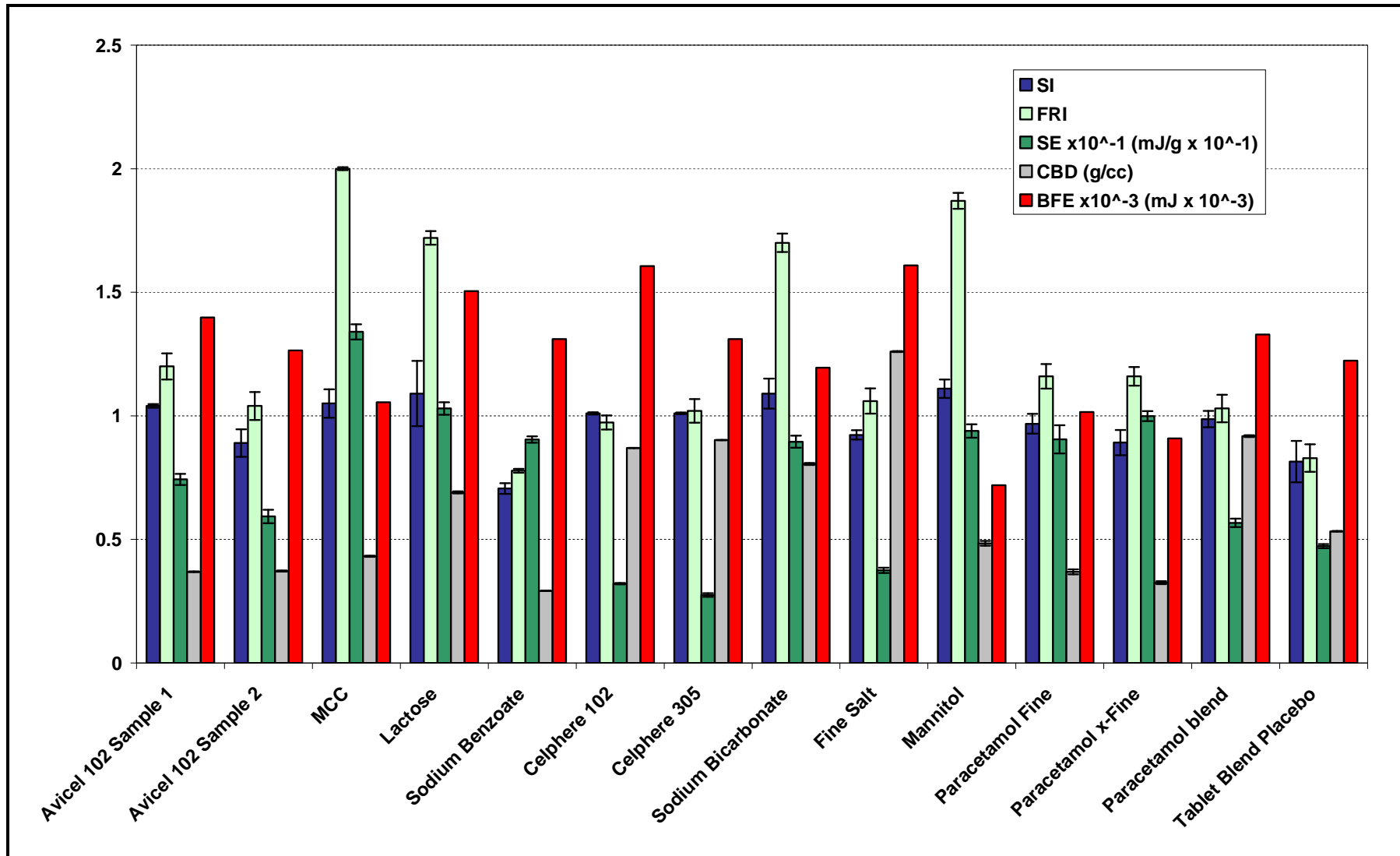


Figure 2.55: Dynamic test data generated by the FT4 Powder Rheometer

Each of the tests describes relative powder behaviour and this can be related to flowability depending on the magnitude of the result. Table 2.18 is a generalised view, with respect to dry powder, provided by Freeman Technology which indicates whether a high or low result can (generally) be interpreted as cohesive or non-cohesive behaviour. This ranking is, like all of the other rankings presented for other testers/instruments reviewed in this thesis, to be used as guidance and whilst it may be substantially correct there are invariably instances where the ranking is flawed due to some specific property of the particles or due to an outside influence such as moisture or electrostatics. Indeed, the exceptions to the norm clearly reinforce the viewpoint that there is no single, universal measurement that will characterise the combination of every possible powder in every possible circumstance.

These interpretations are, of course, simplified and it is accepted that they are not universal. For example, permeability is related to the packing regime of the powder system. If fine particles, such as those added to aid flowability (such as fumed silica), are present in significant quantities, then the interstices are likely to be filled creating a much denser packing regime which can greatly increase the resistance to the passage of air through the powder column – but the flowability of such a sample would more than likely be good due to the presence of the flow aid. The presence of such flow aids will also affect the wall friction result if significant amounts of fines are present at the shearing plane – as will the presence of moisture, which would, in this test, also tend to act as a lubricant rather than as an inter-particulate ‘glue’ as is the case in many other flowability tests.

In many ways these exceptions reinforce the concept that a number of measurements are required to fully characterise a powder and that a single measure of flowability is insufficient to predict behaviour in all circumstances.

Table 2.18: Interpretation of FT4 Powder Rheometer parameters for dry, unlubricated powders

Sub Group	Test	Parameter	Relative flowability
Dynamic	Stability and Variable Flow rate	Basic Flowability Energy (BFE)	See text
		Stability Index (SI)	See text
		Specific Energy (SE)	Low – flowable High – cohesive
		Flow Rate Index (FRI)	Low – flowable High – cohesive
		Conditioned Bulk Density (CBD)	N/A
	Aeration	Aeration Ratio (AR_n)	High – flowable Low – cohesive
		Aeration Energy (AE_n)	Low – flowable High – cohesive
		Normalised Aeration Energy (NAE)	Low – flowable High - cohesive
		Aeration Sensitivity (AS)	High – flowable Low – cohesive
	Bulk Properties	Compressibility	Compressibility (CPS_n)
Bulk Density (BD_n)			N/A
Permeability		Permeability ($Perm_n$)	High – flowable Low – cohesive
		Pressure Drop (PD_n)	Low – flowable High – cohesive
Shear	Powder Shear Testing	Flow Function (FF or ff_c)	High – flowable Low – cohesive
		Cohesion	Low – flowable High – cohesive
	Wall Friction Testing	Angle of wall friction (φ)	Low – flowable High – cohesive

The standard Dynamic test generates a range of parameters, as described in Table 2.18, but the signature parameter is the Basic Flowability Energy or BFE. It is a complex test and interpretation of the resultant information has been described by Freeman as ‘often not straightforward’ (Freeman 2007).

The flow pattern established during the BFE test is a downward anticlockwise motion – often described as a ‘bulldozing’ action. This ensures the powder is pushed forwards and downwards in front of the blade, in a relatively high stress flow mode. The resulting resistance to flow is dependant on the many physical characteristics of the powder and the way in which they interact – size; shape; surface texture; electrostatics; moisture etc, but especially packing structure.

It is often assumed that a low BFE represents a powder with “good” flow properties and a high BFE, a powder that will flow poorly. In many cases this is true, particularly if the difference between powder samples is due to particle surface texture or amount of flow additive. However, the opposite can also be true, where powders that flow freely under gravity result in a high BFE and powders that are cohesive, a low BFE.

One of the most influential physical property variables is particle size and it is well understood that powders consisting of small particles are often more cohesive. Conversely, powders with a larger particle size behave in a less cohesive way and the particles typically pack in an efficient manner. The competition between inter-particulate and gravitational forces significantly influences the packing efficiency of the powder bulk.

The shape of the blade is such that this downward motion is highly compressive and because the powder is “confined” due to the closed base of the vessel, the compressibility of the powder plays a major role in the BFE.

Figures 2.56 and 2.57 show how the flow pattern is transmitted through cohesive and less compressible powders.

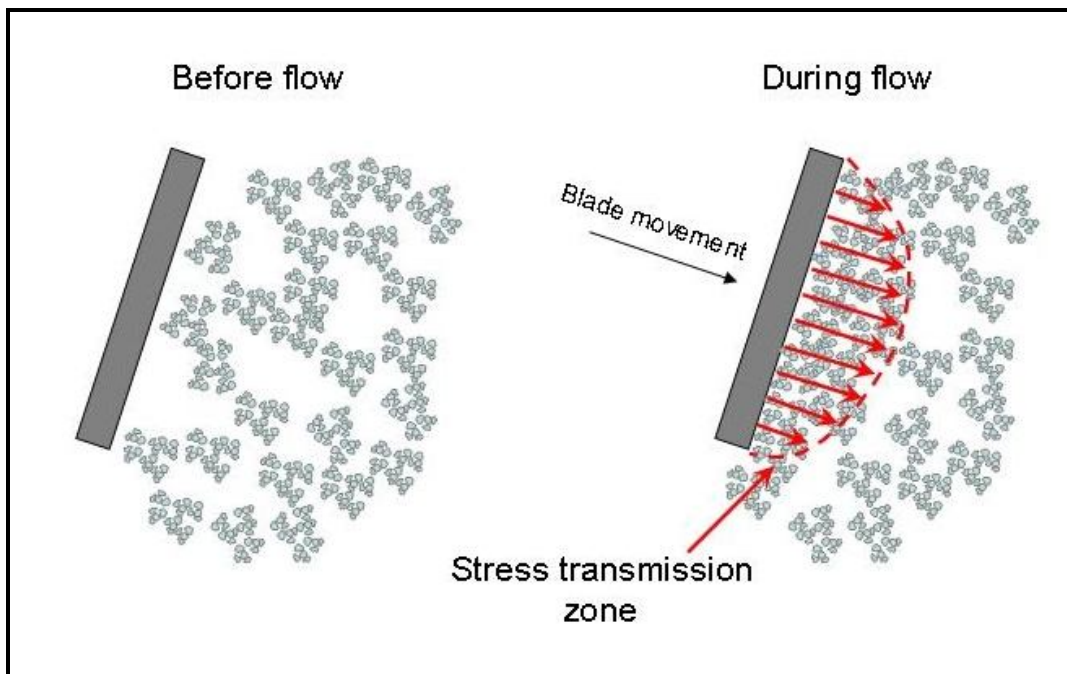


Figure 2.56: Action of test blade on a cohesive/compressible powder

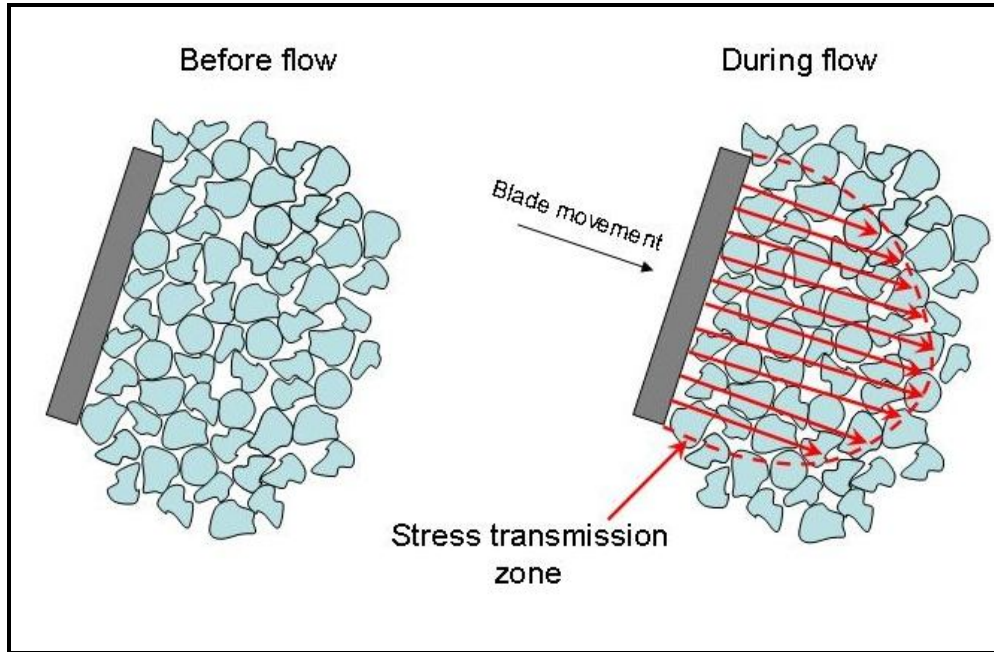


Figure 2.57: Action of test blade on a non-cohesive/non-compressible powder

For cohesive powders, the particles forced to flow at the blade face can be accommodated by the air pockets that exist between agglomerates. The resulting flow or stress transmission zone is relatively localised.

For non-cohesive powders which are packed efficiently, flow induced in particles at the blade face can not be accommodated by pockets of excess air as they are not present in efficiently packed powders. Therefore the flow zone is transmitted far ahead of the blade, deep into the powder bulk. The resulting high number of friction surfaces and high contact stresses contribute significantly to the BFE.

These modes of flow have been observed and videoed and are presented on the Freeman Technology website (www.freemantech.co.uk).

It is for this reason that a counter-intuitive trend of “good” flow – high BFE is sometimes observed. However, this trend is only seen when comparing powders of very different natures – less compressible powders compared to compressible powders.

For nearly all other variables (apart from size) the trend observed with the BFE is intuitive.

This rationalisation by Freeman is arguably, just that – a rationalisation of observed trends without the ability to quantify the behaviour fully or to predict behaviour from the knowledge of other parameters. This is a potential weakness of powder rheometry as the interpretation of the results is not clear cut. However, behaviour of powders is also not clear cut, and Freeman would argue that the characterisation of powder absolutely requires a dynamic insight, especially as they are processing in a dynamic fashion in mixers, dryers, transfer systems etc where an understanding of the resistance to flow in an unconfined state where the powder can move and flow in a less restrictive environment (compared to that of a shear cell, for example) is extremely useful.

Recent Discrete Element Modelling (DEM) of the FT4 Powder Rheometer (Bharadwaj, Ketterhagen, & Hancock) has opened the way to a more detailed explanation of the results generated by powder rheometers based on the physical properties of the powder. Their results showed good agreement with the

experimental data, within the limitations of the modelling capabilities (number of particles, surface interactions etc) and the test materials – glass ballotini.

This uncertainty of the meaning of the data is also apparent when in the interpretation of the Flow Function of some powders, where the flowability of the powder improves at higher consolidating stresses – most of the data presented in Table 2.9 and Figure 2.13 displays this pattern. This can be quite easily rationalised if one considers the balance between the mass acting on the powder with respect to the additional gain in strength achieved due to this additional mass, but for the non-expert this is not an obvious progression. Indeed how does one know what stress to consider as being relevant to any of the particular processes that might be used to handle or modify a powder? Such calculations are available for the filling and emptying of storage vessels,

2.4. Comparative evaluation of powder testers

The direct comparison of the how each of the powder testers ranks the exemplar powders is shown in Table 2.19 and graphically in Figure 2.58.

Presented with such a Table of rankings many people will be tempted to generate a single, all encompassing, number to summarise the results – or suggest that one tester is better than another because its results conform to the users preconceptions of which powders flow better than others.

As has been mentioned earlier in this thesis, this is an inappropriate way to consider these testers and data. All of the results – as long as the test methodology is robust and the data repeatable – have specific uses and describe the powder behaviour under specific conditions. The shear tester generally looks at high stress conditions; the powder rheometer looks at dynamic behaviour in loosely packed structures; the Jolting Volumeter shows how powders will pack when subjected to vibration; the AOR shows the shape of a pile that will be formed when the powder falls under gravity; the Aeration Energy describes the effect of air on the powder.

**Table 2.19: Ranking of exemplar powders according to flowability defined by the test method
– low values indicating greater relative flowability**

Test Material	Angle of Repose	Carr's Index	Flow through an orifice	Cohesion	ff _c	Basic Flowability Energy	Specific Energy	Aerated Energy	Permeability	Compressibility	Total
Avicel 102 Sample 1	5	5	6	5	3	4	7	4	5	6	50
Avicel 102 Sample 2	6	6	5	6	7	8	6	3	4	7	58
MCC	9	11	7	13	13	11	14	9	10	10	107
Lactose	11	9	9	9	9	3	13	10	11	11	95
Sodium Benzoate	10	8	11=	11	10	6=	9	8	3	8	67
Celphere 102	2	3	2	2	1	2	2	2	6	3	25
Celphere 305	1	2	3	4	5	6=	1	14	1	2	33
Sodium Bicarbonate	8	10	8	8	8	10	8	5	12	9	86
Fine Salt	3	1	4	3	6	1	3	6	2	1	30
Mannitol	14	14	11=	14	14	14	11	11	14	12	118
Paracetamol Fine	13	12	11=	10	11	12	10	12	8	13	101
Paracetamol Extra Fine	12	13	11=	12	12	13	12	13	9	14	110
Paracetamol blend	7	7	10	7	4	5	5	7	13	5	70
Tablet Blend Placebo	4	4	1	1	2	9	4	1	7	4	37

An interesting comparison is shown in Figure 2.58 which compares the two universal testers – the shear cell and the powder rheometer – with, arguably, the most reliable of the restricted tests, Carr's Compressibility Index. There are some clear similarities between the results of the three tests where samples are categorised in broadly the same way – the two grades of paracetamol show poor flow characteristics for all three tests, however the inter-relationship of the test results for the freer flowing powders is not as clear cut. In addition, the CCI value for the Sodium Bicarbonate indicates poor flowability, which is not replicated by shear or powder rheometry testing.

In order to show these inter-relationships more clearly, the data has been normalised relative to each particular tests' value for the paracetamol extra fine such that all three data sets present a high value as more free flowing according to their typical descriptors presented earlier in this Chapter. Figure 2.59 shows these interrelationships and it is clear that the low stress powder rheometry test has a relatively small spread of results, whereas the high stress tests (shear and CCI) have a much larger spread for the range of samples. The three tests also seem to rank the more cohesive samples similarly and it is the freer flowing samples that generate disparate flowability results – for example the fine salt and Celphere 305 are shown as the freest flowing by their CCI values whereas the shear test indicates that the Tablet Placebo is by far the freest flowing.

Again what this demonstrates is that the testing conditions have a significant influence on the relative outcome and that multiple types of tests should be conducted to ensure the gamut of powder behaviour is captured.

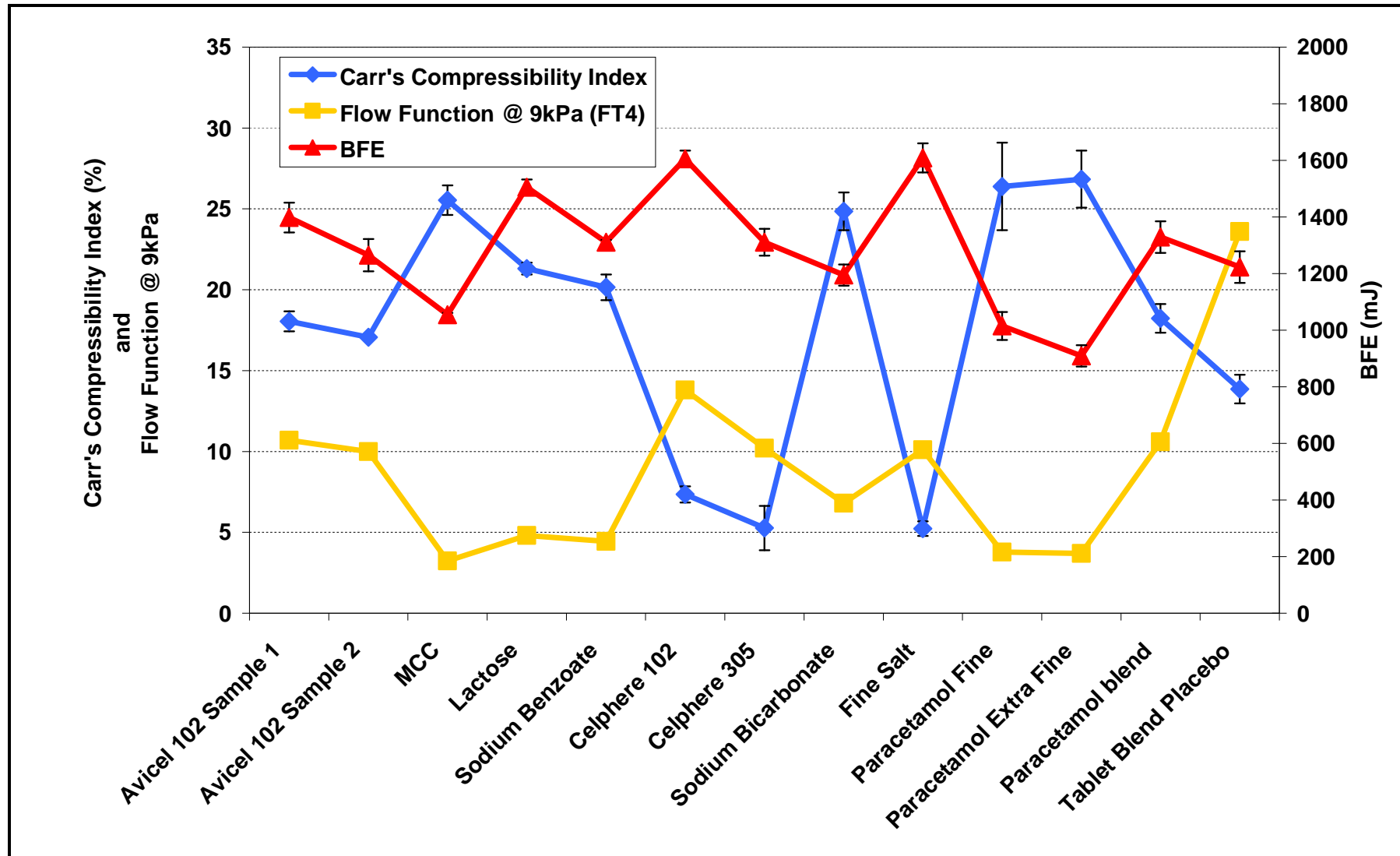


Figure 2.58: Comparison of the Flow Function, BFE and Carr's Compressibility Index for the exemplar powders

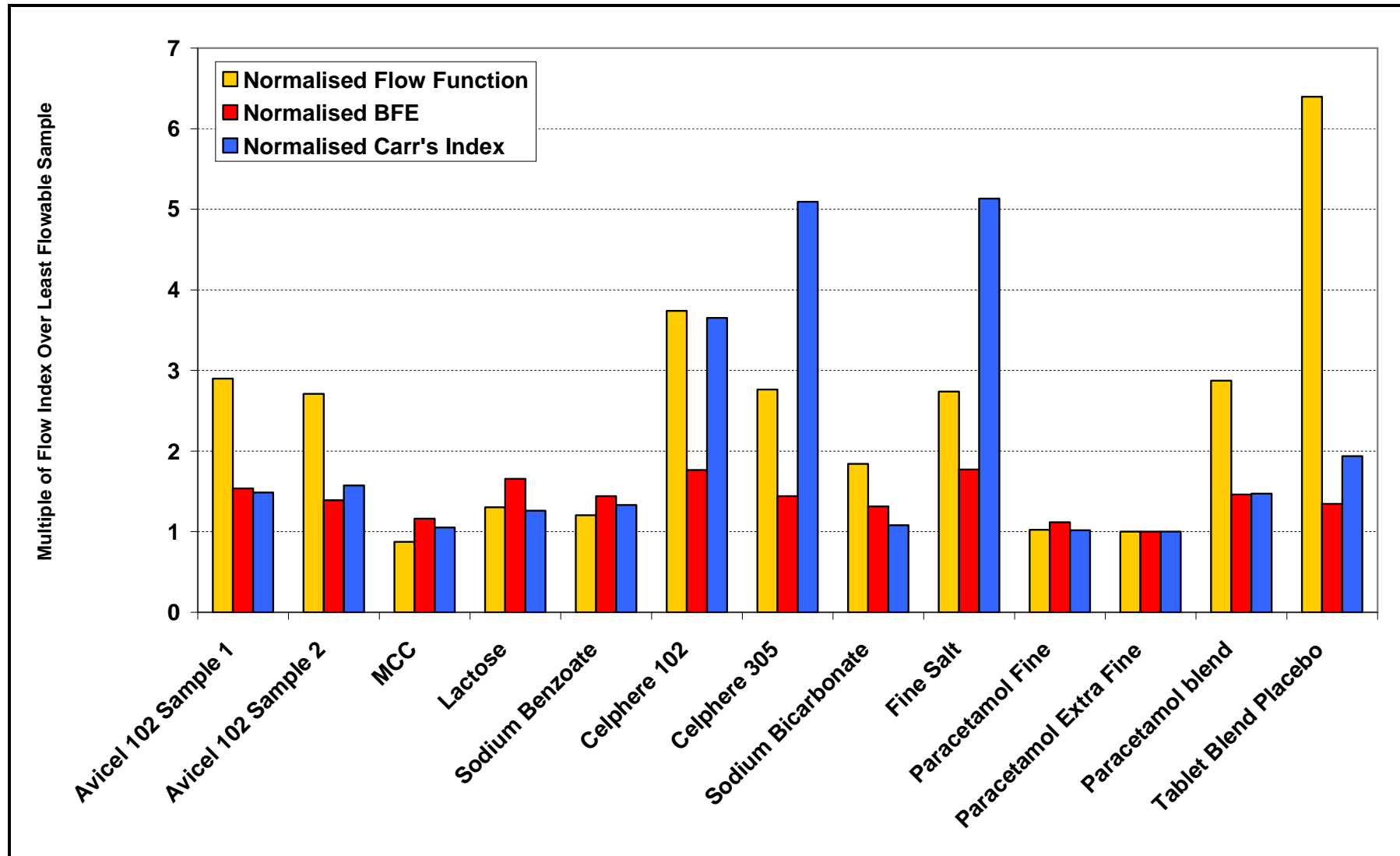


Figure 2.59: Comparison of results from shear cell, powder rheometer and Jolting Volumeter

The ability to visualise several relative properties of a number of powders is difficult – as seen in Figures 2.55 and 2.60 (which is almost impossible to read).

An alternative might be the combination of all the relative rankings for all the tests, as shown in the last column of Table 2.19 which is visually presented in Figure 2.61. As long as the rankings are configured in the same direction (say, ‘bad to good’) for each test method, the use of such a summation should provide a consistent relative view of the materials. In this instance a low value indicates a powder is freer flowing over the entire range of tests. This approach was taken by Taylor (Taylor *et al.* 2000), however there are inherent dangers as it may mask the powder characteristic specific to a particular operation or transfer process and powder combination, thus limiting the usefulness as an investigative tool.

Thus a more suitable form of presentation of large quantities of multivariate data is also required and this will be discussed further in Chapter 4.

Analysing what happens to a powder as it progresses through any given unit operation, or set of unit operations, will identify the range of tests that may directly relate to the stress condition, air flows, vibration, shear rates etc. Thus work has confirmed that no single test or ranking can adequately describe all the ranges of behaviour, (Prescott & Barnum 2000b), (de Silva 2000) (Krantz, Zhang, & Zhu 2009b). All of these tests will give an insight into the likely behaviour of the powder. This analysis is also discussed more thoroughly in Chapter 4.

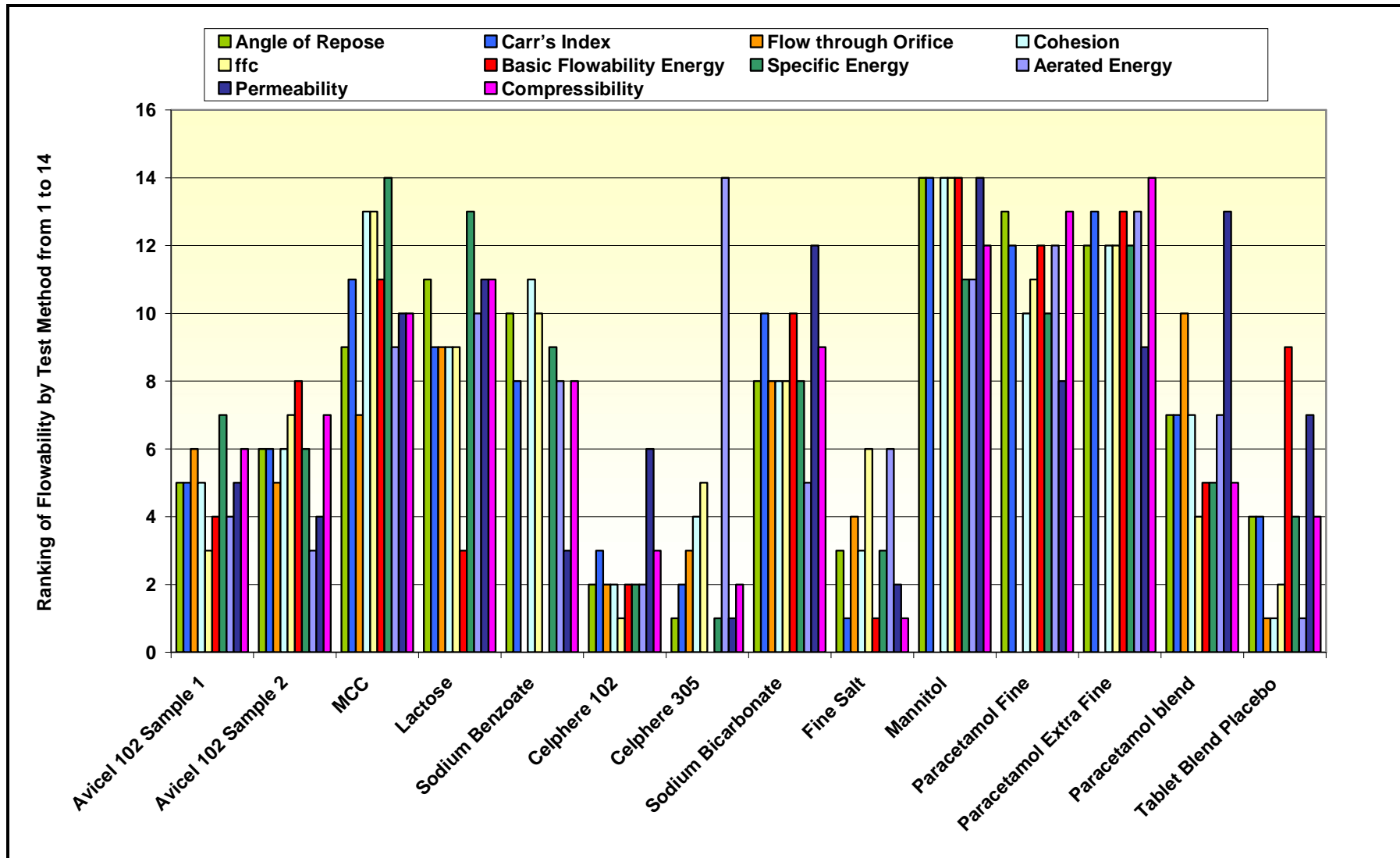


Figure 2.60 Ranking of exemplar powders according to flowability defined by the test method
 - low values indicating greater relative flowability

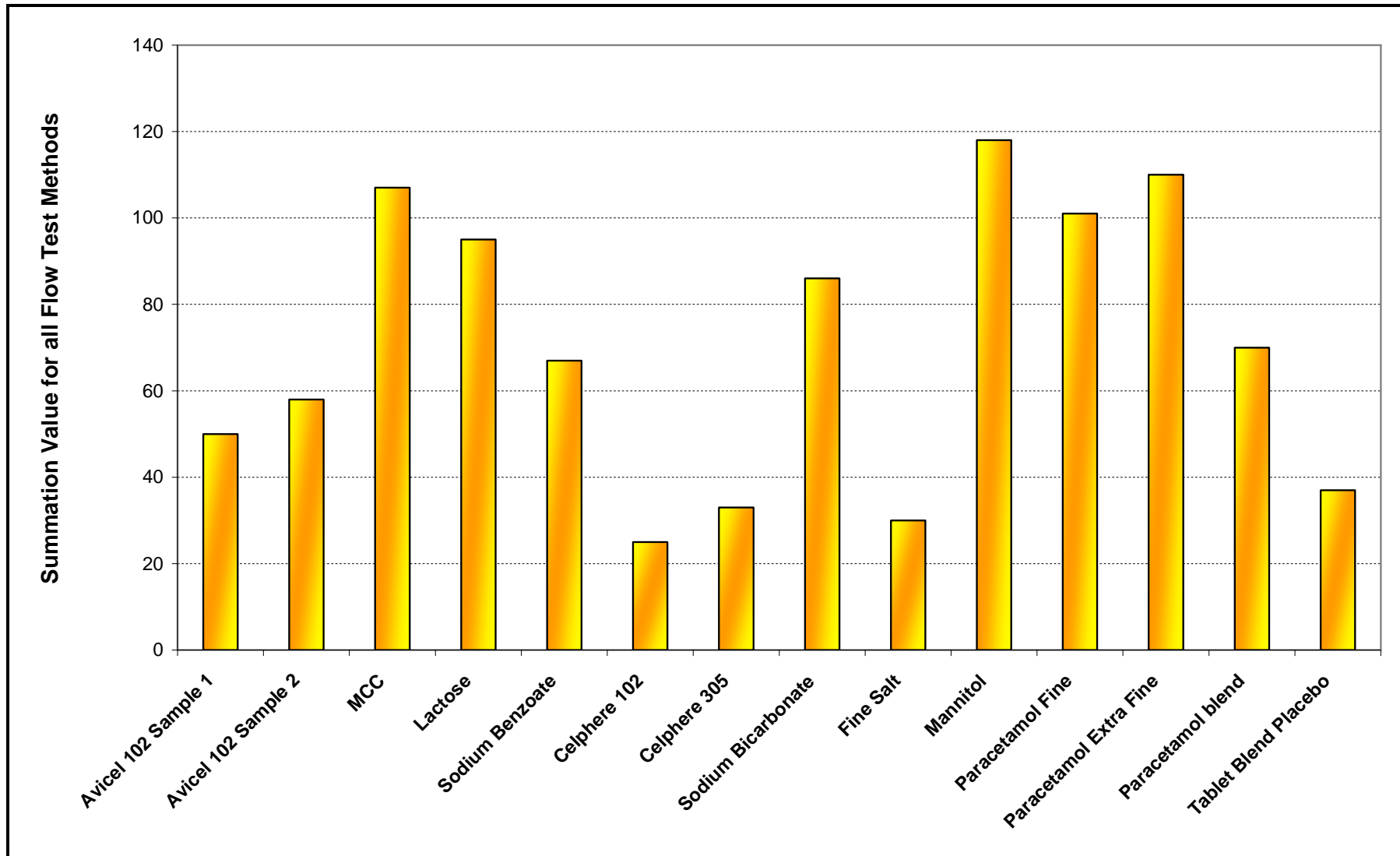


Figure 2.61: Comparison of relative flowability by additive combination of ranking levels for all tests shown in Table 2.19

2.5. *An evaluation of the comparative effectiveness of universal powder testers*

It is clear from the evaluation of the testers and instruments that there are two main categories into which each can be placed;

- **Universal testers** – these instruments can evaluate any powder which can be practically loaded into their test environment.
- **Restricted testers** – these devices cannot generate data on all powders even if they can be practically loaded into their test environment.

In realistic terms, it is likely that GEA/Niro would require some, or all, of the Pharmacopoeia specified testers in order to have a ‘frame of reference’ with which they could discuss powder behaviour with clients who use such devices on a regular basis. Having said that, the limitations of simple testers has been demonstrated, especially with respect to their universality and their inability to differentiate powders. There is, therefore, a need to utilise the capability of one or more of the universal testers because, as previously indicated, the new FDA initiatives dictate a need to gain greater insight into bulk powder properties. The choice of tester falls between

- the PFA,
- a dedicated shear cell such as the RST-XS and
- the FT4 which features the functionality of both testers noted above plus additional bulk property measurement capability.

Despite the strong theoretical basis of the shear cell, there are many instances where such a device alone is insufficiently sensitive to capture differentiating behaviour as for example, described by Tuley *et al* (Tuley *et al.* 2008) with regard to characterising the shear dispersal of inhalable pharmaceuticals. In these cases the powder rheometry approach has significant advantages as some of the following examples will demonstrate. Other examples will show where the shear cell does indeed provide the best representation of differences in powder property, and cases where permeability is the best measure of difference.

There is also the issue of the variability between shear cells with different configurations and/or supplied by different manufacturers (Schmitt & Feise 2004; Schwedes 2003), which has not been the case for the samples and instruments tested in this thesis but could still be a potential issue with respect to choice of supplier.

The question might be asked however 'what use is being able to differentiate between powder samples if you don't know what that differentiation means?' The ability to identify a difference between feedstocks or products which either give processing problems or out-of-spec product is the vital first step if you are to trace and solve the problem. If ones methods of testing powder show no difference between batches which will process and those that will not, then the problem cannot be addressed. Sensitivity and reproducibility are, therefore, key attributes for any instrument.

A series of examples are presented using materials that have not been part of the previous study, but have minor formulation changes which have resulted in reported processing problems. One of the major requirements of any testing system is the ability to differentiate such, apparently, identical materials when they engender anomalous processing behaviour. Complete details of the processes or powders were not provided due to commercial sensitivities, but for all the examples below the differences in process and product performance could not be rationalised from the suite of testing available to the commercial entities (typically size distribution by laser diffraction; angle of repose; Carr's compressibility index; flow through and orifice).

2.5.1. Pharmaceutical grade Zinc Oxide

Two examples of zinc oxide from different suppliers were being used as part of a continuous processing development programme, the initial step of which was to reliably feed a number of excipients into a continuous granulator and examine the limits of the granulator process performance with respect to the feed rate. The feed of the excipients into the granulator was undertaken by single screw loss-in-weight feeders. It was noticed that the quality of the product, both in terms of content uniformity and granule friability varied significantly, not only depending on which zinc oxide was used but also how fast each sample was processed through the loss-in-weight feeder. As this was a development project, exact details of the granulation process and the other excipients were restricted.

Samples which had undergone processing through a loss-in-weight feeder at two extremes of the feeder's operational speed range were evaluated. These processed samples, together with unprocessed samples, of both materials were tested using the dynamic and shear capabilities of the FT4 Powder Rheometer. The sample details are shown in Table 2.20.

Table 2.20: Summary of Zinc Oxide materials tested

Powder Description	Material A			Material B		
Material I/D	Unprocessed	Low Speed	High Speed	Unprocessed	Low Speed	High Speed
Sample Number	2	4	1	6	3	5

The size distributions of both materials are virtually identical and are 99.95% below 42microns, based on the supplier's specifications. No detailed size distributions were provided. They are both white powders with a tendency to form weak agglomerates.

The results of the dynamic test are shown in Figure 2.62 and exhibit several interesting points. The test can easily differentiate between the three processing conditions within each sample and between the two materials. All material A samples have a lower flow energy than material B samples for the equivalent condition – unprocessed: processed high speed; processed low speed.

When comparing dissimilar materials, high flow energy can indicate a more free flowing material, however when comparing minor physical or formulation changes in

the same material, as is the case here, then higher flow energy usually means poorer flow properties.

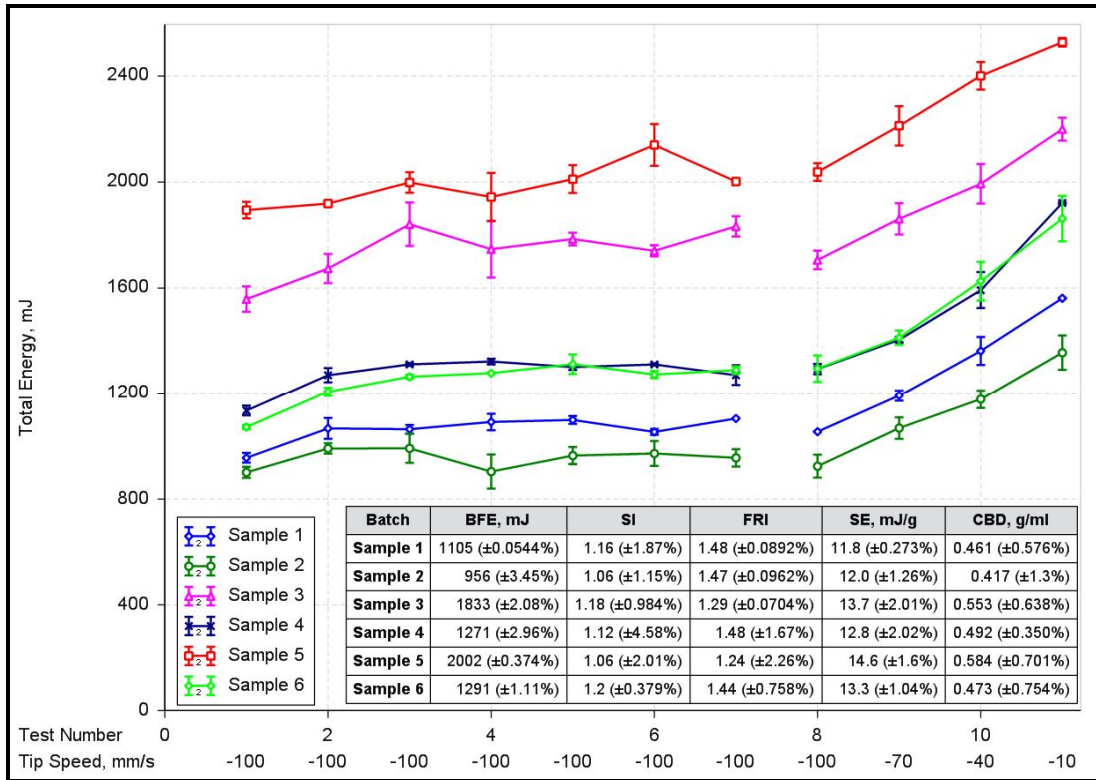


Figure 2.62: A dynamic test for the zinc oxide powders showing 7 repeat tests at a blade tip speed of 100mm/s to evaluate the powders flow stability, followed by 4 tests at reducing blade tip speed from 100mm/s to 10mm/s

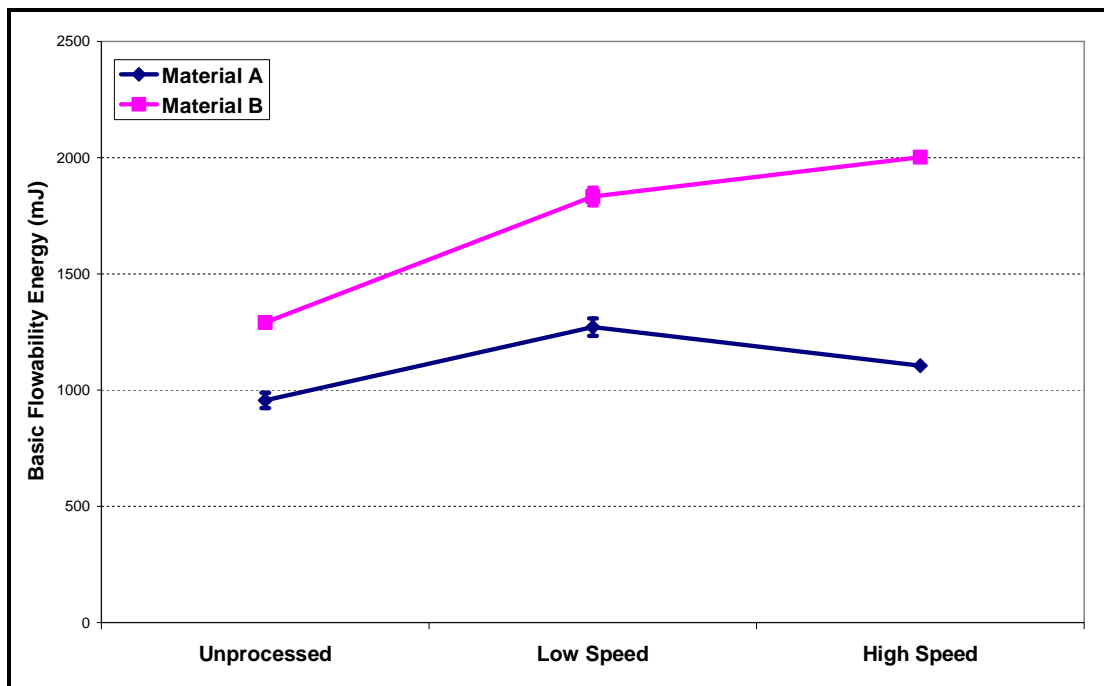


Figure 2.63: Comparison of the Basic Flowability Energy for the two Zinc Oxide materials at three different feeder speeds.

Figure 2.63 shows the relative behaviour of the two samples and, as can be seen, this test clearly differentiates the two materials both in terms of each other but also with respect to each materials processed state.

Interestingly the order of flow energies for the two samples is different as shown schematically in Figure 2.64.


	Material A	Material B
Increasing flow energy 	Unprocessed	
	High Speed	
	Low Speed	Unprocessed
		Low Speed
		High Speed

Figure 2.64: Relative Flow Energies of the two Zinc Oxide materials

The unprocessed samples are always lower than the processed samples for both materials, but the impact of processing each material through the loss-in-weight feeder shows that the rate at which each sample has been sheared ('speed' of loss-in-weight feeder) affects the BFE differently for each material.

In contrast the shear testing does not show this relationship as demonstrated in Figures 2.65 and 2.66.

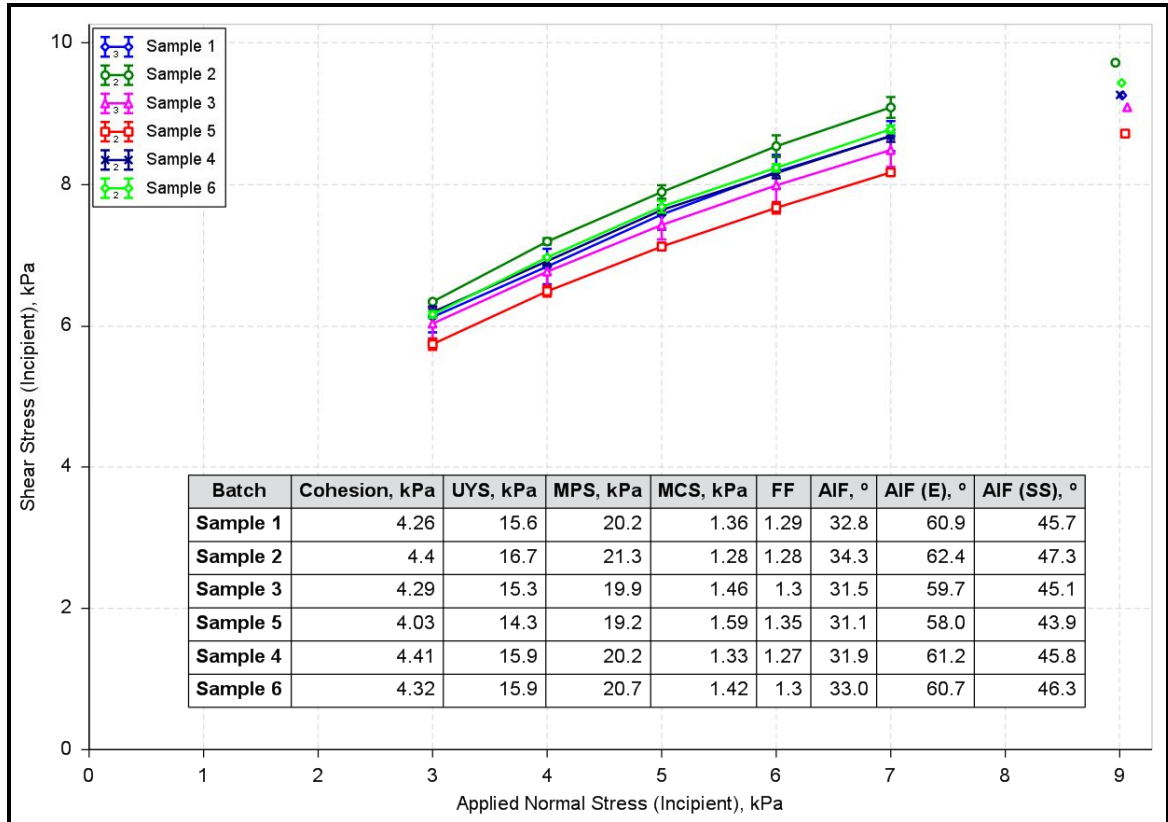


Figure 2.65: Yield loci for Zinc Oxide samples generated using the FT4 shear cell at 9kPa consolidating load

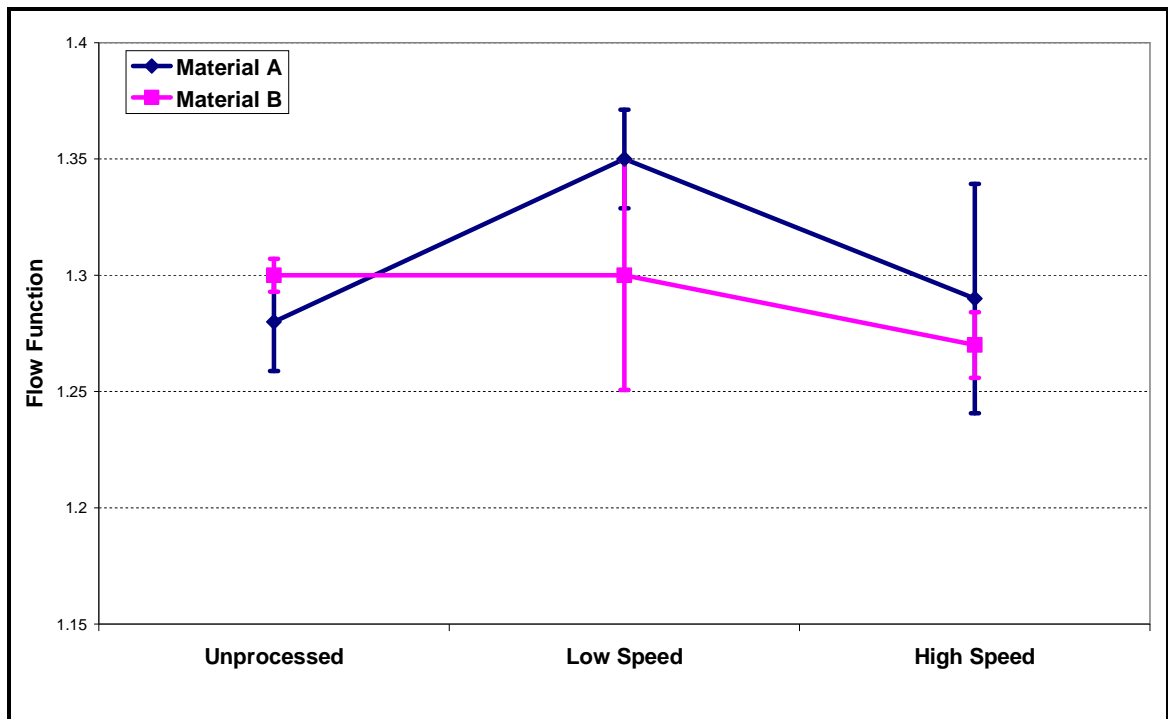


Figure 2.66: Comparison of the Flow Function for the two Zinc Oxide materials at three different feeder speeds.

The yield loci or the derived parameters do not represent clear distinctions between the different samples and thus their interpretation is less straight forward. This is due to the relatively high normal stress and pre-shearing regime which removes most of the influence of variability between the samples, previously observed with the unconfined testing methodologies, as any agglomerates are unlikely to survive these conditions. Material B processed at high speed (sample 5) arguably shows lower shear stresses than the other samples and would likely show slightly improved flow at this higher stress than the other samples, but it is very difficult to differentiate between the other samples.

This also illustrates one of the more frustrating aspects of the interpretation of shear data – which of the outputs of the curve fitting routine actually tells the user which powder will behave better in a given situation; absolute shear stress values?; cohesion?; flow function?; angle of internal friction? None of these parameters, displayed in the embedded table in Figure 2.65, can provide the degree of differentiation that can be seen for the dynamic testing in this particular instance. Indeed, despite the obvious positional variation of the yield loci, the derived parameters show surprisingly little differentiation as demonstrated by the plot of Flow Function against feeder speed in Figure 2.66.

The processing of the material B through a loss-in-weight feeder appears to have a more pronounced effect on its powder characteristics than it does for the material A. It is likely that the screw speed in the loss-in-weight feeder will greatly affect the

population balance of agglomerates. Considering the data presented in Figure 2.63, material B shows a steady increase in BFE with respect to feeder speed, which, as described earlier in this Chapter, usually relates to an increase in the particle size or number of agglomerates. In this instance the rate of creation of agglomerates caused by the stress regime imposed by the loss-in-weight feeder is greater than the rate of destruction of agglomerates in the same regime. Material A reaches a maximum BFE for the low speed feeder configuration, so it can be surmised that the rate of destruction of agglomerates is greater than the rate of creation for the high speed condition due to the lower BFE. Although there are no supporting size analyses for this evaluation (size measurement of agglomerates is notoriously difficult due to their fragility), the resultant reported (confidential) dispersion of this material within the downstream granulation environment supports this analysis.

In this case the Dynamic testing of the powders has shown a significant insight into the processing of these powders.

2.5.2. Pharmaceutical excipients

The evaluation of two excipients Vanillin and Ethyl Vanillin have also been studied. These materials are used as flavouring agents in tablet manufacture and both materials were being considered for a new formulation, but the relative flow behaviour of the two samples was unknown. The formulator therefore decided to have the samples tested to see if there was any indication of potential issues to using either material in the existing process train.

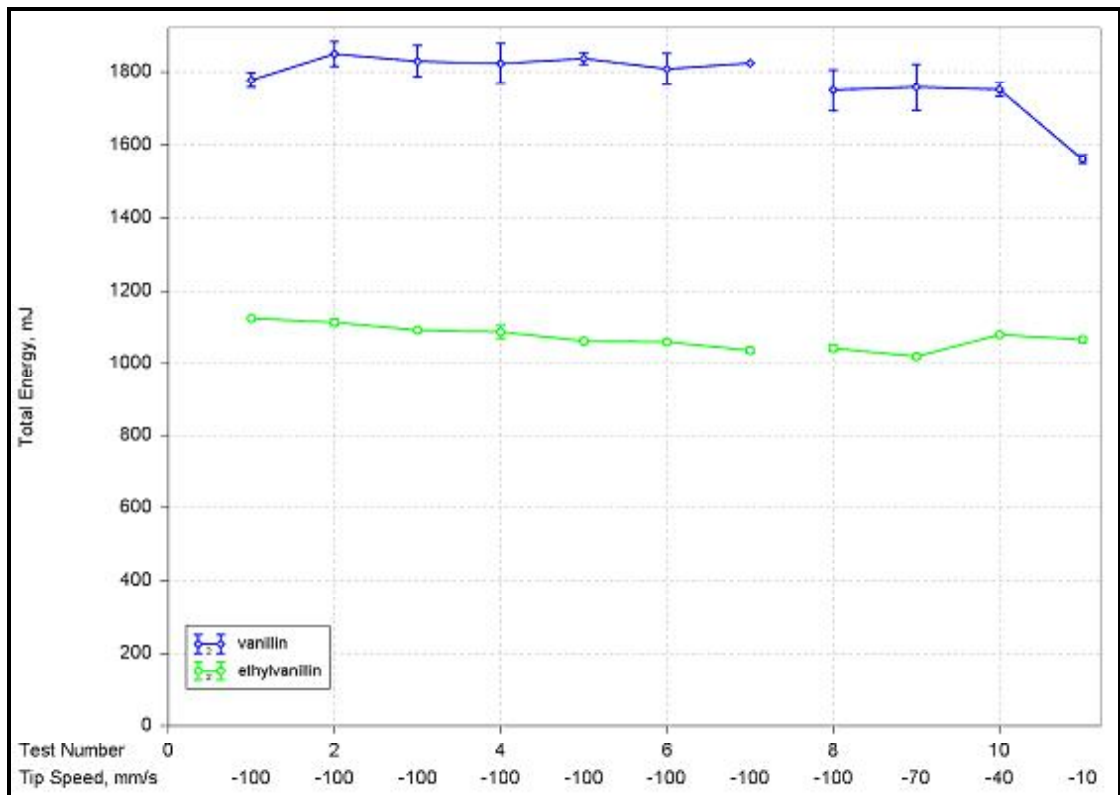


Figure 2.67: A dynamic test for the Vanillin and Ethyl Vanillin powders showing seven repeat tests at a blade tip speed of 100mm/s to evaluate the powders flow stability, followed by 4 tests at reducing blade tip speed from 100mm/s to 10mm/s

As can be seen from Figure 2.67, there is a distinct, 800mJ, difference in the flow energies measured, but the yield loci shown in Figure 2.68 are, for all intents and purposes, identical.

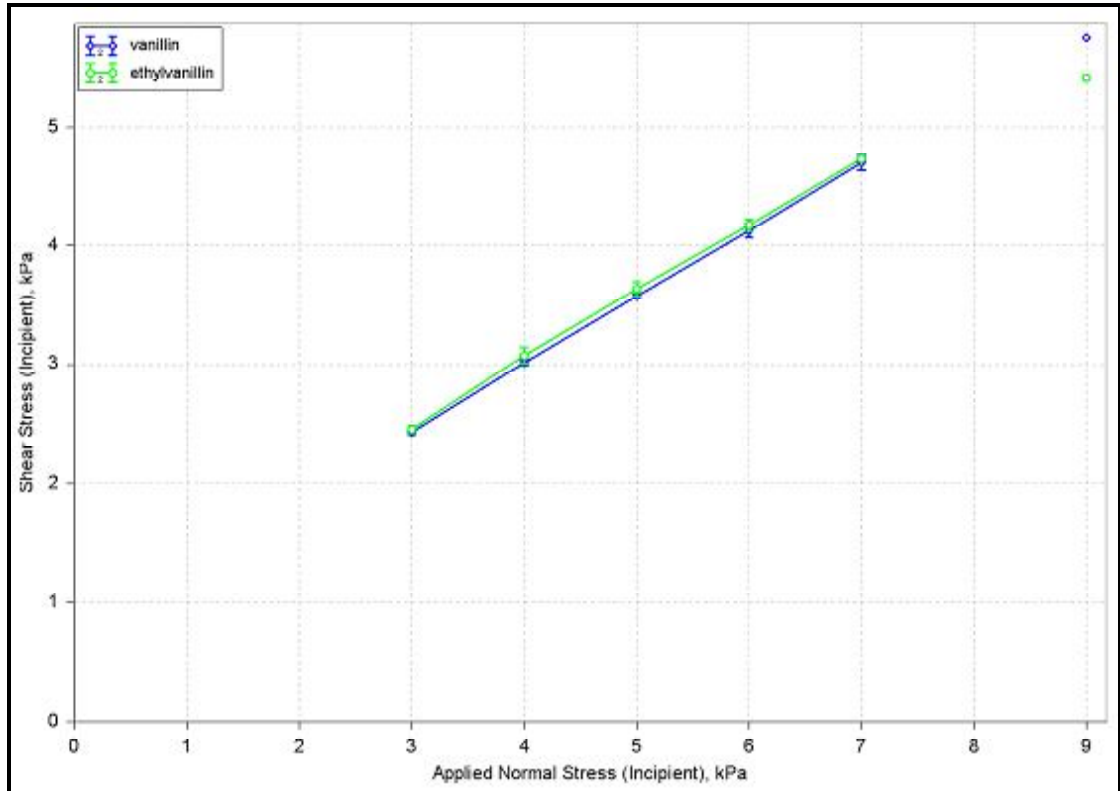


Figure 2.68: Yield loci for Vanillin and Ethyl Vanillin samples generated using the FT4 shear cell at 9kPa consolidating load

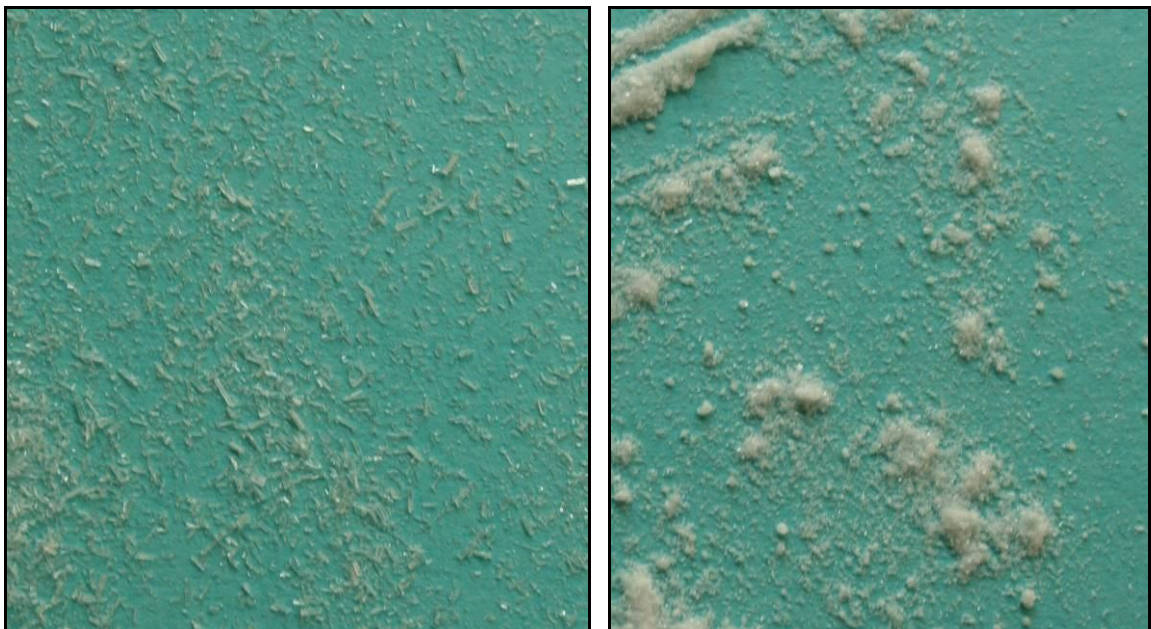


Figure 2.69: Photographs of the particles of Vanillin (l) and Ethyl Vanillin (r)

The photographs of the particles in Figure 2.69 indicate the two materials have significantly different morphologies. The Vanillin has long crystalline needles with a high aspect ratio; the Ethyl Vanillin has spherical particles of a much smaller particle size.

In addition, size and shape data was evaluated using a Sympatec Qicpic instrument. Figures 2.70 and 2.71 show a selection of the typical shapes evaluated for the Vanillin and Ethyl Vanillin respectively. Figure 2.72 shows the shape vs. size variation for three repeat tests of the two materials.

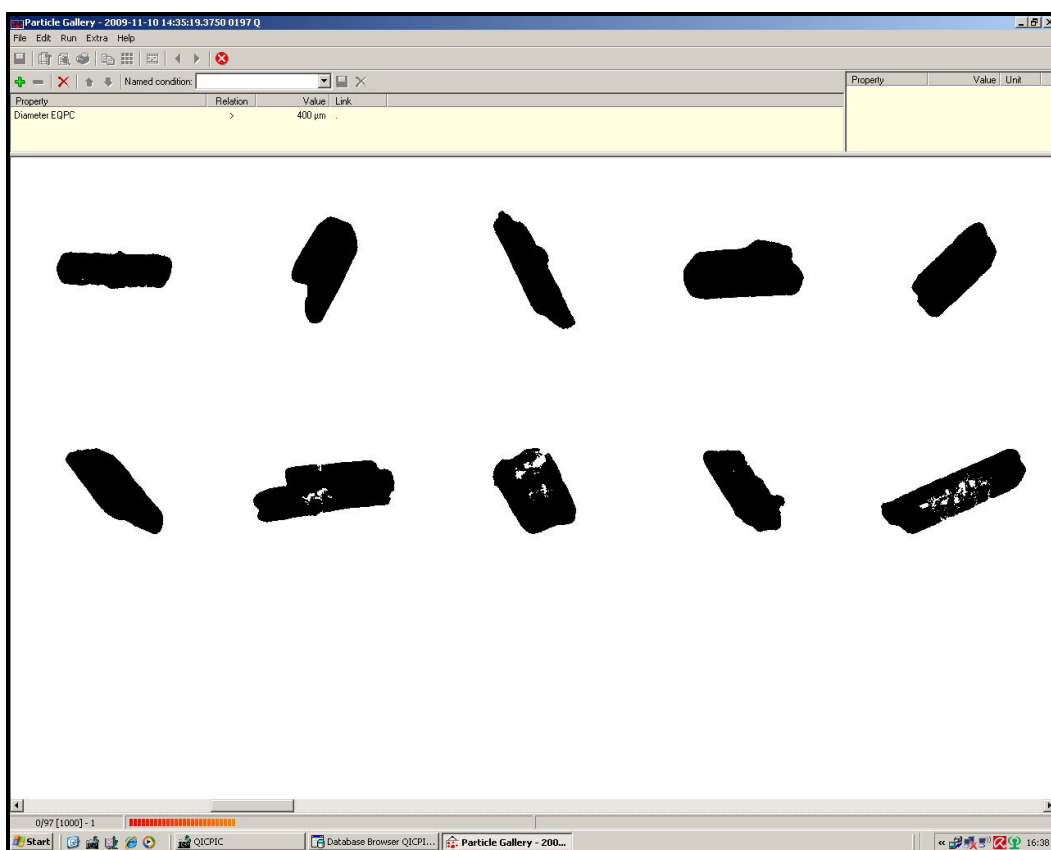


Figure 2.70: Selection of CCD images of Vanillin generated by Sympatec Qicpic

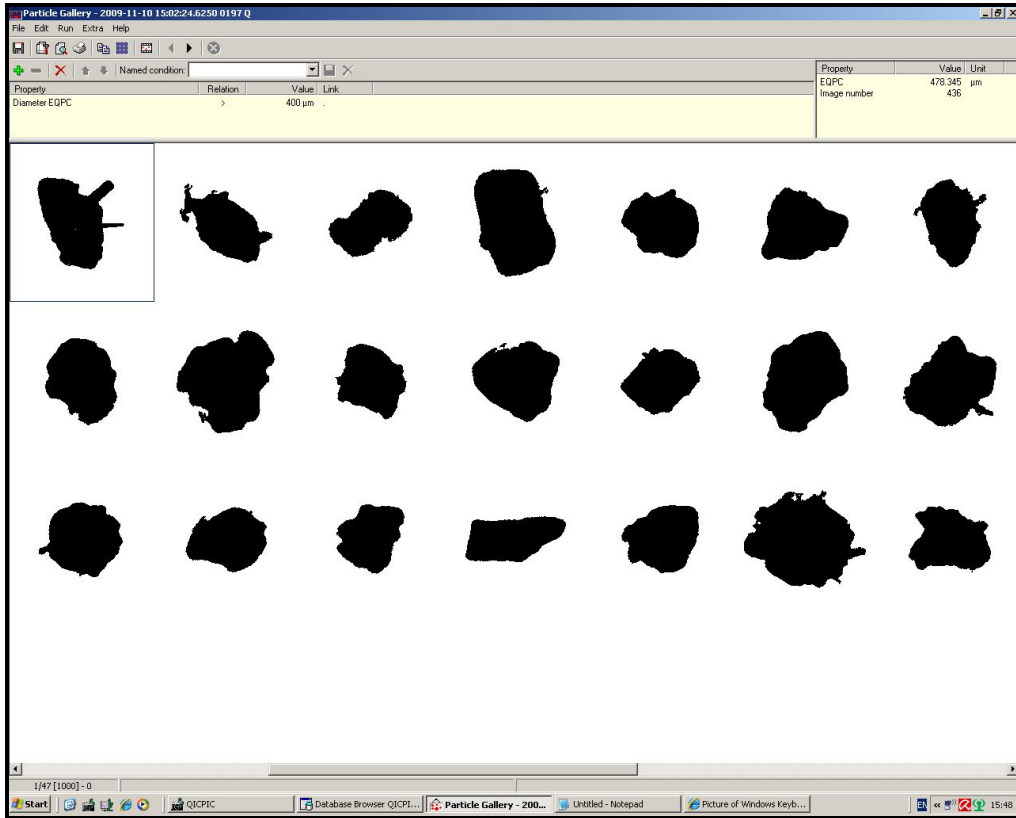


Figure 2.71: Selection of CCD images of Ethyl Vanillin generated by Sympatec Qicpic

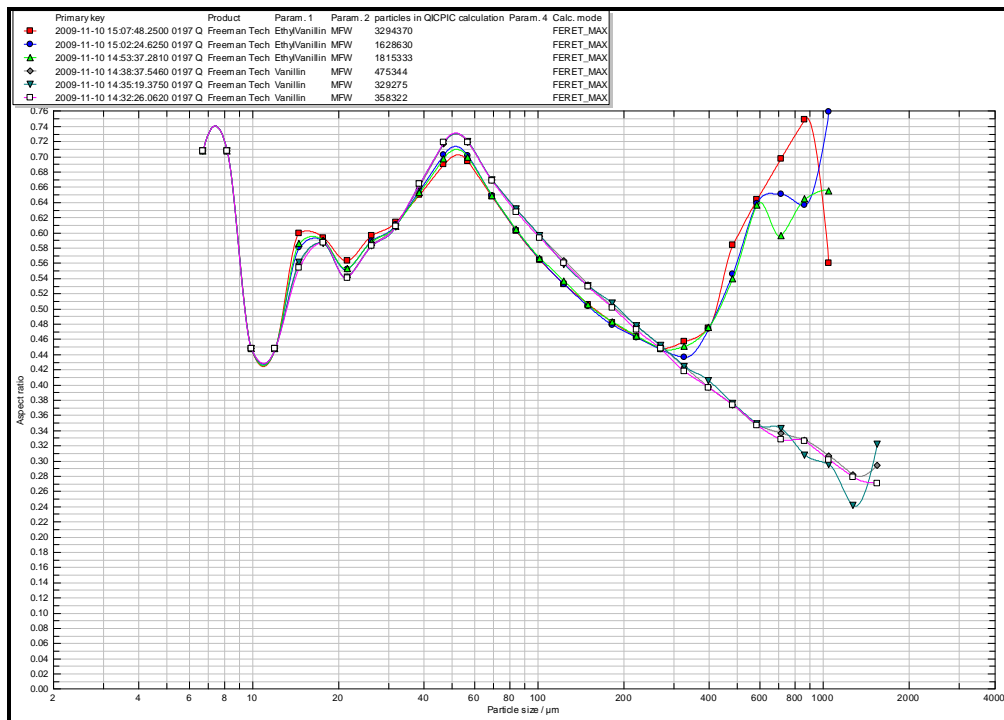


Figure 2.72: Aspect ratio vs particle size for three tests each of Ethyl Vanillin & Vanillin collected by Sympatec Qicpic – note the dramatic split at 300microns between the high aspect ratio Vanillin and the low aspect ratio Ethyl Vanillin

In this instance a simplistic size distribution would not adequately represent the two distinct shape profiles of the two crystal types and could easily give a misleading view of the relative influence that each crystal type would present to a process.

Clearly the difference in performance between the low stress dynamic and high stress shear testing is a function of the stress condition under which the powders are evaluated – the shear cell evaluates the high stress, confined state at incipient flow; the powder rheometer evaluates the unconfined, low stress state during motion. In this case it is probable that the interlocking of the needle-like profile of the particles will be all but destroyed during the pre-shearing process of a shear cell test where the development of directionality of the needles can occur at the shear plane, thus making the sample easier to shear (anisotropy) (Schulze 2007). The unconfined dynamic testing captures the effect the shape has on the flow behaviour. Interestingly the Vanillin has lower flow energy when the blade is traversing slower through the test sample in the FRI test – this again can be attributed to the shape of the particles and was observed with the sodium benzoate mentioned earlier. The likely mechanism is rotational/translational frustration. The needles have significantly larger surface contacts and more mechanical interlocking due to their particle morphology than the spherical particles – they can overlap each other. The ability of the needles to pass over each other and the blade (due to mechanical interlocking/interference) during higher rates of shear is clearly reduced and has been described as ‘rotational (and translational) frustration’ (Santamarina & Cho 2004). The needles have a reduced ability to be mobilised and thus interstitial spaces are not promoted with increased blade speed. In contrast, the spherical

particles can move over each other with greater ease, creating interstitial gaps (i.e. more air is entrained within the powder) when mobilised.

Thus the information generated tells the formulator that there would be little difference in the flow behaviour from storage between formulations containing either material, but there may be significant differences between blending performance, for example.

2.5.3. Pharmaceutical blends

In some instances, there are cases where the dynamic test does not differentiate samples but the shear cell does.

Figure 2.73 shows the yield loci and Figure 2.74 the dynamic evaluation for two tablet blends composed of, ostensibly, the same materials in the same proportions. The difference between the two batches is that one of the excipients has been sourced from two different suppliers. The results from tableting tests showed that there was a slight, but statistically significant increase in the number of rejected tablets (based on their strength) for one of the suppliers. There were no obvious differences in the two blends based on the tests available to the tablet manufacturer.

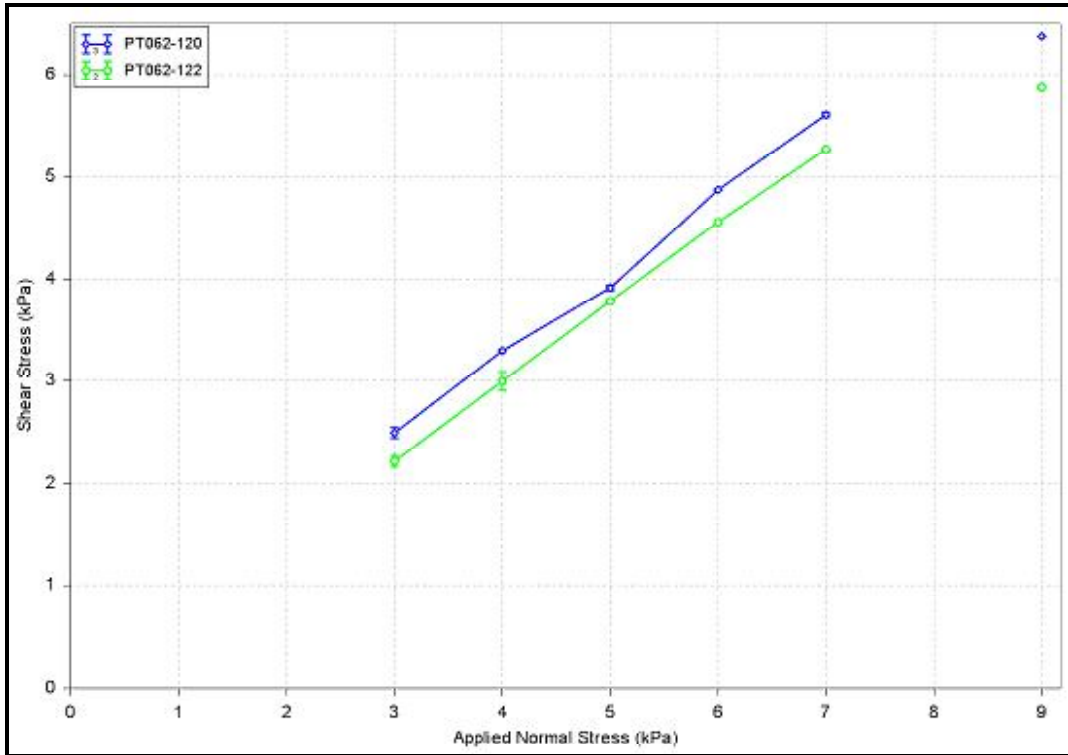


Figure 2.73: Yield loci for two tablet blends generated using the FT4 shear cell at 9kPa consolidating load

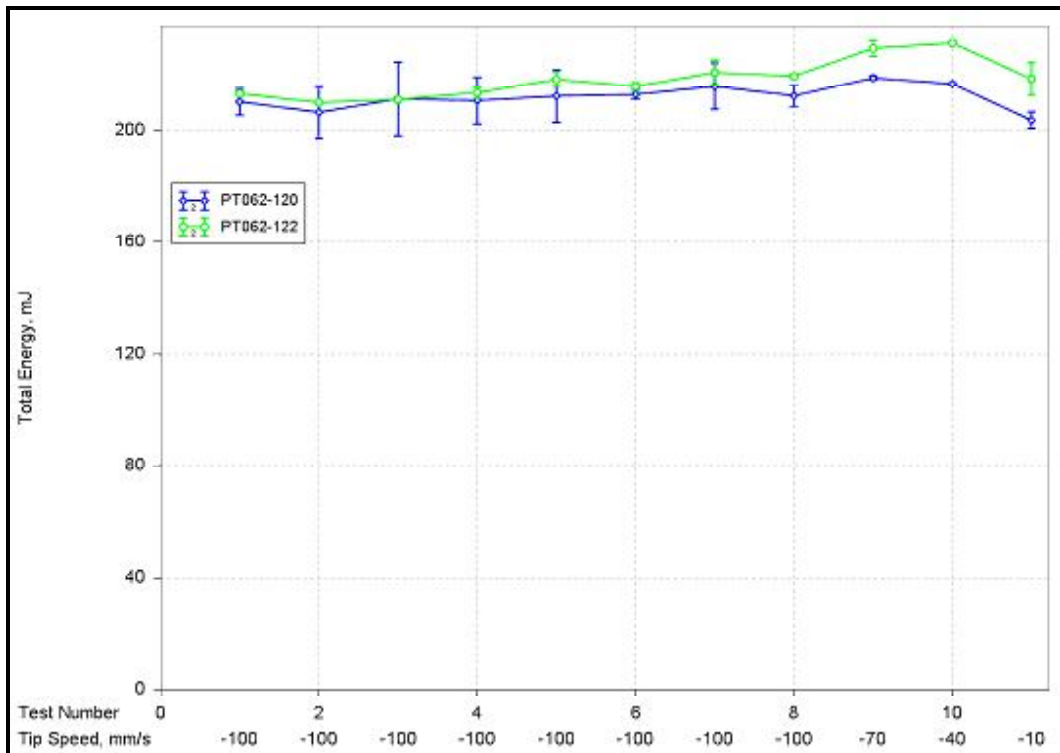


Figure 2.74: A dynamic test for two tablet blends showing 7 repeat tests at a blade tip speed of 100mm/s to evaluate the powders flow stability, followed by 4 tests at reducing blade tip speed from 100mm/s to 10mm/s

In this case it is very difficult to differentiate the two materials by their flow energy values, but the yield loci show a distinct separation. It is likely that a good correlation between the shear properties, the flow into the tablet press and the resultant tablet friability for the existing process configuration could be established.

2.5.4. Pharmaceutical Excipient

Another tablet manufacturing operation, using a different excipient a specific grade of dibasic calcium phosphate (DCP), showed significant weight variability for one particular grade of the material. Trials showed that this weight variation was significantly reduced when the DCP was briefly oven dried. This would usually suggest that some surface moisture was being driven off by the drying process and that the moisture was acting to increase the inter-particulate cohesion. However, when tested using shear (Figure 2.75) and dynamic methods (Figure 2.76), very little (if any) change could be seen between the results for both materials.

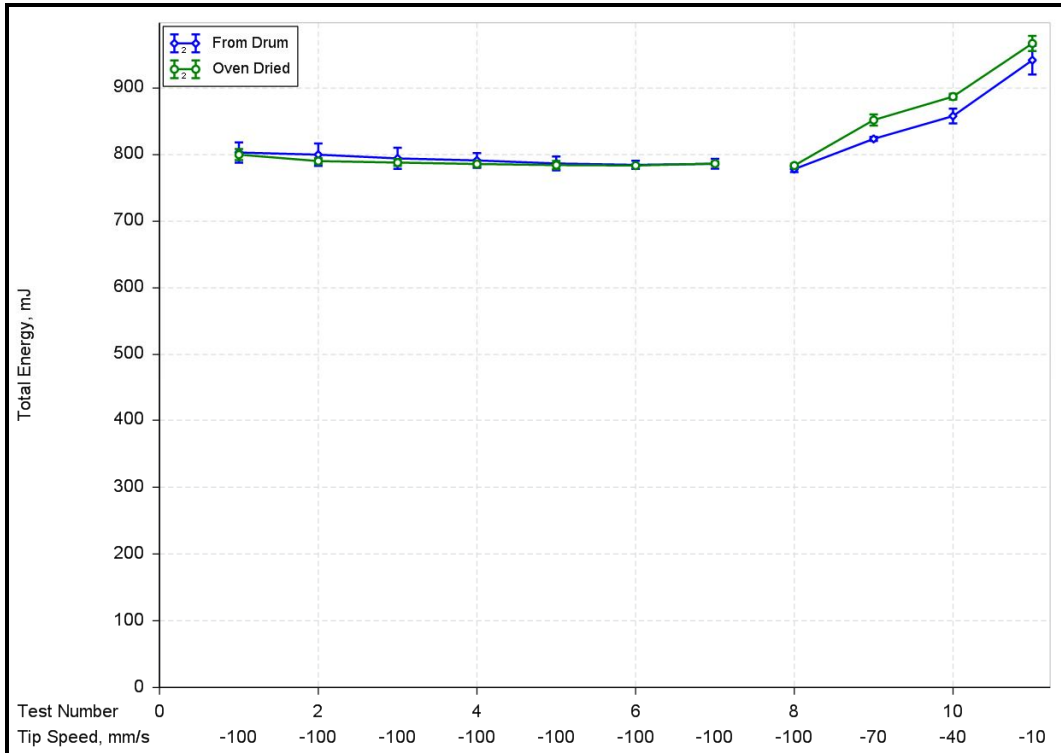


Figure 2.75: A dynamic test for two samples of DCP showing 7 repeat tests at a blade tip speed of 100mm/s to evaluate the powders flow stability, followed by 4 tests at reducing blade tip speed from 100mm/s to 10mm/s

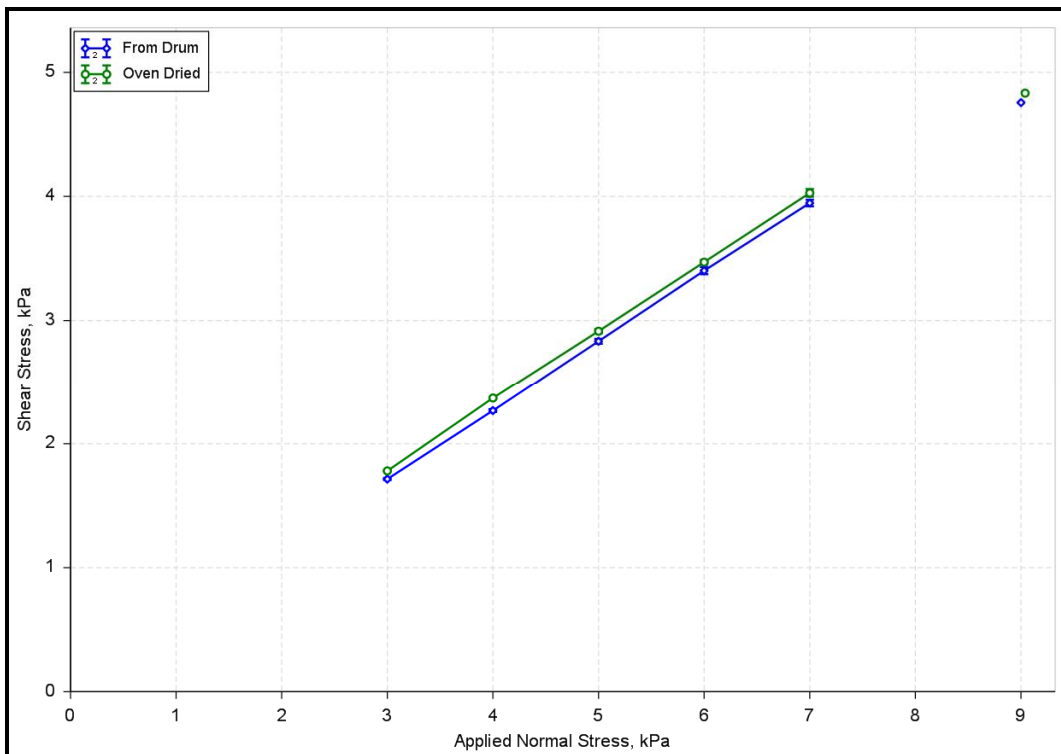


Figure 2.76: Yield loci for for two samples of DCP generated using the FT4 shear cell at 9kPa consolidating load

However, upon the evaluation of the compressibility of the two samples, significant, measurable difference could be identified (shown in Figure 2.77).

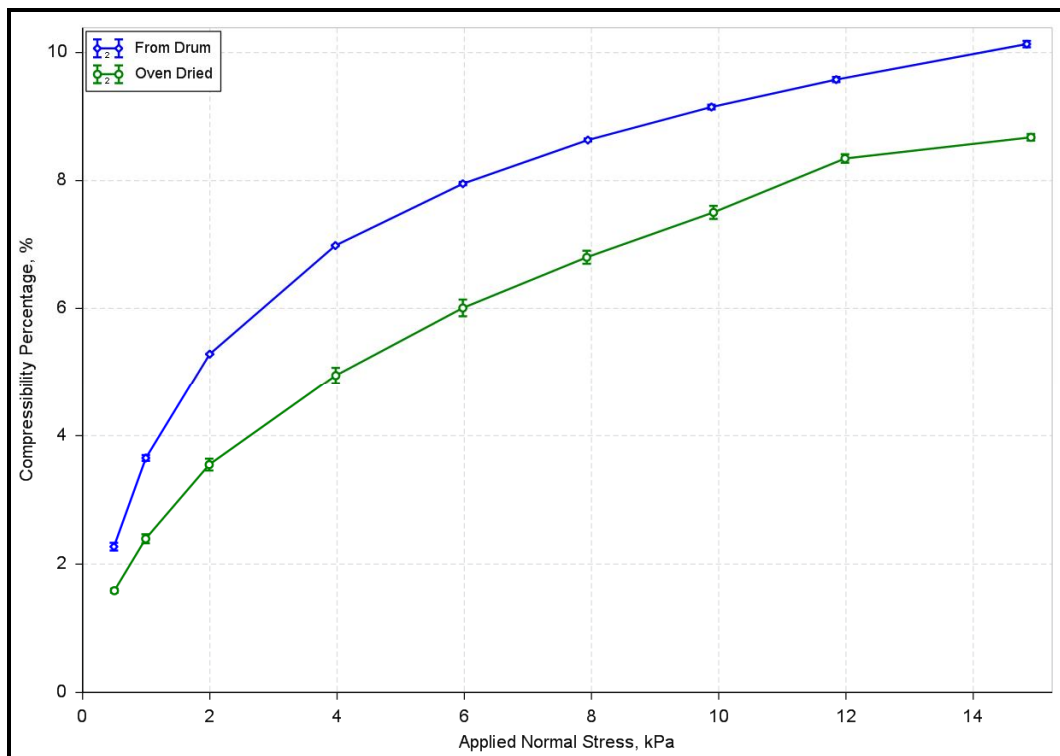


Figure 2.77: The compressibility of samples evaluated by change in volume with respect to an applied normal stress for two samples of DCP

In this instance, the compressibility of the two powders was shown to be different, which correlates well with process experience in the tablet press – the oven dried powder being less compressible over the entire range of normal forces used in the test. This additional compressibility of the ‘drum’ sample explains the variability of the powders flow into the tablet die as it was compacting in the feed system and creating loose agglomerates which prevent even filling of the dies under the evaluated processing conditions.

2.5.5. Summary of comparison testing

The five cases studied in this section, coupled with the results from the exemplar powders, reinforce the concept that a single test, no matter how technically robust, sensitive or repeatable, can be expected to solve every flow or processing problem. Given that GEA operates in an industry that processes thousands of formulations using an equally diverse number of processes and equipment types, in a regulatory environment that is now looking for process understanding, it seems logical that a wide range of testing methodologies be used.

2.6. Summary & conclusions

As most powders undergo a wide range of stress conditions when they progress through a typical powder processing environment, it would seem logical that one should be able to quantify their behaviour as they traverse the entire system and develop design equations and protocols based on their measurable physical assembly characteristics. However, there are very few robust design techniques currently available for powder systems, possibly due to the lack of characterisation techniques in the marketplace, as was noted at the start of this Chapter.

Every powder exhibits a number of behavioural traits relating to its condition and the situation in which it is to be processed/transported. No single test or ranking can adequately describe all the ranges of behaviour, a phenomenon endorsed by Prescott and Barnum (Prescott & Barnum 2000a), de Silva (de Silva 2000) and Krantz *et al* (Krantz, Zhang, & Zhu 2009a). It is necessary, therefore, to have a large

range of simple, rapid tests that will provide a basic language with which engineers can converse. In addition, these basics must be supplemented by specific measurements that relate to individual company products as appropriate. For example, the size distribution of a powder is an invaluable frame of reference and many behavioural properties stem from this basic measurement, but for dry powder blending, a dynamic test provided by the powder rheometry, for example, is likely to provide a rapid evaluation of a blend's suitability for Buck Systems equipment as will be demonstrated in Chapter 3.

The ability to relate to clients methods for testing powders using simple tests (most pharmaceutical companies will have Jolting Volumeters and AOR devices somewhere in their organisation) is important – even if more advanced methods are subsequently introduced into the discussion. Many pharmaceutical textbooks (Aulton & *et al* 2002;Howard 2007) & pharmacopoeia (British Pharmacopoeia Commission 2005;Council of Europe European (COE) - European Directorate for the Quality of Medicines (EDQM) 2007) refer to these sorts of tests and the pharmacists who are employed to undertake powder testing will rely heavily on their training.

In terms of advanced testers, it would be sensible to employ shear testing as one of the main pillars of powder characterisation. But the frequent insensitivity of this test, together with the questions raised about the derivation and analysis of the data, must be considered and it is recommended that additional characteristics should be used to provide a full picture of how the powder will behave over the wide range of stress conditions experienced by the powder during its processing.

However, this Chapter has shown particular issues with the testing of powders relating to universal test instruments as well as significant complexities in the analysis of the measurements and the interpretation of the derived parameters.

- Shear cell has a strong theoretical basis and generates repeatable data, but the results can often be inconclusive as the relatively high stress environment (compared to some unit operations) and the measurement of the incipient flow condition limits the sensitivity of the test – especially where fragile or non-spherical particles are present.
 - Furthermore, there are issues with testing of non-cohesive samples
 - Derived parameters (UYS, MPS, AIF, FF, C) are very sensitive to slight deviations of yield locus and restrict the usefulness of shear cell testing of these materials.
 - For such a well studied test methodology there are, arguably, still a large number of poorly explained operational variations between testers and methodologies that mean that a significant degree of experience is required in the interpretation of both the raw data and the mathematical analysis of the results.
 - The interpretation of what a flow function is actually imparting is complex – especially when the FF varies significantly with stress level
 - The interpretation of the FF/ff results as well a hopper outlet diameter and hopper half angle for mass flow will be discussed in Chapter 4.

- Other than hopper design, there are very few published correlations between shear cell data and process performance.
 - It is, however, still the most respected technique because it produces a scale independent state function of the powder.
- Interpretation of data from powder rheometry can provide a more sensitive and repeatable evaluation of a powder's response to stimulus.
 - There are issues with the understanding and interpretation of the information provided, especially with regard to what the test result means in purely particle mechanics terms.
 - The data is not scale independent and, as yet, there are no scaling factors available from the suppliers.
 - There are no published correlations between the data produced by powder rheometry and actual process performance. This means that a considerable amount of effort will be required to link rheometric data to specific processes – however this is no different to most tests.
- Additional testing methods, such as permeability, aeration and compressibility, enhance and complement main testing methodologies of shear and unconfined/dynamic testing (in powder rheometry) by providing additional insight into the nature of powder assemblies.
- And, whilst often insensitive to changes in the powder assembly characteristics, Carr's Compressibility Index, Angle of Repose and Flow Through and Orifice can permit the correlation of historical performance data and provide a link to GEA's clients testing information.

The main conclusions are therefore

- Simplistic interpretations of 'good' or 'bad' flowability, without reference to the process environment, will not allow a robust evaluation of a system, especially in the pharmaceutical industry where significant numbers of formulations are the norm.
- Recent advances in powder characterisation instrumentation will enable the capture of the variance in powder assembly properties which can be related to the variance in process and/or product performance. This can be done quickly and reliably thus enabling researchers to be confident in the repeatability of data.

2.7. Instrument Manufacturers

- Freeman Technology, Boulters Farm Centre, Castlemorton Common, Welland, Malvern, Worcestershire, WR13 6LE, UK, <http://www.freemantech.co.uk/> (FT4 Powder Rheometer)
- Sci-Tec Inc, 27 Glen Road, Sandy Hook, CT 06482, <http://www.sci-tec-inc.com/> (ShearScan Shear Tester)
- Dr.-Ing. Dietmar Schulze, Schüttgutmesstechnik Am Forst 20 D-38302, Wolfenbüttel, Germany, <http://www.dietmar-schulze.de/fre.html>, (RST-XS Shear Tester)
- Hosokawa Micron Ltd. Rivington Road, Whitehouse Industrial Estate, Runcorn, Cheshire, WA7 3DS, <http://www.hosokawa.co.uk/powdtest.php> (Powder Characteristics Tester PT-S)
- Copley Scientific Ltd., Colwick Quays Business Park, Private Rd. No. 2, Colwick, Nottingham, NG4 2JY, UK. <http://www.copleyscientific.co.uk/> (Jolting Volumeter, Flowability Tester Model BEP2)
- Johanson Innovations Inc., 102 Cross Street, Suite #110, San Luis Obispo, CA 93405, USA. <http://www.indicizer.com/contact.html> (Johanson Indicizer)
- Stable Micro Systems Ltd., Vienna Court, Lammas Rd, Godalming, Surrey, GU71YL, UK. <http://www.stablemicrosystems.com/> (Powder Flow Analyser)
- Brookfield Engineering Laboratories Inc., 11 Commerce Boulevard, Middleboro, Massachusetts, 02346, USA.
<http://www.brookfieldengineering.com/products/pft/powder-flow-tester.asp>
(Powder Flow Tester)

- Shear-Test.com, info@shear-test.com, <http://www.shear-test.de/index.php> (Peschl shear tester)
- E&G Associates Inc., PO Box 681268, Franklin, TN 37068, USA, http://www.powdernotes.com/frameset_ipowder.html (i-Shear Tester)
- Powder Research Ltd., Burn Bridge, Harrogate, North Yorkshire HG3 1LU, UK (Geldart Angle of Repose Tester) <http://www.powderresearch.com/index.html>

2.8. References

Akers, R. J. 1992, *The certification of a limestone powder for Jenike shear testing CRM116* Commission of the European Communities.

ASTM 2005, *Standard Test Method for Measuring the Angle of Repose of Free-Flowing Mold Powders (Withdrawn 2005)* C1444-00.

Aulton, M. E. & et al 2002, *Pharmaceutics, The Science of Dosage Form Design*, 2nd edn, Churchill Livingstone.

Berry, R. J. & Bradley, M. S. A. 2005, "Investigation of the effect of test procedure factors on the failure loci and derived failure functions obtained from annular shear cells", in *Particulate Systems Analysis 2005*.

Bharadwaj, R., Ketterhagen, W. R., & Hancock, B. C. "Discrete element simulation study of a Freeman powder rheometer", *Chemical Engineering Science*, vol. In Press, Corrected Proof.

British Pharmacopoeia Commission 2005, *The British Pharmacopoeia 2005* Stationery Office Books.

Bundalli, N. 1973, "The application of a computer to hopper design", *Computer-Aided Design*, vol. 5, no. 4, pp. 224-227.

Carr, R. L. 1965a, "Classifying Flow Properties of Solids", *Chemical Engineering*, vol. 72, no. 3, pp. 68-72.

Carr, R. L. 1965b, "Evaluating Flow Properties of Solids", *Chemical Engineering*, vol. 72, no. 2, pp. 163-168.

Cheng, D. C. H. & Farley, R. 1968, "Some consequences of the correlation of powder properties on the design of hoppers", *Powder Technology*, vol. 2, no. 2, pp. 131-132.

Council of Europe European (COE) - European Directorate for the Quality of Medicines (EDQM) 2007, *European Pharmacopoeia*, 6 edn.

de Silva, S. R. 2000, "Characterisation of Particulate Materials", *powder handling & technology*, vol. 12, no. 4, pp. 355-363.

EFCE. Standard Shear Testing Technique. 1989. The Institution of Chemical Engineers.
Ref Type: Pamphlet

Ennis, B. J., Witt, W., Weinekoter, R., Sphar, D., Gommeran, E., Snow, R. H., Allen, T., Raymus, G. J., & Litster, J. D. 2007, "Solid-Solid Operations and Processing," in

Perry's Chemical Engineers' Handbook, 8 edn, D. W. Green & R. H. Perry, eds., McGraw-Hill Professional.

Faqih, A. M., Mehrotra, A., Hammond, S. V., & Muzzio, F. J. 2007, "Effect of moisture and magnesium stearate concentration on flow properties of cohesive granular materials", *International Journal of Pharmaceutics*, vol. 336, no. 2, pp. 338-345.

Fayed, M. E. & Otten, L. 1984, *Handbook of Powder Science and Technology* Van Nostrand Reinhold.

Feise, H. J. 1998, "A review of induced anisotropy and steady-state flow in powders", *Powder Technology*, vol. 98, no. 3, pp. 191-200.

Fitzpatrick, J. J., Barringer, S. A., & Iqbal, T. 2004, "Flow property measurement of food powders and sensitivity of Jenike's hopper design methodology to the measured values", *Journal of Food Engineering*, vol. 61, no. 3, pp. 399-405.

Freeman, R. E. 2007, "Measuring the flow properties of consolidated, conditioned and aerated powders -- A comparative study using a powder rheometer and a rotational shear cell", *Powder Technology*, vol. 174, no. 1-2, pp. 25-33.

Geldart, D., Abdullah, E. C., Hassanpour, A., Nwoke, L. C., & Wouters, I. 2006, "Characterization of powder flowability using measurement of angle of repose", *China Particuology*, vol. 4, no. 3-4, pp. 104-107.

Geldart, D., Abdullah, E. C., & Verlinden, A. 2009, "Characterisation of dry powders", *Powder Technology*, vol. 190, no. 1-2, pp. 70-74.

Howard, S. A. 2007, "Solids: Flow Properties," in *Encyclopedia of Pharmaceutical Technology*, Informa Healthcare, pp. 3275-3297.

Janssen, R. J. M., Verwijs, M. J., & Scarlett, B. 2005, "Measuring flow functions with the Flexible Wall Biaxial Tester", *Powder Technology*, vol. 158, no. 1-3, pp. 34-44.

Jenike, A. W. 1964, *Storage and Flow of Solids*, University of Utah, Bulletin 123.

Kalson, P. A. & Resnick, W. 1985, "Angles of repose and drainage for granular materials in a wedge-shaped hopper", *Powder Technology*, vol. 43, no. 2, pp. 113-116.

Kamath, S. & Puri, V. M. 1997, "Measurement of powder flow constitutive model parameters using a cubical triaxial tester", *Powder Technology*, vol. 90, no. 1, pp. 59-70.

Krantz, M., Zhang, H., & Zhu, J. 2009a, "Characterization of powder flow: Static and dynamic testing", *Powder Technology*, vol. 194, no. 3, pp. 239-245.

Krantz, M., Zhang, H., & Zhu, J. 2009b, "Characterization of powder flow: Static and dynamic testing", *Powder Technology*, vol. 194, no. 3, pp. 239-245.

Liu, L. X., Marziano, I., Bentham, A. C., Litster, J. D., E.T.White, & Howes, T. 2008, "Effect of particle properties on the flowability of ibuprofen powders", *International Journal of Pharmaceutics*, vol. 362, no. 1-2, pp. 109-117.

Liu, X. Y., Specht, E., & Mellmann, J. 2005, "Experimental study of the lower and upper angles of repose of granular materials in rotating drums", *Powder Technology*, vol. 154, no. 2-3, pp. 125-131.

Mankoc, C., Janda, A., Arévalo, R., Pastor, J., Zuriguel, I., Garcimartín, A., & Maza, D. 2007, "The flow rate of granular materials through an orifice", *Granular Matter*, vol. 9, no. 6, pp. 407-414.

McGlinchy, D. 2005, *Characterisation of Bulk Solids* Blackwell.

Pechl, I. & Colijn, H. "New Rotational Shear Testing Technique", in *Bulk Solids Handling and Processing*.

Prescott, J. K. & Barnum, R. A. On Powder Flowability. *Pharmaceutical Technology* [October 1984], 60-84. 1-10-2000a.
Ref Type: Magazine Article

Prescott, J. K. & Barnum, R. A. On Powder Flowability. *Pharmaceutical Technology* [October 1984], 60-84. 1-10-2000b.
Ref Type: Magazine Article

Rhodes, M. 1998, *Introduction to Particle Technology* John Wiley & Sons.

Roberts, A. W. 1993, *Basic Principles of Bulk Solids Storage, Flow & Handling* TUNRA Bulk Solids Research Associates.

Rowe, R. C., Sheskey, P., & Owen, S. C. 2005, *Handbook of Pharmaceutical Excipients*, 5 edn, Pharmaceutical Press.

Santamarina, J. C. & Cho, G. C. 2004, "Soil Behaviour: Role of particle shape", in *Skempton Memorial Conference*, British Geotechnical Association.

Schmitt, R. & Feise, H. 2004, "Influence of Tester Geometry, Speed and Procedure on the Results from a Ring Shear Tester", *Particle and Particle Systems Characterisation*, vol. 21, pp. 403-410.

Schulze, D. 2007, *Powders and bulk solids. Behavior, characterization, storage and flow*, 2 edn.

Schulze, D. & Pechl, I. Forum discussion regarding the merits of different shear cell instruments and methodologies. <http://www.bulk-online.com/Forum/showthread.php?threadid=1661> . 2009.
Ref Type: Electronic Citation

Schwedes, J. 2002, "Consolidation and flow of cohesive bulk solids", *Chemical Engineering Science*, vol. 57, no. 2, pp. 287-294.

- Schwedes, J. 2003, "Review on testers for measuring flow properties of bulk solids", *Granular Matter*, vol. 5, no. 1, p. 43.
- Schwedes, J. & Schulze, D. 1990a, "Measurement of flow properties of bulk solids", *Powder Technology*, vol. 61, no. 1, pp. 59-68.
- Schwedes, J. & Schulze, D. 1990c, "Measurement of flow properties of bulk solids", *Powder Technology*, vol. 61, no. 1, pp. 59-68.
- Schwedes, J. & Schulze, D. 1990b, "Measurement of flow properties of bulk solids", *Powder Technology*, vol. 61, no. 1, pp. 59-68.
- Spink, C. D. & Nedderman, R. M. 1978, "Gravity discharge rate of fine particles from hoppers", *Powder Technology*, vol. 21, no. 2, pp. 245-261.
- Stainforth, P. T., Ashley, R. C., & Morley, J. N. B. 1971, "Computer analysis of powder flow characteristics", *Powder Technology*, vol. 4, no. 5, pp. 250-256.
- Taylor, M. K., Ginsburg, J., Hickey, A. J., & Gheyas, F. Composite Method to Quantify Powder Flow as a Screening Method in Early Tablet or Capsule Formulation Development. *Pharmaceutical Technology* 1[3]. 2000.
Ref Type: Magazine Article
- Thalberg, K., Lindholm, D., & Axelsson, A. 2004, "Comparison of different flowability tests for powders for inhalation", *Powder Technology*, vol. 146, no. 3, pp. 206-213.
- Tuley, R., Shrimpton, J., Jones, M. D., Price, R., Palmer, M., & Prime, D. 2008, "Experimental observations of dry powder inhaler dose fluidisation", *International Journal of Pharmaceutics*, vol. 358, no. 1-2, pp. 238-247.
- United States Pharmacopeia 2007, "<1174> Powder Flow," USP 29/NF24 edn, US Pharmacopial Convention, Inc..
- Velasco, M. V., Munoz-Ruiz, A., Monedero, M. C., & Jimenez-Castellanos, M. R. 1995, "Study of Flowability of Powders. Effect of the Addition of Lubricants", *Drug Development and Industrial Pharmacy*, vol. 21, no. 20, pp. 2385-2391.
- Wu, C.-Y., Armstrong, B., Vlachos, N. X., Seville, J. P. K., Chang, I., & Cocks, A. C. F. "A comparative study on characterization of powder flowability using different techniques", in *PARTEC 2007*.
- Zhou, Y. C., Xu, B. H., Yu, A. B., & Zulli, P. 2002, "An experimental and numerical study of the angle of repose of coarse spheres", *Powder Technology*, vol. 125, no. 1, pp. 45-54.

Chapter 3 – Powder Mixing

Abstract

Three tomographic techniques have been used to non-invasively evaluate the mixedness of binary and ternary pharmaceutical powder systems. Positron Emission Tomography has been uniquely applied to powder mixing systems and has been shown to evaluate content uniformity at volumes significantly below a typical dosage unit.

3.1. Introduction

The mixing of powders is a long established practice and is undertaken in most industrial applications where powders are handled. The quality of the mixture has a significant impact on the end product; for example the efficacy of pharmaceuticals or the strength of a sintered metal component. The measurement of the quality of a mixture is not without debate, and many ways of determining 'mixedness' have been proposed.

Tomographic techniques – as represented in this Chapter by Positron Emission Tomography (PET) and Positron Emission Particle Tracking (PEPT) – have been used extensively to follow process behaviour in dynamic solid/liquid and solid/gas systems, but the evaluation of batch solid/solid blending systems has been under represented.

This Chapter presents some tomographic studies to evaluate mixedness in batch blenders with a view to developing comparisons with established techniques for evaluation of blend quality and determination of end point.

3.2. *Mixing in the pharmaceutical industry*

For sound reasons of quality control and containment, solid dose pharmaceutical formulations are generally blended from their component powders in batch blenders. The use of intermediate bulk containers (IBCs) as the primary batch storage, transport and processing/blending vessel is common and is the primary product of Buck Systems. Figure 3.1 shows a range of IBCs and Figure 3.2 shows a tumble blender in operation.



Figure 3.1: Examples of IBCs



Figure 3.2: A tumble blender in operation

The way in which powders with differing physical properties mix in batch IBC blenders is still not well understood, mainly because the mechanisms of mixing are complex and this is compounded by the difficulty of evaluating the mixedness of a powder blend without compromising the blend consistency through invasive sampling. Variability of individual powder properties in a formulation, through manufacturing variation or changes in environmental factors, can also affect the mixedness of a processed blend.

Many ways have been devised to qualitatively and quantitatively calibrate the mixedness of a blend. These include the use of coloured feedstocks (Sudah, Coffin-Beach, & Muzzio 2002); solidification, slicing and image analysis (Wightman, Muzzio, & Wilder 1996); thief sampling and assay (Hausman, Cambron, & Sakr 2005) and on-line spectroscopic techniques (Cho *et al.* 1997; Hailey *et al.* 1996).

The main technique used in industrial processes and research laboratories is thief sampling followed by appropriate assay. Although this technique is well suited to the evaluation of large blending systems, it has several shortcomings that have been thoroughly studied and are described in a number of papers by Muzzio *et al.* (Muzzio *et al.* 1997; Muzzio *et al.* 2003).

The recent introduction of the PAT initiative by the US FDA (Food & Drug Administration 2004), combined with a range of other protocols described in Chapter

1 has led to the development and introduction of a range of new sensors to evaluate blend mixedness on-line. These include near infrared spectroscopy (NIR) (Blanco, Gozalez Bano, & Bertran 2002; Cho *et al.* 1997b; Hailey *et al.* 1996; Sekulic *et al.* 1998; Shi *et al.* 2008); effusivity (Leonard *et al.* 2008); Raman spectroscopy (Hausman, Cambron, & Sakr 2005) and laser induced fluorescence spectroscopy (Lai *et al.* 2001). Figure 3.3 shows a recently developed laboratory blending system utilising a NIR sensor to establish mixedness and a production scale equivalent. Such systems are also used on larger bin blenders in production facilities as indicated by Berntsson *et al.* (Berntsson *et al.* 2002).

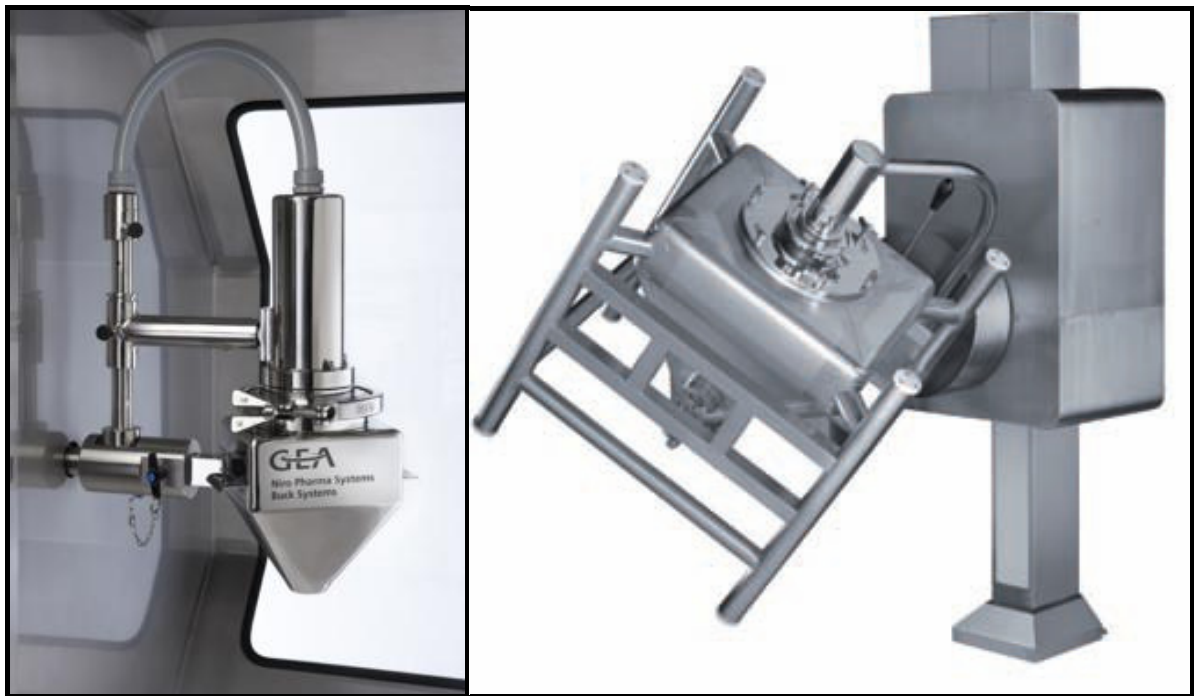


Figure 3.3: Laboratory scale (left) and production scale (right) blenders equipped with NIR sensing head (GEA Pharma Systems 2010a)

Though these new sensor systems have clear process advantages, the validation of the end point is still made using thief sampling as indicated in the paper by Hausman

et al (Hausman, Cambron, & Sakr 2005), and as such these advanced sensors make little or no impact on the improvement of the quality of the blend and can be viewed as technologically advanced thief samplers. This is because NIR systems, for example, necessarily use a single point measurement taken when powder covers the sensor during a rotational cycle – as can be seen in Figure 3.3, there is only a single NIR sensor located on the lid of each bin. Fitting multiple sensors would be complex as the transmission of data has to be routed through the rotating coupling (see Figure 3.3) or transmitted wirelessly from each sensor – neither option is, at present, easy to implement due to mechanical limitations or band width considerations. Thus a decision has to be made as to when this single measurement per rotation relates to the mixing end point, which in turn can only be validated using extractive sampling and assay. Effectively the surface measurement has to be related to what is happening in the entire volume of the powder – requiring the transformation of a 2D measurement into a 3D measurement. Thus there is a requirement for validation by thief sampling to ensure that the observed trend in dispersion is not just an assumption of mixedness.

Therefore, an improved way of studying the blend structure during the actual blending process is required. Such a method needs to be able to produce a 3D image of the blend that can be interrogated to reveal the mixedness down to the appropriate scale of scrutiny – which should be, as a minimum, the dose volume for a tablet. Non-invasive sensors are preferable to invasive sampling and such sensors have recently begun to be used for powder blends, for example the work of Yang & Fu (Yang & Fu 2004). The X-ray technique used by Yang & Fu is not, however, as

versatile as the Positron Emission Tomographic techniques described in Section 3.3 due, mainly, to the limited scale of the vessels (a V blender with a longest dimension of 18mm was used) that can be integrated with the X-ray system. Therefore, it is intended to use PET to evaluate blend mixedness on a laboratory scale to improve the understanding of the relationship between the powder properties and mixing performance. This approach will be consistent with the 'design space' concept described in Chapter 1.

3.2.1 Influences on blending

Typically, pharmaceutical formulations contain a wide range of component materials. Often the active ingredient is only a small proportion of the entire mass – the rest of the formulation is composed of ingredients that assist with the formation of the tablet (flow aids, lubricants and release agents) or the delivery of the active ingredient once the tablet has been ingested (disintegrants, diluents, binders, flavourings, colourings). The largest component is often just a bulking agent, such as lactose, but not always – paracetamol, for example, has very limited potency and most of a standard dose tablet is the active ingredient.

The rate of achievement of a suitable blend is dependent on a range of variables outlined below (Harnby, Edwards, & Nienow 2001;Kaye 1997;Muzzio *et al.* 2004;Poux *et al.* 1991).

- **Process type**
 - **High Shear Mixers (usually as part of granulation process)**
 - Roller compactors (in conjunction with a milling stage)
 - Bottom driven high shear mixers – e.g. Aeromatic Fielder PMA
 - Top driven high shear mixers – e.g. Collette UltimaGral
 - **Fluidised mixers**
 - e.g. Aeromatic Fielder FlexStream
 - **Convective Mixers – Low to medium shear**
 - Paddle mixer
 - Ribbon mixer
 - Planetary mixer
 - Nauta Mixer
 - **Tumble Mixers – Low shear**
 - IBC mixer
 - V blender
 - Double cone
 - Schatz principle
- **Material**
 - Particle size distribution
 - Particle shape
 - Cohesion
 - Adhesion
 - Surface texture
 - Permeability
 - Shear behaviour
 - Aeration properties
- **Operational**
 - Fill proportion
 - Number of powders to be blended
 - Rotational speed
 - Total processing time (number of rotations)
 - Baffles
 - Relative flow properties of constituent powders
 - Initial loading condition

In this instance only IBC tumble mixers will be studied as this is the main product of GEA Buck Systems. In a production context, these systems are typically in the range 150 to 3000litres (GEA Pharma Systems 2010a;GEA Pharma Systems 2010b) and rotate in the range of 2-15rpm (variable) (GEA Pharma Systems 2010c). A laboratory scale blender fitted with a 10litre mini-IBC (GEA Pharma Systems 2010a), Figures 3.4 & 3.5, was used for this work as this was the largest vessel size that was compatible with the PET camera. The maximum rotation speed of this unit was also 15rpm.



Figure 3.4: Laboratory Scale Blender in-situ prior to PET experiment

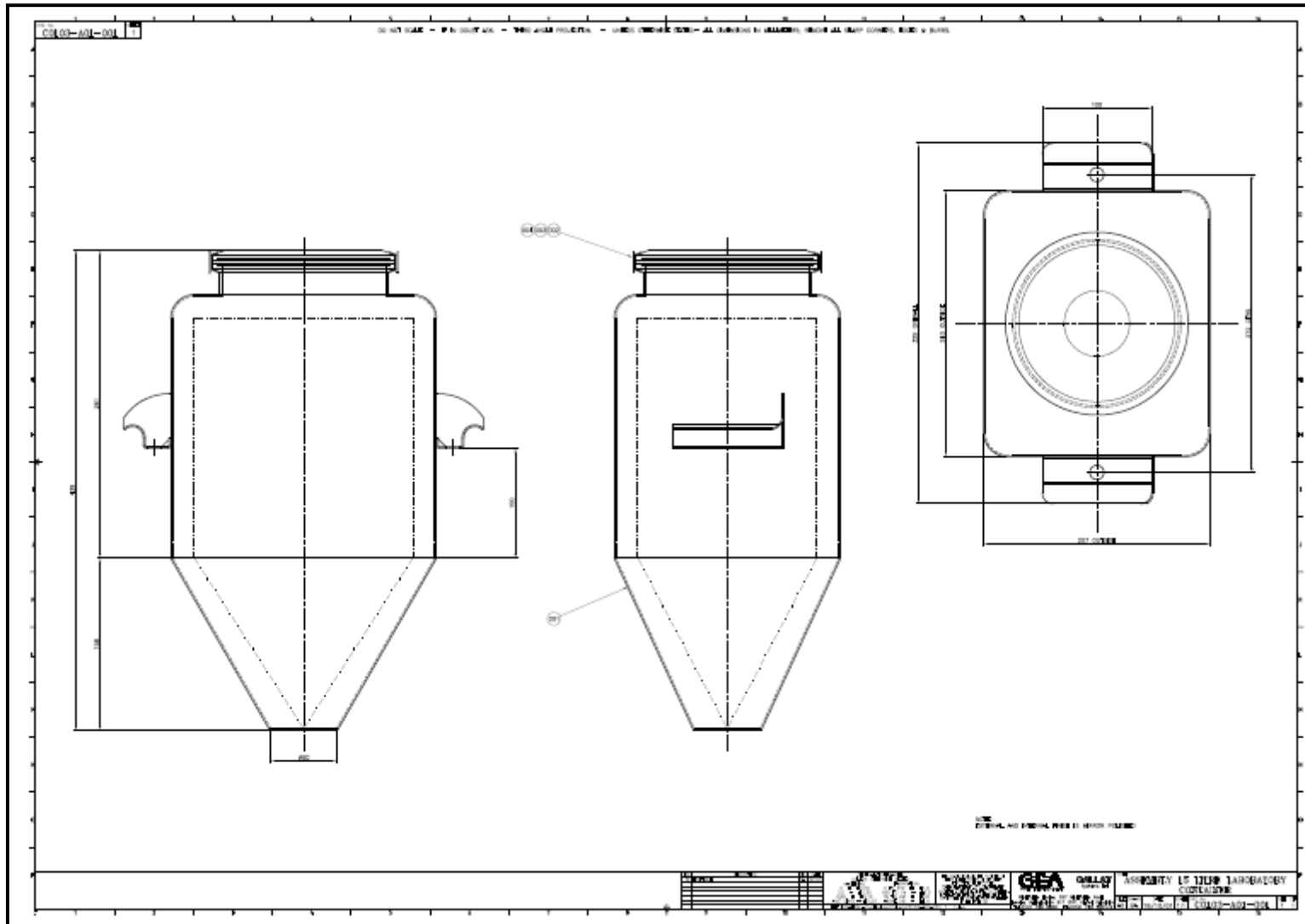


Figure 3.5: Isometric drawing of the 10litre mini-IBC

3.2.2. Modes of flow & mechanisms of dispersal in a tumble blender

The main body of work to investigate the mechanism in tumbling mixers has been undertaken with reference to the simplest type of mixer – the rotating drum (Chaudhuri & Fuerstenau 1971; Finnie *et al.* 2005; Parker *et al.* 1997; Peratt & Yorke 1998; Pirard *et al.* 2009; Wightman & Muzzio 1998). Several modes of flow have been identified and are shown in Figure 3.6.

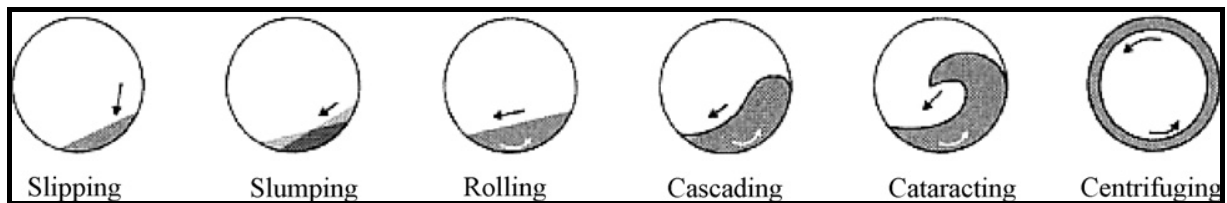


Figure 3.6: Modes of flow in a rotating drum with respect to rotational speed – fastest to slowest, R to L – after (Pirard *et al.* 2009)

These modes of flow impact how the components within the mixer will disperse as well as how quickly the dispersion occurs in the two major axes of the mixer (axial and radial). Although not identical, tumble mixers will generally generate the same modes of flow (Alexander *et al.* 2004). The mode of flow is dictated by the speed of rotation of the mixer and, to a lesser extent, the shape of the mixer, and can be described by the dimensionless Froude number.

$$Fr = \frac{R\omega^2}{g}$$

Equation 3.1

where R is the radius of rotation (m)
 ω is the angular velocity (rad/s)
 g is the acceleration due to gravity (ms^{-2})

Rearranging Equation 3.1 allows the critical speed to be identified (Hogg 2009). Above this critical speed, where $Fr=1$, the sample is believed to be centrifuging in the vessel [although there is evidence to the contrary (Finnie, Kruyt, Ye, Zeilstra, & Kuipers 2005)] as the centripetal and gravitational forces are balanced.

$$\omega_c = \sqrt{\frac{g}{R}} \quad \text{Equation 3.2}$$

where ω_c is the critical angular velocity (rad/s)

The radius of rotation of the mini-IBC used in these experiments is 258mm which gives a critical angular velocity of 6.2 rad/s or 59rpm. Given the speed limit of 15rpm on the experimental blender system this gives a Froude number of 0.065 – 25% of the critical speed – which indicates that the flow modes would include rolling and cascading. Cataracting may be possible due to the offset angle of the bin in its place holder (Figure 3.4) which enables the bin to precess and this eccentric motion exaggerates the axial slide and flow of the powder.

Cascading or cataracting mechanisms ('throw and splash') are more likely at higher Froude numbers and it can be seen that in some cases this approach may improve the initial dispersion of the components by enhancing the diffusive mechanism caused by random motion of particles at the free surface (Bozzone 2001). However, this aggressive approach to mixing is not appropriate in cases where fine, low density particles are to be dispersed – these fines can be thrown into the head space and

result in segregation either at the top of the bin or the sides/perimeter. Indeed Portillo (Portillo *et al.* 2008) lists the Froude numbers for a range of tumble mixer experiments for vessels from 14litres to 283litres and here the Froude numbers have been calculated to be between 4.1×10^{-4} and 8.4×10^{-4} which are significantly lower than those used for these experiments. Additionally the high velocity regimes of cataracting and cascading have not been well analysed (Muzzio, Alexander, Goodridge, Shen, Shinbrot, Manjunath, DhodapKar, & Jacob 2004) and as such, combined with the rotational speed limitations of the laboratory scale blender and the issues with segregation previously mentioned, it was considered acceptable to study the mixing due to rotational speeds up to the maximum of 15 rpm.

The three main dispersive mechanisms that occur in powder mixing have been characterised by many workers (Finnie, Kruyt, Ye, Zeilstra, & Kuipers 2005; Harnby, Edwards, & Nienow 2001; Hogg *et al.* 1966; Hogg 2009; Kaye 1997; Lacey 1997; Martin, Seville, & Parker 2007; Miyanami 2006; Muzzio *et al.* 2004; Parker *et al.* 1997; Wightman & Muzzio 1998) are

- Diffusive mixing – random motion of particles over a free surface
- Convective mixing – when large portions of powder move from one section of the mixing vessel to another
- Shear mixing – when particles exchange across shearing powder beds set up by the motion of the mixer

The terms diffusive and convective are still used in the context of powder mixing, but are more usually used in the context of liquid or gas mixing where diffusion and convection can occur spontaneously. For powder mixing, however, these mechanisms require the input of energy as no mixing will occur without the powder being put in motion and some dilation occurring.

These mechanisms do not occur independently, and each in mixing process the balance between the mechanisms will be determined by the range of equipment, process and powder variable described in Section 3.2.1. Indeed Miyanami (Miyanami 2006) has suggested that there is also a time dependency for the mechanistic balance, as shown in Figure 3.7.

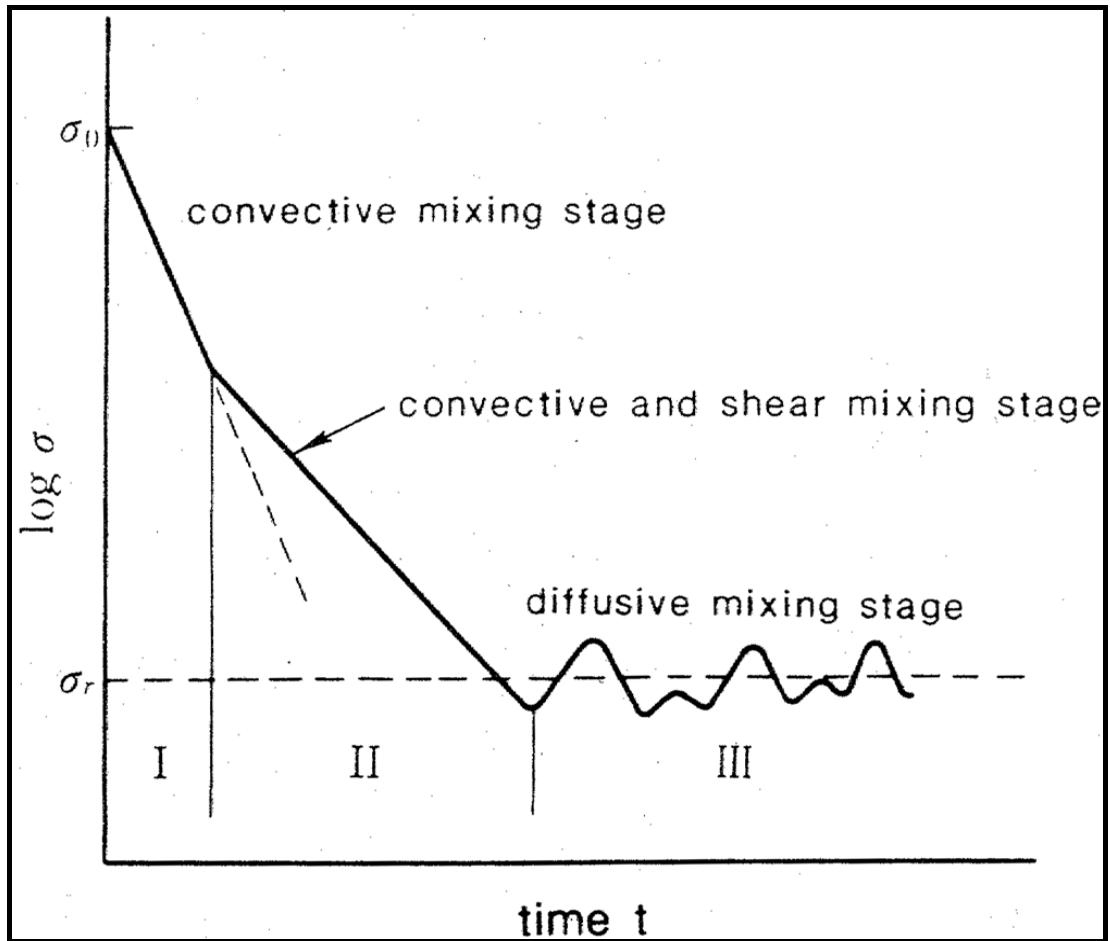


Figure 3.7: Example of the balance of the mechanisms occurring within a mixing process after (Miyanami 2006)

Given that the modes of flow within the mixer are likely to be rolling and cascading regimes, as determined by the Froude number, it is likely that shear at the surface is a major contributor to the rate of dispersion. Thus it would be sensible to understand where the shear occurs and have an estimate of the normal stress levels that will occur.

3.2.3. Stress levels in IBC blenders

Assuming that shear mixing is a significant mechanism that influences the overall mixing rate, then the typical depth of the semi-ellipsoidal flowing layer is around 1-22% of the depth of the bed at a Froude number of 0.064 according to the experimental and modelling work of Khakhar (Khakhar, Orpe, & Ottino 2001). Thus knowledge of the stress level at these depths within the powder bed would be helpful in determining the stress regime and the likely levels of cohesion that are present at these conditions.

The stress levels within a stationary IBC can be relatively easily calculated using the Janssen equation (Fayed & Otten 1984) shown in Equation 3.3.

$$P_v = \left(\frac{\rho_b g D}{4\mu K} \right) \left(1 - e^{\left(\frac{-4H\mu K}{D} \right)} \right) \quad \text{Equation 3.3}$$

where

- μ is angle of internal friction
- D is the diameter of the cylinder
- ρ_b is the poured bulk density of the powder
- g is the acceleration due to gravity
- H is height of the powder
- K is a the ratio of horizontal to vertical pressure and is assumed constant – 0.4

The likely loads at the base of a (full and level) flat bottomed bin of aspect ratio 2:1 have been calculated for three of the pharmaceutical excipients previously tested for

flowability and the results shown in Figure 3.8 indicate the pressure on the bin floor due to the head of powder with respect to increasing bin diameter.

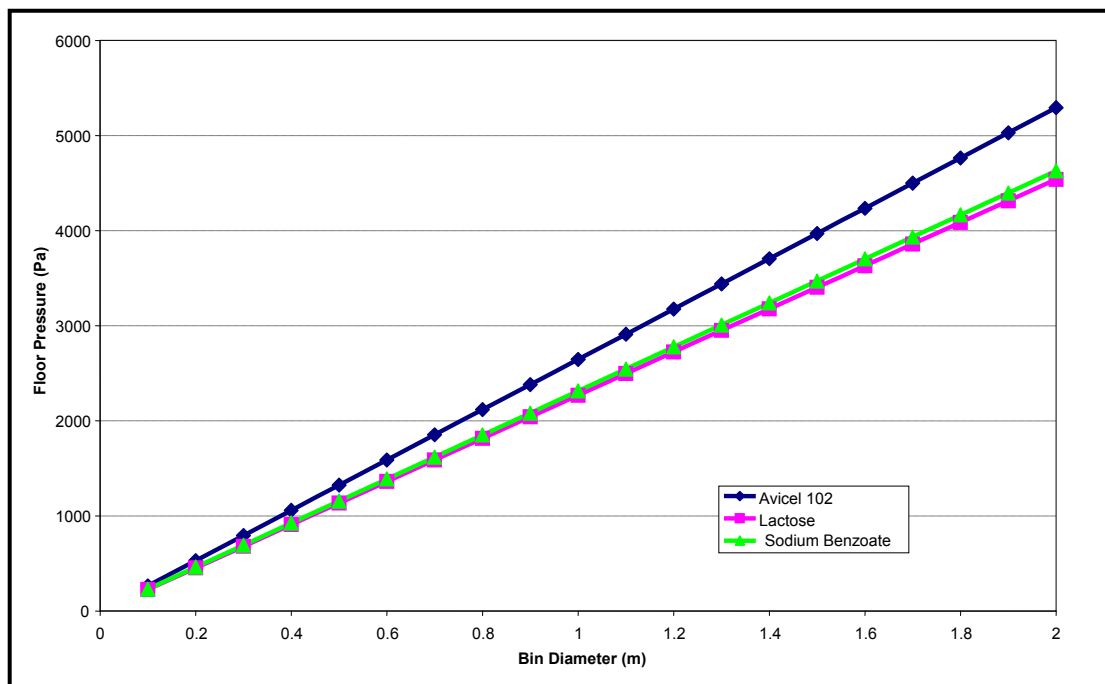


Figure 3.8: Normal loads generated at the base of a column of powder derived for three common pharmaceutical excipients using Janssen's equation

Although it not strictly accurate to assume K is constant – it is a function of the angle of internal friction (Roberts 1993), which in turn is a function of the consolidating load and thus varies through the bin – this approximate calculation shows the order of magnitude of the normal stresses that are likely to be experienced by a low density pharmaceutical powder in a typical IBC/small silo. Typically loads between 2 and 5 kPa are not uncommon for larger bins or IBC's, but intermediate hoppers (within a tablet press for example) are likely to be much smaller and thus floor/outlet stresses are commensurately lower.

However, these calculations refer to the stationary state. The actual shear mixing does not take place whilst the bin is stationary but when the surface layers of the powder are in motion during rotation of the IBC, as described previously. The stress levels on these layers are considerably less than that of the base even when stationary. Using the Janssen equation again and considering the stress levels in a 2m high by 1m diameter cylindrical vessel for the lactose sample used in these experiments, it can be seen that the stress levels at the top of the powder can be generally be defined by the simple hydrostatic convention ($\rho.g.h$) and are of the order of a few tens to a few hundreds of Pascals only (Figure 3.9).

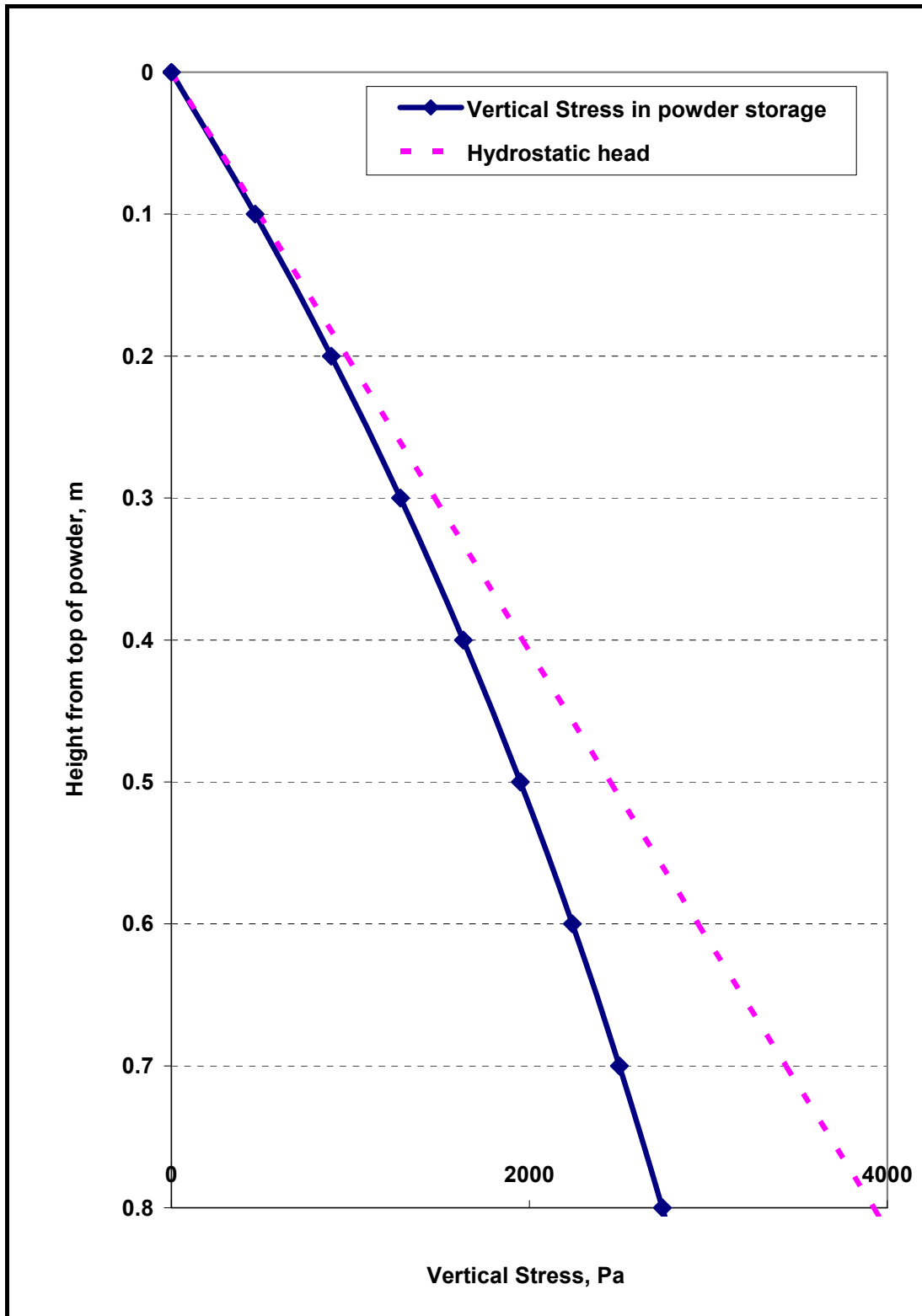


Figure 3.9: The vertical stress in a half filled 1.35mx1.6m cylinder with respect to the depth in the cylinder for lactose, using a wall friction angle of 25° derived from a wall friction test using stainless steel coupon ($R_a = 0.28\mu\text{m}$) from Janssen's Equation.

This fact coupled with the dilation of the sample that will occur during rotational motion make it clear that the shear mixing and convective mixing will take place when the powder is at low normal stresses and it can be stated that an understanding of the flowability/cohesiveness of powders at low stresses is a key requirement to predicting the blendability of a given material.

3.2.4. The measurement of powder cohesion and its influence on tumble blender performance

The terms cohesive and non-cohesive are used widely to distinguish classes of powders that have different flow & blending characteristics in batch pharmaceutical operations.

One of the limits to the application of tumble blenders is the level of cohesiveness of the materials to be blended. This low shear process struggles to de-agglomerate cohesive particles and can therefore be prone to developing areas of very low dispersion of, say, an active ingredient. This can be ameliorated to some extent by the inclusion of a baffle – usually referred to as an ‘intensifier bar’ – such as the GEA Prism™ (GEA Pharma Systems 2010a) shown in Figure 3.10.

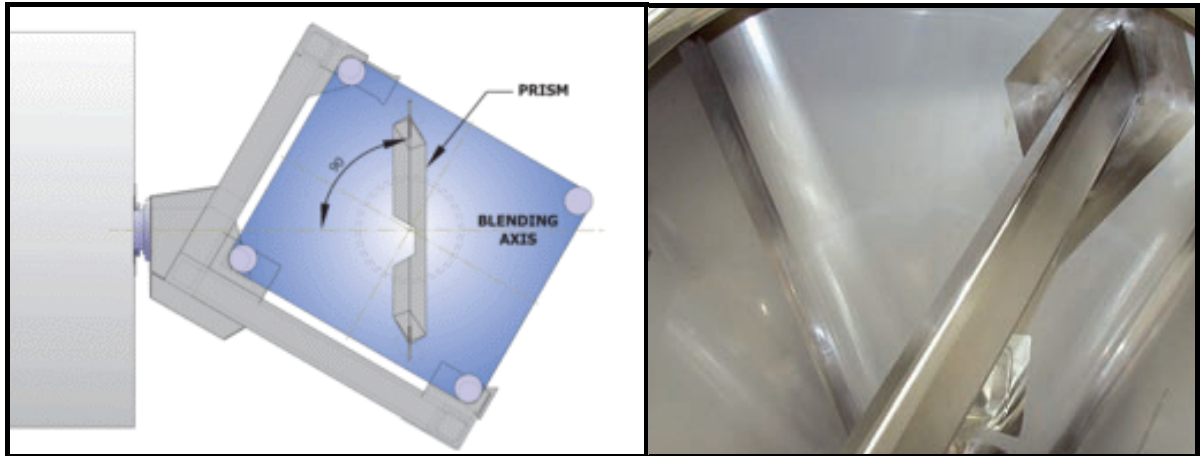


Figure 3.10: The GEA Prism™ intensifier bar shown schematically in plan view in an IBC fitted to a post hoist (left) and a photo of the Prism™ in-situ (right)

However, there is little in the way of quantitative evaluation of what ‘cohesive’ means in the context of low shear tumble blending systems and, perhaps more importantly, whether it is the correct term, or indeed which measurement or measurements to use when evaluating powders for blend development purposes?

A series of articles (Alexander A W *et al.* 2004; Alexander, Arratia, Goodridge, Sudah, Brone, & Muzzio 2004a; Alexander *et al.* 2004b) from the Rutgers Mixing Group, headed by Prof. Muzzio, highlighted a number of issues that they believed required further investigation – cohesion was one area given special mention (Muzzio & Alexander 2005).

“Cohesion is the most important property and determining the relationship among cohesion, shear, mixing rates and blender particulars is the ultimate goal.”

Clearly, the cohesion of a powder is important, and the use of the term 'cohesive' is widespread (Fitzpatrick *et al.* 2004;Khoe, Ip, & Grace 1991;Klausner, Chen, & Mei 2000;McCarthy 2003;Orband & Geldart 1997;Peleg & Mannheim 1973;Rennie *et al.* 1999;Visser 1989;Yamashiro, Yuasa, & Kawakita 1983). Finding any authors who actually attribute a definable measured parameter to the descriptor, or define a relationship to performance is difficult.

The Concise Oxford English Dictionary (Sykes 2005) definition of cohesion is:

“Sticking together; force with which molecules cohere; tendency to remain united;”

In comparison, the definition of adhesion is given as:

“Stick fast to (substance)”

So cohesion could be described as a sub definition of adhesion where the 'particles' stick to themselves rather than anything else. Given that the number of particles that are present in assemblies of fine powders, the number of cohesive contacts certainly outweighs the number of adhesive ones.

There are other technical definitions for cohesion, including:

“(Cohesion is the) resistance to shear in the absence of a normal load acting on the plane of failure” (Orband & Geldart 1997)

“(Cohesion is the) shear stress at yield under zero normal stress, i.e. the intersection of the yield locus with the ordinate”

These technical definitions are synonymous with the shear cell testing of powders based on the work of Jenike in the early 1960’s (Jenike 1964). The minimum level of normal consolidation stress suggested by the EFCE standard technique (EFCE 1989) is 1.5kPa. Cohesion is determined by reference to the normal stress/shear stress yield curve for a given consolidation load as described in Chapter 2, Figure 2.10. The area of concern here is that the cohesion is measured at incipient flow at a stress level that is likely to be significantly above those experienced by the powder in a rotating IBC as was described in Section 3.2.2.

Muzzio has also provided a definition in his 2005 paper (Muzzio & Alexander 2005);

“...a cohesive powder can be defined as a material in which the adhesive forces between the particles exceed the particle weight by at least an order of magnitude.”

Although this is perhaps a more useful descriptor, Muzzio does not, however, expand on how this would be measured. He also refers to a dimensionless cohesion number, a term used frequently in civil engineering, given by;

$$\Pi_c = \frac{\sigma}{\rho g R}$$

Equation 3.4

where Π_c is dimensionless cohesion

σ is the effective surface averaged cohesion stress (Pa or Nm^{-2} or $\text{kgm}^{-1}\text{s}^{-2}$)

ρ is the powder density at flow conditions (kgm^{-3})

g is gravitational acceleration (ms^{-2})

R is the vessel volume (m^3)

The first problem with this formula is that it is not dimensionless! This 'dimensionless cohesion' appears to have dimensions of m^{-2} . Most of the civil engineering texts that refer to this dimensionless factor have a depth value in the denominator [for example (Pack, Tarboton, & Goodwin 1998)] rather than a volume term which would produce a dimensionless number.

The second issue is one of measurement, as the frame of reference seems to be based around an un-measurable condition during flow for both the cohesion stress and the powder (bulk) density. Additionally the problem of what material is being measured is not resolved – does this equation refer to the fully homogenous blend; some intermediate blend state; the major component; the average of all the components etc? However, this is certainly a starting point as the values could, potentially, be measured with a shear cell, assuming it can operate at the low normal consolidation loads alluded to by Muzzio. Alternatively, the use of powder rheometry measurements may be useful in that they are generated by testing powders in a low stress, unconfined state which mimics the condition of powders in most blenders – especially tumble blenders.

To investigate this further, if one now compares this concept to the pull off force that would be generated in an Atomic Force Microscopy (AFM) experiment, as shown in Table 3.1 from the work by Lam & Newton (Lam & Newton 1992).

Table 3.1: Results of AFM experiment after Lam and Newton (Lam & Newton 1992) for spray dried lactose for the pull off forces required to remove a particle from a steel surface following an initial press-on force

Sieve Fraction (micron)	Particle mass (μg)	Mass standard deviation ($\times 10^3 \mu\text{g}$)	Geometric Mean Adhesion Force ($\times 10^{-7}\text{N}$)	Geometric standard deviation ($\times 10^{-7}\text{N}$)	Ratio of adhesion force to particle weight
-40+32	0.0383	1.48	2.72	0.4857	724
-45+40	0.0572	0.6	3.21	0.4092	572
-56+45	0.116	3.06	4.33	0.4670	380
-63+56	0.207	5.03	4.98	0.4326	245
-75+63	0.251	4.73	5.52	0.4698	224

It can be seen that for a spray dried lactose the measured adhesion force is $5.52 \times 10^{-7}\text{N}$ per particle for (average) 69micron particles whose weight per particle is $2.46 \times 10^{-9}\text{N}$. This means that the adhesive forces exceed the weight of the largest particles by 224 times. As expected the ratio increases with decreasing particle size which would confirm the general rule that fines are more cohesive.

Given the fact that this is a particle/surface pull off force (rather than a particle/particle pull off force), it would appear that Muzzio's characterisation of the term cohesion is likely broadly correct. However, this needs to be validated further with a range of different samples, ensuring that the AFM measurements relate to particle/particle pull off forces.

That still leaves the issue of the practicality of generating the data simply to define the cohesiveness for a large variety of powders, as AFM is still an esoteric technique largely confined to academia. There are a large number of other techniques, described in Chapter 2 that can do this much more cost effectively.

3.3. *Positron Emission Tomography*

Positron Emission Tomography is well established in medicine for the non-invasive imaging of the internal structure of patients. The technique relies on the tracking of a radioisotope that is administered to the patient in a formulation that will allow it to reach the part of the body that is of interest.

The application of these techniques to medical imaging is widely used (Bailey *et al.* 2004), but equally their use in the process industries would provide significant insight into many opaque systems. To this end the University of Birmingham Positron

Imaging Centre was formed as an interdisciplinary research centre run jointly by the School of Physics and Astronomy and the Department of Chemical Engineering. The Centre provides an international resource for studying a wide range of process systems, through application of the techniques of Positron Emission Tomography (PET) and Positron Emission Particle Tracking (PEPT). PET enables an individual component of multiphase flow to be radioactively labelled and visualised, and PEPT is a refinement of the PET technique invented at The University of Birmingham whereby a single labelled particle is tracked in real time. The papers by Parker and by Seville provide an overview of PET and PEPT (Parker *et al.* 2005; Seville, Parker, & Ingram 2005).

The principles of operation depend on a very specific property of a radio isotope. The isotopes typically used in radio-medical applications involve carbon-11, nitrogen-13, oxygen-15 and fluorine-18, which can be incorporated into compounds that can be easily biologically assimilated. The isotope used mainly for PEPT and PET studies is fluorine-18, which has a short half-life of 109minutes enabling it to be safely used in patients and for these experiments. These unstable isotopes are usually created in a cyclotron by bombardment of a substrate with positrons and neutrons. They decay by positron emission (also known as β^+ decay), and emit a positron (the antimatter counterpart of an electron). After travelling a very short distance, the positron encounters and annihilates an electron within the atom and produces a pair of annihilation (gamma) photons moving in almost opposite directions at a specific energy (511keV). It is this 'back-to-back' property of the photons that allows them to be used to pin point the location of the disintegration

along a straight line of coincidence known as the "line of response" or LOR. Multiple disintegrations result in multiple back-to-back photons and hence triangulation of the location of the radioactive source can be achieved. In PEPT, detection of a few such events can locate the position of the single tracer particle, whereas in PET, where a labelled bolus¹ is used, it is necessary to detect a large number of events from which the spatial distribution of the (dispersed) tracer can be inferred.

The photons are detected by photomultiplier tubes or silicon avalanche photodiodes (Si APD). Figure 3.11 shows a diagram of a detector block and the ring arrangement within a scanner, Figure 3.12 shows a schematic of the overall data handling process (Langner 2008).

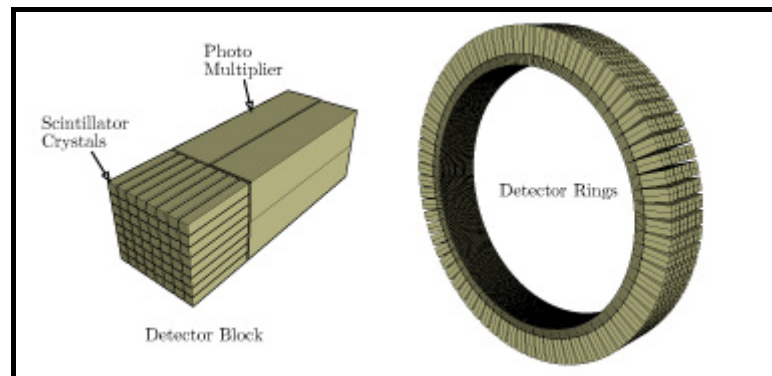


Figure 3.11: Detector block and the ring block of a PET camera

¹ A bolus usually refers to a single large dose of radioactivity in medial tomography applications and in this instance will be used to describe the irradiated sample of powder used in PET studies

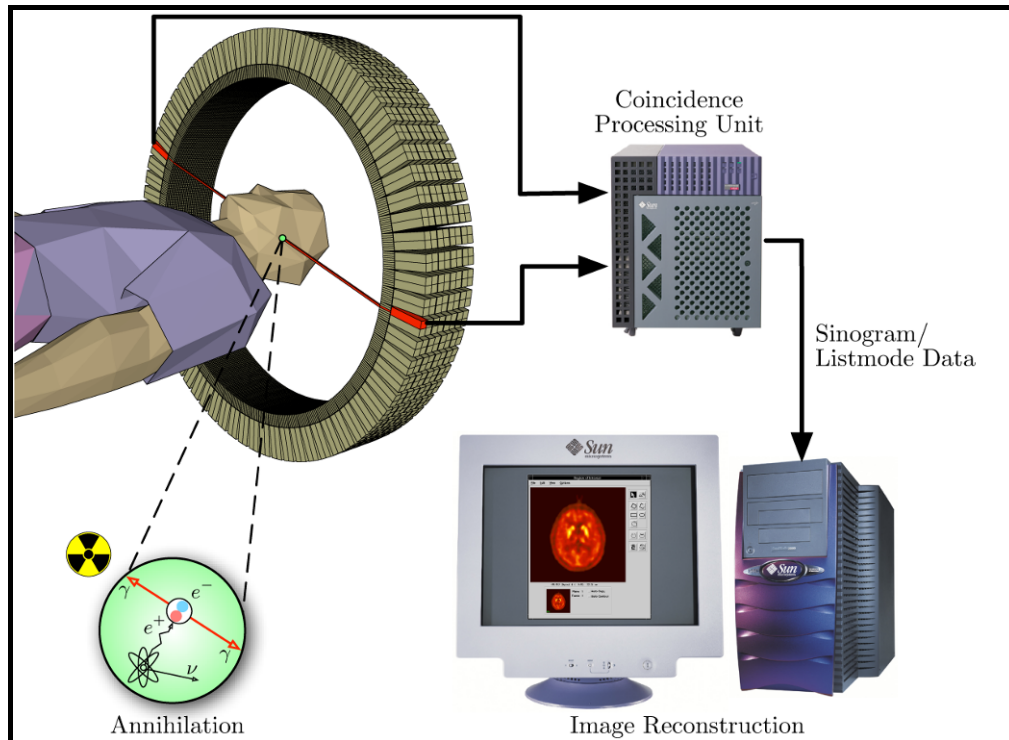


Figure 3.12: The data collection process from a PET camera

When two gamma particles are detected by opposed detectors within a certain time frame, this generates coincidence events which can be grouped into projection images, called sinograms.

The filtered back projection technique (Bailey, Townsend, Valk, & Maisey 2004) is used to reconstruct the image from the sinogram, however, 'shot noise' in the raw data is prominent in the reconstructed images and areas of high tracer uptake can form streaks across the image. This can be minimised in post processing by means of 'masking' which is described in Section 3.3.5.2.

Figure 3.13 shows the Forte dual-headed gamma camera manufactured by ADAC Laboratories that has been the primary scanning device within the centre. Its open

structure allows quite large process equipment to be located within the imaging zone, but its ability to reconstruct a full 3D image from multiple sources is limited as it requires the rotation of the camera plates (the lobes shown in Figure 3.13).



Figure 3.13: The ADAC gamma camera

Additionally, a Siemens ECAT scanner has also been commissioned during this project. The ECAT scanner is the most widely used PET scanner and Figure 3.14 shows the camera in-situ in a medical imaging suite. Unlike the two plate design of the ADAC camera, it is a whole-body system providing 2D and 3D volume measurements of an object by using the ring arrangement of detectors shown in Figure 3.11. The advantages of this machine are improved resolution of the radioactive material, but the size of the opening limits the size of process equipment that can be characterised.



Figure 3.14: ECAT scanner in a medical application

The system consists of the ECAT scanner, an integrated computer workstation and a patient couch.

Siemens indicate that the main characteristics of the tomograph are²:

- It is composed from 24 rings of 784 crystals each. Crystals are organized in blocks (7x8) read by 2 dual phototubes. In 2D mode, the sinogram size is 336 bins x 196 angles x 47 planes (which takes up about 6 Mbyte/frame). In 3D mode, up to 90% of the whole solid angle can be acquired and is re-binned (phi and theta) to 23 Mbyte/frame. The bin size is 1.65 mm (3.125 mm) in the tomographic (axial) direction.
- The spatial resolution is about 3.6 mm (in-plane) and 4 mm (axially).
- The bed can be adjusted in height to optimize acquisition solid angle and whole body scans are performed on 180 cm in one shot.

² Taken from Siemens promotional literature and equipment documentation

- The sensitivity in 2D and current 3D modes are 177 kcps and 1460 kcps, respectively.

3.3.1. Tomographic evaluation of mixing behaviour

A series of experimental studies has been undertaken to develop methods for imaging a laboratory scale tumble blender for a two component system. These include PEPI, PET and PEPT. The PEPI and PEPT studies were carried out on the existing ADAC camera, the PET studies on the ECAT camera which was installed and commissioned during the project.

The main reason for choosing PET as the primary evaluation technique, over the well established PEPT technique, was resource usage. Positron Emission Particle Tracking (PEPT) has been evaluated as a technique to evaluate randomness of movement has been developed and validated for extended mixing periods (Jones *et al.* 2002; Martin 1998). However, the mixing of two substrates within a lab scale tumble blender was likely to achieve a fully blended condition within 100 revolutions or, typically, 8-10 minutes of operation. The evaluation of the dispersion of a small volume of secondary substrate with a single tracer particle could not be completed in such a short time period, as the analysis methodology requires a large number of motions of the particle through the vessel. In addition, it would not be known during any given time if the particle was passing through one substrate or another which may significantly affect its behaviour if the substrates flow properties were different. Thus, to characterise a single system would require a considerable amount of

camera time as well as a large quantity of the test materials. Given that the availability of the ADAC camera was limited and the results would be complex – combined with the waste disposal issue – it was decided to generate most of the data using the ECAT camera.

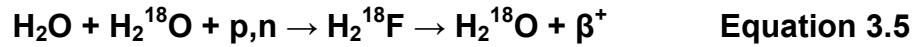
The advantages of combining the PET scan with the tumble blender are that the scan evaluates the entire process volume which can then be studied to evaluate the content uniformity by measuring the radioactivity down to a small proportion of the vessel volume. The process also lends itself to the use of this camera as the tumble process can be stopped and started without significantly disturbing the state of the powder in the vessel. This would be less feasible for a paddle mixer, for example, where powder is continually being lifted and dropped and stopping the process would significantly change the state of the material.

The vessel used throughout the mixing studies was a cube/pyramid laboratory scale, 10litre mini IBC, shown in Figure 3.5 and fitted to a laboratory blender shown in Figure 3.4, manufactured by Buck Systems.

3.3.2. Sample preparation

In all the experiments reported here, the tracer is a pharmaceutical grade of microcrystalline cellulose (chosen because of its low water solubility) which has been doped with radioactive water generated in the University's cyclotron housed in the Department of Physics. Water is bombarded with protons and neutrons which are absorbed by oxygen nuclei to create ^{18}F which then rapidly decay by β^+ emission

(described earlier), the reaction can be described by the simplified equation given below;



This isotope has a half life of 109 minutes and means that it can be used safely within a laboratory environment as there is no detectable radiation from a sample within 24hours of an experiment (Fan, Parker, & Smith 2006a; Fan, Parker, & Smith 2006b; Parker & Fan 2008).

For PEPT studies a small number of particles are placed in a container of the radioactive water, allowed to absorb the radioactivity (as H_2^{18}F), removed and dried. A single particle is then abstracted and its activity measured. If it achieves an acceptable level of radioactivity (dependant on the opacity of the system and the time required for operation) it can be used in an experiment. If not, another particle is evaluated. This procedure is well understood and has been utilised for several years and in many successful studies (Hoomans *et al.* 2001; Jones & Bridgwater 1998; Parker *et al.* 1997; Parker *et al.* 2002; Waters *et al.* 2008; Wildman *et al.* 1999; Yang *et al.* 2008) where the tracking of single particles is appropriate for the (steady state) nature of the process.

The preparation of the radioactive sample for PEPI and PET studies requires the doping of a large number of particles to create a radioactive bolus. To prepare the sample, the target powder is gently stirred in a vessel whilst radioactive water is added slowly to the sample. Only a small quantity of material – typically only 100-

150ml of powder – can be prepared to limit exposure of the technician who is preparing the sample to this radioactive source.

The particular issue with this sample preparation technique is the uniformity of the uptake of the radioactivity between the many particles that have been exposed the radioactive water. Isolating a single particle and evaluating its activity, as performed for a PEPT study is relatively simple, evaluating the evenness of the distribution of activity over many thousands of particles is clearly a much more complex task, which was not resolved during this study. A simple spreading of the active powder (as close to a mono-layer as practicable) and evaluating the radioactivity using a laboratory hand held Geiger counter was attempted, but the size of the measurement head and the poor instrument sensitivity meant it was unrealistic to be able to quantify any variation in activity. In addition, and more importantly, such a measurement exposed the operator to a significant radiation dose and for health and safety reasons the development of this technique was curtailed. It was therefore assumed that each radioactively doped particle in a given bolus possessed the same level of activity for the purposes of these experiments.

3.3.3. PEPI Studies

Before the commissioning of the ECAT camera had been completed, a series of experiments were undertaken to gauge the methods chosen for sample preparation, evaluating the levels of radioactivity that could be achieved using the labelling

technique described in Section 3.3.2, and assessing the experimental methodologies using the PEPI method of data capture/interpretation available for the ADAC camera.

This method can only generate single 2D images of the sample volume.

Two sets of tests were undertaken. The first used a simple round tub, into which ~0.75 litres of MCC microcrystalline cellulose (MCC) was added. A small portion, approximately five cc, of radioactive MCC was then added as the tracer. It was placed as a small pile into the centre of the un-doped MCC in the tub which gave an approximate volumetric concentration of 0.33%. The tub was then rotated by hand for 10 revolutions and then placed into the camera and data was collected for ~2 minutes. An example of the data collected is shown in Figure 3.15.

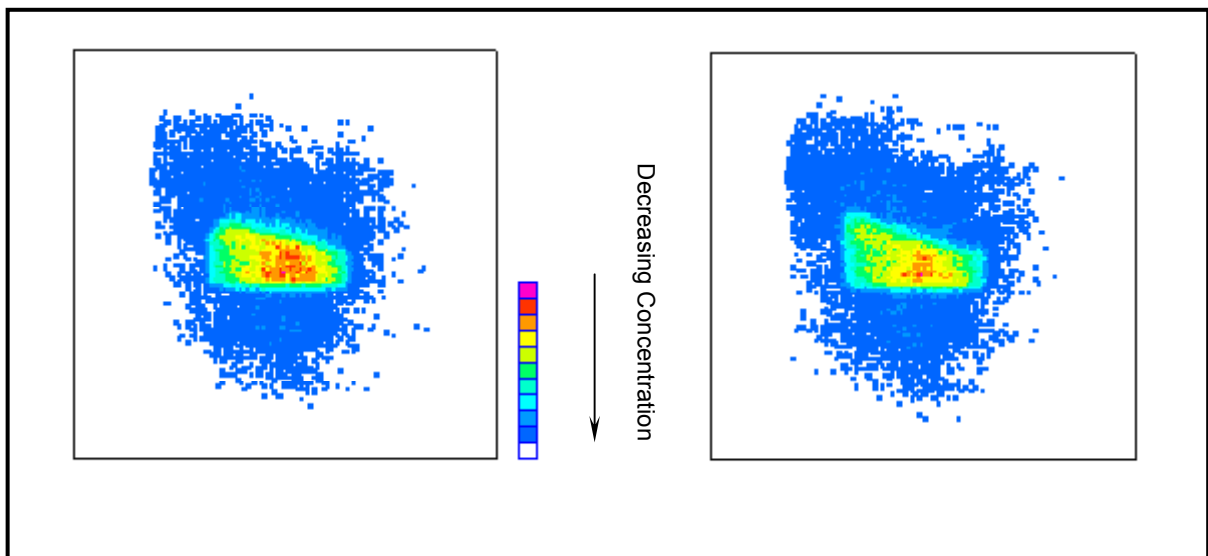


Figure 3.15: Example of PEPI test using MCC in plastic tub showing two orthogonal views of the system – colours at the bottom of the scale show (relatively) lower concentration to those at the top of the scale.

The following should be noted when viewing the results. The data have been fully processed and no account of the shape of the tub has been factored into the picture. Additionally the background level (the blue haze around the more concentrated areas) has not been removed from the pictures for this scoping run.

Both sets show the considerable concentration of doped material in the centre of the image, close to where it was originally placed. Clearly very little quantitative data can be gleaned from these results, but qualitatively the effect (or lack thereof due to limited operational capabilities) can be seen.

The second set of tests was undertaken using a lab scale blender, provided by Buck Systems. The unit has a 10litre mini IBC shown in Figure 3.5. Its operational envelope is; 2-15 rpm in 1 rpm increments; 10 degrees offset for the rotation; manual or automatic control with 0-900 revs or 0-1800 (max) seconds limit per operational cycle.

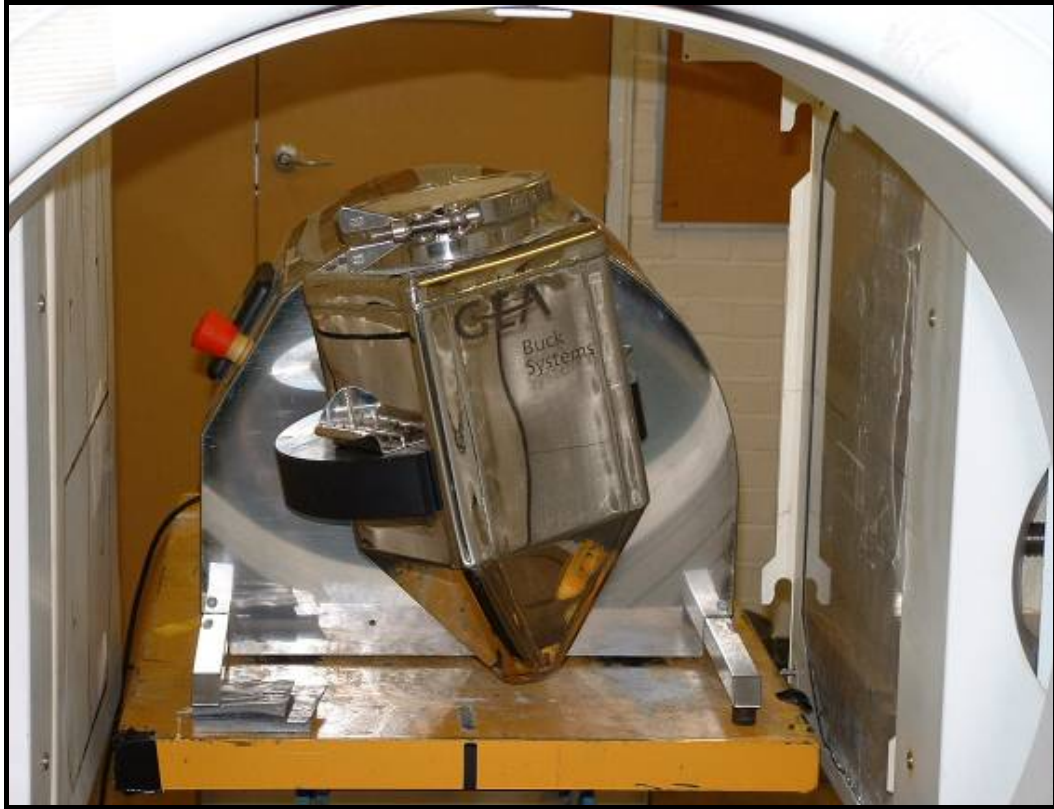


Figure 3.16: Experimental set up for PEPI testing

The test runs utilised the twin plates to take readings in the horizontal and vertical orientation so that a more complete picture of the distribution could be observed.

The measurements on each photo image relate to the average radiation that the camera sees from its fixed position. In effect the image is the sum of activity through the vessel. It would therefore be necessary to take account of the shape of the vessel to moderate the effect of the camera averaging the radiation from more material at the centre of the bin for example. This can be achieved by rotating the plates and taking images from a range of positions (in effect to mimic a ring PET camera), this takes a considerable amount of time and it would not be practicable to fully monitor a blending experiment.

Additionally, as the experiment progresses there is a need to account for the decay of the isotope. Scintillation data (when back to back gamma rays are detected by the instrumentation in the plate) generated by the radioactive materials in the vessel are collected during the 360° rotation of the plates to generate a single image of how the radioactivity has been dispersed within the vessel. However, there is a balance between the length of time required to collect enough scintillations to ensure a well focussed image and the decrease in activity of the radioactive material during the measurement period, which for this isotope is significant. Thus the distribution of radioactivity will seem much 'brighter' at the start of the rotation compared with end of the rotation. The current software for the ADAC camera does not account for this automatically. Thus data from a scan has to be moderated in the post processing to normalise the result with respect to the maximum value obtained in the test. Figures 3.17 and 3.18 show data that have been normalised, with intensities in the range 0-100% of the maximum of the radioactivity that was measured during the test.

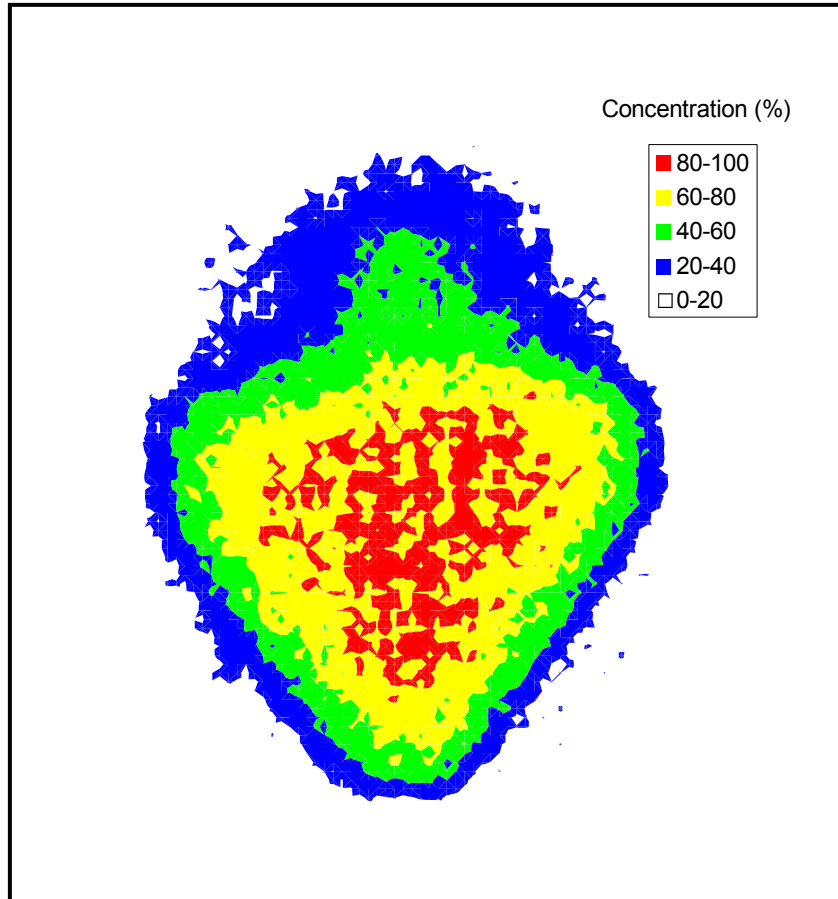


Figure 3.17: Normalised PEPI image showing side view of the 10litre lab blender

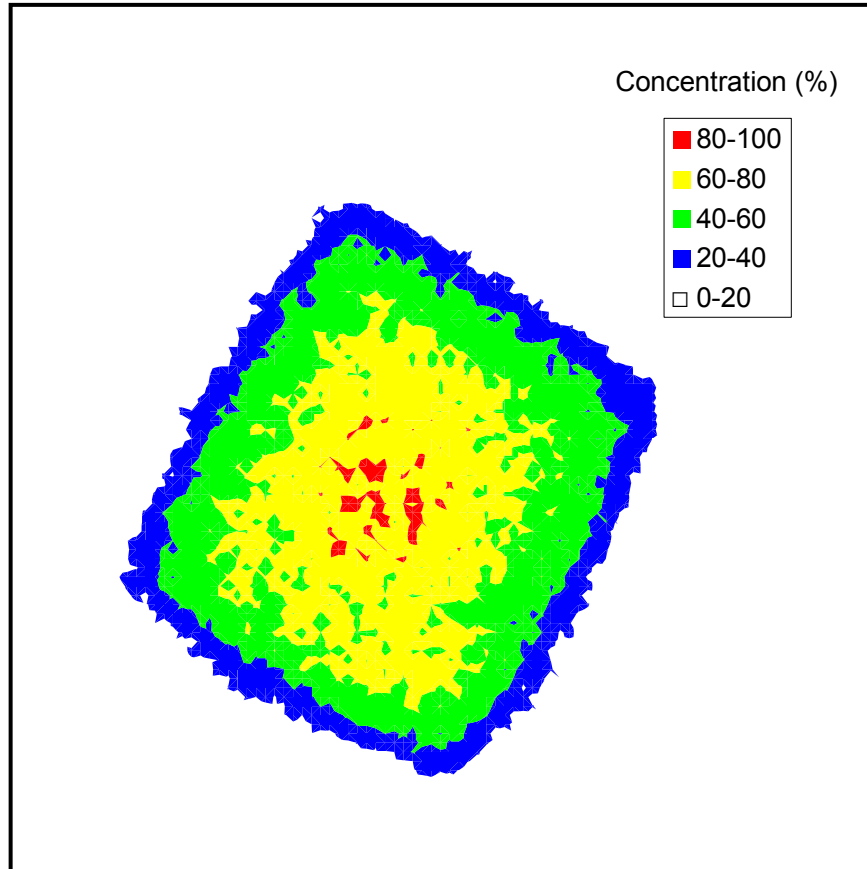


Figure 3.18: Normalised PEPI image showing top view of the 10litre lab blender

As can be seen from Figures 3.17 and 3.18 there is a distinct edge to the image that defines the limit of the powder mass and the inner wall of the IBC (except for the top surface). The concentration is derived from the averaging of the radioactivity across the entire plane of view. Thus for Figure 3.18 this is an average through the entire IBC – top to bottom. This of course biases the interpretation of the image as there is more powder being imaged at the centre of the vessel (due to the hopper section) than at the periphery.

To achieve a complete visualisation and hence understanding of the process, more detailed scans with the ECAT camera were undertaken.

3.3.4. PEPT studies

A series of PEPT studies was also carried out using the ADAC camera. The experimental set up is identical to that for PEPI, shown in Figure 3.16, but does not require the multiple positioning of the plates as a single particle is being tracked in real time to evaluate the dynamic behaviour of the system.

The reasons for undertaking additional testing using PEPT were twofold.

- Pilot scale testing using the recently developed large scale mobile positron camera may be possible using PEPT, which could enable scaling criteria to be developed in the future, and it was therefore useful to obtain an understanding of the information that could be obtained.
- To investigate how data could be collected and interpreted using this method, as the PEPT technique typically relies on a statistical distribution of locations and velocities to generate process behaviours. This usually requires several hours of monitoring of the motion of the tracer particle, with the process at steady state, to ensure it has reached all locations sufficiently often to allow confidence in the data. Therefore the usefulness of this technique to evaluate the 5 or 6 minutes it takes for the unmixed powders to achieve an acceptable mixedness (as will be demonstrated during the PET experiments) needed to be resolved.

Two tests were undertaken using Sodium Benzoate and Lactose as the substrates and a 200 μm Microcrystalline Cellulose particle was used as the tracer. Approximately 5 litres of substrate was used in each experiment.

The data is analysed in the computer programme TRACK (Positron Imaging Centre 2000) which has been updated to include the dispersion analysis programme derived from the work by Martin (Martin 1998).

The analysis is based on the concept of measuring the distance travelled by the tracer particle from a given location in a given time. During any experiment it is likely that the tracer will pass through the location many times and the loci of the end points can be determined as shown in Figure 3.19.

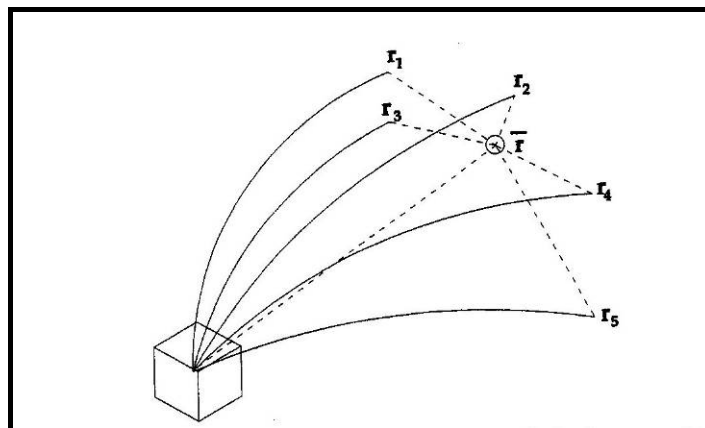


Figure 3.19: Schematic of dispersion calculation method

This process is undertaken for all parts of the system under observation and can provide the variance between the mean end location and the end points as shown in the equation below.

$$\sigma^2 = \frac{1}{n} \sum_{i=0}^n (x_i - \bar{x})^2$$

Equation 3.6

where σ^2 is the variance
 x_i is value of the i th measurement
 \bar{x} is the mean of all the measurements
 n is the number of measurements

The higher the variance, the greater the spread of the particle as it passes through a given location and thus the greater the dispersion.

There is, of course, a time dependency on this information. The longer the time that is allowed to pass for the particle to leave the start point and arrive at the range of end points then the greater the dispersion is going to be for a given set of process parameters. Typically the time base used is around 50 milliseconds and is a compromise to allow an acceptable number of dispersions to occur for each position within the blender for a statistically meaningful standard deviation to be calculated.

The dispersion analysis, Figure 3.20, shows the cumulative dispersion of the tracer particle in the Sodium Benzoate substrate after 500s at 15rpm (125 revs).

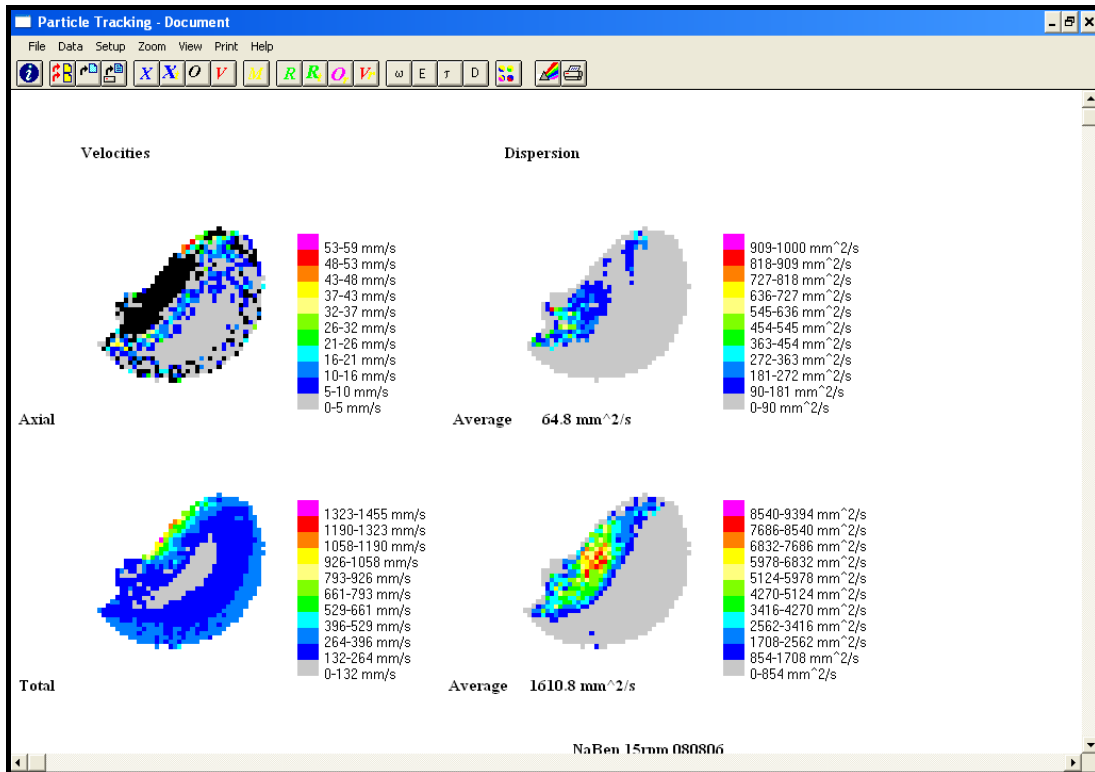


Figure 3.20: Screen shot of dispersion analysis for Sodium Benzoate at 15rpm after 500s

It should be noted that this is NOT an image of the powder in motion, which it might appear to be at first interrogation. The dispersions appear to resemble the motions of a drum blender, as depicted in Figure 3.6, but this not the case. The data represents the positions where the radioactive tracer has been and its dispersion can be measured (as described by Figure 3.19 and Equation 3.6). The overall shape of the locations of where the particle has passed is, not surprisingly described by a truncated circular path, but no implication as to mode of flow can be ascertained from this data, merely that certain velocities can be identified when the tracer is at certain locations within the bin.

Additionally it appears there are some issues with the velocity analysis. With respect to the velocity diagram, the large patch of black is not represented in the

measurement scale because this relates to 'negative' velocities i.e. those which the data analysis programme deems to be in the opposite direction to the general flow of the bin and material – this is quite useful as it confirms that there is a significant level of axial flow at the powder surface during mixing – which is of particular issue for some mixer types (Brone *et al.* 1997; Brone & Muzzio 2000).

The analysis of these data has concentrated on the analysis of the dispersion information provided by TRACK. The data was analysed by evaluating the total cumulative dispersion with respect to the duration of the experiment for Sodium Benzoate and the Lactose (Figures 3.21 and 3.22).

The cumulative dispersions show that there is a rapid increase in the average cumulative dispersion with respect to the total number of revolutions which then slows down dramatically or even levels off to a steady state, as previously shown by Martin (Martin 1998). This is where the particle has reached most of the likely locations within the described volume during the experiment. The dispersion can increase with the increasing length of the experiment due to the statistical likelihood that the particle will reach the extremities of the bin more often, increasing the total dispersion and the expansion of the powder bed due to the interaction with the air in the bin to increase the total volume. The point to note therefore is the change in the rate of dispersion, not the slow increase in dispersion that occurs after longer blending periods.

Specifically for the Sodium Benzoate substrate, the point of rate change appears to increase with bin rotational speed, as hypothesised following the tests on the SMS PFA and FT4 powder rheometers. This is likely to be due to the shape of the particles. The form of Sodium Benzoate used for these tests has a significant proportion of plate like particles whereas the lactose is predominantly spheroid. Thus it is possible that higher rotational speed may limit the movement of these platy particles; there is not sufficient time for them to slide over each other during a rotation and the small increase in centripetal force with increasing rotational speed may also increase the frictional resistance.

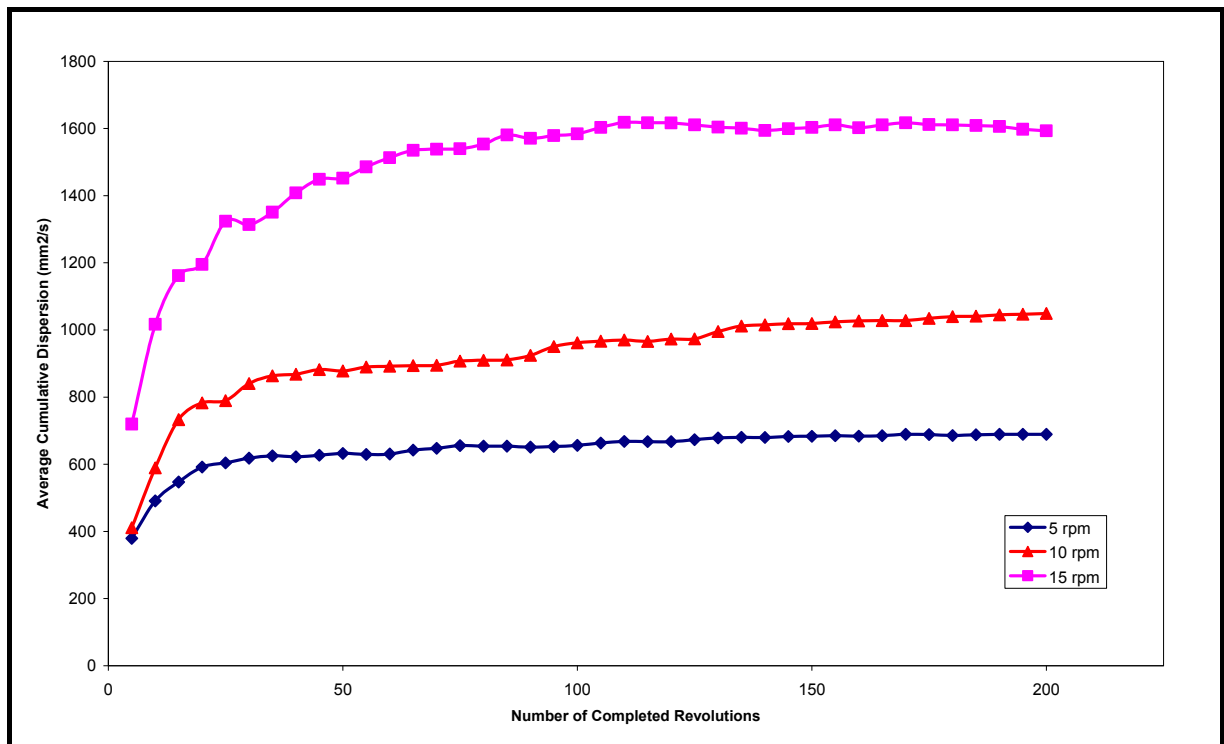


Figure 3.21: Cumulative dispersion for MCC tracer in Sodium Benzoate

The Lactose, which is composed of more spherical particles, shows very similar behaviour for the 5 and 10 rpm experiments, Figure 3.22. The 15rpm experiment is

also, arguably, similar but shows some discontinuities which may be due to agglomerate disintegration during the test.

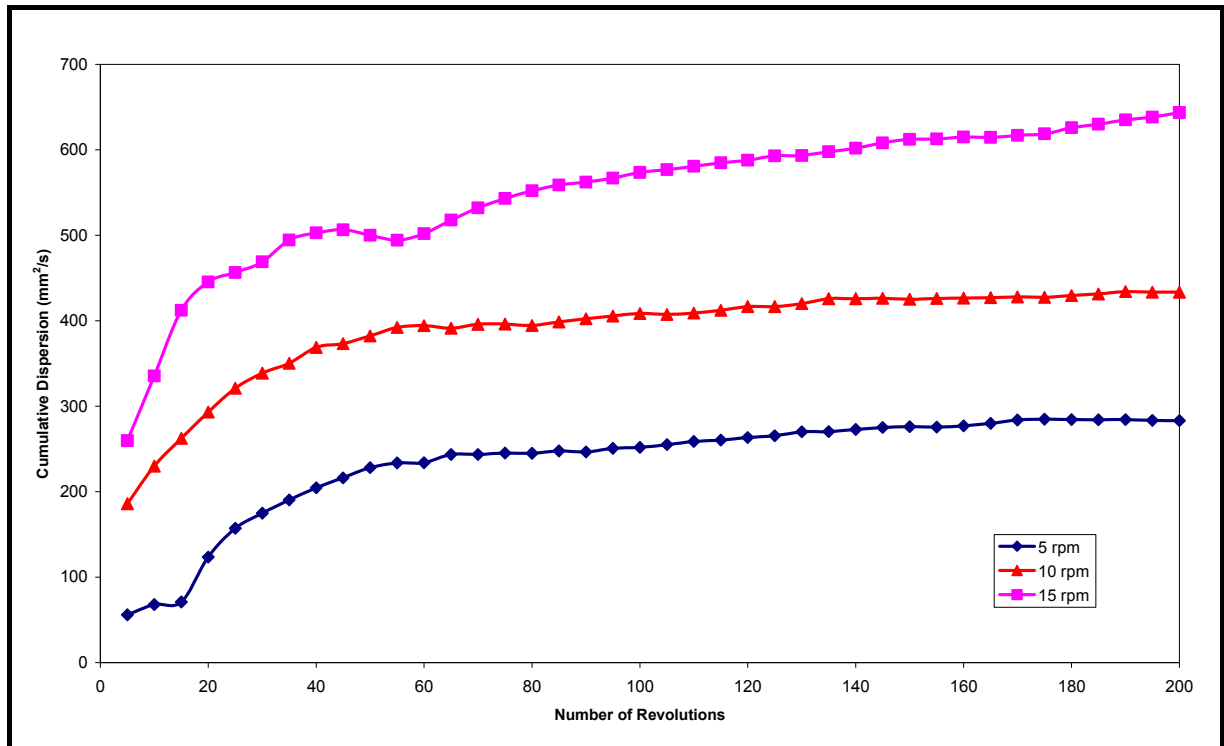


Figure 3.22: Cumulative dispersion for MCC tracer in Lactose

Additionally a method for the analysis of the dispersion at 5 rev intervals based on a simple statistical analysis of the data (shown in Figures 3.23 & 3.24) was undertaken. The statistical evaluation also shows significant differences between the two substrates. The standard deviation of the dispersion data for the Sodium Benzoate increases with bin rotation speed whereas the standard deviation of the Lactose remains constant showing its more repeatable dispersion with respect to bin speed. The much larger standard deviation observed at high IBC rotation speed describes the inconsistent dispersion of the tracer particle through this material, indicating the flow of the tracer through the substrate powder is not uniform. This is not due to the

cohesiveness of the sample but is likely attributable to the shape factor of the Sodium Benzoate and the rotational and translational frustration described in Chapter 2, Section 2.5.2.

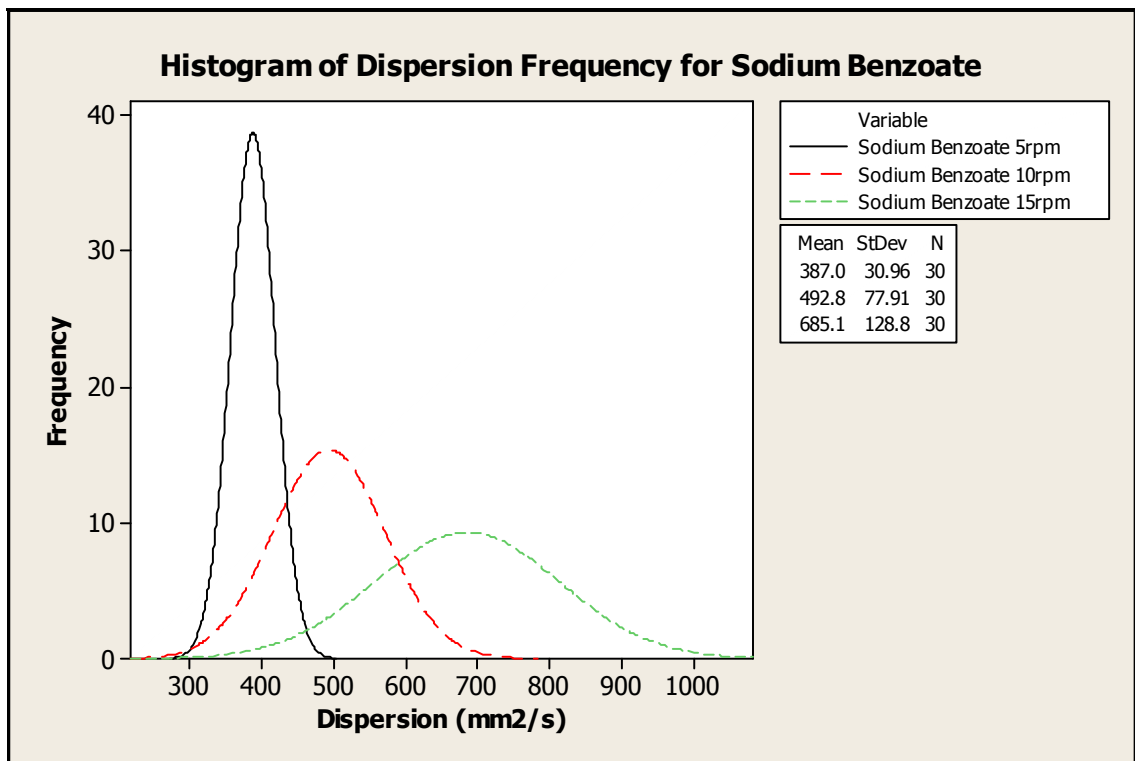


Figure 3.23: Statistical representation of dispersion in 5 rev intervals for Sodium Benzoate

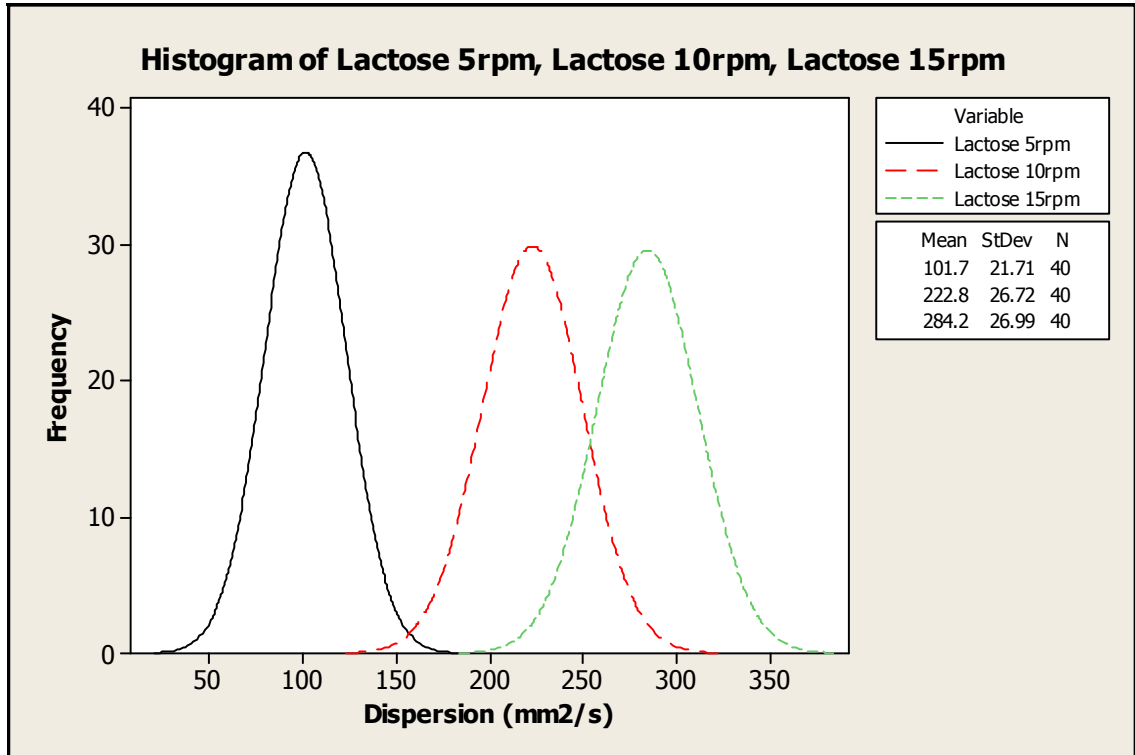


Figure 3.24: Statistical representation of dispersion in 5 rev intervals for lactose

A further series of tests to investigate how PEPT would work with two component systems was also undertaken. Previous work using PEPT for mixing systems has concentrated on particle dynamics and no blending has actually been undertaken. Here two extremes of minor component concentration were evaluated – 1% and 40%, Figure 3.25.

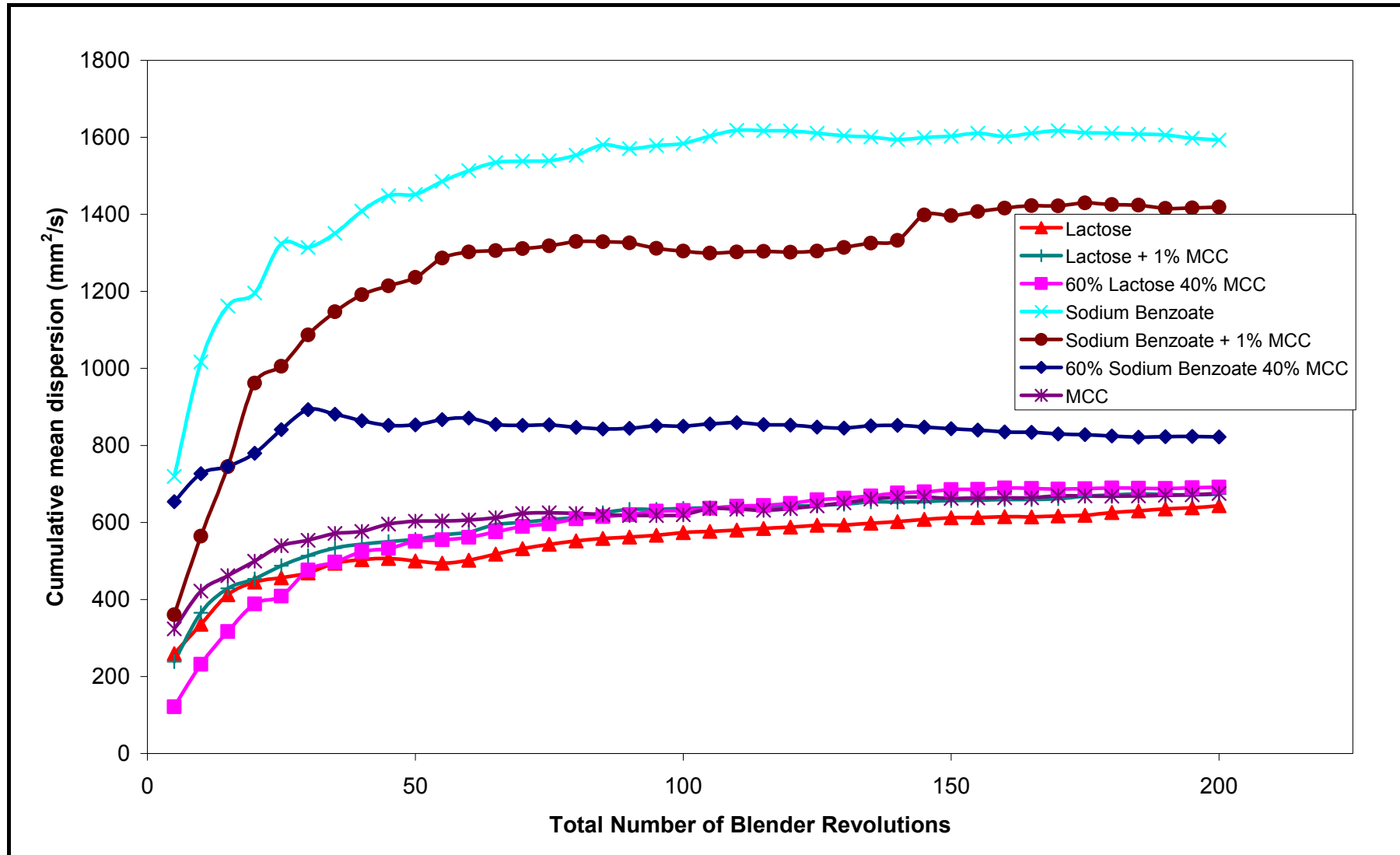


Figure 3.25: Cumulative dispersion of a tracer particle in binary systems

The interesting point of note is that the lactose/MCC system (two very similar materials in terms of their particle size and shape) showed very little change in absolute and rate of rise of dispersion, whereas the Sodium Benzoate/MCC system (two very dissimilar materials with respect to particle shape) gave dramatically different results with respect to the proportion of MCC. The increase in MCC significantly lowered the cumulative dispersion and moved the dispersion levels closer to that of pure MCC. This shows quite dramatically the influence of particle shape on the ability of a system to allow a minor component (in this case a single tracer particle) to disperse within a larger volume of powder.

Overall, however, PEPT has some shortcomings with respect to its ability to describe the mixing of one or more powders with respect to the determination of the end point.

- It can only follow the dispersion of a single particle – it cannot quantify the overall dispersion of a component or when that dispersion has achieved the appropriate target level.
- In order to provide statistically valid interpretations of the entire behaviour of a process that is in a steady state – e.g. a fluidised bed – the PEPT experiment needs to run in excess of an hour. This is well beyond the point at which a two component mixture will have gone from completely un-mixed to fully mixed – as will be shown with the PET experiments in the next section.

3.3.5. PET Studies – Siemens ECAT Camera

The development of a robust, non-invasive, practical and simple technique to characterise the composition of the contents of a blender is central to understanding the processes that are occurring and eventually the development of a predictive capability. The trials using PEPI & PEPT, described in Sections 3.3.3 and 3.3.4, reinforced the view that PET undertaken using the ECAT camera would provide a more detailed evaluation of the vessel contents that would be simpler to analyse and more repeatable.

3.3.5.1. Experimental

The experimental procedure followed the same methodology as the earlier PEPI tests, namely a small quantity of radioactively doped material was placed on top a much larger quantity of different powder in a laboratory scale blender. This mimics the typical operation of industrial blenders.

From a practical point of view, the scope of the tests was limited by the length of the experiment. This was dictated by several factors. The main issue was the amount of the radioactivity added to the substrate. The ECAT camera has a compensation algorithm that adjusts the exposure time in line with a reduction in radioactive count rate during an experiment. If too little was radioactivity was added, the exposure time was extremely long – typically 40+ minutes – per image, which would become longer

every time the IBC was tumbled and the ECAT camera had to acquire the next image, due to the radioactive decay of the ^{18}F .

The size of the IBC meant that its entire volume could not be imaged in a single frame, but required that the IBC was fitted to the computer controlled patient couch which could then be moved further into the camera cavity once the first part of the image had been captured.

Thus following some initial scoping studies, it was decided to limit the rotational speeds to 10 and 15rpm, where 15rpm was the maximum speed achievable by the blender. This allowed a reasonable balance between the time taken to complete a study, the decay of the radioactivity over this time and the exposure during sample preparation. The scoping studies also highlighted the need for keeping the IBC rigid and a frame was constructed that would hold the IBC and was fitted to the patient couch (Figure 3.26)



Figure 3.26: Mini-IBC located in its support frame prior to insertion into the measurement cavity inside the camera

Prior to testing a transmission scan of the vessel and the non-radioactive powder is taken. This scan is stored within the control computer and is then subtracted from any subsequent scans so that only the radioactive powder is evaluated. Large quantities of metal, in this case the stainless steel of the vessel, have their own signature when in the measurement field and would be seen as a bright line interfering with any subsequent evaluation of the intensity of the radiation within the measurement field due the irradiated bolus.

The chosen substrate was loaded into the mini IBC and the radioactive bolus of MCC was gently tipped onto the surface of the substrate. The vessel was sealed and was rotated at the designated speed for 5 revolutions and stopped. The positron camera was then used to acquire a 3D tomographic scan of vessel contents, a process that takes approximately 20-40 minutes per scan. This variation in acquisition time is controlled by the ECAT camera operating system which automatically compensates for the decay of the ^{18}F isotope during the measurement (but not between measurements). This was repeated a further 10 times at 10, 15, 20, 25, 35, 45, 55, 70, 85 and 100 revolutions. Typically this resulted in a 6-7 hour experiment.

The tracer used in all experiments was microcrystalline cellulose, in this case Avicel 102, which has a mean particle size of about 100 microns and could be easily doped with the ^{18}F that was used as the tracer. The size of the MCC bolus was 85-345ml in 3-7litres of substrate which is typical of pharmaceutical blending where the active ingredient, or minor component, is a very small proportion of the overall powder volume, which in turn is between one-third to two-thirds the vessel volume.

During the project there were a number of system failures with the camera and the control computer. This limited the number of useful data that were collected to nine which are detailed in Table 3.3 in Section 3.3.5.3.

3.3.5.2. Image analysis

The data collected from the ECAT camera was exported in a form that could be read by and processed using a public domain Java image-processing program ImageJ, (Abramoff, Magelhaes, & Ram 2004). Figure 3.27 shows a screenshot of experimental data being processed using this programme.

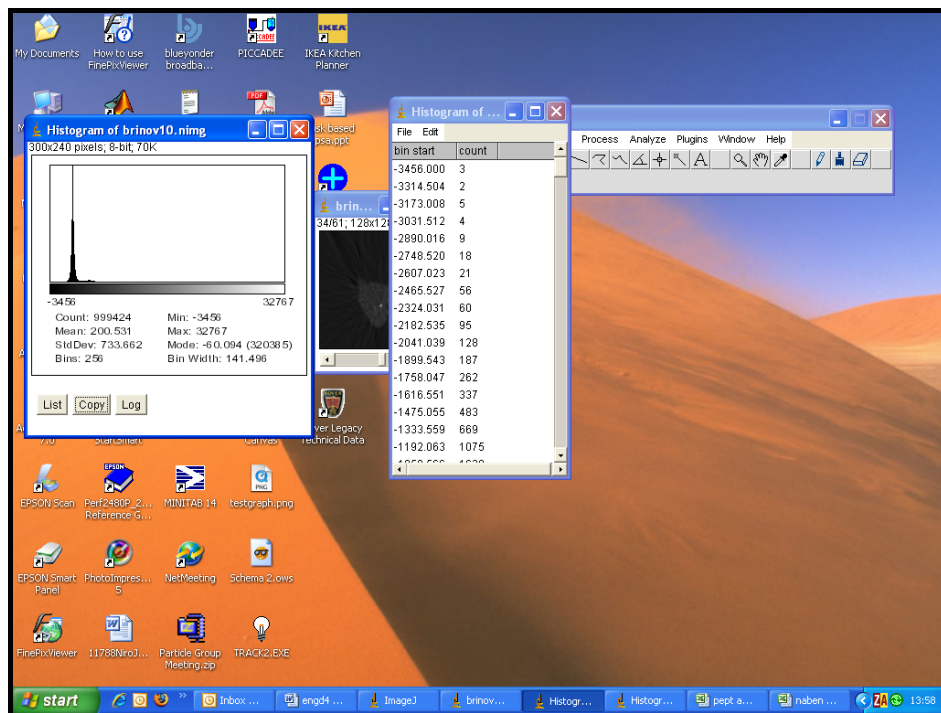


Figure 3.27: Screenshot of ImageJ software

The raw data was collected on the UNIX control computer for the ECAT system and pre-processed prior to export for interpretation using the ImageJ. This procedure prevented the hard disc of the UNIX machine from being saturated and also freed up the control system allowing further experimentation to continue.

The data file was exported in a form that could be imported into ImageJ as a bitmap 62 slices of 128x128 pixels using a software applet developed in the Department of Physics. This gives a voxel size of $\sim 43\text{mm}^3$, considerably smaller than the uncompressed tablet volume of most pharmaceutical excipient mixtures. Based on poured densities of the test powders, 43mm^3 represents 10 to 90% of a typical tablet dose volume assuming a 200mg tablet weight.

A single blending experiment consisted of 11 separate data sets taken at 5, 10, 15, 20, 25, 35, 45, 55, 70, 85 and 100 revs. Each data set, or stack, consists of 62 slices or images showing the concentration of the radioactivity within the powder as relative brightness on the screen. Figure 3.28 shows a stack of slices from a Lactose experiment at 15rpm.

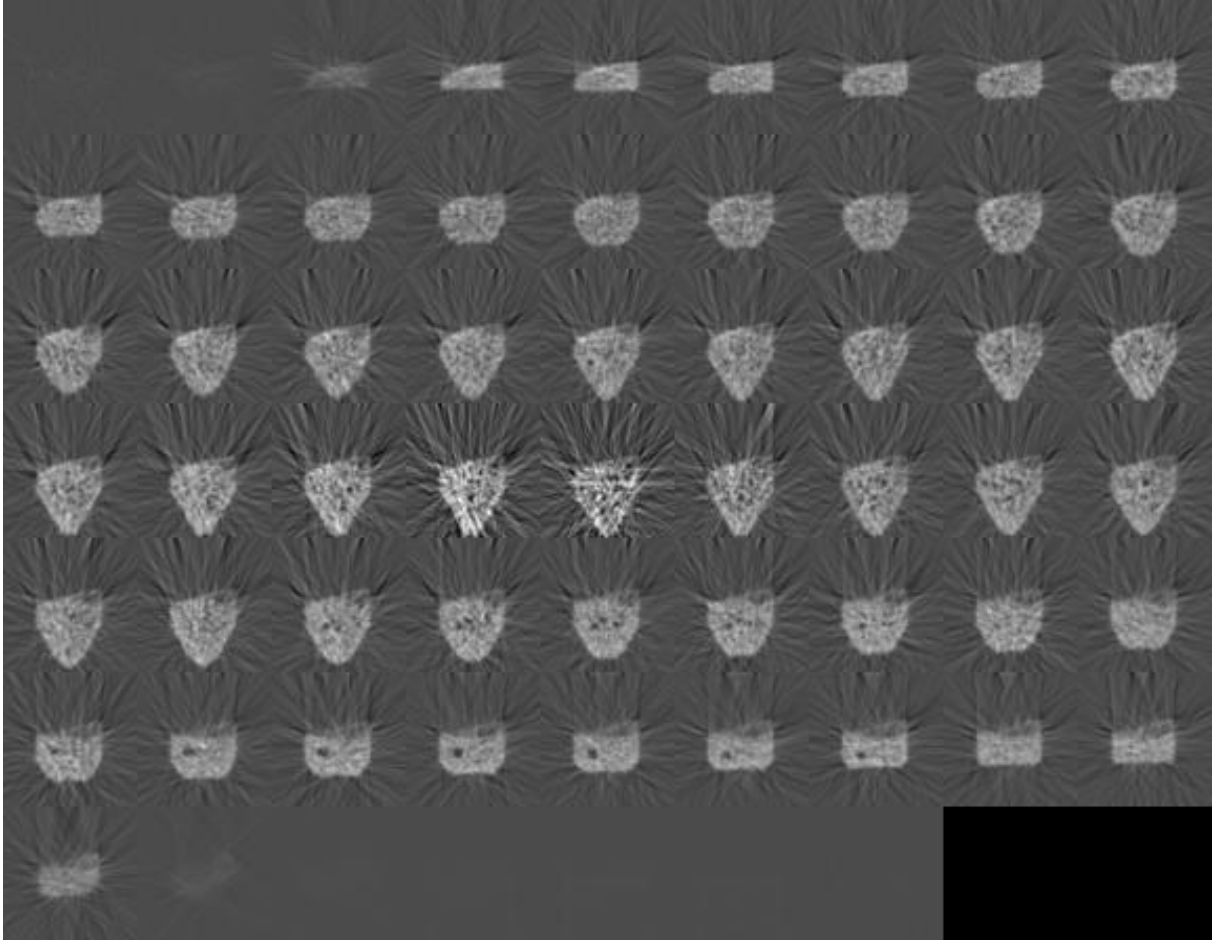


Figure 3.28: Re-constructed sinogram of a blending experiment showing the 62 slice images of the powder in the test vessel moderated for the background and vessel transmission scans

As can be seen from the Figure 3.28, the images appear quite noisy, but this is common in unprocessed data as seen in the Figure 3.29 below of a medical application.

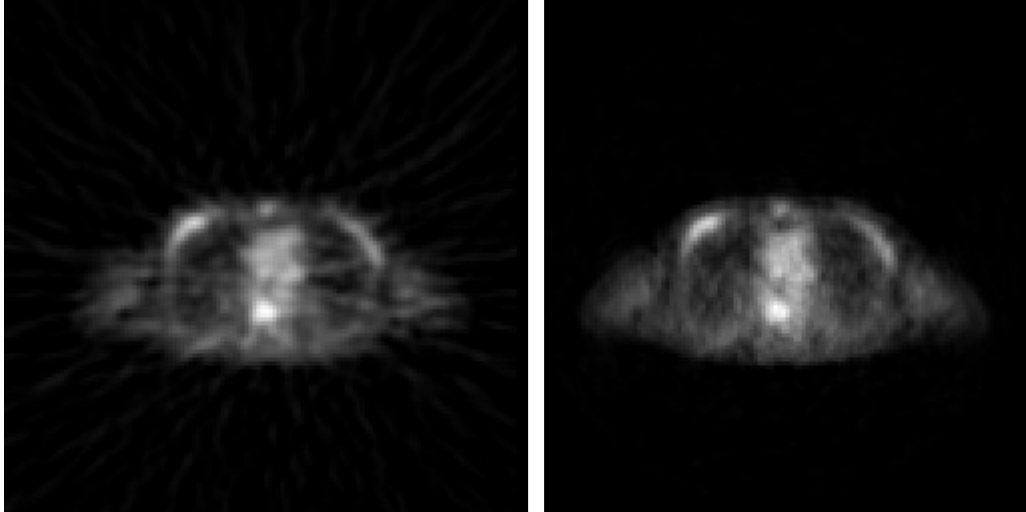


Figure 3.29: An example of the image noise on a medical scan (left) and the resultant processed image (right)

To clean up the data, the final data set is used to create a mask which is then applied to all the data sets so that only the grey scale information from the area occupied by the powder is evaluated. This final data set is used because the radioactive material has reached its most disperse condition (within the confines of the experimental procedure) and will occupy the largest volume within the vessel and can thus define the entire powder volume with reasonable certainty. Additionally, several slices at the start and end of the stack of images, which do not actually image the powder in the vessel, are also removed to further sharpen the data set.

This results in cleaner images which can then be evaluated for the concentration distribution of the radioactivity. Figure 3.30 shows how the radioactivity has been distributed over the course of a single experiment. The same central slice of the mini-IBC is displayed for 5, 20, 55 and 100 revolutions.

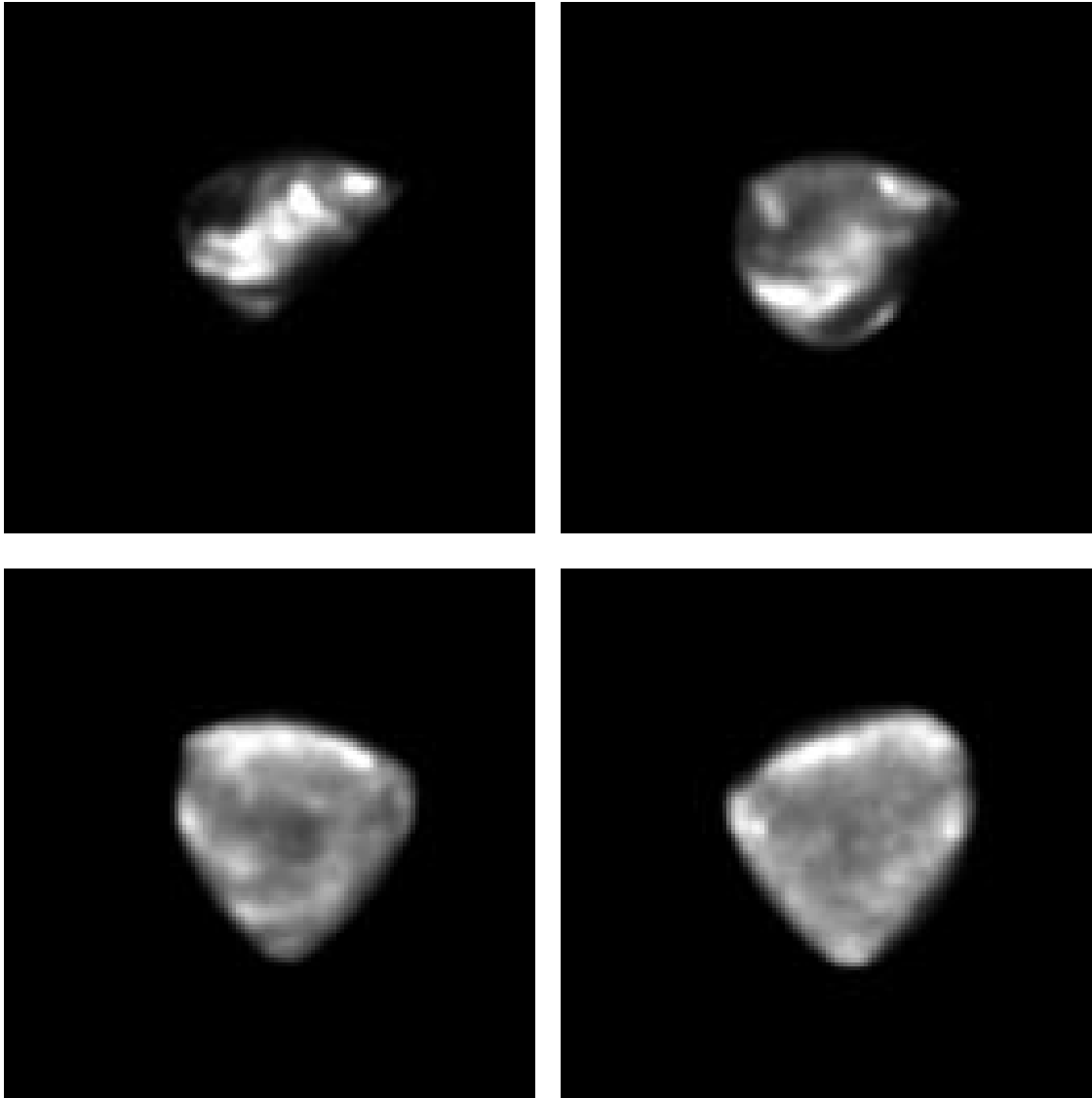


Figure 3.30: Views of the blender contents after 5, 20 (top left, top right) 55 & 100 revolutions (bottom left, bottom right)

Typical histograms of unmasked and masked data sets as direct screenshots from ImageJ are shown in Figures 3.31 and 3.32 respectively. These histograms represent the pixel intensity on the x-axis and the number of pixels with this intensity on the y-axis.

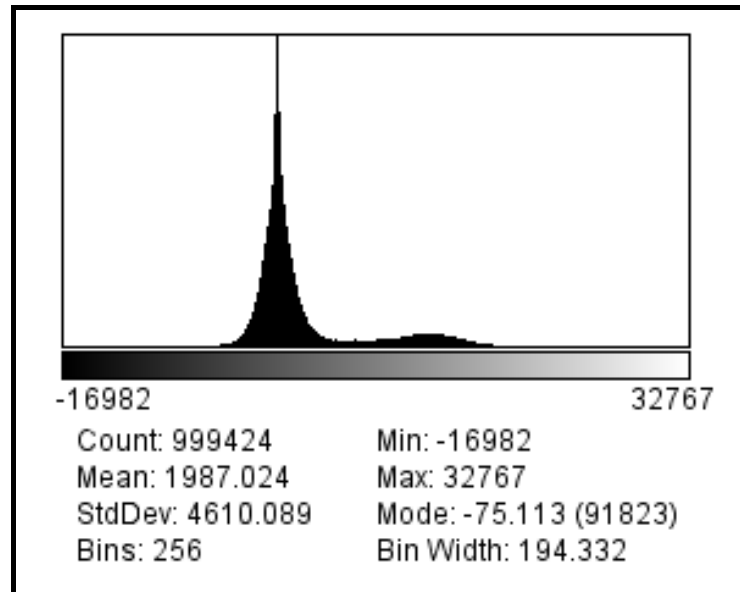


Figure 3.31: Pixel intensity for an unmasked data set, taken after 15 revs, for an experiment where a 2% MCC bolus was mixed in 5litres of Lactose at 15rpm

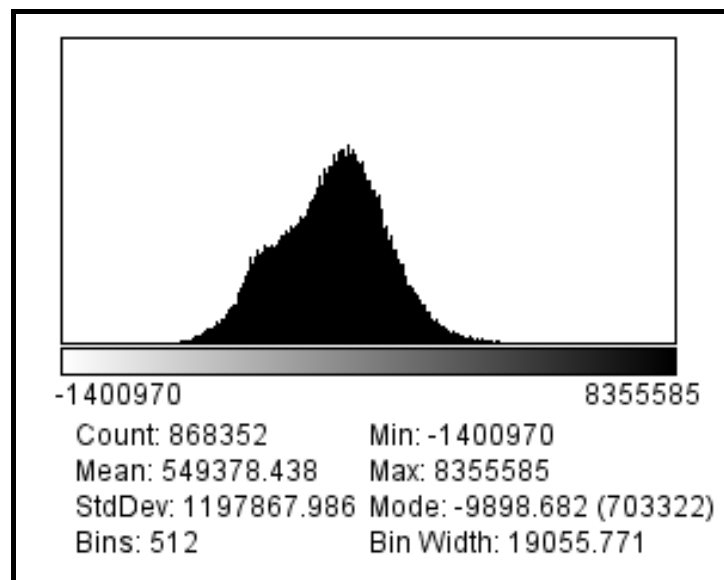


Figure 3.32: Pixel intensity for a masked data set, taken after 15 revs, for an experiment where a 2% MCC bolus was mixed in 5litres of Lactose at 15rpm

As can be seen there is a considerable improvement in the definition of the distribution. Each data set, representing the various stages of the blending operation

mentioned earlier, is masked and analysed. The resulting data are transferred to a spreadsheet for further evaluation.

A typical data set exported from ImageJ to a spreadsheet is shown in Figure 3.33.

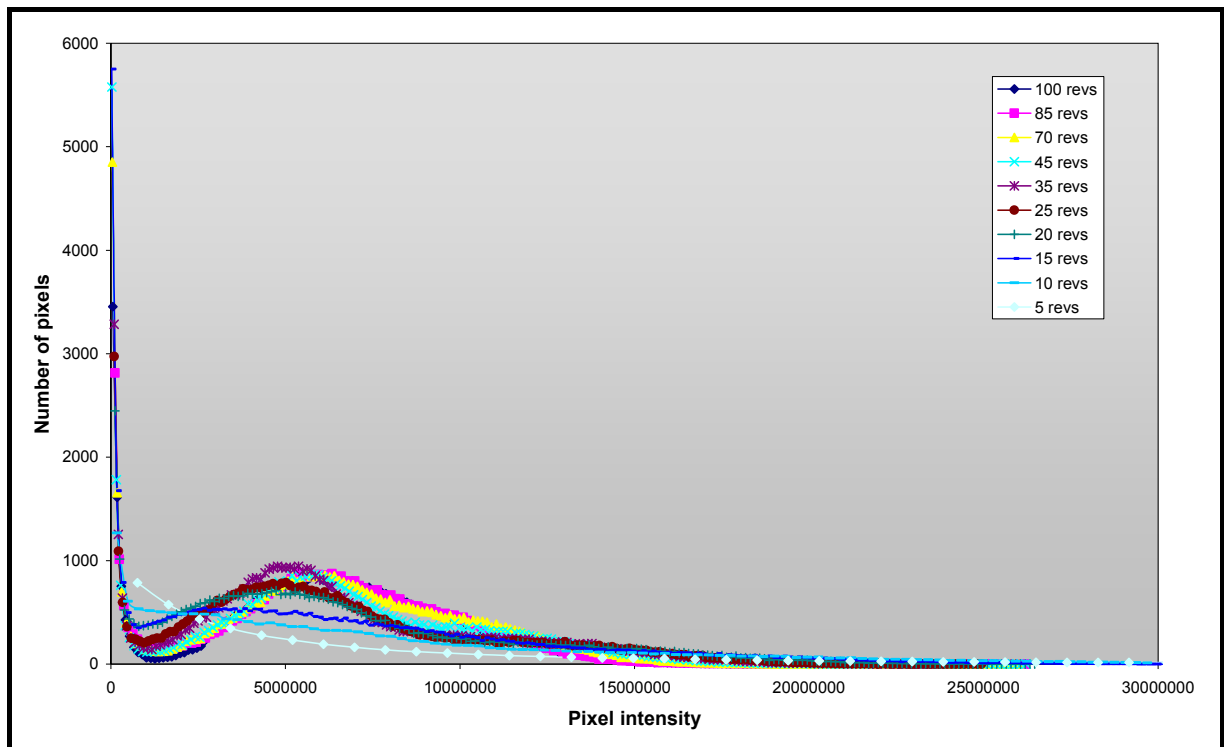


Figure 3.33: Raw data set exported from ImageJ into a spreadsheet for 2% MCC bolus in 5 litres of Lactose at 10rpm

At this point all the zero pixels were eliminated which improved the calculation of the modal value and the standard deviation and a single data set is shown in Figure 3.34. Figure 3.35 shows all the conditions for a Lactose experiment after the removal of the zero pixels.

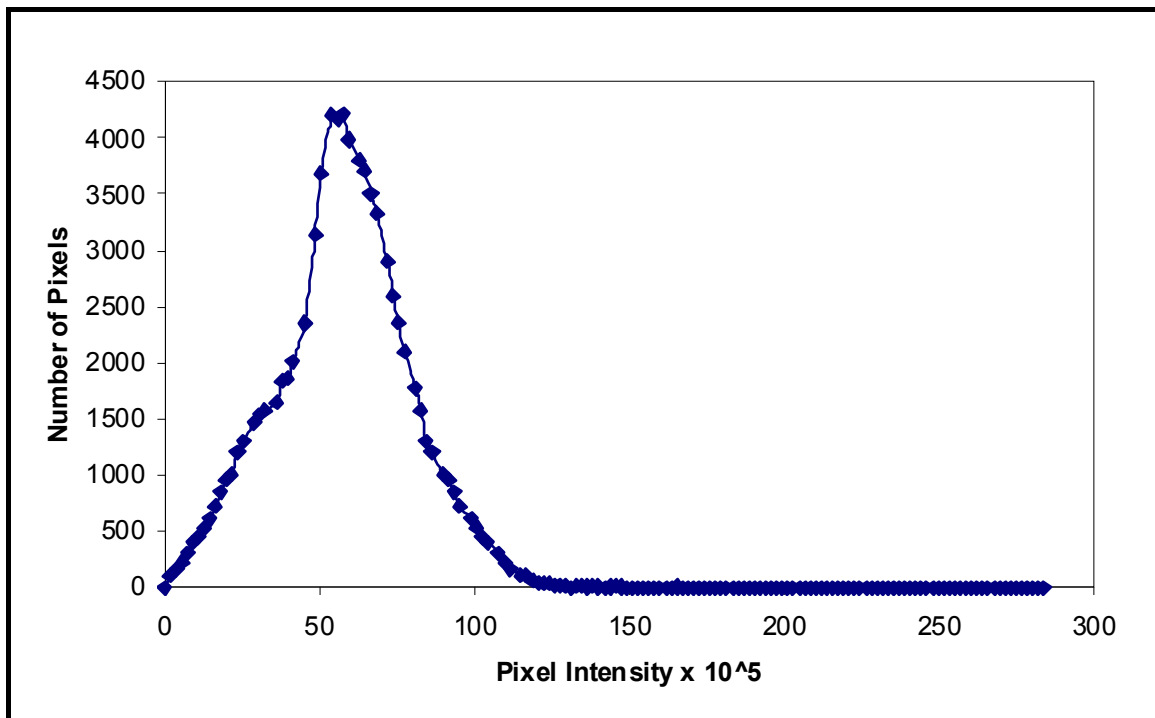


Figure 3.34: Normalised data set for 2% MCC bolus in 5litres of Lactose at 10rpm after 85 revs

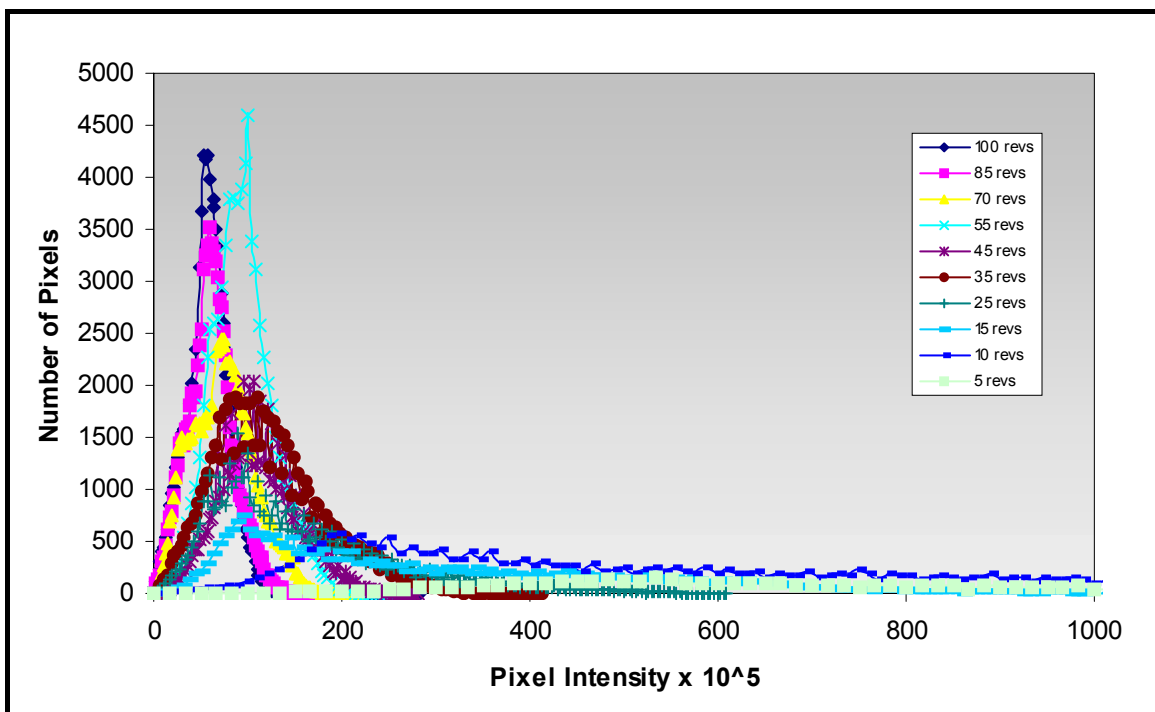


Figure 3.35: All normalised data sets for 2% MCC bolus in 5litres of Lactose at 10rpm

The trend is from a very flat curve, representing a wide spread of concentrations within the vessel corresponding to little dispersion of the radioactive bolus, to a series of much taller, sharper peaks as the pixel intensity becomes less diffuse and lower, representing the more even spread of the radioactivity within the vessel.

Thus, ImageJ can relate the number of pixels with given intensities as provided by the PET camera picture, which in turn allows an evaluation of the concentration. Summing the number of pixels with a given intensity for each data set within a given experiment allows an evaluation of the spread of MCC through the substrate.

In order to determine a measure of mixedness, it is necessary to make a further assumption. The area under each curve is considered to represent the total amount of radiation present and thus the total volume of MCC present. This allows the normalisation of each condition and thus allows the development of a concentration value based on the modal value as a proportion of the total quantity of the radiation. Given the conservation of mass of the system, the modal value can be represented as a most likely concentration. Figure 3.36 shows the continuity graph for the Lactose experiment at 15rpm prior to normalisation. The radioactivity level can vary by up to 6%, which is considered acceptable. There is a slight increase in the 'number x intensity' over the course of an experiment which can be ascribed to the increased dispersion of the radioactivity through more of the voxels.

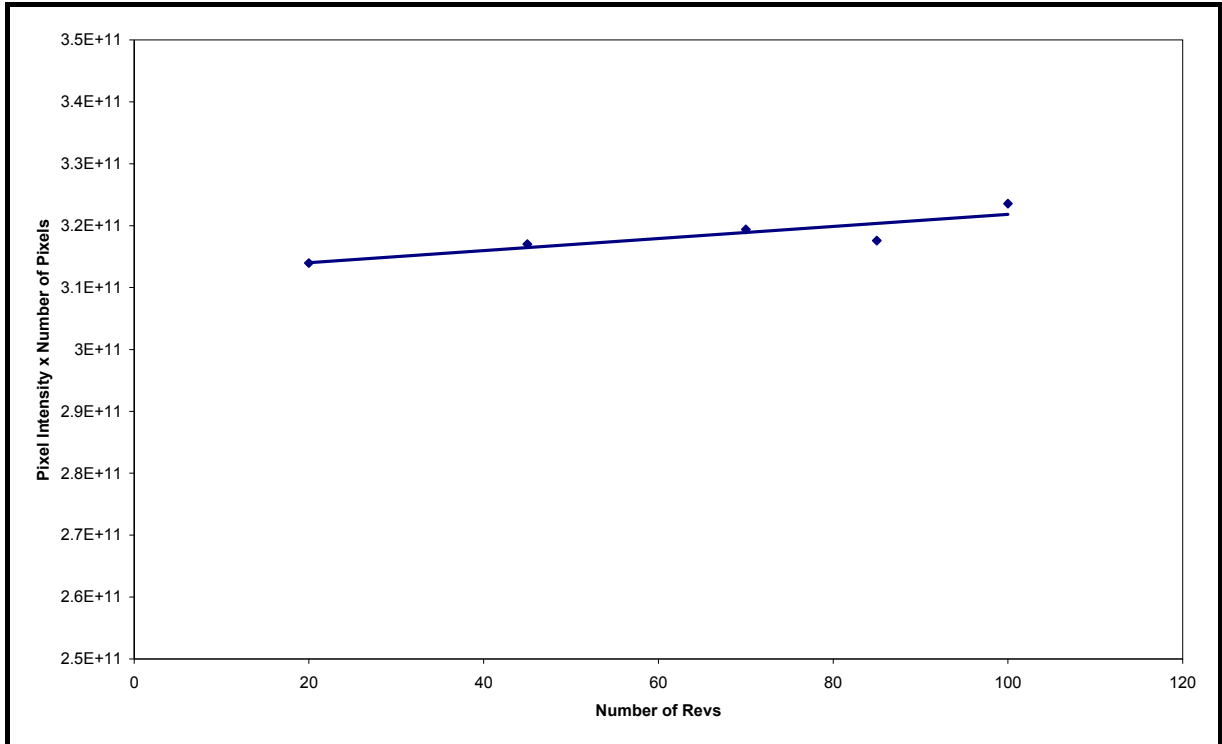


Figure 3.36: Continuity graph for 2% MCC bolus in 5 litres of Lactose at 15rpm

As the total concentration of the radioactive material is fixed at the start of the experiment (a known volume of minor component in a known volume of substrate), the mixedness has to be evaluated by looking at the spread of the pixel intensity in the sample. A wide distribution of intensities indicates that there is a large variation of concentration; a narrow distribution indicates a narrow spread of concentration – i.e. the sample is moving towards content uniformity.

The results are presented as the residual standard deviation (about the modal value) – i.e. the most likely concentration that will be found within the mass of the powder as identified by the peak on the pixel vs. intensity graphs. The residual standard deviation values are also a common way of expressing content uniformity in the pharmaceutical industry when evaluating mixedness by abstraction and assay.

3.3.5.3. Blending results

Once the RSD values for each measurement point in each experiment had been calculated it was then possible to plot the data and derive the expected exponential blending decay curve, as shown for Sodium Carbonate Light in Figure 3.37.

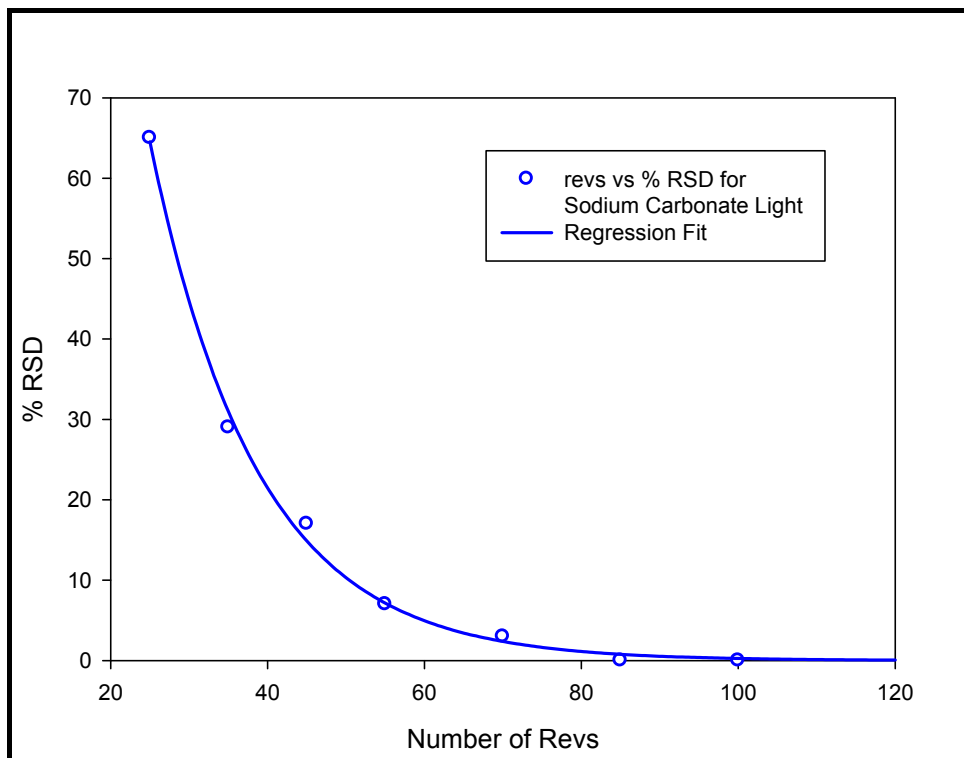


Figure 3.37: Regression fit to data from blending experiment using ~2% labelled MCC in 5.5litres of Sodium Carbonate Light at 15rpm

The form of the regression fit used to characterise the blending experiments is

$$y = ae^{-bx} \quad \text{Equation 3.7}$$

Table 3.2 shows the values of a and b as well as the 'goodness of fit' value. As can be seen, the data are a very good fit to this model.

Table 3.2: Results of exponential regression fit to PET data sets

Material	a	b	R²
Fine Salt	170.99	0.17	0.97
Lactose Run 1	231.84	0.08	0.96
Lactose Run 2	316.10	0.11	0.91
Sodium Carbonate Light	403.37	0.07	1.00
Sodium Benzoate Run 1	106.76	0.07	0.94
Sodium Benzoate Run 2	274.86	0.08	1.00
MCC Run 1	667.10	0.06	1.00
MCC Run 2	465.16	0.19	0.99
Ternary System – 3 litres of lactose + 2 litres of MCC	161.76	0.05	0.97

It should be noted that the early data points are discarded. This is because at the start of any blending cycle, the RSD of the bolus – because it has not had chance to disperse – is actually quite low. The spread of concentrations for the measured radioactivity is small if all the activity is concentrated in a small volume. As the experiment progresses the bolus becomes more disperse and the %RSD goes up dramatically as there are now some areas of high concentration where the radioactive material concentrates coupled with areas where some radioactive powder has been displaced from the rest of the radioactive powder leading to low concentrations. When the bolus becomes completely dispersed the %RSD of the concentration again becomes small as the radioactivity is now evenly spread through the sample.

There are several ways of analysing the blending curves derived from the PET data. Firstly, as the data is clearly exponential in form, it is possible to use the concept of the 'half-life'

$$C_t = C_0 e^{-\lambda t} \quad \text{Equation 3.8}$$

where C_0 is the initial concentration
 C_t is the concentration after time t
 λ is the decay constant
 t is the time that has passed after C_0 was evaluated

This then leads to the derivation of the half life – the time period after which the measured quantity has reached half its initial value.

$$t_{\frac{1}{2}} = \frac{\ln(2)}{\lambda} \quad \text{Equation 3.9}$$

where $t_{\frac{1}{2}}$ is the half life of the system

The 'characteristic time' is a concept derived from resistor-capacitor (RC) circuit theories, in which it is the time taken for a capacitor to discharge by $1/e$ – i.e. 63.2% of the original value.

The third way is to select a suitable blend quality criterion and use the time taken to achieve this target as the characteristic of the blend. In this case a typical

pharmaceutical acceptance criterion of 5% residual standard deviation (RSD) is used.

The results are shown in Table 3.3 together with the process data for each experiment and graphically in Figure 3.38.

Table 3.3: Summary of process conditions and results for PET blending experiments

Material	Process Data							Results		
	Volume of substrate (ml)	Mass of substrate (g)	Volume of bolus (ml)	Mass conc ^a . (%)	Volume conc ^a . (%)	Fill proportion (%)	RPM	'Half life' (revs)	Characteristic Time (revs)	Time to achieve 5% RSD (revs) ³
Fine Salt	3221	3968	123	1.05	3.68	33.5	10	4.04	5.90	21
Lactose Run 1	5463	3795	120	1.07	2.15	55.8	10	8.20	12.50	46
Lactose Run 2	2928	2034	132	2.16	4.31	30.6	15	6.42	9.10	39
Sodium Carbonate Light	5517	3106	120	1.30	2.13	56.4	15	9.45	14.30	60
Sodium Benzoate Run 1	5486	1601	85	1.78	1.53	55.7	10	9.19	12.50	45
Sodium Benzoate Run 2	5109	1491	126	2.80	2.41	52.4	15	9.98	13.57	54
MCC Run 1	6915	2359	120	1.71	1.71	70.4	10	11.99	16.70	85
MCC Run 2	6569	2241	345	5.00	5.00	69.1	15	3.69	5.30	25
Ternary System – 3 litres of lactose + 2 litres of MCC	3121 + 2843	2168 + 970	117	1.26	1.93	59.6	15	15.04	55.21	76

³ The 'Time to achieve 5% RSD' are rounded up to the next complete revolution to present a practicable result

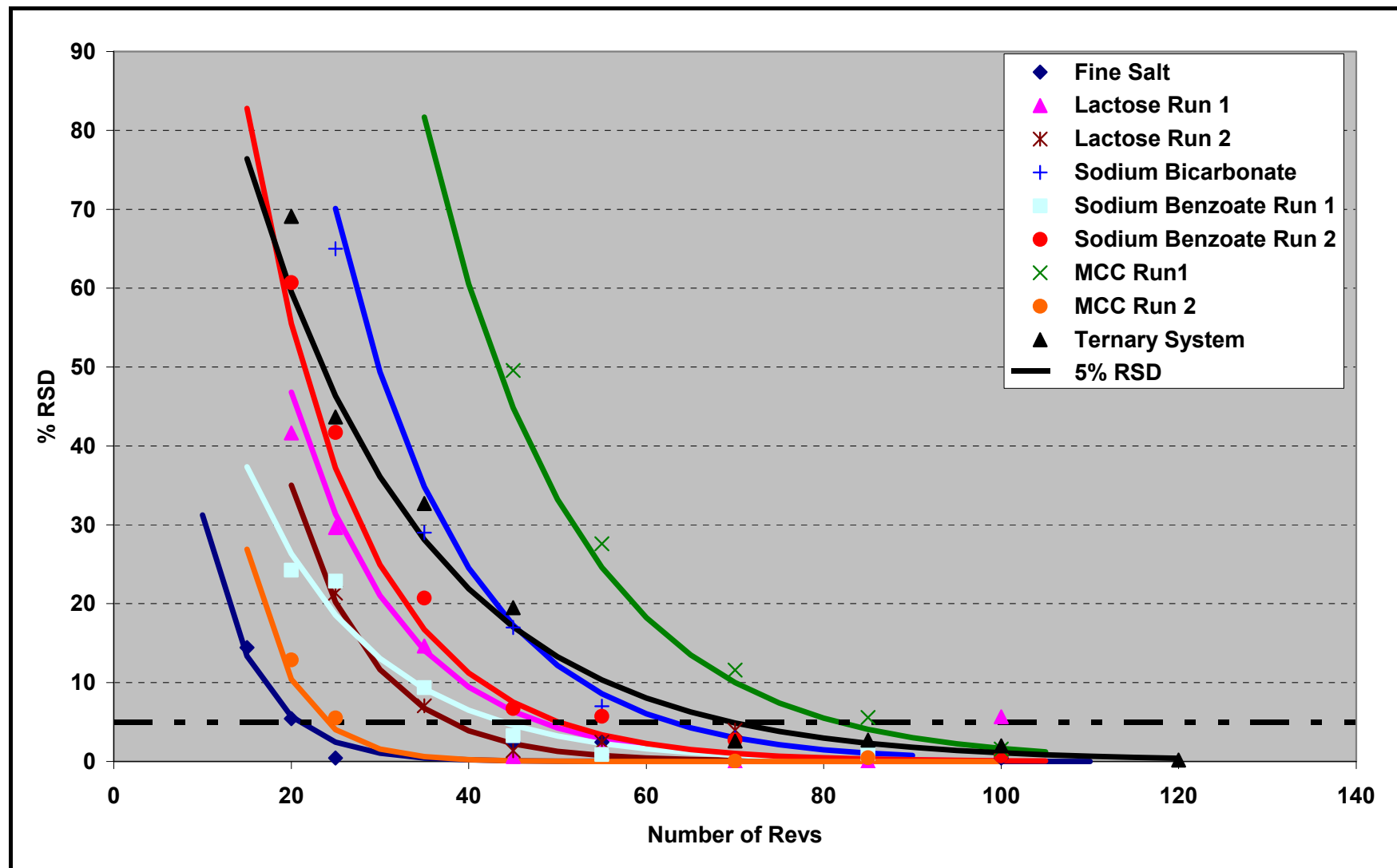


Figure 3.38: Summary graph of all the mixing experiments

The limited number of data sets that could be collected, due to the computer and equipment breakdown mentioned previously, have precluded a fully detailed analysis of the blending performance with respect to the powder characteristics as was intended. There are, however, several notable relationships that can be described by the data.

There are some obvious relationships that can be confirmed with these data. Firstly, if there is an increase in the proportion of substrate within a given vessel then, as the material has less room to expand and allow the minor component to disperse, the rate of blending should decrease. This is seen in Figure 3.39 when two different volumes of lactose are placed in the IBC and blended with the MCC bolus. The number of revs required to achieve 5%RSD is lower for the dispersal in 3litres of substrate than 5 litres by 7revs at the same rotational speed.

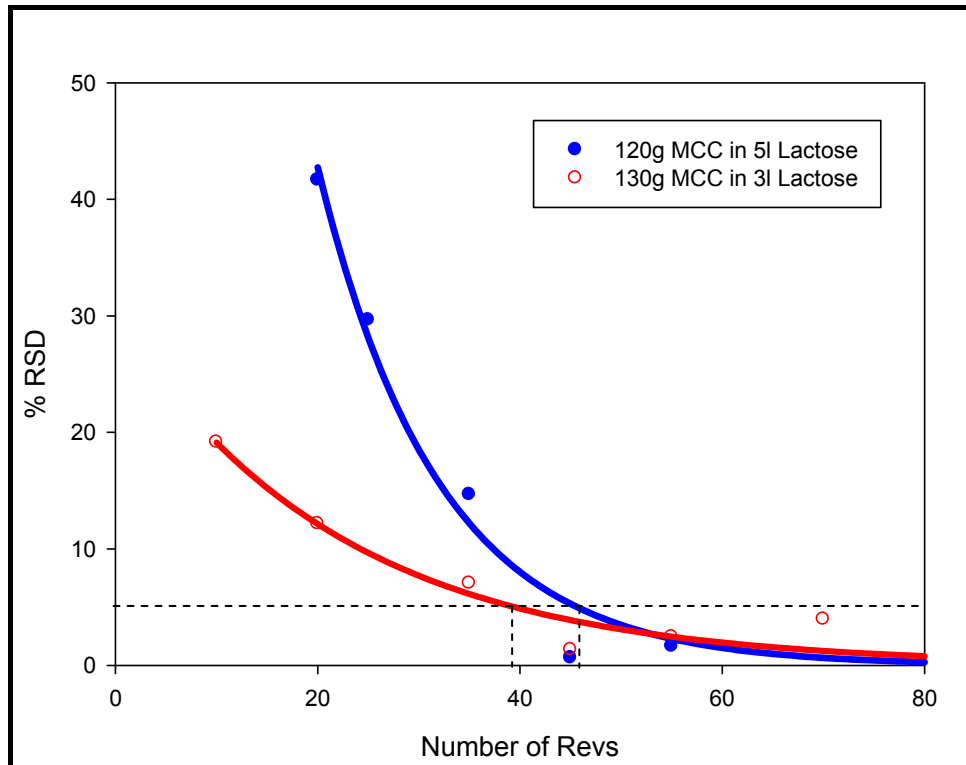


Figure 3.39: Effect of substrate volume on blending rate at 15rpm

Secondly, the effect of the rotational speed of the blender should also be obvious. Increase the blender speed and the minor component should disperse much faster because more energy is being put into the system and there is likely to be a change in the mode of flow, Figure 3.6, from rolling/cascading to cascading/cataracting. This will change the balance of the mechanisms that are acting to disperse the powder from a mostly convective to a convective and shearing balance because the powder is experiencing greater dilation which allows enhanced interaction of different zones of powder. Equally, increased rotational speed coupled with the offset of the bin will improve the diffusional mixing of the system. This is indeed the case when the Lactose tests are compared as shown in Figure 3.40.

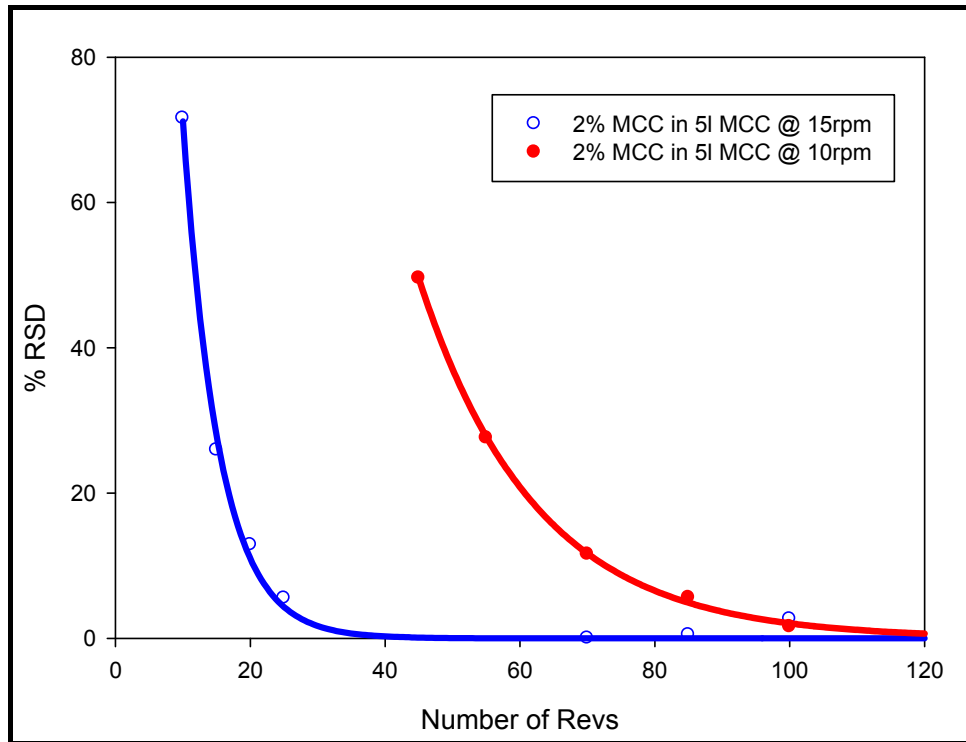


Figure 3.40: Effect of IBC rotational speed on blending rate

However, as has been previously mentioned in Section 3.3.4, the Sodium Benzoate has a different shape to the (broadly) spherical Lactose and this can be seen in the photograph shown in Figure 3.41.

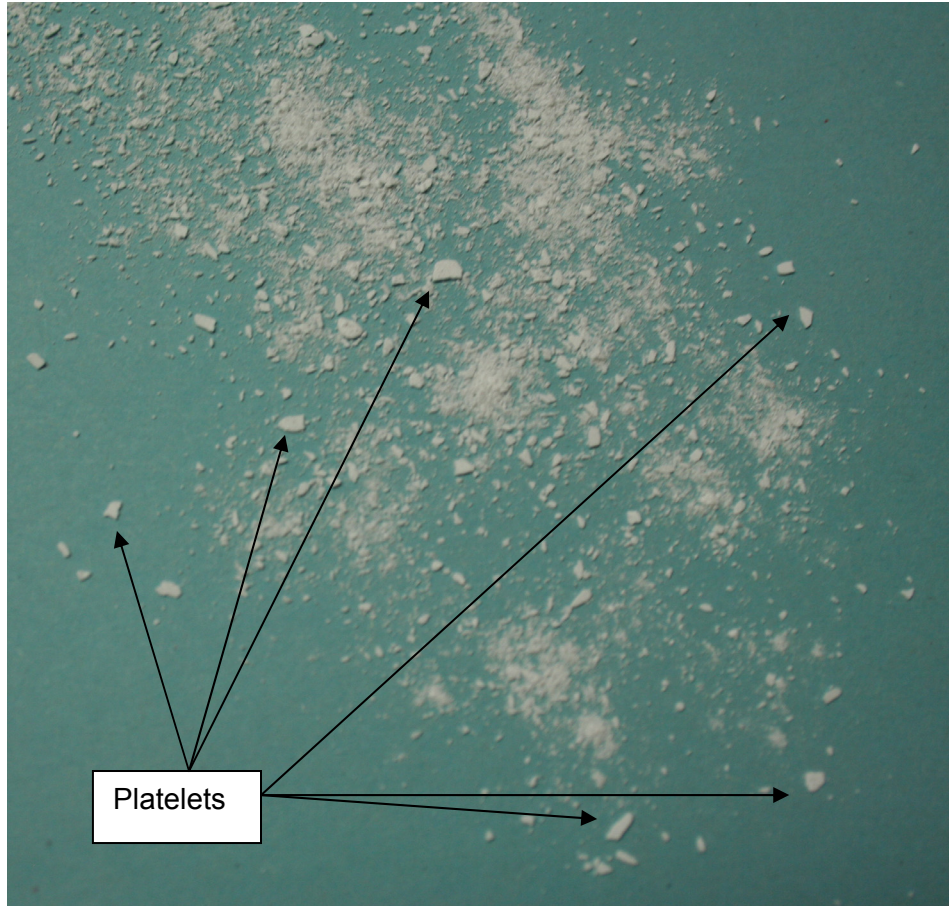


Figure 3.41: Photograph of the Sodium Benzoate powder showing the high concentration of platelets within the sample

Its 'platy' structure gives it a different dynamic response when in motion as was suggested in Chapter 2 Section 2.3.5. Figure 3.42 shows how the MCC bolus disperses within the Sodium Benzoate at the two speeds used to evaluate the irradiated MCC in MCC in Figure 3.40.

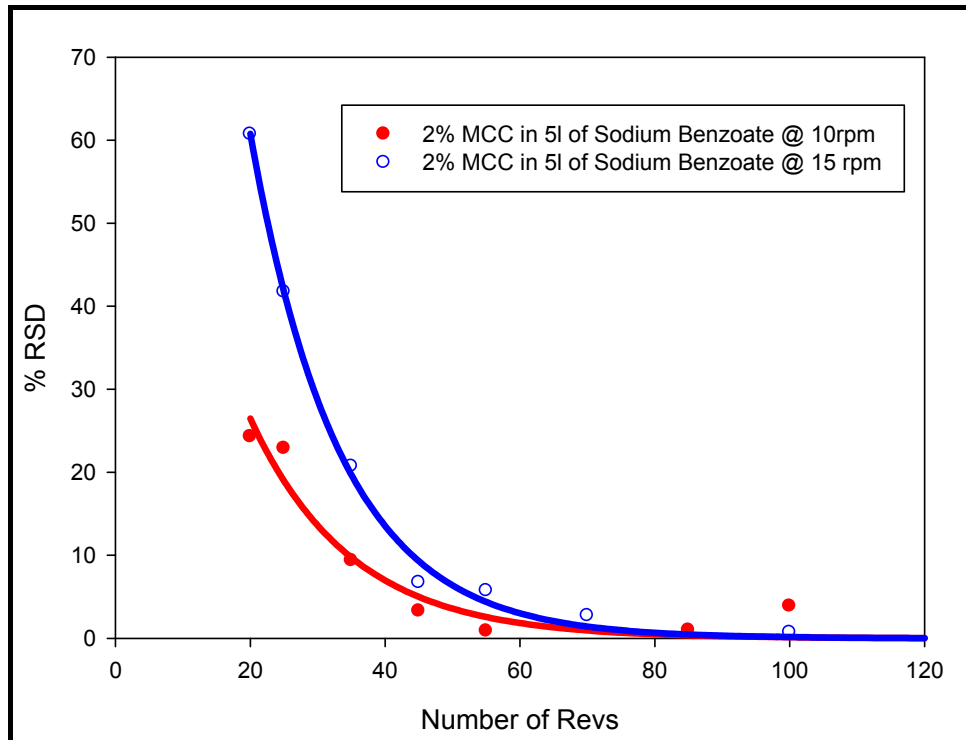


Figure 3.42: Effect of IBC rotational speed on plate like particles

The radioactive bolus actually disperses more slowly with increasing IBC rotational speed which can only be attributed to the shape of the Sodium Benzoate particles and the rotational and translational frustration described in Chapter 2 Section 2.5.2. It should also be noted that the %RSD at 100revs for the 10rpm conditions shows a distinct rise. This may be due to the system undergoing de-mixing, but insufficient radioactivity prevented data being collected beyond the 100revs test. It would be possible to undertake an experiment that started at, say, 40revs for the first data set and continued beyond 100revs to confirm this observation.

A ternary system was also evaluated of MCC and Lactose in the ratio of 3:2, again using of a bolus of MCC. It would perhaps be expected, given the hypothesis promoted by Muzzio and described in Section 3.2.4, that cohesion is a fundamental

influence on mixing rate and that the rate of dispersion of the ternary system, compared to the two substrates on their own, would be related to their relative cohesiveness (however this was to be measured) of each system. Thus it would be expected that the minor component would find it more difficult to inter-disperse in a system where the particles would separate less easily (more cohesive). In this instance, it will be assumed that because of the small size of the radioactive bolus that it will have no influence the flow properties of any of the systems.

There have been some studies that look at how, when mixed, the relative proportion of different components or different size fractions (bou-Chakra & Tüzün 2000; Zhong, Ooi, & Rotter 2005; Zulfiqar, Moghtaderi, & Wall 2006) can affect the flowability of powders, but this author, at the time of writing, is unaware of any published studies relating how the proportion of different components affects the mixing rate.

The comparative blending curves are shown in Figure 3.43, and it can be seen that the radioactive bolus of MCC disperses more slowly in a substrate comprised of both Lactose and MCC than it does in either pure substrate thus one might expect that the relative cohesiveness of the three samples would be ordered:-

MCC<Lactose<Lactose:MCC blend

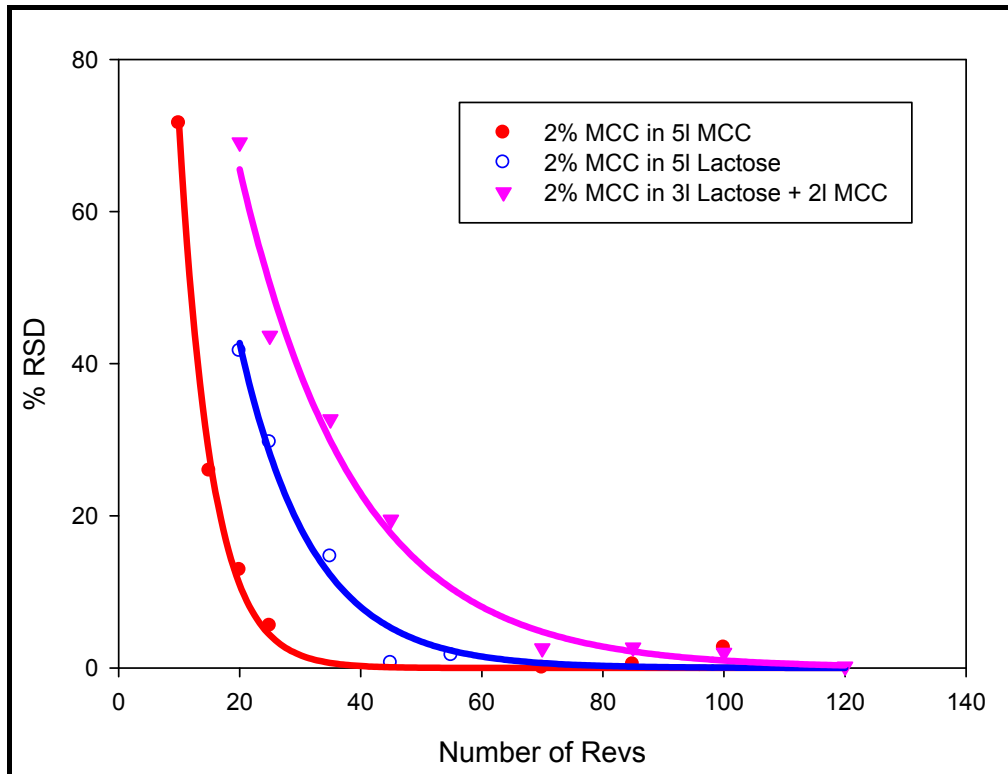


Figure 3.43: Comparison of binary and ternary systems at 15rpm

If one compares the results from the rheometry and shear performance of the individual powders and the (well mixed) blend, as shown in Figures 3.44 to 3.47, it can be seen that the dynamic test using the powder rheometer provides an obvious paralleling of the mixing rate (Figures 3.44 and 3.45). If one considers the yield loci presented in Figure 3.46, the shear test appears on first evaluation to correlate the increased mixing rate with lower levels of shear stress (indicating a lower cohesion, more free flowing system). When the derived functions are considered, Figure 3.47, then a relationship between mixing rate with cohesiveness cannot be correlated. It is entirely possible that testing these samples at a much lower stress in the shear cell may generate a more sensible relationship between shear properties and mixing rate, but this pre-disposes confidence in very low stress shear testing, which has not yet been successfully demonstrated.

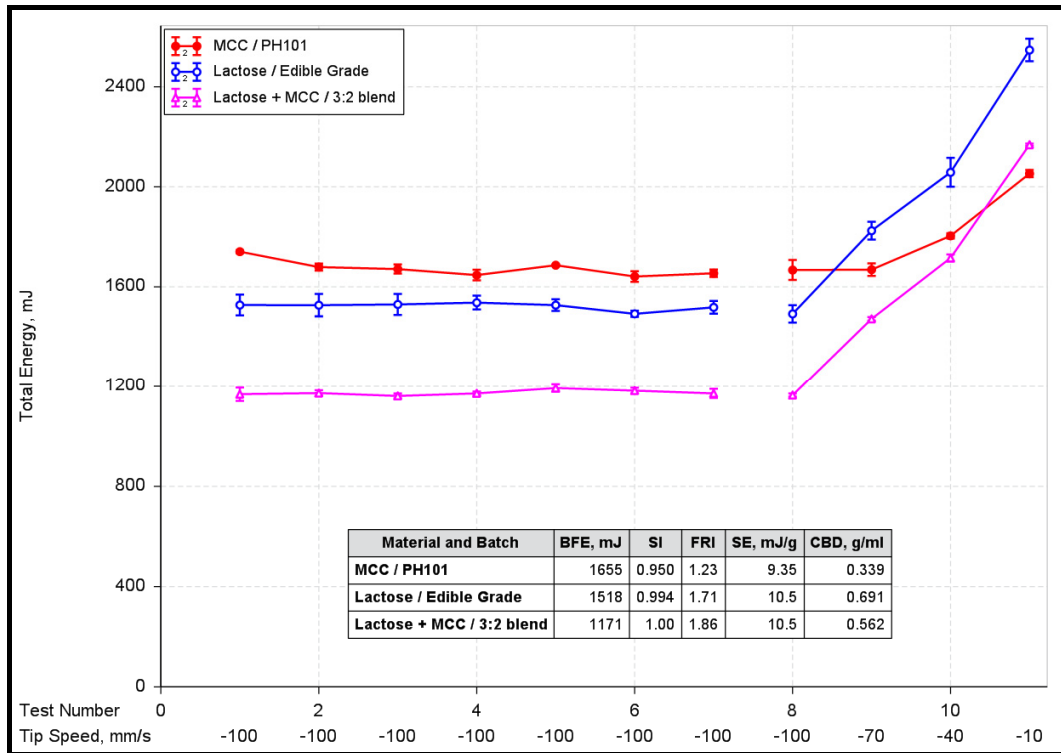


Figure 3.44: Graphical representation of the standard Dynamic test using the FT4 Powder Rheometer comparing three substrates

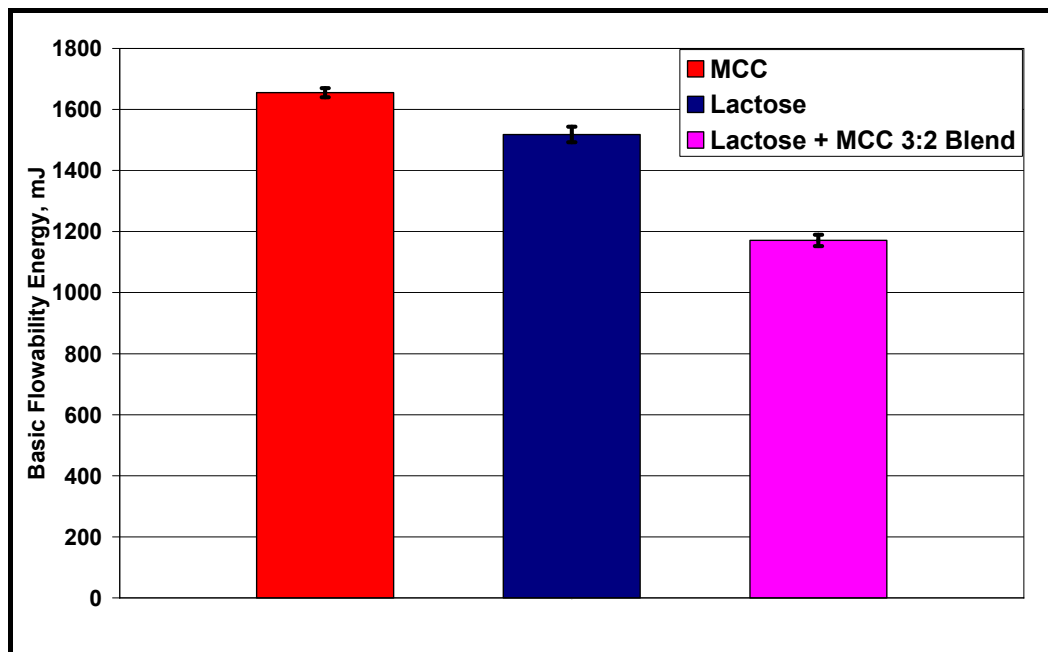


Figure 3.45: The BFE values from the standard Dynamic test using the FT4 Powder Rheometer comparing three substrates

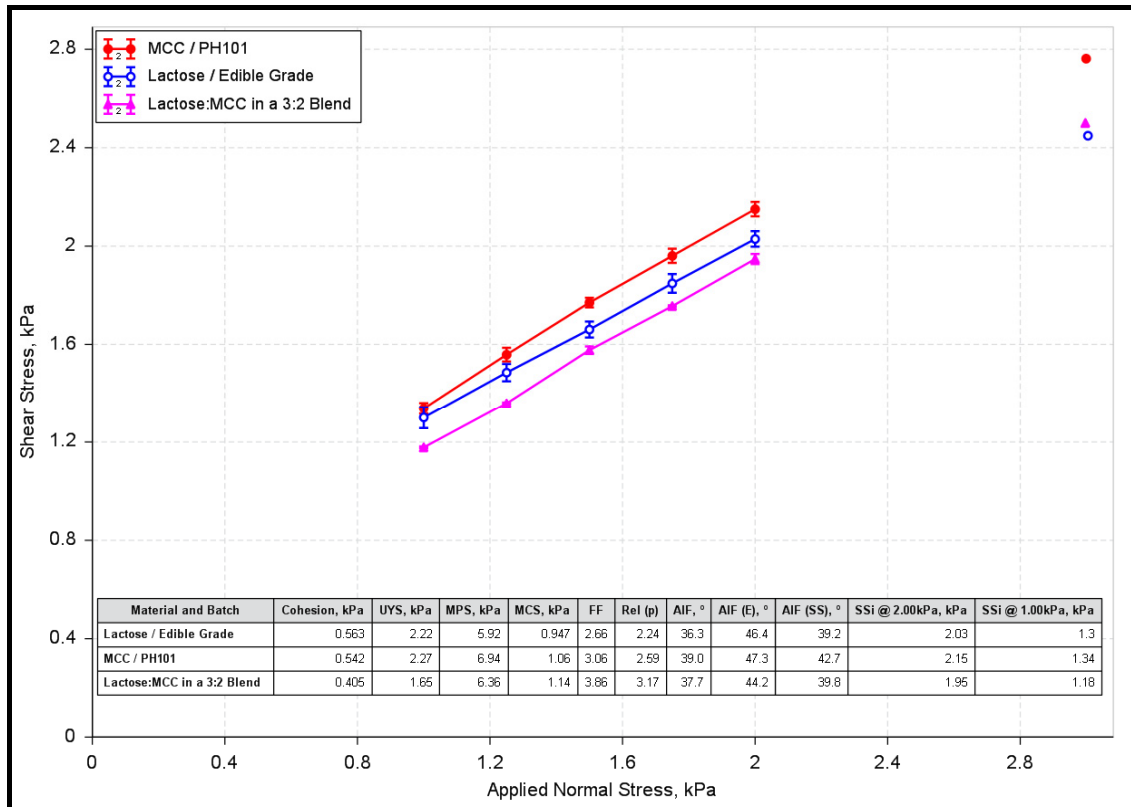


Figure 3.46: Graphical representation of the shear test at 3kPa consolidating stress using the FT4 Powder Rheometer comparing three substrates

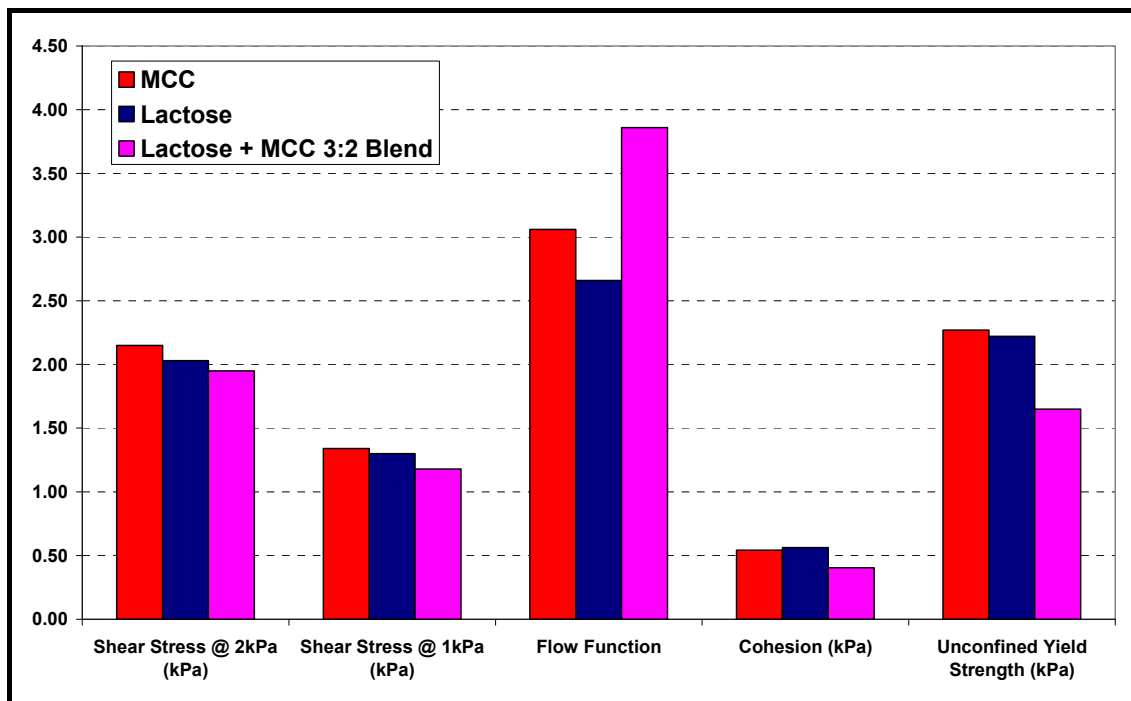


Figure 3.47: the shear stress from the first and last shear points together with the derived functions (FF, C, and UYS) comparing three substrates

Thus the concept that cohesion plays a significant part in the determination of the rate of mixing may be well founded, but it may be dependant on the matching the stress conditions in the powder testing instrument to the process conditions. In this instance the Basic Flowability Energy shows that the Lactose:MCC system is more cohesive – lower BFE – and as such a lower rate of mixing would be expected. Such a relationship has not been specifically determined elsewhere, and it is recommended that work be extended to confirm this initial finding.

3.3.5.4. Scale of scrutiny

The scale of scrutiny is important for all blending exercises. No mixing exercise will produce the ideal/perfect mixture where one particle of component A is exactly adjacent to a particle of component B throughout the entire mixture. There will always be a degree of randomness as one looks at smaller portions of the mixture. Figure 3.48 shows an example of the effect of the scale of scrutiny.

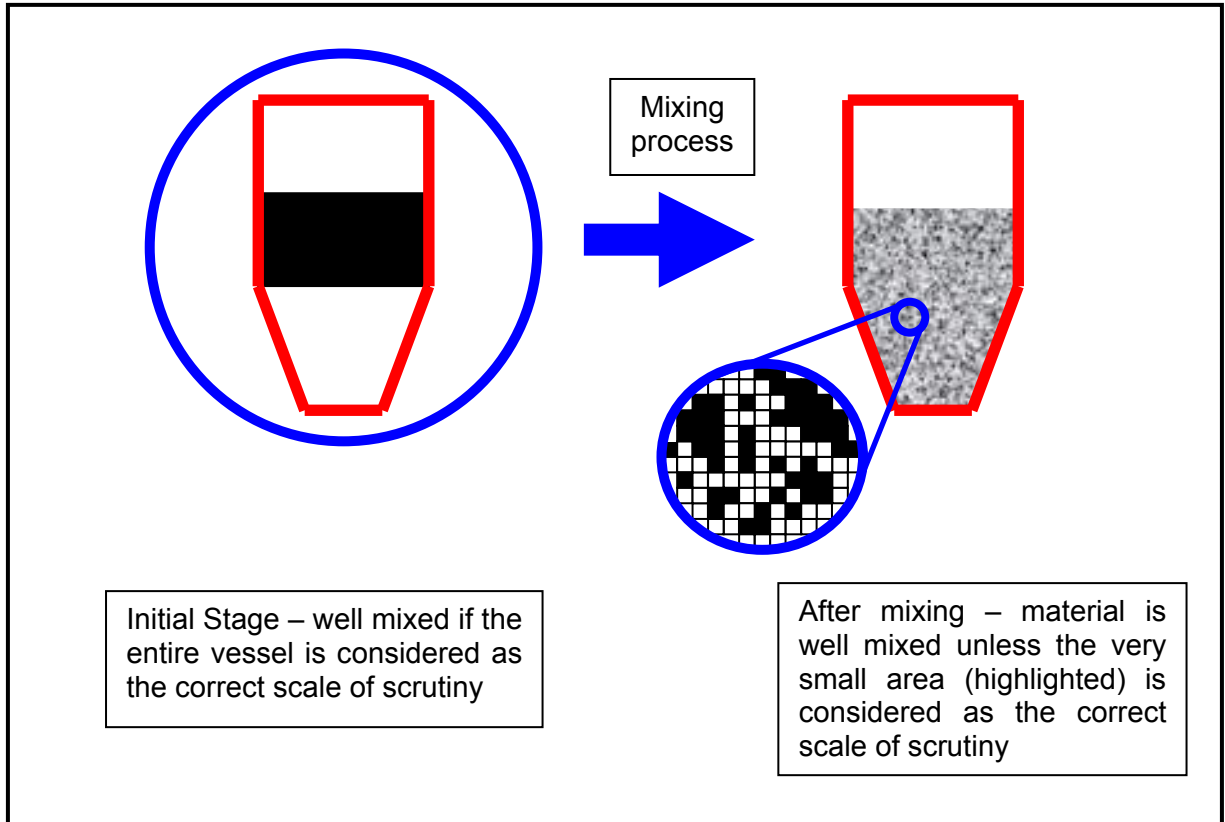


Figure 3.48: How scale of scrutiny can effect the perception of mixedness

The quality of the mixture must be defined at the start of any mixing process and is usually a function of the required downstream form – in the case of most pharmaceutical formulations this is a tablet. Thus, to ensure that the mixture is acceptable it should, ideally, be sampled and analysed at or below the size of the solid dose that it will eventually form. For practical reasons this is not always the case (Muzzio *et al.* 1997; Muzzio *et al.* 2003) and the sample size is a (large) multiple of the dosage volume, leading to a degree of assumption about the mixture quality until QA analysis of the final tablets is carried out. Poor sampling combined with poor mixing can result in the need to scrap or re-work an entire batch.

Within ImageJ it is possible to manipulate the size of the area over which it calculates the grey scale intensity. Thus by changing the area of the nominal 'pixel', it is possible to investigate how the change in the scale of scrutiny from the finest to a coarser scale affects the data set. Figure 3.49 shows this for the Lactose experiment at 10rpm.

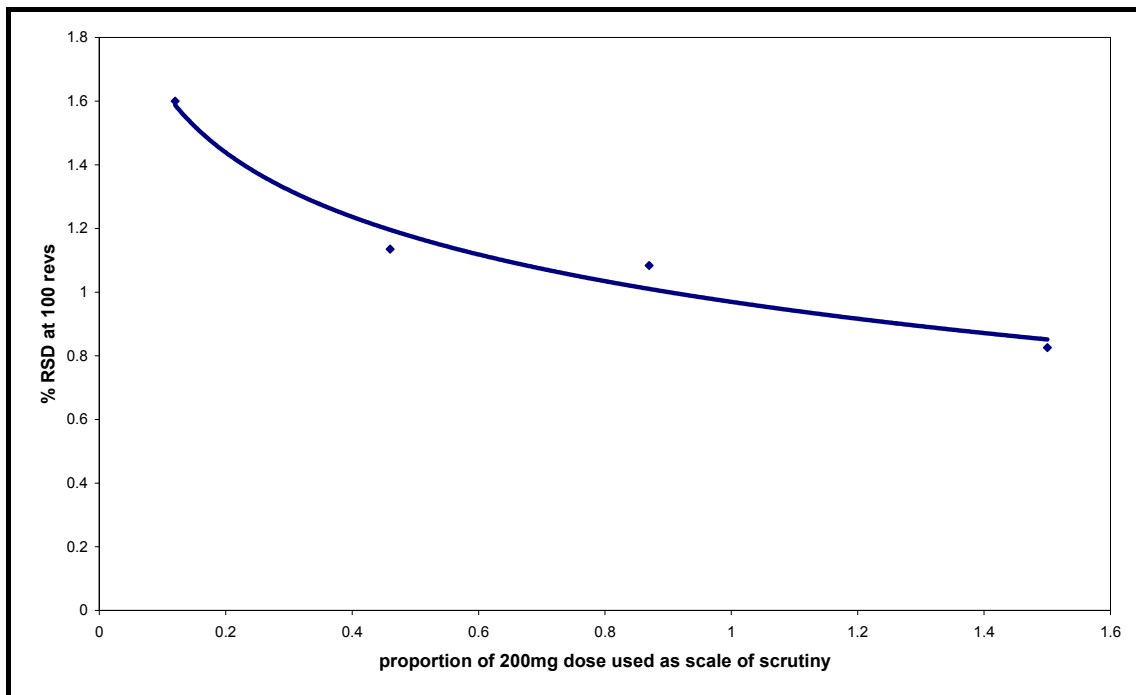


Figure 3.49: Effect of scale of scrutiny for 5 litres of Lactose + 120ml of irradiated MCC, blended at 10rpm, after 100revs

As can be seen there is a distinct improvement in the perceived quality of the mix as a larger (virtual) sample is evaluated. The 0.12 times the dose sample size is the default state for the PET evaluation of this system, assuming that the final dose is (an arbitrarily chosen, but typical) 200mg. As the scale of scrutiny is expanded from 0.12 to 1.5 times the dose the %RSD after 100 revs falls from 1.6% to 0.82 – virtually 50%.

This shows that PET can evaluate the contents of mixing vessel to a fine scale of scrutiny and that this scale of scrutiny can be virtually expanded to assist with the generating the 'design space' criteria mixing systems.

3.4 Summary

This Chapter has presented three tomographic techniques to observe and evaluate the mixing of dry powders in a typical pharmaceutical tumble blending system.

PEPI has been shown to have significant limitations in quantifying behaviour in the powder blender. Both PET and PEPT have, however, shown the ability to generate data that can both quantify blending and differentiate between differing powder systems. The development of the large scale PEPT scanner should also provide the scope to measure dispersion in larger vessels in the near future.

However it is PET that provides the most appropriate measure of mixedness for this type of tumble blender. This unique application of this technique has been shown to generate mixing data well below the typically required scale of scrutiny for pharmaceutical applications. Data collected has also shown the relationship between particle shape and mixing rate which can be characterised by powder rheometry.

Additionally PET has provided the opportunity to investigate some powder and process related phenomena, although these will need further confirmation at different scales and rotational speeds. Direct comparison with a proportion of the industrial operational range was restricted by the limits of the available laboratory blender.

To summarise:

- Increasing the speed of rotation of the blender significantly improves the rate of mixing for spherical/spheroidal particles
- Increasing the relative fill level of the mixing vessel from 30 to 50% has a minor effect on reducing the blending rate
- The shape of particles has a distinct influence on the blending rate such that a powder with a high proportion of platelets will experience rotational and translational frustration when induced to move, resulting in a slight reduction in blending rate with increased blender rotational speed. There appears to be a relationship between this effect and the response of this powder to blade tip speed in a powder rheometer compared to the response from powder with spherical particles. This correlation will require further investigation to confirm its validity.
- The concept that the cohesiveness of a substrate will influence the blending rate for a minor component has been demonstrated for one system but requires further investigation.

3.5. References

- Abramoff, M. D., Magelhaes, P. J., & Ram, S. J. 2004, "Image Processing with ImageJ", *Biophotonics International*, vol. 11, no. 7, pp. 36-42.
- Alexander, A. W., Arratia, P., Goodridge, C., Sudah, O., Brone, D., & Muzzio, F. J., 2004a, "Characterization of the Performance of Bin Blenders, Part 1 of 3: Methodology". *Pharmaceutical Technology*, 70-86.
- Alexander A W, Sudah O, Arratia P, Goodridge C, Alani L, & Muzzio F J. 2004b, "Characterization of the Performance of Bin Blenders, Part 2 of 3: Free-Flowing Mixtures". *Pharmaceutical Technology*, 56-68.
- Alexander, A. W., Sudah, O., Arratia, P., Duong, N.-H., Reynolds, S., & Muzzio, F. J., 2004c, "Characterization of the Performance of Bin Blenders, Part 3 of 3: Cohesive Powders". *Pharmaceutical Technology*, 54-74.
- Bailey, D. L., Townsend, D. W., Valk, P. E., & Maisey, M. N. 2004, *Positron Emission Tomography: Basic Sciences*, 1st Edition edn, Springer-Verlag.
- Berntsson, O., Danielsson, L.-G., Lagerholm, B., & Folestad, S. 2002, "Quantitative in-line monitoring of powder blending by near infrared reflection spectroscopy", *Powder Technology*, vol. 123, no. 2-3, pp. 185-193.
- Blanco, M., Gozalez Bano, R., & Bertran, E. 2002, "Monitoring powder blending in pharmaceutical processes by use of near infrared spectroscopy", *Talanta*, vol. 56, no. 1, pp. 203-212.
- bou-Chakra, H. & Tüzün, U. 2000, "Microstructural blending of coal to enhance flowability", *Powder Technology*, vol. 111, no. 3, pp. 200-209.
- Bozzone, S. 2001, "Solid Oral Dosage Forms: Powder Mixing", in *IKEV Validation Seminar*.
- Brone, D. & Muzzio, F. J. 2000, "Enhanced mixing in double-cone blenders", *Powder Technology*, vol. 110, no. 3, pp. 179-189.
- Brone, D., Wightman, C., Connor, K., Alexander, A., Muzzio, F. J., & Robinson, P. 1997, "Using flow perturbations to enhance mixing of dry powders in V-blenders", *Powder Technology*, vol. 91, no. 3, pp. 165-172.
- Chaudhuri, P. K. & Fuerstenau, D. W. 1971, "The effect of mixing aids on the kinetics of mixing in a rotating drum", *Powder Technology*, vol. 4, no. 3, pp. 146-150.
- Cho, J., Gemperline, P. J., Aldridge, P. K., & Sekulic, S. S. 1997, "Effective mass sampled by NIR fiber-optic reflectance probes in blending processes", *Analytica Chimica Acta*, vol. 348, no. 1-3, pp. 303-310.

- EFCE. Standard Shear Testing Technique. 1989. The Institution of Chemical Engineers.
- Fan, X., Parker, D. J., & Smith, M. D. 2006a, "Enhancing ^{18}F uptake in a single particle for positron emission particle tracking through modification of solid surface chemistry", *Nuclear Instruments and Methods in Physics Research Section A: Accelerators, Spectrometers, Detectors and Associated Equipment*, vol. 558, no. 2, pp. 542-546.
- Fan, X., Parker, D. J., & Smith, M. D. 2006b, "Labelling a single particle for positron emission particle tracking using direct activation and ion-exchange techniques", *Nuclear Instruments and Methods in Physics Research Section A: Accelerators, Spectrometers, Detectors and Associated Equipment*, vol. 562, no. 1, pp. 345-350.
- Fayed, M. E. & Otten, L. 1984, *Handbook of Powder Science and Technology* Van Nostrand Reinhold.
- Finnie, G. J., Kruyt, N. P., Ye, M., Zeilstra, C., & Kuipers, J. A. M. 2005, "Longitudinal and transverse mixing in rotary kilns: A discrete element method approach", *Chemical Engineering Science*, vol. 60, pp. 4083-4091.
- Fitzpatrick, J. J., Iqbal, T., Delaney, C., Twomey, T., & Keogh, M. K. 2004, "Effect of powder properties and storage conditions on the flowability of milk powders with different fat contents", *Journal of Food Engineering*, vol. 64, no. 4, pp. 435-444.
- Food & Drug Administration 2004, *Guidance for Industry PAT — A Framework for Innovative Pharmaceutical Development, Manufacturing, and Quality Assurance*.
- GEA Pharma Systems. Blending Technology. 2010a.
- GEA Pharma Systems. Intermediate Bulk Containers. 2010b.
- GEA Pharma Systems. Post Hoists. 2010c.
- Hailey, P. A., Doherty, P., Tapsell, P., Oliver, T., & Aldridge, P. K. 1996, "Automated system for the on-line monitoring of powder blending processes using near-infrared spectroscopy part I. System development and control", *Journal of Pharmaceutical and Biomedical Analysis*, vol. 14, no. 5, pp. 551-559.
- Harnby, N., Edwards, M. F., & Nienow, A. W. 2001, *Mixing in the Process Industries*, 2 edn, Butterworth-Heinemann.
- Hausman, D. S., Cambron, R. T., & Sakr, A. 2005, "Application of Raman spectroscopy for on-line monitoring of low dose blend uniformity", *International Journal of Pharmaceutics*, vol. 298, no. 1, pp. 80-90.
- Hogg, R. 2009, "Mixing and Segregation in Powders: Evaluation, Mechanisms and Processes", *Kona*, vol. 27, pp. 3-17.

- Hogg, R., Cahn, D. S., Healy, T. W., & Fuerstenau, D. W. 1966, "Diffusional mixing in an ideal system", *Chemical Engineering Science*, vol. 21, no. 11, pp. 1025-1038.
- Hoomans, B. P. B., Kuipers, J. A. M., Mohd Salleh, M. A., Stein, M., & Seville, J. P. K. 2001, "Experimental validation of granular dynamics simulations of gas-fluidised beds with homogenous in-flow conditions using Positron Emission Particle Tracking", *Powder Technology*, vol. 116, no. 2-3, pp. 166-177.
- Jenike, A. W. 1964, *Storage and Flow of Solids*, University of Utah, Bulletin 123.
- Jones, J. R. & Bridgwater, J. 1998, "A case study of particle mixing in a ploughshare mixer using Positron Emission Particle Tracking", *International Journal of Mineral Processing*, vol. 53, no. 1-2, pp. 29-38.
- Jones, J. R., Davies, C. E., Fallon, S. J., Fenton, K., Brown, N., & Parker, D. J. 2002, "Comparison of Sampling and PEPT on Mixing in a Tote Blender", in *Asian-Pacific Conference of Chemical Engineering (APCChE)*.
- Kaye, B. H. 1997, *Powder Mixing* Chapman & Hall.
- Khakhar, D. V., Orpe, A. V., & Ottino, J. M. 2001, "Surface Granular flows: Two Related Examples", *Advanced Complex Systems*, vol. 4, pp. 407-417.
- Khoe, G. K., Ip, T. L., & Grace, J. R. 1991, "Rheological and fluidization behaviour of powders of different particle size distribution", *Powder Technology*, vol. 66, no. 2, pp. 127-141.
- Klausner, J. F., Chen, D., & Mei, R. 2000, "Experimental investigation of cohesive powder rheology", *Powder Technology*, vol. 112, no. 1-2, pp. 94-101.
- Lacey, P. M. C. 1997, "The mixing of solid particles", *Chemical Engineering Research and Design*, vol. 75, no. Supplement 1, p. S49-S55.
- Lai, C. K., Holt, D., Leung, J. C., Cooney, C. L., Raju, G. K., & Hansen, P. 2001, "Real time and noninvasive monitoring of dry powder blend homogeneity", *A.I.Ch.E. Journal*, vol. 47, no. 11, pp. 2618-2622.
- Lam, K. K. & Newton, J. M. 1992, "Influence of particle size on the adhesion behaviour of powders, after application of an initial press-on force", *Powder Technology*, vol. 73, no. 2, pp. 117-125.
- Langner, J. 2008, *Event-Driven Motion Compensation in Positron Emission Tomography: Development of a Clinically Applicable Method*, PhD, Technische Universität Dresden.
- Leonard, G., Bertrand, F., Chaouki, J., & Gosselin, P. M. 2008, "An experimental investigation of effusivity as an indicator of powder blend uniformity", *Powder Technology*, vol. 181, no. 2, pp. 149-159.

- Martin, T. W. 1998, *Studies of Particle Motion in Mixers*, PhD, The University of Birmingham.
- Martin, T. W., Seville, J. P. K., & Parker, D. J. 2007, "A general method for quantifying dispersion in multiscale systems using trajectory analysis", *Chemical Engineering Science*, vol. In Press.
- McCarthy, J. J. 2003, "Micro-modeling of cohesive mixing processes", *Powder Technology*, vol. 138, no. 1, pp. 63-67.
- Miyayami, K. 2006, "Mixing," in *Powder Technology Handbook, Third Edition*, CRC Press.
- Muzzio, F. J., Alexander, A., Goodridge, C., Shen, E., & Shinbrot, T. 2004, "Solids Mixing Part A: Fundamentals of Solids Mixing," in *Handbook of Industrial Mixing*, E. L. Paul, V. A. Atiemo-Obeng, & S. M. Kresta, eds., Wiley Interscience, pp. 887-923.
- Muzzio, F. J. & Alexander, A. W. 2005, "Scale Up of Powder Blending Operations". *Pharmaceutical Technology [Scaling up Manufacturing 2005]*, s34-s44..
- Muzzio, F. J., Goodridge, C. L., Alexander, A., Arratia, P., Yang, H., Sudah, O., & Mergen, G. 2003b, "Sampling and characterization of pharmaceutical powders and granular blends", *International Journal of Pharmaceutics*, vol. 250, no. 1, pp. 51-64.
- Muzzio, F. J., Robinson, P., Wightman, C., & Dean, B. 1997, "Sampling practices in powder blending", *International Journal of Pharmaceutics*, vol. 155, no. 2, pp. 153-178.
- Orband, J. L. R. & Geldart, D. 1997a, "Direct measurement of powder cohesion using a torsional device", *Powder Technology*, vol. 92, no. 1, pp. 25-33.
- Pack, R. T., Tarboton, D. G., & Goodwin, C. N. 1998, "The SINMAP Approach to Terrain Stability Mapping", in *8th Congress of the International Association of Engineering Geology*.
- Parker, D. J., Dijkstra, A. E., Martin, T. W., & Seville, J. P. K. 1997, "Positron emission particle tracking studies of spherical particle motion in rotating drums", *Chemical Engineering Science*, vol. 52, no. 13, pp. 2011-2022.
- Parker, D. J., Fan, X., Forster, R. N. G., Fowles, P., Ding, Y., & Seville, J. P. K. 2005, "Positron Imaging Studies of Rotating Drums", *The Canadian Journal of Chemical Engineering*, vol. 83, no. 1, pp. 83-87.
- Parker, D. J., Forster, R. N., Fowles, P., & Takhar, P. S. 2002, "Positron emission particle tracking using the new Birmingham positron camera", *Nuclear Instruments and Methods in Physics Research Section A: Accelerators, Spectrometers, Detectors and Associated Equipment*, vol. 477, no. 1-3, pp. 540-545.
- Parker, D. J. & Fan, X. 2008, "Positron emission particle tracking--Application and labelling techniques", *Particuology*, vol. 6, no. 1, pp. 16-23.

- Peleg, M. & Mannheim, C. H. 1973, "Effect of conditioners on the flow properties of powdered sucrose", *Powder Technology*, vol. 7, no. 1, pp. 45-50.
- Peratt, B. A. & Yorke, J. A. 1998, "Modeling continuous mixing of granular solids in a rotating drum", *Physica D: Nonlinear Phenomena*, vol. 118, no. 3-4, pp. 293-310.
- Pirard, S. L., Lumay, G., Vandewalle, N., & Pirard, J. P. 2009, "Motion of carbon nanotubes in a rotating drum: The dynamic angle of repose and a bed behavior diagram", *Chemical Engineering Journal*, vol. 146, no. 1, pp. 143-147.
- Portillo, P., Ierapetritou, M., Tomassone, S., Mc Dade, C., Clancy, D., Avontuur, P., & Muzzio, F. 2008, "Quality by Design Methodology for Development and Scale-up of Batch Mixing Processes", *Journal of Pharmaceutical Innovation*, vol. 3, no. 4, pp. 258-270.
- Positron Imaging Centre 2000, '*Track*' Manual, Version 3 School of Physics & Astronomy, University of Birmingham.
- Poux, M., Fayolle, P., Bertrand, J., Bridoux, D., & Bousquet, J. 1991, "Powder mixing: Some practical rules applied to agitated systems", *Powder Technology*, vol. 68, no. 3, pp. 213-234.
- Rennie, P. R., Chen, X. D., Hargreaves, C., & Mackereth, A. R. 1999, "A study of the cohesion of dairy powders", *Journal of Food Engineering*, vol. 39, no. 3, pp. 277-284.
- Roberts, A. W. 1993, *Basic Principles of Bulk Solids Storage, Flow & Handling* TUNRA Bulk Solids Research Associates.
- Sekulic, S. S., Wakeman, J., Doherty, P., & Hailey, P. A. 1998, "Automated system for the on-line monitoring of powder blending processes using near-infrared spectroscopy: Part II. Qualitative approaches to blend evaluation", *Journal of Pharmaceutical and Biomedical Analysis*, vol. 17, no. 8, pp. 1285-1309.
- Seville, J. P. K., Parker, D. J., & Ingram, A. 2005, "Probing Processes Using Positrons", *Chemical Engineering Research & Design*, vol. 83, no. A7, pp. 788-793.
- Shi, Z., Cogdill, R. P., Short, S. M., & Anderson, C. A. 2008, "Process characterization of powder blending by near-infrared spectroscopy: Blend end-points and beyond", *Journal of Pharmaceutical and Biomedical Analysis*, vol. 47, no. 4-5, pp. 738-745.
- Sudah, O. S., Coffin-Beach, D., & Muzzio, F. J. 2002, "Effects of blender rotational speed and discharge on the homogeneity of cohesive and free-flowing mixtures", *International Journal of Pharmaceutics*, vol. 247, no. 1-2, pp. 57-68.
- Sykes, J. B. e. 2005, *The Concise Oxford Dictionary*, Six edn, Oxford University Press.
- Visser, J. 1989, "Van der Waals and other cohesive forces affecting powder fluidization", *Powder Technology*, vol. 58, no. 1, pp. 1-10.

- Waters, K. E., Rowson, N. A., Fan, X., Parker, D. J., & Cilliers, J. J. 2008, "Positron emission particle tracking as a method to map the movement of particles in the pulp and froth phases", *Minerals Engineering*, vol. 21, no. 12-14, pp. 877-882.
- Wightman, C. & Muzzio, F. J. 1998, "Mixing of granular material in a drum mixer undergoing rotational and rocking motions I. Uniform particles", *Powder Technology*, vol. 98, no. 2, pp. 113-124.
- Wightman, C., Muzzio, F. J., & Wilder, J. 1996, "A quantitative image analysis method for characterizing mixtures of granular materials", *Powder Technology*, vol. 89, no. 2, pp. 165-176.
- Wildman, R. D., Blackburn, S., Benton, D. M., McNeil, P. A., & Parker, D. J. 1999, "Investigation of paste flow using positron emission particle tracking", *Powder Technology*, vol. 103, no. 3, pp. 220-229.
- Yamashiro, M., Yuasa, Y., & Kawakita, K. 1983, "An experimental study on the relationships between compressibility, fluidity and cohesion of powder solids at small tapping numbers", *Powder Technology*, vol. 34, no. 2, pp. 225-231.
- Yang, C. Y. & Fu, X. Y. 2004, "Development and validation of a material-labeling method for powder process characterization using X-ray computed tomography", *Powder Technology*, vol. 146, no. 1-2, pp. 10-19.
- Yang, Z., Fan, X., Bakalis, S., Parker, D. J., & Fryer, P. J. 2008, "A method for characterising solids translational and rotational motions using Multiple-Positron Emission Particle Tracking (Multiple-PEPT)", *International Journal of Multiphase Flow*, vol. 34, no. 12, pp. 1152-1160.
- Zhong, Z., Ooi, J. Y., & Rotter, J. M. 2005, "Predicting the handlability of a coal blend from measurements on the source coals", *Fuel*, vol. 84, no. 17, pp. 2267-2274.
- Zulfiqar, M., Moghtaderi, B., & Wall, T. F. 2006, "Flow properties of biomass and coal blends", *Fuel Processing Technology*, vol. 87, no. 4, pp. 281-288.

Chapter 4 – Powder Systems Evaluation

Abstract

This chapter investigates the application of enhanced powder characterisation capability, with particular respect to hopper design methodologies, and introduces methodologies for evaluation of powder processing systems so that appropriate testing can be targeted. A novel way of representing the multivariate data such as that described in Chapter 2 is evaluated.

4.1. Introduction

The previous chapters have shown that it is necessary for companies operating in the pharmaceutical industry, both manufacturers and suppliers, to better understand their processes; and that, in the context of powder handling and processing, a range of characterisation techniques are necessary and are now readily available to evaluate powder properties; furthermore these properties can be used to help study process systems. This chapter will endeavour to provide a framework that will allow process engineers to systematically evaluate their process such that the goal of quantifying the 'design space' can be achieved. It will also critically review issues relating to the most common powder processing design routine – generating the specifications for a mass flow hopper. Finally a worked example will be presented to link all the threads of this thesis.

4.2. Powder systems and their analysis

The inability of industry to generate reliable processes that meet their design specifications is a long standing issue. In the late 1980's Merrow (Merrow 1986) produced a report that outlined some of the outstanding challenges relating to solids processing R&D, and the paper by Ennis *et al* in 1994 (Ennis, Green, & Davies 1994) both indicate the poor performance of powder and bulk solids processing systems. Although there is no recent discussion on this subject, the issues and challenges remain.

Some of the reasons why powder systems perform poorly are the inability to generate reliable and meaningful powder characteristics in a cost effective manner, and the significant recent improvements in this field have been discussed in Chapter 2. Additionally, the development of measurement techniques that can be used to generate behavioural models and provide on- and in-line measurements in (opaque) powder processing systems have also improved significantly and this has been discussed in Chapter 3. These improvements also require a framework on which to pin the concepts generated by this work and to look at areas where issues such as feedstock variability will impact on process performance.

The engineering and physico-chemical sciences which are practised when designing and installing systems for manipulating particulate materials are the domain of many traditionally defined interest groups, which have been loosely summarised in Table 4.1.

Table 4.1: Disciplines associated with powder processing

Chemical Engineering	⇒	Reactor design; separation processes; macroscopic effects; (increasingly) microscopic effects
Mechanical Engineering	⇒	Equipment design; transfer processes; macroscopic effects
Civil Engineering	⇒	Soil mechanics and flow, storage vessels; macroscopic effects
Physics	⇒	Surface phenomena; microscopic effects
Chemistry	⇒	Surface reaction phenomena; molecular effects; formulation design
Pharmacy	⇒	Design of pharmaceutical formulation
Control Engineering	⇒	Control of operations

Much cross disciplinary research is undertaken, but it is apparent that no one specialism 'owns' the field of particulate processing, which perhaps goes some way to explain the lack of a coherent approach to particulate systems.

The processing of particulate materials is frequently based upon standard flowsheeting and piping and instrumentation (P&I) techniques (Himmelblau 1996). This invariably leads to reactor-centric systems; all the design effort is focused on the vessel which 'creates' the product with limited attention on the ancillary systems which supply, store & blend the raw materials and remove, transfer & store the finished product. This is perhaps understandable as most flowsheeting is a legacy of the oil and petrochemical industries, where the raw (fluid) materials are easily pumped between reactors – the pipelines have little effect on the materials transported and flow is invariably guaranteed and thus ignored, hence the 'reactors connected to each other by thin black lines' appearance of the typical flowsheet.

A typical bulk solid processing flowsheet is shown in Figure 4.1

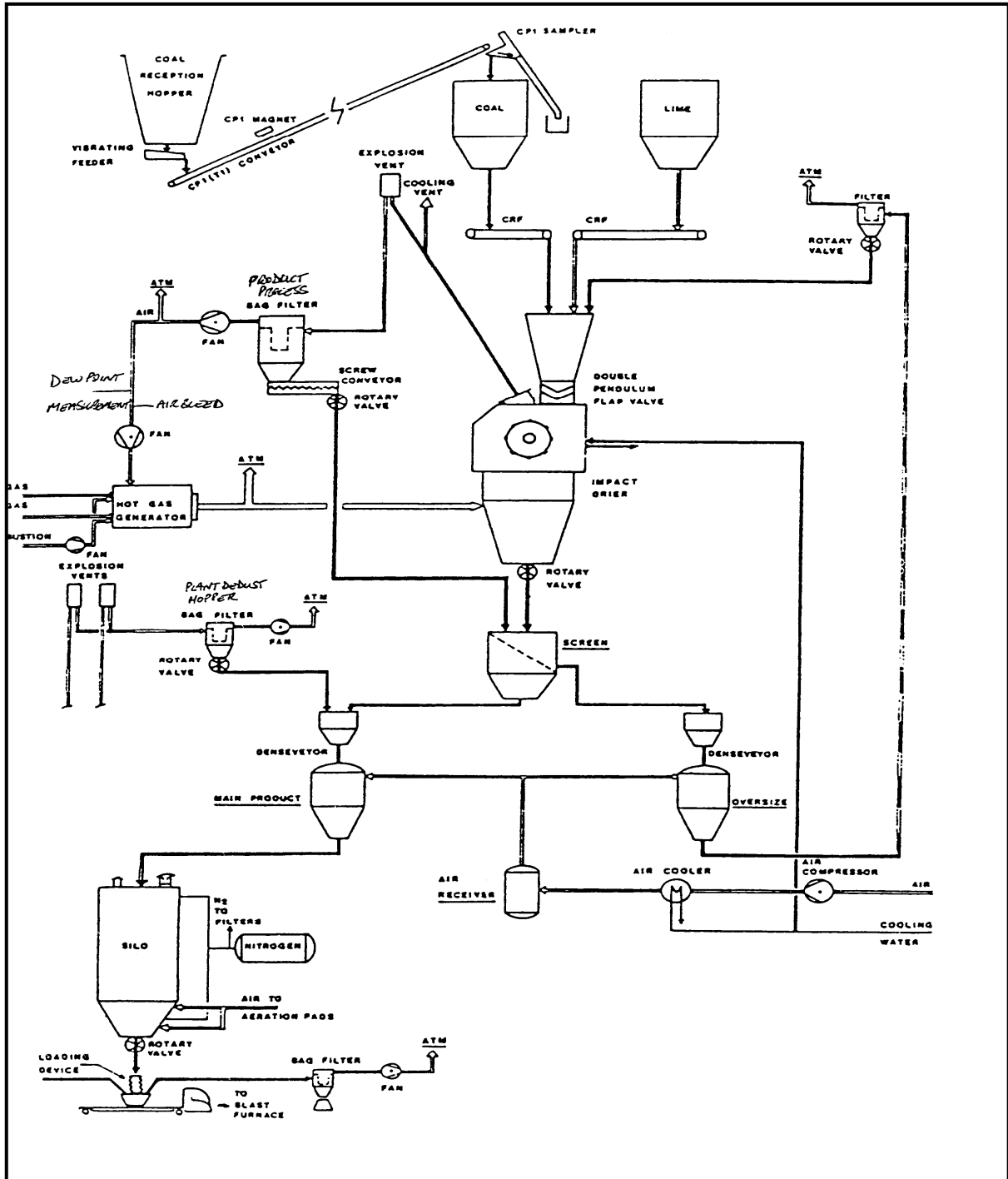


Figure 4.1: Flowsheet for a coal processing facility

In particulate processing these ancillary transport functions cannot be assumed to be simple - particulate solid flow cannot be guaranteed. Ostensibly simple operations can dramatically disturb the balance of the system by preventing flow or by creating

unwanted effects in raw materials, intermediates or finished products. Typically poor initial design, the fitting of low quality equipment to save cost, incorrect interfacing or poor control methodologies are the root causes of these problems. As can be seen from this flowsheet, on which the preliminary the Hazard & Operability Study (HAZOP) is usually undertaken, there are many horizontal lines which link vessels through which powders flow by gravity. This is not to suggest that the HAZOP team are not aware of this issue, it just provides a mind set in which the 'operability' part of the test can be overlooked or sidelined.

In general, the approach to creating a particulate processing system is akin to playing with Meccano on a larger scale. Reactors, feeders and transfer systems are often bought off the shelf and bolted or butted together with little thought given as to whether they will perform in unison. The legacy of the flowsheet manifests itself in the attitude to construction and operation.

The contracting out of 'turnkey' projects based on price also does little to benefit powder and bulk processing systems. It is not unknown for contract engineering concerns to bid low with generalised designs in order to win a contract, with the view of making up the profit with variation orders when specifications are not achieved. This can often result in a poor working relationship between the two parties which, in extreme circumstances, ends in legal proceedings. Equally, companies who provide poor information to contractors and hold them to unreasonable specifications for materials which do not match the initial process design samples are also acting in a disingenuous manner. Invariably both parties loose out; the contractor can be sued

or subjected to stringent penalty clauses and thus squeezed to the point where there is no profit in the contract whilst trying to solve problems not of his making; the company letting the contract can be left with an underperforming process which was delivered late and liable for expensive variation orders. The reality is often in the middle and both sides end up with additional costs which hurt their bottom lines. Thus no amount of contractual red tape will make up for the aggravation and loss of earnings from a poorly designed and under performing plant.

Like the flowsheet, the contractual models assume that it will be (relatively) simple to design the process, which will be based around robust design calculations such that the specifications can be easily met. As has been shown in Chapters 2 & 3, very few design calculations that encompass the entire spectrum of bulk solid materials exist due to the difficulties measuring, quantifying and representing the huge range of physical, chemical and environmental variations that apply to particulate solids.

In order to achieve consistency of product with low processing costs and minimal waste for all particulate processes, it is, perhaps, intuitive that the whole process be approached systematically to consider all the effects that are brought to bear on the particulates involved. However this is not often the case.

Evaluating the literature produces a number of reactor focussed 'expert systems' (Klinzing & Dhodapkar 1993; Lerou & Ng 1996; Regli *et al.* 2000; Toebermann *et al.* 2000) – specific (software) tools based on specific models – which allow an expert to rapidly generate optimal designs for specific reactors. They do not, however, answer

a number of fundamental questions of how to analyse a process to enable a rational appraisal of how variation in the powder feedstock will affect the operation of the process.

These expert systems usually only relate to a single process or operation, and a more encompassing approach is required to evaluate a whole process plant. Such an approach does already exist and is very familiar to chemical engineers – the Hazard & Operability Study (HAZOP) – but it is usually undertaken as part of a safety exercise and the emphasis is most definitely (and quite correctly) on the HAZard aspect. Section 4.2.1 will show that, with some minor extensions to the usual methodology, HAZOP can be employed to systematically detail the operability of powder processing systems and improve the levels of plant availability and achieving a higher proportion of the design throughput where applicable.

4.2.1. *The extension of the HAZOP methodology*

Most chemical engineers are familiar with the standard HAZOP methodology (Coulson, Richardson, & Sinnott 1991;Kletz 1992) whereby a flowsheet from a proposed or existing process plant is systematically analysed by means of guide words and process parameters for each and every reactor and process line present on the diagram, however there will be more of an emphasis on the ‘OPerability’ rather than the ‘HAZard’ in this instance.

Table 4.2 shows the guide words that are typically used and Table 4.3 shows a series of parameters that are used in conjunction with guide words to inject theoretical perturbations into the process, the outcomes of which the HAZOP team will identify as possible or impossible outcomes (IBC Technical Services Limited 1994). The possible outcomes will then be assessed for their likelihood and their consequences and the team members will be tasked with eliminating or moderating the outcomes by changes to design, operating procedures and/or feedstock.

Table 4.2: Range of Guide Words Used in HAZOP Studies

Guide Word	Meaning
NO or NOT	Complete negation of the design intent
MORE	Quantitative increase
LESS	Quantitative decrease
AS WELL AS	Qualitative modification/increase
PART OF	Qualitative modification/decrease
REVERSE	Logical opposite of the design intent
OTHER THAN	Complete substitution
EARLY	Relative to the clock time – batch operation
LATE	Relative to the clock time – batch operation
BEFORE	Relating to order or sequence – batch operation
AFTER	Relating to order or sequence – batch operation

Table 4.3: Examples of the Combination of Parameters, Guide Words and perturbations Used in HAZOP Studies

Parameter	Guide Word						
	More	Less	None	Reverse	As well as	Part of	Other than
Flow	high flow	low flow	no flow	reverse flow	deviating conc ^a	contamination	deviating material
Pressure	high pressure	low pressure	vacuum		delta-p		explosion
Temperature	high temperature	low temperature					fire
Level	high level	low level	no level		different level		
Time	too long / too late	too short / too soon	sequence step skipped	backwards	extra actions	missing actions	wrong time
Agitation	fast mixing	slow mixing	no mixing				
Reaction	fast reaction / runaway	slow reaction	no reaction				unwanted reaction
Start-up / Shut-down	too fast	too slow			actions missed		wrong recipe
Draining / Venting	too long	too short	none		deviating pressure	wrong timing	
Inerting	high pressure	low pressure	none				wrong material
Utility failure (instrument air, power)			failure			contamination	
Maintenance		low quality part	none		part left in system		wrong part
Vibrations	too low	too high	none				wrong frequency

If one considers the specific problems that can be observed in powder processing systems, there are a number of factors, both as a function of the powder and of the environment, which impact the system operability, some of which are listed below;

- Mean particle size
- Size distribution
- Shape effects
- Segregation
- Degradation
- Agglomeration
- Moisture absorption/adsorption
- Electrostatic charging
- Time effects – consolidation/caking
- Plant vibration
- Aeration/de-aeration
- Permeability
- Gravity induced pressure effects – consolidation/caking

Thus when the HAZOP study group applies the guide words to the parameter, the possible factors can be assessed as plausible or implausible causes for a reduction ('less') or prevention ('none') of powder moving within the designated vessel or pipeline. It should be noted that occasionally a powder's ability to retain air may

allow it to exhibit the other extreme case of an increase over specification ('more') of flow.

In the case where the guide words are applied to the 'flow' parameter, for example, it can be seen that 'less flow' (by far and away the most likely scenario for this parameter) can be influenced by many of the powder properties, or a change therein, such as particle size distribution, segregation, moisture, vibration etc., however the ability to assess the impact of such variability has been limited by the small number of test methods that could cost effectively evaluate powder properties. Equally the lack of use of any of the available test methodologies in such situations, perhaps through lack of awareness, may also contribute to a failure to identify and quantify potential flow issues.

The significantly expanded range of laboratory tests described and employed in Chapter 2 enable the rapid (and therefore relatively low cost) evaluation of the sensitivity of a particular powder characteristic – say cohesion or permeability – to a change in size distribution or moisture content or segregation, for example. Thus the ability to quantify the effect of any variation in powder property is available, and this can be related, either through standard design equations or through empirical methods, to a deviation in process performance – making the job of the designer and the HAZOP team much easier.

Once the issues have been determined during the HAZOP procedure, the next stage is to determine how likely these parameters are to change and, perhaps more

importantly how much they have to change, such that the process is compromised – this is the risk assessment element that should be present in all process evaluation. Typically a risk assessment matrix is used to correlate the likelihood of an event – such as a ‘no flow’ issue – with the estimate of the consequences in a visual matrix, and is shown in Table 4.4.

Table 4.4: Risk Assessment Matrix

Likelihood	Consequences				
	Insignificant (minor problem easily handled by normal operation)	Minor (some disruption possible)	Moderate (significant time/resource required)	Major (operations severely damaged)	Catastrophic (business survival at risk)
Almost certain (>90% chance)	High	High	Extreme	Extreme	Extreme
Likely (between 50% & 90%)	Moderate	High	High	Extreme	Extreme
Moderate (between 10% & 50%)	Low	Moderate	High	Extreme	Extreme
Unlikely (between 3% & 10%)	Low	Low	Moderate	High	Extreme
Rare (<3% chance)	Low	Low	Moderate	High	High

Once this is completed and the possible (operational) risk is deemed to be high or extreme, then there are usually three options to allow the moderation of the risk;

- Control the specification of the powder. This usually involves the purchase/manufacture of a sample with a tighter size distribution (for example); the specification of a flow aid; or, in extremis a change to the formulation. There is clearly an operational cost and time implication here which will need to be assessed.
- Change the system design to cope with the potential variation in the powder. This can involve larger hopper outlets; steeper chutes; steeper hopper half angles; low friction materials of construction etc. which can significantly impact storage volumes or the overall height of the process plant. There are clearly capital and operational cost implications here which will need to be assessed.
- Keep the design and allow for periodic production stoppages caused by the variability of the powder. There is also an operational cost implication with this option which will need to be assessed.

The choice of corrective action is clearly related to the system and powder combination and the philosophy of the company commissioning the process.

4.2.2. Additional considerations

Although many chemical engineering processes are batch operations, the necessarily intermittent operation of most bulk handling systems is often not considered. Even if the main 'reactor' is a continuous process, the feedstocks are often held in a main storage vessel which batch transfers material to a local feed hopper.

In addition, the history of the particles frequently has a significant effect on the characteristics and behaviour of the bulk.

Similarly the item of processing equipment may have a transitory but significantly different effect on the powder during start up and shut down operations than during normal operation. The development of complementary 'start-up', 'shut-down' and 'extended wait cycle' flowsheets may be appropriate for difficult materials.

The HAZOP study is usually composed of a review at various stages within the development of a project, as summarised in Table 4.5.

Table 4.5: Various stages of Hazard and Operability Study

HAZOP Stage	Description
1	Identify major hazards and check for availability of key hazard data
2	Coarse HAZOP using flowsheet and block diagram
3	Full HAZOP on frozen P&I diagram
4	Check that all intended actions have been implemented, including hardware and software
5	Pre-commissioning check including statutory requirements
6	Safety audit after a few months operation

However, it is extremely important to include a further stage for powder processing systems. As most powder systems rely on gravity for a significant number of transfer processes, any powder system must include a review of the isometric drawings (or as

a minimum orthographic drawings) of the process plant. This is not an issue with all but the most viscous fluid based systems but, as has been already mentioned, flow in powder systems cannot be guaranteed. Poorly specified chute angles and unnecessary reductions in pipeline diameter can severely compromise flow in any powder processing system, and it is vital that such discrepancies are identified and corrected before the steelwork is installed and it becomes very difficult to correct. This is also relevant for pneumatic transfer processes where inclined pipework, sharp bends ($r/d < 4$) or just too many changes of direction (Bradley 1990) can dramatically limit throughput. With reference to Table 4.5, this review of the isometric drawings should take place at the same time as the HAZOP on the frozen P&I diagram to ensure that any equipment that will be ordered is specified correctly.

4.2.3. Summary

Utilising the flowsheet approach for powder processing plant and equipment can impose some severe restrictions to the engineer's conception of powder behaviour in the process. The block and line representation, derived from the petrochemical industry, implies guaranteed flow, which is never the case with powder systems. A more detailed review using an enhanced HAZOP methodology can significantly improve the quality of the approach to designing powder processing systems.

4.3. Sensitivity analysis of storage system design

Most industrial powder processing systems include at least one storage element, whether this is buffer storage between processing steps or bulk storage of raw materials, and/or intermediates and/or finished product, so there is a clear advantage in evaluating the methodology for hopper design, especially in light of the advances in shear cell automation and methodology reviewed in Chapter 2, making it much quicker to generate repeatable data and to analyse that data more fully. In addition, it is one of the very few robust design methodologies that is available for powder systems.

The development of hopper design criteria is almost always taken as read. It is probably the most common design methodology associated with powder analysis and is presented in many textbooks (EFCE 1989;Fayed & Otten 1984;McGlinchy 2005;Rhodes 1998;Schulze 2007;Wood 1986). However, there are some limitations to the usefulness of the data. The criteria set down by Jenike (Jenike 1964) and refined by Roberts *et al* (Roberts 1993) have to be considered in respect to the testing equipment available at the time – namely the Jenike type translational shear cell. There is little published about the sensitivity of the design methodology to slight variations in the test data that are always present even in the most repeatable of powders, again mainly due to the time costs of undertaking Jenike shear cell tests.

The work done by Roberts and co-workers was to develop a more analytical solution to the arching criteria. Although this is not the only analytical solution to the problem,

as indicated by Drescher (Drescher, Waters, & Rhoades 1995a; Drescher, Waters, & Rhoades 1995b), it is, arguably, the most accessible and also has been recently presented in McGlinchy's book (McGlinchy 2005). This solution has been adopted by Freeman Technology, in conjunction with this authors input, to develop a software design tool that provides a way of giving the shear cell data, derived from its FT4 Powder Rheometer, a more tangible result that is more easily understandable to non-specialist engineers. A hopper outlet and wall angle can be much more readily conceptualised than, for example the implication of a Flow Function or an angle of internal friction.

The update to the FT4 post processing software allows the user to import shear, wall friction and compressibility tests and then, using the equations developed by Roberts, calculate a hopper outlet and hopper half angle that will allow the powder to flow out of the hopper in a mass flow regime. A detailed description of this software design tool is presented in Appendix 2. Thus the rapidity of generating test data, coupled with current computer processing power has allowed the rapid generation of hopper design parameters. Using this software design tool allows the engineer to evaluate the sensitivity of the design to the powder properties quickly, easily and repeatably. Variability in moisture content, particle size, alternate feedstocks, can all now be quickly tested and the impact on a real process parameter can be ascertained. Very little regarding computer based silo design processes exists in the public domain. Extensive searches have not revealed commercial or even shareware programs that are currently available. Early work was undertaken by Stainforth *et al* (Stainforth, Ashley, & Morley 1971) and Bundali (Bundalli 1973) but

no longer seems to be available. Clearly such analyses are regularly undertaken by users of shear cells – consultants and academics – as the exercise is reasonably straightforward once the equations (Roberts 1993) have been identified.

However the dichotomy is, historically, that such users who advocate the use of the shear cell and should promote its use have not really made the most of the opportunity. Given the potential market of powder processors (Ennis, Green, & Davies 1994b), this seems a missed opportunity. This is, perhaps, understandable as consultants selling instrumentation will, on the whole, prefer to stick to what they know best – consultancy.

Recently the shear cells by Schulze and (later) Freeman have expanded the market for such devices by making the use of shear cells much simpler, quicker and transparent allowing the end user to generate their own information and sensitivity analyses. The Brookfield Engineering Powder Flow Tester which has entered the market very recently (2009/2010) and been developed in conjunction with the Wolfson Centre at the University of Greenwich, has all the necessary tools for developing bin design parameters as standard (Brookfield Engineering Laboratories Inc. 2010)¹ and, for some, will provide a low cost and rapid solution.

¹ It was not possible during this study to evaluate this device but it appears that it is competitively priced against the shear cells evaluated here, but it should be noted that it cannot perform any of the other functions of the powder rheometers.

However, now that it is possible to rapidly generate the shear cell data used for hopper design and to process the results to provide bin design data, there are some aspects of the design process which have been brought into sharp focus.

- the sensitivity of the derived parameters to slight variations in repeat yield loci (expanded from the analysis provided in Chapter 2),
- the limitations of the models commonly presented in the texts cited earlier and most of the literature for the treatment of
 - the yield locus and
 - the Flow Function.

4.3.1. *Review of bin design using standard protocols*

Before these are evaluated, there are, however, a number of issues with the hopper design procedure with which any user needs to be aware. Firstly, it is useful to understand what sorts of stress levels are likely to be seen in bins in accordance with the methodology set out in Section 4.3 – specifically for typical pharmaceutical excipients studied in this thesis. Secondly, bin designs using the linear fit to the yield loci and a linear fit to the Flow Function will be reviewed with respect to a number of published and recently measured data for a range of common materials.

To illustrate the point, the likely loads at the base of a (full and level) flat bottomed bin of aspect ratio 2:1 have been calculated using the Janssen equation (Fayed & Otten 1984) shown in Equation 4.1 for three common pharmaceutical excipients and the results shown in Figure 4.2.

$$P_v = \left(\frac{\rho_b g D}{4\mu K} \right) \left(1 - e^{\left(\frac{-4H\mu K}{D} \right)} \right) \quad \text{Equation 4.1}$$

where

μ is angle of internal friction

D is the diameter of the cylinder

ρ_b is the poured bulk density of the powder

g is the acceleration due to gravity

H is height of the powder

K is a the ratio of horizontal to vertical pressure and is assumed constant – 0.4

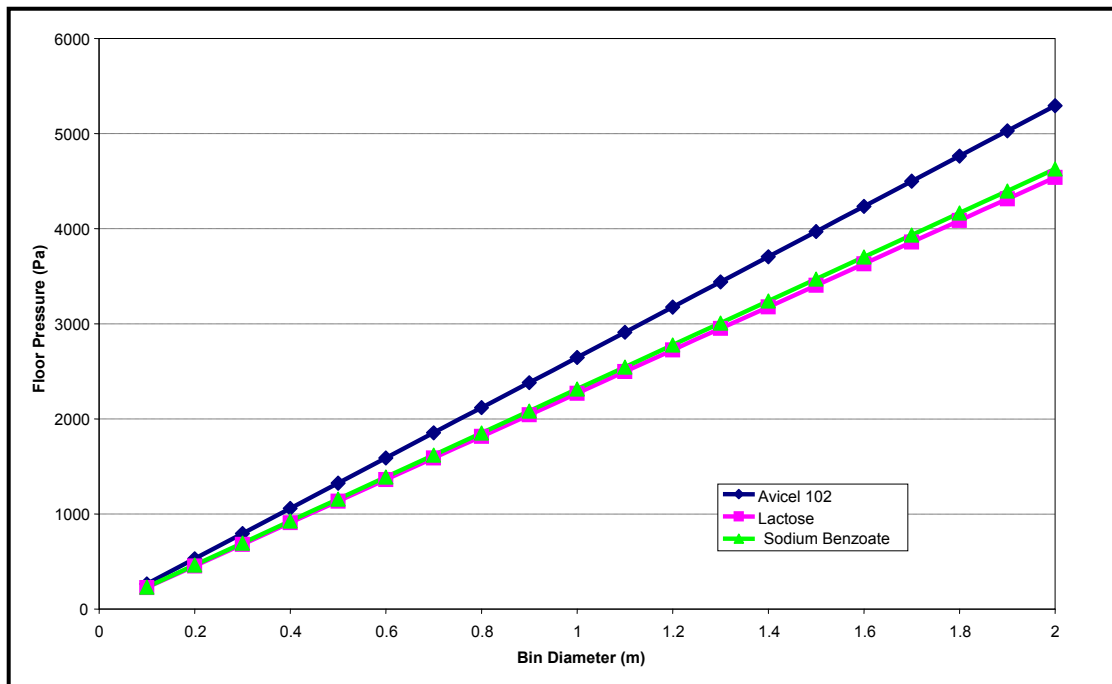


Figure 4.2: Normal loads generated at the base of a column of powder based on Janssen's equation for three common pharmaceutical excipients

Although it not strictly accurate to assume K is constant – it is a function of the angle of internal friction (Roberts 1993), which in turn is a function of the consolidating load and thus varies through the bin – this approximate calculation shows the order of magnitude of the normal stresses that are likely to be experienced by a low density

pharmaceutical powder in a typical IBC/small silo. Typically 5kPa is not uncommon for larger bins or IBC's, but intermediate hoppers (within a tablet press for example) are likely to be, physically, much smaller and thus floor/outlet stresses are commensurately lower.

It is also useful to quantify the order of magnitude of the design parameters, hopper wall angle and outlet size, that are typically generated when using the Jenike design procedure. A paper by Fitzpatrick *et al* (Fitzpatrick, Barringer, & Iqbal 2004) presents the hopper half angle and outlet diameter for a range of common foodstuffs and these results are reproduced in Table 4.6.

Table 4.6: Hopper design parameters generated by Fitzpatrick *et al* using a Stainless Steel 304 wall materials (Ra unknown)

Powder	Flow index (FF or ff _c)	Bulk density (g/cc)	ff	θ (deg)	$\overline{\sigma}_1$ or CAS (kPa)	D (m)
Salt 200	1.2	0.87	1.15	16	3.36	0.88
Tomato	1.2	0.89	1.26	23	No flow	No flow
Cocoa	1.5	0.36	1.35	27	0.6	0.41
Corn flour	1.5	0.73	1.34	32	-0.02	0.17
Sugar 140	1.6	0.71	1.31	25	0	0.17
Wheat flour	1.6	0.71	1.47	33	1.1	0.39
Soy flour	2	0.6	1.37	26	0.09	0.2
Corn starch	2.1	0.76	1.46	31	0.21	0.21
Tea	2.6	0.91	1.39	15	0.1	0.12
Non Fat Milk	3.8	0.69	1.31	28	-0.23	0.18
Maltodextrin	4.9	0.6	1.33	24	0.1	0.17
Cellulose	6.1	0.41	1.49	35	0.24	0.31
Salt 140	6.3	1.17	1.3	15	0.34	0.1

These data presented by Fitzpatrick *et al* have some anomalies which are not reconciled within the text. Firstly the negative results for $\overline{\sigma}_1$, or Critical Applied Stress (CAS), (highlighted in Red in Table 4.6) are not physically realistic values and there is no explanation given for this anomalous behaviour or why they were included! How it would be possible to process these anomalous results to obtain a bin outlet size is also unclear. The 'tomato' sample was classified as 'No Flow' so

why were the Non Fat Milk and Cornflour not classified in this way? In addition the FF and bulk densities are presented as single values, but as both vary with the consolidation level of the sample, and it is not clear at what stress level these data were generated, these results are of little use.

When considering the results as a whole, however, what is striking is the size of the outlet generated using the routine data processing methodology. There is nothing smaller than 0.1m (100mm or ~4 inches) and the largest outlet is 0.88m (880mm or ~35inches). Interestingly both are for different grades of salt! Although the Salt 200 sample is very fine and dry – a mean size of 5.6μ and a moisture content of 0.04% (as indicated in the paper) – these properties do not entirely explain the result, as powders which one might consider cohesive, such as cocoa (which is shown in the text as having a mean particle size of 7.6μ and a moisture content of 4.4%) has a indicated bin outlet size of 0.41m – less than half that of the Salt 200. It may be that this particular grade of salt is particularly cohesive, it may be a milled product rather than derived from small crystals (thus with a very rough surface texture), but equally some issues with the testing procedure may have occurred or there may have been some caking of the sample during testing that was not immediately obvious to the operator.

As is evidenced by this paper, the hopper design procedure is not always easy to carry out but, in addition, the results are often difficult to interpret.

This large scale of outlet is also generated when FT4 data for a range of free flowing and cohesive industrial powders, including Standard Limestone CRM/BCR116 (Akers 1992), is evaluated using the hopper design software tool described in Appendix 2.

Table 4.7: Typical hopper design parameters generated from the FT4 hopper design software tool

Powder	ff²	θ (deg)	$\bar{\sigma}_1$ or CAS (kPa)	D (m)
Limestone CRM116	1.22	4	2.10	0.54
Manganese Dioxide	1.52	28	2.48	0.34
Aluminium Hydroxide	1.13	5	2.09	0.78
Potato powder	1.29	16	1.79	0.74
Spray Dried Lactose	1.84	24	0.36	0.16
Talc	1.33	12	0.70	0.23
Gypsum	1.22	12	1.36	0.38

Both sets of hopper design data show a requirement for a large outlet to achieve mass flow. This would suggest that large feeders and steep hopper sections are required and, if large quantities are to be stored, this can also mean very tall storage vessels. An actual hopper test could be carried out to determine the arching dimension, but this could prove costly.

If the one considers the alternative flow regime, core flow, the design theory (Roberts 1993) indicates even larger outlets are required than those derived for the mass flow

² ff derived from stainless steel wall friction testing coupon with a surface roughness of 1.2microns

regime. There is some discussion of the applicability of shear testing to free flowing, 'non-continuum' materials in Chapter 2 which would go some way to explain the limits of applying this procedure to free flowing powders, but does not explain it fully.

This seems possible as there are two factors at play here. Firstly the historical use of the Jenike cell means that the consolidating stresses used to develop a full Flow Function are quite high due to instrumental limitations. This has implication for the intersection of the FF and ff curves which is described later in Section 4.3.3.

The second possible factor is the concatenation of safety margins, of which there are three. There is an initial level of safety derived from the use of a linear fit to the yield locus which leads to a higher cohesion value and a higher UYS due to the size of the minor Mohr's circle required to be tangential to the higher yield locus, which in turn leads to a higher Flow Function, higher intersection with the flow factor and thus higher outlet value compared to the parameters generated using the Warren Springs equation, for example. Figure 4.3 shows the variation in the derived Cohesion value (44% uplift) and UYS (22% uplift) when using a linear and non-linear curve for a 7 point yield locus.

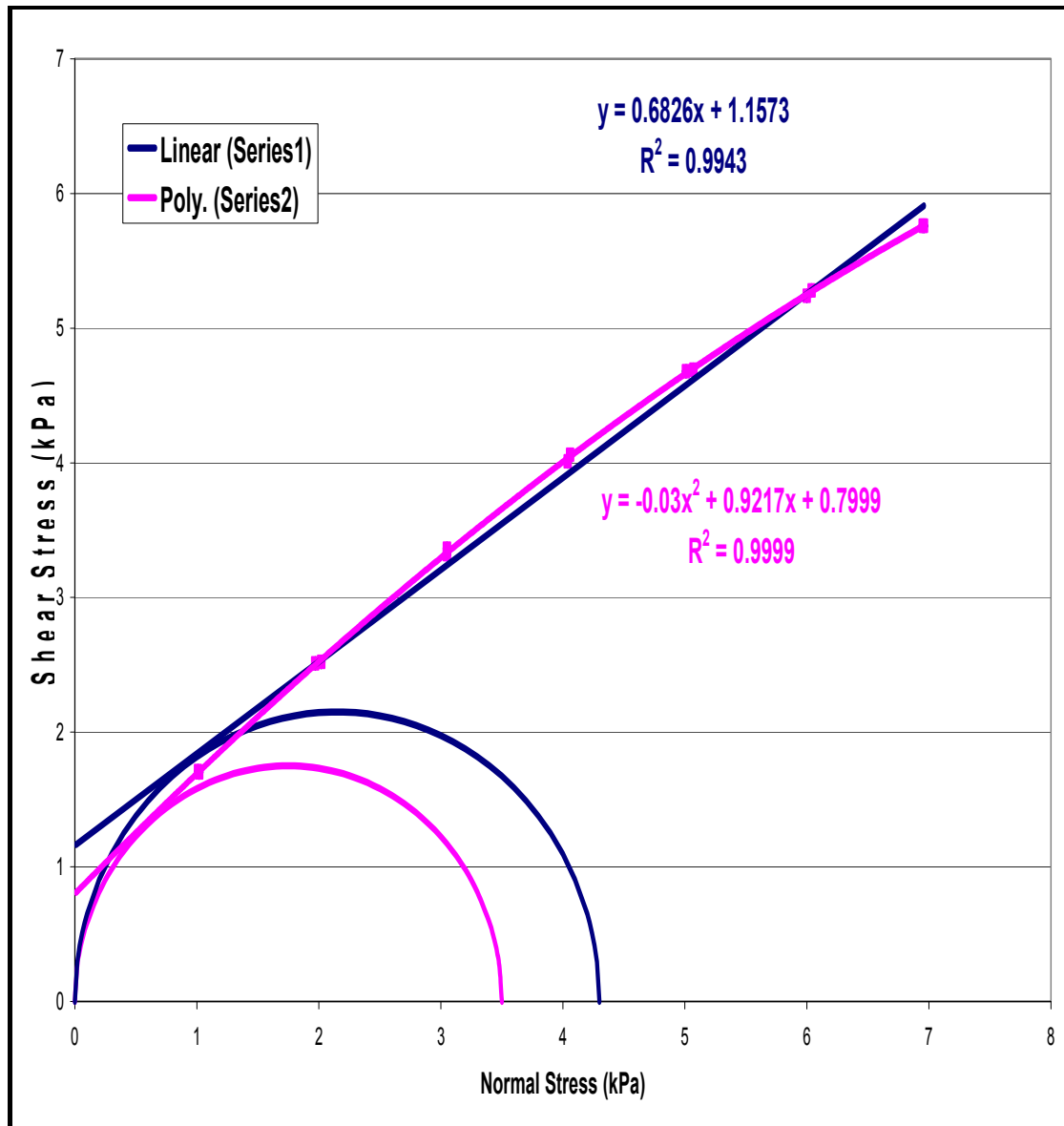


Figure 4.3: Example of linear and polynomial curve fitting to two repeat 7 point yield loci for Limestone

In addition there is a level of safety from the use of a linear fit for the Flow Function, which will be analysed in detail later in this section. Finally there is a recommended 20% uplift in the outlet size as an 'engineering safety margin' (Roberts 1993). All of these three choices for the design method are additive, but, as will be shown, it is the

use of a linear fit to the Flow Function data that leads to the largest uplift in the outlet size.

From the viewpoint of the design consultant, the enhanced level of safety margin could be seen as an advantage. It allows for the presentation of a robust design to the client, but more importantly it provides an allowance for the inevitable variability of the powder used in the field from the (probably unrepresentative) sample that was provided for testing. It also will allow a margin for changes in the environmental variables, especially time and moisture³.

The downside is that the design will call for a much larger outlet than is probably necessary, which in turn means a larger valve/feeder for the interface and possibly a more complex control interface for the (larger specified) feeder due to the increased turn down ratio necessary to hit the required feed rate (which is invariably much smaller than the unmetered gravity discharge rate). This means increased capital cost for the client which may be unnecessary. The upside is that a more compact vessel design may result, which will reduce capital cost for stabilising and providing feeders to reach a tall bin. Clearly there is a balance between the cost of the extra testing required to generate a more comprehensive, risk based assessment of powder flow properties and the additional cost of the feed system. However to exploit such a risk based system it is necessary to understand where variability will

³ The author has been given sight of confidential bin design reports from a notable US consultant prepared for a major chemical manufacturer where single yield loci consisting of three measurement points at each of three consolidating stresses, for which the client was charged \$10,000 without any sensitivity analysis. Equally, the author is aware of European consultants charging €5000 for shear testing of 2 powder samples (prices as at 2007).

occur and how it will propagate into the design process. Sections 4.3.2 and 4.3.3 will to analyse and evaluate the variability due to the design methodology.

4.3.2. Sensitivity of outlet size to variations in yield loci

Section 2.3.1.3 in Chapter 2 described how slight variations in the yield locus can generate large differences in the parameters derived from the fitting of a (linear) yield locus and the Mohr's circles. In this section the analysis will be extended to look at the effect of yield locus variability on bin outlet size.

For this analysis two sets of data are used for gypsum and for Standard Limestone CRM/BCR116 (Akers 1992). The bin outlet results will be compared when multiple yield loci for a fixed consolidating stress are used both individually for the calculation and as an averaged set of data – thus the Flow Function will be calculated using⁴

- $YL_{9,1} + YL_6 + YL_3$;
- $YL_{9,2} + YL_6 + YL_3$; and
- $YL_{9,3} + YL_6 + YL_3$ as well as
- $\text{avg}(YL_{9,1} YL_{9,2} YL_{9,3}) + YL_6 + YL_3$.

The data sets for compressibility and wall friction, required to run the hopper design software tool, also remain constant.

⁴ $YL_{9,1}$ refers to the first yield locus measured at 9kPa consolidating stress etc

Figure 4.4 shows the three individual yield loci for the Gypsum that were measured for a consolidating load of 9kPa. These were repeat tests using material extracted and discarded from the same well mixed, 1 litre sub-sample of material, as were the additional shear tests, wall friction test and compressibility test used for this analysis.

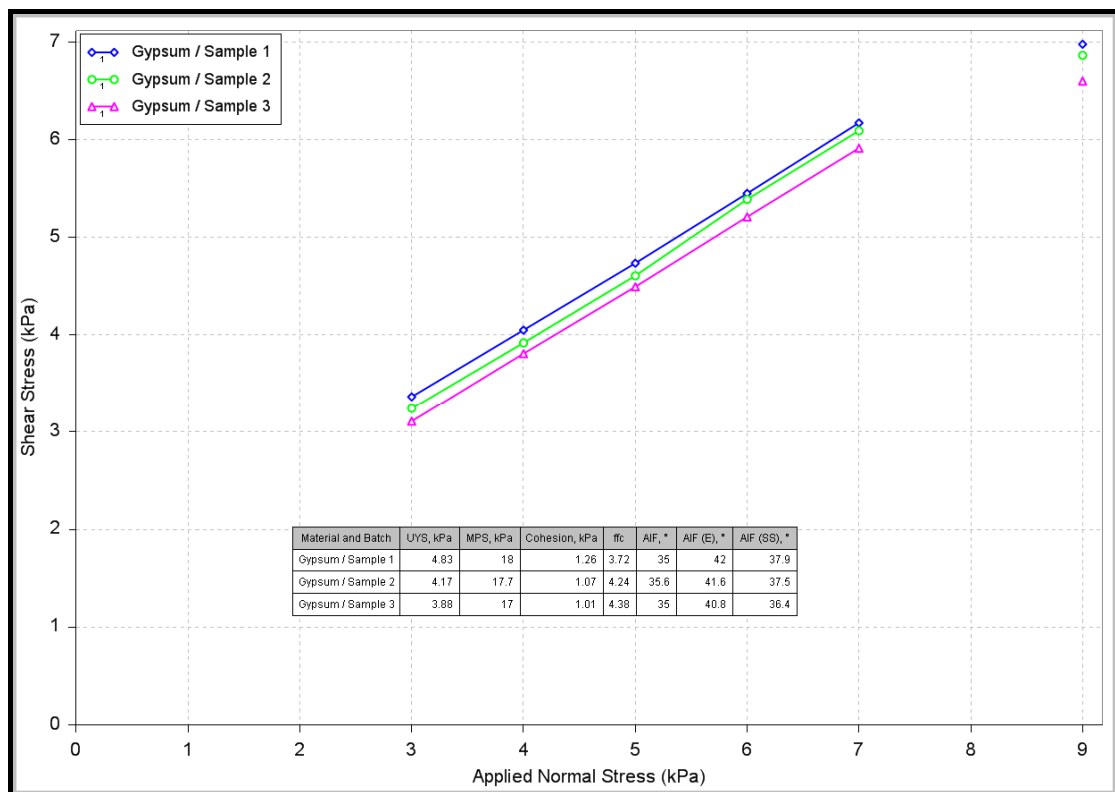


Figure 4.4: Three repeat shear tests of Gypsum at 9kPa consolidating load

These loci indicate some variability of material during testing although the flow functions are similar as are the cohesion values.

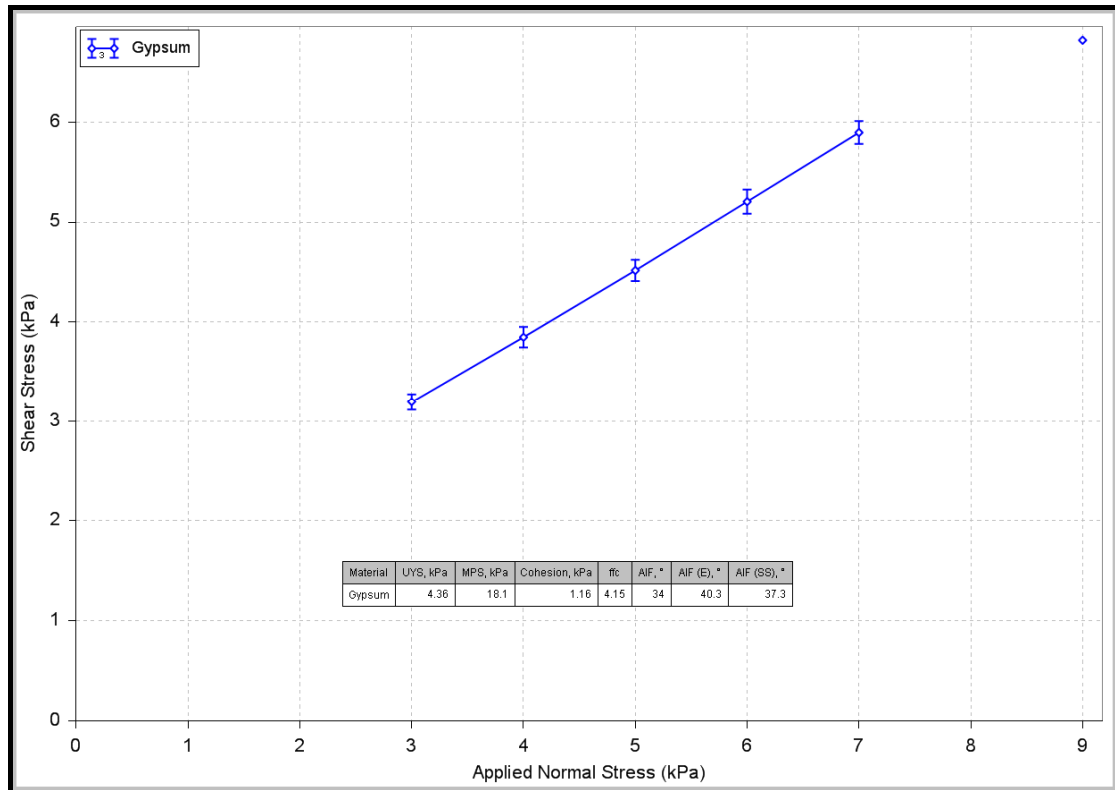


Figure 4.5: Averaged data sets from three yield loci

If the three loci are averaged – as shown in Figure 4.5 – the repeatability is acceptable. The standard deviation at the 3kPa applied normal stress point is ± 0.0788 kPa or 2.41%; standard deviation at the 7kPa applied normal stress point is ± 0.115 kPa or 1.82%. This would be generally considered very repeatable and well within acceptable experimental error.

Similarly for the Limestone example, these loci indicate some variability of material during testing although the flow functions are similar as are the cohesion values. Figure 4.6 shows the three individual yield loci that were measured for a consolidating load of 9kPa.

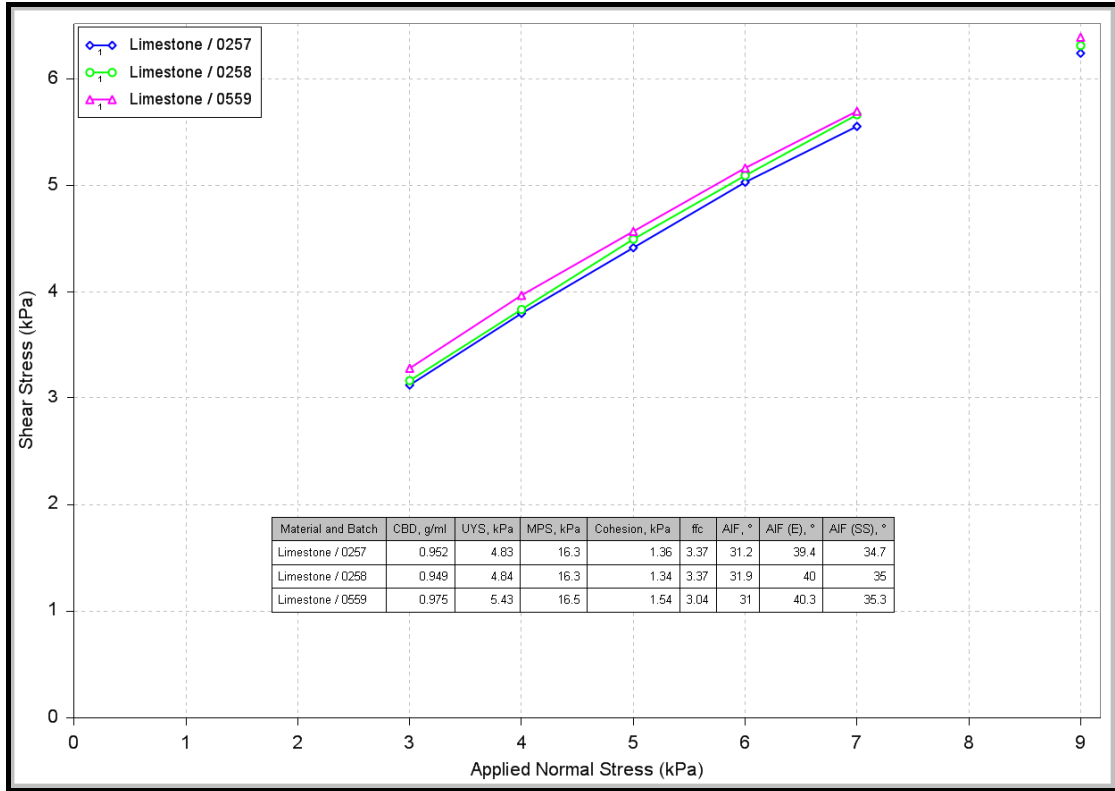


Figure 4.6: Three repeat shear tests of Limestone at 9kPa consolidating load

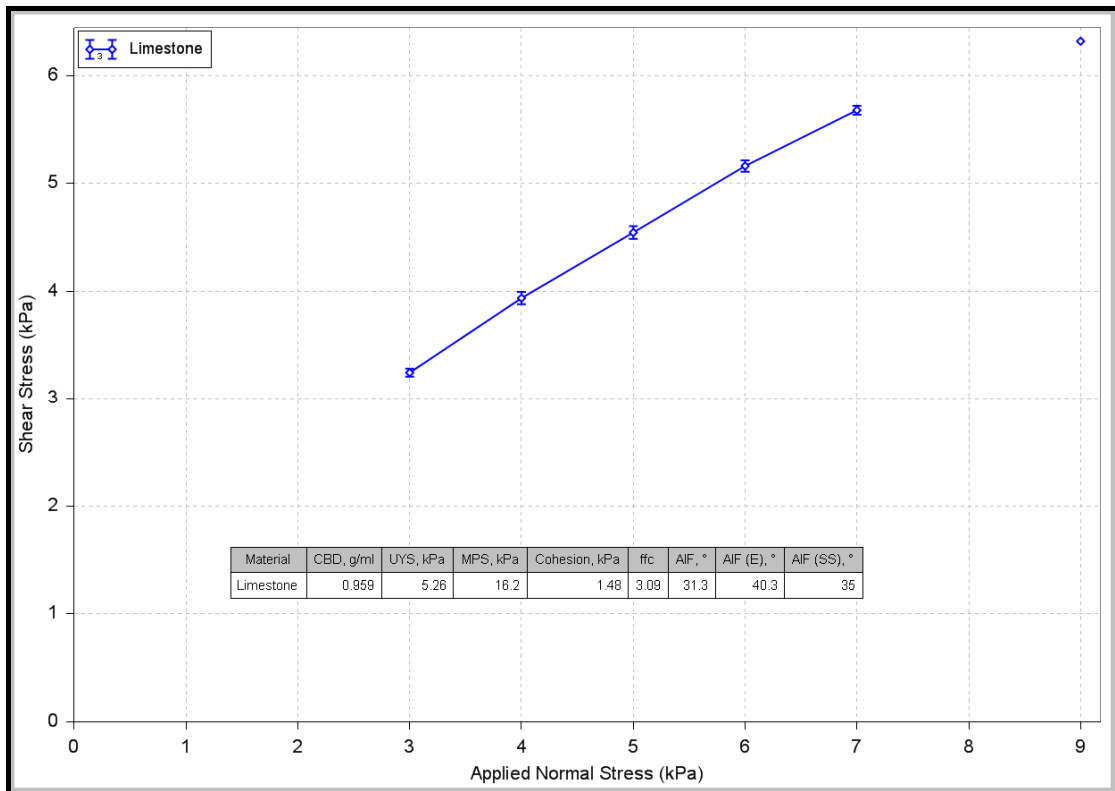


Figure 4.7: Averaged data sets from three yield loci

If the three loci are averaged – as shown in Figure 4.7 – the repeatability is even better than the gypsum example. The standard deviation at the 3kPa applied normal stress point is ± 0.0258 kPa or 0.81%; standard deviation at the 7kPa applied normal stress point is ± 0.0581 kPa or 0.971%.

If these data are then processed through the hopper design software tool, as individual loci and as an average of the three loci, the following results are produced.

Table 4.8: Sensitivity of derived hopper design parameters to variation in the yield locus for an axi-symmetric conical hopper using a stainless steel wall friction material with a 1.2micron surface roughness

Material	Batch Reference	Calculated Outlet (m)	Calculated Wall Angle ($^{\circ}$)
Gypsum	Average	0.44	12
	YL _{9,1}	0.38	12
	YL _{9,2}	0.48	12
	YL _{9,3}	0.51	12
Limestone CRM116	Average	0.54	4
	YL _{9,1}	0.47	4
	YL _{9,2}	0.57	4
	YL _{9,3}	0.59	4

Clearly the choice of yield locus has a significant effect on the size of the outlet. There is a 25% uplift in outlet between the smallest and largest dimensions for the limestone and a 13% uplift for the gypsum. What is not clear from any reference source is how to treat this data. Is this purely a function of the sensitivity of the mathematical model for the derivation of first the flow function and then the hopper

outlet, or is it the slight changes within the sample that cause a difference in the yield locus and the model/test method is suitably robust in representing these changes in the sample?

There is not sufficient time within the remit of this thesis to fully investigate the ramifications of the treatment of the data on the hopper design process, but it is clear that a sensitivity analysis is a sensible undertaking given the variation produced from what are regarded as well behaved materials. Multiple testing is easily and cost effectively attainable with modern automatic shear testers. Rapid evaluation of the results is now possible with the development of software tools which can produce bin designs within seconds of assimilating the shear data.

In terms of the actual design such variation, 120mm for the limestone and 130mm for the gypsum, may not significantly alter the choice of feeder or the specification of outlet size for fabrication, especially when experienced consultants suggest that specifying the outlet to within 50mm is acceptable⁵.

4.3.3. *The use of alternate evaluations of the Flow Function on hopper design parameters.*

The use of a linear Flow Function is common in most treatments of the hopper design. Although the EFCE guide to shear testing (EFCE 1989) does recommend the fitting of a 'smooth curve' through the data points, it does not specify any mathematical form that this smooth curve should take, making any determination of

⁵ Private communication with Prof MSA Bradley at the University of Greenwich.

the intersection with the flow factor dependent on the ability to draw such a 'smooth curve' and how the curve is extrapolated backwards towards the Y-axis. As with most data sets with only three or four x-y measurements, it is relatively easy to fit a linear trendline and obtain a reasonable least-mean-squares R^2 value. However, as will be shown this is a very safe but ultimately flawed way to interpret the data.

The value of the hopper outlet size is directly proportional to the value of the UYS ($\bar{\sigma}_1$) at the intersection, as given by Equation 4.2, the evaluation of this intersection (designating the flow/no flow boundary) is the crux of the entire design procedure.

$$B = \frac{\bar{\sigma}_1 H(\alpha)}{\rho g} \quad \text{Equation 4.2}$$

where B is the calculated hopper outlet (for a conical, axi-symmetric hopper)
 $\bar{\sigma}_1$ is the stress generated in an arch at the outlet under the action of the major consolidating pressure (kPa)
 $H(\alpha)$ is a function that takes account of variation in arch thickness, hopper half angle & hopper geometric configuration
 ρ is the bulk density of the powder at the consolidating stress imposed at the outlet
 g is the acceleration due to gravity

The extrapolation of any curve fitting is thus the most significant part of the derivation of the bin design and the most ill-defined. It is further complicated by the distance between the lowest data point in the Flow Function and the typical position of the flow factor. Figure 4.8 shows an example Flow Function for FlowLac 100 spray dried lactose, derived from data collected at 3, 6, 9 and 15kPa, together with flow factors of 1.1 and 1.9 (the typical extremes of the flow factor shown in Jenike (Jenike 1964) and Roberts(Roberts 1993)) are also plotted. As can be seen the Flow Function has

to be considerably extrapolated (~21% of the span of the data) to intersect with origin, and with either flow factor.

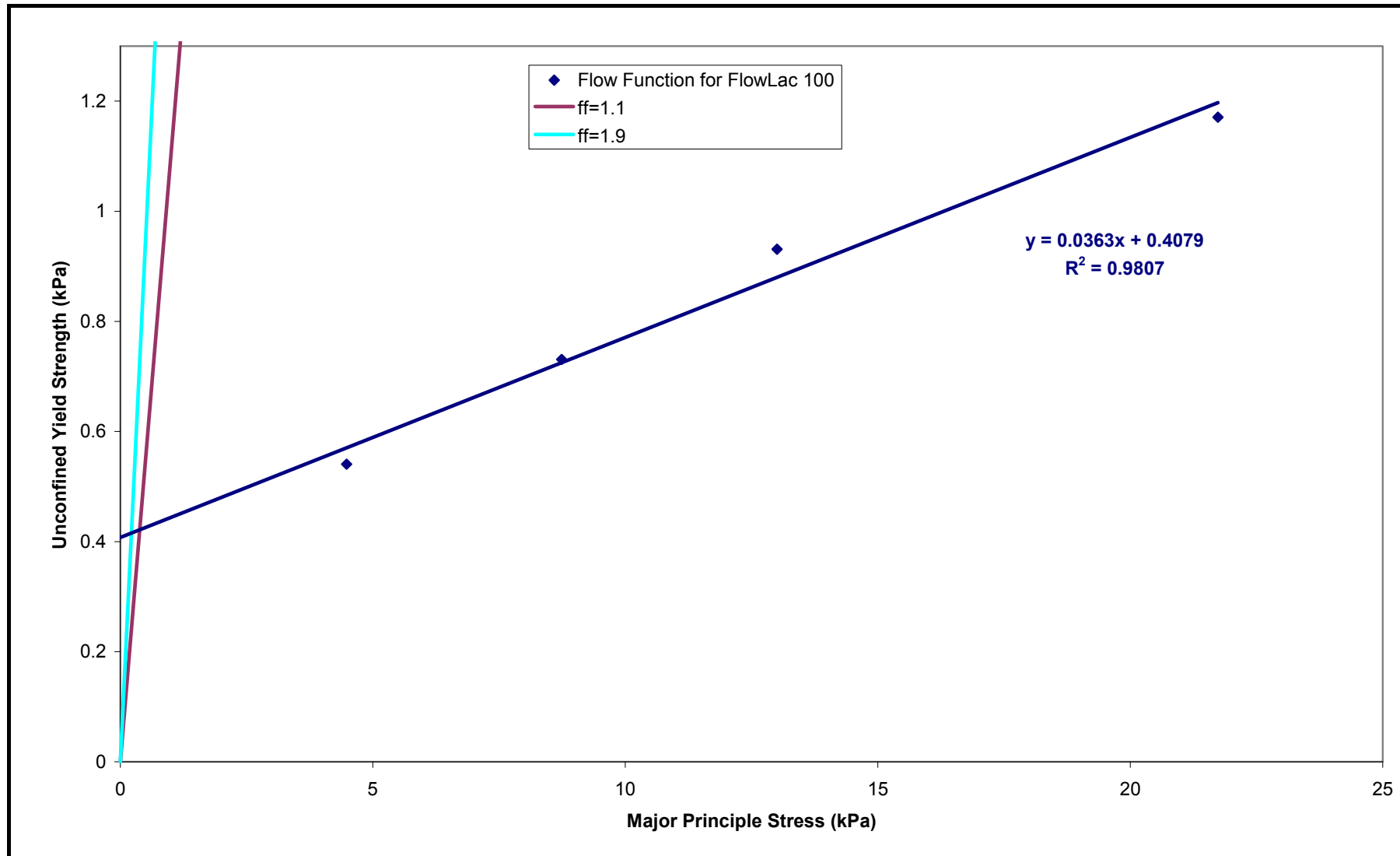


Figure 4.8: Extent of extrapolation required for linear fit Flow Function (derived from yield loci measured at 3, 6, 9 and 15kpa) to achieve intersection with maximum and minimum flow factor limits expressed in Roberts (Roberts 1993).

The main reason for this has been postulated in Chapter 2 and is thought to be related to the complexity and time penalties involved with shear testing. This meant that the derivation of a Flow Function was a very time intensive process. This time factor, coupled with the limitations of the shear cell in generating data at low consolidating stresses meant that the majority of Flow Functions were generated from three or four single (non-repeated) shear tests from the range 3-15kPa. Indeed, this is the format recommended in the EFCE Guide to shear testing with the consolidating stresses moderated to take account of the powder bulk density. Fitzpatrick *et al* commented in 2004 on the time/cost of undertaking this level of work with a Jenike type translational shear cell (Fitzpatrick, Barringer, & Iqbal 2004). Schulze recommends testing at lower stresses (Schulze 2007), as does Berry (Berry *et al.* 2007; Berry & Bradley 2003), but to date no reworked European standard is available.

Thus in order to improve the confidence of the Flow Function, two areas need to be addressed; testing at low consolidating loads to minimise the uncertainty introduced by the extrapolation of the curve; and a more realistic way of expressing the Flow Function curve.

Very little work appears to have been undertaken at low stress conditions with shear cells (Schulze & Wittmaier 2003), which is believed to be primarily due to the mechanical restrictions imposed during loading for most 'dead weight' testers. It has been previously noted that the RST-XS shear tester struggled to control low normal stresses below about 1kPa. The larger shear cell manufactured by Schulze (Model

RST) may have better force control than the unit available during this work, but for pharmaceutical applications such a large unit is not, ultimately, practicable.

This is arguably where the FT4 shear cell assembly can provide enhanced testing. Several low stress tests have been undertaken using improved force and torque measurement/control, which has allowed testing at much lower consolidating loads than was previously possible – typically down to 500Pa – greatly improving the accurate development of the Flow Function closer to its intersection point with the flow factor.

The use of a non-linear fit to σ_c/σ_1 data was postulated by Singhal & Hogg (Singhal & Hogg 1986). They indicated that the FF should pass through the origin as a physical necessity – when there is no major principal stress there can be no unconfined yield strength. A power law fit, as described by Equation 4.3, was postulated and this seemed to fit the data that was available – given the previously mentioned limitation of the Jenike shear cell that was employed.

$$\sigma_c = m\sigma_1^n \quad \text{Equation 4.3}$$

This approach was used to evaluate FT4 shear cell data and was combined with additional shear testing at consolidating stresses of 1.5, 0.75 and 0.5kPa such that there were 7 data sets used to describe the Flow Function curve.

Figures 4.9 and 4.10 show the Flow Functions generated from testing a cohesive powder (Limestone) and a non-cohesive powder (spray dried lactose – FlowLac 100)

using this approach coupled with both the best linear fit (in blue) and the power law fit (in pink).

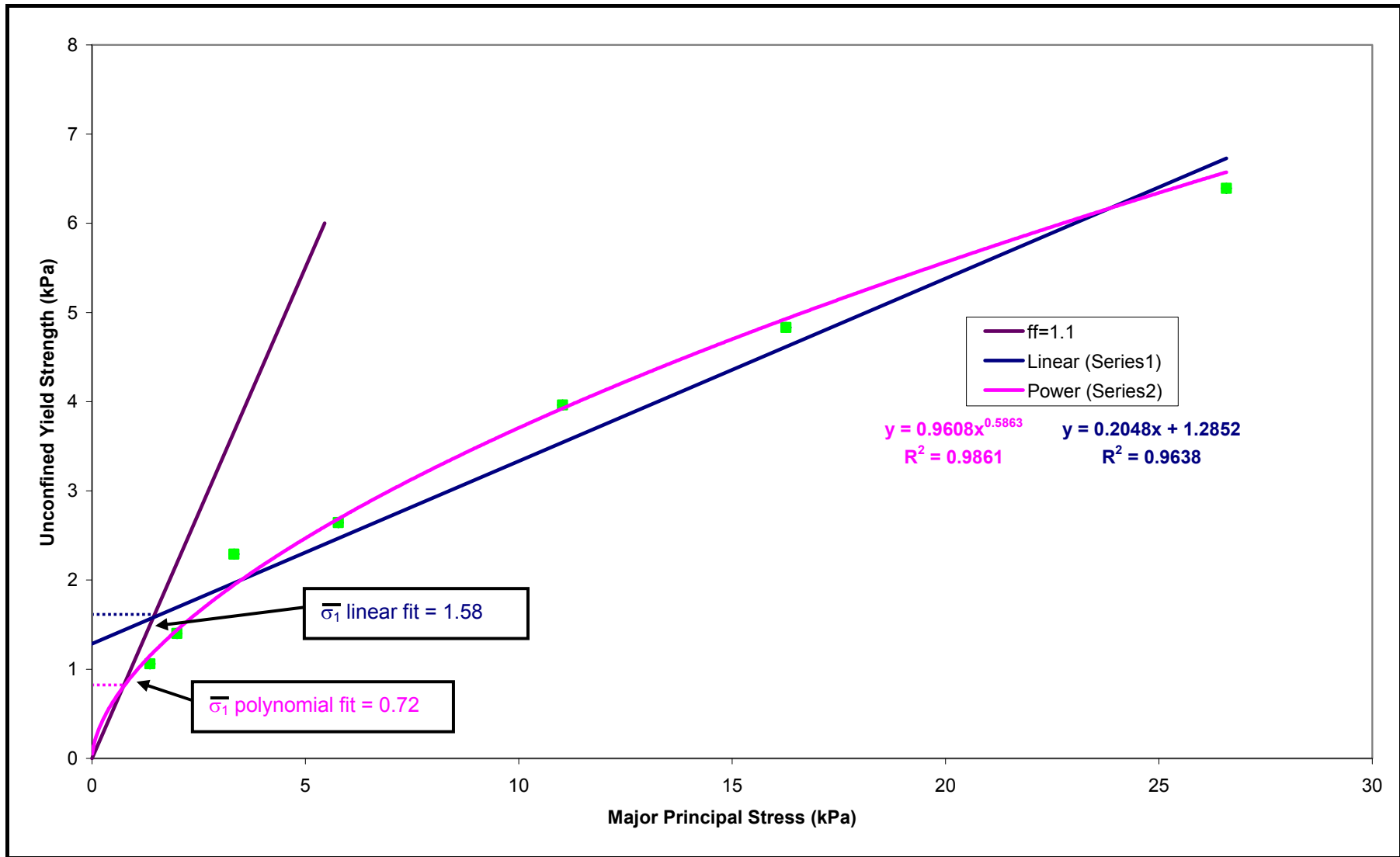


Figure 4.9: Flow Function for Limestone CRM116 derived from yield loci generated at consolidating loads of 0.5kPa to 15kPa

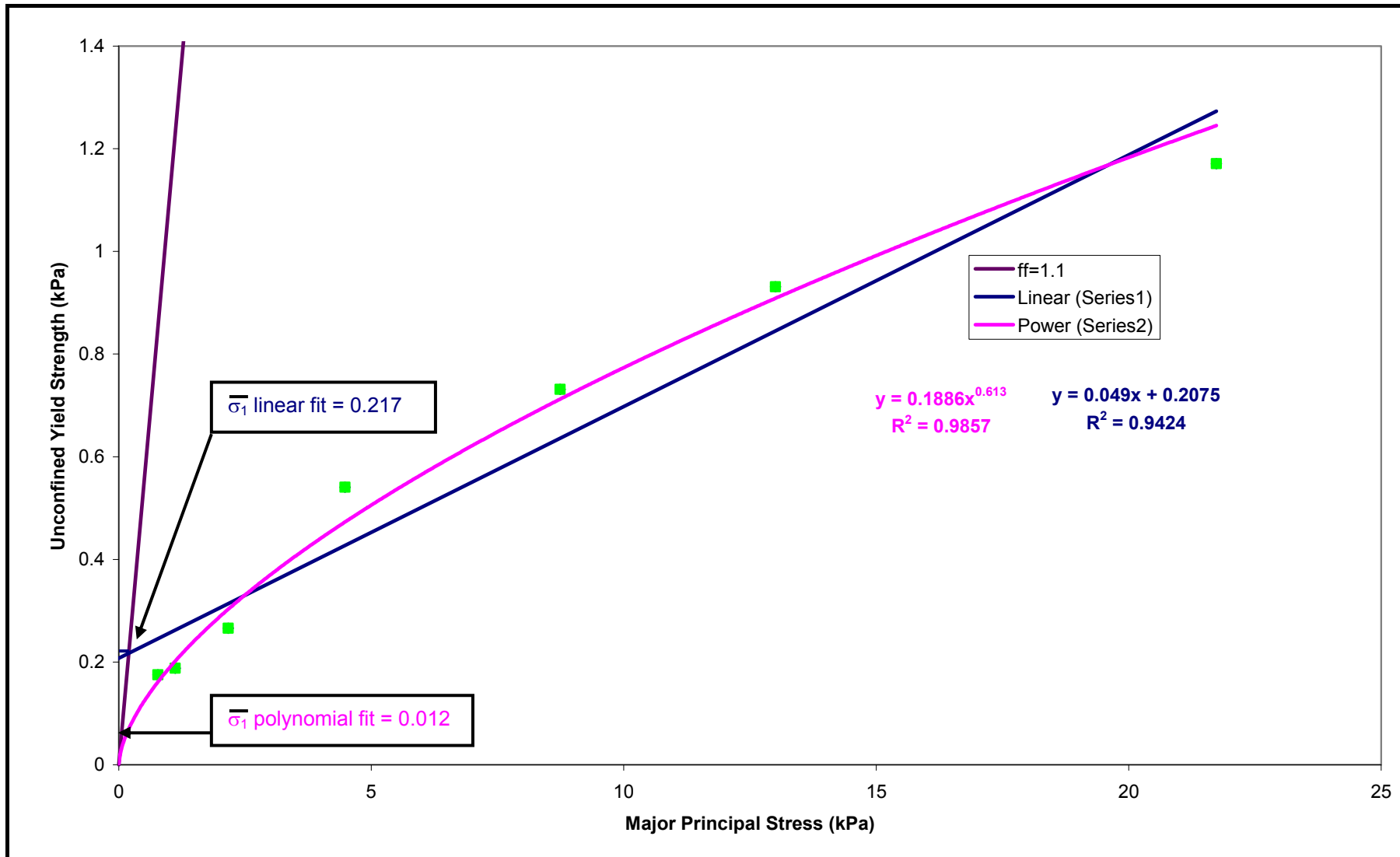


Figure 4.10: Flow Function for FlowLac 100 derived from yield loci generated at consolidating loads of 0.5kPa to 15kPa

It can be seen that the use of a non-linear power law fit provides a more compelling argument as a model for the data for both cohesive and free flowing samples.

It should also be noted that a wide range of consolidating stresses is required to enable the fully developed Flow Function to be visualised. If only a few data points are taken, it is quite possible that a linear fit once again becomes a viable option – whether those points are from the lower end of the FF curve, the top end, or a limited selection of any of the points. Given the linearity of the data generated at lower consolidating loads, it could be argued that a linear fit to these data points alone would be sufficient to fully inform a valid flow function. However, testing at lower stresses can still suffer from issues relating to normal force control, as described in Chapter 2, and at this stage moving to solely testing at low stresses as an option cannot be fully recommended without further study on a wider range of powders.

Once the value of $\overline{\sigma}_1$ has been determined using the hopper design software tool, the hopper outlet size for mass flow can be recalculated (using the same flow factors that were used in the original calculations). These results are presented in Table 4.9.

Table 4.9: Comparison of derived outlet sizes from two Flow Function models

	Outlet size (m) [with 20% safety uplift]	
	3 data points; linear FF	7 data points; power law FF
Limestone CRM116	0.54	0.23
FlowLac 100	0.16	0.0024

As can be seen the difference is dramatic and would provide a significant change in the overall capital cost for building storage vessels for either of these materials. The effect of the change in intersection gives an outlet size for the Limestone which is 42% of the linear derived value and 15% of the linear derived value for the FlowLac 100. The result for the FlowLac 100 is, arguably, another example of the limitations of relying on protocols derived for the Jenike shear tester when applied to more granular materials.

A more complete study by Drescher *et al* (Drescher, Waters, & Rhoades 1995a; Drescher, Waters, & Rhoades 1995b) also suggested that a power law fit was applicable which they based on a variant of the Warren Springs equation.

$$\left(\frac{f_c + E}{E}\right)^q = \frac{\sigma_1}{F} + 1 \quad \text{Equation 4.4}$$

Drescher *et al* also combined their analysis with practical experiments and the conclusion was that the predicted outlet sizes were between 2.4 and 4.1 times bigger than the experimentally derived values, which he attributes to inaccuracies in the powder testing procedure (with the caveat that his

experimental results were for the first opening of the outlet only) and limits on low stress testing with Jenike type shear testers.

However, Drescher *et al* discount the effect of the form of the Flow Function (linear or power law evaluation) on the calculation of the outlet size in their second 1995 paper (Drescher, Waters, & Rhoades 1995b). This is at odds with the diagrams presented in their first 1995 paper (Drescher, Waters, & Rhoades 1995a) which clearly show that the power law form would give a significantly lower value for $\overline{\sigma}_1$ when the flow factor that was used in his calculation is applied. As shown in Equation 4.2, $\overline{\sigma}_1$ is directly proportional to B, the outlet diameter, and the reductions that would be attainable appear to match his experimental data. No additional information in either of the papers appears to support this postulate that the form of the Flow Function does not affect the outlet, and the data appears to support the analysis presented earlier in this thesis that the power law form gives significantly lower outlet diameters.

Drescher *et al* do point out that these analyses only refer to the first discharge after filling for any silo system, as the stress regime does change dramatically upon initiation of flow as is shown in Figure 4.11.

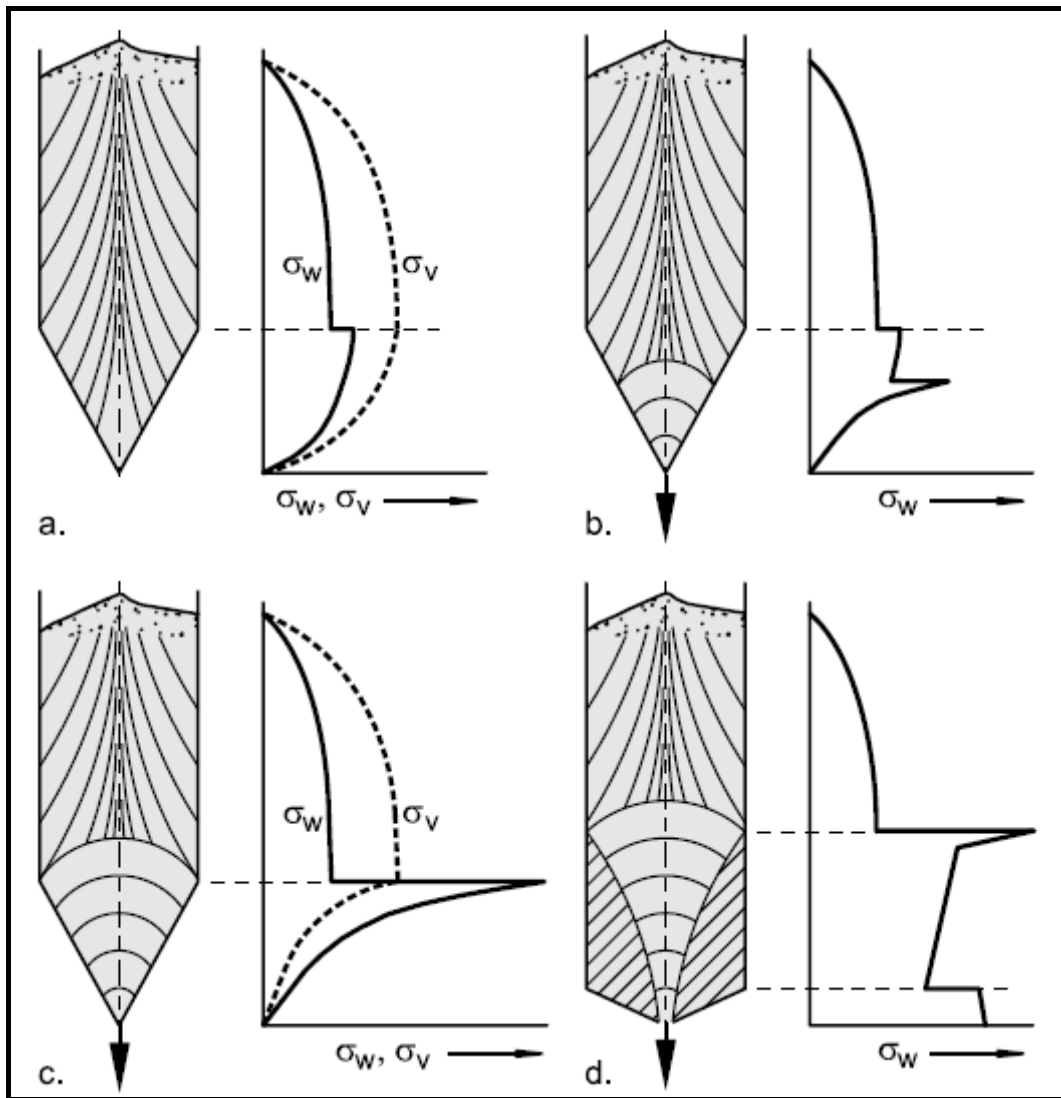


Figure 4.11: Assumed trajectories of the major principal stress respectively for filling state of stress (a), for initiation of discharge state stress for the mass flow regime (b), the fully developed discharge stress state for the mass flow regime (c) and for discharging state of stress for the core flow regime (d) (where the 'dead zone' is also shown) (Schulze 2007)

Normally this would present an issue and the results of the study generally discarded as the mass flow models presented here relate to the assumed radial stress field that is produced when powder begins to move within the silo (Jenike 1964; Roberts 1993; Schulze 2007). Whether Drescher *et al* have actually achieved this radial stress field in their hopper tests is unknown.

Berry (Berry, Birks, & Bradley 2003) have shown that the arches generated in plane flow hoppers may be far from the idealised notion presented in the texts and Figure 4.11 and suggests that significant caution be exercised with this in mind. Berry concludes that the reasons such variability has not been frequently observed is that

‘.....using the Jenike method of design over a few decades is the considerable over-design that occurs partly in the design, but mainly in the measurement and the analysis of results’.

These results need to be confirmed with an additional study similar to that carried out by Drescher *et al* and there is a need to investigate the effect of multiple draws on the hopper contents and how this affects the stress regime and the maintenance of mass flow. Such an investigation is beyond the scope of this thesis and could be the main subject of another entire doctoral study. It should therefore be concluded that although the generation of modified flow function curves appears to provide an alternative to the current linear fits to the data and smaller bin outlet diameters, the stress conditions in the bin in question needs to be carefully considered.

4.3.4. Summary

The analyses carried out on the bin design protocols that are commonly cited within the literature have presented a number challenges on the collection, processing interpretation of the data. These can be summarised as follow:

- The use of automatic shear testers and automated calculation routines dramatically reduces the time required to generate bin designs. It also allows sensitivity analyses to be undertaken at reasonable cost.
- Improvements to the precision of the FF/ff intersection can be made by evaluating the test sample over a much lower range of consolidating stresses.
- The use of a power law fit for the FF provides a more physically correct interpretation (compared to the usual linear fit) and a more compelling model due the improved goodness of fit to the data when low consolidating stresses are employed for testing.
- Linear fit to the yield locus produces lower FF values which in turn results in increased bin outlet sizes
- The variability of generated yield loci when multiple repeat tests are undertaken produces a spread of bin design results. The evaluation of the most appropriate model for the generation of a yield locus from multiple data sets needs to be studied in greater depth
- However, caution must be exercised when applying these conclusions to actual bin designs as the stress state model has been shown to have limitations in its assumptions regarding the radial stress fields upon which the Jenike failure analysis is based.

4.4. Perceptual mapping

The need for multiple measurements in order to properly characterise a powder has been described in Chapter 2. However, it is difficult for the engineer to perceive the relative influence and interaction of a large number of variables for a large number of materials. Figures 2.55 and 2.60 in Chapter 2 show how difficult it is to display multivariate data in standard 2-dimensional graphical forms, and more pertinently, how to perceive interrelationships.

The following quotation from Fisher (Fisher 1990) succinctly explains the usefulness of generating useable diagrams when evaluating (complex) data sets.

“The preliminary examination of most data is facilitated by the use of diagrams. Diagrams prove nothing, but bring outstanding features readily to the eye; they are therefore no substitute for such critical tests as may be applied to the data, but are valuable in suggesting such tests and in explaining conclusions founded upon them.”

Engineers are, perhaps, too keen to develop first principals' models based on a limited set of powders without recourse to the wider picture. This then results in a fragmented representation of powder behaviour where multiple worthy models exist for very narrow categories of materials based on limited ranges of physical properties or specific to industrial groupings (pharma, Fast Moving Consumer Goods, fine chemical, minerals etc).

Such difficulties in evaluating multivariate data sets are common in a number of fields, and several techniques have been developed to best represent the data.

Perceptual mapping has been undertaken in the marketing environment for over 30 years (Hauser & Koppleman 1979) and is commonly used to compare non-numerical data sets, as shown below in the examples presented in Figure 4.12.

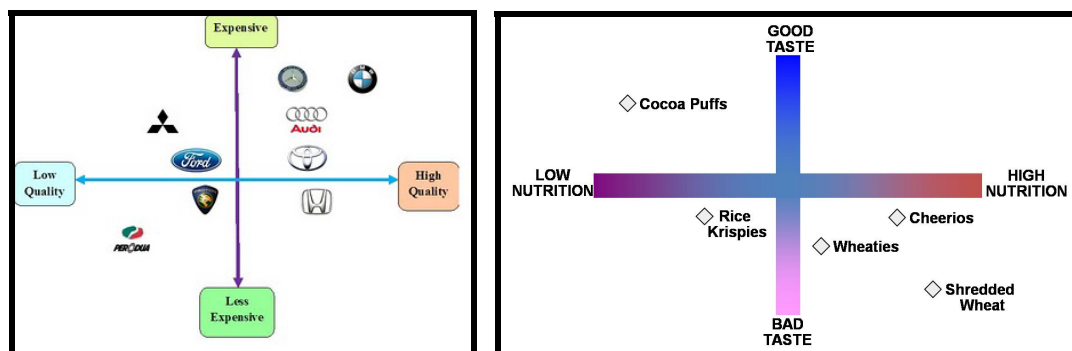


Figure 4.12: Perceptual Maps for Automotive Brands and Breakfast Cereals

However, the benefits of such a perceptual map for numerical systems are obvious, as it allows direct comparison of multiple variables for a number of discrete entities. They can, of course, be developed into three dimensional maps, but these are difficult to draw and hard to interpret.

The use of multivariate mapping in presenting the relative properties of powders is sparse. This may be for two reasons – firstly, as mentioned in Chapter 2, the number of reliable and meaningful tests available to describe powder and/or particle properties has been historically small in number and therefore mapping the limited

number of powder properties, though relatively easy, would not necessarily provide meaningful results; secondly the existence of the hugely successful Geldart fluidisation map has, perhaps, dampened the enthusiasm of researchers to develop perceptual diagrams, in any form, for other systems which were less successful than Geldart's diagram.

Geldart diagram shows the classification powders according to their fluidisation behaviour (Figure 4.13).

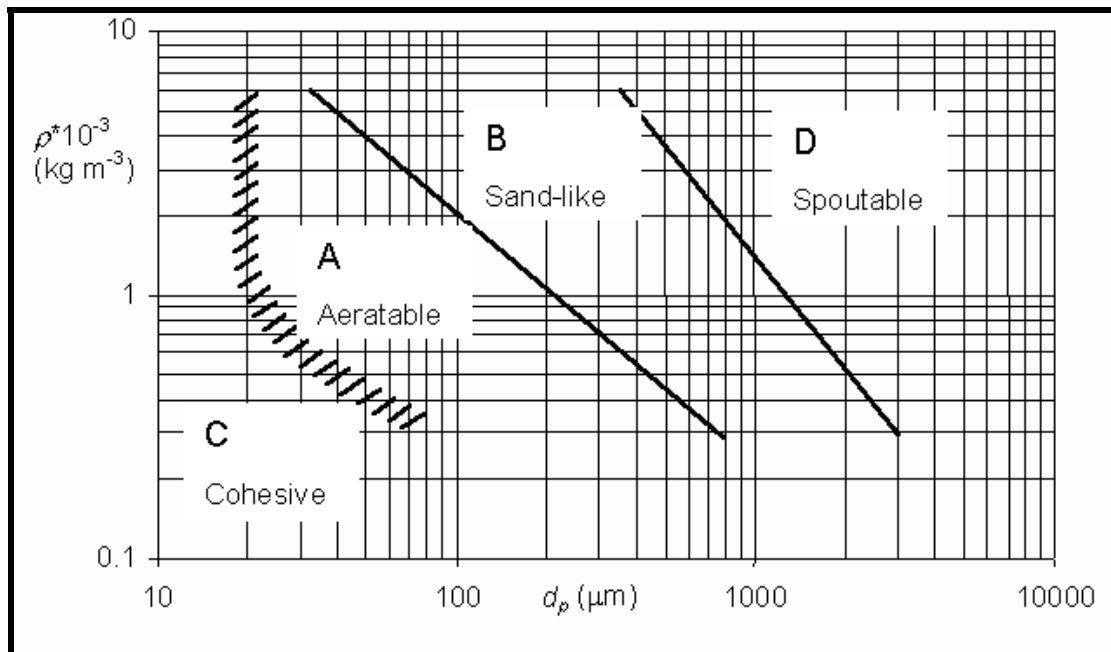


Figure 4.13: Geldart's representation of the relationship between the particle size and density with respect to its likely fluidisation behaviour

This approach was first presented by Geldart in his seminal 1973 paper (Geldart 1973), and has been used extensively ever since (Goossens 2006; Molerus 1982; Shan *et al.* 2003; Wang, Rahman, & Rhodes 2007). Its advantage is that it concisely correlates the particle properties to process behaviour in an easily

interpreted visual map. This remains the 'gold standard' in powder technology for the visualisation and interpretation of data.

Its success is, however, attributable to the chosen process. Fluidisation requires the separation of each particle from its neighbours, thus the influence of inter-particulate interactions is significantly reduced, greatly simplifying the behaviour of the assembly of particles into the balance between long range forces, represented by the particle density, and short range forces, represented by the mean particle size. When one considers more densely packed systems, the interactions are much more complex and a method of mapping such systems (such as a mixing process, for example) has not been derived.

Following on from Geldart's work, many empirical and numerical models relating to fluidisation have been developed and it is certain that all the researchers involved were aware of this perceptual map and would acknowledge its influence.

More recently Lee *et al* (Lee *et al.* 2000) used a perceptual map technique, based on principal component analysis, to visualise the relative differences between different flow property measurement systems – flow-through-orifice; Carr's Compressibility Index; mean time to avalanche (MTA) (Aeroflow device⁶); and a flow pattern moderated mean time to avalanche.

⁶ The Aeroflow device looks at how powders in a rotating drum will avalanche and generates data for the time between avalanches by imaging the shadow cast by the motion of the powder in an enclosed Perspex drum (Kaye 1997). The device is no longer on sale and was thus not considered for this project.

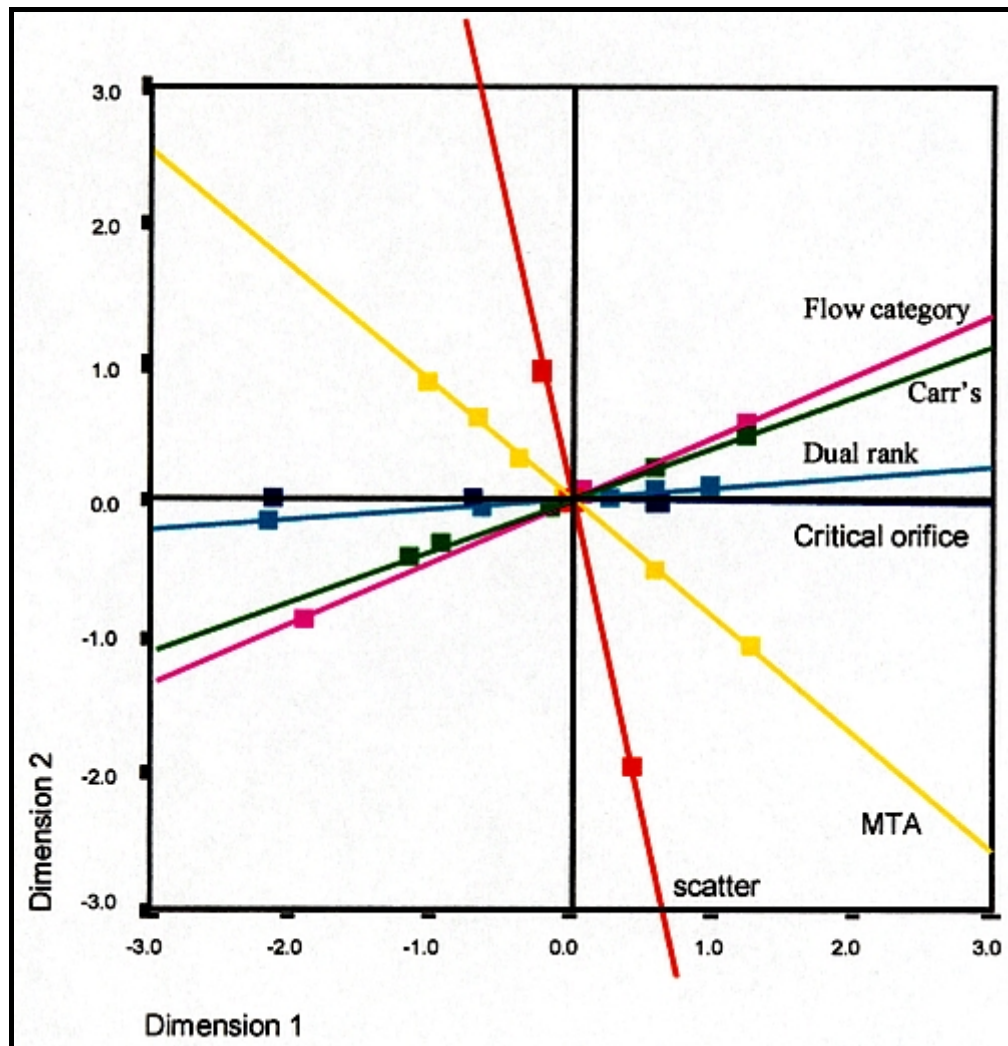


Figure 4.14: Similarities and differences between different methods of powder flow measurement – from Lee et al

Two main nonlinear principal components (Dimensions 1 and 2 in Figure 4.14), the details of which were not presented in the paper, are used to represent the information contained in the data. The information can be condensed to a single point in the coordinate system for each property measured and each powder. It is then possible to construct correlation lines linking the points for each powder, with each line representing a single measured property.

The main problem with this approach is that the diagram is difficult to interpret and largely uninformative. It successfully shows that there ways of presenting complex relationships, but this presentation method is not intuitive and requires a significant level of further deconstruction to show the relative behaviour of materials.

Work done by McGlinchy and McGee (McGee & McGlinchy 2005; McGlinchy 2005) has shown how a spider diagram can be used to generate the relative 'footprint' of a powders behaviour using six normalised characteristics.

“The diagram is built from a series of three concentric circles each divided by an axis for each of the characteristics – wall friction (f_w), shear strength (τ_s), bulk density (ρ_b), hopper mass flow wall angle (β_c), outlet size (strength/bulk density ratio, D_{crit}) and Hausner ratio (H.R.).” (McGee 2009)

The test data for the powder are plotted on the relevant axis which is scaled according to previously derived maxima and minima defined in Table 4.10. These maxima and minima are based on the collected experience of the author and historic data available to him. It is not clear from the published articles whether the axes are scaled between the maxima and minima or whether each measurement is placed given a single value (Easy; Average; Poor) based on how it relates to the ranges shown in Table 4.10. If the latter is the case, then powders with subtle differences in their properties would not be differentiated using this visualisation method.

Table 4.10: Parameters suggested by the tests reported in McGee 2005.

Circle	Bulk Density (kg/m ³) ρ_b	Outlet size (cm) D_{crit}	Shear strength (N/m ²) τ_s	Mass flow Wall angle (deg) β_c	Wall friction (deg) Φ_w	Hausner ratio $H.R.$
Easy flow	1200	15	300	65	< 20	1.1
Average	800	50	1000	73	25	1.25
Poor flow	400	100	2000	80	> 30	1.5

Figure 4.15 shows how idealised easy flowing and poor flowing materials are represented.

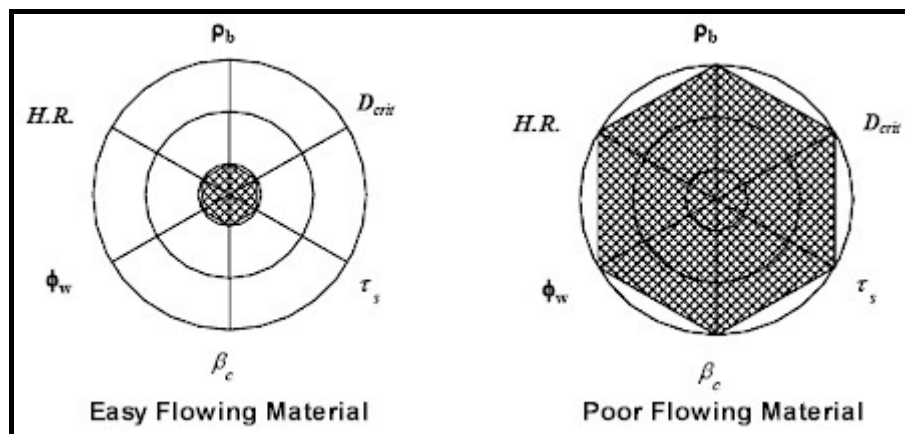


Figure 4.15: McGee's Spider Diagram showing idealised easy flowing (left hand side) and poor flowing (right hand side) materials

Figure 4.16 shows a series of example materials

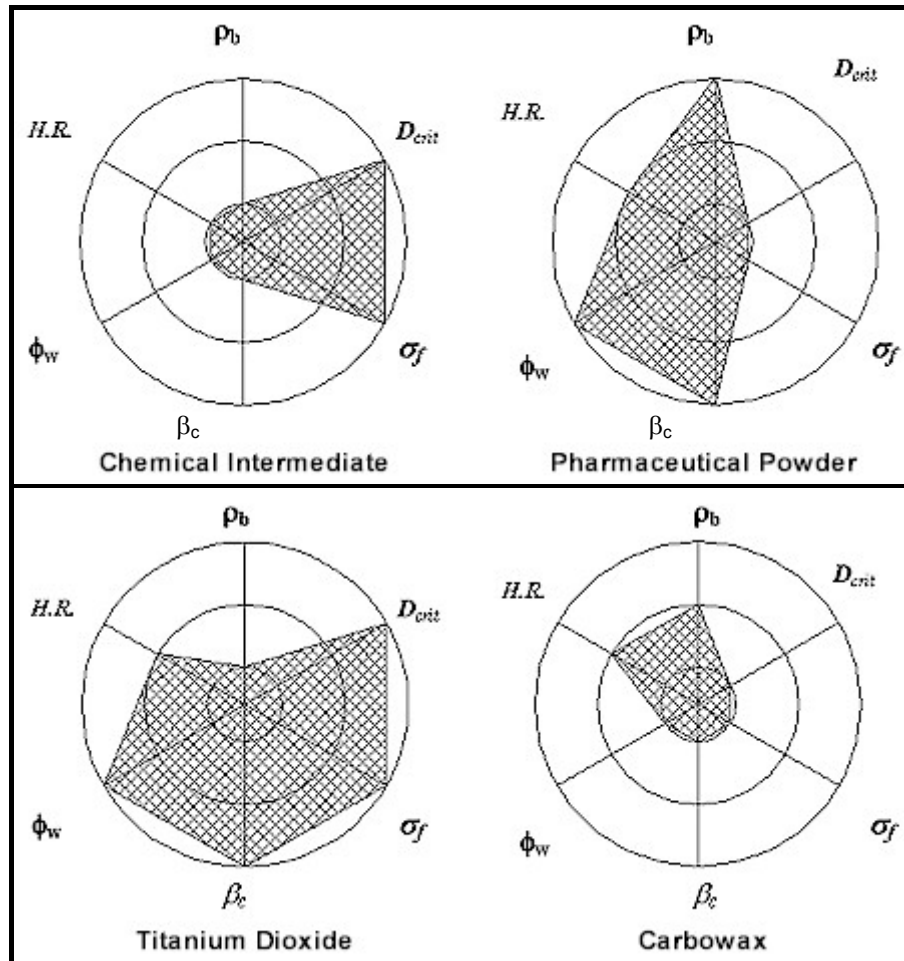


Figure 4.16: Examples of McGee's Spider diagram for four sample materials

What these diagrams do show is that each powder has a characteristic that, if taken on its own, would allow the sample to be described as 'good' or easy flowing – bulk density for the Chemical Intermediate and the Titanium Dioxide; D_{crit} and σ_f for the Pharmaceutical Powder and the Carbowax. Equally each powder has a characteristic that, if taken on its own, would allow the sample to be described as 'bad' or poor flowing (intermediate in the case of the Carbowax). This therefore reinforces the concept, described in Chapter 2, that no single parameter can be used to describe a powder as having good or bad flow properties.

There are, however, a number of further downsides to this method of presentation. Firstly, McGee's representation is not believed to be currently available in a commercial computerised form. This severely limits the precision of the (hand drawn) diagrams. Additionally, given the data are banded to easy/average/poor values, it is likely that many powders would provide identically bad or good representations of particular properties – for example the Φ_w and β_c values for the Titanium Dioxide and the Pharmaceutical Powder have the same maximum value on their respective diagrams in Figure 4.16, but it is unlikely that, in reality, they have the same value. The question thus becomes does this mode of presentation assist the engineer to better understand the behaviour of the powders being compared – in this instance it does not.

Microsoft Excel does provide a similar graphing option (Figure 4.17) where four samples are displayed on a diagram with four powder characteristic measurements, and is identified as a 'Radar' plot. This is not exactly the same graphing method as that presented by McGee as it can graph more or fewer axes than the six presented in Figures 4.15 and 4.16 and Table 4.10, thus giving the user the opportunity to use characteristics other than those suggested by McGee. The values plotted are the data inputted into the spreadsheet, but normalisation against standard values is, of course, an option. The precision of the graphing process is improved, as is the quality of the graph display.

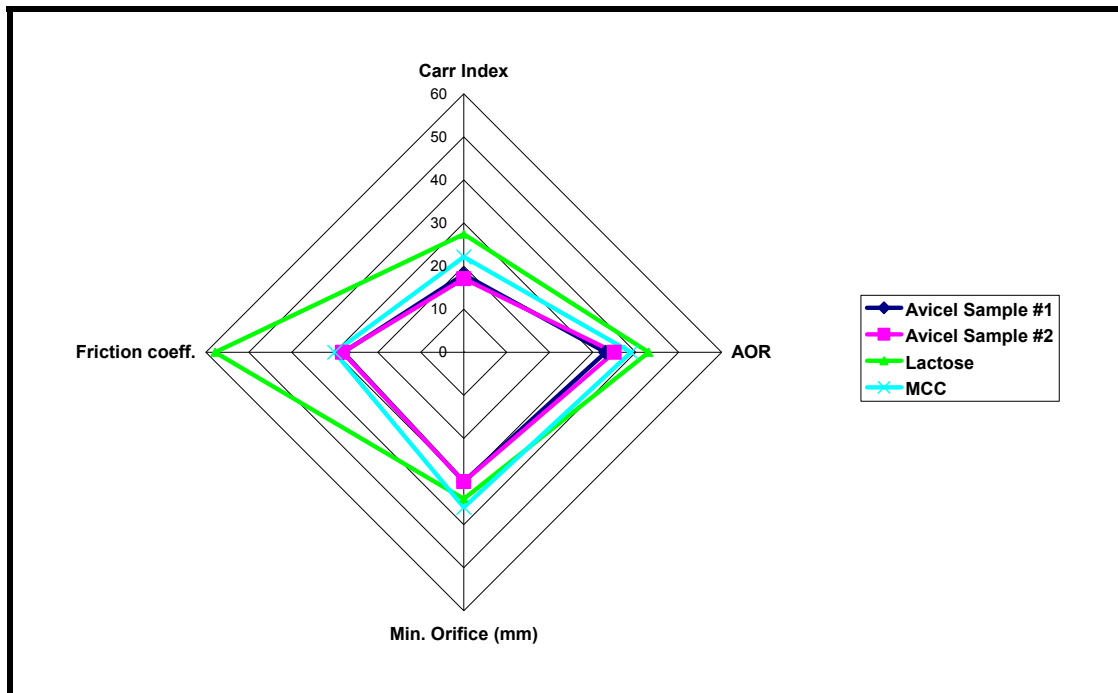


Figure 4.17: A spider diagram created in Microsoft Excel for four materials

As can be seen from Figure 4.17, evaluation of the materials is quite easy and the differences and similarities are obvious.

However, this display method too has limitations (Figure 4.18). It is not easy to compare more than, say, three or four different materials on the same diagram as it makes it much harder to see the differences and similarities. The data sets also have to be normalised when comparing properties which have disparate numerical values. This is the same issue as noted in Figures 2.55 and 2.60.

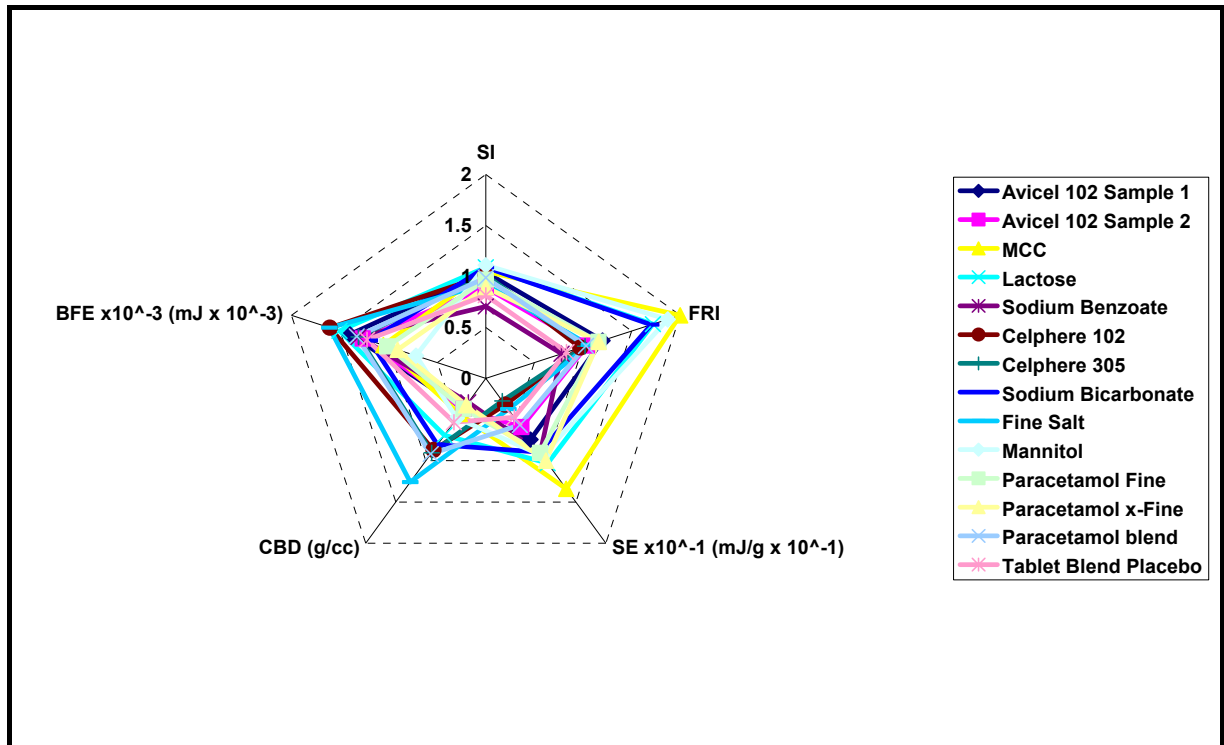


Figure 4.18: Spider diagram representing the powder rheometry data for the exemplar powder set

Additionally the plot cannot show the confidence limits in each measurement, which would assist with understanding the variability of the powder sample.

Summarising the current state of perceptual mapping within powder technology

- The Geldart diagram is effective, but only relates to a (relatively) simple process case.
- Lee *et al* have shown that more complex relationships can be visualised, but the interpretation of the resulting diagram is not straightforward.
- The McGee spider diagram is useful but needs some refinement to enable its practical application. It should also not be limited to the six variables chosen by McGee but be more flexible to allow for wider application to powder processing unit operations.

Finding an effective representation of a multivariate data set is a hard problem to solve. As the number of measurable characteristics increases, so does the complexity of finding an effective visual representation that promotes insight into the underlying meaning of the relative performance of multiple powders.

Clearly this difficulty relates to the number of dimensions that can be represented – three spatial dimensions (more ideally two dimensions for ease of visualisation) are available, the remaining variables of the data space have to be mapped to other dependent variables of the visual space such as shape, colour, orientation, texture, etc.

There are a number of visualisation methods that are routinely employed in fields such as medical and biological statistical analysis and social sciences.

Perhaps the most accessible open source data visualisation system is provided by the Laboratory of Artificial Intelligence in the Faculty of Computer and Information Science at the University of Ljubljana, Slovenia (<http://www.ailab.si/orange/>). Their free to use 'Orange' software is a component based machine learning library that uses visual programming and Python scripting/programming language to undertake data mining. Other systems exist, but they are considerably less accessible than the visualisation techniques available within Orange.

The method that shows most potential is Radviz (Fisher 1990; Hoffman *et al.* 1997; Hoffman 1999), a nonlinear visualization method developed from Hoffmans doctoral work, which presents visualized features as anchor points equally spaced around the perimeter of a circle. Data points are shown as points inside the circle, each point is held in place with 'virtual springs' that are attached at the other end to the feature anchor points. The stiffness of each spring is proportional to the value of the corresponding feature and the point ends up at the position where the spring forces are in equilibrium. Prior to visualization, feature values are scaled to lie between 0 and 1. Data instances that are close to a set of feature anchors have higher values for these features than for the others.

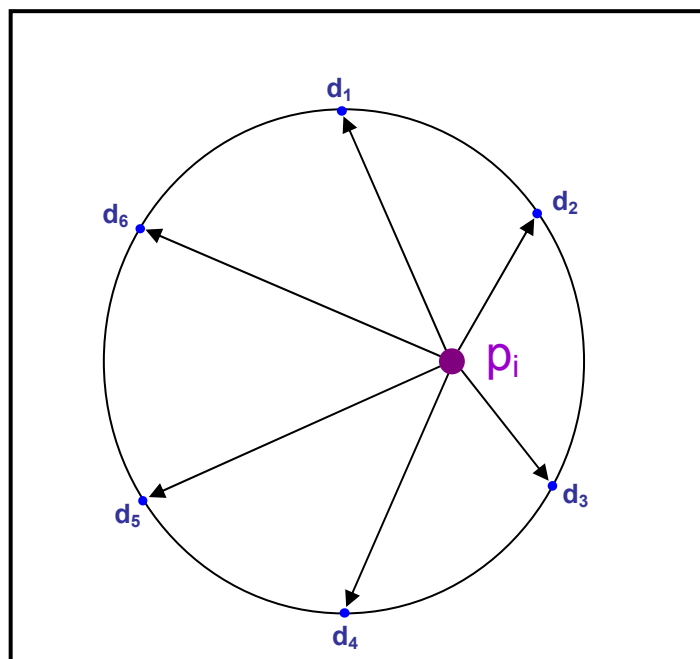


Figure 4.19: The representation of the features of a single substrate as a function of 6 characteristics d_1 to d_6

Albuquerque *et al* (Albuquerque *et al.* 2010) have presented the calculation of each point p_i such that it is connected by n springs to the n respective dimensions of the dataset (in this example d_1 to d_6) and the spring constant K_i is equal to the j -th coordinate of x_i , namely $x_{i,j}$. The final position of p_i in the visualization is determined by the point where the sum of all spring forces is zero and can be computed as:

$$p_i = \frac{\sum_{j=1}^n d_j x_{i,j}}{\sum_{j=1}^n x_{i,j}} \quad \text{Equation 4.5}$$

Polyviz is a variation of the Radviz visualization technique. However, instead of single fixed attribute anchors, data points are now attracted to anchors with value-dependent positions. The side of the polygon is scaled to represent the maxima and minima of the data set under evaluation. Figure 4.20 shows an example of a PolyViz display of all of the shear cell and powder rheometry results for the exemplar powders. The lines show how each point – representing a single powder – are linked to the relevant axis. These lines can be switched out for clarity if necessary. The position of each point relates to balance of each powders test performance relative to the maxima/minima of the entire class for all the given measurements. The test notation is the same as that presented in Table 2.8, 2.16 and 2.17.

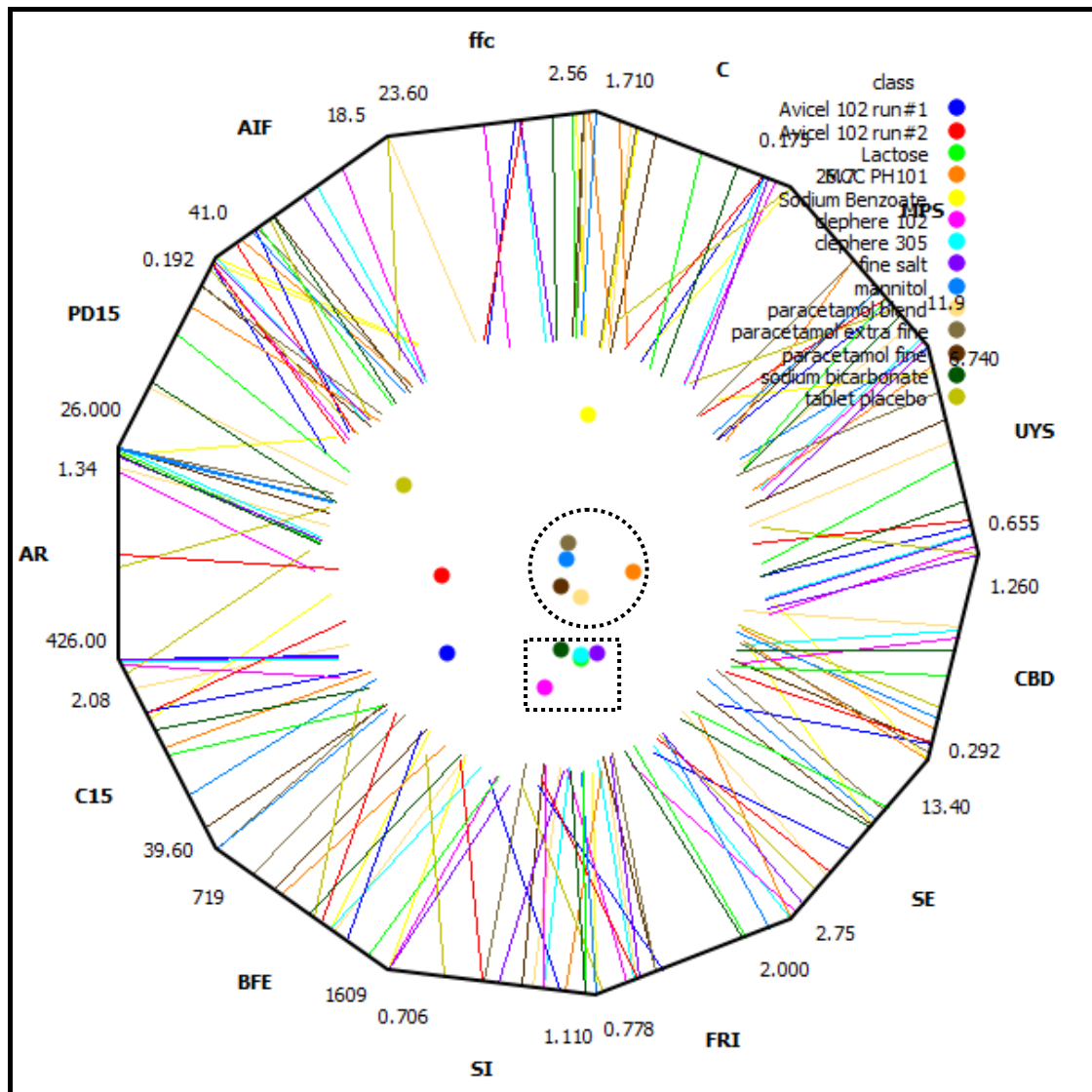


Figure 4.20: PolyViz representation of all the powder rheometry and shear cell results for all the exemplar powders

As can be seen, the presentational aspects of Orange are somewhat below the best commercial graphing software, but it does plot the data accurately even if the key which identifies the data overlaps the plot for large data sets such as those investigated here.

What can be noted from Figure 4.20 are various relative groupings of the powders and where certain powders stand out. The conventionally cohesive powders are

located in the centre of the plot (indicated by the dotted circle). The conventionally free flowing materials are lower on the plot as indicated by the dotted rectangle. Interestingly, the most free flowing material, the tablet placebo, is located on its own at the top right of the graph, and the platy sodium benzoate is located on its own at the top just right of centre. These positions relate to how one or two properties can make these particular samples stand out from the crowd and this is what these types of representations of multivariate data are good at doing. The two Avicel 102 powders (which were materials used in a specific equipment qualification trial described in the next section) are shown to be quite distant in their location on the PolyViz map.

Not all the information that is in the main data set needs to be represented and it is possible to display partial sets such as the powder rheometry set in Figure 4.21. Here there seems to be a clear delineation between those samples which would be classified as cohesive (dotted circle) and those which would be classified as freer flowing (dotted square). The mannitol stands out the main cluster of cohesive materials and it could be argued that this is the most difficult sample tested using powder rheometry.

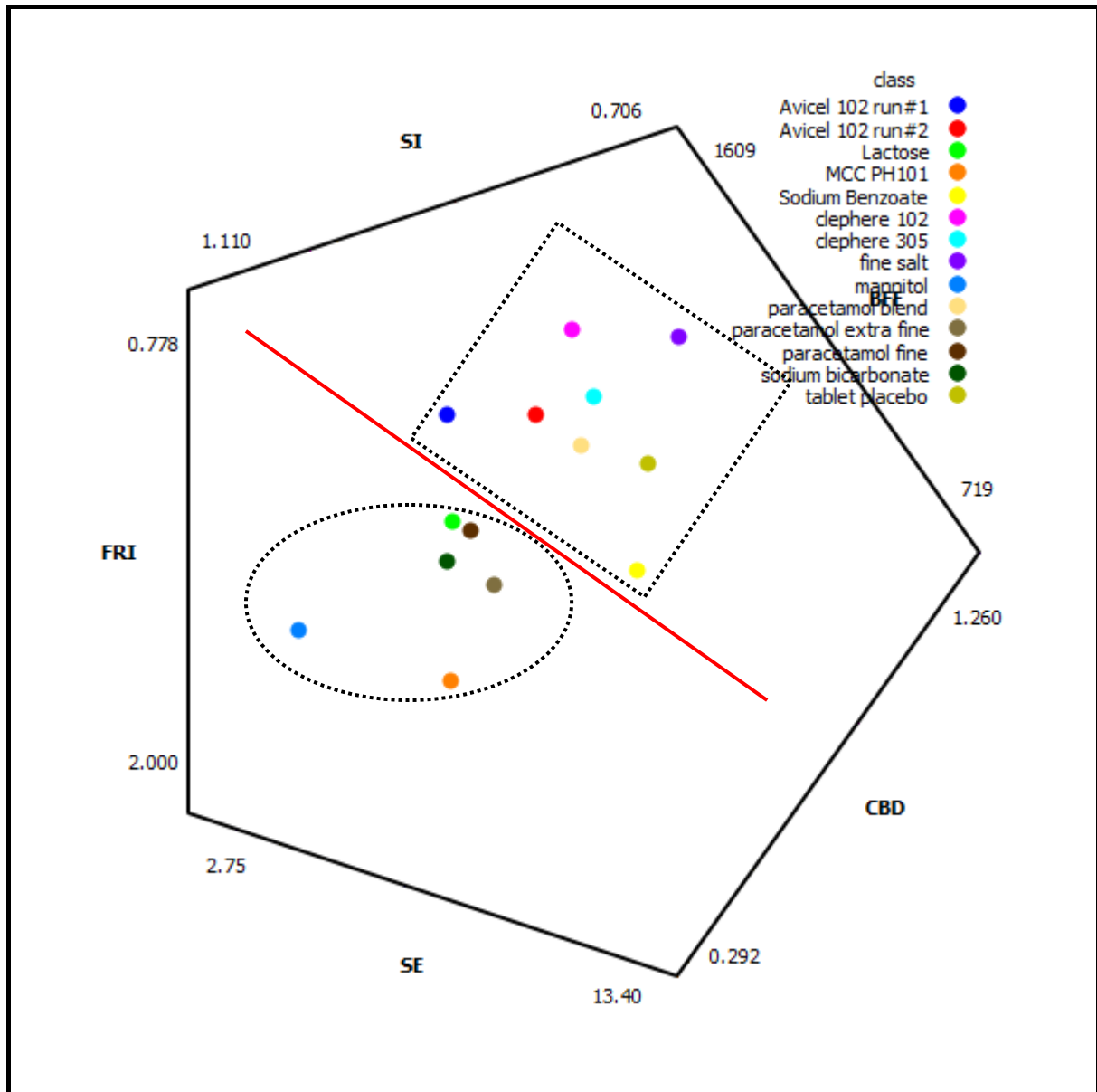


Figure 4.21: PolyViz representation of all the powder rheometry results for all the exemplar powders

If one were to look at shear data, for example, other relevant parameters such as permeability could be included, Figure 4.22. In this instance, it would seem that the shear cell PolyViz indicates that the Sodium Benzoate and paracetamol blend are more likely to be cohesive materials, which is not really the case.

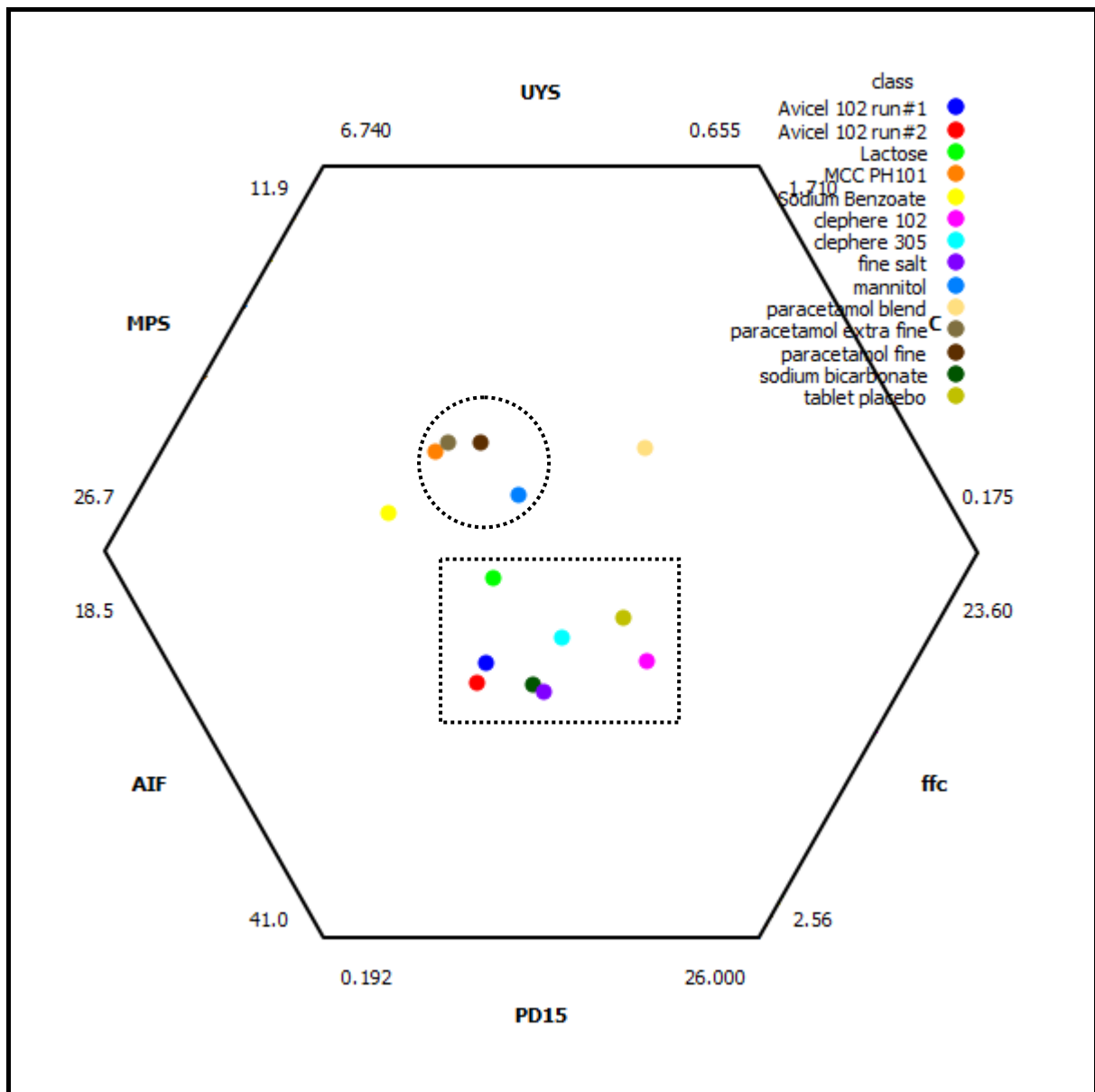


Figure 4.22: PolyViz representation of all the shear cell results for all the exemplar powders

Comparing the two representations of the shear data and the powder rheometry data it can be seen that they group the powders slightly differently, which is to be expected given their different modes of mobilising the powders, but in general there are more similarities than there are differences. Each representation picks out one or

two 'outliers' which are not part of the main clusters. This is where the visualisation of the data sets is very useful and can show up powders with slightly different behaviour, enabling the engineer to predict how any new powders will perform – given that he knows the process performance of the base data set. Once such performance can be correlated it will be possible to build more detailed models of processes with respect to more specific powder properties. To paraphrase the Fischer quote at the start of this section – it helps if you can see all the results of a multivariate data set to help you to decide the next step. Powders require multiple measurements to enable a full picture to be developed and PolyViz appears to be a useful tool to display the picture. Clearly there is more work that needs to be done in this area, but this appears to be a possible way for GEA to take advantage of any data they may collect.

4.5. Evaluation of the Decel system

To combine the concepts developed during this thesis would require several in depth studies of pharmaceutical powder processing systems. Time and equipment availability precluded this, but the concepts were applied to one case study, outlined in this section, and to the blending study, as previously described.

The Decel system fitted to Buck System discharge stations is designed to manage the flow of powder from an IBC to a reception point located vertically below – typically between different levels of a building. This configuration is common in many pharmaceutical manufacturing facilities and the uncontrolled discharge of powder through a long, say 5m, vertical pipe can lead to aeration and segregation of a blend as it impacts the base (and then powder) in the receiving vessel. In extreme circumstances, if the API is very fine, then such uncontrolled discharge can lead to a significant proportion of the active material settling on the top surface of the powder bed or even adhering to the inside of the top of the receiving vessel. Clearly this is an issue that will severely impact on the content uniformity of the powder and the resultant solid dose form, potentially leading to the batch being reworked or even scrapped.

Controlled flow should minimise segregation and dusting of the product and the Decel system is designed to do this. It operates by inflating a rubber sheath within the discharge tube, which in turn compresses a replaceable plastic 'layflat' tube that comes into contact with the powder. When a proximity sensor detects that powder

has started to flow from the IBC, the rubber sheath is allowed to deflate and the weight of the powder pushes air out of the sheath which slows the fall through the vertical discharge tube.

Vibration can be used to assist the flow of powder out of the vessel. In the first instance it is applied to a Buck Systems 'Vibroflow™' (GEA Pharma Systems 2010) device fitted to the inside of the vessel (Figure 4.23).



Figure 4.23: GEA Vibroflow™ flow promoter

It is fixed to the IBC between the outlet valve and the IBC flange. Vibrating the valve allows vibration to be transmitted through the 'Vibroflow™' into the powder. An additional out of balance motor vibrator, fitted to the discharge station frame, can also be activated.

In order to meet customer qualification protocols a demonstration of the system can be required. This usually entails the construction of a test rig at the same scale as

the final installation and an operational demonstration to confirm the capability of a specific item of process equipment and/or an appropriate installation.

In this instance the client requested a Qualification Demonstration of the Decel system which would be required to work under sealed conditions due to the highly toxic nature of the API. This meant that either the system had to operate fully sealed and that the air balance between the top and bottom vessel was maintained by the transit of air through the powder, or suitable venting and filtering mechanisms were in place to prevent discharge of dust into the work area surrounding the discharge and receiver vessels.

Figure 4.24 shows the test rig and Figure 4.25 shows the discharge point. The outlet diameter of the IBC was 100mm and the length of the Decel tube assembly was 5.3m. A small stainless steel conical section with a 100mm inlet, a 20mm outlet and a 70° wall slope was located at the bottom of the Decel tube to restrict flow to a manageable level. A load cell frame was relocated to a position under the discharge point to monitor the flow rate of the powder.



Figure 4.24: Discharge Station and Decel Tube with IBC containing the placebo located in position before operation with a load cell frame located under the discharge point to monitor the flow rate of the powder



Figure 4.25: Detail of the discharge point of the Decel test rig

The test material provided by the client was Avicel 102 and was supplied direct by the manufacturers, FMC, in five 20kg cardboard boxes fitted with a plastic liner.

Prior to testing, the question was asked ‘how do the flow properties of this placebo compare to those of your actual material?’ As was demonstrated with the mixing of binary and ternary systems in Chapter 3, the relationship between properties of single components compared to their performance as part of a mixture is not always obvious. Equally, there was no indication of typical loading and standing periods prior to discharge, whether the powder had been tumbled in the IBC or not, or distance and mode of transport between filling/tumbling and discharging stations. All

of these process conditions can have a profound effect on whether the powder will flow from the IBC outlet as many powders gain strength through periods of storage or through being vibrated as they are being stored.

Such questions had clearly not ever been asked of the GEA engineering staff or the clients engineering and compliance staff, and there were no procedures in place to generate simulation data. Due to the time and protocol constraints, the test was carried out with the placebo provided by the client and no attempt to find a compatible simulant or process conditions was made.

This is clearly an unaddressed issue within GEA and the client organisation (and possibly all of their clients) and is a clear indicator of why the FDA regulations relating to process understanding, described in Chapter 1, are necessary and why the modified HAZOP procedure, described earlier in this Chapter, should be adopted. Simply put, neither party had any significant understanding of the system or how it could be affected. Both parties appeared to be undertaking the trial so a box could be ticked in a New Drug Application, or similar bureaucratic evaluation, and so had to be seen to have been done. The author had little input into the trials and could not change the methods or protocols significantly.

The experimental plan was to carry out a series of four tests to investigate the ability of the system to discharge material under closed vessel conditions. The four test conditions to be investigated were:

- Closed system
- Open vessel system
- Closed system with discharge valve venting
- Closed system with discharge valve venting & vibration assistance

The only mode of validation/differentiation that was provided by GEA was that each condition could be differentiated by variation in flow rate. Given that a restrictor had been fitted to the outlet it was difficult to envisage that, should reasonable flow be possible for one or more conditions, how the flow rate would vary for the same powder.

4.5.1. Results and observations

Test 1

The first test was as indicated above – closed vessel; no vent; no vibration. Flow from the IBC was poor and intermittent. The Decel tube was never filled and the test was stopped after approximately 6 minutes after a total discharge of 12kgs. On investigation, it was observed that the powder had ratholed in the IBC – Figure 4.26.

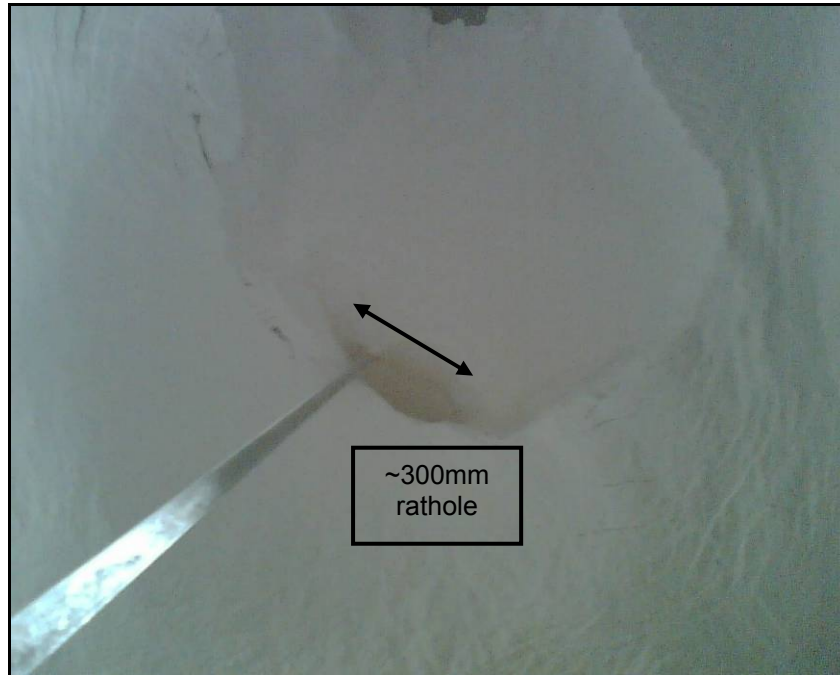


Figure 4.26: Rathole formed in IBC containing Avicel 102 during Test 1

It was also noted that the powder volume had increased by about 10-15% as more containers were required to hold the measured mass of discharged powder.

The remainder of the powder was assisted through the system manually and returned to the IBC via a 'dump load' method from the collection vessels.

Test 2

Following the expected poor performance in Test 1, it was decided to keep the bin sealed but to use the vent system that had been added to the discharge station valve assembly.

Initially the Decel tube was filled and there was a steady, but slow, flow of powder for approximately 10 minutes at a mean rate of ~0.6kg/min. Flow then ceased and was

re-initiated manually by gently tapping the outside of the Decel tube. Intermittent flow aided by gentle tapping of the tube persisted over the next 8 minutes, after which the test was halted. Again the powder had ratholed in the bin (Figure 4.27).



Figure 4.27: Rathole formed in IBC containing Avicel 102 during Test 2

The remainder of the powder was assisted through the system manually and returned to the IBC.

Test 3

In Test 3, following the poor flow in Test 2, it was decided to use all the flow aids available and with the lid seal unlocked to provide a fully vented condition such that a base set of data could be generated. The flow of powder was still intermittent with no real periods of consistent discharge.

It was noted that a vacuum could easily form in the lower, transparent section of the Decel tube as there was an observable vertical void formed between upper and lower horizontal material faces – as shown schematically in Figure 4.28.

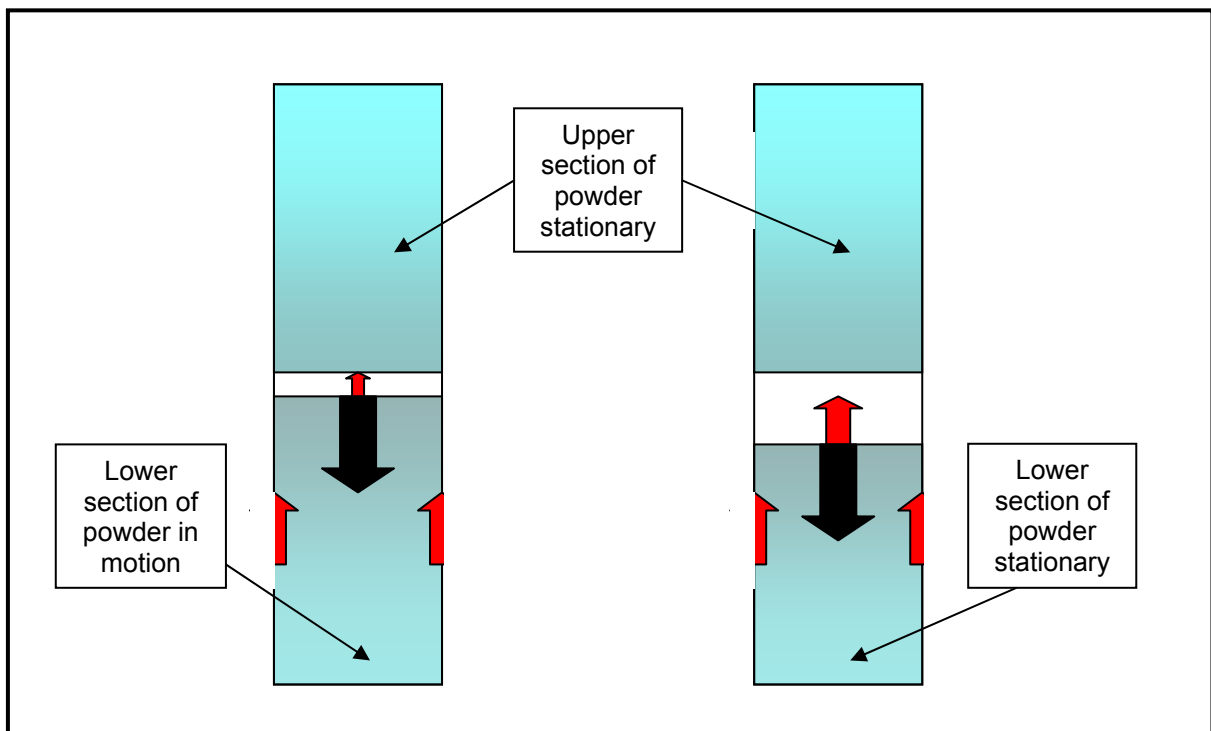


Figure 4.28: Schematic of the 'vacuuming' of the powder

In order for the powder to discharge, gas has to pass from the bottom of the column to the top. Within the column there are frictional and gravitational forces acting on the material to a greater or lesser extent depending on the position in the column. In order for flow to occur the gravitational force must overcome the frictional forces, but when gas cannot pass through the powder bed there is a tendency to create a separation between two portions of the column. This then can create the void shown in Figure 4.28 where there is a low pressure (vacuum) zone formed which generates a suction that also helps to balance the gravitational force acting on the lower portion of the powder. This suction can be broken in one of two ways; air finally percolates

up through the lower mass and relieves the low pressure (observed in the transparent section of the Decel tube); or the upper section of the powder column fails and powder falls from the upper surface to the lower surface, allowing air to percolate upwards, usually in waves of small surface failures.

In extremis the layflat was pulled inwards (Figure 4.29). It was likely that this was occurring elsewhere in the (opaque) section of the tube. Ratholing was again observed in the IBC (Figure 4.30).



Figure 4.29: Contraction of the layflat due to ‘vacuuming’ in the tube

The remainder of the powder was assisted through the system manually and returned to the IBC.

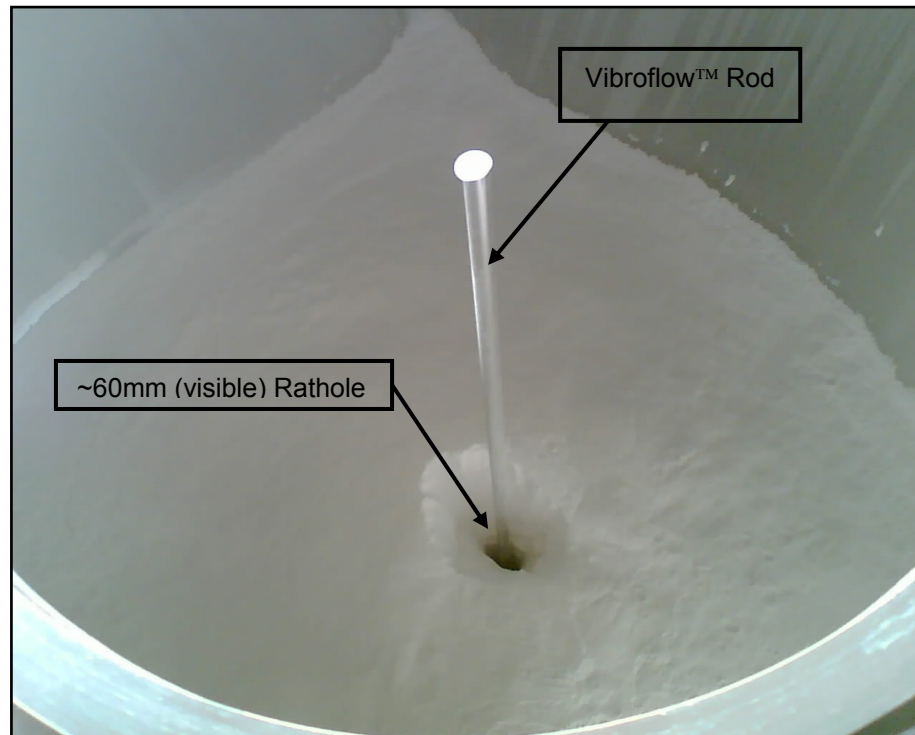


Figure 4.30: Rathole formed in IBC containing Avicel 102 during Test 3

Test 4

Test 4 was a repeat of Test 3, except that the vessel lid was removed to ensure that a vented condition was used. Flow was now negligible and the test was halted almost immediately. At this stage it was necessary to rod the powder in the IBC to create some flow.

It was felt that the powder had been 'overworked' and that the amount of aeration and compaction had led to a significant worsening of the flow over the series of tests despite the operational conditions being modified to assist the flow.

The remainder of the powder was assisted through the system manually and returned to the IBC where it was left overnight to de-aerate.

Test 5

Test 5 was a repeat of Test 3 undertaken the following day to allow the powder to de-aerate overnight.

Initially there was a good flow of powder out of the bin, but the rate slowly began to reduce and manual assistance was required to maintain flow. Vacuuming was also observed. The test was halted after 45kg had been discharged and flow had again become difficult. The remainder of the powder was assisted through the system and collected in the original boxes and additional bins.

Second Sample

Following the first test of the Decel unit and the provision of a report on the test, the client determined it necessary to undertake a repeat of the first test, this time using a different sample of the powder. Buck Systems also modified the vent system for the bin to improve the movement of air through the system by increasing the diameter of the vent orifice (from 25mm to 50mm) and providing a disposable filter cartridge. The new test material was presented as fresh batch of Avicel 102 microcrystalline cellulose. The sample of powder provided appeared to be drier than the previous sample tested (although subsequent moisture analysis showed no significant

difference) and visually flowed more freely with fewer agglomerates than the previous sample.

250kg of the new test material was loaded into the test vessel and the vessel positioned on the discharge station. As before, the IBC was fitted with a Vibroflow[®] system, and the discharge station fitted with the novel venting device.

Upon initiation of the discharge cycle, the powder appeared to flow poorly as the Decel tube was deflated. There followed a rush of powder as the material began to discharge some 30-45 seconds after cycle initiation. The powder then flowed smoothly for several minutes. Examination of the discharged powder sampled from the flow at the bottom of the Decel tube, revealed some loose agglomerates approx. 10-20mm in size. After several more minutes of regular flow, the vacuum effect described above, became evident. Flow was monitored for 30 minutes and the rate of discharge, although irregular, but never failed to flow – in marked contrast to the previous tests. The flow did eventually fail after ~100kg had been discharged. When the lid was removed there was evidence of core flow and perhaps some ratholing. The remainder of the material was then allowed to discharge with the vessel fully vented and showed significantly improved flow over the powder trialled previously.



Figure 4.31: Rathole formed in IBC containing Avicel 102 during test of second sample

Clearly the two samples behaved differently during processing, despite being presented as identical by the client. The two questions that these behaviours pose are

- What are the powder characteristics of the samples and how do they relate to the process behaviour?
- How can the process/powder system be analysed to improve flow?

4.5.2. Powder characterisation study

In order to evaluate the powder characteristics, a full suite of tests was carried out using the methods described in Chapter 2. Table 4.10 shows the results from the restricted testers.

Table 4.11: Results from Restricted Powder Testing Methods

Test Result	Material	
	Avicel Sample 1	Avicel Sample 2
Hausner Ratio	1.22	1.21
AOR	33.4	35.0
Min. Orifice (mm)	30	30
Friction coefficient	2829	2800

As can be seen there is very little difference in the results from restricted measurement systems and it would be difficult to differentiate the two samples on the basis of these data despite the difference in system performance – a result that also follows the conclusions from Chapter 2.

The samples were then tested using universal testers – the FT4 Powder Rheometer and the Schulze RST-XS shear cell.

The permeability and dynamic testing provide clear evidence of the difference between the two samples. The dynamic testing (Figure 4.32) indicates that the second sample is not stable and the result is suggestive of the presence of a flow aid thus any determination of relative flowability of these two samples cannot be definitively made with this test.

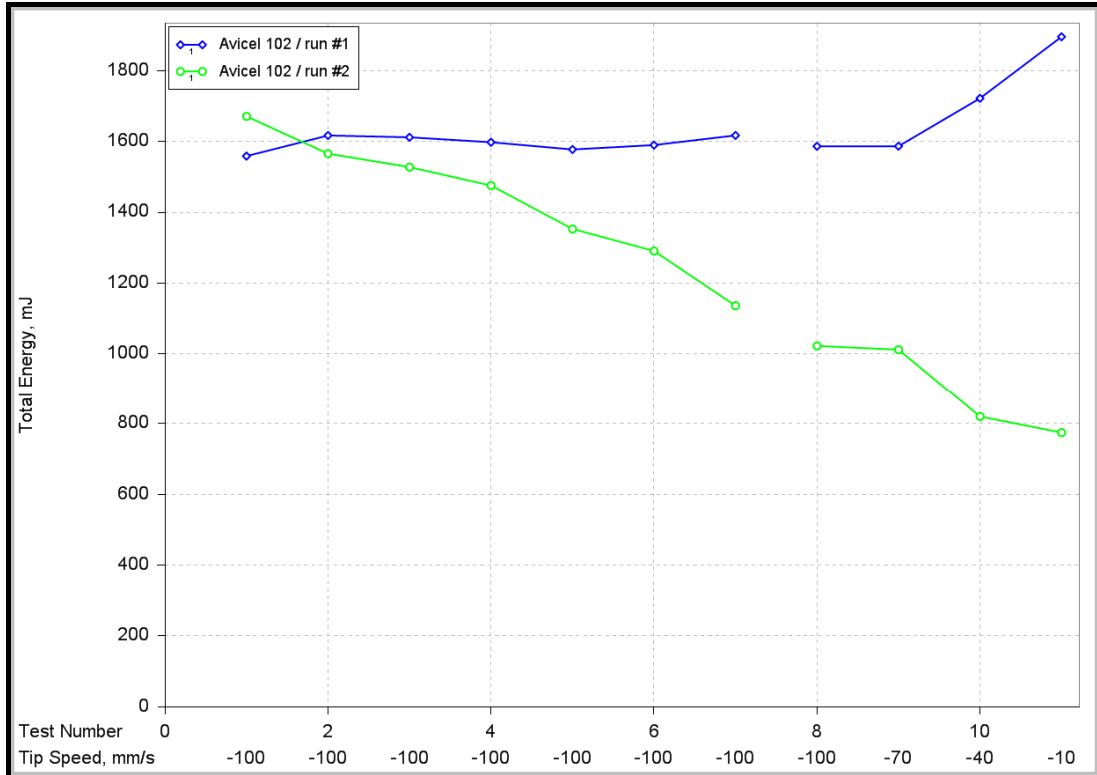


Figure 4.32: Dynamic testing for Avicel Samples

The permeability testing (Figure 4.33) shows that the first sample has a higher pressure drop than the second sample. This would indicate that air would pass through the second sample slightly more easily and should aid the discharge through a long discharge tube, as is the case here.

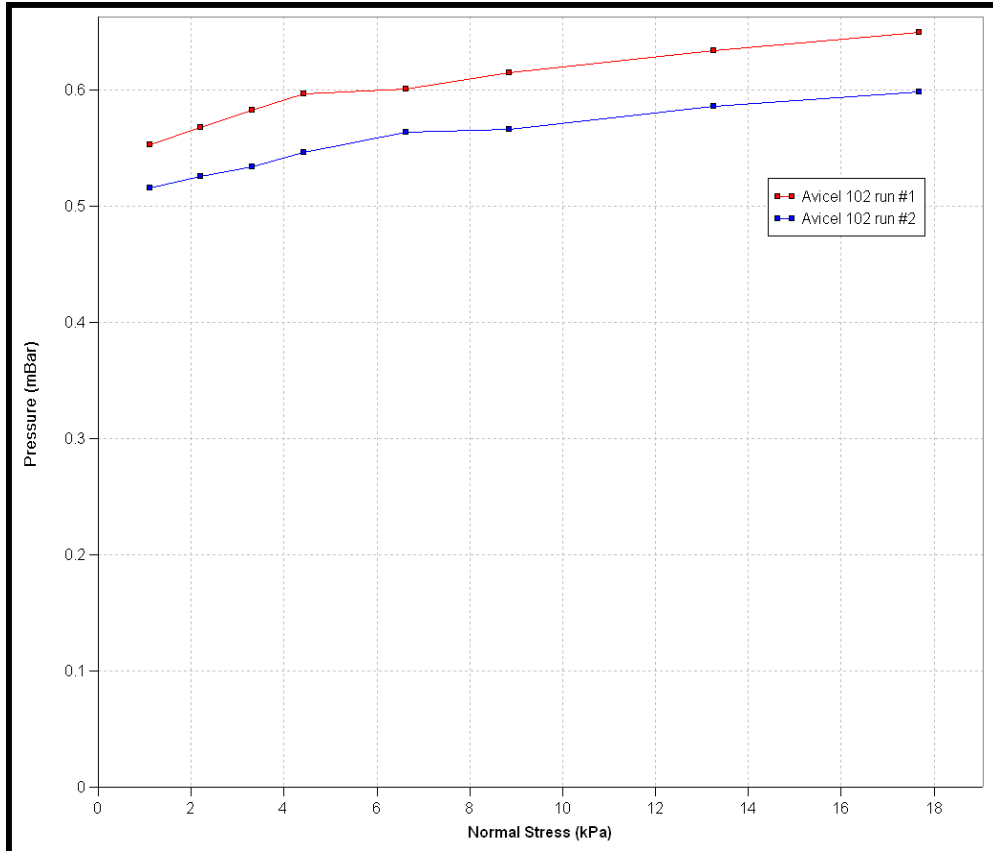


Figure 4.33: Permeability for Avicel Samples

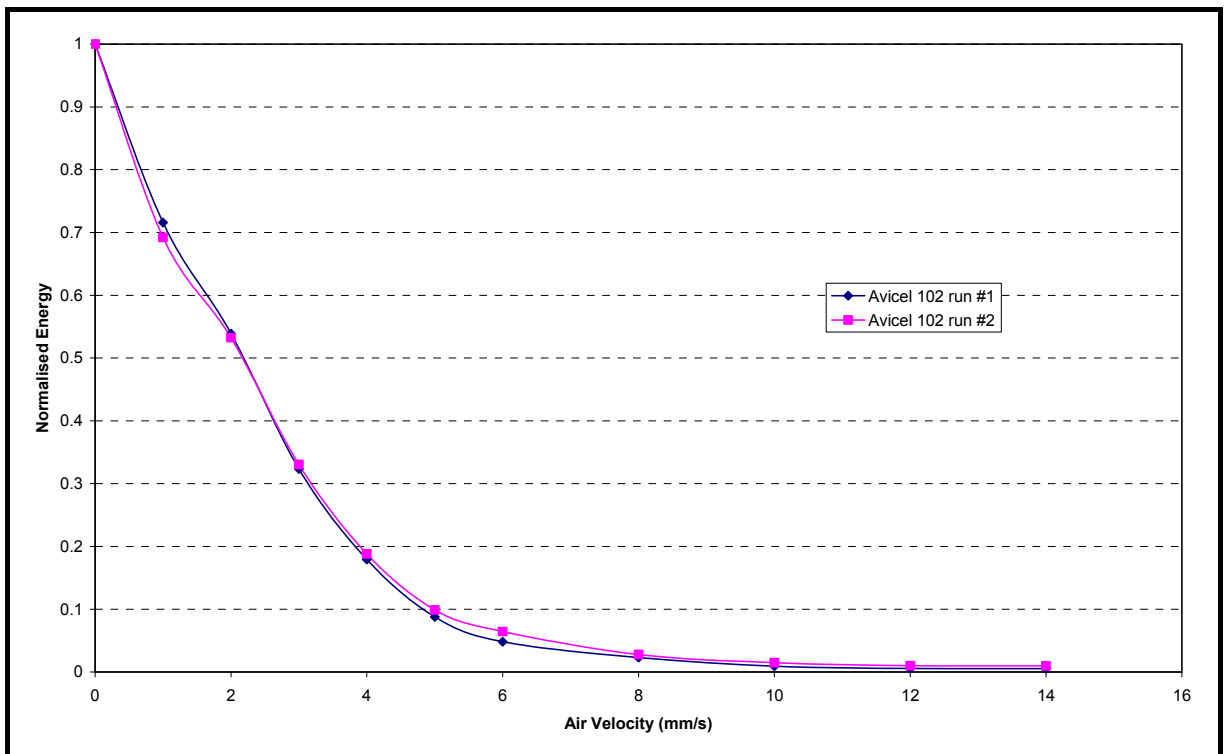


Figure 4.34: Normalised Aeration Energy for Avicel Samples

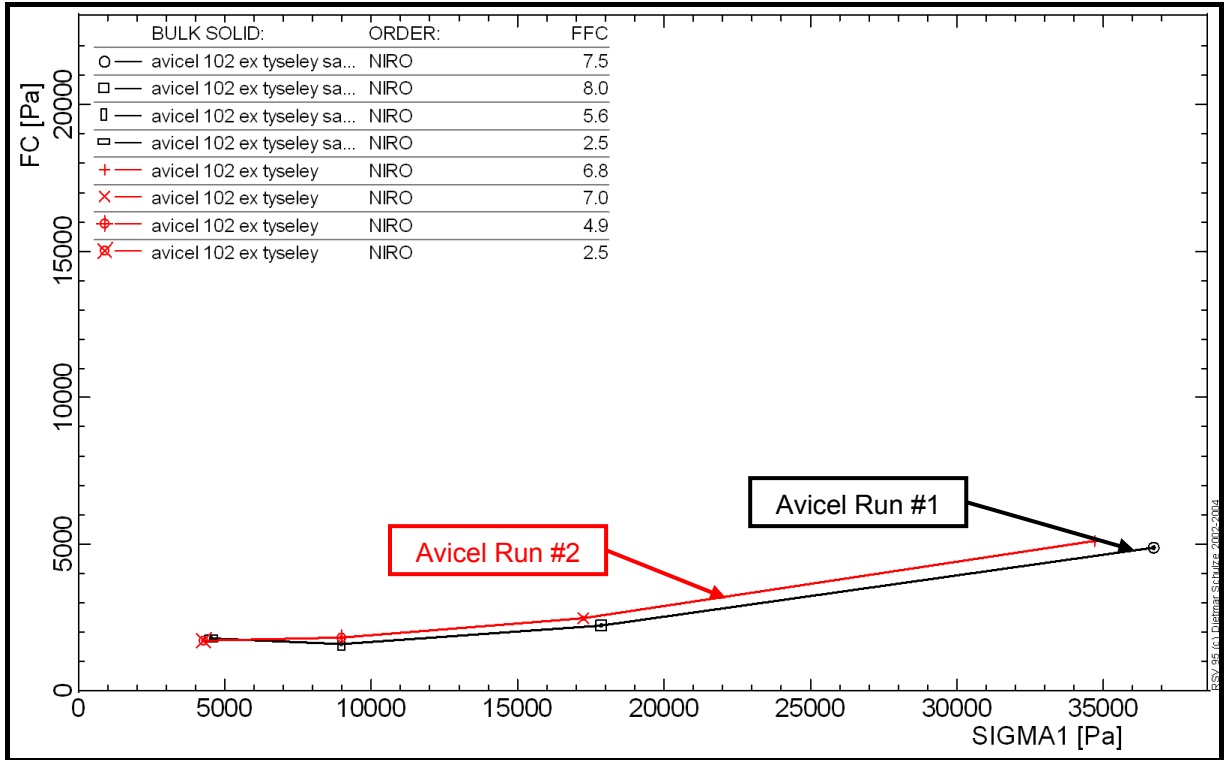


Figure 4.35: Flow Functions for Avicel Samples

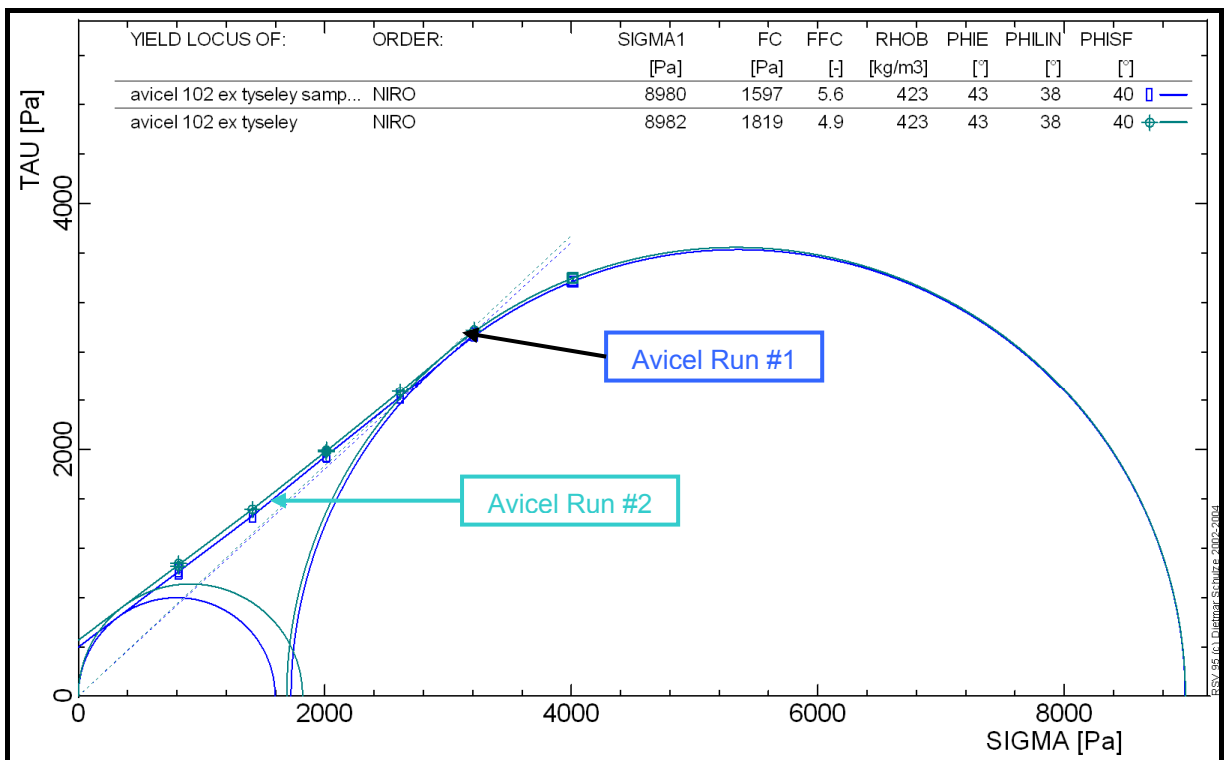


Figure 4.36: Yield loci for Avicel Samples generated by the RST-XS shear cell @ 4kPa consolidating stress

Figures 4.34, 4.35 and 4.36 show the normalised aeration ratio, the Flow Function and typical yield loci respectively for the two samples. As can be seen, these particular test methods do not differentiate the two samples.

In this case the testing of the samples at high stress (shear cell, Flow Function) and extremely low stress (aeration) does not enable any correlation with the system performance. The standard dynamic test did not differentiate the samples either – the flow aid merely making the Avicel Run#2 sample unstable within the test procedure.

4.5.3. Powder system analysis

If one examines the flowsheet/P&I diagram for the discharge station, as shown in Figure 4.37, it appears to be fairly straightforward. However, as has been noted in Section 4.1 there are a number of areas that require a more considered approach.

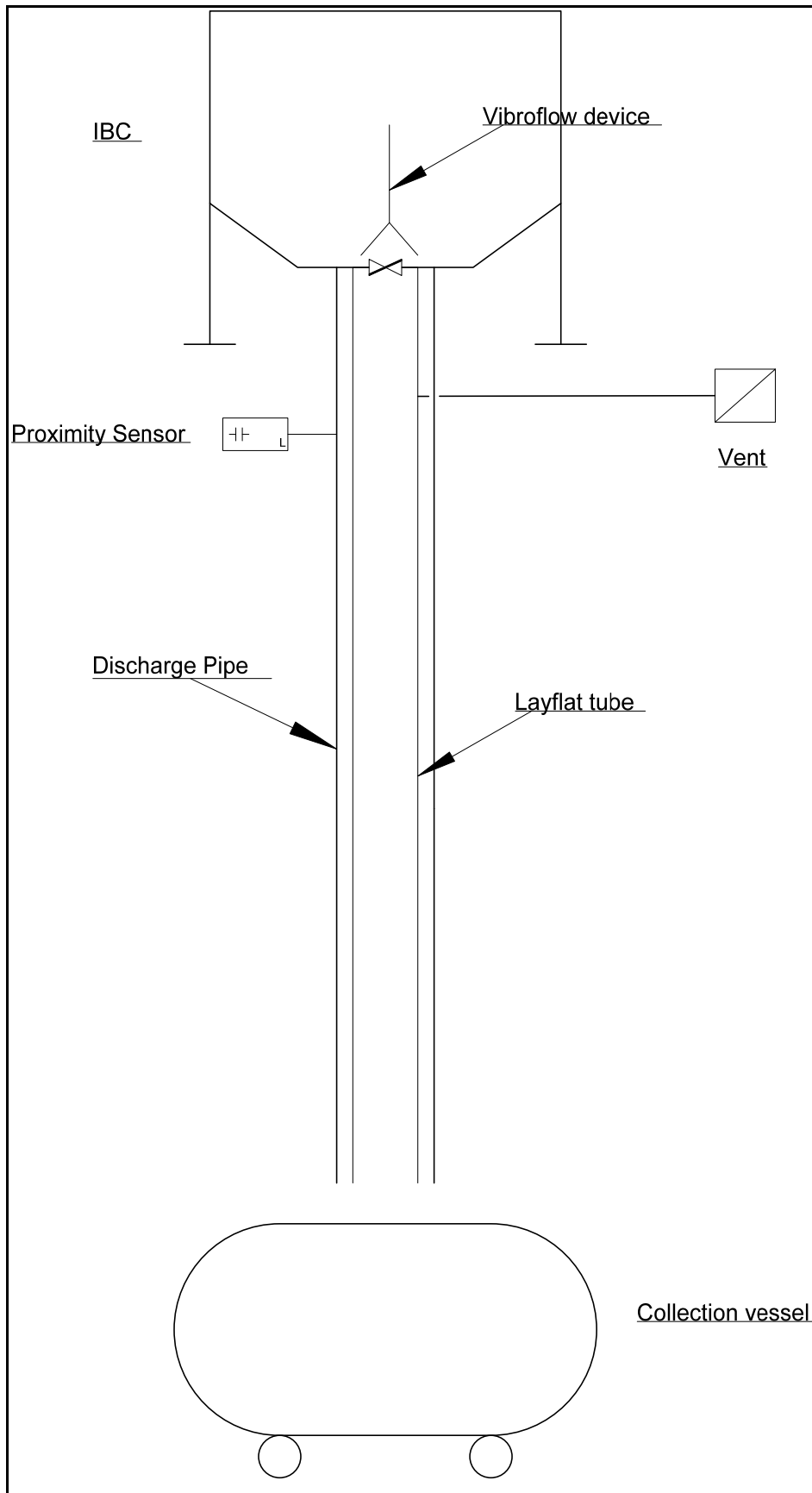


Figure 4.37: Flowsheet/P&I schematic for the Decel discharge station

Applying the guide words to the flow parameter generates several 'no-flow' conditions.

- I. IBC design will not allow mass flow from the vessel with these powders
- II. The frictional properties of the layflat tube may hinder the passage of the powder
- III. Any kinks or creases in the layflat tube may hinder the flow of the powder
- IV. The permeability of the powder may not allow air to pass easily through the column of powder, limiting its ability to dilate and hence flow in a regular manner.
- V. The application of vibration compacts the powder if
 - a. The level/flow sensor is in a void in the powder
 - b. The vibration is applied before or during the opening of the IBC outlet valve

Addressing each of these particular conditions in turn

- I. When the two samples were shear tested and the results run through the hopper design software tool (described in Chapter 2 and Appendix 2), the results showed that the outlet diameter, albeit for a cylinder and cone design, required a very small outlet to allow mass flow to occur – much smaller than the 150mm diameter outlet present on the IBC. However, the point at issue here is that the system, as set up, will not follow a mass flow regime. This is because the powder/vessel system does not conform to one of the basics of mass flow – the powder has to be able to flow at the vessel wall, which clearly

it does not. The best that can be expected is that a fully self emptying core flow regime can be achieved. Any IBC system has a number of issues relating to its general shape and capacity which make designing mass flow difficult. Firstly the usual shape is square with a pyramidal hopper section (purely due to manufacturing costs) – this is a difficult shape for even the freest flowing materials to mass flow against because of the narrow valley angles created where the walls meet and it is where powder tends to hang. Secondly mass flow usually requires a reasonable head of material to generate enough ‘weight’ to break the arch at the outlet. IBCs often have very shallow vertical sections and mass flow generally requires an overburden height of 0.75 to 1 x vessel diameter (Appendix 2). As the critical rathole dimension is considerably larger than the outlet of the IBC, the first sample did not flow uniformly and the second sample only flowed sporadically due to the addition of a flow aid.

- II. This aspect was not tested as the frictional qualities of the plastic appeared low, but could easily be evaluated by modification of a wall friction test coupon
- III. During discharge, the visible section of the layflat tube was not creased and this was thought an unlikely scenario
- IV. The permeability of the samples was tested (Figure 4.22) and the indicated difference would account for the difference in flow behaviour.
- V. The application of vibration to a system is poorly understood with only some rough empirical guidance in the public domain (Roberts 1993; Woodcock & Mason 1987). What can definitely be stated is that the application of vibration to a powder that does not have the space to dilate will generate a more compacted material which, in the majority of cases, will prevent flow entirely.

In this case, the hang up of the powder in the discharge tube created observable voids

4.5.4. Summary and discussion

Once the report of the Decel system evaluation had been supplied to the client, a number of details about the test and the proposed installation became apparent. The second sample that had been supplied was indeed mixed with a flow aid – confirming the laboratory evaluation of the flow properties. Secondly the actual Decel tube to be used in the process was of the order of 2m – significantly shorter than the test rig configuration of 5.3m which, given that permeability of a powder column is inversely proportional to the depth of the powder column, testing with an accurately sized shorter Decel tube would have greatly increased the likelihood of sustained steady powder flow. Finally, the design of the IBC was different to the unit that was employed for the test programme, although the exact differences were never elucidated by GEA.

If one was looking to apply the FDA guidance regarding process understanding and the development of the correct design and control spaces, there are several areas where both the client and GEA would not be able to show that they understood their process.

The first point that needs to be made is that the test material is a placebo and the differences between it and the real material need to be quantified before any test can

be assumed to be representative. The placebo may reasonably replicate behaviour under some conditions, but not necessarily all conditions. The client may suggest that the test material behaviour is close to that of the real material, but such differences need to be identified and quantified and the test methods established and validated. Secondly, the test rig built by GEA was not representative of the equipment designed and installed at the client facility in terms of the discharge distance and hopper type – as mentioned above.

If the details of the system are considered, the main issue that the modified HAZOP appraisal identified was the application of vibration. The proximity/flow sensor appears to be of limited value in these conditions. The material tended to bridge over and around the sensor, which believed that material was flowing and thus did not activate the vibration system. However, initiation of vibration may not have been a good thing. If the powder cannot dilate down the tube, any activation of the vibration system will simply pack the powder in the IBC, making it even more difficult for the powder to exit the vessel. It is likely that this was caused when a void was created around the vibrating flow indicator (located in the discharge tube just below the discharge valve) and the material was already struggling to dilate and exit the vessel – when the sensor supplied the control signal for the vibration its effect was most likely to further compact the powder in the IBC, as evidenced by the ratholing observed in all tests, especially for the first sample where a flow aid was not present. The use of a vibrating flow sensor to generate the control signal is inappropriate – these probes are best suited to high/low level switching and it is recommended that a system to monitor mass change be trialled to replace the current system. Load cells

are available in small, bolt-on configurations and a precise weight is not required – just a change in weight. The point of application of vibration also needs to be considered. A long discharge tube such as that tested may also need some additional vibration along the length of the tube to promote powder dilation and allow air to pass along the tube.

4.6. Conclusions

The ability to generate a more considered evaluation of powder processing systems using a modified HAZOP approach has been demonstrated. This approach allows the team member, specifically a powder systems expert, to identify clearly operability issues that require further investigation and which tests that can practicably be undertaken to evaluate the sensitivity of the design to potential variability in feedstocks and intermediates. The improvement in powder characterisation methodologies greatly enhances the understanding of the material behaviour and hence the ability to predict risk factors.

The use of advanced perceptual mapping methods has shown some promise for the elucidation of relative behaviour from a wide range of powders combined with a wide range of test data. It may be possible that this technique can be used for specific process behaviour maps and help to focus on the measurable powder properties that can influence a particular processing performance parameter.

It has also been shown that the models for generating hopper design are extremely sensitive to test variability, but the use of concatenated safety margins from the traditional employment of linear curve fitting to yield locus and Flow Function data, combined with an engineering safety factor, leads to over specification of hopper outlets, as argued by Berry.

The application of these techniques to a full scale discharge station test rig has shown that a number of problems encountered during evaluation of two sample materials could have been predicted using the modified HAZOP approach and that the relative performance of the two materials could be related to certain powder characterisation techniques, but not others, for this specific process. It has also highlighted the issues of designing IBC vessels for flow. The general shape is not conducive to mass flow and thus the powder properties must be considered in this context, with greater attention paid to the core flow design method than was possible during this project.

4.7. References

Akers, R. J. 1992, *The certification of a limestone powder for Jenike shear testing CRM116* Commission of the European Communities.

Albuquerque, G., Eisemann, M., Lehmann, D. J., & Theisel, H. 2010, "Improving the Visual Analysis of High-dimensional Datasets Using Quality Measures", in *IEEE Symposium on Visual Analytics Science and Technology*.

Berry, R. J., Birks, A. H., & Bradley, M. S. A. 2003, "Arching behaviour of cohesive powders in a pilot scale plane flow silo", *Task Quarterly*, vol. 7, no. 4, pp. 479-498.

Berry, R. J. & Bradley, M. S. A. 2003, "Comparisons between observed powder behaviour in industrial feeders and measured powder failure properties obtained using a short cut silo design procedure", in *The 5th International Conference for Conveying and Handling of Particulate Solids*.

Berry, R. J., Bradley, M. S. A., Reed, A. R., Farnish, R. J., & Angulo, O. A. 2007, "Effect of Machine Dependence on Wall Failure Property Measurements, Jenike versus an Annular Shear Tester", in *9th International Conference on Bulk Materials Storage, Handling and Transportation*.

Bradley, M. S. A. 1990, "Pressure losses caused by bends in pneumatic conveying pipelines", *Powder Handling and Processing*, vol. 2, no. 4.

Brookfield Engineering Laboratories Inc. 2010, Think Powder. Think Brookfield PFT™.

Bundalli, N. 1973, "The application of a computer to hopper design", *Computer-Aided Design*, vol. 5, no. 4, pp. 224-227.

Coulson, J. M., Richardson, J. F., & Sinnott, R. K. 1991, "Safety and Loss Prevention," in *Chemical Engineering Design*, 1 edn, vol. 6 pp. 274-304.

Drescher, A., Waters, A. J., & Rhoades, C. A. 1995a, "Arching in hoppers: I. Arching theories and bulk material flow properties", *Powder Technology*, vol. 84, no. 2, pp. 165-176.

Drescher, A., Waters, A. J., & Rhoades, C. A. 1995b, "Arching in hoppers: II. Arching theories and critical outlet size", *Powder Technology*, vol. 84, no. 2, pp. 177-183.

EFCE. Standard Shear Testing Technique. 1989. The Institution of Chemical Engineers.

Ennis, B. J., Green, J., & Davies, R. 1994, The Legacy of Neglect in the U.S. *Chemical Engineering Progress*, 32-43.

Fayed, M. E. & Otten, L. 1984, *Handbook of Powder Science and Technology* Van Nostrand Reinhold.

Fisher, R. A. 1990, *Statistical Methods, Experimental Design, and Scientific Inference: A Re-issue of Statistical Methods for Research Workers, The Design of Experiments, and Statistical Methods and Scientific Inference* Oxford University Press, USA.

Fitzpatrick, J. J., Barringer, S. A., & Iqbal, T. 2004, "Flow property measurement of food powders and sensitivity of Jenike's hopper design methodology to the measured values", *Journal of Food Engineering*, vol. 61, no. 3, pp. 399-405.

GEA Pharma Systems. Blending Technology. 2010.

- Geldart, D. 1973, "Types of gas fluidization", *Powder Technology*, vol. 7, no. 5, pp. 285-292.
- Goossens, W. R. A. 2006, "The onset of bubbling fluidisation to distinguish the class A from the class B", *Powder Technology*, vol. 161, no. 1, pp. 59-64.
- Hauser, J. R. & Koppleman, F. S. 1979, "Alternative Perceptual Mapping Techniques: Relative Accuracy and Usefulness", *Journal of Market Research*, vol. 16, pp. 495-509.
- Himmelblau, D. M. 1996, *Basic Principles and Calculations in Chemical Engineering*, 6th edn, Prentice Hall.
- Hoffman, P. E. 1999, *Table Visualisations: A Formal Model and Its Applications*, University of Massachusetts Lowell.
- Hoffman, P. E., Grinstein, G. G., Marx, K., Grosse, I., & Stanley, E. 1997, "DNA visual and analytic data mining", *Computer Society and ACM*, pp. 437-441.
- IBC Technical Services Limited 1994, *A Guide Word Approach to Hazard and Operability Studies*.
- Jenike, A. W. 1964, *Storage and Flow of Solids*, University of Utah, Bulletin 123.
- Kaye, B. H. 1997, *Powder Mixing* Chapman & Hall.
- Kletz, T. 1992, *HAZOP and HAZAN, Identifying and Assessing Process Industry Hazards*, 3rd edn, Institution of Chemical Engineers.
- Klinzing, G. & Dhodapkar, S. V. 1993, "Expert Systems in Solids Handling," in *Particulate Two-Phase Flow*, M. C. Roco, ed., Butterworth-Heinemann, pp. 743-777.
- Lee, Y. S. L., Poynter, R., Podczeck, F., & Newton, J. M. 2000, "Development of a Dual Approach to Assess Powder Flow from Avalanching Behavior", *AAPS PharmaSciTech*, vol. 1, no. 3.
- Lerou, J. J. & Ng, K. M. 1996, "Chemical Reaction Engineering: A Multiscale Approach to a Multiobjective Task", *Chemical Engineering Science*, vol. 51, no. 10, pp. 1595-1614.
- McGee, E. The Benefits of Powder Characterisation. 2009. Solids Handling and Processing Association.
- McGee, E. & McGlinchy, D. 2005, "Characterising bulk solids: a profiling technique that helps solve flow problems", in *Particulate Systems Analysis 2005*.
- McGlinchy, D. 2005, *Characterisation of Bulk Solids* Blackwell.
- Merrow, E. W. 1986, *A Quantitative Assessment of R&D Requirements for Solids Processing Technology*, The Rand Corporation, R-3216-DOE/PSSP.

Molerus, O. 1982, "Interpretation of Geldart's type A, B, C and D powders by taking into account interparticle cohesion forces", *Powder Technology*, vol. 33, no. 1, pp. 81-87.

Regli, W. C., Hu, X., Atwood, M., & Sun, W. 2000, "A Survey of Design Rationale Systems: Approaches, Representation, Capture and Retrieval", *Engineering with Computers*, vol. 16, pp. 209-235.

Rhodes, M. 1998, *Introduction to Particle Technology* John Wiley & Sons.

Roberts, A. W. 1993, *Basic Principles of Bulk Solids Storage, Flow & Handling* TUNRA Bulk Solids Research Associates.

Schulze, D. 2007, *Powders and bulk solids. Behavior, characterization, storage and flow*, 2 edn.

Schulze, D. & Wittmaier, A. 2003, "Flow properties of highly dispersed powders at very small consolidation stresses", *Chemical Engineering Technology*, vol. 26, no. 2, pp. 133-137.

Shan, J., Sheng, H., Fan, M., Yu, B., Jinfu, W., & Yong, J. 2003, "Experimental study on the hung-up regime in hopper-standpipe systems for Geldart-A powders", *Chemical Engineering and Processing*, vol. 42, no. 1, pp. 39-43.

Singhal, I. K. & Hogg, R. 1986, "Evaluation of Shear Cell Test Procedures for the Characterization of Powder Flow", in *Second International Conference on Bulk Materials Storage, Handling and Transportation*, Wollongong, pp. 89-93.

Stainforth, P. T., Ashley, R. C., & Morley, J. N. B. 1971, "Computer analysis of powder flow characteristics", *Powder Technology*, vol. 4, no. 5, pp. 250-256.

Toebermann, J.-C., Rosenkranz, J., Werther, J., & Gruhn, G. 2000, "Block-oriented process simulation of solids processes", *Computers & Chemical Engineering*, vol. 23, no. 11-12, pp. 1773-1782.

Wang, X. S., Rahman, F., & Rhodes, M. J. 2007, "Nanoparticle fluidization and Geldart's classification", *Chemical Engineering Science*, vol. 62, no. 13, pp. 3455-3461.

Wood, P. A. *Fundamentals of bulk solids flow*. 1986. London, IEA Coal Research.

Woodcock, C. R. & Mason, J. S. 1987, *Bulk Solids Handling: An Introduction to the Practice and Technology*, 1 edn, Chapman Hall.

Chapter 5 – Final conclusions & suggested future work

5.1. Main conclusions

The regulatory framework in which pharmaceutical companies have to work has changed significantly since the late 1990's. The development and implementation of risk based approaches to processing pharmaceutical powders allows the pharmaceutical manufacturers the freedom to adopt real-time release for their products whilst reducing the regulatory burden for both the statutory bodies and the manufacturers.

This clearly has an impact on the way GEA/Buck Systems approaches the design, development and tendering process for their clients – the pharmaceutical companies. The ability to develop systems that show an understanding of the 'design space' concept will be essential for the long term health of the company.

The characterisation of bulk powder flow properties is a vital tool for any company that manufactures powder or produces equipment that processes such powders. Historically the use of simple measurement approaches, as depicted in many pharmaceutical textbooks & pharmacopoeia, has been prevalent in this sector. However, the development of far more advanced powder property measurement systems, such as the automated shear cells and powder rheometers evaluated in this thesis, will allow much more robust data to be generated quickly with significantly enhanced reproducibility.

Such a universal approach using modern instrumental methods can also be adopted by the other companies within NIRO Pharma Systems/GEA Group to further enhance the company's ability to better understand their processes to comply with the regulatory framework.

Although the ability for Buck Systems to relate to clients methods for testing powders using simple tests (most pharmaceutical companies will have Jolting Volumeters, 'flow through an orifice' and AOR devices somewhere in their organisation) is important, more advanced methods are required to develop strong relationships between the measured properties of the powders and the process design and operating conditions. In particular, the use of AOR and 'flow through an orifice' devices are not recommended. It has been shown that they provide inconsistent data; AOR devices can generate multiple angles of repose within a single test for some materials and the variety of commercial testers will fail to provide interchangeable data as they have significantly different configurations, methodologies and materials of construction; the inability of 'flow through an orifice' devices to generate data for cohesive samples is a significant limitation. Of the other simple methods evaluated, only the Jolting Volumeter has any merit, but even this has significant drawbacks with respect to its repeatability, limitations with cohesive samples and occasional unusual result (c.f. sodium bicarbonate – Figure 2.58)

Buck Systems main product line is IBC tumble blending systems which are employed throughout the pharmaceutical industry for sound reasons of quality control and containment of solid dose pharmaceutical formulations as they combine primary

batch storage with in-plant transport and processing/blending. This thesis has presented three tomographic techniques to observe and evaluate the mixing of dry powders in a typical pharmaceutical tumble blending system. PEPI has been shown to have significant limitations in quantifying behaviour in the powder blender. Both PET and PEPT have, however, shown the ability to generate data that can both quantify blending and differentiate between differing powder systems. The development of the large scale PEPT scanner could also provide the scope to measure dispersion in larger vessels in the near future.

However, it is PET that provides the most appropriate measure of mixedness for this type of tumble blender. This unique application of this technique has been shown to generate mixing data well below the typically required scale of scrutiny for pharmaceutical applications. Data collected has also shown the influence of particle shape on the mixing rate, a property which can be characterised by powder rheometry.

The ability to generate a more considered evaluation of powder processing systems using a modified HAZOP approach has been demonstrated. This approach allows the team member, specifically a powder systems expert, to clearly identify operability issues that require further investigation and which tests that can practicably be undertaken to evaluate the sensitivity of the design to potential variability in feedstocks and intermediates. The improvement in powder characterisation methodologies greatly enhances the understanding of the material behaviour and

hence the ability to predict risk factors associated with common variations in powder properties such as particle size, size distribution, moisture content etc.

It has also been shown that the models for generating hopper design can be incorporated into a computer based software tool, greatly reducing the time required to evaluate design options, this simplicity has, however, highlighted the sensitivity of the model to test data variability. It has also been shown how the influence of concatenated safety margins from the traditional employment of linear curve fitting to yield locus and Flow Function data, combined with an engineering safety factor, leads to probable over specification of hopper outlets.

However, it should be noted that the typical IBC size and shape may often not be compatible with the ideal mass flow regime with some of the poorer flowing formulations. In such instances the manufacturer and the client need to understand this at the earliest stage of design so that either bespoke, rather than existing designs of IBC are considered or that establishing a self emptying core flow regime is possible or that some external influence (such as GEA's Vibroflow device) can ensure discharge. Segregation during any of these processes has also to be considered and accounted for. Working within the FDA's QbD framework will require such an approach by manufacturer and client alike.

Finally the application of the these techniques to a full scale discharge station test rig has shown that a number of problems encountered during evaluation of two sample materials could have been predicted using the modified HAZOP approach. The

relative performance of the two materials could be related to certain powder characterisation techniques (particularly permeability) for this specific process.

Thus the outcomes of this project will allow Buck Systems to establish their credentials for understanding of the design space of their powder processing products with the pharmaceutical manufacturers and the regulatory bodies by;

- A more complete knowledge of how to evaluate the assembly properties of pharmaceutical powders including the limits of the testing procedures
- Having a better appreciation of the way shear cell data are developed and the limitations of the design criteria relating to hopper design including the sensitivity to powder properties
- A greater awareness of the issues relating to the blending of multi-component systems through the tomographic study of the content uniformity of mixtures
- Ways of using the data generated from powder testing to improve the operation of their powder processing systems and troubleshoot problems generated in existing installations.

There have been many studies and reports urging companies who deal with powdered or bulk materials (both processors and equipment suppliers) to develop a better understanding of the materials they work with to inform and improve the processing equipment and operating systems. They have mostly been well received but ultimately ignored. The reasons for this are that there needs to be very strong technical (i.e. we have never worked with such a cohesive sample before) or fiscal

(i.e. if we do not show our understanding of the powder/process relationship, we will not win the contract) incentives to change behaviour.

Why then should GEA take greater notice of this study in particular and then invest in powder characterisation equipment at all, given that the company has historically prospered without access to such to this data? The main driver, as discussed in Chapter 1 is the regulatory pressure for a better understanding of manufacturing processes which is being promoted by the FDA. Companies working in the pharmaceutical sector who do not incorporate this new ethos may, ultimately go out of business – if equipment manufacturers cannot show a reasoned specification for an item of process equipment then the customers will, of regulatory necessity, have to purchase from a supplier who can.

To that end it is gratifying to report that GEA have purchased a Jolting Volumeter and 'Flow through an Orifice' tester in 2007 and an FT4 Powder Rheometer in 2010, based on the results and recommendations presented in this thesis.

5.2. Suggested Future Work

The use of PET techniques to image the operation of a laboratory scale IBC tumble blender has been extremely successful. However, the reliability of the ECAT camera has limited the extent of the work due to a range of camera and control system failures. Another, more modern, ECAT camera has been recently commissioned in the Department of Physics and it is recommended that further studies with this more reliable system be carried out. The main areas of focus should be

- Extending the evaluation of binary systems with further studies on materials with a wider range of flow properties. This will allow a better understanding of the powder characteristics that affect mixing rates in order to inform a suitable model.
- More detailed study of mixtures containing multiple components to further assist with the development of a mixing rate model and investigate the concept of the system cohesion being the rate governing property that has been proposed by Muzzio. Cohesion in this case may be defined by powder rheometry methods or potentially by shear cell methods at very low consolidating stresses.
- Evaluating mixing rates at higher Froude numbers than was possible during this work due to the rotational speed limitation of the available mixer. This will enable a fuller evaluation of the relationship between mechanistic behaviour and powder properties to influence mixing rates.

- Developing a method to evaluate the distribution of radioactivity within a doped powder bolus such that the preparation technique can be validated or improved to ensure homogeneity.

The development of powder characterisation techniques should be focused on the universal testers evaluated during this thesis. With respect to the shear cell and the hopper design protocols:

- Greater understanding of the limitations of the theories underpinning this technique needs to be developed – especially where free flowing, less cohesive materials ($FF > 8$) are to be tested.
- The application of linear/non-linear models to yield loci needs to be developed further.
- Testing at lower consolidating stresses is essential to better understand the limitations of the curve fitting to yield loci and to provide better location of the FF/ff intersection.
- Further investigation of the hopper design model, especially in the way it applies to smaller systems (IBCs) where there are issues with the hopper shape, fill and discharge modes and the amount of powder overburden and how it relates to the particular discharge regime that can actually be achieved.

Powder rheometry has proved to be a useful tool, especially for differentiating powders which appear identical when subjected to other testing methods. It too requires further development

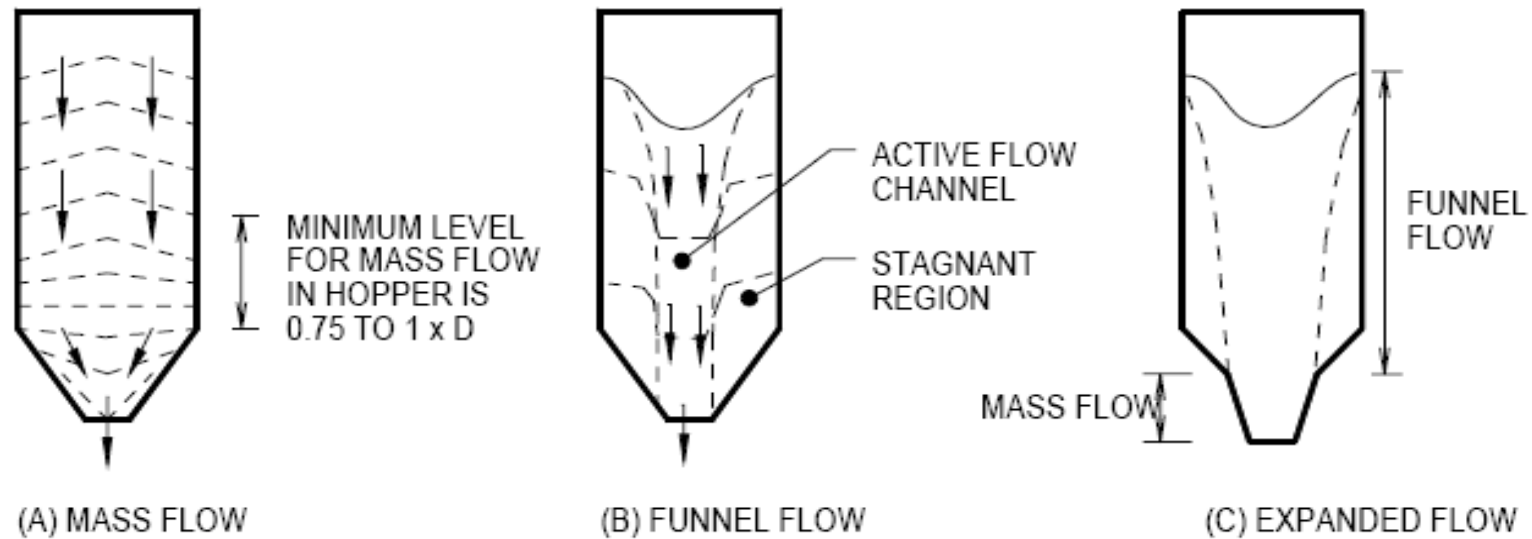
- Finding a suitable model which describes the data in a realistic way
- Developing a suitable scaling factor which will allow the instrument to be scale independent, which it is currently not – unlike the shear cell

In parallel to these suggested improvements, it is imperative that all the stake holders in the sector (pharmaceutical manufacturers, equipment suppliers and academia) improve and extend the knowledge of how powder flow properties affect their processes.

Appendix 1

Background to Shear Cell Testing

Silo Flow Modes

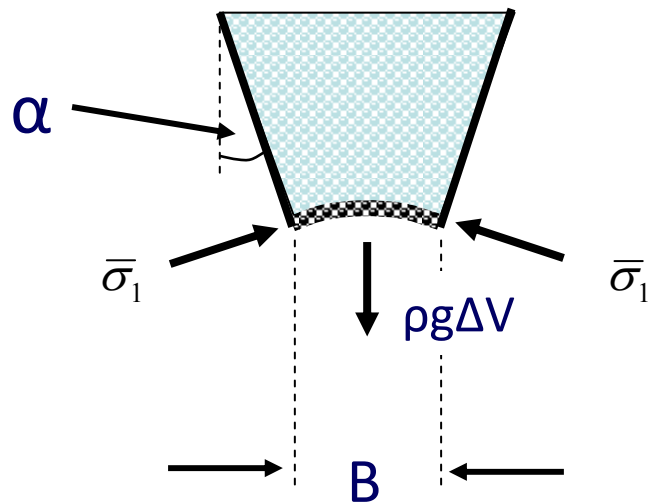


Mass flow is the preferred mode in the majority of operations

- ❑ Provides 'first in, first out' regime
- ❑ Flow is more consistent
- ❑ Full bin capacity is used

Need a methodology to allow hopper sections of silos to be designed so that mass flow can be achieved

Methodology



$\bar{\sigma}_1$ = stress in the arch

ρ = density

g = acceleration due to gravity

ΔV = volume of arch

The stress in the arch, $\bar{\sigma}_1$, is a function of both the span and the major consolidating pressure, σ_1

For flow to occur, the stress in the arch must be less than the unconfined yield strength, σ_c , of the powder

Thus there is a need to identify the unconfined yield strength and the major principal stress so that the stress in the arch can be defined

What needs to be measured?

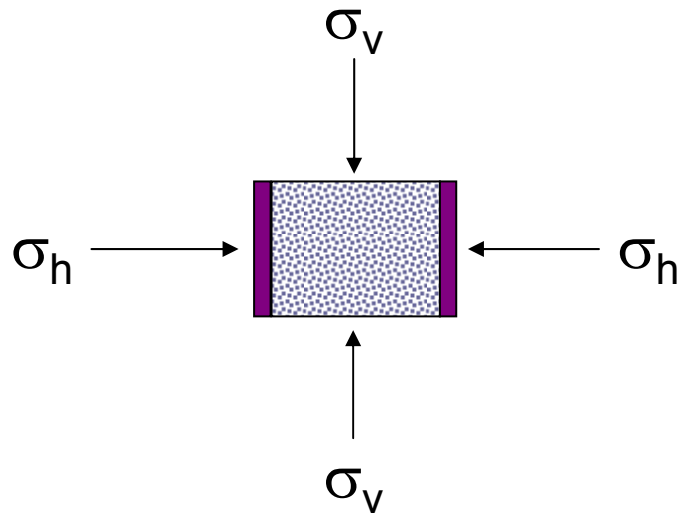
- ❑ Shear properties – how easily the powder will flow over itself
- ❑ Wall friction – how easily the powder will flow over the inner surface of the hopper
- ❑ Density – how this changes with consolidation stress

Methodology set out in...

'Standard Shear Testing Technique for particulate solids using the Jenike shear cell', IChemE/EFCE, 1989

Stresses in Powders

Considering a 2D element of powder

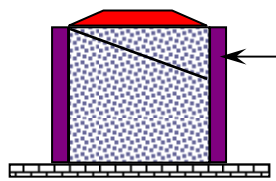


$$K = \lambda = \frac{\sigma_h}{\sigma_v}$$

Liquids $\lambda = 1$ (hydrostatic)

Solid $\lambda \approx 0$

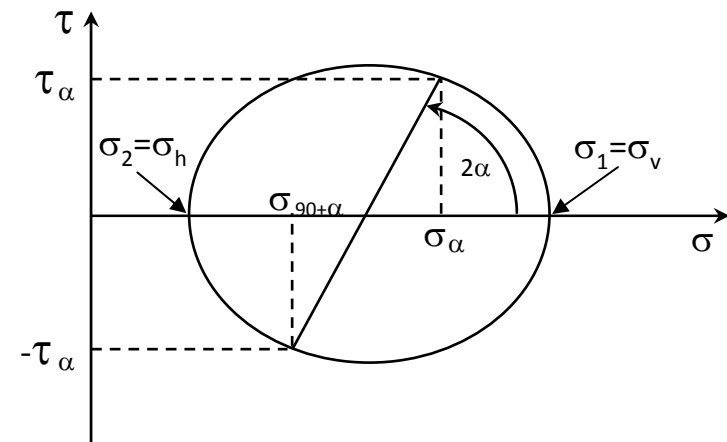
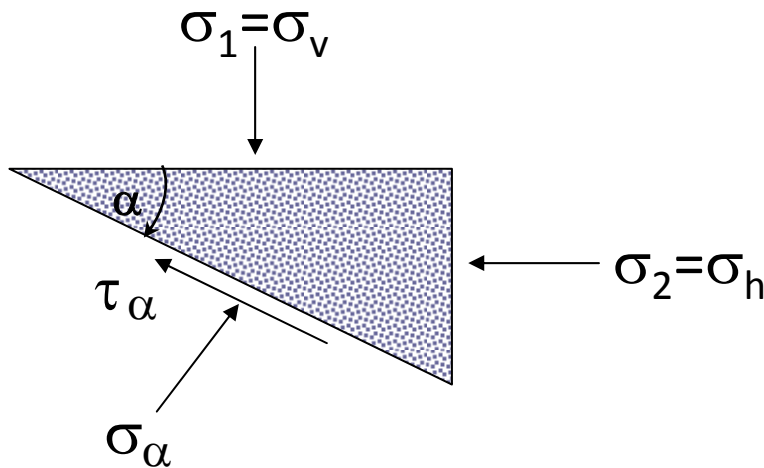
Powders $0.3 < \lambda < 0.6$



Triangular element defined by a cutting plane

$$\sigma_{\alpha} = \frac{\sigma_v + \sigma_h}{2} + \frac{\sigma_v - \sigma_h}{2} \cos(2\alpha)$$

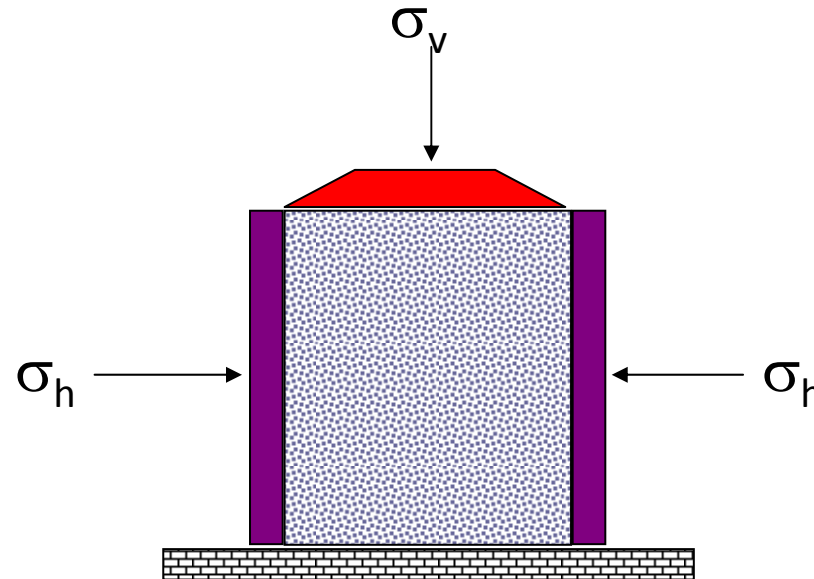
$$\tau_{\alpha} = \frac{\sigma_v - \sigma_h}{2} \sin 2\alpha$$



Mohr Stress Circle

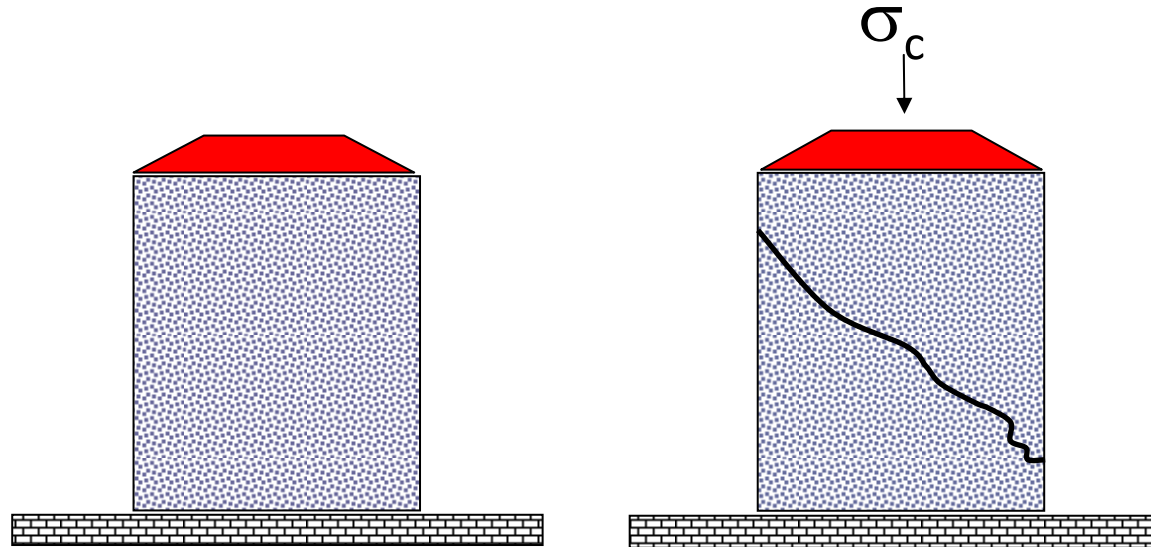
The Mohr's circle represents the stresses in all cutting planes for a given consolidating stress when the powder is stationary

Understanding principle stresses using the uni-axial method



Powder is contained in a hollow cylinder and consolidated with stress σ_v
The application of stress σ_v results in the build up of the minor principle stress σ_h
The Major Mohr circle shows the stresses in the consolidated powder

Note: upper and lower surfaces and walls assumed to be frictionless

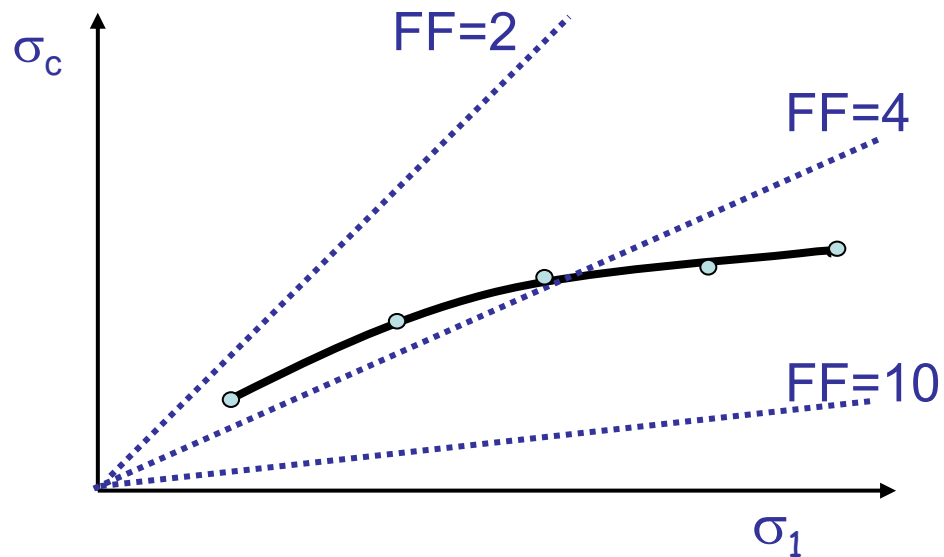


Next the consolidation stress σ_v is removed and the cylinder is taken away
Vertical stress is reapplied and increased until failure occurs (powder flows)

Stress required to cause failure is called Unconfined Yield Strength, σ_c

The horizontal stress is the minor principle stress and must be equal to zero when the powder is unconfined

$$\text{Flow function, } FF = \frac{\sigma_1}{\sigma_c}$$



The Flow Function, as defined by the equation on the left, can be determined for a given consolidation stress level. When the Flow Functions for a number of levels of consolidation stress are combined, a Flow Function graph can be described.

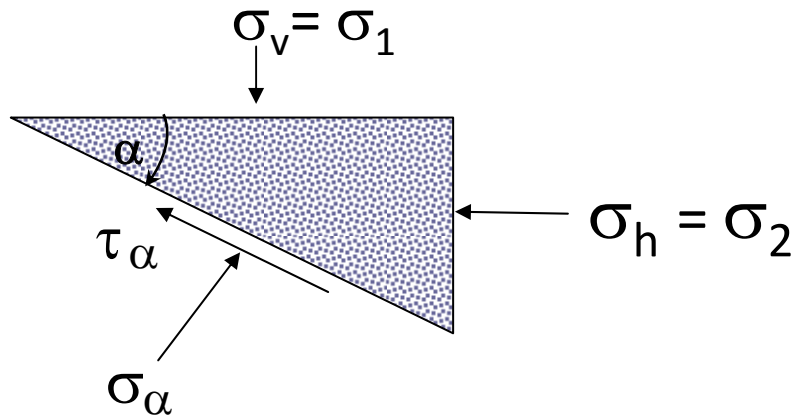
Limitations of unconfined yield test

- The unconfined yield test is not the simplest test to conduct. It requires
 - A powder column that remains intact following the compaction and vessel wall removal stages
 - this usually involves very high consolidating stresses (with respect to the stresses found in a hopper arch) for less cohesive powders
 - Uniform stress throughout the powder column which is achieved by a progressive fill and compaction regime
 - typically upwards of 5 steps depending on the consolidating stress
 - A powder column that fails along a single cutting plane which is achieved by having a column $L/D = \tan(45^\circ + \phi/2)$
 - This requires a knowledge of the angle of internal friction, ϕ , which requires a knowledge yield locus which, in turn, requires a shear test to have been completed – thus the whole process becomes iterative and lengthy

Benefits of shear cell testing

- More control over the definition of the shear plane
- Does not require pre-determination of powder properties to define test parameters – not iterative
- Universal test that will evaluate powder properties at much lower consolidating stresses (important for hopper design method)

Derivation of Mohrs circle for shear testing



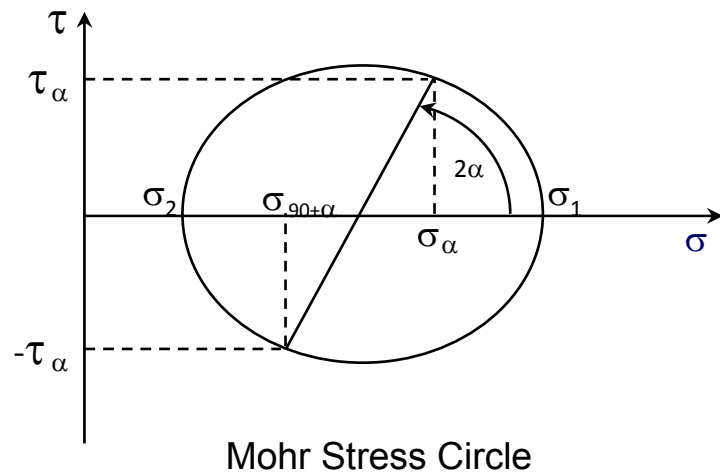
If one then considers a triangular element of bulk material, the forces acting on it are shown left.

The Mohr circle is a representation of all the stresses acting on the element for all possible cutting plane angles of α .

For angles $\alpha = 0$ and $\alpha = \pi/2$, the *shear stresses*, $\tau = 0$.

The *normal stresses* acting in these planes are called the Principle Stresses.

The larger stress is called the Major Principle Stress σ_1 and the smaller one the Minor Principle Stress, σ_2



At equilibrium, the sum of the forces acting on the triangular element of bulk solid can be represented by Equations 1 and 2

$$\sum F_x = \sigma_v l \cos \alpha - \sigma_\alpha l \cos \alpha - \tau_\alpha l \sin \alpha = 0 \quad \text{Equation 1}$$

$$\sum F_y = \sigma_v l \sin \alpha - \tau_\alpha l \cos \alpha - \sigma_h l \sin \alpha = 0 \quad \text{Equation 2}$$

These can be simplified by dividing by l (the length of the plane) and rearranging

$$\tau_{\alpha} = \frac{\sigma_v \cos \alpha - \sigma_{\alpha} \cos \alpha}{\sin \alpha}$$

Equation 3

$$\sigma_{\alpha} = \frac{\tau_{\alpha} \cos \alpha - \sigma_h \sin \alpha}{\sin \alpha}$$

Equation 4

These expressions include both σ_{α} and τ_{α} which cannot be explicitly defined, and thus further manipulation is required to isolate equations for each variable which do not depend on the other variable

Combining Equations 3 & 4

$$\sigma_{\alpha} = \frac{\sigma_v (\cos \alpha)^2 - \sigma_{\alpha} (\cos \alpha)^2}{(\sin \alpha)^2} + \sigma_h$$

Equation 5

Rearranging Equation 5

$$\Rightarrow \sigma_{\alpha} \left(1 + \frac{(\cos \alpha)^2}{(\sin \alpha)^2} \right) = \sigma_v \frac{(\cos \alpha)^2}{(\sin \alpha)^2} + \sigma_h$$

Equation 6

Multiplying through by $(\sin \alpha)^2$

$$\Rightarrow \sigma_{\alpha} \left((\sin \alpha)^2 + (\cos \alpha)^2 \right) = \sigma_v (\cos \alpha)^2 + \sigma_h (\sin \alpha)^2$$

Equation 7

Given that

$$(\sin X)^2 + (\cos X)^2 = 1$$

Equation 8

Then equation 7 becomes

$$\sigma_{\alpha} = \sigma_v (\cos \alpha)^2 + \sigma_h (\sin \alpha)^2$$

Equation 9

Also given that

$$(\sin X)^2 = \frac{1}{2}(1 - \cos 2X)$$

Equation 10

$$(\cos X)^2 = \frac{1}{2}(1 + \cos 2X)$$

Equation 11

Thus, substituting Eqns 10 and 11 into Eqn 9

$$\sigma_{\alpha} = \frac{1}{2} \sigma_v (1 + \cos 2\alpha) + \frac{1}{2} \sigma_h (1 - \cos 2\alpha) \quad \text{Equation 12}$$

$$\Rightarrow \sigma_{\alpha} = \frac{\sigma_v + \sigma_h}{2} + \frac{\sigma_v - \sigma_h}{2} \cos 2\alpha \quad \text{Equation 13}$$

Thus Equation 13 explicitly defines the normal stress acting on the cutting plane as a function of the vertical and horizontal stresses acting on the element for all angles of the cutting plane between 0 and 2π radians.

Substituting Equation 9 into Equation 3 gives

$$\tau_{\alpha} = \frac{\sigma_v \cos \alpha - \sigma_v (\cos \alpha)^3 - \sigma_h (\sin \alpha)^2 \cos \alpha}{\sin \alpha} \quad \text{Equation 14}$$

$$\Rightarrow \tau_{\alpha} = \frac{\sigma_v \cos \alpha (1 - (\cos \alpha)^2) - \sigma_h (\sin \alpha)^2 \cos \alpha}{\sin \alpha}$$

Equation 15

$$\Rightarrow \tau_{\alpha} = \frac{\sigma_v \cos \alpha (\sin \alpha)^2 - \sigma_h (\sin \alpha)^2 \cos \alpha}{\sin \alpha}$$

Equation 16

$$\Rightarrow \tau_{\alpha} = (\sigma_v - \sigma_h) \cos \alpha \sin \alpha$$

Equation 17

Since $\cos X \sin X = \frac{1}{2} \sin 2X$

Equation 18

Then substituting Equation 18 into Equation 17

$$\tau_{\alpha} = \frac{\sigma_v - \sigma_h}{2} \sin 2\alpha$$

Equation 19

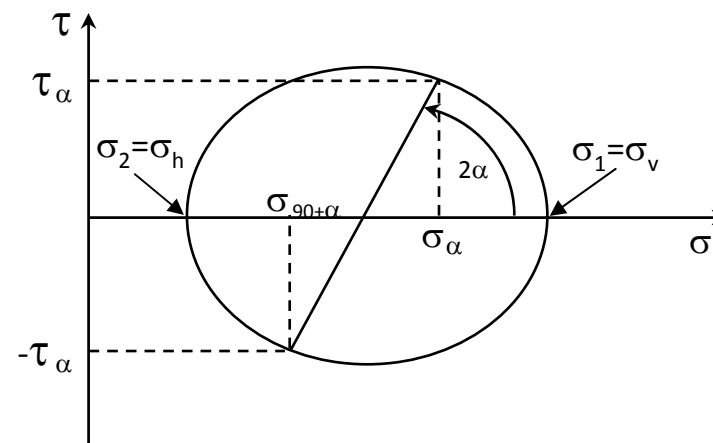
Thus the pair of values are explicitly defined as functions of the vertical and horizontal stresses acting on the element for all angles of the cutting plane between 0 and 2π radians as shown on the diagram shown below.

$$\sigma_{\alpha} = \frac{\sigma_v + \sigma_h}{2} + \frac{\sigma_v - \sigma_h}{2} \cos(2\alpha)$$

Equation 13

$$\tau_{\alpha} = \frac{\sigma_v - \sigma_h}{2} \sin 2\alpha$$

Equation 19



Mohr Stress Circle

How a shear cell derives the principal and unconfined yield stresses

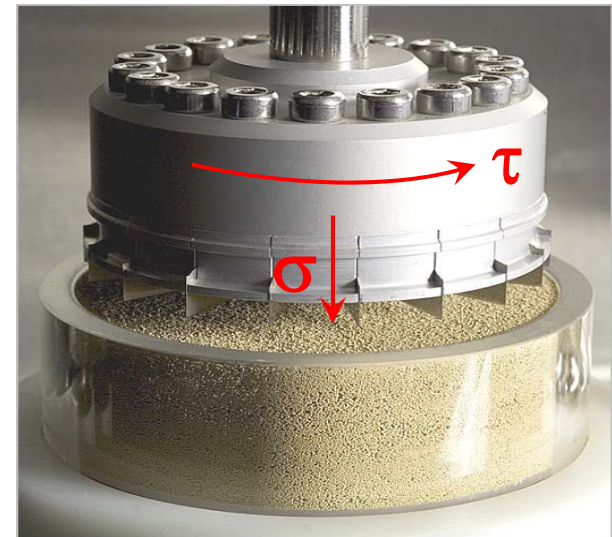
Uni-axial tester not ideal for the many reasons mentioned earlier, so for practical measurements of shear stress for a range of consolidation stresses, a shear cell can be used.

This rotational shear cell example consists of a vessel containing the powder sample and a shear head to induce both vertical and rotational stresses.

The powder sample is subjected to a normal stress σ , whilst slow rotation of the shear head induces a shear stress, τ .

As the powder bed resists the rotation of the shear head, the stress increases until the bed fails or shears, and a maximum shear stress is observed.

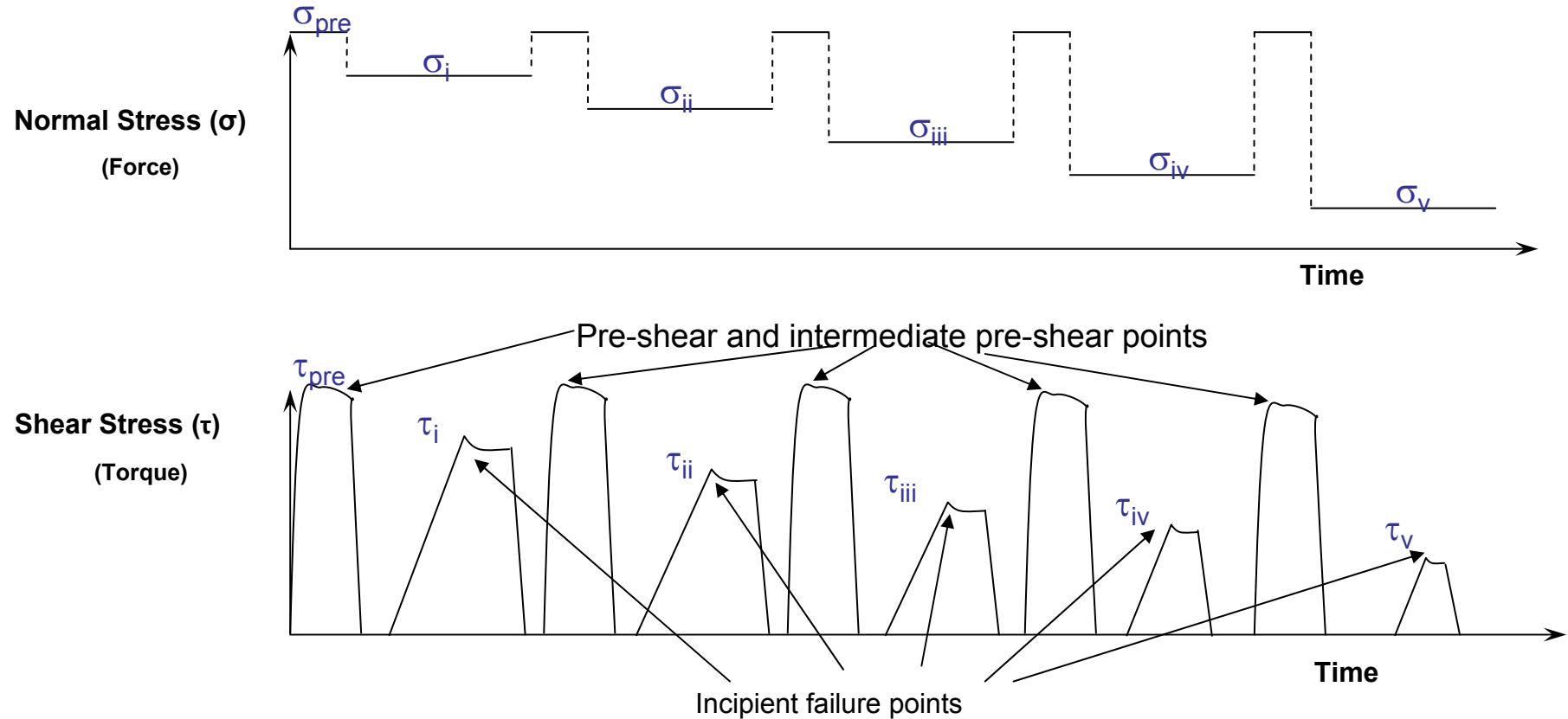
This is the point of *Incipient Failure*



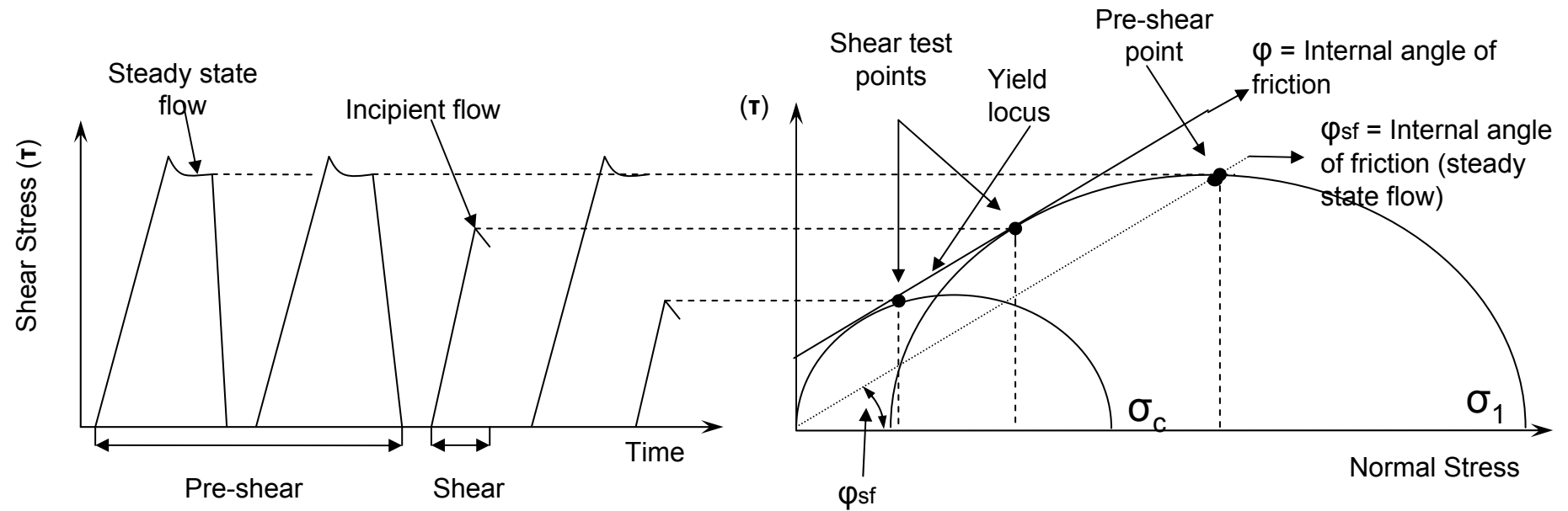
Pre-shearing

- A pre-shearing step is carried out at the start of any test and between each measurement point.
- It is designed to create a uniform shear plane within the powder for the given consolidating stress.
- Intermediate pre-shearing occurs between shear tests to re-establish a uniform shear plane in the powder after the powder has been sheared to failure at the test normal stress (lower than the consolidation stress).

Shear Test



The incipient failure points allow you to define the limits of flow of the powder – the yield locus – to which major and minor Mohr's circles can be fitted



Mohr stress circles can be drawn under the yield loci to determine the unconfined yield strength and the major principle stress.

Pro-rating

- For all types of tester, the pre-shears should, ideally, achieve the same level of shear stress at the same consolidating stress.
- However due to inevitable variability in the shear plane it can often produce a drop of in the pre-shear stress through the test.
- To minimise the effect of this drop off, the shear stress at each shear point (τ_s) is normalised by the use of the equation presented on the right.
- τ_s' is then plotted against the corresponding normal stress.

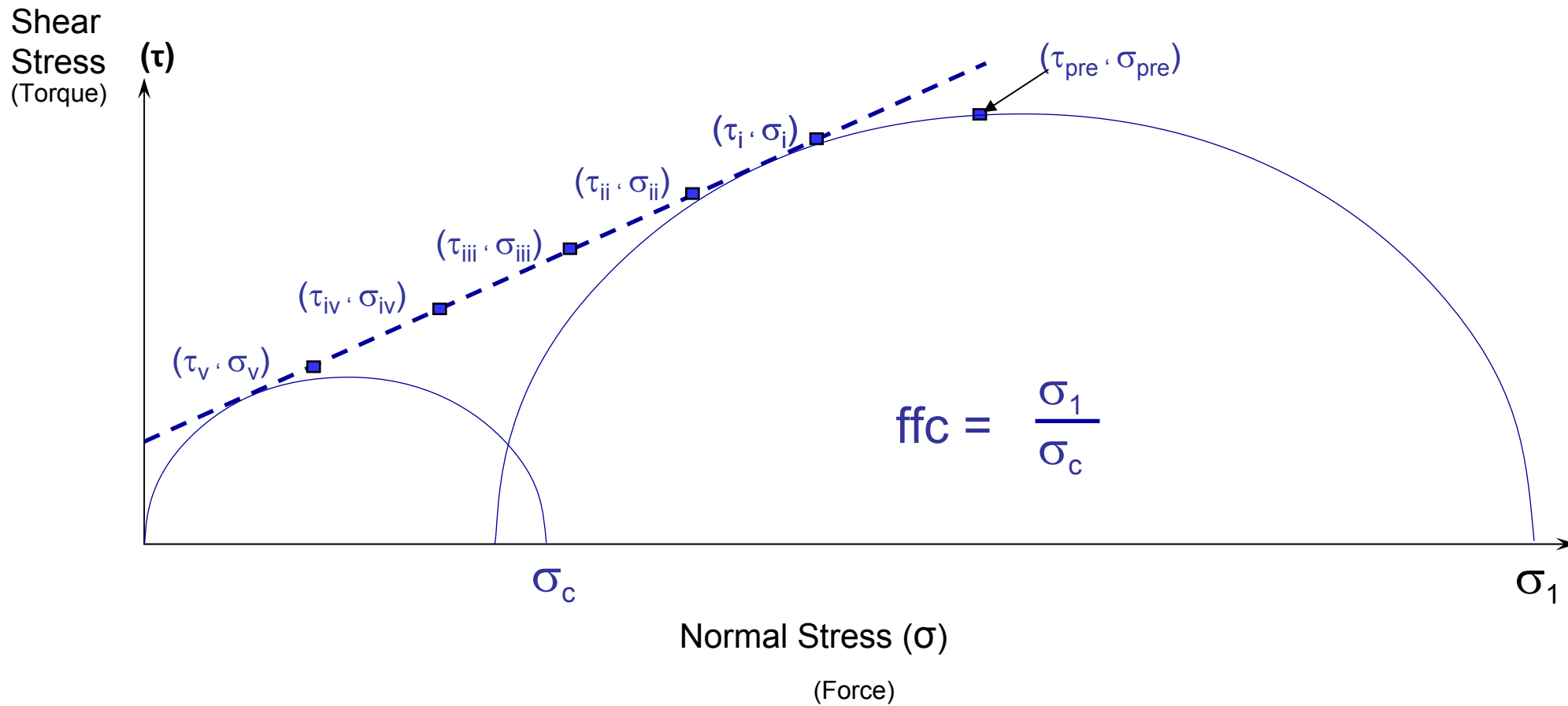
$$\tau_s' = \tau_s \frac{\overline{\tau_p}}{\tau_p}$$

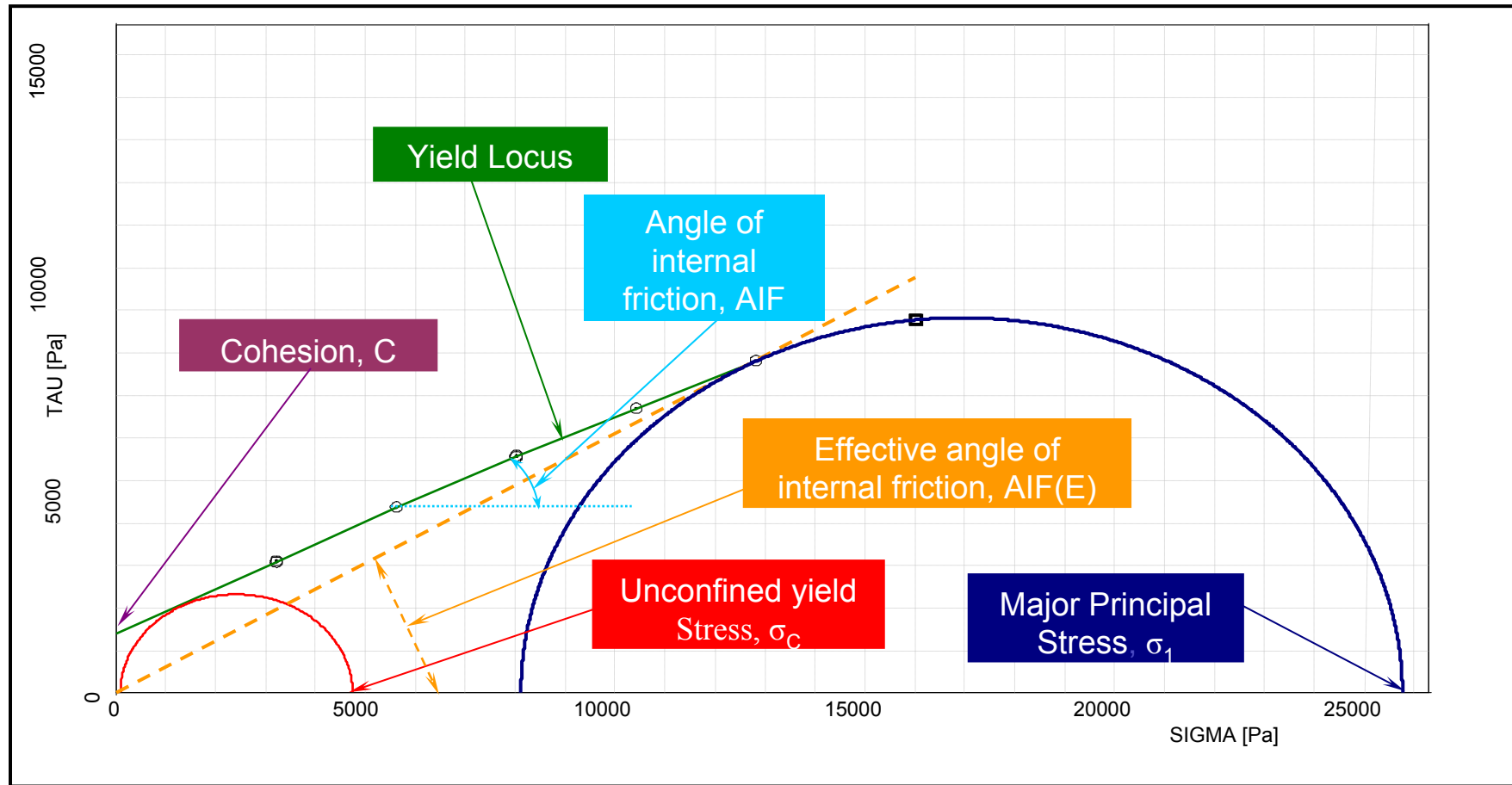
τ_s = measured shear stress

τ_s' = prorated shear stress

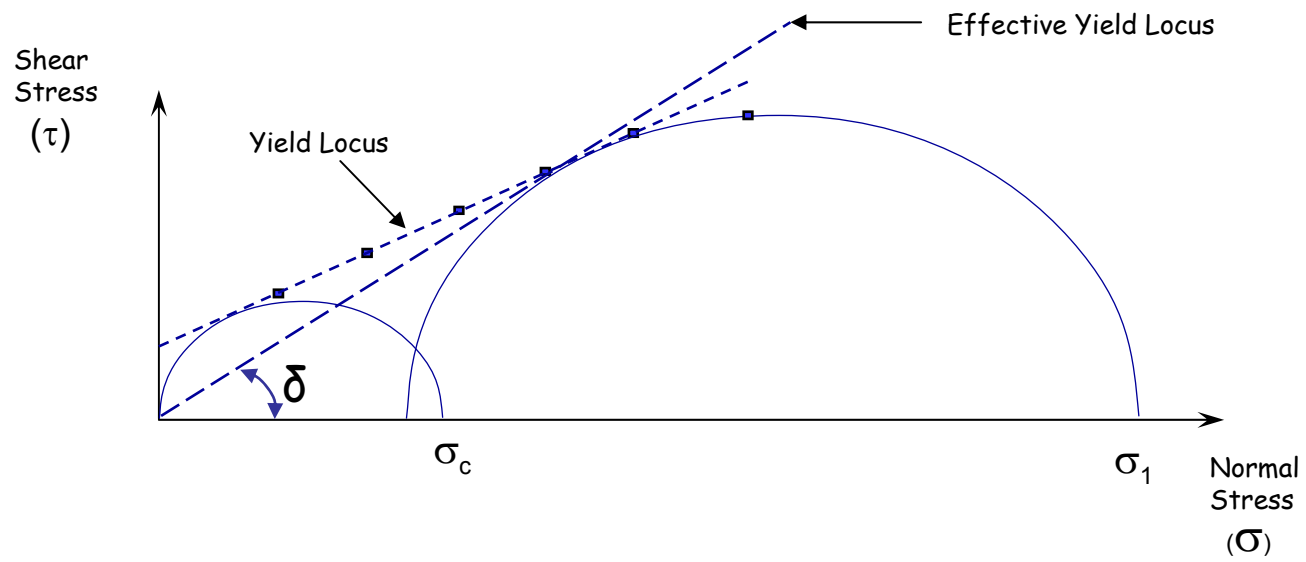
τ_p = pre-shear stress
corresponding to τ_s

$\overline{\tau_p}$ = average of the pre-shear
shear stresses





$$\text{Flow function, } FF = \frac{\sigma_1}{\sigma_c}$$

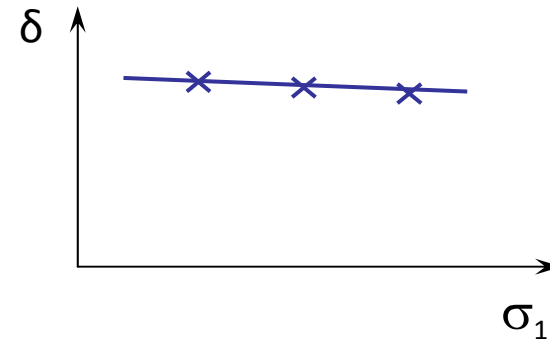
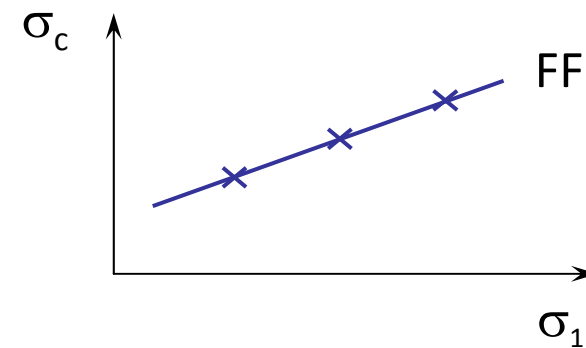
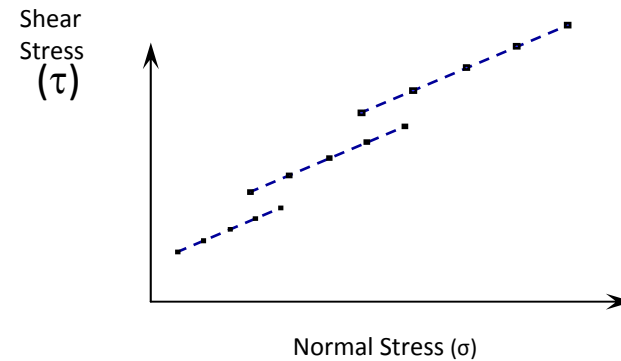


Mohr stress circles and the Yield Locus

Yield Loci can be measured for a range of consolidation stresses (typically 3, 6 & 9kPa) to give σ_1/σ_c data pairs

The Flow Function can then be plotted.....

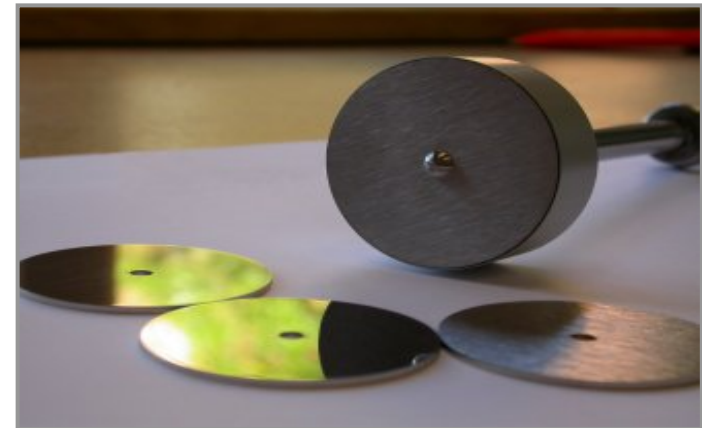
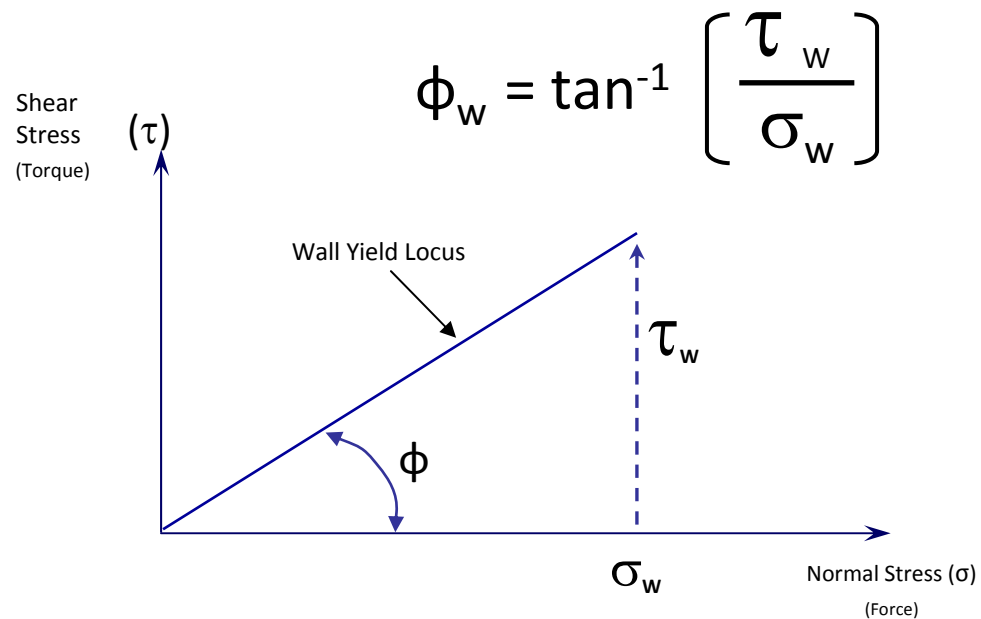
.....as can the effective angle of internal friction versus major consolidating stress



Wall Friction Angle

The Wall Yield Locus can be measured using a representative sample of the material used to construct the vessel containing the powder. This relates the shear stress at the wall of the hopper and the corresponding normal stress.

These two stress can be plotted and define the Wall Friction Angle, ϕ_w



Bibliography

- Jenike, A. W. 1964, *Storage and Flow of Solids*, University of Utah, Bulletin 123.
- Schulze, D. 2008, *Powders and bulk solids. Behavior, characterization, storage and flow*, 2 edn, Springer-Verlag,
- 'Standard Shear Testing Technique for particulate solids using the Jenike shear cell', IChemE/EFCE, 1989
- Roberts, A. W. 1993, *Basic Principles of Bulk Solids Storage, Flow & Handling* TUNRA Bulk Solids Research Associates.
- Williams, J.C., Birks, A.H., Bhattacharya, D., *The direct measurement of the failure function of a cohesive powder*, Powder Technology, 4, 1970/71, 328-327

Appendix 2. Hopper Design Software Tool

A software tool has been developed in conjunction with Freeman Technology. It takes shear, wall friction and compressibility data produced by the FT4 Powder Rheometer and generates hopper designs for axi-symmetric conical and plane flow hoppers.

The program can be accessed from the drop down menus available within the proprietary post processing software package 'Data Analysis' (DA) and the output is a spreadsheet that includes all the intermediate calculations and derived data. It requires a minimum of three sets of shear cell data taken at different consolidating stresses, a set of wall friction data and a set of compressibility for the expert system to operate, but adding repeat data sets to the analysis is possible.

The following pages show a presentation of the method of calculation which is based on the work of Jenike and, later Roberts. In addition a worked example is presented to show the form of the spreadsheet output.

Further expansion of this expert system is possible, to include

- Core flow designs
- Option to use
 - Non-linear fitting of yield locus
 - Non-linear fitting of Flow Function
- Pyramid type bins (e.g. IBC's)

Hopper Design Using FT4 Powder Rheometer Data

Mass Flow Hopper Design

- There are 2 criteria which define the limits of the bin to operate in a mass flow mode
 - Outlet size, B
 - Hopper half angle, α
- Both result from calculations which use data generated from shear cell, wall friction and compressibility testing

The shear properties of the bulk material present a resistance to gravity discharge

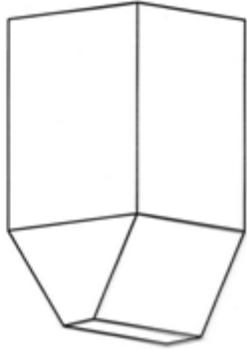
- For flow to occur, the material at the hopper outlet must not have sufficient strength to support the rest of the material (hence the need to correctly define B & α)

Note: the material in the converging section must be able to dilate, so even if B has been calculated correctly, a wrongly sized valve/feeder will destroy the mass flow regime

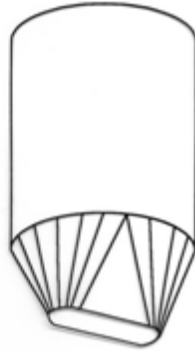
Bin Shapes



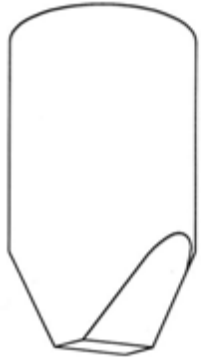
conical



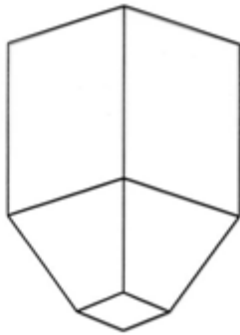
plane flow



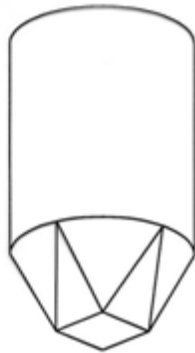
transition



chisel, plane flow



pyramid



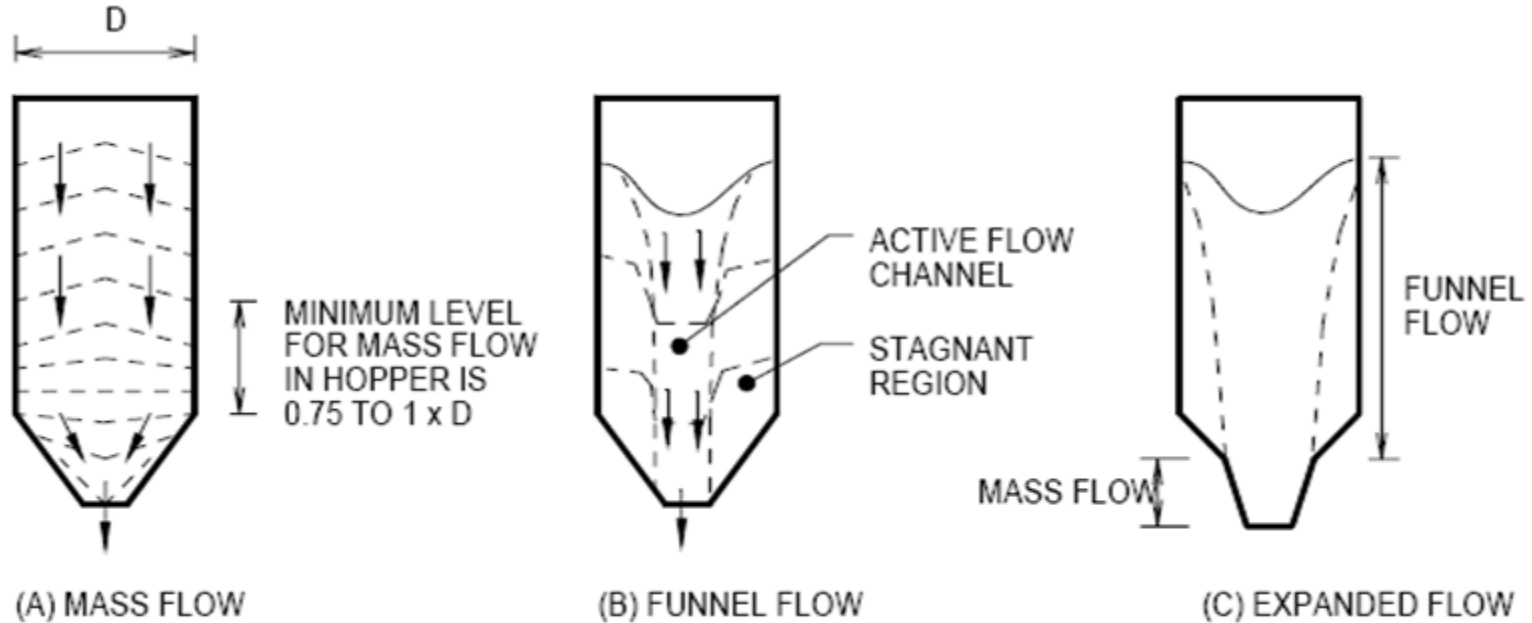
square opening

There are many designs of bin: -

- Conical
- Plane Flow
- Transition
- Chisel, plane flow
- Pyramid
- Square

The calculations on the following slides are based on a conical design

Modes of Flow



Mass flow is the preferred mode in the majority of operations

- Provides 'first in, first out' regime
- Flow is more consistent
- Full bin capacity is used

Shear testing program

- Based on knowledge of operational & spatial requirements, powder can be tested appropriately
 - evaluate bulk density
 - define consolidation loads
 - select hopper wall material
- Methodology set out in
 - ‘Standard Shear Testing Technique for particulate solids using the Jenike shear cell’, IChemE/EFCE, 1989

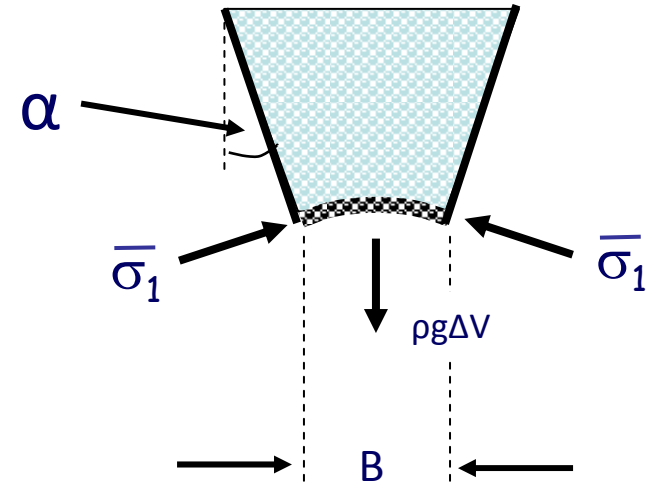
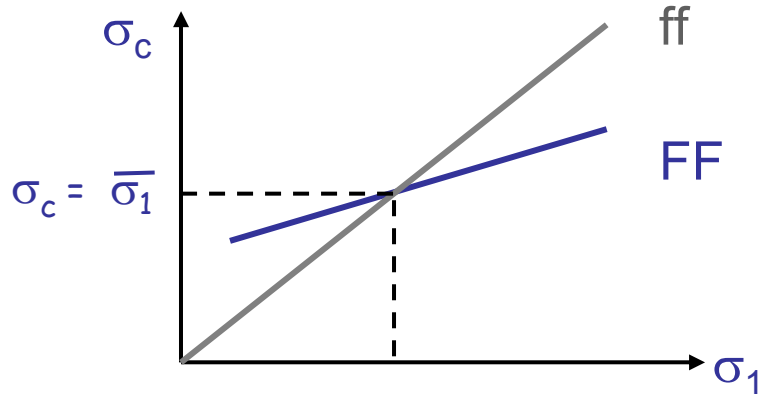
- Measure properties of the material
 - Shear – how easily the material will flow over itself
 - Wall friction – how easily the material will flow over the inner surface of its container
 - Density – how this changes with consolidation stress

Theory

The illustration on the right shows a hopper containing powder.

The stress in the arch $\bar{\sigma}_1$ is a function of both the span and the major consolidating pressure, σ_1

The critical opening dimension, B , for the “flow / no flow” condition is obtained for defined by the intersection of the Flow Function (FF) and Flow Factor (ff) plot, $\sigma_c = \bar{\sigma}_1$



α = Hopper half angle

ρ = density

g = acceleration due to gravity

ΔV = volume of arch

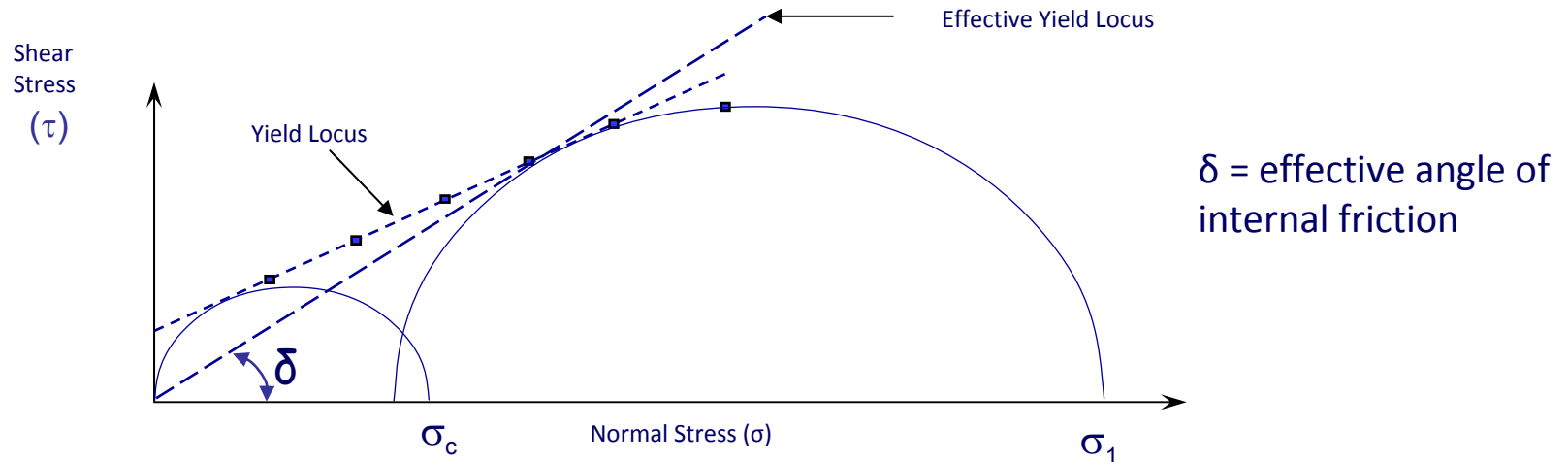
where σ_c = Unconfined Yield Strength

Deriving the Flow Function, FF

The bulk strength, represented by the Flow Function, is the relationship between the Unconfined Yield Strength, σ_c and the Major Consolidation Stress, σ_1 , where: -

$$FF = \frac{\sigma_1}{\sigma_c}$$

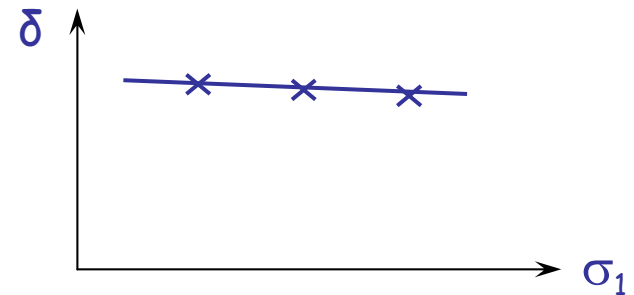
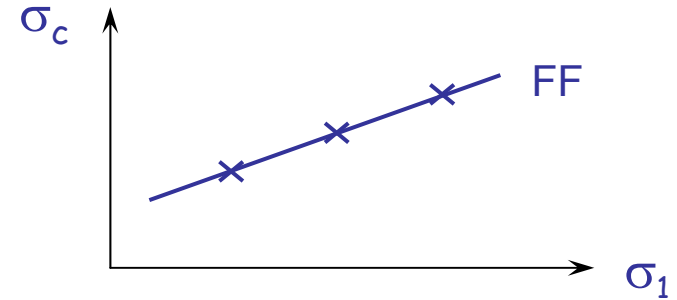
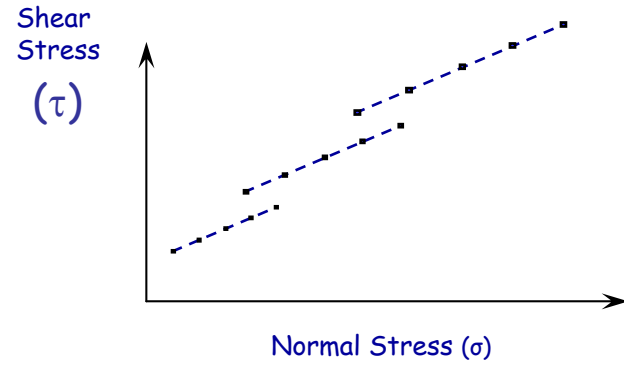
Using the FT4 Shear Cell, Yield Loci can be measured and Mohr circle stress analysis applied for the derivation of σ_c and σ_1



Yield Loci can be measured for a range of consolidation stresses (typically 3, 6 & 9kPa)

The Flow Function can then be plotted.....

.....as can the effective angle of internal friction versus major consolidating stress

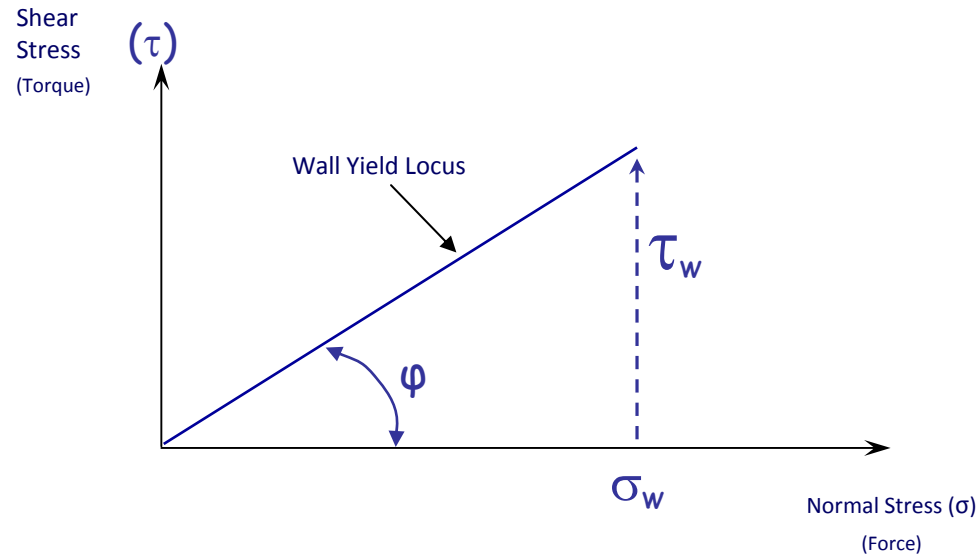


Measuring Wall Friction

Using the FT4 Wall Friction module, the Wall Yield Locus can be measured. This relates the shear stress at the wall of the hopper and the corresponding normal stress.

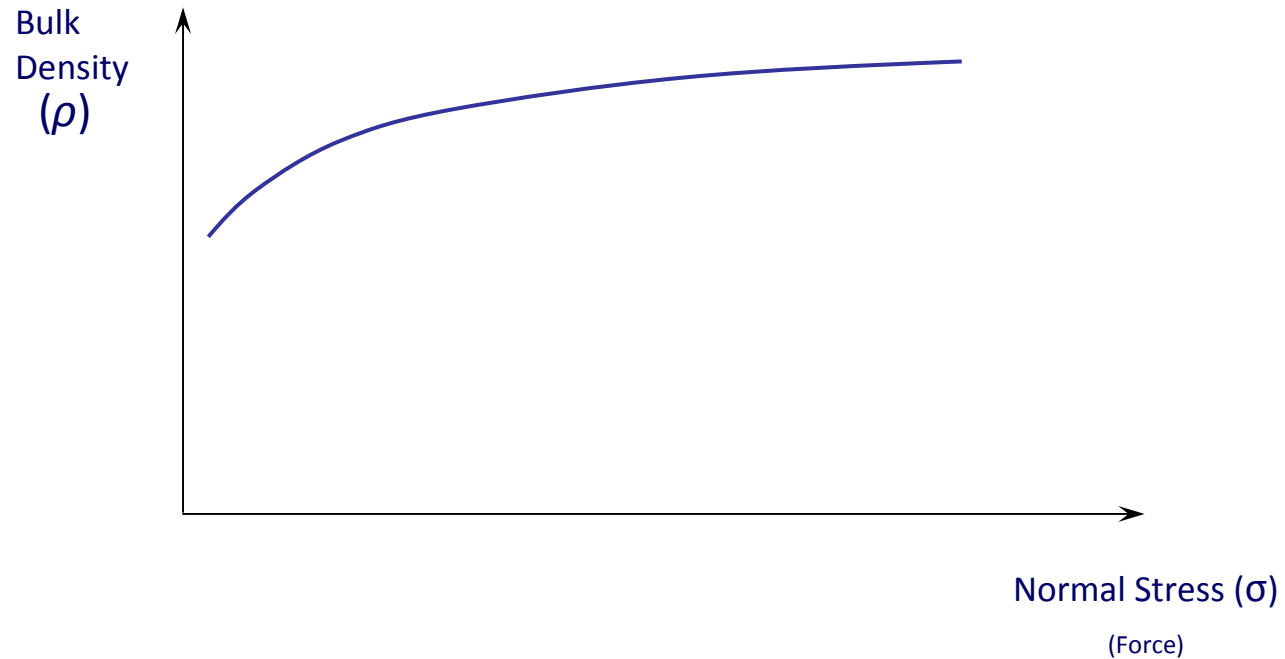
These two stress can be plotted and define the Wall Friction Angle, ϕ

$$\phi = \tan^{-1} \left[\frac{\tau_w}{\sigma_w} \right]$$



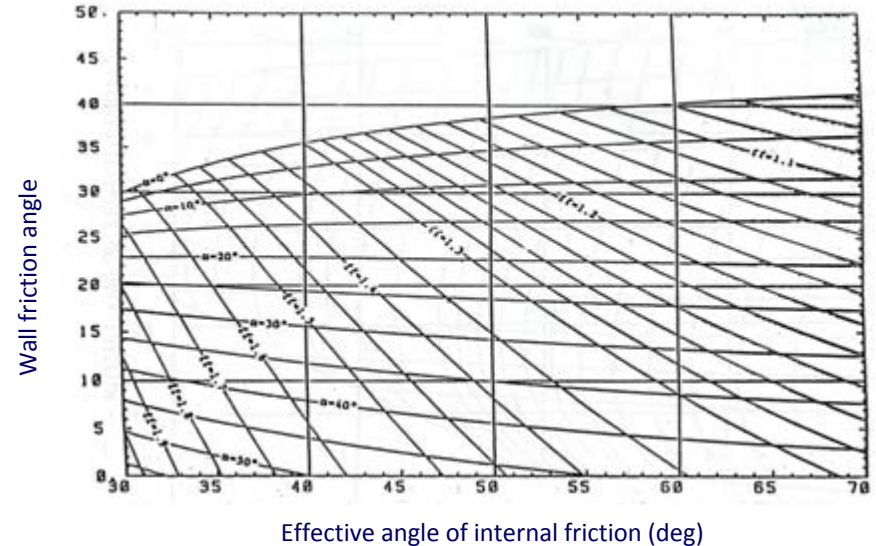
Measuring Bulk Density

Using the FT4 Compressibility method, the powder density can be measured as a function of applied normal stress



Calculating Hopper Half Angle

Hopper half angle (α) can be generated graphically from the relationship between wall friction angle (ϕ) and the effective angle of internal friction (δ)



It can also be calculated using the following equations: -

$$\alpha = \frac{\pi}{2} - \frac{1}{2} \cos^{-1} \frac{(1 - \sin \delta)}{2 \sin \delta} - \beta$$

where

$$\beta = \frac{1}{2} \left\{ \phi + \sin^{-1} \frac{\sin \phi}{\sin \delta} \right\}$$

Calculating Flow Factor, ff

The Flow Factor (ff) is a function of the effective angle of internal friction (δ), the hopper half angle (α) and the wall friction angle (ϕ).

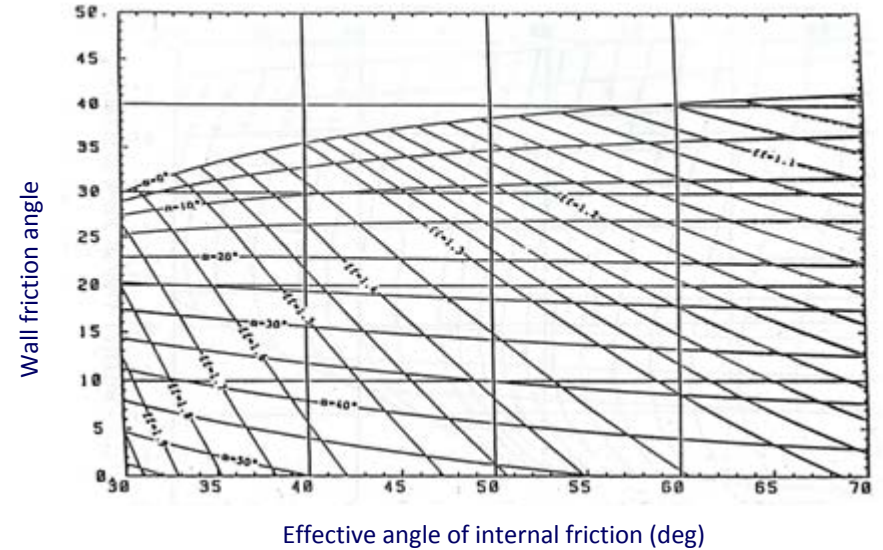
It is based on the flow stress field in the hopper and can be derived graphically or calculated from the following equations: -

$$ff = \frac{Y(1 + \sin \delta)H(\alpha)}{2(X - 1)\sin \alpha}$$

where

$$X = \frac{2^m \sin \delta}{1 - \sin \delta} \left[\frac{\sin(2\beta + \alpha)}{\sin \alpha} + 1 \right]$$

$$Y = \frac{[2(1 - \cos(\beta + \alpha))]^m (\beta + \alpha)^{1-m} \cdot \sin \alpha + \sin \beta \cdot \sin^{1+m}(\beta + \alpha)}{(1 - \sin \delta) \cdot \sin^{2+m}(\beta + \alpha)}$$

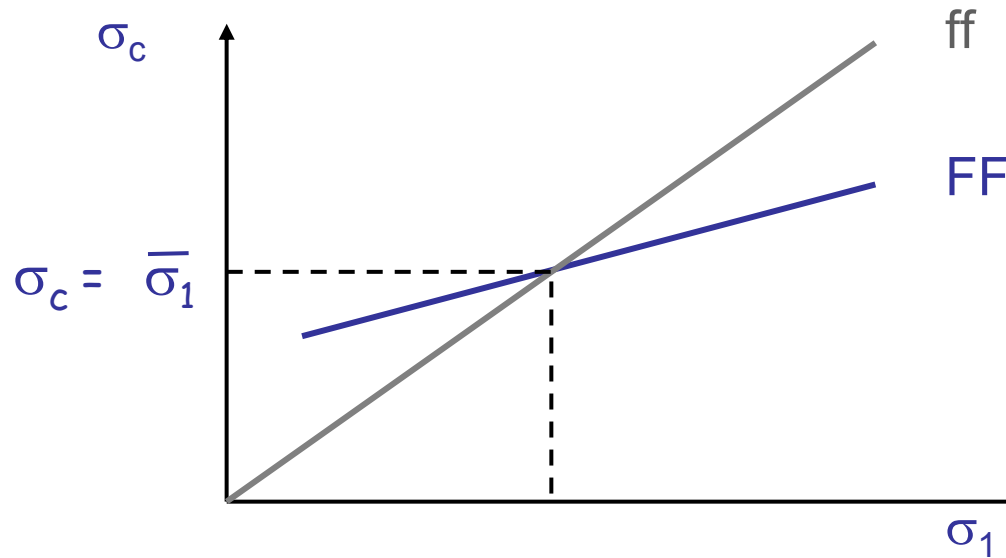


$$H(\alpha) = \left[\frac{(130 + \alpha)}{65} \right]^m \left[\frac{(200 + \alpha)}{200} \right]^{(1-m)}$$

Note: All Angles in the equations are in Radians apart from H(α) which uses Degrees

Calculating the stress in the arch

Plotting the Flow Function and Flow Factor on the same graph allows the intercept to be identified. At this point $\sigma_c = \bar{\sigma}_1$, the stress in the arch at the boundary of the “flow / no flow” condition.



Force Balance

Force balance on the arch
reduces to :-

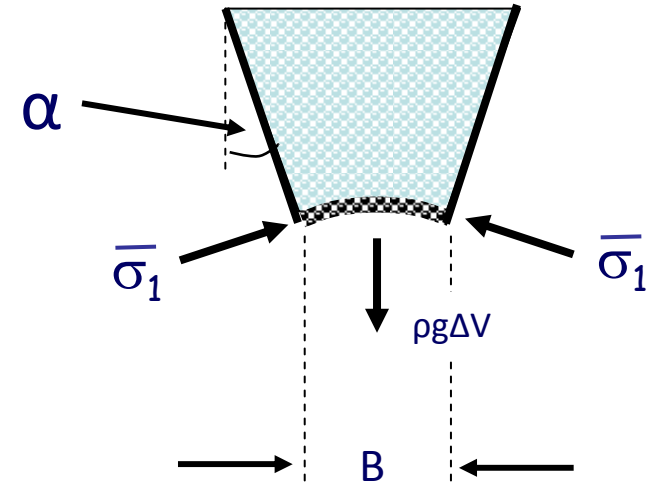
$$\frac{\bar{\sigma}_1}{\rho g} = 2R$$

$$R = \frac{A}{P} = \text{'Hydraulic Radius'}$$

$$R = \frac{\text{Area of Cross-section}}{\text{Effective Perimeter}} = \frac{B}{2(m+1)}$$

Where m is the symmetry factor

- m = 1 for axi-symmetric
- m = 0 for plane-flow



α = Hopper half angle

ρ = density

g = acceleration due to gravity

ΔV = volume of arch

Basic design equation

$$B = \frac{\bar{\sigma}_1 H(\alpha)}{\rho g}$$

- B is the outlet diameter (metres)
- $\bar{\sigma}_1$ is the consolidating stress generated in an arch at the outlet (kPa)
- $H(\alpha)$ is a function that takes account of variation in arch thickness, hopper half angle & hopper geometric configuration
- ρ is the bulk density when consolidated at $\bar{\sigma}_1$ (kg/m³ or g/ml)
- g is the accⁿ due to gravity (9.81m/s²)

Considerations

Effective angle of internal friction

- As part of the analysis, a yield locus is measured for each consolidating stress
- From each yield locus an effective angle of internal friction (δ) is derived
- However, it is typical that there is some variation in δ with consolidating stresses
- The standard approach is to take an average of the three values of δ and use this in the calculations of hopper half angle, α and Flow Factor, ff

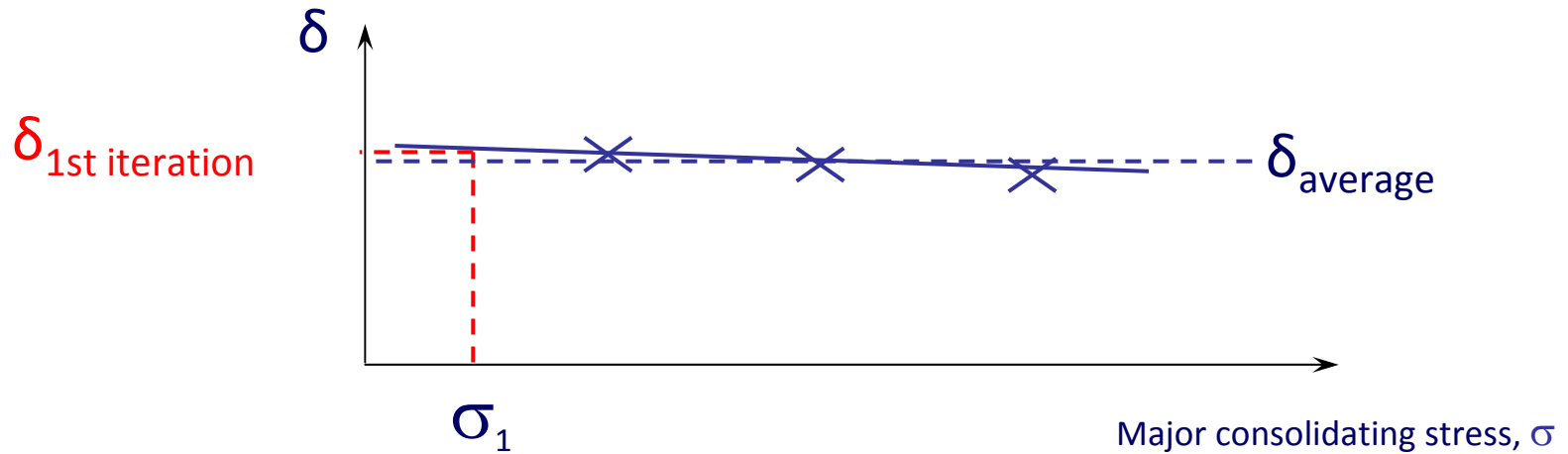
Flow Function

- The intersection of the Flow Function, FF and Flow Factor, ff is normally at a stress level below the those stresses actually measured in the shear cell tests
- Therefore the point of intersection is subject to variability as a result of the fact that the FF is extrapolated backwards
- If the Flow Function is substantially linear, then this variability is typically small,

Iteration

In order to minimise errors as a result of using the average of the effective angle of internal friction, one or more iterations can be completed, as follows:-

Having calculated the stress in the arch, $\bar{\sigma}_1$, and the corresponding major consolidation stress, σ_1 , using the average value of δ and an extrapolation of the Flow Function, σ_1 , can be fed back into the plot of effective angle of internal friction versus major consolidation stress, to provide a new value of effective angle of internal friction, $\delta_{1st\ iteration}$



If the difference between the first value of δ used and $\delta_{1st\ iteration}$ is less than 1 degree, then this is unlikely to have much of an effect on the hopped half angle and outlet size.

However, iterations should be repeated until the values of α and B do not change significantly.

Design Factors Post Calculation

- An increase in outlet size of 20% is typically introduced to allow for some variation in powder properties and environment
- Also a 3° decrease in the hopper half angle, for the same reasons

Note that a significant change in flow properties of the powder or frictional properties of the bin may prohibit mass flow operation

Worked example

Using the FT4.....

Generate **shear cell** data for (typically) 3, 6, 9kPa consolidating loads. This gives: -

- Flow Function (FF)
- Effective Angle of Internal Friction (δ)

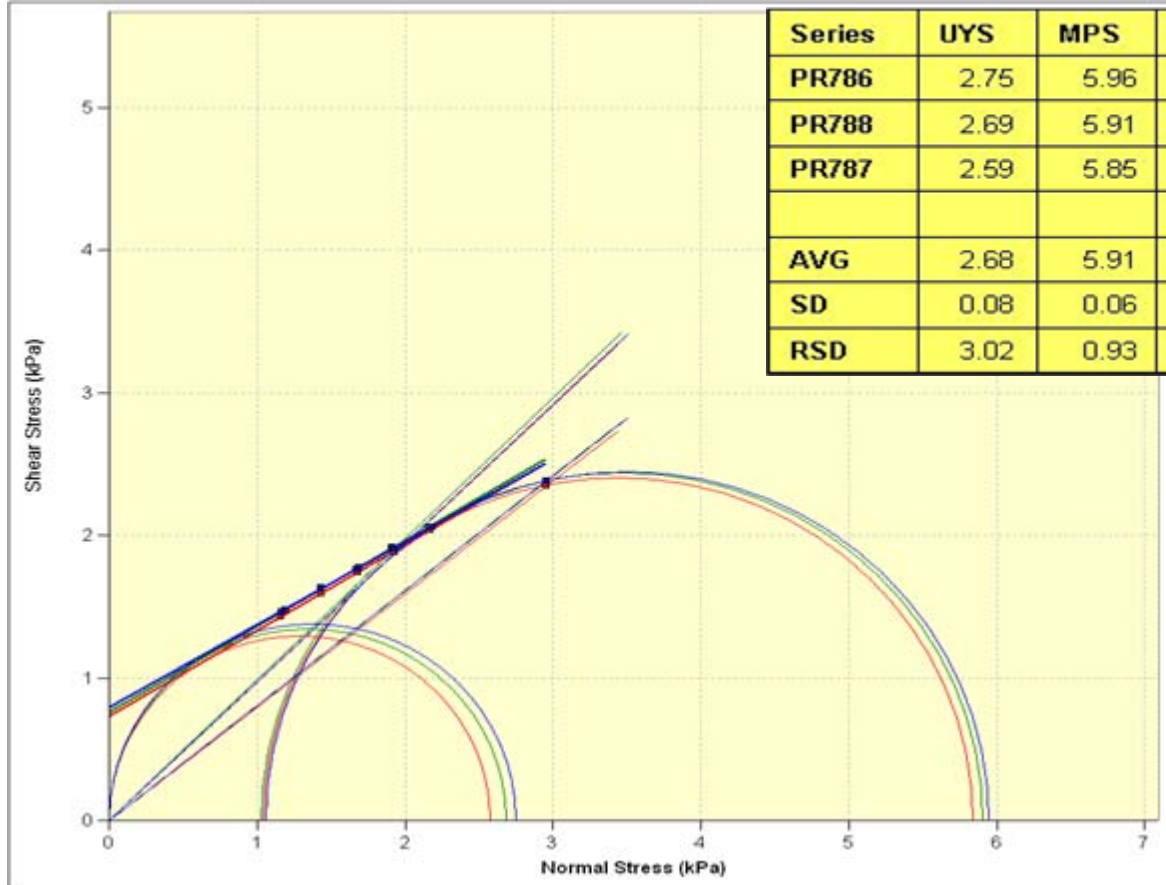
Generate **wall friction** data with the materials likely to be used for the bin. This gives: -

- Wall Friction Angle (ϕ)

Generate compressibility data to characterise the relationship between bulk density and consolidating load. This gives: -

- Bulk Density (ρ)

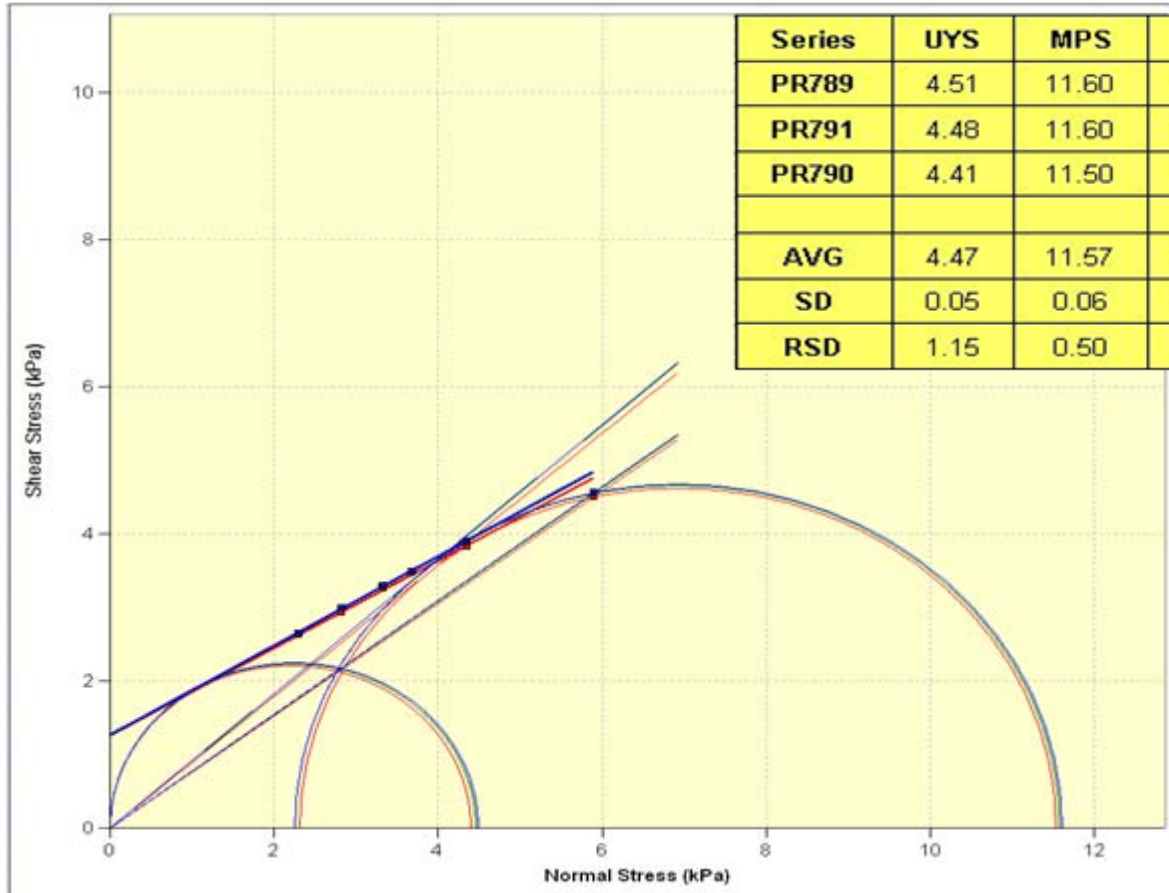
Typical Shear Cell data – 3kPa



Series	UYS	MPS	C	f_f	AIF	AIF (E)	AIF (SS)	BD
PR786	2.75	5.96	0.79	2.16	30.10	44.20	38.90	0.66
PR788	2.69	5.91	0.76	2.20	31.00	44.70	38.90	0.66
PR787	2.59	5.85	0.73	2.26	31.00	44.20	38.50	0.66
AVG	2.68	5.91	0.76	2.21	30.70	44.37	38.77	0.66
SD	0.08	0.06	0.03	0.05	0.52	0.29	0.23	0.00
RSD	3.02	0.93	4.01	2.28	1.69	0.65	0.60	0.32

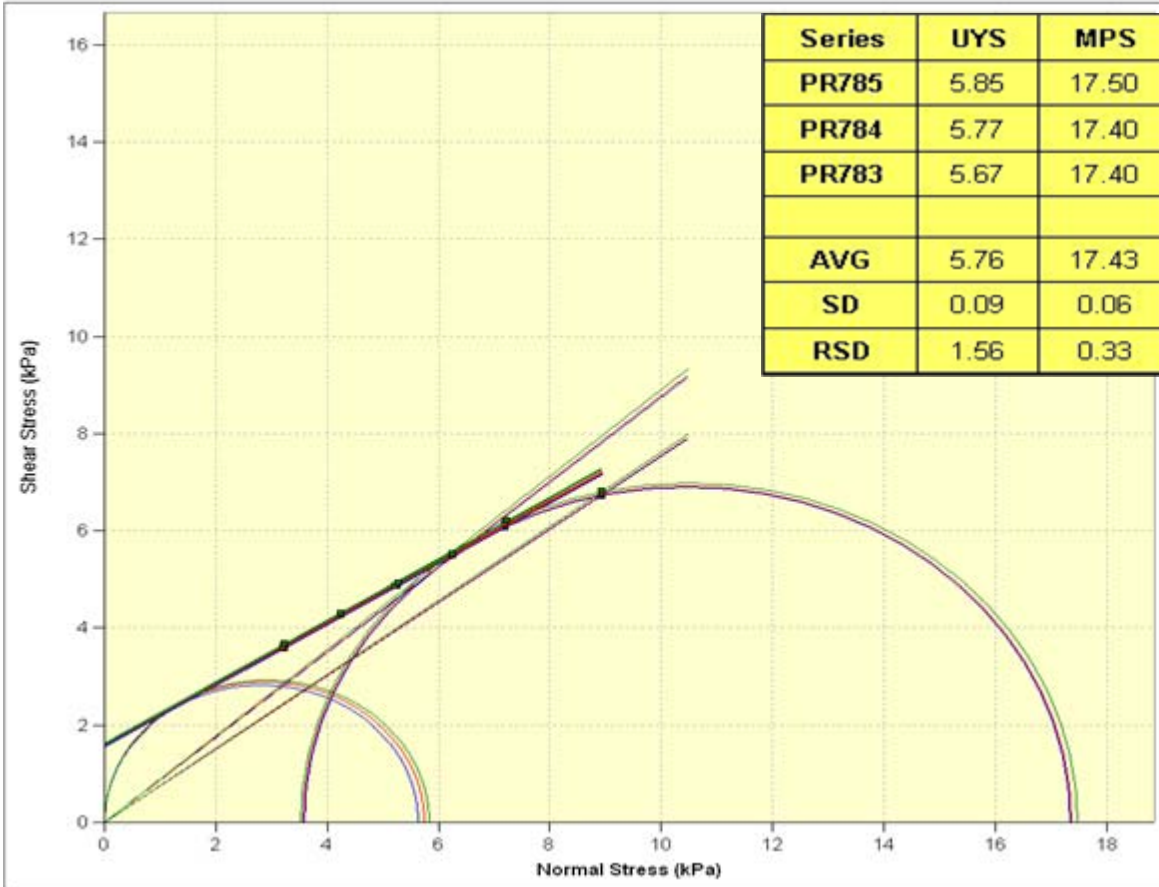
Data shows results of shear test run on three separate samples

Typical Shear Cell data – 6kPa



Data shows results of shear test run on three separate samples

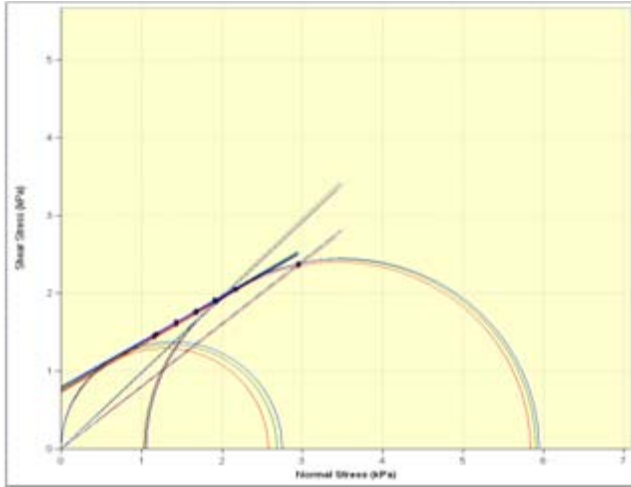
Typical Shear Cell data – 9kPa



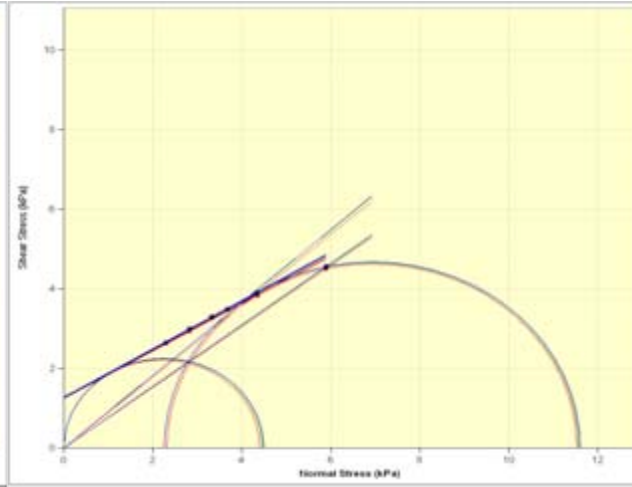
Series	UYS	MPS	C	ffc	AIF	AIF (E)	AIF (SS)	BD
PR785	5.85	17.50	1.61	2.99	32.40	41.60	37.30	0.71
PR784	5.77	17.40	1.60	3.01	32.10	41.30	37.00	0.72
PR783	5.67	17.40	1.57	3.07	32.10	41.10	37.00	0.72
AVG	5.76	17.43	1.59	3.02	32.20	41.33	37.10	0.72
SD	0.09	0.06	0.02	0.04	0.17	0.25	0.17	0.00
RSD	1.56	0.33	1.31	1.38	0.54	0.61	0.47	0.29

Data shows results of shear test run on three separate samples

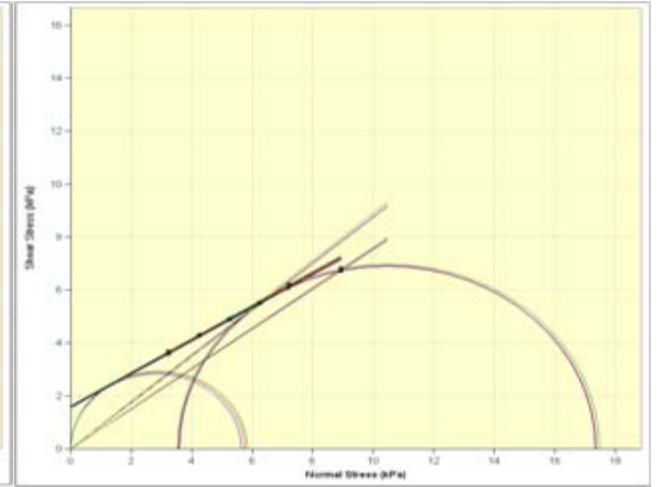
All Yield Loci



3kPa Consolidating Load

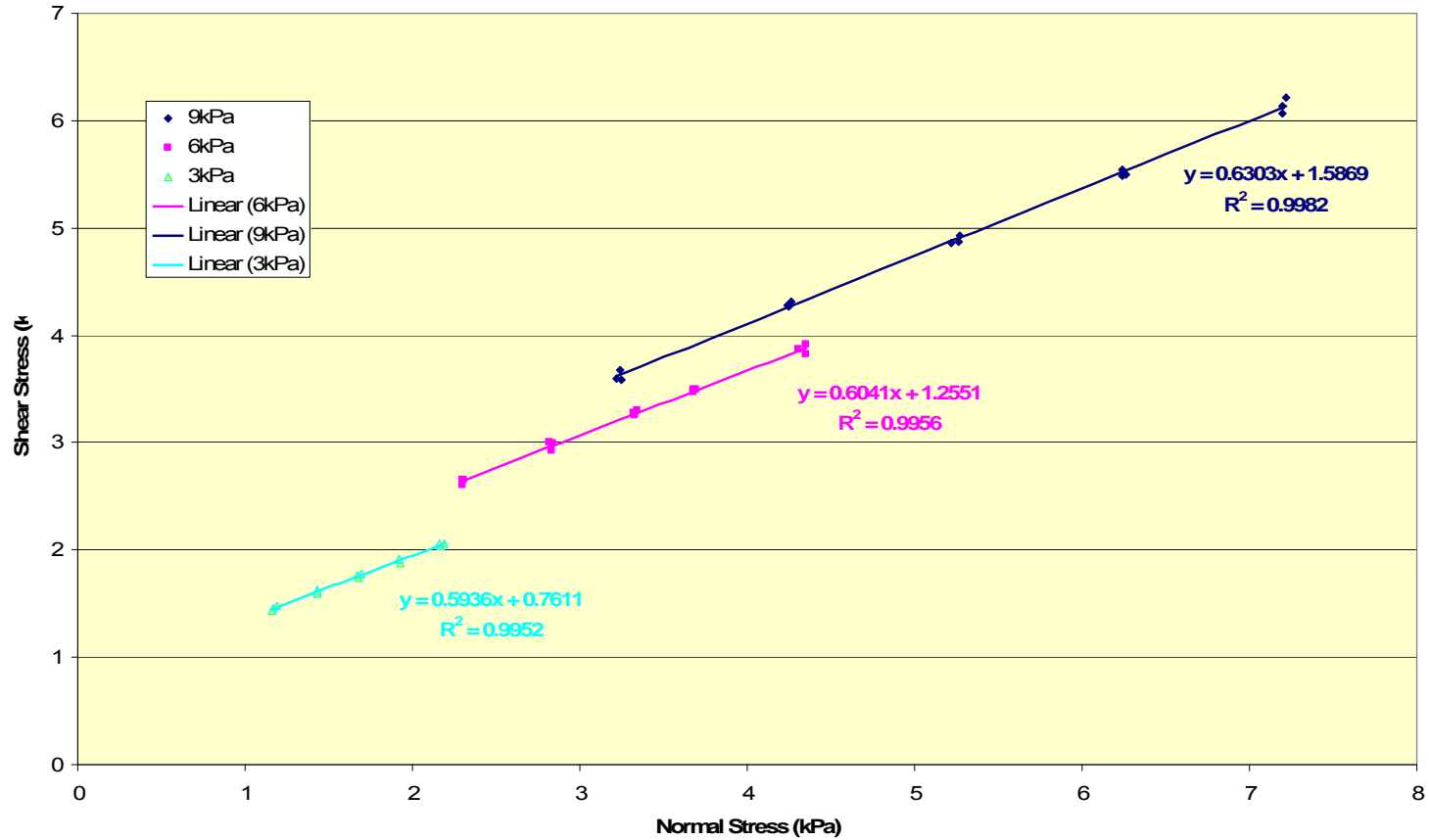


6kPa Consolidating Load

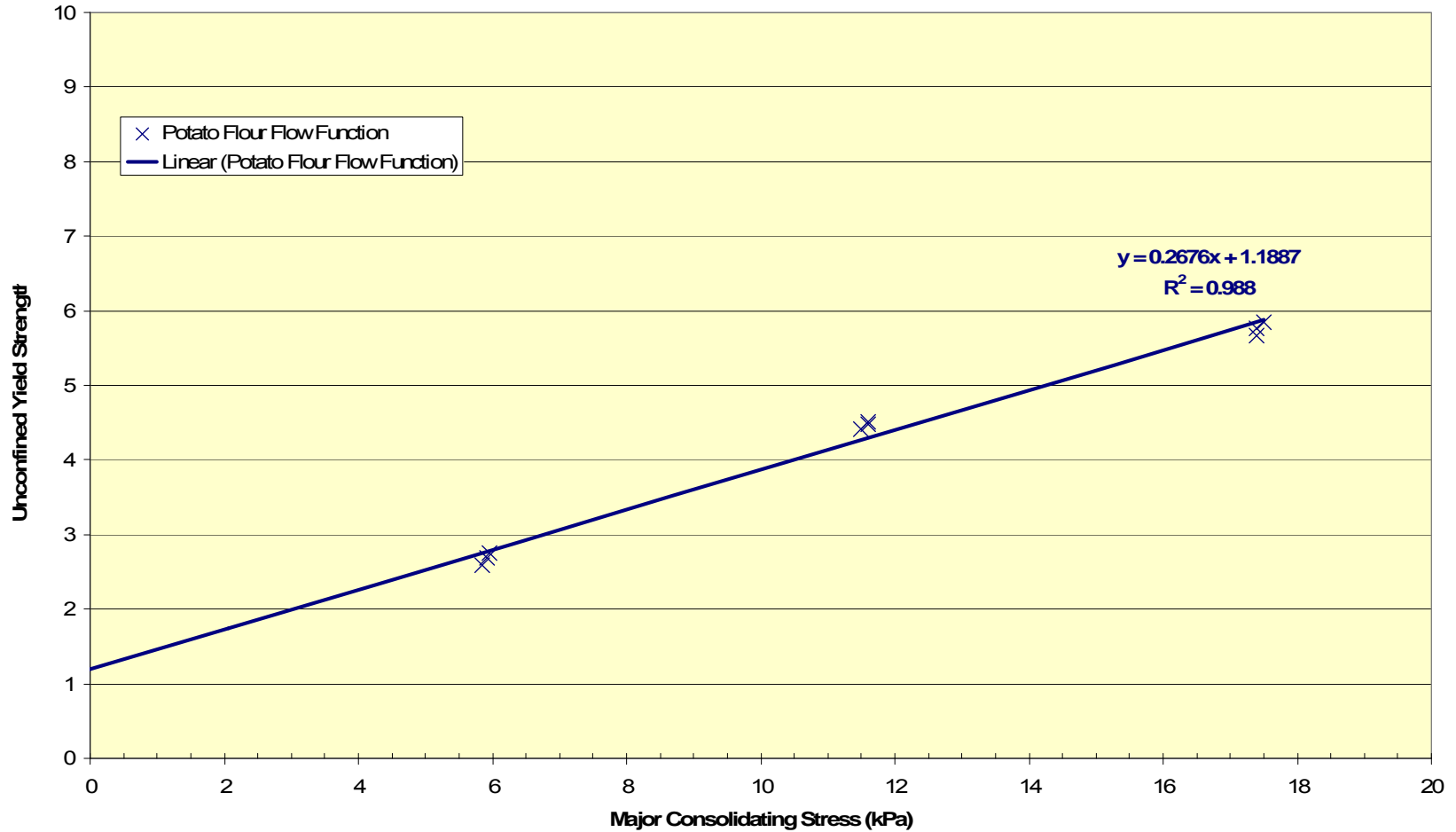


9kPa Consolidating Load

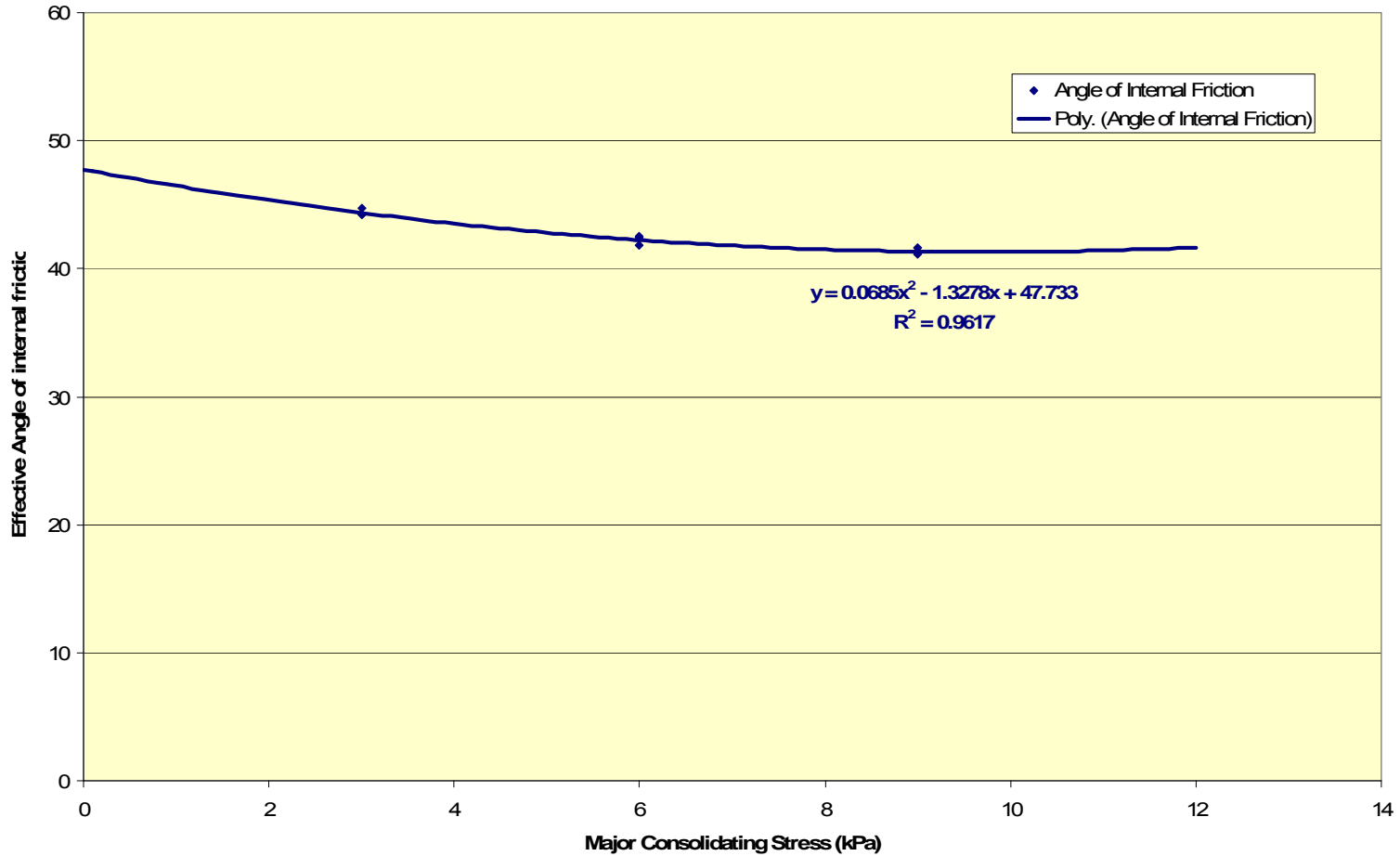
All yield loci plotted on the same graph



Plotting the Flow Function



Effective Angle of Internal Friction vs Major Consolidating Stress



Worked example

Using the FT4.....

Generate **shear cell** data for (typically) 3, 6, 9kPa consolidating loads. This gives: -

- Flow Function (FF)
- Effective Angle of Internal Friction (δ)

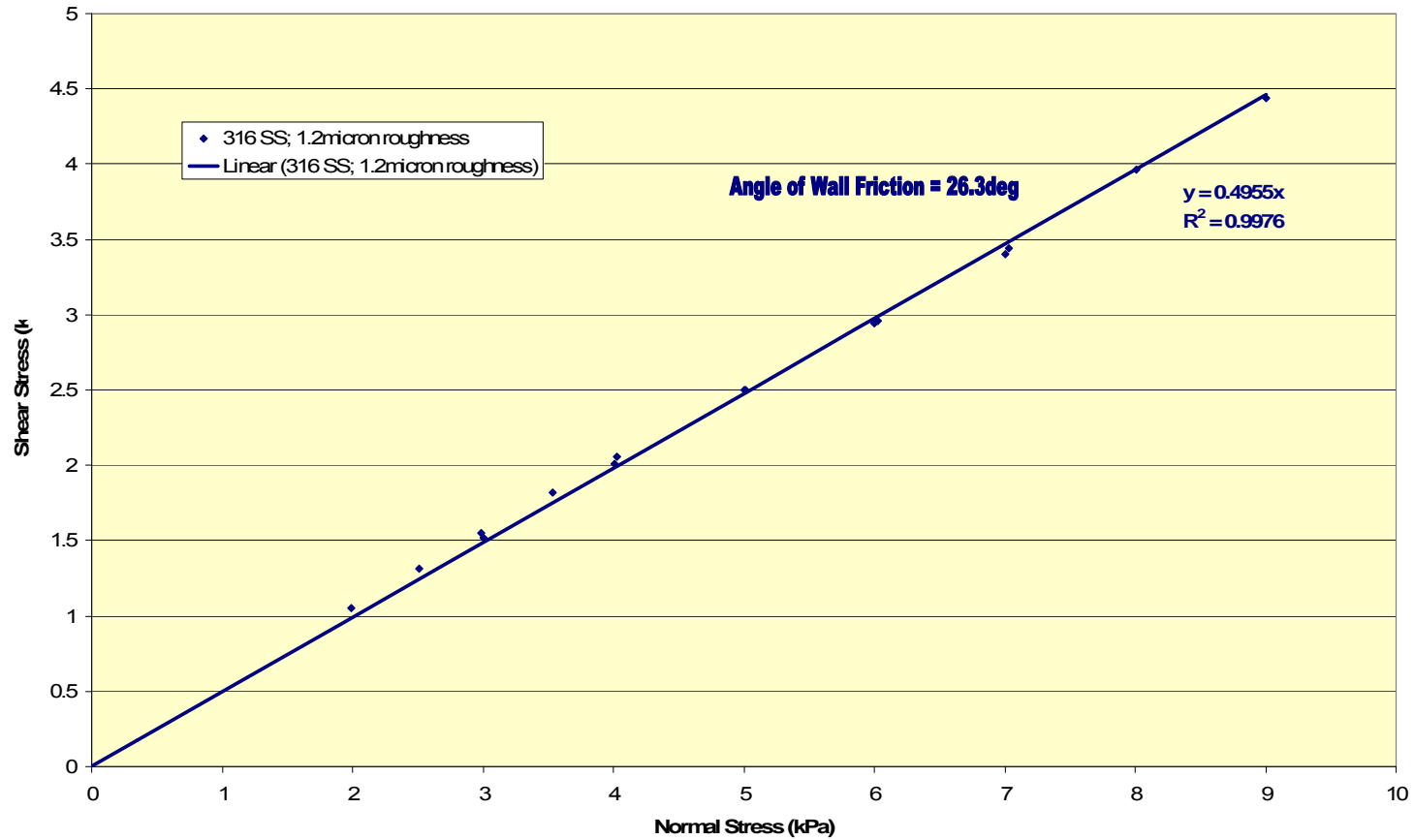
Generate **wall friction** data with the materials likely to be used for the bin. This gives: -

- Wall Friction Angle (ϕ)

Generate compressibility data to characterise the relationship between bulk density and consolidating load. This gives: -

- Bulk Density (ρ)

Wall Friction Angle (ϕ)



Worked example

Using the FT4.....

Generate **shear cell** data for (typically) 3, 6, 9kPa consolidating loads. This gives: -

- Flow Function (FF)
- Effective Angle of Internal Friction (δ)

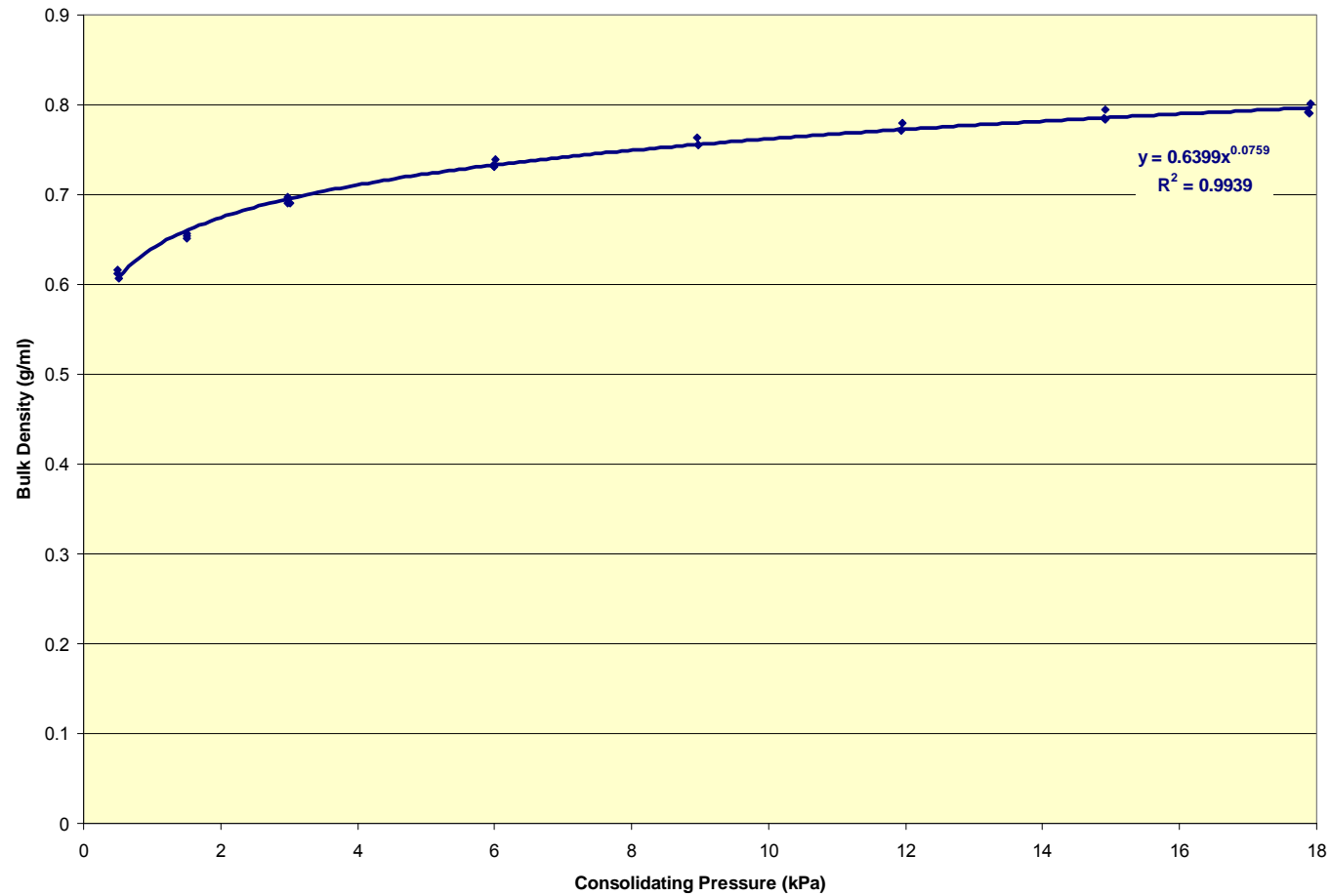
Generate **wall friction** data with the materials likely to be used for the bin. This gives: -

- Wall Friction Angle (ϕ)

Generate compressibility data to characterise the relationship between bulk density and consolidating load. This gives: -

- Bulk Density (ρ)

Determining Bulk Density



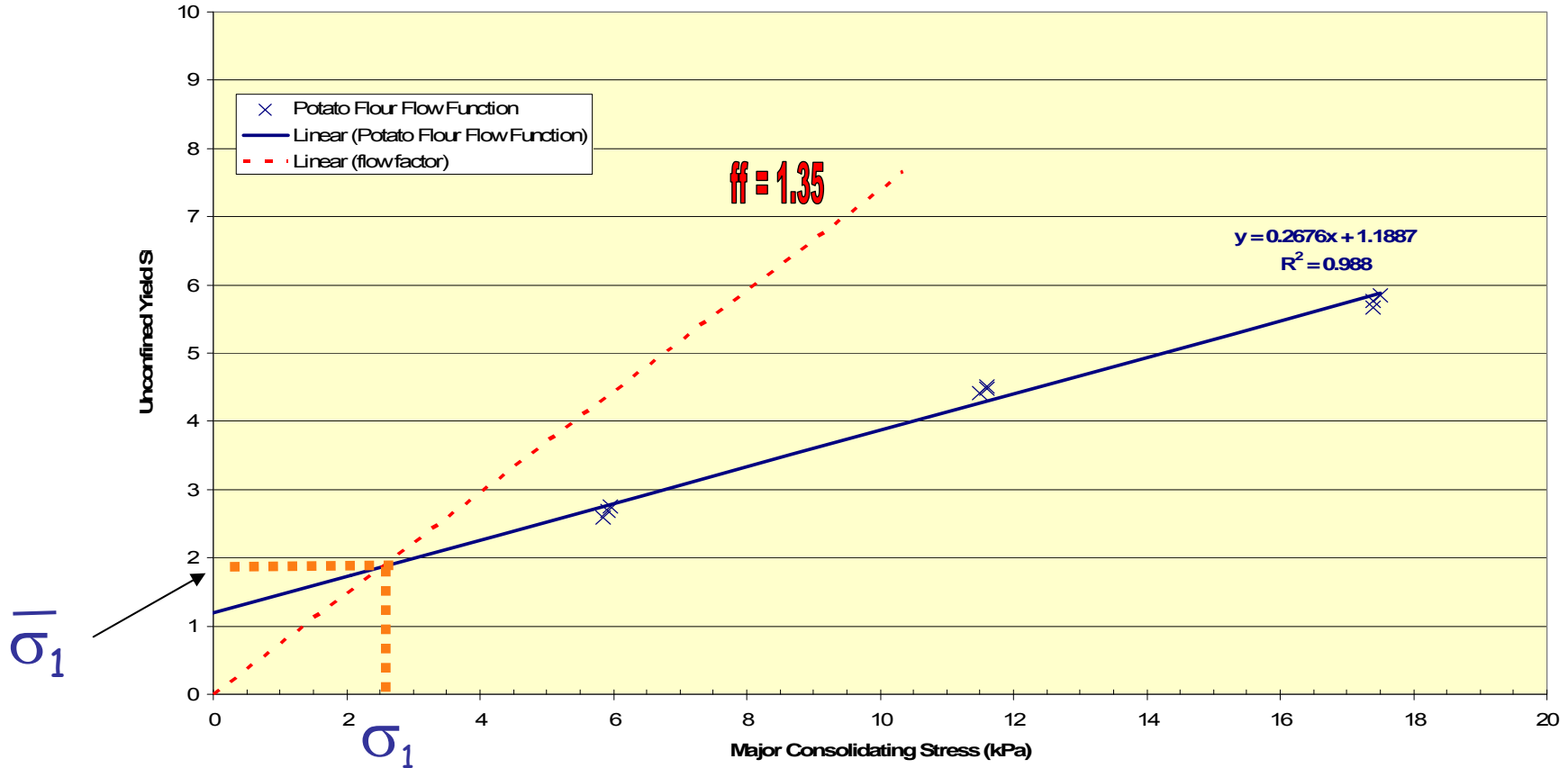
Using the wall friction angle and the average value of the effective angle of internal friction, calculate all other parameters.....

ϕ	δ
26.3	42.7

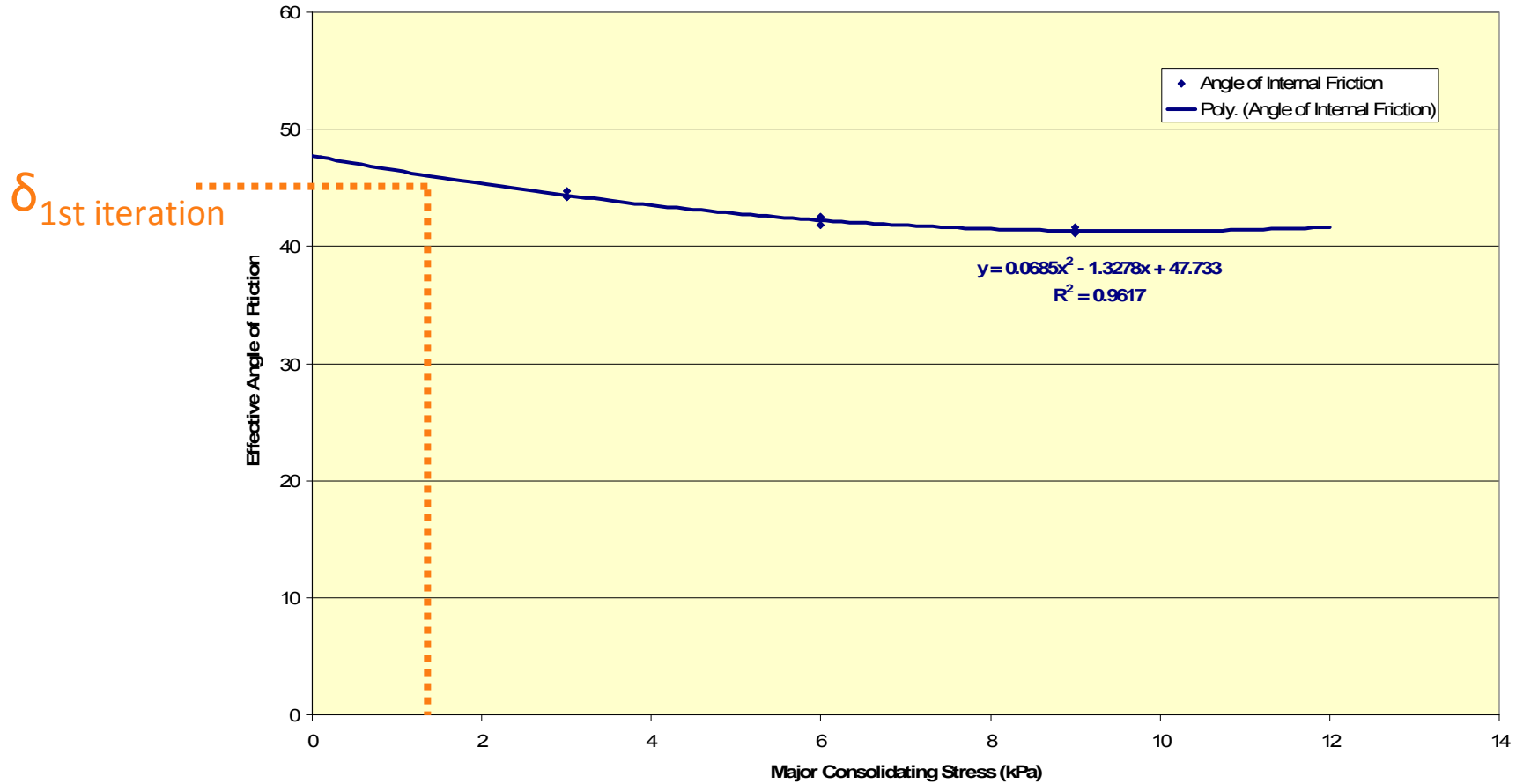


α	$H(\alpha)$	ff
15	2.22	1.35

Draw the flow factor ($\sigma_1 / \bar{\sigma}_1$) on the flow function plot, to derive the stress in the arch, σ_1 , and the corresponding major consolidation stress, $\bar{\sigma}_1$, at the “flow / no flow” boundary



Using the major consolidating stress, σ_1 , corresponding to the stress in the arch $\overline{\sigma_1}$, derive the effective angle of friction (first iteration)



Then, using the new value of the effective angle of internal friction, again calculate all other parameters.....

φ	$\delta_{1st\ iteration}$
26.3	45.5



α	$H(\alpha)$	ff
15	2.25	1.25

Therefore.....

$$\bar{\sigma}_1 \text{ (original)} = 1.86$$

$$\bar{\sigma}_1 \text{ (after first iteration)} = 1.78$$

In this case, further iterations have little affect on the value of $\bar{\sigma}_1$. Therefore this value can now be used in the following calculation, along with the value of density at the major consolidation stress corresponding to $\bar{\sigma}_1$

$$B = \frac{\bar{\sigma}_1 H(\alpha)}{\rho g}$$

$$B = 0.59\text{m}$$

$$\alpha = 15 \text{ degrees}$$

Therefore, after applying 20% increase to B and subtracting 3 degrees from the hopper half angle, the design criteria are.....

$$\underline{B = 0.71\text{m}}$$

$$\underline{\alpha = 12 \text{ degrees}}$$